

**The Caspase-like Cell Cycle Protease  
Separase:  
Upstream Regulations  
and Downstream Functions**

**DISSERTATION**

zur Erlangung des akademischen Grades einer Doktorin der  
Naturwissenschaften (Dr. rer. nat.)  
an der Fakultät für Biologie, Chemie und Geowissenschaften  
der Universität Bayreuth

vorgelegt von

**Susanne Hellmuth**

aus Quedlinburg

**Bayreuth, 2020**

This doctoral thesis was prepared at the department of Genetics at the University of Bayreuth from August 2011 until February 2020. It was supervised by Prof. Dr. Olaf Stemmann and is represented in front of the faculty II by Prof. Dr. Benedikt Westermann.

This is a full reprint of the dissertation submitted to obtain the academic degree of Doctor of Natural Sciences (Dr. rer. nat.) and approved by the Faculty of Biology, Chemistry and Geosciences of the University of Bayreuth.

Date of submission: 12.02.2020

Date of defense: 25.06.2020

Acting dean:

Prof. Dr. Matthias Breuning

Doctoral committee:

Prof. Dr. Benedikt Westermann (reviewer)

Prof. Dr. Andreas Möglich (reviewer)

Dr. Claus Kuhn

Prof. Dr. Stefan Heidmann (chairman)

## Table of contents

Abbreviations.....	1
Zusammenfassung .....	3
Summary.....	5
Introduction and state of the art .....	7
The cohesin cycle .....	7
Late mitotic events are driven by proteolysis.....	9
Late mitotic events are supervised by the spindle assembly checkpoint (SAC) .....	10
The separase-securin complex .....	11
Securin-independent regulation of separase .....	13
Non-canonical substrates and functions of separase .....	13
Aims of this thesis.....	15
Synopsis .....	16
Separase regulatory mechanisms .....	16
Investigating the positive effect of securin on separase .....	16
Protein phosphatase 2A times the liberation of separase from securin .....	17
Positive and negative regulation of separase by Cdk1-Cyclin B1.....	20
The peptidyl-prolyl-isomerase Pin1 regulates separase by enabling its Cdk1-Cyclin B1-dependent inhibition and limiting its proteolytic half-life .....	22
A second branch of spindle assembly checkpoint-dependent anaphase control: Inhibition of Separase by Mad2-activated shugoshin.....	27
Non-canonical separase functions.....	32
Local activation of human separase in interphase facilitates repair of double strand breaks by homology directed repair .....	32
Nek2A- and separase constitute a checkpoint that transforms anti- into pro-apoptotic factors when early mitosis falls below a minimal duration .....	36
References .....	43
Own contributions .....	52
Manuscripts .....	53
Hellmuth, S., Bottger, F., Pan, C., Mann, M. & Stemmann, O. PP2A delays APC/C-dependent degradation of separase-associated but not free securin. EMBO J 33, 1134-1147 (2014). .....	53
Hellmuth, S., Pohlmann, C., Brown, A., Bottger, F., Sprinzl, M. & Stemmann, O. Positive and negative regulation of vertebrate separase by Cdk1-cyclin B1 may explain why securin is dispensable. J Biol Chem 290, 8002-8010 (2015a). .....	82

Hellmuth, S., Rata, S., Brown, A., Heidmann, S., Novak, B. & Stemmann, O. Human chromosome segregation involves multi-layered regulation of separase by the peptidyl-prolyl-isomerase Pin1. Mol Cell 58, 495-506 (2015b). .....	91
Hellmuth, S., Gutierrez-Caballero, C., Llano, E., Pendas, A. M. & Stemmann, O. Local activation of mammalian separase in interphase promotes double-strand break repair and prevents oncogenic transformation. EMBO J 37, e99184 (2018). .....	122
Hellmuth, S., Gomez-H, L., Pendas, A. M. & Stemmann, O. Securin-independent regulation of separase by checkpoint-induced shugoshin-Mad2. Nature, 580, 536-541 (2020). .....	153
Hellmuth, S. & Stemmann, O. Separase-triggered apoptosis enforces minimal length of mitosis. Nature, 580, 542-547 (2020). .....	172
List of all own publications .....	195
Danksagung .....	196
Eidestattliche Erklärung .....	197

## Abbreviations

53BP1 = p53-binding protein 1

Ac = acetyl-

APC/C = anaphase promoting complex or cyclosome

APD = active protease domain

ATM = ataxia telangiectasia mutated

Bad = BCL2 associated agonist of cell death

Bak = BCL2 antagonist/killer

Bax = BCL2 associated X, apoptosis regulator

Bcl2 = B-cell lymphoma 2

Bcl-xL = B-cell lymphoma-extra large (gene: BCL2-like 1)

BH-domain = Bcl-2 homology domain

Bim = BCL2-interacting mediator of cell death

Bub3 = budding uninhibited by benzimidazole

BubR1 = Bub1 related kinase 1

CAD = caspase activated DNase

Cdc20 = cell division cycle 20

Cdk1 = cyclin dependent kinase

ChIP = chromatin immunoprecipitation

Chk2 = checkpoint kinase 2

CLD = Cdc6-like domain

D-box = destruction box

DDR = DNA damage response

DiM = death in mitosis

DMBA = 7,12-Dimethylbenzo[a]anthracen

DMC = minimal duration of early mitosis checkpoint

DMSO = dimethyl sulfoxide

DRB = doxorubicin

DSB = double strand break

E1A = adenovirus early region 1A

EGCG = Epigallocatechin gallate

ER = estrogen receptor

GFP = green fluorescent protein

$\gamma$ H2AX = H2A histone family member X phosphorylated at Ser-139

HCT116 = human colonic carcinoma tumorigenic 116

HDR = homology directed repair

Hek293 = human embryonic kidney 293

Hek293T = Hek293 expressing SV40 large T antigen

hRas (V12) = transforming protein p21 (a GTPase), Val instead of Gly at position 12

hTERT = human telomere reverse transcriptase

ICAD = inhibitor of CAD

IFM = immunofluorescence microscopy

IP = immunoprecipitation

KEN = Lys-Glu-Asn

Mad1/2 = mitotic arrest deficient 1/2

MCC = mitotic checkpoint complex

Mcl1 = myeloid cell leukemia 1

MDC1 = mediator Of DNA Damage Checkpoint 1  
Me = methyl-  
MEF = mouse embryonic fibroblasts  
mKEB/mBD = mutated KEN- and destruction boxes  
Mms21 = Methyl methanesulfonate-sensitivity protein 21  
MOM = mitochondrial outer membrane  
MOMP = mitochondrial outer membrane permeabilization  
M-phase = mitosis + cytokinesis  
MPS1 = monopolar spindle protein 1 (Ser/Thr-protein kinase required for SAC)  
MR tail = C-terminal Met-Arg  
Nek2a = NIMA Related Kinase 2a  
NES = nuclear export signal  
NHEJ = non-homologous end joining  
NPC = nuclear pore complex  
OHT = 4-Hydroxytamoxifen  
PARP = poly ADP-ribose polymerase  
PBE = polar body extrusion  
PCS = premature sister chromatid separation  
Pin1 = peptidyl prolyl cis/trans isomerase, NIMA-interacting 1  
PP2A = protein phosphatase 2A  
PPD = pseudo protease domain  
PPIase = peptidyl-prolyl isomerase  
PRMT1 = protein arginine N-methyltransferase 1  
PTM = posttranslational modification  
qPCR = quantitative polymerase chain reaction  
RG-repeat = Arg-Gly-repeats  
RNAi = RNA interference  
RNC = ribosome nascent chain complex  
RPE = retinal pigment epithelium  
SAC = spindle assembly checkpoint  
Scc1 = sister chromatid cohesion 1  
Sgo1/2 = shugoshin 1 or -2  
SILAC = stable isotope labeling with amino acids in cell culture  
SIM = structured illumination microscopy  
siRNA = small interfering RNA  
SPD = alpha-solenoid protease domain  
SMC = structural maintenance of chromosomes  
SUMO = small ubiquitin-like modifier  
Tev = tobacco etch virus  
TM = transmembrane  
Tom20 = Translocase of the outer membrane 20  
TPA = 12-O-Tetradecanoylphorbol-13-acetate  
TPR = translocated promoter region (nuclear basket protein) or tetratricopeptide repeat  
Trip13 = thyroid hormone receptor interacting protein 13  
UPS = ubiquitin-proteasome-system  
Wapl = Wings apart-like protein homolog  
WW = Trp-Trp

## Zusammenfassung

Separase löst alle eukaryotischen Anaphasen aus, indem sie kohäsionsvermittelndes Cohesin spaltet. Bis dahin wird diese essentielle Protease durch Securin inhibiert. Separase kann alternativ durch Assoziation mit Cdk1-Cyclin B1 gehemmt werden, aber der entsprechende Komplex ist in der frühen Mitose wenig abundant und kann nicht erklären, warum Securin in Vertebraten entbehrlich ist. Die Proteinphosphatase 2A (PP2A) bindet Separase ebenfalls, aber die physiologische Rolle dieser Interaktion bleibt rätselhaft. Durch die Inaktivierung des 'spindle assembly checkpoint' (SAC) in der Metaphase kann die Ubiquitin-Ligase APC/C die proteasomale Zerstörung von Securin (und Cyclin B1) vermitteln und dadurch Separase aktivieren.

Obwohl sie strukturell mit Caspasen verwandt ist, wurde Separase bisher nicht mit der Apoptose in Verbindung gebracht. Stattdessen wurde in zwei Studien eine Rolle der Hefe-Separase bei der Reparatur von DNS-Schäden vorgeschlagen. Die Frage, ob diese nicht-kanonische Interphase-Funktion von Separase in Säugern konserviert ist, blieb jedoch unbeantwortet.

Meine Untersuchung von Regulationsmechanismen und Funktionen der Wirbeltier-Separase ergab die folgenden Ergebnisse:

- 1) Securin assoziiert kotranslational mit Separase und verhindert ihre Aggregation. Dies legt nahe, dass es die korrekte Faltung dieser riesigen Protease unterstützen könnte, und bietet eine erste mechanistische Erklärung für den genetischen Nachweis, dass Securin nicht nur ein Inhibitor, sondern auch ein Aktivator von Separase ist.
- 2) APC/C bevorzugt als Substrat phosphoryliertes gegenüber unphosphoryliertem Securin. Während freies Securin in der Mitose phosphoryliert wird, wird das an Separase gebundene Securin durch assoziierte PP2A in einem unphosphorylierten Zustand gehalten. Dies bewirkt, dass überzähliges Securin zuerst abgebaut wird und weitgehend verschwunden ist, wenn die Proteolyse von Separase-assoziiertem Securin beginnt. Dadurch wird eine vorzeitige Aktivierung der Separase verhindert und der Metaphase-Anaphase-Übergang geschärft.
- 3) Einmal freigesetzt, unterliegt Separase einer Konformationsänderung durch die Peptidyl-Prolyl-Isomerase Pin1. Dies macht sie gegen restliches Securin resistent. Gleichzeitig wird dadurch die Aktivität von Separase zeitlich begrenzt, so dass Cohesin bereits in Telophase erneut auf Chromatin geladen werden kann ohne gespalten zu werden.
- 4) Die Pin1-katalysierte Separase-Isomerisierung von *trans* nach *cis* ist für die Cdk1-Cyclin B1-abhängige Inhibition essentiell und erklärt, warum die Kinase und Securin nicht gleichzeitig mit Separase assoziieren können.
- 5) Die Bildung des Cdk1-Cyclin B1-Separase-Komplexes wird durch Phosphorylierung von Cyclin B1 in der frühen Mitose gehemmt. Die Dephosphorylierung führt zu einem zweiten Maximum von Cdk1-Cyclin-B1-Separase in der späten Mitose, obwohl zu diesem Zeitpunkt das meiste Cyclin B1 bereits abgebaut ist.
- 6) Bei der Zerstörung dieses letzten Cyclin B1 in der frühen G1-Phase wird Separase aus dem späten Cdk1-Cyclin B1-Separase-Komplex freigesetzt und löst dann die Entkopplung der

Zentriolen aus, wodurch eine spätere Zentrosomen-Duplikation lizenziert wird.

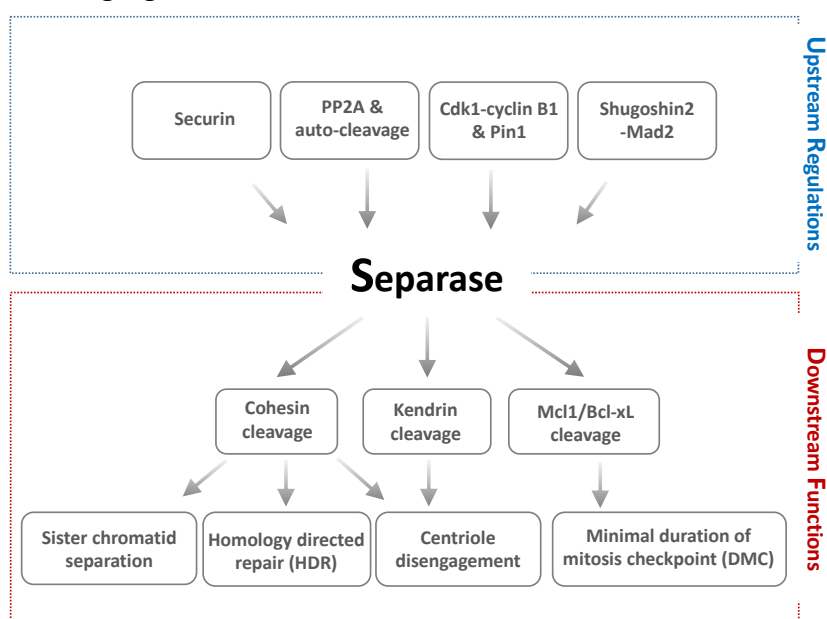
7) Humanes Shugoshin 2 (Sgo2), ein Protektor von meiotischem Cohesin mit bisher unbekannter Funktion in somatischen Zellen, stellt einen entscheidenden zweiten Zweig der Anaphasenregulation dar. Es wird durch SAC-aktiviertes Mad2 in die Lage versetzt, Separase inhibitorisch zu binden und kann Securin funktionell ersetzen. Eine akute Depletion von Sgo2 und Securin (aber nicht die einzelnen Verluste) führen zu einer Deregulierung von Separase gefolgt von vorzeitigem Verlust der Schwesterchromatid-Kohäsion.

8) Der AAA-ATPase-Trip13 disassembliert den Separase-Sgo2-Mad2-Komplex nach SAC-Inaktivierung in der Metaphase. Während also der kanonische, Securin-abhängige Zweig der Anaphasekontrolle Proteolyse erfordert, tut dies die Freisetzung aktiver Separase von Sgo2-Mad2 nicht.

9) Humane Separase fördert die Reparatur von DNS-Doppelstrangbrüchen (DSBs) durch homologe Rekombination. Eine Reihe von posttranslationalen Modifikationen führt zur Rekrutierung von Separase aus dem Zytoplasma hin zu DSBs. Hier wird Separase aktiviert und spaltet lokal Cohesin. Dies könnte der Reparaturmaschinerie den Zugang zur beschädigten DNS erleichtern.

10) Die Spaltung von Mcl1 und Bcl-xL durch Separase wandelt diese anti-apoptotischen Faktoren in pro-apoptotische Fragmente um und löst über den intrinsischen Weg der Apoptose den Tod in Mitose aus. Das C-terminale Spaltfragment von Mcl1 bildet Cytochrom c leitende Poren in der mitochondrialen Außenmembran, eine Fähigkeit, von der man bisher annahm, dass sie auf Bak und Bax beschränkt ist.

11) Mcl1 und Bcl-xL sind nur dann Substrate für Separase, wenn sie durch Nek2a phosphoryliert vorliegen. Eine gleichzeitige Aktivität beider Enzyme tritt nur dann auf, wenn die Zellen aufgrund eines pathologischen Verlustes des SAC ungehindert schnell durch die Mitose gehen. Nek2a und Separase stellen daher einen 'minimal duration of early mitosis checkpoint' (DMC) dar, welcher die Apoptose von Zellen auslöst, die ansonsten zur Chromosomen-Fehlseggregation verdammt wären.



## Summary

Separase universally triggers eukaryotic anaphases by cleavage of sister chromatid cohesion mediating cohesin. Until then, this essential protease is kept inactive by association with securin. Separase can alternatively be inhibited by association with Cdk1-cyclin B1 but the corresponding complex is scarce in early mitosis and cannot explain why vertebrate securin is dispensable. Protein phosphatase 2A (PP2A) also binds separase but the physiological role of this interaction remains enigmatic. Silencing of the spindle assembly checkpoint (SAC) in metaphase enables the ubiquitin ligase APC/C to mediate the proteasomal destruction of securin (and cyclin B1), thereby activating separase.

Despite being structurally related to caspases, separase has not been previously linked to apoptosis. Instead, two studies suggested a role of yeast separase in DNA damage repair but left unanswered whether this non-canonical interphase function of separase is conserved in mammals.

Studying upstream regulations and downstream functions of vertebrate separase, I discovered the following:

- 1) Securin associates co-translationally with separase and prevents its aggregation. This suggests that it might assist the proper folding of this giant protease and offers a first mechanistic explanation for the genetic evidence that securin is not only an inhibitor but also an activator of separase.
- 2) APC/C prefers phosphorylated securin over un-phosphorylated securin as a substrate. While free securin is phosphorylated in mitosis, separase-bound securin is kept in an un-phosphorylated state by associated PP2A. This effecuates supernumerous securin to be degraded first and largely gone by the time separase-associated securin is targeted for proteolysis. Thereby, premature activation of separase is prevented and the metaphase-to-anaphase transition sharpened.
- 3) Once liberated, separase is subject to conformational change by the peptidyl-prolyl isomerase Pin1 and thereby rendered resistant against residual securin. At the same time, this limits separase's proteolytic half-life and allows cohesin to be reloaded onto telophase chromatin without being cleaved.
- 4) Pin1 catalyzed *trans*-to-*cis* isomerization of separase is essential for Cdk1-cyclin B1-dependent inhibition and explains why the kinase and securin bind separase in a mutually exclusive manner.
- 5) Formation of the Cdk1-cyclin B1-separase complex is counter-acted by phosphorylation of cyclin B1 in early mitosis. Dephosphorylation results in a second peak of Cdk1-cyclin B1-separase complex formation in late mitosis when most cyclin B1 has already been degraded.
- 6) Upon destruction of this last cyclin B1 in early G1 phase, separase is released from the late

Cdk1-cyclin B1-separase complex and triggers centriole disengagement, thereby licensing later centrosome duplication.

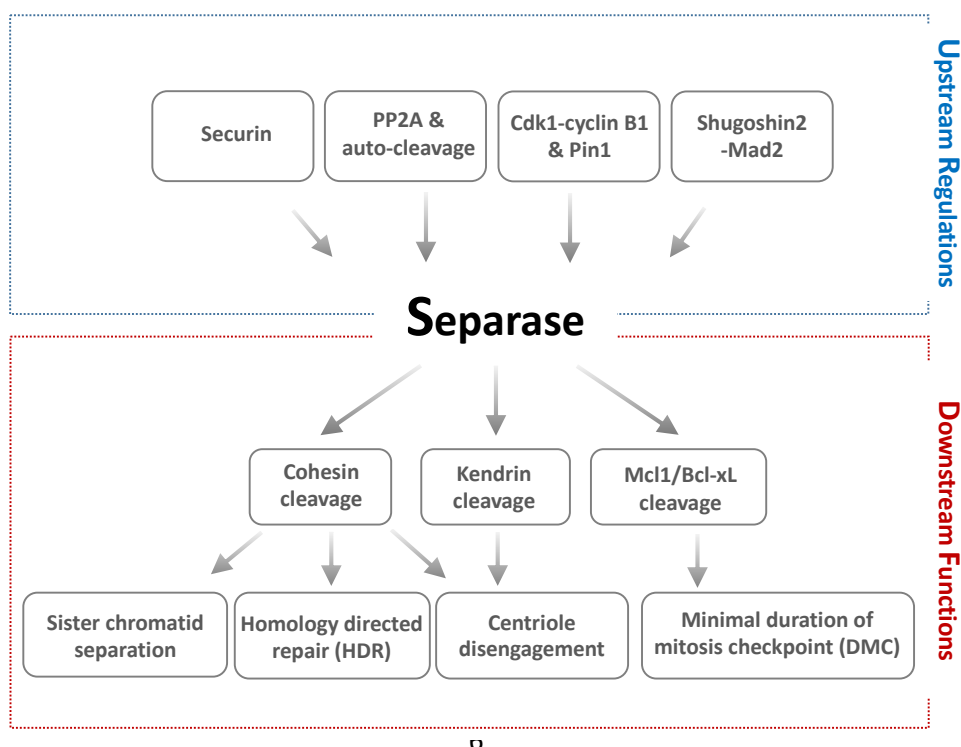
7) Human shugoshin 2 (Sgo2), a protector of meiotic cohesin with hitherto unknown function in somatic cells, represents a crucial second branch of anaphase regulation. It is enabled by SAC-activated Mad2 to bind and inhibit separase and can functionally replace securin. Acute depletion of Sgo2 and securin (but not the individual knock-downs) result in separase deregulation and premature loss of cohesion.

8) The AAA-ATPase Trip13 actively disassembles the separase-Sgo2-Mad2 complex upon SAC silencing in metaphase. Thus, while the canonical, securin-dependent branch of anaphase control requires proteolysis, the release of active separase from Sgo2-Mad2 does not.

9) Human separase facilitates the repair of DNA double strand breaks (DSBs) by homologous recombination. A number of post-translational modifications result in the recruitment of separase from the cytoplasm to DSBs. Here, separase is activated and locally cleaves cohesin, which might grant the repair machinery access to the damaged DNA.

10) Cleavage of Mcl1 and Bcl-xL by separase transforms these pro-survival factors into pro-apoptotic fragments and triggers death in mitosis via the intrinsic pathway of apoptosis. The C-terminal cleavage fragment of Mcl1 forms cytochrome c conducting pores into the mitochondrial outer membrane, an ability which was previously thought to be limited to Bak and Bax.

11) Mcl1 and Bcl-xL are substrates for separase only when phosphorylated by Nek2a. Simultaneous activity of both enzymes only occurs when cells rush through mitosis due to pathological loss of the SAC. Nek2a and separase therefore represent a 'minimal duration of early mitosis checkpoint' (DMC), which triggers apoptosis of cells that are doomed to chromosome missegregation.



## Introduction and state of the art

### The cohesin cycle

The invention of sister chromatid cohesion enabled eukaryotic (as opposed to prokaryotic) cells to timely separate the reduplication of chromosomes in S-phase from their segregation in M-phase (Nasmyth and Haering, 2009). Cohesion is established in a co-replicative manner and mediated by a ring-shaped multi-protein complex, cohesin, which encircles and thereby pairs the two copies of each chromosome (Figure 1) (Gruber et al., 2003; Haering et al., 2008; Uhlmann and Nasmyth, 1998). Cohesion facilitates the tension-dependent monitoring of proper microtubule-kinetochore interactions in early mitosis and, as such, is instrumental for the error-free distributive halving of the genetic material during cell division.

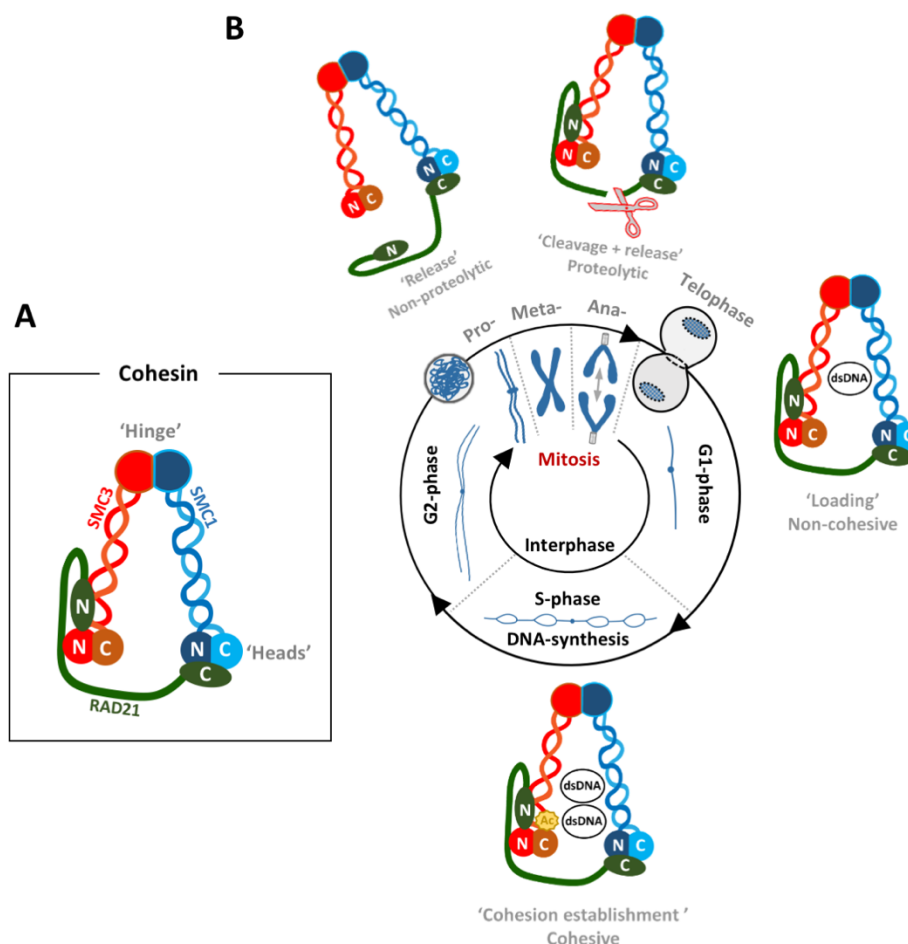


**Figure 1: Establishment and dissolution of cohesin throughout the chromosome cycle.**

**A)** Structure of the cohesin ring (see Gligoris and Lowe, 2016; Nasmyth and Haering, 2009 for details). Smc1 and Smc3 are highly elongated SMC (structural maintenance of chromosomes) proteins, in which an ATPase head domain is connected via an antiparallel coiled-coil to a hinge domain that mediates their heterodimerization. Binding of the ATPase to the kleisin subunit Rad21/Scc1 closes the ring. Note that ATP hydrolysis, which impacts loading and non-proteolytic release of cohesin, requires the head domains to come together (not shown). Rad21 serves as landing platform for interacting Scc3/stromal antigen and Pds5, which in turn bind to either Sororin and shugoshin or Rad61/Wapl (not shown). **B)** Starting in late telophase, vertebrate cohesin is loaded onto DNA. Upon entry into S-phase, sister chromatid cohesion is established in a co-replicative manner and stabilized by acetylation (Ac) of Smc3, which leads to recruitment of the cohesin protector sororin (not shown). In early mitosis, cohesin is removed from chromosome arms in a non-proteolytic manner, i.e. by opening of the Smc3-Rad21 'gate'. A small pool of cohesin is preserved at centromeres. Sister chromatids finally separate when this centromeric cohesin is opened by Separase-dependent cleavage of Rad21 at anaphase (see figure 2 for details).

However, before the two sister chromatids of each chromosome can separate, cohesin has to be quantitatively removed from chromatin, which, in metazoans, occurs in two waves (Figure 2) (Waizenegger et al., 2000). Activation of mitotic kinases results in phosphorylation-dependent inactivation of the cohesin protector sororin in prophase (Liu et al., 2013). Phosphorylated sororin is displaced by anti-cohesive Wapl, which causes ring opening by dissociation of the cohesin subunits Smc3 and Rad21/Scc1 (Buheitel and Stemmann, 2013; Chan et al., 2012; Eichinger et al., 2013; Kueng et al., 2006; Ouyang and Yu, 2017). This removes cohesin from chromosome arms. However, sister chromatid cohesion within (peri-)centromeric regions is preserved because, here, protein phosphatase 2A (PP2A), which is recruited to cohesin by the adaptor protein shugoshin 1 (Sgo1), keeps sororin in the active, de-phosphorylated state (Kitajima et al., 2006; Liu et al., 2013; Riedel et al., 2006). Triggering of anaphase essentially requires destruction of this remaining centromeric cohesin by separase, a caspase-related Cys-endopeptidase that cleaves Rad21 (Figure 2) (Uhlmann et al., 1999; Uhlmann et al., 2000; Wirth et al., 2006). Already shortly thereafter, in telophase, cohesin is reloaded onto the decondensing chromatin (Losada et al., 1998; Sumara et al., 2000). (This reloading does not require cohesin re-synthesis because only a very small fraction of total Rad21 is cleaved by separase.)

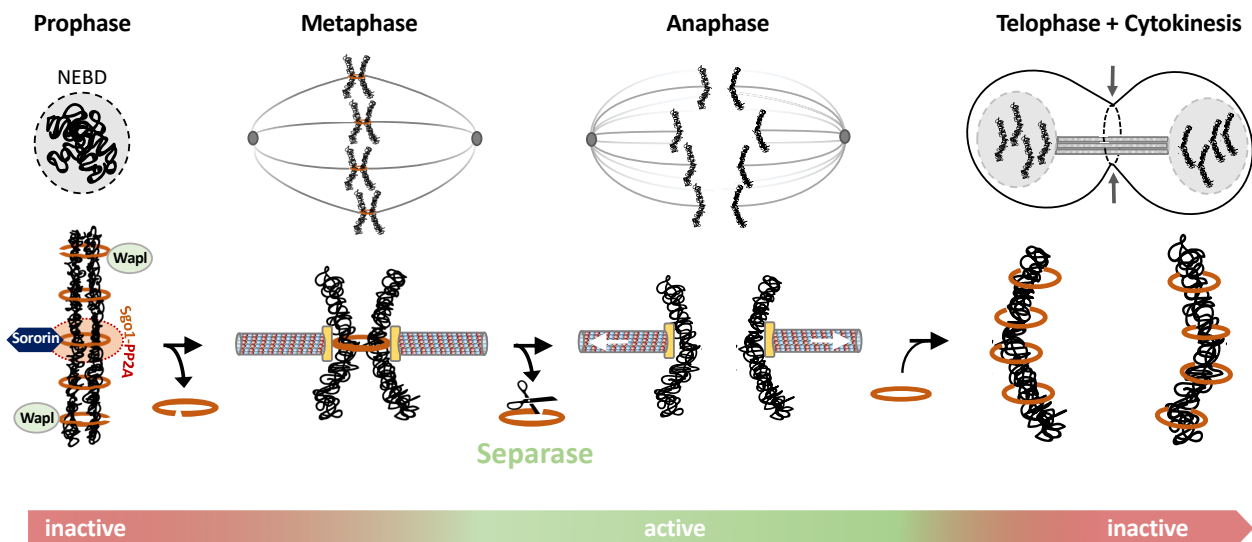


**Figure 2: Stepwise removal of cohesin from metazoan chromosomes in mitosis.**

In early mitosis sororin at chromosome arms is inactivated by phosphorylation, thus enabling the cohesin-release factor Wapl to open the Smc3-Rad21 gate. Sgo1-dependent recruitment of PP2A ensures continued dephosphorylation of sororin at centromeres, thereby preserving cohesion. Sister chromatids are finally separated and anaphase is triggered when the Rad21 subunit of centromeric cohesin is cleaved by Separase. Kollerin (not shown) reloads vertebrate cohesin onto chromatin in late telophase. (Note that cohesin is not drawn to scale in this cartoon and does embrace chromatin loops rather than entire, condensed chromatids. Note also that mammalian kinetochores bind 15-30 microtubules rather than just 1, as depicted here for sake of clarity.)

## Late mitotic events are driven by proteolysis

Despite its essential function as universal trigger of eukaryotic anaphase, separase is also a dangerous protease. Its proteolytic activity must be tightly controlled in order to prevent premature sister chromatid separation (PCS) which would be followed by chromosome missegregation and/or cell death. Prior to anaphase onset, vertebrate separase is inhibited by (mutually exclusive) association with securin or Cdk1-cyclin B1 (Figure 3, left) (Gorr et al., 2005; Stemmann et al., 2001; Zou et al., 1999). Securin may not have separase-independent functions. In contrast, Cdk1-cyclin B1 is the master regulatory kinase of mitosis and phosphorylates a multitude of proteins. Its activation and inactivation, respectively, is necessary and sufficient for entry into and exit from mitosis (Murray and Kirschner, 1989; Murray et al., 1989). Separase is activated at the metaphase to anaphase transition when both securin and cyclin B1 are degraded via the ubiquitin-proteasome pathway (Figure 3, right) (Ciosk et al., 1998; Glotzer et al., 1991). The corresponding ubiquitin-ligase (E3) is the anaphase-promoting complex or cyclosome (APC/C) in conjunction with its essential co-activator Cdc20 (Holloway et al., 1993; Irniger et al., 1995; King et al., 1995; Sudakin et al., 1995). APC/C<sup>Cdc20</sup> recognizes an amino acid motif of the consensus sequence R-x-a-L-g-x-l-x-n, the so-called destruction box (or D-box), which is located close to the N-termini of securin and cyclin B1 (King et al., 1996; Zou et al., 1999). In addition (or alternatively), the APC/C recognizes a second degron, the so-called KEN-box, which is located upstream of securin's D-box (but is missing from cyclin B1) (Pfleger and Kirschner, 2000).

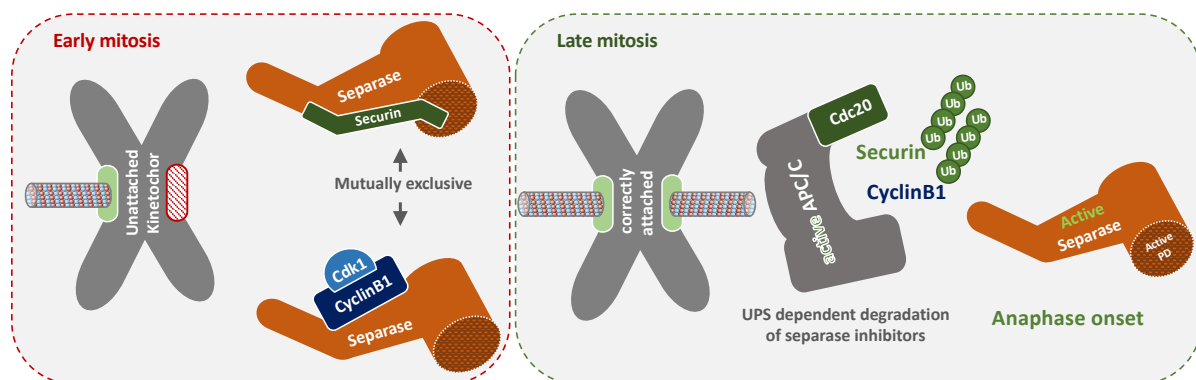


**Figure 3: Regulation of separase throughout mitosis.**

Early in mitosis, separase is still held inactive by mutually exclusive interaction with either securin or Cdk1-cyclin B1. At the metaphase-to-anaphase transition, activation of the E3 ligase APC/C<sup>Cdc20</sup> results in the degradation of securin and cyclin B1 via the ubiquitin-proteasome-system (UPS), thus releasing separase in its proteolytically active form.

## Late mitotic events are supervised by the spindle assembly checkpoint (SAC)

APC/C<sup>Cdc20</sup> activity is controlled by the spindle assembly checkpoint (SAC), which is of prime importance for timing of mitosis and chromosome segregation fidelity in metazoans (Michel et al., 2001; Taylor and McKeon, 1997). As long as chromosomes have not yet properly attached to microtubules of the spindle, this essential surveillance mechanism generates a diffusible 'wait-anaphase' signal at kinetochores, which inhibits APC/C<sup>Cdc20</sup> (Musacchio, 2015; Nasmyth, 2005). How does this work? A multitude of factors, among them the kinases Aurora B and Mps1, mediate the recruitment of a Mad1-Mad2 complex to un- or mis-attached kinetochores (Ditchfield et al., 2003; Tighe et al., 2008; Yamagishi et al., 2012). This kinetochore-bound Mad2 catalyzes the conformational activation of soluble Mad2, thereby enabling it to bind and sequester Cdc20 (Musacchio, 2015; Nasmyth, 2005). The subsequent recruitment of the checkpoint factors BubR1 and Bub3 results in formation of the heterotetrameric mitotic checkpoint complex (MCC), and the continued inactivation of APC/C (Figure 4, upper panel) (Alfieri et al., 2016; Chao et al., 2012; Sudakin et al., 2001).

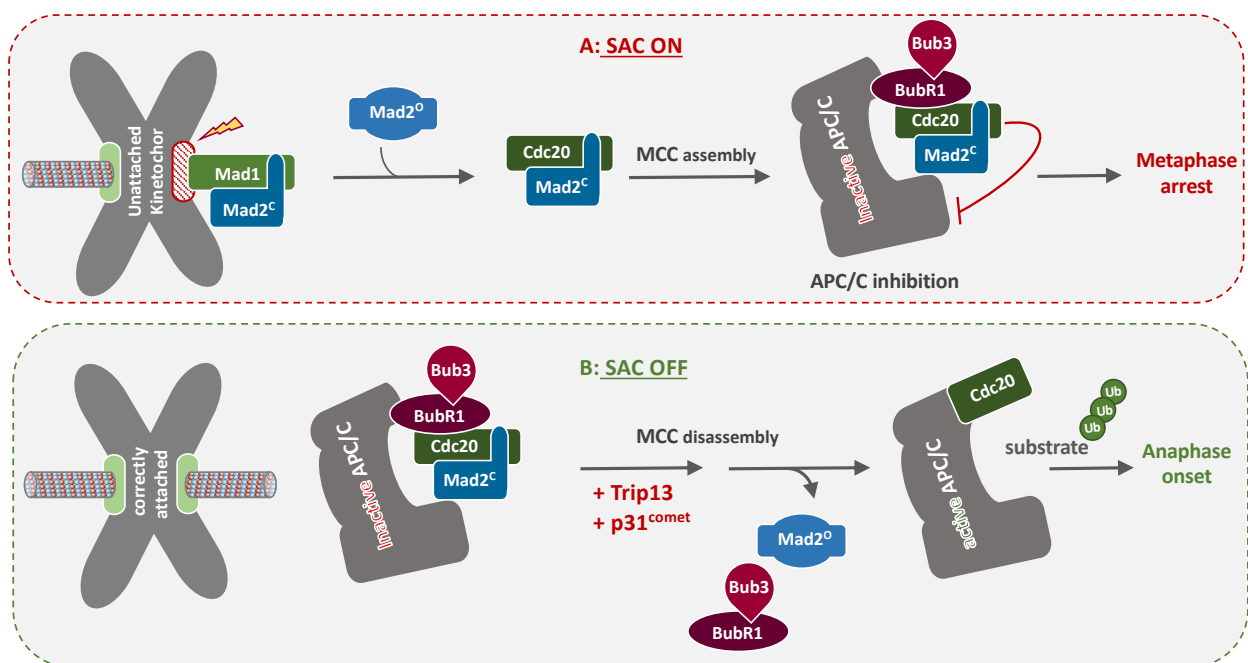


**Figure 4: The spindle assembly checkpoint (SAC) and its silencing.**

**A)** Unattached kinetochores are decorated with Mad1-bound Mad2, which catalyzes the conversion of diffusible Mad2 from its inactive 'open' (o) into its active 'closed' (c) conformation. Sequestration of Cdc20 by Mad2<sup>c</sup> and the SAC components BubR1 and Bub3 results in the formation of the mitotic checkpoint complex (MCC) and hinders Cdc20 to activate the anaphase-promoting complex/cyclosome (APC/C). **B)** Bi-orientation of all sister-kinetochore pairs by proper amphitelic attachment to microtubules displaces Mad1-Mad2 and terminates the conformational activation of Mad2. Subsequent disassembly of the MCC by the AAA-ATPase Trip13 and the Mad2-specific adaptor protein p31<sup>comet</sup> liberates Cdc20 and activates APC/C.

Upon proper amphitelic attachment of the chromosomes, Mad1-Mad2 is displaced from kinetochores and the generation of active Mad2 ceases (Musacchio, 2015). Mechanisms that constitutively challenge the SAC then quickly lead to the de-repression of Cdc20. Of prime importance here is the AAA-ATPase Trip13. With the aid of p31<sup>comet</sup>, a Mad2-specific adapter molecule, this molecular machine actively dismounts the MCC, thereby liberating Cdc20 (Figure 4, lower panel) (Alfieri et al., 2018; Eytan et al., 2014). Cdc20-activated APC/C then mediates the ubiquitin-dependent proteasomal degradation of securin and cyclin B1, thereby releasing separase in its proteolytically active form.

### **The separase-securin complex**

Separase is a large Cys-endopeptidase which, like caspases, belongs to the CD superfamily of proteases (Uhlmann et al., 2000). It is encoded by an essential gene and represents the universal trigger of eukaryotic anaphase (Wirth et al., 2006). Separase varies greatly in length and sequence between different eukaryotes with the exception of its conserved C-terminal protease domain. Human separase is a 233 kDa protein and consists of 2120 amino acids. It starts with a vertebrate-specific  $\alpha$ -helical domain (residues 1-650) that is followed by a structurally conserved, large tetratricopeptide repeat (TPR)-like domain (residues 651-1641, see Figure 5) (Boland et al., 2017). This  $\alpha$ -solenoid domain contains two disordered insertions (residues 1070-1140 and 1307-1561) that are of relevance for separase regulation (see below). A nuclear export sequence (NES) centered around amino acid 1665 separates the  $\alpha$ -solenoid- from the C-terminal protease domain (SPD). The SPD can be subdivided into a pseudoprotease domain (PPD, residues 1755-1890) and the active protease domain (APD, residues 1891-2120), with the latter containing the catalytic dyad consisting of His-2003 and Cys-2029. The APD is similar in fold to caspases, which are activated by re-organization of loop 4 (L4) upon homo-dimerization and auto-cleavage (Boland et al., 2017; Lin et al., 2016). Interestingly, L4 of separase structurally resembles the activated conformation of L4 in caspases - even when separase is in complex with securin. Consistently, after the removal of securin separase does not need further processing in order to become proteolytically active.

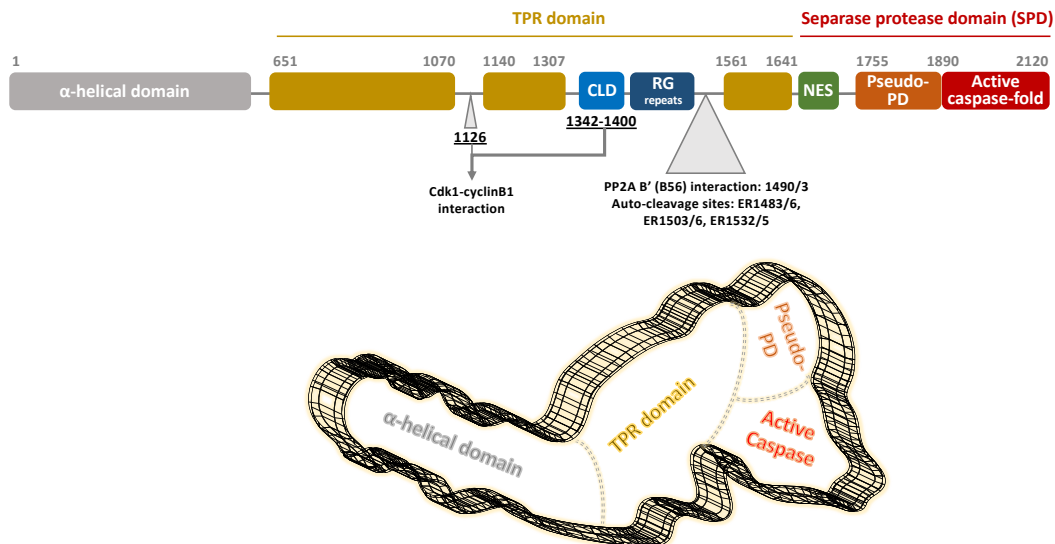


**Figure 5: Separate structure.**

**A)** Domain structure and important regulatory elements of human separase (modified from Boland et al., 2017). TPR = tetratricopeptide repeat; CLD = Cyclin B interacting Cdc6-like domain; RG = Arg-Gly or PP2A interaction; NES = nuclear export signal. **B)** Overall shape of human separase in complex with securin as revealed by electron microscopy (Boland et al., 2017; Viadiu et al., 2005).

Securin, which by itself is an intrinsically disordered protein, binds separase in a highly elongated, antiparallel fashion and entertains contacts to all domains of the protease (with the possible exception of the N-terminal domain that is specific for vertebrates) (Boland et al., 2017; Viadiu et al., 2005). Importantly, securin employs a pseudo-substrate sequence to competitively inhibit separase (Lin et al., 2016; Nagao and Yanagida, 2006). While cohesin is cleaved by separase after an E-x-x-R motif, the Arg is missing in securin and - depending on the species - replaced by Pro, Met or Phe. This exchange distorts the arrangement of residues within the catalytic site of separase, thereby explaining why the pseudo-substrate sequence is not cleaved (Boland et al., 2017; Lin et al., 2016).

Genetics tells us that securin also exerts a positive effect on separase, which, curiously, is even more important than the inhibitory effect. In species like *S. pombe* and *D. melanogaster*, in which securin is essential, the loss of function phenotypes of securin and separase are the same (Funabiki et al., 1996; Stratmann and Lehner, 1996). And when securin is not essential, like in *S. cerevisiae* and mammals, its absence does not result in premature cleavage of cohesin but instead in reduced amount/activity of separase (Pfleghaar et al., 2005; Yamamoto et al., 1996). It has been suggested that securin might act as a separase specific chaperone and assists proper folding of the giant protease (Hornig et al., 2002). However, this hypothesis has never been experimentally addressed, which is why, mechanistically, the positive effect of securin on separase remains enigmatic.

## Securin-independent regulation of separase

A study on chromosome segregation in *Xenopus* egg extracts, first identified separase inhibition by Cdk1-cyclin B1-dependent phosphorylation (Stemmann et al., 2001). Subsequent work revealed that phosphorylation of separase is necessary but not sufficient for its inhibition by Cdk1-cyclin B (Gorr et al., 2005). The kinase also has to stably associate with the protease. Securin and Cdk1-cyclin B cannot bind to separase at the same time and, thus, represent co-existing rather than synergistic inhibitory mechanisms at the molecular level. Somewhat unexpected, the stable binding of the kinase to separase is not mediated by the catalytic subunit itself but rather by the regulatory cyclin. Crosslinking experiments demonstrated that cyclin B is in direct contact with the so-called CLD motif centered around position 1370 of human separase (Boos et al., 2008). Why this explained the need of CLD phosphorylation, it left the essential requirement of Ser-1126 phosphorylation for complex formation unresolved (Boos et al., 2008; Stemmann et al., 2001).

Interestingly, metazoan separase cleaves itself upon activation (Waizenegger et al., 2000; Zou et al., 2002). In human separase three auto-cleavage sites were mapped between residues 1486 and 1535 (Zou et al., 2002). The auto-cleavage sites overlap with a binding site for protein phosphatase 2A (PP2A). Thus, it comes at no surprise that auto-cleavage prevents PP2A binding and *vice versa* (Holland et al., 2007). Furthermore, it was demonstrated 1) that auto-cleavage is dispensable for the proteolytic activity of separase *in vitro* and 2) that within the separase-PP2A complex both enzymes retain activity (Holland et al., 2007; Zou et al., 2002). There were two reports about putative functions of auto-cleavage and PP2A binding (Holland et al., 2007; Papi et al., 2005) but the Stemmann lab was unable to reproduce these results.

## Non-canonical substrates and functions of separase

As outlined above, separase cleaves mitotic and meiotic cohesin and - in metazoans - itself. In addition, a total of three additional substrates were reported so far. 1) *C. elegans* expresses two versions of CENP-A, the centromer-specific histone H3 variant: HCP-3 and CPAR-1. Of these, CPAR-1 is cleaved by separase at the end of meiosis I. However, no function could be assigned to this cleavage (Monen et al., 2015). 2) *S. cerevisiae* separase cleaves a non-essential, yeast specific protein, Slk19. Preventing its cleavage results in

minimal destabilization of the mitotic spindle (Sullivan et al., 2001). 3) As first demonstrated in *Xenopus* egg extracts, separase has a role in centriole disengagement, which constitutes a licensing step for later centrosome duplication (Tsou and Stearns, 2006). While the Stemmann group reported that cleavage of centrosomal cohesin triggers centriole disengagement (Schockel et al., 2011), two other groups claimed that kendrin/pericentrin-B is the relevant substrate (Lee and Rhee, 2012; Matsuo et al., 2012). Moreover, it remains unclear how separase could trigger centriole disengagement, which occurs in early G1 phase, whereas the reloading of cohesin in telophase suggests rapid inactivation of the protease after anaphase. Finally, yet another study reported that the absence of separase merely delays but does not prevent centriole disengagement (Tsou et al., 2009). Recent data from the Stemmann group suggest that the cleavage of centrosomal cohesin or kendrin is each sufficient for centriole disengagement (Kahlen and Stemmann, unpublished). This observation could (partially) resolve the contradiction and, important in this context, it confirms kendrin as a *bona fide* substrate of vertebrate separase.

In addition, two yeast studies reported an unexpected function of separase in interphase rather than M-phase (McAleenan et al., 2013; Nagao et al., 2004). The authors found that DNA double strand breaks (DSBs) result in the activation of separase and cleavage of cohesin in the vicinity of the break. However, overwhelming evidence shows that in response to DSBs cohesin is re-loaded onto chromatin and accumulates especially around the damaged sites (Kim et al., 2010; Strom et al., 2004; Unal et al., 2007). Given this seeming contradiction, the field did not believe the two reports mentioned above.

Finally, metazoan separase seems to play a role in cytokinesis. Data from *C. elegans* demonstrate that separase is required for the fusion of vesicles with the plasma membrane at the cleavage furrow and midbody (Bembenek et al., 2010). Furthermore, vertebrate separase is required for the highly asymmetric cytokinesis during polar body extrusion at the end of female meiosis I (PBE I). Interestingly, PBE I in the absence of separase is restored by proteolytically inactive variants, thereby revealing the first function of separase that is independent of its proteolytic activity (Gorr et al., 2006; Kudo et al., 2006). Cdk1-cyclin B-separase might play a role, here, because within the complex the kinase, which is a known antagonist of cytokinesis, is also inhibited (Gorr et al., 2005).

In summary, finding additional substrates and functions of separase has proven exceedingly difficult. Whether this is due to technical reasons or whether there are simply no more substrates/functions to be discovered for this protease was not clear.

### **Aims of this thesis**

Given the many unresolved issues outlined above, the goal of this thesis was simply to 1) unravel hitherto unknown upstream regulations of separase and 2) identify novel downstream functions and substrates of this essential protease. In doing so, I hoped to better understand how a complete and undamaged complement of chromosomes is maintained in a healthy cell and what might go awry during disease.

## Synopsis

### Separase regulatory mechanisms

#### Investigating the positive effect of securin on separase (Hellmuth et al., 2015a)

Genetics clearly shows that securin not only antagonizes separase but simultaneously exerts a positive effect on the protease (Funabiki et al., 1996; Stratmann and Lehner, 1996). However, what molecular mechanism is behind this positive effect has remained enigmatic. Given that securin was reported to function in transcriptional regulation, we tested whether it promoted separase expression. Using an electrochemical chip developed by the Sprinzl group, we could show that the *SEPARASE* mRNA levels were the same in human *SECURIN*<sup>-/-</sup> cells and parental HCT116s. Moreover, based on Western analysis of total cell contents separase protein levels were also very similar between *SECURIN*<sup>-/-</sup> and parental HCT116 cells. Thus, securin does not seem to affect transcription, mRNA stability, or translation efficiency of separase. Interestingly, strong differences between both cell lines appeared when total cell lysates were cleared by centrifugation prior to immunoblotting: While most separase from *SECURIN*<sup>-/-</sup> cells ended up in the insoluble pellet, most separase from wild type cells was found in the soluble supernatant. Likewise, co-expression of securin greatly increased the solubility of transgene encoded, over-expressed separase. The Uhlmann lab had proposed - but never experimentally addressed - that 'securin might act as a chaperone, possibly facilitating proper folding of the large separase polypeptide' (Hornig et al., 2002). Misfolding and aggregation of separase could well explain its insolubility in *SECURIN*<sup>-/-</sup> cells. To clarify whether securin might bind to the protease co-translationally, I studied whether recombinant securin would co-purify with ribosome-nascent chain-complexes (RNCs) in a separase-dependent manner. Indeed, securin co-purified with separase translating RNCs, and this association was specific because it did not occur when a stop codon within the mRNA allowed dissociation of separase from ribosomes or when exportin instead of separase was being translated. (Exportin was chosen as control because, similar to the N-terminal half of separase, it also contains a superhelical structure.) Based on these results we proposed that the co-translational association of securin with separase serves the dual purpose of assisting proper folding of the giant protease while simultaneously ensuring its immediate inhibition. This situation is reminiscent of caspase activated DNase (CAD)

requiring co-translational association with its inhibitor, ICAD, to reach a natively folded state, from which it can later be activated by caspase-dependent cleavage of ICAD (Sakahira et al., 2000; Sakahira and Nagata, 2002). Thus, use of an inhibitor as a folding helper seems to be a recurrent mechanism in Nature to ensure tight regulation of dangerous enzymes.

### **Protein phosphatase 2A times the liberation of separase from securin (Hellmuth et al., 2014)**

When I started my thesis, it remained controversial whether PP2A (and which isoform thereof) was interacting with securin or separase or both (Gil-Bernabe et al., 2006; Holland et al., 2007). To clarify this issue, I conducted consecutive immunoprecipitation (IP) experiments: Separase was immuno-depleted from lysates of mitotic cells before excessive, free securin was immuno-precipitated from the corresponding supernatants. (Securin is about 5 fold more abundant than separase.) Subsequent immunoblotting analyses clarified that 1) PP2A associates with human separase-securin complex but not free securin and that 2) it is the B56 (B') and not the B55 isoform that does so (Figure 6A, right). Catalytic activity of separase-securin associated PP2A suggested separase and/or securin as putative substrates of the phosphatase (Holland et al., 2007). The previous identification of a PP2A binding deficient separase variant (Holland et al., 2007) enabled us to use SILAC and mass spectrometry to quantitatively assess phosphorylation of separase and securin in the absence and presence of bound PP2A. This approach identified four phosphorylation sites within securin that were substrates of separase-associated PP2A. The relevant Ser/Thr residues were changed to Ala or phosphorylation mimicking Asp, and the resulting securin-4A and -4D were compared to wild type securin in terms of their degradation kinetics. To this end, single transgene copies were stably integrated into parental Hek293 cells such that both alleles were expressed at the same, near physiological level upon induction with doxycycline. In addition, a C-terminal tag allowed to discern securin-4A and -4D from endogenous securin, which served as an internal control. (Controls had previously shown that the C-terminal tag had no effect on securin stability.) Both cell lines were then supplemented with the translation inhibitor cycloheximide and synchronously released from a prometaphase arrest. Time-resolved consecutive IP-Western analyses (see above) revealed that in its free form securin-4A was stabilized relative to wild type, whereas securin-4D was turning over with normal kinetics. This picture changed when separase-associated securin

was looked at: Here, securin-4D exhibited a shortened half-life relative to wild type and securin-4A, which were degraded with similar kinetics. Together, these observations led to a model, in which free securin is rendered short-lived by phosphorylation whereas separase-associated securin is stabilized by PP2A-dependent dephosphorylation (Figure 6). Consistently, free and separase-associated wild type securin were destroyed with the same kinetics when endogenous separase was replaced by the PP2A binding deficient variant.

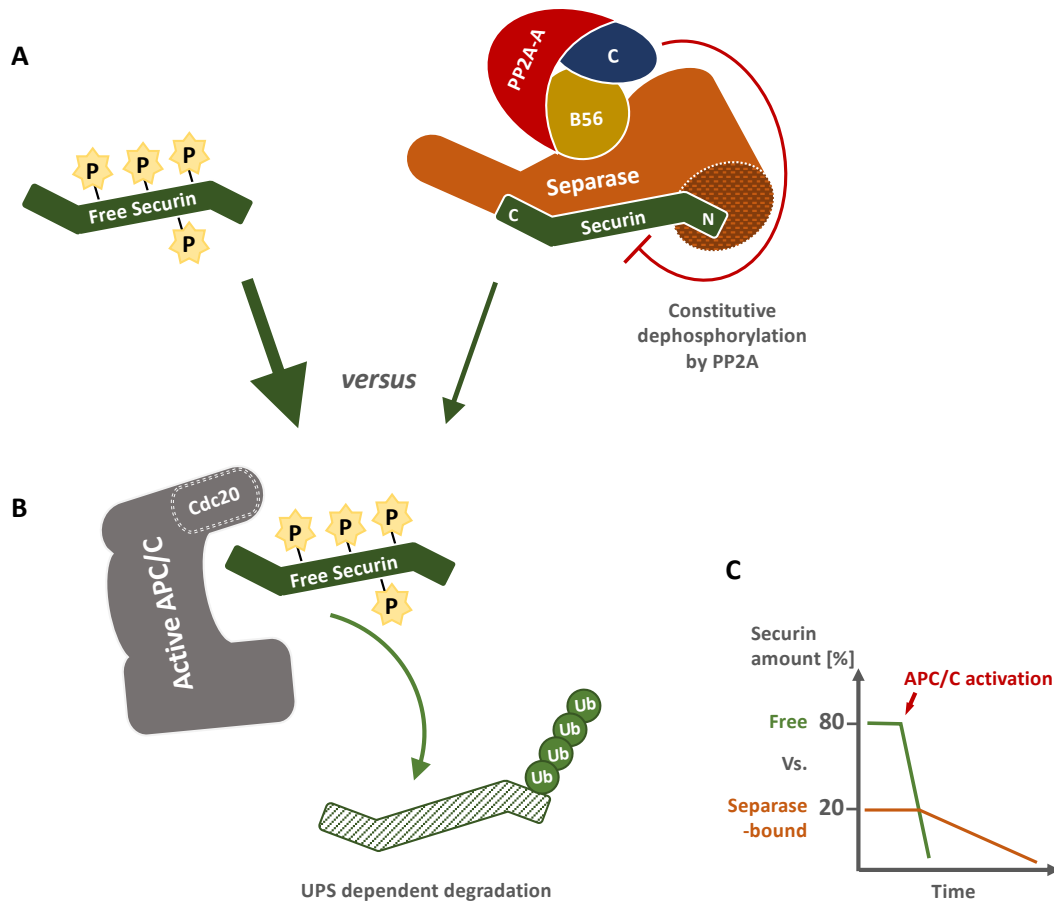


**Figure 6: Separase-bound PP2A stabilizes associated securin.**

**A)** The B56 isoform of PP2A interacts with separase and constitutively dephosphorylates bound securin. In contrast, free securin is hyperphosphorylated in mitosis. **B)** APC/C<sup>Cdc20</sup> prefers phosphorylated over de-phosphorylated securin as a substrate. **C)** As a consequence of A) and B), free securin is largely degraded before the ubiquitylation of separase-bound securin commences.

Phosphorylation-dependent protein degradation is typically mediated by ubiquitin ligases of the SCF family and, indeed, it had been reported that SCF<sup>βTrCP</sup> mediates proteasomal destruction of securin in UV irradiated cells (Limon-Mortes et al., 2008). However, the canonical E3 of securin clearly is the APC/C, which recognizes a KEN- and destruction box within the N-terminal 3rd of human securin (Zou et al., 1999). To clarify which ubiquitin ligase is responsible for the phosphorylation-dependent degradation of securin, the KEN-

and D-box were destroyed by point mutations; this did not affect any putative phosphorylation sites. Importantly, the corresponding securin-mKEN/mDB was dramatically stabilized in anaphase. Cycloheximide-shut off experiments revealed that wild type securin was slowly turned over even in cells that were arrested in G2 or prometaphase, when APC/C activity is very low. Still, securin-mKEN/mDB was stable also during these cell cycle phases. Consistently, the half-life of wild type securin was profoundly extended by siRNA-mediated depletion of the essential APC/C co-factor Cdc20. In order to underline my findings also with some biochemical data, I established a new method for the isolation of active APC/C from anaphase human cells. (This method also resulted in a fruitful collaboration, in which we studied how mutational inactivation of APC/C subunits suppressed the otherwise lethal loss of the SAC component Mad2 (Wild et al., 2018).) Using the purified APC/C for *in vitro*-ubiquitylation assays, I was able to show that pre-phosphorylated wild type securin and securin-4D are better APC/C<sup>Cdc20</sup> substrates than un-phosphorylated wild type securin or securin-4A, respectively. Thus, while I did not study and therefore cannot exclude a minor contribution of SCF, my experiments clearly demonstrate that the preferred proteolysis of phosphorylated human securin chiefly depends on APC/C. My finding that APC/C-dependent protein degradation kinetics is modulated by phosphorylation on the level of the substrates was unexpected. However, a recent study reports that the APC/C-dependent destruction of human FBXO31 is also regulated by its phosphorylation (Choppara et al., 2018). Furthermore, *S. cerevisiae* APC/C requires some of its substrates (like Clb5) to be de-phosphorylated and others (like Cdc5) to be phosphorylated (Simpson-Lavy et al., 2015). Curiously, the ubiquitin-dependent degradation of *S. cerevisiae* securin (Pds1) is boosted by de-phosphorylation (Holt et al., 2008). However, given that there is no sequence homology between yeast and human securin, this poses no contradiction to the findings reported here. The common denominator is that the phosphorylation status of APC/C substrates impacts the degradation timing of proteins and sub-pools thereof, thereby contributing to the proper order of downstream events in late mitosis.

To study the physiologic relevance of securin stabilization by separase-associated PP2A, endogenous securin was knocked-down by RNAi and replaced by doxycycline-induced expression of securin-4D. Importantly, corresponding cells suffered from premature activation of separase both during a G2- and a prometaphase arrest. Thus, prolonging the half-life of separase-bound securin seems to be important to prevent the unscheduled

unleashing of separase's essential but dangerous proteolytic activity during cell cycle arrests. The same approach was used to replace endogenous securin with securin-4A and to study the consequences of slowed degradation of free securin. Interestingly, cell that relied solely on this phosphorylation site mutant securin exhibited delayed separase activation as revealed by expression of a fluorescent separase activity sensor (Hellmuth et al., 2014; Shindo et al., 2012). This went along with a prolonged early anaphase and the formation of anaphase bridges indicative of difficulties to separate sister chromatids of individual chromosomes. Free securin is expected to compete with separase-bound securin for APC/C when both are degraded at the same time, and this offers an explanation for the observed phenotypes. Alternatively or in addition, lingering of free securin should result in repeated re-inhibition of separase, thereby increasing the effective size of the separase-associated pool and retarding overall separase activation. Consistent with this explanation, the share of securin-4A in the separase-bound securin pool transiently increased after APC/C activation when it was expressed on top of endogenous securin. In this context, it is interesting to note that the PP2A binding site on separase overlaps with the auto-cleavage sites, which is why PP2A binding and self-cleavage are mutually exclusive (Holland et al., 2007). Auto-cleavage of once activated separase would prevent further recruitment of PP2A, thereby ensuring that any residual securin that might re-inhibit this separase molecule would stay phosphorylated and, hence, be degraded more quickly. In this manner, auto-cleavage might contribute to the abruptness of anaphase onset.

In summary, I could show that the separase-PP2A interaction constitutes an additional layer of separase regulation that operates through stabilization of complexed securin by de-phosphorylation. This renders securin-dependent inhibition of separase more robust and helps to sharpen the metaphase-to-anaphase transition (Figure 6).

### **Positive and negative regulation of separase by Cdk1-Cyclin B1 (Hellmuth et al., 2015a)**

Viability of *SECURIN*<sup>-/-</sup> human cells and mice demonstrate that the aforementioned co-translational association of securin with separase is not essential. A small but large enough fraction of separase obviously reaches a natively folded state in the absence of securin. Moreover, this separase must still be regulated because *SECURIN*<sup>-/-</sup> cells do not suffer from premature sister chromatid separation (PCS) but rather undergo anaphase with normal

timing. Here, an obvious candidate was Cdk1-cyclin B1 because this master regulatory mitotic kinase had previously been identified as a securin-independent inhibitor of vertebrate separase (Stemmann et al., 2001). I made the interesting observation that the insolubility of separase under securin-limiting conditions (see above) was more pronounced in mitosis than interphase, which suggested that mitotic phosphorylation renders separase particularly prone to aggregation/precipitation. Work from our lab had suggested that Ser1126 phosphorylation induces a conformational change that exposes a Cdc6-like domain (CLD) on separase (Boos et al., 2008; Gorr et al., 2005; Stemmann et al., 2001). Subsequent binding of Cdk1-cyclin B1 via its regulatory cyclin to phosphorylated CLD then results in separase inhibition (Figure 5). To relate these findings to the behavior of separase in the above pelleting assay, I assessed the effects of a Ser1126Ala exchange and of a CLD-deletion. Although both variants are resistant to inhibition by Cdk1-cyclin B1, they behaved very differently here: While separase-S1126A was much more soluble than the wild type, the insolubility of separase- $\Delta$ CLD was aggravated. To correlate solubility with proteolytic activity, both variants were affinity-purified under securin-limiting conditions from prometaphase-arrested Hek293T cells before equal amounts were compared in their ability to cleave  $^{35}$ S-labeled Rad21. This analysis revealed cohesin cleaving activity of separase-S1126A but not  $\Delta$ CLD and demonstrated good accordance of solubility and proteolytic activity. All these results are best explained by the following model: Upon entry into mitosis, Cdk1-dependent phosphorylation of Ser1126 triggers a conformational change that renders securin-less separase even more aggregation-prone. (See below for further mechanistic insight on this conformational change.) Precipitation and irreversible inactivation are prevented, however, by association of phosphorylated separase (via its CLD) with Cdk1-bound cyclin B1. This preserved pool of separase then becomes liberated and proteolytically active when cyclin B1 is degraded at the metaphase-to-anaphase transition. Thus, much like securin, Cdk1-cyclin B1 also acts as both inhibitor and specific chaperone of separase. Unlike securin, however, it does not assist in folding but rather protects from a 'phosphorylation shock' (by analogy to 'heat shock') that the kinase itself inflicts onto separase at mitotic entry. In this manner, it is ensured even in the absence of securin that any separase, which can later be activated, is first held inactive by association with Cdk1-cyclin B1.

**The peptidyl-prolyl-isomerase Pin1 regulates separase by enabling its Cdk1-Cyclin B1-dependent inhibition and limiting its proteolytic half-life (Hellmuth et al., 2015b)**

Pin1 is a phosphorylation specific peptidyl-prolyl-cis/trans-isomerase with important mitotic functions (Liou et al., 2011; Lu et al., 1996; Shen et al., 1998; Yaffe et al., 1997). It consists of a catalytic PPIase and a regulatory WW domain, both of which bind to phosphorylated Ser/Thr-Pro motifs (Lu et al., 1999). Given that Cdk1-dependent phosphorylation of Ser1126 likely induces a conformational change in separase (see above) and given that this residue is followed by a Pro, I asked myself whether Pin1 might be involved in the regulation of separase by Cdk1-cyclin B1. Indeed, Pin1 co-purified with separase from mitotic but not interphase cells. Binding studies with isolated PPIase and WW domains subsequently showed that Pin1's affinity to separase is chiefly mediated by its WW domain. Mapping experiments further revealed that the PPIase domain bound to *phosphoSer1126-Pro1127*, as expected, but that the WW domain, surprisingly, did not recognize this motif but rather *phosphoSer1153-Pro1154* (whose phosphorylation had not even been previously recognized).

Incubation of separase-securin complex in an anaphase-like *Xenopus* egg extract with high Cdk1 activity results in APC/C-dependent securin degradation and inhibition of separase by Cdk1-cyclin B1 (Stemmann et al., 2001). I could show that prior immunodepletion of Pin1 from the egg extract abrogated the inhibitory binding of the kinase to separase. This effect was specific because Cdk1-cyclin B1-separase complex formation was re-installed and cohesin cleavage again prevented when bacterially expressed, purified Pin1 was added back to depleted extract prior to separase. To test for the requirement of Pin1 *in vivo*, I capitalized on the previous finding that Cdk1-cyclin B1 becomes crucial for separase regulation when securin is titrated out by overexpression of the protease (Boos et al., 2008; Holland et al., 2007). Indeed, overexpression of wild type separase in Hek293 cells, which on its own did have no detrimental effects, caused profound PCS when Pin1 had been depleted by RNAi. This phenotype was rescued by expression of Pin1 from an siRNA resistant transgene and mimicked by chemical inhibition of Pin1 with EGCG (Urusova et al., 2011). Moreover, overexpression of WW-binding deficient separase-S1153A also caused PCS and this phenotype was suppressed by simultaneous over-expression of wild type but not catalytically inactive PPIase domain. Thus, Pin1 in its catalytically active form is required for Cdk1-cyclin B1

dependent inhibition of separase not only *in vitro* but also in living cells.

The requirement of Pin1's catalytic activity was consistent with the long proposed conformational change of separase but did still not prove it. I therefore isolated securin-free separase from anaphase egg extract supplemented with either EGCG or just carrier solvent, removed any bound Cdk1-cyclin B1 by a high salt wash (Gorr et al., 2005), and then subjected both preparations to limited proteolysis with trypsin. Notably, this resulted in different separase digestion patterns, thus lending the first experimental support to the (up to then speculative) conformational change and, further, to its catalysis by Pin1.

These and previous results taken together lead to the following multi-step model of Cdk1-dependent separase inhibition: Initial phosphorylation of separase by Cdk1 is followed by docking of Pin1 via its WW domain onto phosphorylated Ser1153. This places the PPIase domain at the right position to then catalyze the isomerization of the phosphorylated Ser1126-Pro1127 peptide bond - likely from *trans* into *cis*. The resulting different conformation of *cis*-separase enables Cdk1 to stably bind via its regulatory cyclin B1 to the CLD, thereby blocking separase's proteolytic activity (Figure 7).

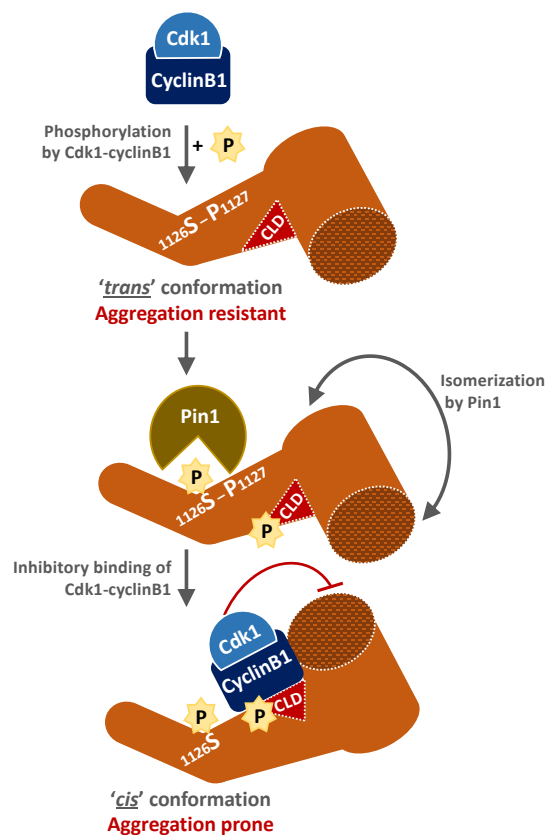


**Figure 7: Pin1 facilitates Cdk1-cyclin B1-separase complex formation and destabilizes separase.**

Cdk1-cyclinB1 mediated phosphorylation at serine 1126 recruits Pin1, which subsequently catalyzes isomerization of separase from its *trans*- into its *cis*-conformer. This renders separase aggregation prone but, at the same time, de-masks the CLD, thereby enabling binding of cyclin B1 to separase.

Does Pin1 act also on separase that is regulated by securin instead of Cdk1-cyclin B1? Beginning to address this issue, I conducted (co-)IP experiments, which demonstrated that a Pin1-separase-securin complex does not exist, whereas Pin1 and Cdk1-cyclin B1 can simultaneously associate with separase. This left me with the question of whether Pin1 might act on separase that has just been liberated from securin's grip? I noted that in cells, which were synchronously driven through anaphase, liberated separase did not associate with free securin-mKEN/mDB whose expression had just been induced. In the presence of EGCG, however, separase was sequestered almost quantitatively by the newly produced, stable securin. Thus, once the SAC is silenced and APC/C activated, Pin1 converts the majority of separase into a securin-resistant state, which we propose corresponds to the *cis*-conformer.

Next, I scrutinized the mutually exclusive binding of securin and Cdk1-cyclin B1 to separase by a biochemical approach: Phosphorylated separase that was in complex with securin was unable to bind Cdk1-cyclin B1, as expected. However, when the securin was cut in half by cleavage of an engineered site with human rhinovirus 3c protease and when active Pin1 was present at the same time, then Cdk1-cyclin B1 (and Pin1) interacted with separase (despite the securin fragments remaining associated with the protease). Thus, Cdk1-dependent phosphorylation of Ser1126 (which is quantitative in mitotic cells, (Stemmann et al., 2001)) renders the *cis*-conformation of separase energetically favorable. Isomerization of the *phospho*Ser1126-Pro1127 peptide bond within separase-securin complexes is impossible, however, because securin locks separase in the *trans*-conformation. Once securin is destroyed by site specific proteolysis (here) or ubiquitin-dependent degradation (*in vivo*), Pin1 converts the 'spring-loaded', phosphorylated separase from *trans* into the Cdk1-cyclin B1-binding *cis* conformer.

What - if any - are the physiological consequences of *trans*-to-*cis* isomerization of separase in late mitosis? Although free securin is preferentially degraded over separase-bound securin (see above), it is much more abundant. Hence, when separase-associated securin is being destroyed, some residual, free securin still persists (Hellmuth et al., 2014). Pin1 dependent conversion of separase into the securin-resistant *cis*-isomer prevents its re-inhibition by this lingering securin, which should otherwise slow overall separase activation. *Cis*-separase, while being resistant to securin, can be sequestered by Cdk1-cyclin B1, of course. But for the

reasons given below, separase, which has been liberated from securin, associates with residual Cdk1-cyclin B1 only after it has cleaved cohesin (Hellmuth et al., 2015b; Shindo et al., 2012). It is therefore tempting to speculate that resistance of once activated separase to persisting, free securin helps to sharpen the transition into anaphase (although I did not yet investigate this further).

A second consequence of the *trans*-to-*cis* isomerization of separase should be a shortened half-life of separase's catalytic activity because my previous experiments suggested an increased propensity of the *cis*-conformer to aggregate (Hellmuth et al., 2015a). To investigate whether isomerization would affect the stability of separase *in vitro*, I produced active separases, which were either in the *trans* or the *cis* conformational state. Subsequent incubations followed by time-resolved cohesin cleavage assays demonstrated that, indeed, the activity of *cis*-separase rapidly declined, while *trans*-separase proved a stable enzyme. Next, I asked whether presence of separase-S1126A or chemical inhibition of Pin1 during late mitosis would have any cellular phenotypes. As I suspected prolonged proteolytic activity of separase under these conditions, I analyzed cohesin, which in unperturbed cells reloads onto chromatin already in telophase without being cleaved (Losada et al., 2000; Sumara et al., 2000). I performed immunofluorescence microscopy and immunoblotting of chromatin isolated in a time-resolved manner from synchronized cells. Control Hek293Ts, which expressed separase- $\Delta$ CLD or had been treated with DMSO instead of EGCG, behaved as expected - reloading cohesin in telophase. However, cohesin failed to re-associate with telophase chromatin in cells, in which the *trans*-to-*cis* isomerization of separase was blocked. This is likely explained by the continued cleavage of cohesin in these cells and suggests that a normal cohesin cycle requires that the burst-like activation of separase at the end of metaphase is followed by rapid inactivation of the protease in anaphase.

In summary, Pin1 is not only essential for the inhibition of separase by Cdk1-cyclin B1. The Pin1-facilitated conformational switch of separase also acts like a time fuse that leads to rapid, aggregation-driven self-inactivation of most separase in late mitosis.

When cells are synchronously released from prometaphase, then the Cdk1-cyclin B1-separase complex first disappears to then appear again in late mitosis, i.e. at a time when most of securin and cyclin B1 has already been degraded. Mathematical modeling could not explain why the Cdk1-cyclin B1-separase complex would transiently disappear prior to its re-

accumulation, hence predicting that we were missing 'something'. This 'something' turned out to be phosphorylation/de-phosphorylation of cyclin B1. I could show that early mitotic phosphorylation of cyclin B1 at multiple sites weakens its affinity for separase, thereby explaining why in prometaphase cells only a small fraction of separase is in complex with Cdk1-cyclin B1. With the advent of APC/C activity and the concomitant degradation of cyclin B1, the Cdk1-cyclin B1-separase complex totally disappears at the metaphase-to-anaphase transition. Then, however, the continued decay in activity of Cdk1 and other mitotic kinases results in de-phosphorylation of residual cyclin B1 during anaphase (by hitherto unknown phosphatases). Because this dramatically increases cyclin B1's affinity for separase, the Cdk1-cyclin B1-separase complex forms anew despite the fact that only trace amounts of cyclin B1 are left at this late stage of mitosis (Figure 8A). When the phosphorylation/de-phosphorylation parameter is integrated into the mathematical simulation, then the *in vivo* observations can faithfully be recapitulated *in silico*. Moreover, a phosphorylation site mutant cyclin B1-8A out-competes endogenous cyclin B1 and clings to separase even longer than wild type cyclin. Expression of this separase-super-binding cyclin B1-8A also prevented the transient decline in abundance of the Cdk1-cyclin B1-separase complex.

Does the late Cdk1-cyclin B1-separase complex have any biological function? It cannot impact on sister chromatid separation because correlating its presence with cleavage of a fluorescent separase activity sensor showed that it forms when cohesin has already been cleaved by separase (Hellmuth et al., 2015b; Shindo et al., 2012). Within the Cdk1-cyclin B1-separase complex, both the protease and the kinase are held inactive (Gorr et al., 2005). A corollary is that the final disassembly of this late complex will unleash a small pool of active separase. In fact, my data suggest that this delayed, second activation of separase is important for separase-mediated centriole disengagement during early G1 phase (Hellmuth et al., 2015a). While this reveals one function of the Cdk1-cyclin B1-separase complex that forms in late mitosis, it might serve yet another purpose during cytokinesis at the end of female meiosis I (Gorr et al., 2006).

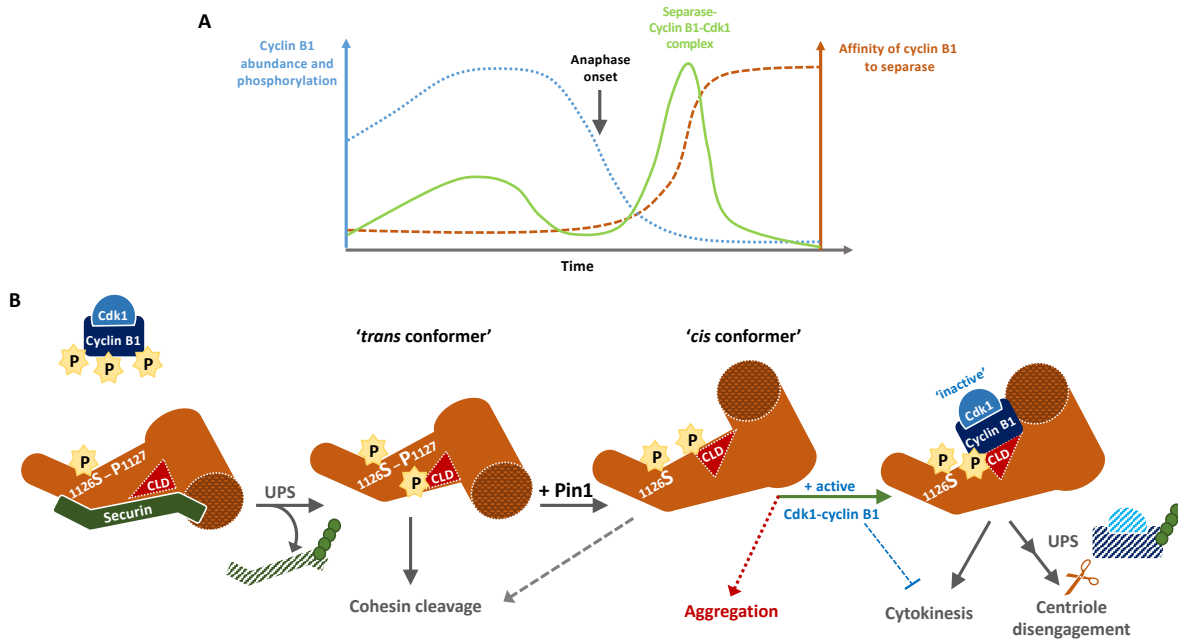


**Figure 8: Formation of the Cdk1-cyclin B1-separase complex after sister chromatid segregation suggests late functions for the complex.**

**A)** The Reciprocal relation between abundance and phosphorylation of cyclin B1 (blue curve) and its affinity towards separase (red curve) explains why Cdk1-cyclin B1-separase complex re-forms late in mitosis (green curve). **B)** After separase activation by securin and cyclin B1 degradation Rad21 is cleaved and sister chromatids are segregated. Pin1-dependent isomerization of separase and de-phosphorylation of remaining cyclin B1 then facilitates late Cdk1-cyclin B1-separase complex formation. This stabilizes the otherwise aggregation-prone cis-separase and holds it in a re-activatable state. At the same time, remaining Cdk1 kinase activity is inhibited. Formation of this late Cdk1-cyclin B1-separase complex might facilitate cytokinesis during murine female meiosis I, and its disassembly in early G1 phase is important for separase-dependent centriole disengagement.

### **A second branch of spindle assembly checkpoint-dependent anaphase control: Inhibition of separase by Mad2-activated shugoshin (Hellmuth et al., 2020)**

Double knock-out mice lacking the APC/C activator Cdc20 and securin terminally arrest as two cell embryos with separated sister chromatids (Li et al., 2007). Loss of cohesion is suppressed, however, by constitutive SAC activation. This observation was surprising because APC/C<sup>Cdc20</sup> (back then the only known downstream target of the SAC) was defective in these embryos to begin with. It therefore suggested the existence of a securin-independent but SAC-dependent inhibitor of separase. Cdk1-cyclin B1 was an unlikely candidate here because its separase inhibitory capacity is debilitated by early mitotic phosphorylation of cyclin B1 (Hellmuth et al., 2015b). However, our lab subsequently identified human Sgo2 as a Cdc20-like interactor of the key SAC effector component Mad2 suggesting that Sgo2 might be the sought-after SAC-activated regulator of separase (Orth et al., 2011). What seemed to contradict this hypothesis, however, was that Sgo2 localizes to kinetochores/pericentromeres where the soluble separase is not to be found. Shugoshins

bind via their conserved, C-terminal SGO-C box to Bub1-phosphorylated histone H2A at kinetochores/pericentromeres (Kawashima et al., 2010; Liu et al., 2013). To my surprise I found that binding of a phosphorylated H2A peptide to Sgo2 is mutually exclusive with Mad2-Sgo2 complex formation. *Vice versa*, pre-loading of Sgo2 with Mad2 blocked phospho-H2A binding. This suggested the existence of two Sgo2 pools: A kinetochore/peri-centromere-associated one and a soluble, Mad2-associated one, which might regulate separase. Indeed, separase and Sgo2 interacted as judged by co-IP experiments. Importantly, this interaction depended on the prior association of Sgo2 with Mad2 and did not take place, for example, when the Mad2-interaction motif of Sgo2 had been destroyed by mutation of Arg-153 to Asp.

The separase-Sgo2-Mad2 complex was present in G1-, early S-, G2-, and prometaphase arrested cells, which coincides with the presence of Cdc20-Mad2 throughout the cell cycle. This is consistent with the re-localization of Mad1-Mad2 from kinetochores to nuclear pore complexes (NPC) in interphase and the continued conformational activation of Mad2 (Rodriguez-Bravo et al., 2014). Consistently, separase-Sgo2-Mad2, like Cdc20-Mad2, became (almost) undetectable upon depletion of Mad1 and/or the NPC component TPR. Importantly, addition of *in vitro*-expressed Sgo2 and *E. coli*-expressed, purified Mad2 to active, recombinant separase prevented it from cleaving Rad21. Sgo2-R153D and a C-terminally truncated, Sgo2-binding deficient Mad2 were both inactive in this separase inhibition assay, which demonstrated that - at least *in vitro* - Sgo2 is enabled to inhibit separase only upon association with Mad2.

When highly overexpressed, the hypermorphic, Cdk1-resistant Separase-S1126A triggers PCS (Boos et al., 2008; Holland and Taylor, 2006). This phenotype was partially rescued by overexpression of Sgo2 and exacerbated by its siRNA-mediated depletion, which made it possible to assess Sgo2 variants for their ability to restrict separase activity in living cells. Confirming the biochemical results, Sgo2-R153D was unable to suppress PCS in this system. The above results implied Sgo2-Mad2 as a 3rd separase inhibitor - next to securin and Cdk1-cyclin B1. Do these inhibitors bind separase simultaneously or in a mutually exclusive manner? Inability to detect any interaction between securin, Sgo2-Mad2 and Cdk1-cyclin B1 in IP-experiments suggested the latter, i.e. that these anaphase inhibitors act in parallel rather than synergistically on one and the same separase molecule. But how much separase is sequestered by each of the three inhibitors? IPs of securin, cyclin B1, and Sgo2 from

various human cell lines were compared by immunoblotting in terms of the amount of associated separase. These analyses revealed that on average 59, 6, and 35% of total separase is sequestered by securin, cyclin B1, and Sgo2, respectively, in a prometaphase-arrest. These quantifications suggested that Sgo2-Mad2 is a much more important regulator of separase than Cdk1-cyclin B1, and, indeed, 85% of separase was in complex with Sgo2 in *SECURIN*<sup>-/-</sup> cells. (Interestingly, Sgo2 and Mad2 appear to be overexpressed in *SECURIN*<sup>-/-</sup> relative to parental HCT116 cells.)

Based on their prominent association with separase, I next tested whether loss of securin and Sgo2 was sufficient to induce untimely separase activity. Consistent with this proposal, co-depletion of securin and Sgo2 1) was highly cytotoxic as judged by colony formation assay, 2) triggered premature centriole disengagement in G2-phase arrested cells, 3) caused an otherwise uncommon absence of cohesin from early mitotic chromatin, 4) strongly compromised the cell's ability to form proper metaphase plates, and 5) resulted in marked PCS, which could be further enhanced by preventing also the Cdk1-cyclin B1-dependent inhibition of separase. Importantly, simultaneous absence of securin and Sgo2 was also associated with 6) premature cleavage of Rad21 and the separase activity sensor in prometaphase-arrested cells. Moreover, individual depletions of either securin or Sgo2 were well tolerated and did not cause any of these phenotypes. Thus, while securin and Sgo2 can functionally replace each other, the acute loss of both renders (most) separase constitutively active.

The remote possibility remained that the redundancy of Sgo2 with securin was due not to direct inhibition of separase but some other function of this shugoshin. (In fact, the Watanabe lab had reported that somatic Sgo2 contributed to the protection of centromeric cohesion from the prophase pathway (Kitajima et al., 2006; Tanno et al., 2010), although several publications challenge this statement (Llano et al., 2008; Orth et al., 2011; Wolf et al., 2018).) Importantly, when endogenous separase was replaced by either one of two Sgo2-binding deficient variants, then the depletion of securin alone was sufficient to cause profound PCS.

What is the mechanism of Sgo2-Mad2-dependent separase inhibition? The protection of Rec8 by Sgo2 throughout meiosis I essentially depends on its ability to recruit PP2A to pericentromeric cohesin (Kitajima et al., 2006; Rattani et al., 2013; Riedel et al., 2006).

However, a PP2A-binding deficient Sgo2-N58I (Orth et al., 2011) retained the ability to inhibit separase both *in vitro* and *in vivo*, thus indicating that PP2A-mediated dephosphorylation is not involved in this newly discovered function of Sgo2. Securin acts as a competitive inhibitor and is turned into a separase substrate when a cleavage-resistant pseudo-substrate sequence, which occupies the protease's active site, is changed into a consensus cleavage site (Boland et al., 2017; Lin et al., 2016; Nagao and Yanagida, 2006). To test whether the same might apply to Sgo2, I screened several  $\phi$ ExxX-to- $\phi$ ExxR variants of Sgo2 for their cleavage by separase. Indeed, Sgo2-M114R (but no other variant) was cleaved by separase both *in vitro* and *in vivo*. Thus, Sgo2 resembles securin in that it is a competitive separase inhibitor but differs in that it essentially requires Mad2 binding in order to do so.

Another difference between securin and Sgo2-Mad2 is that the former is degraded in metaphase whereas the latter are stable proteins. This begs the question of whether and - if yes - how Sgo2-Mad2-inhibited separase is liberated upon silencing of the SAC? When prometaphase-arrested cells were synchronously driven through late mitosis by chemical inhibition of an essential SAC kinase, then the degradation of securin and the auto-cleavage of separase coincided with dissociation of Sgo2 and Mad2 from the protease. Thus, the separase-Sgo2-Mad2 complex is indeed dismantled at the metaphase-to-anaphase transition. At this time, the Cdc20-Mad2 containing MCC is actively disassembled by the AAA-ATPase Trip13 in conjunction with the Mad2-specific adaptor p31<sup>comet</sup> (Eytan et al., 2014). Inspired by this insight, I incubated isolated, immobilized separase-Sgo2-Mad2 complex with bacterially expressed, purified Trip13 and p31<sup>comet</sup> and then analyzed, which proteins were mobilized and which ones remained bound to the beads. Remarkably, wild type Trip13 and p31<sup>comet</sup> quantitatively displaced Sgo2 and Mad2 from separase, thereby leaving it proteolytically active towards Rad21. This effect was specific because Sgo2-Mad2 stayed bound and separase inhibited, when wild type Trip13 was replaced by Walker-A or -B mutant variants or when wild type p31<sup>comet</sup> was replaced by Mad2- or Trip13-binding deficient variants. In addition, siRNA mediated depletion of Trip13 and p31<sup>comet</sup> prevented the usual disassembly of separase-Sgo2-Mad2 in anaphase cells.

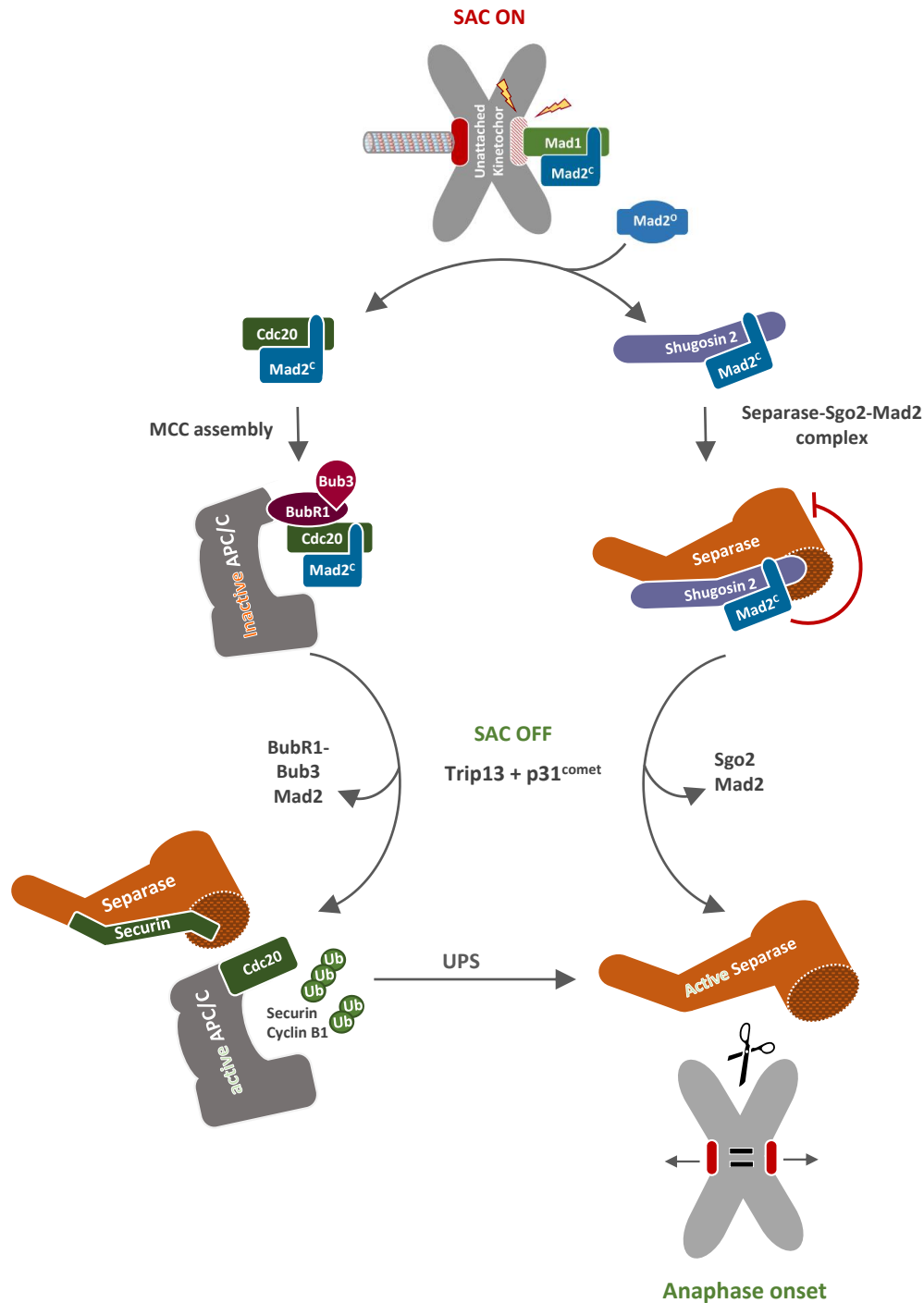


**Figure 9: The SAC controls separase activity by two different mechanisms.**

Both branches of anaphase regulation are controlled by the balance between SAC signaling and Trip13-dependent silencing of the checkpoint. They differ, however, in that only the canonical pathway essentially requires proteolysis for separase activation.

The above results suggest that under condition when separase is chiefly controlled by Sgo2-Mad2, like in *SECURIN*<sup>-/-</sup> cells, sister chromatid separation should (at least partially) be uncoupled from APC/C. To test this prediction, *SECURIN*<sup>-/-</sup> and parental HCT116 cells were released from a SAC arrest in presence of APC/C inhibitors. In both cell lines this blocked the degradation of securin and cyclin B1 but not the dissociation of Sgo2-Mad2 from separase.

Notably, separase cleaved itself and sister chromatids separated in *SECURIN*<sup>-/-</sup> cells, while both processes were largely prevented in parental HCT116s.

The SAC-shugoshin link is conserved in *Xenopus* with the curious difference that here Sgo1 rather than Sgo2 binds Mad2 (Orth et al., 2011). I could confirm and extend these earlier findings by showing that *Xenopus laevis* Sgo1 also binds separase in a Mad2-dependent manner and also uses a non-cleavable pseudo-substrate sequence (131-LEmaS-135) to competitively inhibit the protease.

Despite the high divergence of human Sgo2 and *X.l.* Sgo1 in length and sequence, the Mad2 and separase interaction sites are conserved in position and distance relative to the coiled coil domain and SGO-C box. This argues that Mad2 binding and separase inhibition are characteristics that evolved prior to duplication of the primordial vertebrate *SHUGOSHIN* gene.

In summary, I discovered an unanticipated, second branch, by which the SAC controls separase activity. This branch is (largely) independent of securin and APC/C-mediated proteolysis. It is represented by shugoshin (Sgo2 in mammals and Sgo1 in amphibians), which is turned into a direct, competitive inhibitor of separase by SAC-activated Mad2.

## **Non-canonical separase functions**

### **Local activation of human separase in interphase facilitates repair of double strand breaks by homologous recombination (Hellmuth et al., 2018)**

Motivated by two yeast studies (McAleenan et al., 2013; Nagao et al., 2004), I started to investigate whether separase might play a role in the DNA damage response of human cells. Expression of a restriction endonuclease, the 8-bp cutter AsiSI, in fusion with an estrogen receptor (ER) results in defined DSBs upon treatment of cells with 4-Hydroxytamoxifen (OHT) (Caron et al., 2012; Iacovoni et al., 2010). Using this system enabled me to perform ChIP experiments, which I then analysed by multiplex- or qPCR. These analyses demonstrated that human separase - much like the established DNA damage marker  $\gamma$ H2AX - is recruited to DSBs. IP of separase from total cell lysates containing benzonase-fragmented

chromatin extended this finding because it exemplified the DNA damage-dependent co-purification of  $\gamma$ H2AX with separase. In a complementary approach, cells treated with the topoisomerase II inhibitor doxorubicin (DRB) to inflict DSBs were analyzed by immunofluorescence microscopy (IFM). In some cells, anti-separase labeled nuclear foci stained positive also for  $\gamma$ H2AX. The signals were specific because they were absent from separase-depleted or undamaged cell cultures. Interestingly, most DRB treated cells exhibited  $\gamma$ H2AX- but no separase foci. DRB treatment and subsequent IFM of pre-synchronized cell populations unraveled that separase was recruited to DSBs only in G2- but not G1-phase. DSBs are repaired by one of two major pathways, error-prone non-homologous end-joining (NHEJ) or error-free homology directed repair (HDR). While NHEJ can take place at any time during interphase, HDR depends on presence of an undamaged sister chromatid and, hence, is possible only after replication (Polo and Jackson, 2011). Might separase take part only in HDR but not NHEJ? To clarify this issue, I capitalized on pathway specific reporter cell lines, in which repair of a single, specific DSB gives rise to GFP only if it occurs by either NHEJ or HDR (Gunn and Stark, 2012; Pierce et al., 1999). Using these two reporter lines, I could show that siRNA-mediated depletion of separase left NHEJ unaffected but compromised HDR.

Next, I investigated whether separase becomes proteolytically active during HDR. To this end, AsiSI-ER expressing Hek293 cells were synchronized in G2-phase, treated with OHT or carrier solvent, and then subjected to IP using a Rad21 antibody (or unspecific IgG as control) to enrich putative cleavage fragments. Final Western analysis demonstrated that separase-specific Rad21 fragments were indeed present in DSB containing cells but absent from undamaged cells. By the same approach, I could further show that a chromatin associated separase activity sensor was likewise cleaved in a DNA damage-dependent manner. When cells expressing this fluorescent separase sensor were treated with DRB and nocodazole in G2 phase and subjected to chromosome spreading some hours later, then some condensed chromosomes with  $\gamma$ H2AX-positive foci were detectable indicating that the corresponding cells had slipped from the DNA damage checkpoint into a SAC-mediated mitotic arrest. Importantly,  $\gamma$ H2AX-foci coincided with regions of separase activity as judged by fluorescence microscopy. Thus, during HDR separase is activated only locally at/around DSBs.

Separase contains an active nuclear export signal (NES) and is usually restricted to the cytoplasm in interphase (Sun et al., 2006). How then does it get into the nucleus during DNA damage response (DDR) to begin with? Furthermore, the active protease does not seem to diffuse, thus raising the question of how it is tethered to the sites of damage? Numerous experiments that were inspired by known recruitment mechanisms of established DDR factors led to the following answers (Galanty et al., 2009; Sacher et al., 2006; Thandapani et al., 2013; Zhang and Xiong, 2001): Separase's NES is inactivated by phosphorylation of Ser1660. In addition, separase is sumoylated at Lys1034 and Arg-methylated at an RG-repeat motif centered around position 1426 in response to DSBs (Figure 10). Enzymatic assays with recombinant proteins showed that *in vitro* these post-translational modifications (PTMs) can be put onto separase by the DNA damage relevant ATM kinase, the SUMO-ligase Mms21, and protein arginine methyltransferase 1 (PRMT1), respectively (Boisvert et al., 2005a; Boisvert et al., 2005b; Potts and Yu, 2005; Zhang and Xiong, 2001).

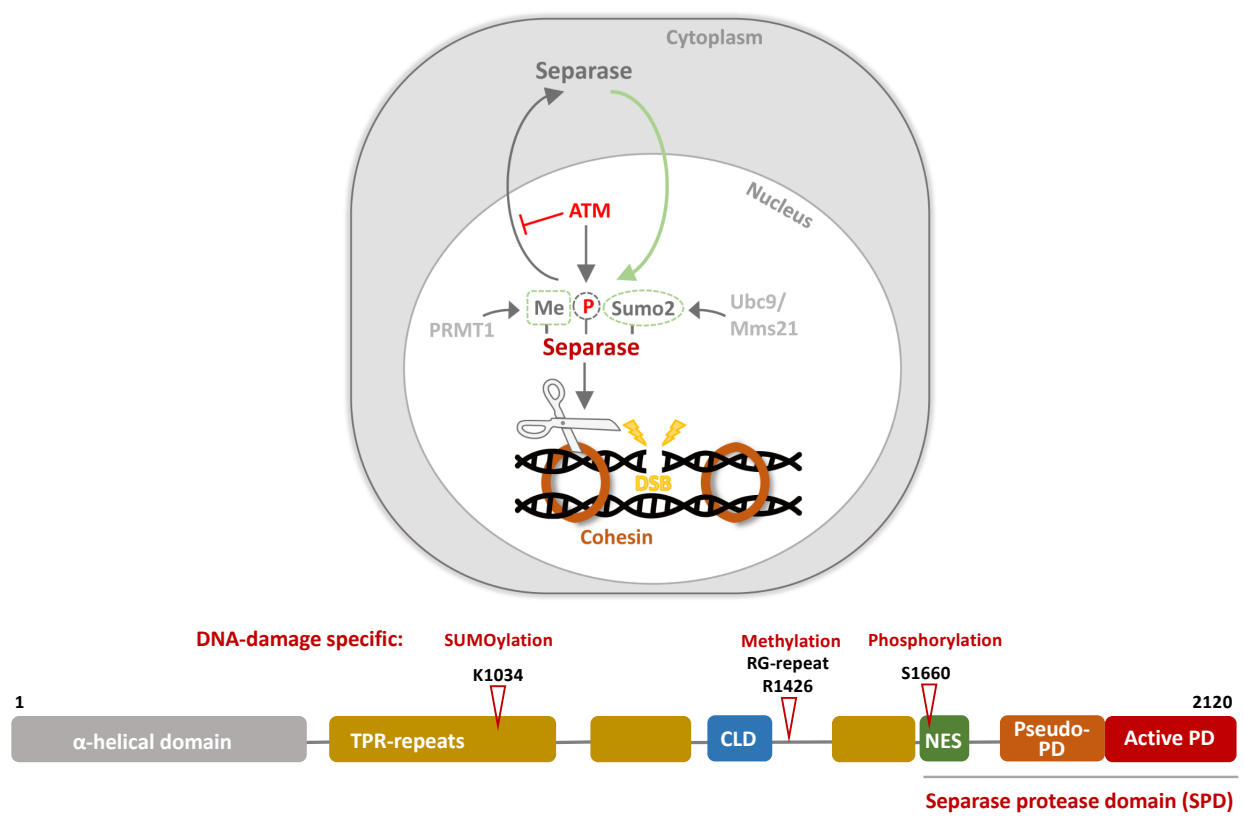


**Figure 10: Post-translational modifications direct separase to DSBs where it cleaves cohesin to support homology directed repair.**  
 In undamaged interphase cells separase is excluded from the nucleus. In response to DSBs, the nuclear export signal (NES) of separase is inactivated by ATM-dependent phosphorylation. Once in the nucleoplasm, PRMT1-dependent methylation (Me) of RG-repeats and Mms21-dependent sumoylation of Lys-1034 direct separase to DSBs. Here, it is locally activated, cleaves cohesin around the damaged sites and facilitates HDR - possibly by granting DNA access to the repair machinery.

Preventing these PTMs by corresponding point mutations prevented separase from associating with damaged chromatin and to interact with  $\gamma$ H2AX. Following the wash-out of DRB,  $\gamma$ H2AX- and MDC1-positive foci disappeared from wild type separase expressing cells, which then also continued to progress through the cell cycle. In contrast, cells that solely relied on the above separase variants exhibited continued presence of  $\gamma$ H2AX- and MDC1-positive foci and arrest in G2 phase. Thus, preventing these PTMs not only prevented the recruitment of separase to DSBs but also rendered it unable to support HDR. In parallel to our investigation of human separase in HDR, the Pendás-lab generated and analyzed mice that were heterozygous for *SEPARASE*. Transduction of two oncogenes, E1A and hRas<sup>V12</sup>, into MEFs from *SEPARASE*<sup>+/-</sup> and *SEPARASE*<sup>+/+</sup> mice enabled the former but not the latter to form colonies from single cells, which is indicative of neoplastic transformation of these primary cells. In addition, *SEPARASE*<sup>+/-</sup> and *SEPARASE*<sup>+/+</sup> mice were compared in a two-step skin carcinogenesis assay that uses DMBA as inductor and the mitogen TPA as tumor promoter (Abel et al., 2009). A time-resolved histological assessment revealed a markedly increased number and size of skin lesions for the *SEPARASE*<sup>+/-</sup> over the wild type mice. The Pendás group could not pinpoint a molecular basis for these cancer-relevant haploinsufficiency phenotypes: *SEPARASE*<sup>+/-</sup> mice had a normal life span with no obvious increase in spontaneous tumorigenesis. Moreover, *SEPARASE*<sup>+/-</sup> MEFs exhibited normal proliferation and cell cycle progression rates and did not suffer from any measurable increase in aneuploidies or lagging chromosomes in anaphase relative to wild-type cells. They therefore turned to us, and I studied the proficiency of *SEPARASE*<sup>+/-</sup> MEFs in HDR looking at the cleavage of Rad21 upon DRB addition and the disappearance of the DSB markers  $\gamma$ H2AX, 53BP1, and phosphorylated Chk2 during the recovery from DRB. Importantly, Rad21 cleavage was reduced and DSB repair markedly retarded in the *SEPARASE*<sup>+/-</sup> relative to wild type MEFs. I conclude that 1) taking an active part in DDR is a conserved feature of mammalian separase and 2) this function - in contrast to sister chromatid separation - is strikingly dependent on *SEPARASE* dosage. In summary, *SEPARASE* heterozygosity is hallmarked by both debilitated HDR and propensity to cellular transformation. This correlation suggests that the function of mammalian separase in HDR might help to prevent carcinogenesis.

It is well established that DNA damage results in replication-independent *de-novo* loading of cohesin and that accumulation of cohesin around DSBs is required for efficient HDR (Kim et

al., 2002; Potts et al., 2006; Strom et al., 2004; Unal et al., 2004). Using the aforementioned HDR reporter cell line, I observed a comparable drop in repair efficiency upon depletion of either separase or cohesin subunits, which is in line with these previous findings. Enrichment of cohesin and activation of separase at the same sites seem counterintuitive at first. However, hyper-recruitment of cohesin and its simultaneous separase-dependent removal is not *per se* contradicting each other but will result in DSB-associated cohesin to be more dynamic. This could serve the dual purpose of keeping the sister chromatid close for effective homologous recombination, while still granting the repair machinery access to the DNA. In support of this speculative model, separase-resistant Rad21 was reported to impair DNA end-resection during DSB repair in *S. cerevisiae* (McAleenan et al., 2013).

**Nek2A- and separase constitute a checkpoint that transforms anti- into pro-apoptotic factors when early mitosis falls below a minimal duration (Hellmuth and Stemmann, 2020)**

Securin- and Sgo2 depleted human cells exhibit PCS upon entry into mitosis (Hellmuth et al., 2020). I noted that this was followed by apoptosis shortly thereafter. This phenotype was due to separase deregulation rather than loss of cohesion because Sgo1- or sororin-less cells, which maintain normal separase regulation and suffer from PCS due to quantitative removal of cohesin via the prophase pathway, did not die but exhibited a SAC-mediated mitotic arrest instead. If cohesin cleavage is not the trigger of this death in mitosis (DiM), then what could be the relevant separase target(s)? Taking an educated guess, I tested whether the two anti-apoptotic Bcl2 family proteins Mcl1 and Bcl-xL could be cleaved by active separase *in vitro*. Knowing that Rec8 is recognized by separase as a substrate only when it is phosphorylated (Katis et al., 2010; Kudo et al., 2009), I included various mitotic kinases in the cleavage assays. These experiments revealed that phosphorylation of Mcl1 and Bcl-xL by Nek2a enabled their endo-proteolysis by separase. In addition, cyclin A2-dependent Cdk1/2 facilitated some separase-dependent cleavage of Bcl-xL (but not Mcl1). Subsequent mapping of both the relevant phosphorylation- and cleavage sites by candidate approaches revealed the following: 1) When Mcl1 is phosphorylated by Nek2a at S-60, S-159 and T-163, it can be cleaved by separase after 173-ExxR-176. 2) The separase-dependent cleavage of Bcl-xL after 31-ExxR-34 is enabled by phosphorylation of S-4 and S-164 by Nek2a and of S-62 by Cdk1/2-cyclin A2 (Figure 11).

Immunoblotting of *siSECURIN/siSGO2*-transfected cells confirmed that Mcl1 and Bcl-xL were fragmented also *in vivo* - not only in various human cancer cell lines but also in untransformed hTERT RPE1 and murine NIH/3T3 cells. Mcl1 and Bcl-xL had been reported to be cleaved during apoptosis (Clem et al., 1998; Michels et al., 2004) and, indeed, in my hands caspase 3 cleaved Mcl1 after D-157 and Bcl-xL after D-61 *in vitro*. However, in cells Mcl1 and Bcl-xL are cleaved directly by separase and not by downstream caspases as judged by the following observations: 1) Using *in vitro* expressed fragments as length standards, I could show that the two *in vivo* generated Mcl1 fragments perfectly matched cleavage by separase rather than caspase. 2) Replacing the relevant ExxR by a Tev site, rendered Mcl1 and Bcl-xL resistant to separase and susceptible to Tev protease but did not affect their cleavage by caspase 3 *in vitro*. Importantly, these variants were no longer processed in cells that underwent separase-dependent DiM. 3) A pan-specific caspase inhibitor blocked cleavage of the established caspase substrate PARP but did not affect Mcl1 and Bcl-xL cleavage in Securin- and Sgo2 depleted mitotic cells.

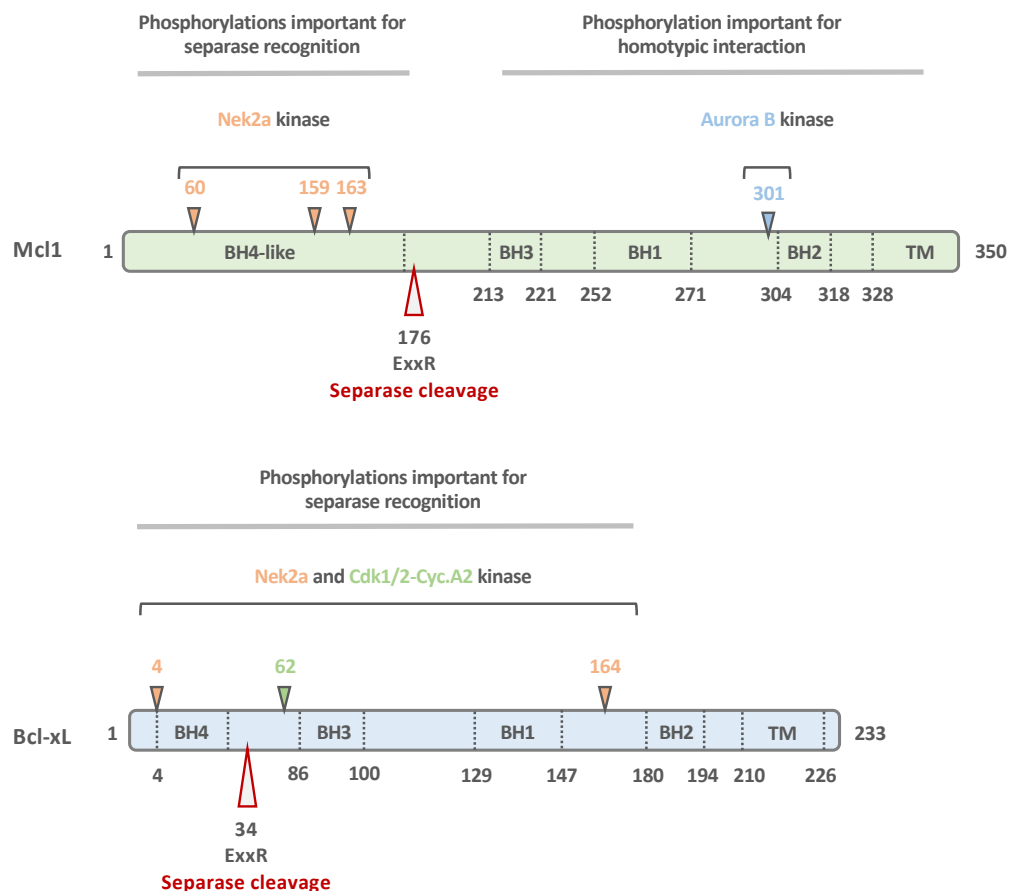


**Figure 11: Cleavage- and phosphorylation sites within the anti-apoptotic Bcl2 family members Mcl1 and Bcl-xL.** Note that it is not clear whether aurora B is the kinase relevant for *in vivo*-phosphorylation of Thr-301; the labeling is merely based on corresponding *in vitro* kinase assays. BH1-4 = Bcl-2 homology domains 1 to -4; TM = transmembrane domain.

What is the functional consequence of Mcl1 and Bcl-xL cleavage by separate? Mcl1 and Bcl-xL interact via their hydrophobic groove with the BH3-domains of Bak or Bax, thereby preventing them from homo-oligomerization and formation of pores into the mitochondrial outer membrane. Pro-apoptotic BH3-only proteins, like Bim and Bad, compete with Bak and Bax for binding to Mcl1 and Bcl-xL but, in healthy cells, Mcl1/Bcl-xL-Bak/Bax complexes prevail (Figure 12). Consistent with the existing literature, I found that full-length Mcl1 interacted with Bak rather than co-expressed Bim. Upon its cleavage at position 176, however, the resulting C-terminal Mcl1 fragment preferred Bim over Bak as binding partner. Similarly, separate-dependent removal of its N-terminus transformed Bcl-xL from a Bak- into a Bad-binder.

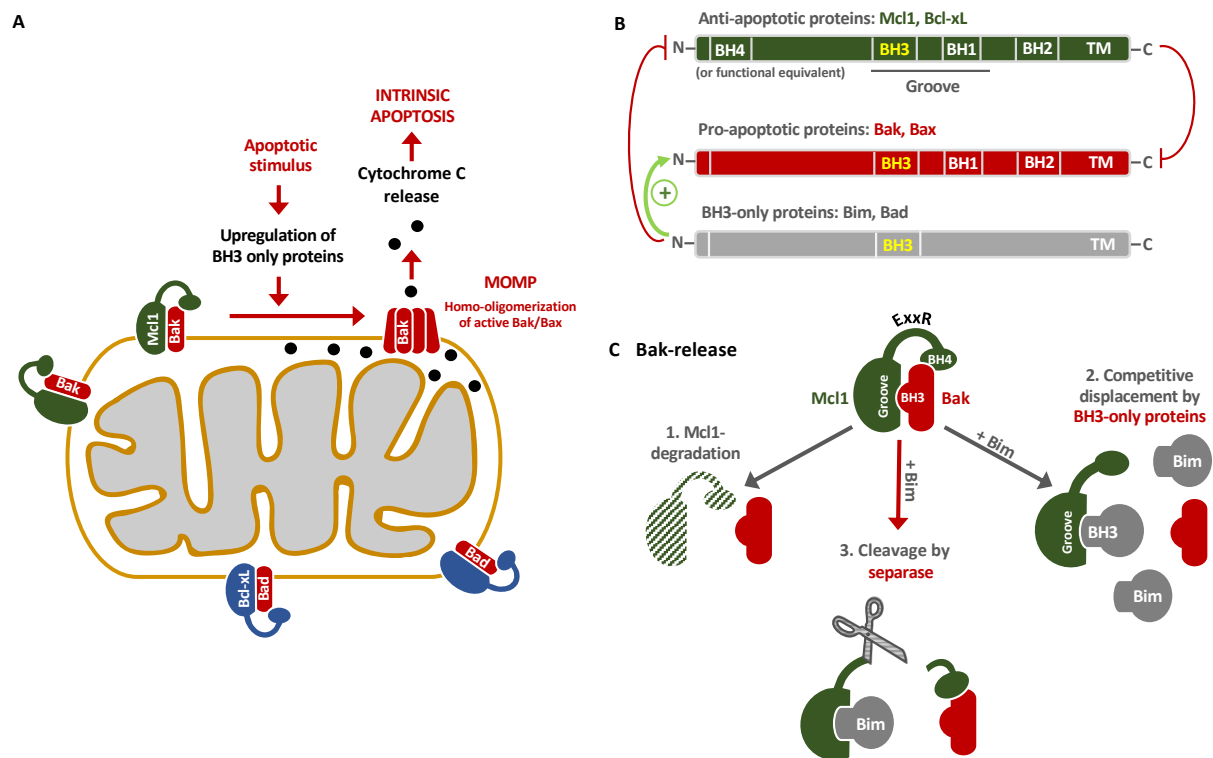


**Figure 12: Cleavage by separate transforms Mcl1's action from anti- into a pro-apoptotic.**

**A)** The mitochondrial intermembrane space contains the electron carrier cytochrome c, which initiates intrinsic apoptosis upon its release into the cytoplasm. In healthy cells, Mcl1 or Bcl-xL sequester pro-apoptotic Bak and Bax, thereby preventing them from pore formation. Apoptotic stimuli frequently result in upregulation of BH3-only proteins like Bim or Bad. These compete for binding to Mcl1 and Bcl-xL, thus releasing Bak and Bax. Alternatively, they transiently interact with Bak and Bax to facilitate their homotypic interaction and mitochondrial outer membrane permeabilization (MOMP). **B)** Schematic composition of the three classes of Bcl-2 family proteins. **C)** Three different mechanisms to release Bak from the inhibitory grip of Mcl1: 1) Decline of Mcl1 levels during extended mitotic arrest (Haschka et al., 2015; Sloss et al., 2016). 2) Increased levels of BH3-only proteins like Bim (Galluzzi et al., 2018; Villunger et al., 2003). 3) Cleavage of Mcl1 by separate, which destroys the cooperative binding of the hydrophobic groove and the N-terminus of Mcl1 to Bak (this work).

Cleavage by separate leaves the hydrophobic groove of Mcl1 and Bcl-xL intact. (It is situated in the C-terminal fragments, Mcl1-C and Bcl-xL-C.) This raises the question of how the

cleavage-dependent change in affinities can be explained? For Mcl1, I found that, interestingly, the N-terminal fragment stayed associated with Bak and was expelled only upon homotypic interaction of the latter. Contact of Mcl1-N with Bak has not been reported before but is consistent with the reported contribution of Bcl-2's BH4 domain to Bax binding (Barclay et al., 2015). I therefore propose that Mcl1 entertains contacts to Bak with both its N-terminal domain and the hydrophobic groove within its C-terminal half. Cleavage by separase between the two contact sites breaks the cooperativity of binding, thereby enabling Bim to out-compete Bak from Mcl1-C (Figure 12C, 2.). The same mechanism presumably applies also to the separase-dependent cleavage of Bcl-xL, although I did not yet test whether Bcl-xL-N interacts with Bak.

I noticed that the depletion of Mcl1 and/or Bcl-xL suppressed DiM in Securin- and Sgo2 depleted mitotic cells. This observation seemed counterintuitive and suggested 1) that these two Bcl-2 family proteins are the crucial - if not the only - targets during separase mediated DiM and 2) that their cleavage might not only inactivate them as Bak/Bax antagonists but transform them from survival into death factors. This possibility was scrutinized further for Mcl1. Indeed, both Mcl1-N and Mcl1-C proved apoptogenic upon their overexpression, with Mcl1-C having the stronger pro-apoptotic effect. Mcl1-N competes with the N-terminal domains of endogenous, full-length Bcl-xL/Mcl1 for the binding to Bak/Bax (Figure 13). Much like cleavage by separase, this destroys avidity and enables BH3-only proteins to supersede Bak/Bax from the hydrophobic groove of Bcl-xL/Mcl1. Moreover, Bcl-xL/Mcl1 seem to be slightly better separase substrates when in complex with a BH3-only protein as opposed to Bak/Bax.

For Mcl1-C, I found the following: 1) Mcl1-C (but not full-length Mcl1) can interact with itself (Figure 13). Homotypic interaction is prevented by addition of a Mcl1-specific BH3-mimetic and by deletion of the C-terminal transmembrane domain. 2) Bim interacts with Mcl1-C only transiently and disengages upon Mcl1-C self-interaction. 3) *BAK/BAX* double knock-out cells were compared to parental HCT116s by time-resolved separation of soluble cytosol from pelleted cell contents including mitochondria. Subsequent immunoblotting analyses revealed that separase induced DiM was delayed but still occurred in the absence of Bak and Bax as judged by release of cytochrome c into the cytosol (and PARP cleavage). Notably, Mcl1-C induced release of cytochrome c from mitochondria was unaffected by the absence

of Bak and Bax. 4) 2D structural illumination microscopy (SIM) showed that at late stages of apoptosis Mcl1-C forms large (200-400 nm) rings, which likely represent macro-pores because they lack the MOM protein Tom20 in their center. All these characteristics were previously reported for the pore formation by Bak/Bax (Brouwer et al., 2014; Czabotar et al., 2013; Dai et al., 2011; Grosse et al., 2016; McArthur et al., 2018; Salvador-Gallego et al., 2016). Thus, Mcl1-C itself permeabilizes the mitochondrial outer membrane by pore formation.

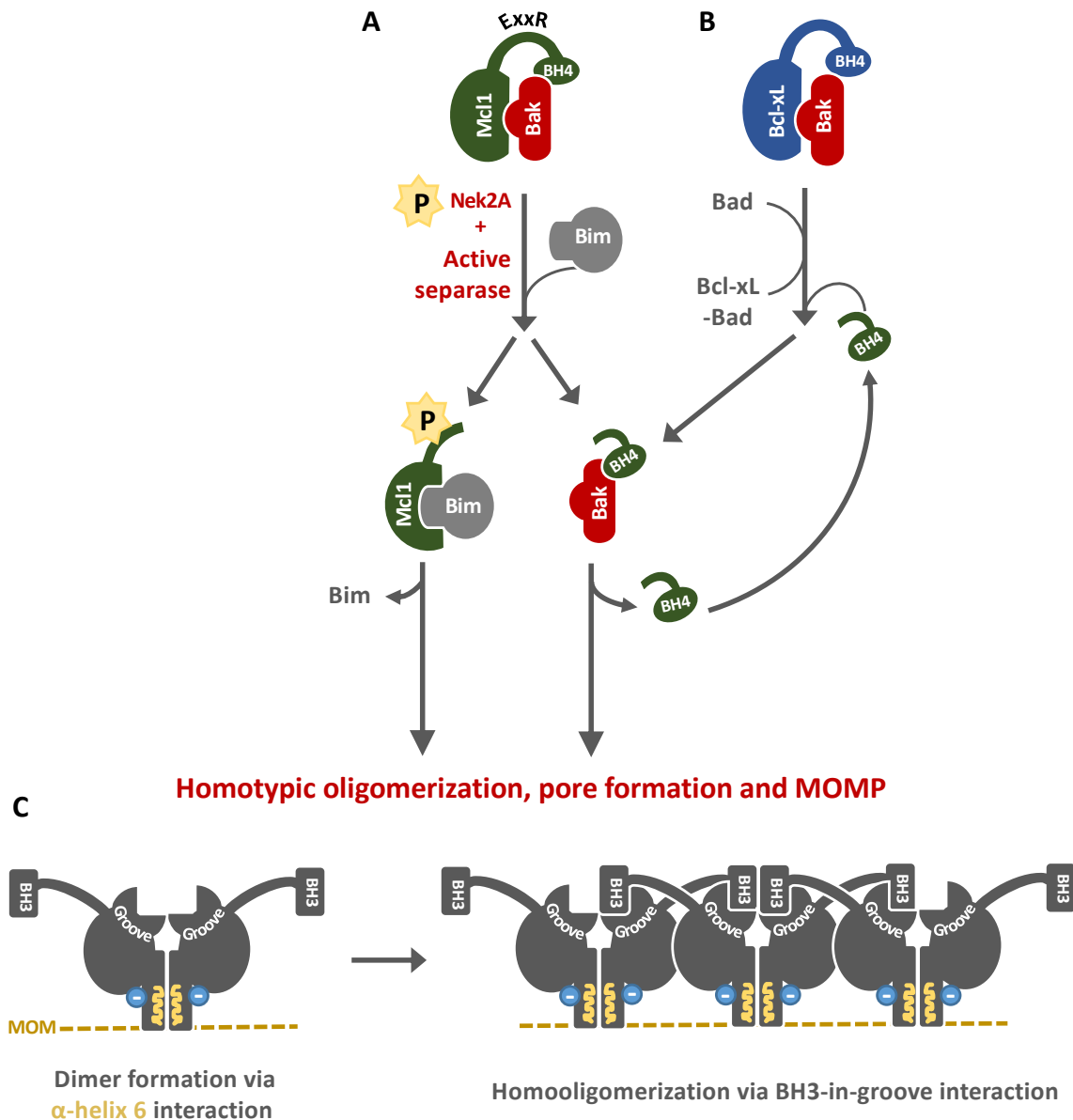


**Figure 13: Both separase cleavage fragments of Mcl1 promote apoptosis.**

**A)** Simultaneous activity of Nek2a and separase result in cleavage of Mcl1 after Arg-176, giving rise to N- and C-terminal fragments. This enables Bim to supersede Bak from Mcl1-C. Both the interaction of Bim with Mcl1-C and of Bak with Mcl1-N are transient. Bim and Mcl1-N are expelled when Mcl1-C and Bak each form homodimers during pore formation. **B)** Like separase-dependent cleavage, Mcl1-N also breaks the cooperative binding of Bcl-xL to Bak. Competitive displacement of Bcl-xL's BH4 domain from Bak by Mcl1-N enables Bad to liberate Bak. **C)** Proposed order of events during MOMP-causing pore formation. Homotypic oligomerization starts with dimerization of  $\alpha$ -helix 6, which requires a negative charge at the end of this  $\alpha$ -helix. This being phosphorylated Thr-301 in Mcl1-C and Glu-146 in Bax explains why Mcl1-C (but not Bax) requires mitotic phosphorylation for pore formation. Multimerization then occurs by BH3-in-groove interaction of dimers.

Despite the many parallels between Bak/Bax and Mcl1-C, one important difference is that Bak and Bax form pores independent of cell cycle stage, while Mcl1-C can trigger MOMP only in mitosis. Furthermore, Mcl1-N's pro-apoptotic effect is also limited to M-phase. I suspected mitotic phosphorylations as a reason and indeed could identify Ser/Thr to Ala mutations that weakened Mcl1-N induced DiM and extinguished Mcl1-C induced DiM. Thus, there are two kinds of phosphorylations: Those that turn Mcl1 and Bcl-xL into separase substrates and those that activate the pro-apoptotic character of the cleavage fragments. While the former are put into place by Nek2a (with a minimal contribution of Cdk1/2-cyclin A2 in case of Bcl-xL), *in vitro* assays suggest that the latter might be mediated by aurora B kinase (Figure 11).

Thr-301 of Mcl1 turned out to be especially interesting: Detection of affinity-purified Mcl1-C by a phospho-Thr specific antibody was possible for mitosis but abolished by Thr-301-Ala mutation, suggesting *in vivo* phosphorylation at this position. Changing this single site into Ala was sufficient to render Mcl1-C unable to self-interact and inactive in MOMP, while changing it to Glu enabled Mcl1-C to induce apoptosis also in interphase. Based on sequence alignments and structural information, the Thr-301 equivalent position in Bax is occupied by a Glu. Interestingly, changing this Glu-146 to Ala inactivates Bax, while changing it to Thr limits Bax's pro-apoptotic effect to mitosis. Thr-301 and Glu-146 reside at the end of  $\alpha$ -helix 6 within Mcl1 and Bax, respectively, and dimerization of this helix was reported to be required for the homo-oligomerization of Bak (Day et al., 2005; Dewson et al., 2009) (Figure 13). I propose that a negative charge (carboxyl- or phosphate group) at this position is required for pore formation and that this explains why MOMP by Mcl1-C is restricted to mitosis.

Mcl1 and Bcl-xL are present when separase becomes active on schedule. This begs the question of why cells do not die when undergoing a normal metaphase to anaphase transition? The explanation must be that Mcl1 and Bcl-xL are no longer cleavable by separase at this stage of mitosis. Consistently, Nek2a and Cyclin A are degraded in early mitosis and gone by the time when SAC inactivation triggers the events that culminate into release of separase (Hayes et al., 2006; Wolthuis et al., 2008). A corollary is that any temporal overlap of the enzymatic activities of Nek2a and separase should kill cells. The early mitotic degradation of Nek2a requires its C-terminal, so-called MR tail (Hayes et al.,

2006) and, indeed, expression of a stabilized Nek2a- $\Delta$ MR (but not the wild type kinase) was sufficient to trigger DiM in anaphase. Cells also died in late mitosis when Nek2a phosphorylation mimicking variants of Mcl1 or Bcl-xL were expressed (instead of Nek2a- $\Delta$ MR). Interestingly, DiM upon Nek2a stabilization was all the more effective, the higher the expression level of Mcl1 was. This graded response is potentially relevant for cancer therapy because Mcl1 is frequently over-expressed in many human tumors (Beroukhim et al., 2010).

If Nek2a and separase are usually not active at the same time, then what - if any - is the physiological role of separase dependent DiM? Does it ever occur *in vivo*, i.e. without highly artificial manipulations like separase deregulation or Nek2a stabilization? Timing of mitotic progression in vertebrates is chiefly determined by the SAC (Taylor and McKeon, 1997). I therefore tested whether SAC abrogation and the consequent shortening of M phase would result in simultaneous activity of Nek2a and separase. To this end, I either depleted the SAC components Mad2 and/or BubR1 by RNAi or supplemented cells with reversine, an inhibitor of the SAC kinase Mps1. As expected, this caused securin/cyclin B1 degradation and separase auto-cleavage to occur earlier than in corresponding controls. At the same time, Nek2a destruction was delayed - probably due to competition by other substrates for the APC/C. Importantly, this was accompanied by cleavage of Mcl1, Bcl-xL and PARP and by fragmentation of genomic DNA. Based on these results, we proposed that Nek2a and separase form a 'minimal duration of early mitosis checkpoint'. The biological function of this DMC would be to supervise the integrity of the SAC or, put differently, to sacrifice cells that have lost this surveillance mechanism. This might protect the organism from tumorigenic chromosome mis-segregations and explain the counter-intuitive observation that mutations in SAC genes are rare in cancer (Hernando et al., 2001; Tighe et al., 2001).

## References

- Abel, T.W., Clark, C., Bierie, B., Chytil, A., Aakre, M., Gorska, A., and Moses, H.L. (2009). GFAP-Cre-mediated activation of oncogenic K-ras results in expansion of the subventricular zone and infiltrating glioma. *Mol Cancer Res* 7, 645-653.
- Alfieri, C., Chang, L., and Barford, D. (2018). Mechanism for remodelling of the cell cycle checkpoint protein MAD2 by the ATPase TRIP13. *Nature* 559, 274-278.
- Alfieri, C., Chang, L., Zhang, Z., Yang, J., Maslen, S., Skehel, M., and Barford, D. (2016). Molecular basis of APC/C regulation by the spindle assembly checkpoint. *Nature* 536, 431-436.
- Barclay, L.A., Wales, T.E., Garner, T.P., Wachter, F., Lee, S., Guerra, R.M., Stewart, M.L., Braun, C.R., Bird, G.H., Gavathiotis, E., *et al.* (2015). Inhibition of Pro-apoptotic BAX by a noncanonical interaction mechanism. *Mol Cell* 57, 873-886.
- Bembenek, J.N., White, J.G., and Zheng, Y. (2010). A role for separase in the regulation of RAB-11-positive vesicles at the cleavage furrow and midbody. *Curr Biol* 20, 259-264.
- Beroukhi, R., Mermel, C.H., Porter, D., Wei, G., Raychaudhuri, S., Donovan, J., Barretina, J., Boehm, J.S., Dobson, J., Urashima, M., *et al.* (2010). The landscape of somatic copy-number alteration across human cancers. *Nature* 463, 899-905.
- Boisvert, F.M., Dery, U., Masson, J.Y., and Richard, S. (2005a). Arginine methylation of MRE11 by PRMT1 is required for DNA damage checkpoint control. *Genes Dev* 19, 671-676.
- Boisvert, F.M., Rhie, A., Richard, S., and Doherty, A.J. (2005b). The GAR motif of 53BP1 is arginine methylated by PRMT1 and is necessary for 53BP1 DNA binding activity. *Cell Cycle* 4, 1834-1841.
- Boland, A., Martin, T.G., Zhang, Z., Yang, J., Bai, X.C., Chang, L., Scheres, S.H., and Barford, D. (2017). Cryo-EM structure of a metazoan separase-securin complex at near-atomic resolution. *Nat Struct Mol Biol* 24, 414-418.
- Boos, D., Kuffer, C., Lenobel, R., Korner, R., and Stemmann, O. (2008). Phosphorylation-dependent binding of cyclin B1 to a Cdc6-like domain of human separase. *J Biol Chem* 283, 816-823.
- Brouwer, J.M., Westphal, D., Dewson, G., Robin, A.Y., Uren, R.T., Bartolo, R., Thompson, G.V., Colman, P.M., Kluck, R.M., and Czabotar, P.E. (2014). Bak core and latch domains separate during activation, and freed core domains form symmetric homodimers. *Mol Cell* 55, 938-946.
- Buheitel, J., and Stemmann, O. (2013). Prophase pathway-dependent removal of cohesin from human chromosomes requires opening of the Smc3-Scc1 gate. *EMBO J* 32, 666-676.
- Caron, P., Aymard, F., Iacovoni, J.S., Briois, S., Canitrot, Y., Bugler, B., Massip, L., Losada, A., and Legube, G. (2012). Cohesin protects genes against gammaH2AX Induced by DNA double-strand breaks. *PLoS genetics* 8, e1002460.
- Chan, K.L., Roig, M.B., Hu, B., Beckouet, F., Metson, J., and Nasmyth, K. (2012). Cohesin's DNA exit gate is distinct from its entrance gate and is regulated by acetylation. *Cell* 150, 961-974.
- Chao, W.C., Kulkarni, K., Zhang, Z., Kong, E.H., and Barford, D. (2012). Structure of the mitotic checkpoint complex. *Nature* 484, 208-213.

Choppara, S., Malonia, S.K., Sankaran, G., Green, M.R., and Santra, M.K. (2018). Degradation of FBXO31 by APC/C is regulated by AKT- and ATM-mediated phosphorylation. *Proc Natl Acad Sci U S A* *115*, 998-1003.

Ciosk, R., Zachariae, W., Michaelis, C., Shevchenko, A., Mann, M., and Nasmyth, K. (1998). An ESP1/PDS1 complex regulates loss of sister chromatid cohesion at the metaphase to anaphase transition in yeast. *Cell* *93*, 1067-1076.

Clem, R.J., Cheng, E.H., Karp, C.L., Kirsch, D.G., Ueno, K., Takahashi, A., Kastan, M.B., Griffin, D.E., Earnshaw, W.C., Veluona, M.A., *et al.* (1998). Modulation of cell death by Bcl-XL through caspase interaction. *Proc Natl Acad Sci U S A* *95*, 554-559.

Czabotar, P.E., Westphal, D., Dewson, G., Ma, S., Hockings, C., Fairlie, W.D., Lee, E.F., Yao, S., Robin, A.Y., Smith, B.J., *et al.* (2013). Bax crystal structures reveal how BH3 domains activate Bax and nucleate its oligomerization to induce apoptosis. *Cell* *152*, 519-531.

Dai, H., Smith, A., Meng, X.W., Schneider, P.A., Pang, Y.P., and Kaufmann, S.H. (2011). Transient binding of an activator BH3 domain to the Bak BH3-binding groove initiates Bak oligomerization. *J Cell Biol* *194*, 39-48.

Day, C.L., Chen, L., Richardson, S.J., Harrison, P.J., Huang, D.C., and Hinds, M.G. (2005). Solution structure of pro-survival Mcl-1 and characterization of its binding by proapoptotic BH3-only ligands. *J Biol Chem* *280*, 4738-4744.

Dewson, G., Kratina, T., Czabotar, P., Day, C.L., Adams, J.M., and Kluck, R.M. (2009). Bak activation for apoptosis involves oligomerization of dimers via their alpha6 helices. *Mol Cell* *36*, 696-703.

Ditchfield, C., Johnson, V.L., Tighe, A., Ellston, R., Haworth, C., Johnson, T., Mortlock, A., Keen, N., and Taylor, S.S. (2003). Aurora B couples chromosome alignment with anaphase by targeting BubR1, Mad2, and Cenp-E to kinetochores. *J Cell Biol* *161*, 267-280.

Eichinger, C.S., Kurze, A., Oliveira, R.A., and Nasmyth, K. (2013). Disengaging the Smc3/kleisin interface releases cohesin from Drosophila chromosomes during interphase and mitosis. *EMBO J* *32*, 656-665.

Eytan, E., Wang, K., Miniowitz-Shevtov, S., Sitry-Shevah, D., Kaisari, S., Yen, T.J., Liu, S.T., and Hershko, A. (2014). Disassembly of mitotic checkpoint complexes by the joint action of the AAA-ATPase TRIP13 and p31(comet). *Proc Natl Acad Sci U S A* *111*, 12019-12024.

Funabiki, H., Kumada, K., and Yanagida, M. (1996). Fission yeast Cut1 and Cut2 are essential for sister chromatid separation, concentrate along the metaphase spindle and form large complexes. *EMBO J* *15*, 6617-6628.

Galanty, Y., Belotserkovskaya, R., Coates, J., Polo, S., Miller, K.M., and Jackson, S.P. (2009). Mammalian SUMO E3-ligases PIAS1 and PIAS4 promote responses to DNA double-strand breaks. *Nature* *462*, 935-939.

Galluzzi, L., Vitale, I., Aaronson, S.A., Abrams, J.M., Adam, D., Agostinis, P., Alnemri, E.S., Altucci, L., Amelio, I., Andrews, D.W., *et al.* (2018). Molecular mechanisms of cell death: recommendations of the Nomenclature Committee on Cell Death 2018. *Cell Death Differ* *25*, 486-541.

Gil-Bernabe, A.M., Romero, F., Limon-Mortes, M.C., and Tortolero, M. (2006). Protein phosphatase 2A stabilizes human securin, whose phosphorylated forms are degraded via the SCF ubiquitin ligase. *Mol Cell Biol* *26*, 4017-4027.

- Glitoris, T., and Lowe, J. (2016). Structural Insights into Ring Formation of Cohesin and Related SMC Complexes. *Trends Cell Biol* 26, 680-693.
- Glotzer, M., Murray, A.W., and Kirschner, M.W. (1991). Cyclin is degraded by the ubiquitin pathway. *Nature* 349, 132-138.
- Gorr, I.H., Boos, D., and Stemmann, O. (2005). Mutual inhibition of separase and Cdk1 by two-step complex formation. *Mol Cell* 19, 135-141.
- Gorr, I.H., Reis, A., Boos, D., Wuhr, M., Madgwick, S., Jones, K.T., and Stemmann, O. (2006). Essential CDK1-inhibitory role for separase during meiosis I in vertebrate oocytes. *Nat Cell Biol* 8, 1035-1037.
- Grosse, L., Wurm, C.A., Bruser, C., Neumann, D., Jans, D.C., and Jakobs, S. (2016). Bax assembles into large ring-like structures remodeling the mitochondrial outer membrane in apoptosis. *EMBO J* 35, 402-413.
- Gruber, S., Haering, C.H., and Nasmyth, K. (2003). Chromosomal cohesin forms a ring. *Cell* 112, 765-777.
- Gunn, A., and Stark, J.M. (2012). I-SceI-based assays to examine distinct repair outcomes of mammalian chromosomal double strand breaks. *Methods in molecular biology* 920, 379-391.
- Haering, C.H., Farcas, A.M., Arumugam, P., Metson, J., and Nasmyth, K. (2008). The cohesin ring concatenates sister DNA molecules. *Nature* 454, 297-301.
- Haschka, M.D., Soratroi, C., Kirschnek, S., Hacker, G., Hilbe, R., Geley, S., Villunger, A., and Fava, L.L. (2015). The NOXA-MCL1-BIM axis defines lifespan on extended mitotic arrest. *Nature communications* 6, 6891.
- Hayes, M.J., Kimata, Y., Wattam, S.L., Lindon, C., Mao, G., Yamano, H., and Fry, A.M. (2006). Early mitotic degradation of Nek2A depends on Cdc20-independent interaction with the APC/C. *Nat Cell Biol* 8, 607-614.
- Hellmuth, S., Bottger, F., Pan, C., Mann, M., and Stemmann, O. (2014). PP2A delays APC/C-dependent degradation of separase-associated but not free securin. *EMBO J* 33, 1134-1147.
- Hellmuth, S., Gomez-H, L., Pendas, A. M. & Stemmann, O. (2020) Securin-independent regulation of separase by checkpoint-induced shugoshin-Mad2. *Nature*, *in press*.
- Hellmuth, S., Gutierrez-Caballero, C., Llano, E., Pendas, A.M., and Stemmann, O. (2018). Local activation of mammalian separase in interphase promotes double-strand break repair and prevents oncogenic transformation. *EMBO J* 37.
- Hellmuth, S., Pohlmann, C., Brown, A., Bottger, F., Sprinzl, M., and Stemmann, O. (2015a). Positive and negative regulation of vertebrate separase by Cdk1-cyclin B1 may explain why securin is dispensable. *J Biol Chem* 290, 8002-8010.
- Hellmuth, S., Rata, S., Brown, A., Heidmann, S., Novak, B., and Stemmann, O. (2015b). Human chromosome segregation involves multi-layered regulation of separase by the peptidyl-prolyl-isomerase Pin1. *Mol Cell* 58, 495-506.
- Hellmuth, S. & Stemmann, O. (2020) Separase-triggered apoptosis enforces minimal length of mitosis. *Nature*, *in press*.
- Hernando, E., Orlow, I., Liberal, V., Nohales, G., Benezra, R., and Cordon-Cardo, C. (2001). Molecular analyses of the mitotic checkpoint components hSMAD2, hBUB1 and hBUB3 in human cancer. *International journal of cancer* 95, 223-227.

- Holland, A.J., Bottger, F., Stemmann, O., and Taylor, S.S. (2007). Protein phosphatase 2A and separase form a complex regulated by separase autocleavage. *J Biol Chem* **282**, 24623-24632.
- Holland, A.J., and Taylor, S.S. (2006). Cyclin-B1-mediated inhibition of excess separase is required for timely chromosome disjunction. *J Cell Sci* **119**, 3325-3336.
- Holloway, S.L., Glotzer, M., King, R.W., and Murray, A.W. (1993). Anaphase is initiated by proteolysis rather than by the inactivation of maturation-promoting factor. *Cell* **73**, 1393-1402.
- Holt, L.J., Krutchinsky, A.N., and Morgan, D.O. (2008). Positive feedback sharpens the anaphase switch. *Nature* **454**, 353-357.
- Hornig, N.C., Knowles, P.P., McDonald, N.Q., and Uhlmann, F. (2002). The dual mechanism of separase regulation by securin. *Curr Biol* **12**, 973-982.
- Iacovoni, J.S., Caron, P., Lassadi, I., Nicolas, E., Massip, L., Trouche, D., and Legube, G. (2010). High-resolution profiling of gammaH2AX around DNA double strand breaks in the mammalian genome. *EMBO J* **29**, 1446-1457.
- Irniger, S., Piatti, S., Michaelis, C., and Nasmyth, K. (1995). Genes involved in sister chromatid separation are needed for B-type cyclin proteolysis in budding yeast. *Cell* **81**, 269-278.
- Katis, V.L., Lipp, J.J., Imre, R., Bogdanova, A., Okaz, E., Habermann, B., Mechtler, K., Nasmyth, K., and Zachariae, W. (2010). Rec8 phosphorylation by casein kinase 1 and Cdc7-Dbf4 kinase regulates cohesin cleavage by separase during meiosis. *Dev Cell* **18**, 397-409.
- Kawashima, S.A., Yamagishi, Y., Honda, T., Ishiguro, K., and Watanabe, Y. (2010). Phosphorylation of H2A by Bub1 prevents chromosomal instability through localizing shugoshin. *Science* **327**, 172-177.
- Kim, B.J., Li, Y., Zhang, J., Xi, Y., Li, Y., Yang, T., Jung, S.Y., Pan, X., Chen, R., Li, W., *et al.* (2010). Genome-wide reinforcement of cohesin binding at pre-existing cohesin sites in response to ionizing radiation in human cells. *J Biol Chem* **285**, 22784-22792.
- Kim, J.S., Krasieva, T.B., LaMorte, V., Taylor, A.M., and Yokomori, K. (2002). Specific recruitment of human cohesin to laser-induced DNA damage. *J Biol Chem* **277**, 45149-45153.
- King, R.W., Glotzer, M., and Kirschner, M.W. (1996). Mutagenic analysis of the destruction signal of mitotic cyclins and structural characterization of ubiquitinated intermediates. *Mol Biol Cell* **7**, 1343-1357.
- King, R.W., Peters, J.M., Tugendreich, S., Rolfe, M., Hieter, P., and Kirschner, M.W. (1995). A 20S complex containing CDC27 and CDC16 catalyzes the mitosis-specific conjugation of ubiquitin to cyclin B. *Cell* **81**, 279-288.
- Kitajima, T.S., Sakuno, T., Ishiguro, K., Iemura, S., Natsume, T., Kawashima, S.A., and Watanabe, Y. (2006). Shugoshin collaborates with protein phosphatase 2A to protect cohesin. *Nature* **441**, 46-52.
- Kudo, N.R., Anger, M., Peters, A.H., Stemmann, O., Theussl, H.C., Helmhart, W., Kudo, H., Heyting, C., and Nasmyth, K. (2009). Role of cleavage by separase of the Rec8 kleisin subunit of cohesin during mammalian meiosis I. *J Cell Sci* **122**, 2686-2698.
- Kudo, N.R., Wassmann, K., Anger, M., Schuh, M., Wirth, K.G., Xu, H., Helmhart, W., Kudo, H., McKay, M., Maro, B., *et al.* (2006). Resolution of chiasmata in oocytes requires separase-mediated proteolysis. *Cell* **126**, 135-146.

Kueng, S., Hegemann, B., Peters, B.H., Lipp, J.J., Schleiffer, A., Mechtler, K., and Peters, J.M. (2006). Wapl controls the dynamic association of cohesin with chromatin. *Cell* *127*, 955-967.

Lee, K., and Rhee, K. (2012). Separase-dependent cleavage of pericentrin B is necessary and sufficient for centriole disengagement during mitosis. *Cell Cycle* *11*, 2476-2485.

Li, M., York, J.P., and Zhang, P. (2007). Loss of Cdc20 causes a securin-dependent metaphase arrest in two-cell mouse embryos. *Mol Cell Biol* *27*, 3481-3488.

Limon-Mortes, M.C., Mora-Santos, M., Espina, A., Pintor-Toro, J.A., Lopez-Roman, A., Tortolero, M., and Romero, F. (2008). UV-induced degradation of securin is mediated by SKP1-CUL1-beta TrCP E3 ubiquitin ligase. *J Cell Sci* *121*, 1825-1831.

Lin, Z., Luo, X., and Yu, H. (2016). Structural basis of cohesin cleavage by separase. *Nature* *532*, 131-134.

Liou, Y.C., Zhou, X.Z., and Lu, K.P. (2011). Prolyl isomerase Pin1 as a molecular switch to determine the fate of phosphoproteins. *Trends in biochemical sciences* *36*, 501-514.

Liu, H., Rankin, S., and Yu, H. (2013). Phosphorylation-enabled binding of SGO1-PP2A to cohesin protects sororin and centromeric cohesion during mitosis. *Nat Cell Biol* *15*, 40-49.

Llano, E., Gomez, R., Gutierrez-Caballero, C., Herran, Y., Sanchez-Martin, M., Vazquez-Quinones, L., Hernandez, T., de Alava, E., Cuadrado, A., Barbero, J.L., *et al.* (2008). Shugoshin-2 is essential for the completion of meiosis but not for mitotic cell division in mice. *Genes Dev* *22*, 2400-2413.

Losada, A., Hirano, M., and Hirano, T. (1998). Identification of Xenopus SMC protein complexes required for sister chromatid cohesion. *Genes Dev* *12*, 1986-1997.

Losada, A., Yokochi, T., Kobayashi, R., and Hirano, T. (2000). Identification and characterization of SA/Scp3p subunits in the Xenopus and human cohesin complexes. *J Cell Biol* *150*, 405-416.

Lu, K.P., Hanes, S.D., and Hunter, T. (1996). A human peptidyl-prolyl isomerase essential for regulation of mitosis. *Nature* *380*, 544-547.

Lu, P.J., Zhou, X.Z., Shen, M., and Lu, K.P. (1999). Function of WW domains as phosphoserine- or phosphothreonine-binding modules. *Science* *283*, 1325-1328.

Matsuo, K., Ohsumi, K., Iwabuchi, M., Kawamata, T., Ono, Y., and Takahashi, M. (2012). Kendrin is a novel substrate for separase involved in the licensing of centriole duplication. *Curr Biol* *22*, 915-921.

McAleenan, A., Clemente-Blanco, A., Cordon-Preciado, V., Sen, N., Esteras, M., Jarmuz, A., and Aragon, L. (2013). Post-replicative repair involves separase-dependent removal of the kleisin subunit of cohesin. *Nature* *493*, 250-254.

McArthur, K., Whitehead, L.W., Heddleston, J.M., Li, L., Padman, B.S., Oorschot, V., Geoghegan, N.D., Chappaz, S., Davidson, S., San Chin, H., *et al.* (2018). BAK/BAX macropores facilitate mitochondrial herniation and mtDNA efflux during apoptosis. *Science* *359*.

Michel, L.S., Liberal, V., Chatterjee, A., Kirchwegger, R., Pasche, B., Gerald, W., Dobles, M., Sorger, P.K., Murty, V.V., and Benezra, R. (2001). MAD2 haplo-insufficiency causes premature anaphase and chromosome instability in mammalian cells. *Nature* *409*, 355-359.

Michels, J., O'Neill, J.W., Dallman, C.L., Mouzakiti, A., Habens, F., Brimmell, M., Zhang, K.Y., Craig, R.W., Marcusson, E.G., Johnson, P.W., *et al.* (2004). Mcl-1 is required for Akata6 B-

lymphoma cell survival and is converted to a cell death molecule by efficient caspase-mediated cleavage. *Oncogene* 23, 4818-4827.

Monen, J., Hattersley, N., Muroyama, A., Stevens, D., Oegema, K., and Desai, A. (2015). Separase Cleaves the N-Tail of the CENP-A Related Protein CPAR-1 at the Meiosis I Metaphase-Anaphase Transition in *C. elegans*. *PLoS One* 10, e0125382.

Murray, A.W., and Kirschner, M.W. (1989). Cyclin synthesis drives the early embryonic cell cycle. *Nature* 339, 275-280.

Murray, A.W., Solomon, M.J., and Kirschner, M.W. (1989). The role of cyclin synthesis and degradation in the control of maturation promoting factor activity. *Nature* 339, 280-286.

Musacchio, A. (2015). The Molecular Biology of Spindle Assembly Checkpoint Signaling Dynamics. *Curr Biol* 25, R1002-1018.

Nagao, K., Adachi, Y., and Yanagida, M. (2004). Separase-mediated cleavage of cohesin at interphase is required for DNA repair. *Nature* 430, 1044-1048.

Nagao, K., and Yanagida, M. (2006). Securin can have a separase cleavage site by substitution mutations in the domain required for stabilization and inhibition of separase. *Genes to cells : devoted to molecular & cellular mechanisms* 11, 247-260.

Nasmyth, K. (2005). How do so few control so many? *Cell* 120, 739-746.

Nasmyth, K., and Haering, C.H. (2009). Cohesin: its roles and mechanisms. *Annu Rev Genet* 43, 525-558.

Orth, M., Mayer, B., Rehm, K., Rothweiler, U., Heidmann, D., Holak, T.A., and Stemmann, O. (2011). Shugoshin is a Mad1/Cdc20-like interactor of Mad2. *EMBO J* 30, 2868-2880.

Ouyang, Z., and Yu, H. (2017). Releasing the cohesin ring: A rigid scaffold model for opening the DNA exit gate by Pds5 and Wapl. *Bioessays* 39.

Papi, M., Berdugo, E., Randall, C.L., Ganguly, S., and Jallepalli, P.V. (2005). Multiple roles for separase auto-cleavage during the G2/M transition. *Nat Cell Biol* 7, 1029-1035.

Pfleger, C.M., and Kirschner, M.W. (2000). The KEN box: an APC recognition signal distinct from the D box targeted by Cdh1. *Genes Dev* 14, 655-665.

Pfleghaar, K., Heubes, S., Cox, J., Stemmann, O., and Speicher, M.R. (2005). Securin is not required for chromosomal stability in human cells. *PLoS Biol* 3, e416.

Pierce, A.J., Johnson, R.D., Thompson, L.H., and Jasin, M. (1999). XRCC3 promotes homology-directed repair of DNA damage in mammalian cells. *Genes Dev* 13, 2633-2638.

Polo, S.E., and Jackson, S.P. (2011). Dynamics of DNA damage response proteins at DNA breaks: a focus on protein modifications. *Genes Dev* 25, 409-433.

Potts, P.R., Porteus, M.H., and Yu, H. (2006). Human SMC5/6 complex promotes sister chromatid homologous recombination by recruiting the SMC1/3 cohesin complex to double-strand breaks. *EMBO J* 25, 3377-3388.

Potts, P.R., and Yu, H. (2005). Human MMS21/NSE2 is a SUMO ligase required for DNA repair. *Mol Cell Biol* 25, 7021-7032.

Rattani, A., Wolna, M., Ploquin, M., Helmhart, W., Morrone, S., Mayer, B., Godwin, J., Xu, W., Stemmann, O., Pendas, A., *et al.* (2013). Sgol2 provides a regulatory platform that coordinates essential cell cycle processes during meiosis I in oocytes. *Elife* 2, e01133.

Riedel, C.G., Katis, V.L., Katou, Y., Mori, S., Itoh, T., Helmhart, W., Galova, M., Petronczki, M., Gregan, J., Cetin, B., *et al.* (2006). Protein phosphatase 2A protects centromeric sister chromatid cohesion during meiosis I. *Nature* **441**, 53-61.

Rodriguez-Bravo, V., Maciejowski, J., Corona, J., Buch, H.K., Collin, P., Kanemaki, M.T., Shah, J.V., and Jallepalli, P.V. (2014). Nuclear pores protect genome integrity by assembling a premitotic and Mad1-dependent anaphase inhibitor. *Cell* **156**, 1017-1031.

Sacher, M., Pfander, B., Hoegge, C., and Jentsch, S. (2006). Control of Rad52 recombination activity by double-strand break-induced SUMO modification. *Nat Cell Biol* **8**, 1284-1290.

Sakahira, H., Iwamatsu, A., and Nagata, S. (2000). Specific chaperone-like activity of inhibitor of caspase-activated DNase for caspase-activated DNase. *J Biol Chem* **275**, 8091-8096.

Sakahira, H., and Nagata, S. (2002). Co-translational folding of caspase-activated DNase with Hsp70, Hsp40, and inhibitor of caspase-activated DNase. *J Biol Chem* **277**, 3364-3370.

Salvador-Gallego, R., Mund, M., Cosentino, K., Schneider, J., Unsay, J., Schraermeyer, U., Engelhardt, J., Ries, J., and Garcia-Saez, A.J. (2016). Bax assembly into rings and arcs in apoptotic mitochondria is linked to membrane pores. *EMBO J* **35**, 389-401.

Schockel, L., Mockel, M., Mayer, B., Boos, D., and Stemmann, O. (2011). Cleavage of cohesin rings coordinates the separation of centrioles and chromatids. *Nat Cell Biol* **13**, 966-972.

Shen, M., Stukenberg, P.T., Kirschner, M.W., and Lu, K.P. (1998). The essential mitotic peptidyl-prolyl isomerase Pin1 binds and regulates mitosis-specific phosphoproteins. *Genes Dev* **12**, 706-720.

Shindo, N., Kumada, K., and Hirota, T. (2012). Separase sensor reveals dual roles for separase coordinating cohesin cleavage and cdk1 inhibition. *Dev Cell* **23**, 112-123.

Simpson-Lavy, K.J., Zenvirth, D., and Brandeis, M. (2015). Phosphorylation and dephosphorylation regulate APC/C(Cdh1) substrate degradation. *Cell Cycle* **14**, 3138-3145.

Sloss, O., Topham, C., Diez, M., and Taylor, S. (2016). Mcl-1 dynamics influence mitotic slippage and death in mitosis. *Oncotarget* **7**, 5176-5192.

Stemmann, O., Zou, H., Gerber, S.A., Gygi, S.P., and Kirschner, M.W. (2001). Dual inhibition of sister chromatid separation at metaphase. *Cell* **107**, 715-726.

Stratmann, R., and Lehner, C.F. (1996). Separation of sister chromatids in mitosis requires the *Drosophila* pimples product, a protein degraded after the metaphase/anaphase transition. *Cell* **84**, 25-35.

Strom, L., Lindroos, H.B., Shirahige, K., and Sjogren, C. (2004). Postreplicative recruitment of cohesin to double-strand breaks is required for DNA repair. *Mol Cell* **16**, 1003-1015.

Sudakin, V., Chan, G.K., and Yen, T.J. (2001). Checkpoint inhibition of the APC/C in HeLa cells is mediated by a complex of BUBR1, BUB3, CDC20, and MAD2. *J Cell Biol* **154**, 925-936.

Sudakin, V., Ganoth, D., Dahan, A., Heller, H., Hershko, J., Luca, F.C., Ruderman, J.V., and Hershko, A. (1995). The cyclosome, a large complex containing cyclin-selective ubiquitin ligase activity, targets cyclins for destruction at the end of mitosis. *Mol Biol Cell* **6**, 185-197.

Sullivan, M., Lehane, C., and Uhlmann, F. (2001). Orchestrating anaphase and mitotic exit: separase cleavage and localization of Slk19. *Nat Cell Biol* **3**, 771-777.

Sumara, I., Vorlaufer, E., Gieffers, C., Peters, B.H., and Peters, J.M. (2000). Characterization of vertebrate cohesin complexes and their regulation in prophase. *J Cell Biol* **151**, 749-762.

Sun, Y., Yu, H., and Zou, H. (2006). Nuclear exclusion of separase prevents cohesin cleavage in interphase cells. *Cell Cycle* 5, 2537-2542.

Tanno, Y., Kitajima, T.S., Honda, T., Ando, Y., Ishiguro, K., and Watanabe, Y. (2010). Phosphorylation of mammalian Sgo2 by Aurora B recruits PP2A and MCAK to centromeres. *Genes Dev* 24, 2169-2179.

Taylor, S.S., and McKeon, F. (1997). Kinetochore localization of murine Bub1 is required for normal mitotic timing and checkpoint response to spindle damage. *Cell* 89, 727-735.

Thandapani, P., O'Connor, T.R., Bailey, T.L., and Richard, S. (2013). Defining the RGG/RG motif. *Mol Cell* 50, 613-623.

Tighe, A., Johnson, V.L., Albertella, M., and Taylor, S.S. (2001). Aneuploid colon cancer cells have a robust spindle checkpoint. *EMBO Rep* 2, 609-614.

Tighe, A., Staples, O., and Taylor, S. (2008). Mps1 kinase activity restrains anaphase during an unperturbed mitosis and targets Mad2 to kinetochores. *J Cell Biol* 181, 893-901.

Tsou, M.F., and Stearns, T. (2006). Mechanism limiting centrosome duplication to once per cell cycle. *Nature* 442, 947-951.

Tsou, M.F., Wang, W.J., George, K.A., Uryu, K., Stearns, T., and Jallepalli, P.V. (2009). Polo kinase and separase regulate the mitotic licensing of centriole duplication in human cells. *Dev Cell* 17, 344-354.

Uhlmann, F., Lottspeich, F., and Nasmyth, K. (1999). Sister-chromatid separation at anaphase onset is promoted by cleavage of the cohesin subunit Scc1. *Nature* 400, 37-42.

Uhlmann, F., and Nasmyth, K. (1998). Cohesion between sister chromatids must be established during DNA replication. *Curr Biol* 8, 1095-1101.

Uhlmann, F., Wernic, D., Poupart, M.A., Koonin, E.V., and Nasmyth, K. (2000). Cleavage of cohesin by the CD clan protease separin triggers anaphase in yeast. *Cell* 103, 375-386.

Unal, E., Arbel-Eden, A., Sattler, U., Shroff, R., Lichten, M., Haber, J.E., and Koshland, D. (2004). DNA damage response pathway uses histone modification to assemble a double-strand break-specific cohesin domain. *Mol Cell* 16, 991-1002.

Unal, E., Heidinger-Pauli, J.M., and Koshland, D. (2007). DNA double-strand breaks trigger genome-wide sister-chromatid cohesion through Eco1 (Ctf7). *Science* 317, 245-248.

Urusova, D.V., Shim, J.H., Kim, D.J., Jung, S.K., Zykova, T.A., Carper, A., Bode, A.M., and Dong, Z. (2011). Epigallocatechin-gallate suppresses tumorigenesis by directly targeting Pin1. *Cancer prevention research* 4, 1366-1377.

Viadiu, H., Stemmann, O., Kirschner, M.W., and Walz, T. (2005). Domain structure of separase and its binding to securin as determined by EM. *Nat Struct Mol Biol* 12, 552-553.

Villunger, A., Michalak, E.M., Coultas, L., Mullauer, F., Bock, G., Ausserlechner, M.J., Adams, J.M., and Strasser, A. (2003). p53- and drug-induced apoptotic responses mediated by BH3-only proteins puma and noxa. *Science* 302, 1036-1038.

Waizenegger, I.C., Hauf, S., Meinke, A., and Peters, J.M. (2000). Two distinct pathways remove mammalian cohesin from chromosome arms in prophase and from centromeres in anaphase. *Cell* 103, 399-410.

Wild, T., Budzowska, M., Hellmuth, S., Eibes, S., Karemore, G., Barisic, M., Stemmann, O., and Choudhary, C. (2018). Deletion of APC7 or APC16 Allows Proliferation of Human Cells without the Spindle Assembly Checkpoint. *Cell Rep* 25, 2317-2328 e2315.

- Wirth, K.G., Wutz, G., Kudo, N.R., Desdouets, C., Zetterberg, A., Taghybeeglu, S., Seznec, J., Ducos, G.M., Ricci, R., Firnberg, N., *et al.* (2006). Separase: a universal trigger for sister chromatid disjunction but not chromosome cycle progression. *J Cell Biol* *172*, 847-860.
- Wolf, P.G., Cuba Ramos, A., Kenzel, J., Neumann, B., and Stemmann, O. (2018). Studying meiotic cohesin in somatic cells reveals that Rec8-containing cohesin requires Stag3 to function and is regulated by Wapl and sororin. *J Cell Sci* *131*.
- Wolthuis, R., Clay-Farrace, L., van Zon, W., Yekezare, M., Koop, L., Ogink, J., Medema, R., and Pines, J. (2008). Cdc20 and Cks direct the spindle checkpoint-independent destruction of cyclin A. *Mol Cell* *30*, 290-302.
- Yaffe, M.B., Schutkowski, M., Shen, M., Zhou, X.Z., Stukenberg, P.T., Rahfeld, J.U., Xu, J., Kuang, J., Kirschner, M.W., Fischer, G., *et al.* (1997). Sequence-specific and phosphorylation-dependent proline isomerization: a potential mitotic regulatory mechanism. *Science* *278*, 1957-1960.
- Yamagishi, Y., Yang, C.H., Tanno, Y., and Watanabe, Y. (2012). MPS1/Mph1 phosphorylates the kinetochore protein KNL1/Spc7 to recruit SAC components. *Nat Cell Biol* *14*, 746-752.
- Yamamoto, A., Guacci, V., and Koshland, D. (1996). Pds1p, an inhibitor of anaphase in budding yeast, plays a critical role in the APC and checkpoint pathway(s). *J Cell Biol* *133*, 99-110.
- Zhang, Y., and Xiong, Y. (2001). A p53 amino-terminal nuclear export signal inhibited by DNA damage-induced phosphorylation. *Science* *292*, 1910-1915.
- Zou, H., McGarry, T.J., Bernal, T., and Kirschner, M.W. (1999). Identification of a vertebrate sister-chromatid separation inhibitor involved in transformation and tumorigenesis. *Science* *285*, 418-422.
- Zou, H., Stemman, O., Anderson, J.S., Mann, M., and Kirschner, M.W. (2002). Anaphase specific auto-cleavage of separase. *FEBS Lett* *528*, 246-250.

## **Own contributions**

**1) Hellmuth, S., Bottger, F., Pan, C., Mann, M. & Stemmann, O.**

**PP2A delays APC/C-dependent degradation of separase-associated but not free securin.**  
**EMBO J 33, 1134-1147, doi:10.1002/embj.201488098 (2014).**

I co-designed and performed all experiments (including corresponding quantifications) except for the ones shown in Figures 1A, 1B, and S4. I also contributed to writing of the manuscript.

**2) Hellmuth, S., Pohlmann, C., Brown, A., Bottger, F., Sprinzl, M. & Stemmann, O.**

**Positive and negative regulation of vertebrate separase by Cdk1-cyclin B1 may explain why securin is dispensable.**

**J Biol Chem 290, 8002-8010, doi:10.1074/jbc.M114.615310 (2015a).**

I co-designed and performed all experiments except for the one shown in Figures 1A. Furthermore, I contributed to writing of the paper.

**3) Hellmuth, S., Rata, S., Brown, A., Heidmann, S., Novak, B. & Stemmann, O.**

**Human chromosome segregation involves multi-layered regulation of separase by the peptidyl-prolyl-isomerase Pin1.**

**Mol Cell 58, 495-506, doi:10.1016/j.molcel.2015.03.025 (2015b).**

I co-designed and performed all 'wet lab experiments' and wrote parts of the manuscript.

**4) Hellmuth, S., Gutierrez-Caballero, C., Llano, E., Pendas, A. M. & Stemmann, O.**

**Local activation of mammalian separase in interphase promotes double-strand break repair and prevents oncogenic transformation.**

**EMBO J 37, e99184, doi:10.15252/embj.201899184 (2018).**

I co-designed the research, carried out all experiments except for those shown in Figures 8 and EV4 and Table EV1. I also contributed to writing of the paper.

**5) Hellmuth, S., Gomez-H, L., Pendas, A. M. & Stemmann, O.**

**Securin-independent regulation of separase by checkpoint-induced shugoshin-Mad2.**  
**Nature 580, 536-541, doi: 10.1038/s41586-020-2182-3 (2020).**

I carried out all experiments except for the one shown in Extended Data Fig. 1a. Furthermore, I co-designed the research and contributed to writing of the manuscript.

**6) Hellmuth, S. & Stemmann, O.**

**Separase-triggered apoptosis enforces minimal length of mitosis.**  
**Nature 580, 536-541, doi: 10.1038/s41586-020-2187-y (2020).**

I carried out all experiments, co-designed the research and contributed to writing of the paper.

# PP2A delays APC/C-dependent degradation of separase-associated but not free securin

Susanne Hellmuth<sup>1,§</sup>, Franziska Böttger<sup>1,\*†,§</sup>, Cuiping Pan<sup>2,‡</sup>, Matthias Mann<sup>2</sup> & Olaf Stemmann<sup>1,\*\*</sup>

## Abstract

The universal triggering event of eukaryotic chromosome segregation is cleavage of centromeric cohesin by separase. Prior to anaphase, most separase is kept inactive by association with securin. Protein phosphatase 2A (PP2A) constitutes another binding partner of human separase, but the functional relevance of this interaction has remained enigmatic. We demonstrate that PP2A stabilizes separase-associated securin by dephosphorylation, while phosphorylation of free securin enhances its polyubiquitylation by the ubiquitin ligase APC/C and proteasomal degradation. Changing PP2A substrate phosphorylation sites to alanines slows degradation of free securin, delays separase activation, lengthens early anaphase, and results in anaphase bridges and DNA damage. In contrast, separase-associated securin is destabilized by introduction of phosphorylation-mimetic aspartates or extinction of separase-associated PP2A activity. G<sub>2</sub>- or prometaphase-arrested cells suffer from unscheduled activation of separase when endogenous securin is replaced by aspartate-mutant securin. Thus, PP2A-dependent stabilization of separase-associated securin prevents precocious activation of separase during checkpoint-mediated arrests with basal APC/C activity and increases the abruptness and fidelity of sister chromatid separation in anaphase.

**Keywords** APC/C; PP2A; securin; separase; ubiquitylation

**Subject Categories** Cell Cycle; Post-translational Modifications, Proteolysis & Proteomics

**DOI** 10.1002/embj.201488098 | Received 1 February 2014 | Revised 19 March 2014 | Accepted 31 March 2014

**The EMBO Journal (2014) 33: 1134–1147**

## Introduction

In eukaryotes, other than in prokaryotes, the duplication and segregation of the genetic material are separated in time, taking place during S- and M-phase, respectively. This decoupling is made possible because the two sister chromatids of each

chromosome are paired and thus treated as one unit beginning from the time of their generation in S-phase until their segregation in mitosis. Sister chromatid cohesion is mediated by the multi-protein complex cohesin. Its long coiled-coil subunits Smc1 and Smc3 together with the kleisin Scc1 (Rad21) form a tripartite ring, 50 nm in diameter, that provides a topological linkage by entrapping both DNA double strands (Haering *et al.*, 2008). In early metazoan mitosis, cohesin rings at chromosome arms are removed by prophase pathway signaling which triggers the phosphorylation-dependent opening of the Smc3-Scc1 gate (Buheitel & Stemmann, 2013; Eichinger *et al.*, 2013). However, sister chromatid cohesion is maintained because protein phosphatase 2A (PP2A) is recruited by shugoshin 1 (Sgo1) to centromeric cohesin and keeps it in a dephosphorylated state (Watanabe, 2005). At metaphase-to-anaphase transition, the Scc1 subunit of remaining cohesin is cleaved by separase and sister chromatids spring apart (Uhlmann *et al.*, 2000). Separase is a large Cys-endopeptidase with a conserved C-terminal catalytic domain. It is encoded by an essential gene and represents the universal trigger of eukaryotic anaphase (Kumada *et al.*, 2006; Wirth *et al.*, 2006). Hyper- or hypo-activity of separase results in premature separation of sister chromatids or chromosome non-disjunction, respectively (Huang *et al.*, 2005; Holland & Taylor, 2006; Boos *et al.*, 2008). Separase also cleaves centrosomal cohesin and pericentrin-B (kendrin), which promotes centriole disengagement and licensing of subsequent centrosome duplication (Schockel *et al.*, 2011; Lee & Rhee, 2012; Matsuo *et al.*, 2012). The well-tuned regulation of separase activity is therefore crucial to ensure a stable inheritance of genomic information and to prevent aneuploidies that might otherwise result in cell death or malignant transformation.

Prior to anaphase onset, vertebrate separase is inhibited by mutually exclusive association with Cdk1-cyclin B1 or securin (Gorr *et al.*, 2005; Stemmann *et al.*, 2006). Cdk1-cyclin B1 is the master regulatory kinase of mitosis and phosphorylates a multitude of proteins. Its activation and inactivation, respectively, is necessary and sufficient for entry into and exit from mitosis. For unknown reasons, the relevance of Cdk1-cyclin B1 versus securin for the inhibition of separase varies in different cells and

<sup>1</sup> Chair of Genetics, University of Bayreuth, Bayreuth, Germany

<sup>2</sup> Department of Proteomics and Signal Transduction, Max Planck Institute of Biochemistry, Martinsried, Germany

\*Corresponding author. Tel: +46 852486311; Fax: +46 8342651; E-mail: franziska.boettger@ki.se

\*\*Corresponding author. Tel: +49 921552702; Fax: +49 921552710; E-mail: olaf.stemmann@uni-bayreuth.de

§These authors contributed equally to this work.

†Present address: Department of Microbiology, Tumor and Cell Biology (MTC), Karolinska Institutet, Stockholm, Sweden

‡Present address: Department of Genetics, Stanford University School of Medicine, Stanford, CA, USA

developmental states. For example, murine post-migratory primordial germ cells and early embryos chiefly rely on Cdk1-cyclin B1 to control separase, whereas in mouse female meiosis II and cultured human cancer cells, most of the protease is held in check by association with securin (Gorr *et al*, 2005; Huang *et al*, 2008, 2009; Nabti *et al*, 2008). Separase is activated at the metaphase-to-anaphase transition when both securin and cyclin B1 are degraded via the ubiquitin-proteasome pathway. The corresponding ubiquitin ligase is a multi-subunit RING E3, the anaphase-promoting complex or cyclosome (APC/C), in conjunction with Cdc20, its mitosis specific co-activator (Peters, 2006). Cdc20 (but also Cdh1, a related co-activator of interphase APC/C) recognizes a motif of the minimal consensus sequence R-x-x-L, the so-called destruction box (or D-box), located close to the N-terminus of securin and cyclin B1. Securin (but not cyclin B1) contains an additional N-terminal motif called KEN-box, which is named after its core amino acid sequence and also binds to Cdc20 (and Cdh1). APC/C<sup>Cdc20</sup> activity is controlled by the spindle assembly checkpoint (SAC), which, in metazoans, is of prime importance for timing of mitosis and chromosome segregation fidelity (Lara-Gonzalez *et al*, 2012). As long as chromosomes have not yet properly attached to spindle microtubules, this essential surveillance mechanism generates a diffusible ‘wait-anaphase’ signal at kinetochores, which inhibits APC/C<sup>Cdc20</sup>.

Despite our knowledge of the basic SAC-APC/C-separase axis, other aspects of separase regulation remain poorly understood. For example, it has recently been noted that, relative to total securin, the separase-bound fraction is proteolysed more slowly (Shindo *et al*, 2012). However, both the putative function and the underlying mechanism of this phenomenon are unknown. Largely unresolved is also the question of why higher eukaryotic separase cleaves itself upon liberation from its inhibitors (Waizenegger *et al*, 2000; Herzig *et al*, 2002). *In vitro* this auto-cleavage does not influence the proteolytic activity or the re-inhibition of separase by securin or Cdk1-cyclin B1 (Stemmann *et al*, 2001; Waizenegger *et al*, 2002; Zou *et al*, 2002). Finally, PP2A was identified as another binding partner of human separase (Holland *et al*, 2007). The separase-PP2A complex seems to exist throughout most of the cell cycle and dissociates only transiently upon auto-cleavage of separase in anaphase until re-synthesis of full-length protease in the next G1 phase. Despite these initial characterizations, the *in vivo* relevance of the separase-PP2A complex formation remains again largely enigmatic. PP2A is a heterotrimeric serine/threonine phosphatase consisting of a scaffolding A subunit, a catalytic C subunit, and a variable regulatory B subunit that mediates subcellular targeting and substrate specificity (Janssens *et al*, 2005). Of the four subfamilies of B subunits that exist (B, B', B'', and B'''), it is B' (also called PR56) in all its isoforms which is found in association with separase (Holland *et al*, 2007).

Here, we show that PP2A restricts separase activity. It does so by dephosphorylation of separase-bound securin, thereby stabilizing it relative to the free, phosphorylated pool of securin. This function of PP2A not only prevents precocious activation of separase in cells that are arrested in G2- or prometaphase. It also ensures that virtually all excess securin is degraded before the separase-associated pool is targeted. In this way, PP2A prevents repeated activation and re-inhibition of separase and increases the overall abruptness and fidelity of anaphase.

## Results

### Separase-bound securin is a substrate for separase-associated PP2A

The B' (PR56) regulatory subunit containing isoform of protein phosphatase 2A (PP2A) was previously identified as an interaction partner of human separase (Holland *et al*, 2007). It was also reported that the B (PR55) isoform of PP2A can directly interact with human securin (Gil-Bernabe *et al*, 2006). Therefore, it remained to be clarified whether PP2A interacts directly with separase, securin, or both, and which isoform of the phosphatase would do so. First, a separase antibody was used for immunoprecipitation (IP) of all separase-securin complexes from a lysate of mitotically arrested HeLa cells. Then, a securin antibody was used in a second step to isolate free securin from the separase-depleted supernatant. Western blot analysis of the immunoprecipitated material revealed that the constitutive PP2A subunits A and C specifically co-purified with separase-securin complexes, but not with free securin (Fig 1A). Similar IP-Western experiments from cells expressing Myc-separase and Flag-tagged versions of either PP2A-B or PP2A-B' furthermore demonstrated that it is only the B' (PR56) containing isoform of PP2A which interacts with separase (Fig 1B).

Within the complex of separase, securin, and PP2A, the phosphatase is catalytically active (Holland *et al*, 2007). This begs the question whether securin might be a direct target of separase-bound PP2A. To address this issue, we capitalized on a separase variant with a small internal deletion ( $\Delta$ ) that largely abrogates PP2A binding without affecting proteolytic activity *in vitro* nor association with securin or Cdk1-cyclin B1 (Holland *et al*, 2007). We used SILAC (stable isotope labeling with amino acids in cell culture) followed by mass spectrometry to quantitatively assess the phosphorylation status of securin associated with either wild-type (WT) or PP2A-binding deficient ( $\Delta$ ) separase affinity-purified from prometaphase-arrested HEK293T cells (Ong & Mann, 2007). This analysis revealed that Ser-31, Thr-66, Ser-87, and Ser-89 of human securin were 2.3- to 4.3-fold hyperphosphorylated when binding of PP2A to separase was compromised (Fig 1C). (Somewhat unexpected, these changes did not coincide with upregulation of separase phosphorylations critical for binding of Cdk1-cyclin B1.) The observed differences in securin phosphorylation likely represent underestimations because the small deletion within separase- $\Delta$  greatly compromises, but does not fully abrogate its ability to recruit PP2A (Holland *et al*, 2007). Thus, securin is a substrate of separase-associated PP2A. Together with the inability of PP2A to bind securin directly (Fig 1A), these findings further suggested that—relative to separase-bound securin—free securin should be in a hyperphosphorylated state.

To test this prediction and whether we had mapped major phosphorylation sites, we used site-specific recombination to generate stable HeLa lines that inducibly expressed either WT securin or a variant that had the Ser/Thr residues at positions 31, 66, 87, and 89 replaced by alanines (securin-4A). Both alleles were expressed to the same and near physiological level upon doxycycline (Dox) addition (Supplementary Fig S1A). C-terminal Flag-tags reduced the motility of the transgene-encoded securins in SDS-

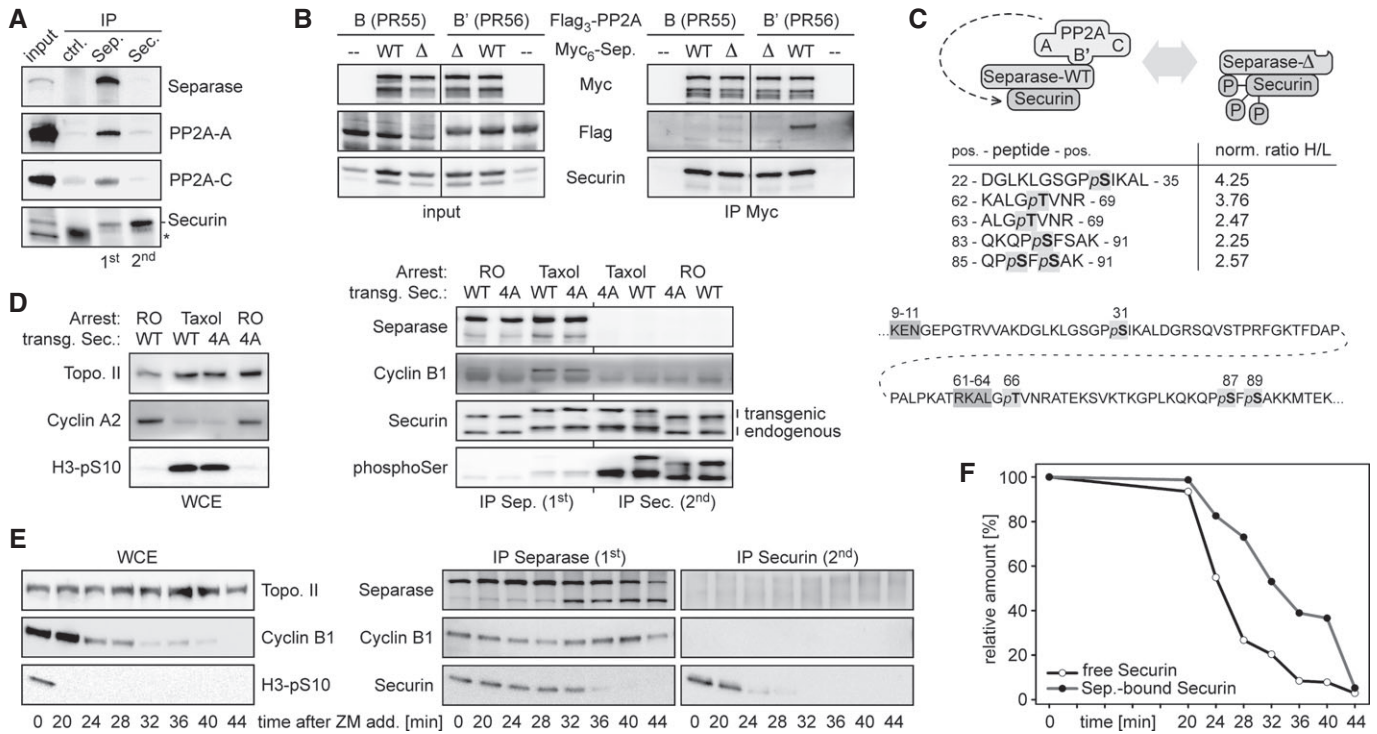


**Figure 1. The indirect association of separase-bound securin with PP2A-B'56 correlates with its hypophosphorylation and increased stability over free securin.**

**A** PP2A associates with separase-securin complex, but not with free securin. Separase antibody was used to immunoprecipitate separase-securin from lysates (input) of mitotic HeLa cells overexpressing separase, securin, PP2A-A, and PP2A-C. Unspecific IgG served as control (ctrl.). Subsequently, free securin was isolated from the separase-depleted lysate using anti-securin. IPs were analyzed by immunoblotting as indicated. \*light chain of unspecific IgG.

**B** The B' - and not the B-isoform of PP2A interacts with separase-securin. Lysates (input) of mitotic HEK293T cells overexpressing Myc-tagged variants of wild-type (WT) separase or a PP2A-binding deficient deletion mutant ( $\Delta$ ) and Flag-tagged versions of either PP2A-B55 ( $\alpha$  isoform) or PP2A-B'56 ( $\delta$  isoform) were subjected to anti-Myc IP and immunoblotting.

**C** Rationale and summary of the SILAC-MS experiment to quantitatively compare the phosphorylation of securin bound to separase-WT or separase- $\Delta$ . The table shows the five phospho-peptides with the largest difference in phosphorylation state. The ratios of heavy (H; separase- $\Delta$ ) and light (L; separase-WT) phospho-peptides were normalized (norm.) to those of unrelated, unphosphorylated peptide pairs. Shown below is the positioning of the mapped phosphorylation sites (bold letters, light gray shading) relative to the APC/C recognition sites (dark gray shading) within securin (amino acid positions given on top).

**D** Separase-less securin is hyper-phosphorylated. Transgenic HeLa cells were induced to express C-terminally Flag-tagged securin-WT or securin-4A and synchronized in prometaphase or late G2-phase by taxol or RO3306 (RO). Whole cell extracts (WCE) and sequential IPs of separase and securin were analyzed by immunoblotting as indicated (H3-pS10 = Ser-10 phosphorylated histone H3).

**E** Accelerated degradation of free over separase-bound securin. Pre-synchronized HeLa cells were released from a taxol arrest by addition of ZM447439 (ZM) and CHX at  $t = 0$  min and harvested in aliquots at the indicated time points. Whole cell extracts and sequential IPs of separase and securin were analyzed by immunoblotting as indicated.

**F** Securin immunoblot signals were quantified relative to the band at  $t = 0$  min. Shown are mean values of three independent experiments.

PAGE, thereby allowing the faster migrating endogenous securin to serve as an internal reference. Cultures of the two lines were pre-synchronized in G2 by the Cdk1 inhibitor RO3306 (RO) or in prometaphase by taxol and used for the consecutive IPs of first separase-bound and then free securin. Comparative Western analysis using an antibody specific for phosphorylated serine revealed (i) that free securin indeed exhibits a pronounced hyperphosphorylation relative to separase-associated securin in both G2- and prometaphase and (ii) that serine phosphorylation in securin-4A is greatly diminished in G2 and virtually undetectable in prometaphase (Fig 1D). These results are consistent with the SILAC-MS analysis and confirm Ser-31, Ser-87, and/or Ser-89 as major phosphorylation sites of securin that are effectively dephosphorylated by separase-associated PP2A.

**Free securin is degraded more rapidly than separase-bound securin**

It has recently been reported that HeLa cells that are released from a prometaphase arrest exhibit delayed degradation kinetics of separase-associated relative to total securin (Shindo *et al*, 2012). Given that in prometaphase-arrested HeLa cells, free securin is 4- to 5-fold more abundant than separase-associated securin (Fig 1A), the accelerated disappearance of total securin might largely be attributed to preferential proteolysis of free over separase-bound securin. To test this prediction, taxol-arrested HeLa cells were treated with cycloheximide (CHX) to prevent re-synthesis of securin and with the aurora B kinase inhibitor ZM447439 (ZM) to synchronously drive them through an anaphase- into a G1-like state (Shindo *et al*, 2012).

Confirming the success of the release, cyclin B1 and Ser10-phosphorylation of histone H3 both disappeared, and separase cleaved itself (Fig 1E). As before, aliquots taken at different time points were used to purify separase-securin complexes and free securin by two consecutive rounds of IP. Quantitative immunoblotting confirmed the predicted faster degradation kinetics of free over separase-associated securin (Fig 1E and F). As a result, about 75% of separase-bound securin still persists when 75% of free securin has already been cleared from the cell. An earlier disappearance of free relative to separase-bound securin is also observed in the absence of CHX albeit with slowed overall kinetics (unpublished observation).

Interestingly, free securin is less stable than separase-associated securin even in checkpoint-arrested cells. Upon CHX addition to nocodazole-treated HeLa cells, free securin started to decline after 2 h and was undetectable after 8 h (Supplementary Fig S2A). In contrast, separase-bound securin remained largely stable over 8 h in these SAC-arrested prometaphase cells and began to slowly disappear only after 10 h, probably as a consequence of apoptosis as judged by the increase in number of cells with sub-G1 DNA content. We also assessed the stability of the two securin pools during a DNA-damage checkpoint-mediated arrest in G2 phase. To this end, HeLa cells were arrested in early S-phase with thymidine, released for 6 h, and then treated with doxorubicin (DRB), which causes DNA double-strand breaks due to poisoning of topoisomerase II. The success of these synchronization procedures was confirmed by flow cytometry and immunoblotting (Supplementary Fig S3). Subsequent CHX shutoff experiments revealed that free securin was short-lived also during a G2 arrest, with a half-life of about 1 h, while separase-bound securin was stable for at least 5 h (Supplementary Fig S2B). Thus, irrespective of the very different degradation kinetics at different cell cycle phases, free securin is always less stable than separase-associated securin.

#### PP2A stabilizes separase-bound securin by dephosphorylation

Is the difference in stability between free and separase-bound securin due to a different phosphorylation status of both pools? If phosphorylation turns securin into a better substrate for the ubiquitin-proteasome system (UPS), then preventing its phosphorylation by mutation should stabilize free securin. *Vice versa*, mimicking constitutive phosphorylation with a negatively charged amino acid might destabilize separase-bound securin, which is normally held in a dephosphorylated state by action of associated PP2A. To test these predictions, we generated also a HeLa line that inducibly expressed a (C-terminally Flag-tagged) securin variant with aspartates at positions 31, 66, 87, and 89 (securin-4D) but was otherwise isogenic with the aforementioned securin-WT and securin-4A lines (Supplementary Fig S1B). When prometaphase cells were released with ZM into CHX-containing medium, strikingly, the free pool of securin-4A exhibited greatly retarded degradation kinetics (Fig 2A). Importantly, the behavior of securin-4D was the exact opposite. This phosphorylation-mimicking variant disappeared with WT kinetics in its free form but was greatly destabilized relative to endogenous securin in its separase-associated form (Fig 2B). Of note, separase-associated securin-4A was detectable even longer than free securin-4A or separase-associated endogenous securin (Fig 2A and Supplementary Fig S7B). This could be due to

additional phosphorylation sites, which escaped our mapping analysis, but the fact that securin-4D is degraded with nearly the same kinetics in its separase-associated and free forms (Fig 2B) argues against this possibility. Instead, we attribute this phenomenon to the association of lingering free securin-4A with separase that has already been stripped of endogenous securin (see Discussion). None of the above effects was caused by the tagging *per se* because transgene-encoded tagged securin-WT was degraded with kinetics identical to the endogenous protein (Fig 2A and B).

A securin variant which lacks its first 100 amino acids retains normal ability to bind and inhibit separase but can no longer be degraded. Given that the N-terminal half of securin contains not only the KEN- and D-box but also the identified PP2A substrate sites (Fig 1C), it is conceivable that phosphorylation of the corresponding residues could impact securin's clearance via the UPS. At this point, it could not be excluded, however, that the changed degradation properties of securin-4A and securin-4D were caused not by blocked or mimicked phosphorylation but rather by the mutations *per se*. To rule out this possibility, we capitalized on separase- $\Delta$  with impaired PP2A binding ability. Securin in association with this separase variant should be phosphorylated and exhibit a reduced half-life if phosphorylation does indeed turn the anaphase inhibitor into a better UPS substrate. Transgenic HeLa cells were induced to express Myc-tagged separase-WT or separase- $\Delta$ , synchronized in prometaphase with taxol, and then released by ZM into medium containing CHX and trace amounts of okadaic acid (OAA) to inhibit residual PP2A still associated with separase- $\Delta$ . Time-resolved anti-Myc IPs followed by quantitative immunoblotting revealed that endogenous securin in complex with transgenic separase-WT and separase- $\Delta$  had mean half-lives of 38 and 29 min, respectively (Fig 2C). This result is fully consistent with the behavior of the phosphorylation site mutant securins and validates the 4A and 4D variants as probes to study the effects of no or constitutive securin phosphorylation, respectively. In summary, the above experiments demonstrate that securin is destabilized by phosphorylation and stabilized by separase-based PP2A-dependent dephosphorylation.

#### Phosphorylation of securin enhances its APC/C-dependent polyubiquitylation

What are the kinases that destabilize securin by phosphorylation? According to a scansite prediction (Obenauer *et al*, 2003), one candidate is Ca<sup>2+</sup>/calmodulin-dependent kinase II (CaMKII) which might target Ser-87 of human securin because this site ranks among the top 0.071% of putative CaMKII motifs across all vertebrate proteins (percentile 0.071). Indeed, recombinant CaMKII readily phosphorylated bacterially expressed, affinity-purified human securin-WT (Fig 3A). The CaMKII-dependent labeling of securin-4A was 3.7-fold less efficient consistent with Ser-87 representing a chief phosphorylation site for this kinase. Next we asked whether chemical inhibition of CaMKII with KN-93 would impact the degradation kinetics of securin *in vivo*. To this end, securin-WT-expressing, taxol-arrested HeLa cells were treated with either KN-93 or its carrier solvent DMSO (control) for 4 h and then released into anaphase with ZM. Time-resolved immunoblotting demonstrated that the CaMKII inhibitor extended the half-life of free securin by about 15 min while leaving the overall exit from mitosis unaffected (Fig 3B). KN-93 treatment had also no overt effect on the proteolysis

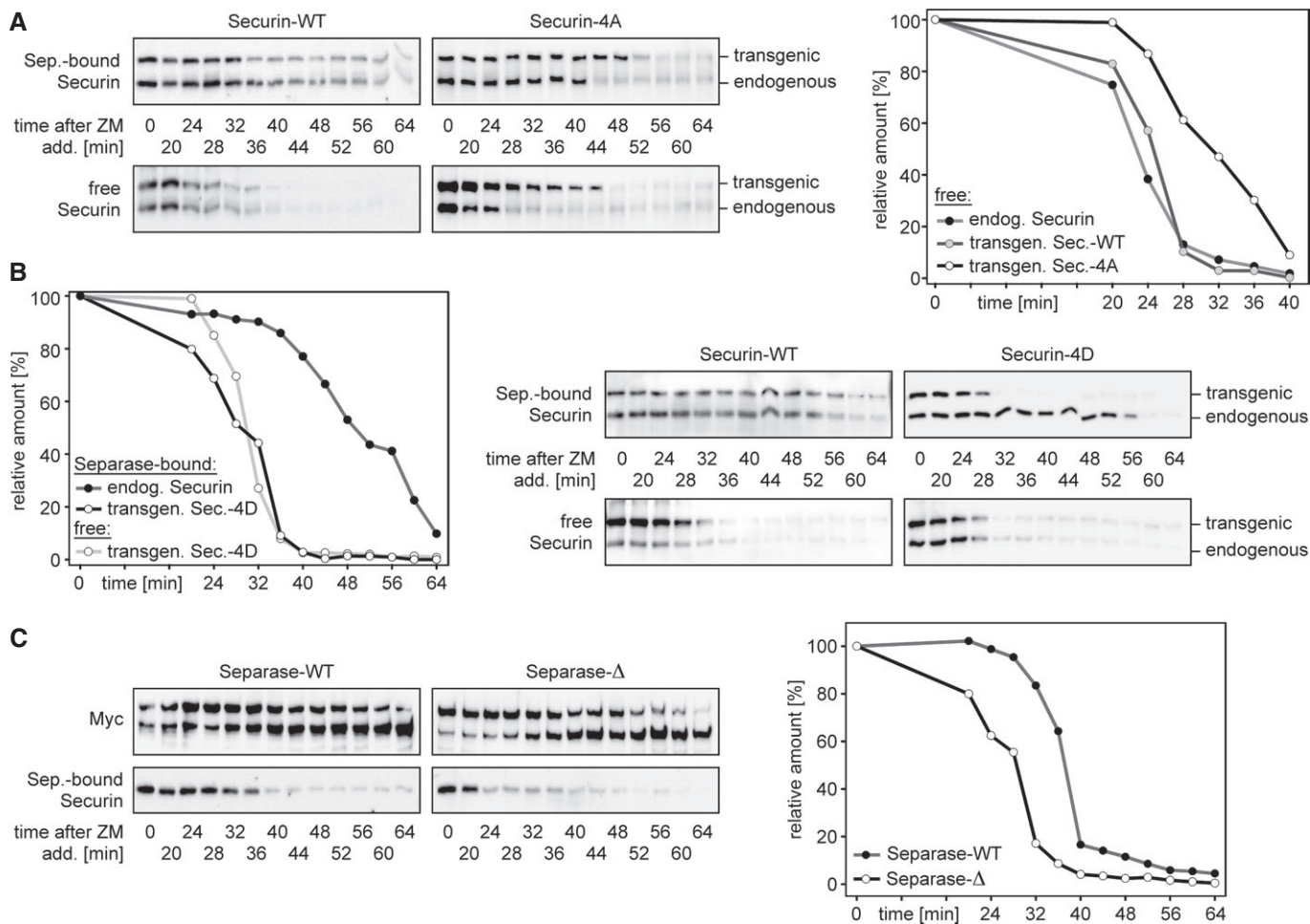


**Figure 2. Securin is destabilized by phosphorylation and stabilized by PP2A-dependent dephosphorylation on separate.**

- A** Preventing its phosphorylation stabilizes free securin. Transgenic HeLa cells induced to express C-terminally Flag-tagged securin-WT or securin-4A were treated as described in Fig 1E and subjected to sequential IPs that separated separate-bound securin (top panels) from free securin (bottom panels). The graph represents the mean degradation kinetics of endogenous and transgenic free securin. Western signals of three independent experiments were quantified by densitometry and blotted as percent of the value at ZM addition ( $t = 0$ ).
- B** Mimicking its phosphorylation destabilizes separate-associated securin. Transgenic HeLa cells induced to express C-terminally Flag-tagged securin-WT or securin-4D were treated and analyzed as described in (A).
- C** Preventing PP2A binding to separate accelerates the degradation of associated securin. Mitotic HeLa cells induced to overexpress Myc-tagged separate-WT or separate- $\Delta$  were incubated with trace amounts of okadaic acid shortly before ZM addition to inactivate residual PP2A on separate- $\Delta$  but leave gross PP2A activity unaffected. Transgenic separates were immunoprecipitated with anti-Myc, and associated endogenous securin was quantified as described in (A).

of separate-bound securin, probably because this pool is constantly being dephosphorylated by PP2A.

Securin is a well-established substrate of APC/C. Its KEN- and D-box are recognized by Cdc20 and Cdh1, APC/C's co-activators in mitosis and interphase, respectively. However, the pronounced phosphorylation dependence of securin degradation is reminiscent of proteolysis mediated by SCF-complexes, another class of multi-subunit ubiquitin ligases. In fact, the same study that reported the existence of a direct interaction between PP2A and securin also claimed that phosphorylated securin was degraded in an SCF-dependent manner (Gil-Bernabe *et al*, 2006). To clarify this issue, we asked whether mutational inactivation of the KEN- and D-box or depletion of Cdc20 by RNAi would affect the rapid degradation of free, phosphorylated securin in late mitosis. When securin with

mutated KEN- and D-boxes (mKEN/mDB) was inducibly expressed in corresponding transgenic HeLa cells, this variant appeared to be fully stable during a ZM-mediated SAC override, that is, at a time when endogenous securin and transgenic securin-WT were rapidly degraded (Fig 3C). Upon its addition to HeLa cells or *Xenopus* egg extracts, the PP2A inhibitor okadaic acid (OAA) induces a pseudo-anaphase state with active APC/C<sup>Cdc20</sup>. While WT securin was rapidly degraded under these conditions, the mKEN/mDB variant was again not proteolysed but merely hyperphosphorylated leading to reduced and less uniform electrophoretic mobility that could be reversed by  $\lambda$ -PPase treatment (Fig S4). Furthermore, upon ZM addition to Cdc20-depleted, taxol-treated cells, separate-free securin did not decline over at least 45 min (Fig 3D). In contrast, mock-depleted control cells fully degraded this securin population within

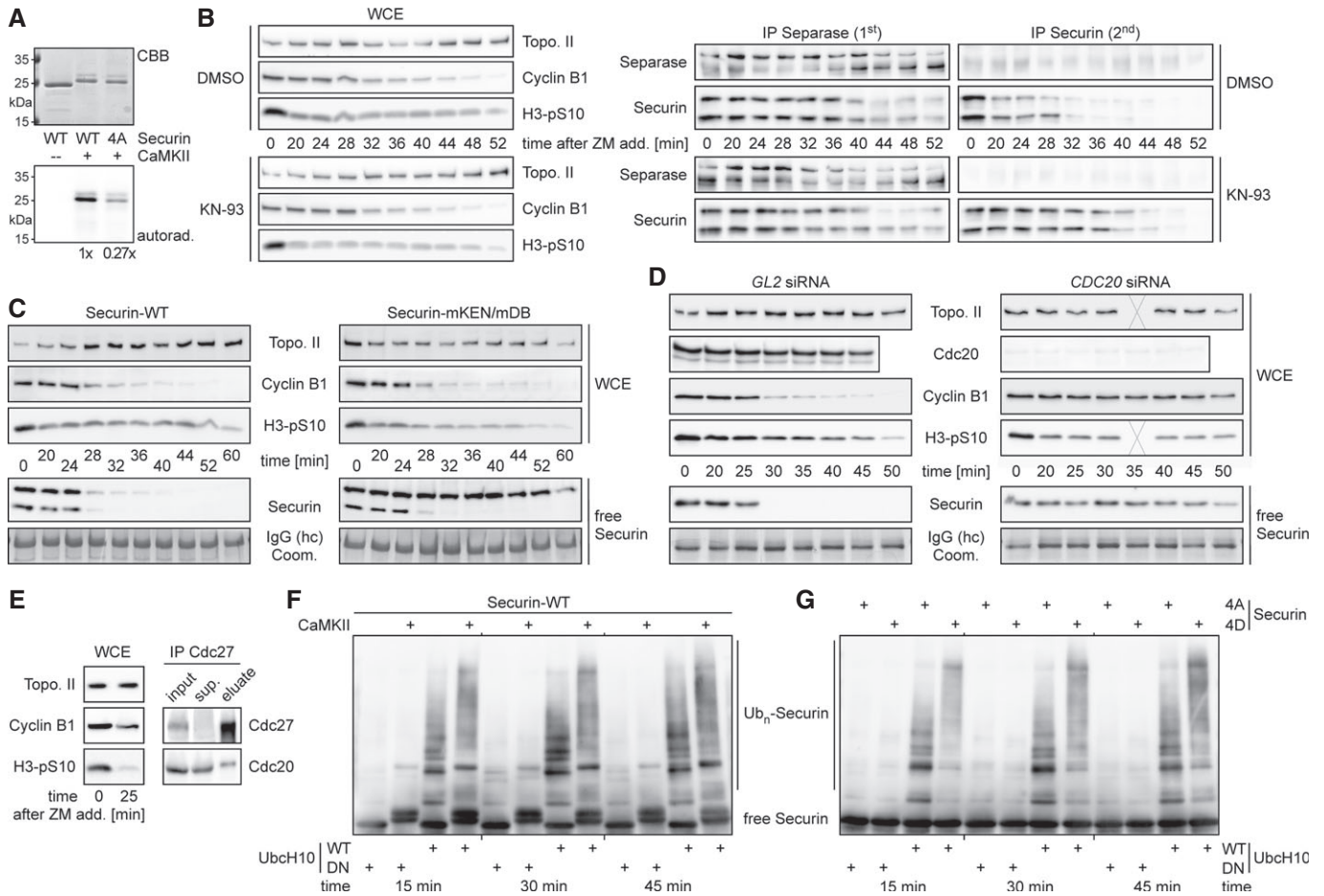


**Figure 3. Rapid degradation of free securin depends on CaMKII and APC/C.**

**A** CaMKII phosphorylates securin at PP2A substrate site(s). Recombinant securin-WT or securin-4A was incubated with active (+) or heat-inactivated (–) CaMKII in presence of  $\gamma$ -<sup>33</sup>P-ATP and then analyzed by SDS-PAGE, auto-radiography, and Coomassie staining (CBB).

**B** Inhibition of CaMKII decelerates the degradation of free securin *in vivo*. Transgenic HeLa cells were induced to express Flag-tagged securin-WT, arrested with taxol and then treated with the CaMKII inhibitor KN-93 or DMSO 4 h prior to addition of ZM and CHX ( $t = 0$  min). Aliquots harvested at the indicated time points were analyzed as described in Fig 1E.

**C** Free securin is stabilized by mutation of its KEN- and D-box. Transgenic HeLa cell lines were induced to express Flag-tagged securin-WT or securin-mKEN/mDB, released from a taxol arrest by ZM (and CHX) at  $t = 0$  min, harvested in aliquots at the indicated times and analyzed as in (B). Coomassie-stained IgG-heavy chain (hc) served as a loading control for the securin IP.

**D** Free securin is stabilized by Cdc20 depletion. HeLa cells transfected with siRNA against *CDC20* or *GL2* were otherwise treated and analyzed as described in (B). Note that the *Cdc20* panels are directly comparable as the corresponding samples were run on one gel and blotted onto the same membrane. Crosses indicate lost samples.

**E** Affinity purification of APC/C<sup>Cdc20</sup>. APC/C<sup>Cdc20</sup> was immunoprecipitated from taxol-ZM-treated HeLa cells with an antibody directed against the C-terminus of Cdc27 and competitively eluted with the antigenic peptide. Sup. = supernatant.

**F** Phosphorylation of securin with CaMKII enhances its APC/C<sup>Cdc20</sup>-dependent polyubiquitylation. Bacterially expressed, purified human securin was pre-phosphorylated with CaMKII where indicated and then incubated for the indicated times in an ubiquitylation assay containing wild-type (WT) or dominant-negative (DN) UbcH10 and APC/C<sup>Cdc20</sup> [from (E)]. Reactions were analyzed by SDS-PAGE and anti-securin Western. Ub<sub>n</sub> = ubiquitin chains.

**G** Increased processivity of multi-ubiquitylation of securin-4D versus securin-4A. An APC/C<sup>Cdc20</sup>-dependent ubiquitylation assay was performed and analyzed as described in (F).

30 min. Securin-mKEN/mDB-expressing or Cdc20-less, taxol-arrested cultures were also supplemented with CHX alone, that is, without simultaneous addition of ZM. These experiments revealed that even the slow degradation of free securin during a prolonged prometaphase arrest required an intact KEN- and D-box as well as the presence of Cdc20 (Supplementary Fig S5A). Finally, we tested the requirements of securin proteolysis in DNA-damage checkpoint-arrested G2 cells. Consistent with APC/C<sup>Cdh1</sup> being the predominant

form of active APC/C at this stage (Bassermann *et al*, 2008), securin degradation was hardly affected by depletion of Cdc20 (unpublished observation). However, securin was again strongly stabilized in DRB-treated cells by mutational inactivation of its KEN- and D-box (Supplementary Fig S5B). Taken together, these experiments demonstrate that, irrespective of kinetic differences, the degradation of securin in G2-, prometa-, and anaphase is largely, if not entirely, dependent on APC/C.

To clarify whether the APC/C-catalyzed ubiquitylation reaction itself or a different step of the degradation pathway is positively influenced by securin phosphorylation, we immuno-affinity-purified the APC/C subunit Cdc27 (Apc3) from HeLa cells that were released from a taxol arrest by treatment with ZM for 25 min (Fig 3E). Combining the resulting APC/C<sup>Cdc20</sup> preparation with ATP, ubiquitin, E1 (Ube1), and UbcH10 (Ube2C) led to ubiquitylation of bacterially expressed, purified securin (Fig 3F). This reaction was specific as it was blocked by replacement of WT UbcH10 with a dominant-negative (DN) variant of this E2. Importantly, ubiquitin chain formation was enhanced if securin was pre-treated with CaMKII and ATP (Fig 3F). Similarly, phosphorylation-mimicking securin-4D was subject to much more pronounced multi-ubiquitylation than phosphorylation site mutant securin-4A under otherwise identical conditions (Fig 3G). Together, these reconstitution assays demonstrate that N-terminal phosphorylations indeed render human securin a better APC/C substrate, a notion that is fully consistent with the observed *in vivo*-degradation kinetics.

### Phosphorylation site mutant securin compromises timing and fidelity of anaphase

Why are separase-bound and free, excessive securin degraded with such different kinetics? And does interference with this phosphorylation-dependent difference have any physiological consequences? To address these questions, we first asked whether expression of securin-4A resulted in any effect on the timing and fidelity of mitosis. Transgenic cells were transiently transfected to label their chromosomes with histone 2B-eGFP and then filmed by video fluorescence microscopy in the presence or absence of Dox (Fig 4A). Subsequent quantification showed that induced expression of securin-4A (but not of securin-WT) caused an averaged lengthening of early anaphase from 3.4 to 9.2 min, while all other phases of mitosis were normal in timing. This specific effect was accompanied by the frequent occurrence of anaphase bridges. Immunofluorescence microscopy (IF) of fixed cells confirmed that individual chromosome arms and/or Hec1-stained kinetochores lagged behind in more than 50% of securin-4A-expressing anaphase cells, while these defects were rarely observed (<13%) in the corresponding controls (Fig 4B). Chromosome segregation defects are associated with an increase in DNA double-strand breaks (DSBs) which is due to lagging chromosomes being frequently damaged through cytokinesis and/or the formation of micronuclei (Janssen *et al*, 2011; Crasta *et al*, 2012). To clarify whether DSBs would also occur as an indirect consequence of blocked securin phosphorylation, transgenic securin-WT or securin-4A were expressed for 3 days or left uninduced before the corresponding cells were analyzed by immunoblotting and IF for DSB-specific phosphorylations of histone variant H2AX on Ser-139 ( $\gamma$ H2AX) and checkpoint kinase 2 on Thr-68 (pChk2). Indeed, long-term expression of securin-4A caused a strong up-regulation of these DSB-markers (Fig 4C). More specifically,  $\gamma$ H2AX- and pChk2-positive nuclear foci were detected in 45% of securin-4A-expressing cells but only in about 10% of uninduced cells or those that expressed transgenic securin-WT. Thus, preventing securin phosphorylation at four key sites results in impaired chromosome segregation followed by DNA damage.

The above phenotypes could be explained by slowed or delayed activation of separase in presence of securin-4A. To test this

directly, we adapted a recently published separase activity sensor (Shindo *et al*, 2012), which consists of a separase-cleavable Scc1 fragment fused N-terminally to histone 2B-mCherry and C-terminally to eGFP (Fig 5A). The chromosomes of sensor-expressing cells fluoresce red and green (yellow in merge) early in mitosis but lose their green fluorescence when separase becomes active (Fig 5B). We used transient transfection to express this sensor in our stable transgenic securin lines, arrested the cells in prometaphase with taxol, and then released them with ZM. Interestingly, the cleavage of the reporter was clearly delayed and less complete in securin-4A relative to securin-WT expressing cells as judged by time-resolved immunoblotting and live cell microscopy (Fig 5C and D). Thus, physiological amounts of a securin variant which can no longer be phosphorylated dampen the otherwise switch-like activation of separase, thereby interfering with the abruptness and accuracy of sister chromatid separation in anaphase.

### Mimicking constitutive securin phosphorylation results in premature activation of separase

Does selective destabilization of separase-associated securin by phosphorylation mimicking also have any cellular consequences? We performed video microscopy as before, which demonstrated that ectopic securin-4D expression by itself did not affect mitotic timing (Fig 6A). Endogenous securin might suppress potential phenotypes by replacing precociously proteolysed securin-4D. Therefore, we combined knockdown of endogenous securin with induction of the (siRNA resistant) transgene (Fig 6B). Consistent with separase-bound securin now being degraded as quickly as free securin (Fig 2B), the replacement of endogenous securin by securin-4D resulted in a modest shortening of metaphase relative to the WT control (Fig 6A). However, despite the slightly earlier advent of anaphase, cells segregated their chromosomes surprisingly normal (data not shown).

Each time a separase-associated securin molecule is degraded, the corresponding separase molecule will briefly become active before being re-inhibited by excessive, free securin. Given that the securin-4D variant has a higher turn-over rate on separase than WT securin, unscheduled cohesin cleavage is expected to be enhanced in cells expressing the former as compared to the latter. To test whether this might cause problems over time, we assessed how well sister chromatid cohesion was maintained in a prometaphase arrest. Replacement of endogenous securin by securin-4D indeed caused partial or complete loss of cohesion in 14% of the cells after 3 h in taxol and in 30% after 9 h (Fig 6C). At these time points, control cells, in which endogenous securin was either replaced by transgenic securin-WT or left undepleted, displayed on average merely 4 and 8% premature sister chromatid separation, respectively. While precocious loss of cohesion was further enhanced by simultaneous CHX treatment, importantly, it did not essentially require inhibition of translation and even occurred without visible decline of securin-4D (Fig 6C and D). Thus, the PP2A-dependent stabilization of the separase-securin complex is crucial to prevent transient activation of the cohesin-cleaving protease in SAC-arrested cells.

Finally, we asked whether replacing endogenous securin by securin-4D might also cause problems in cells that are arrested in G2 phase. Because separase is excluded from the nucleus (Sun *et al*, 2006), cleavage of chromosomal cohesin cannot serve as an

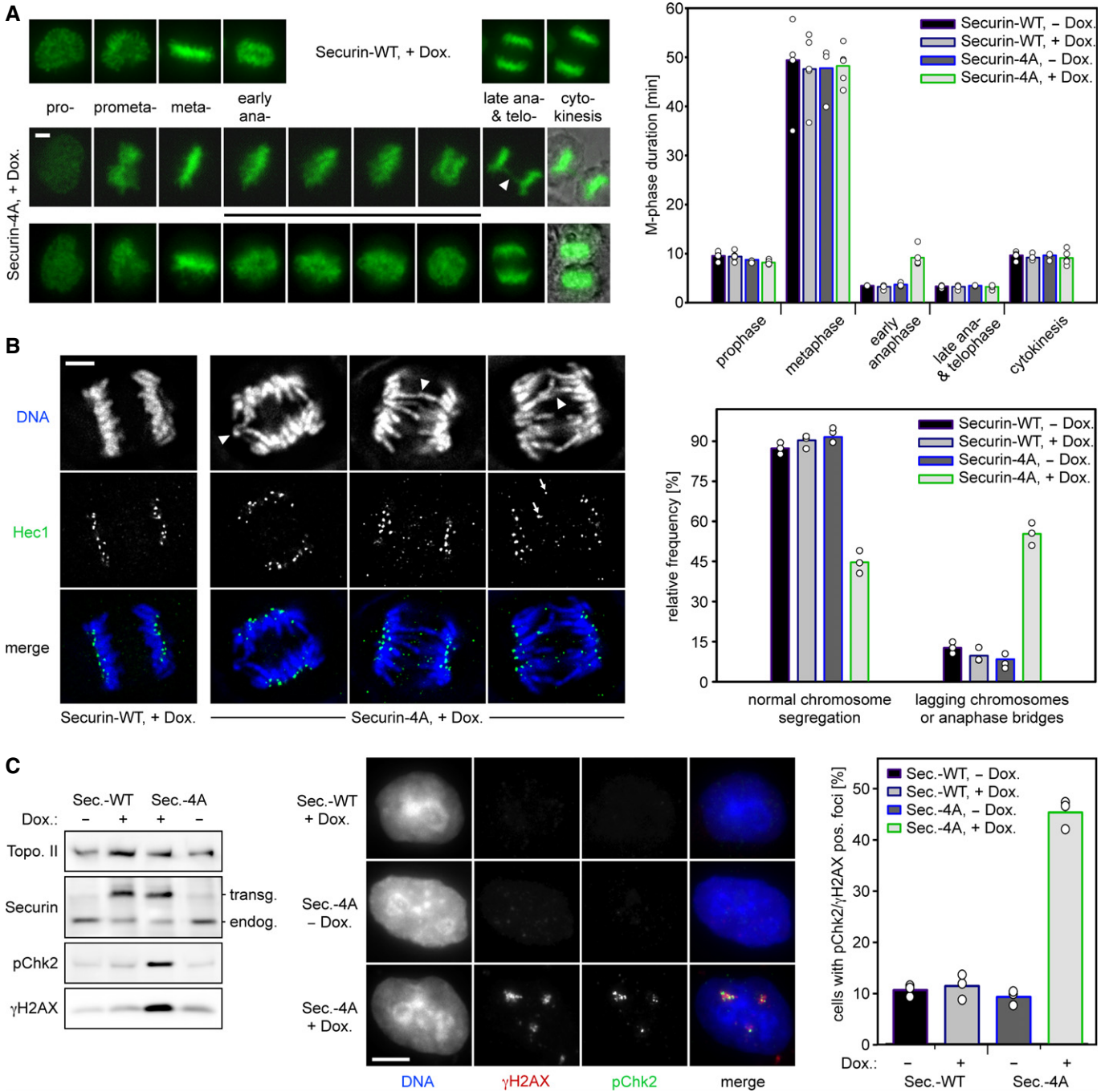


**Figure 4. Phosphorylation site mutant securin compromises proper anaphase and elicits DNA damage.**

**A** Expression of securin-4A (but not of securin-WT) prolongs the process of sister chromatid separation. Transgenic HeLa cells transiently transfected to express histone H2B-eGFP were released from a double-thymidine arrest and induced (+Dox) to express securin-WT or securin-4A or left uninduced. Live cell imaging was started 10 h later and conducted at 180-s intervals over a period of 12 h. Early anaphase was defined as the time between the first broadening of the metaphase plate until the first discernable separation of chromosomes into two masses. Arrowhead labels an anaphase bridge. Lower two panels on right represent merges of green fluorescence and DIC images. The graph shows mean values (bars) of four independent experiments (dots) quantifying at least 100 cells per line and state of induction. Scale bar, 5  $\mu$ m.

**B** Expression of securin-4A (but not of securin-WT) results in anaphase bridges. Cells were released from thymidine for 13 h, fixed, and stained for Hec1 and DNA. Impaired chromosome segregation was identified by lagging DNA (arrowheads) and/or lagging Hec1 signals (arrows) in anaphase cells. The graph shows mean values (bars) out of three independent experiments (dots). Between 250 and 600 cells were analyzed per line and state of induction. Scale bar, 5  $\mu$ m.

**C** Long-term expression of securin-4A (but not of securin-WT) results in DNA-damage. Asynchronous HeLa cells induced to express securin-WT or securin-4A for 3 days were analyzed by immunoblotting and IF as indicated. Foci positive for  $\gamma$ H2AX and phospho-Thr68 Chk2 (pChk2) were counted. Represented are mean values (bars) out of three independent experiments (dots) quantifying at least 200 cells per line and state of induction. Scale bar, 5  $\mu$ m.

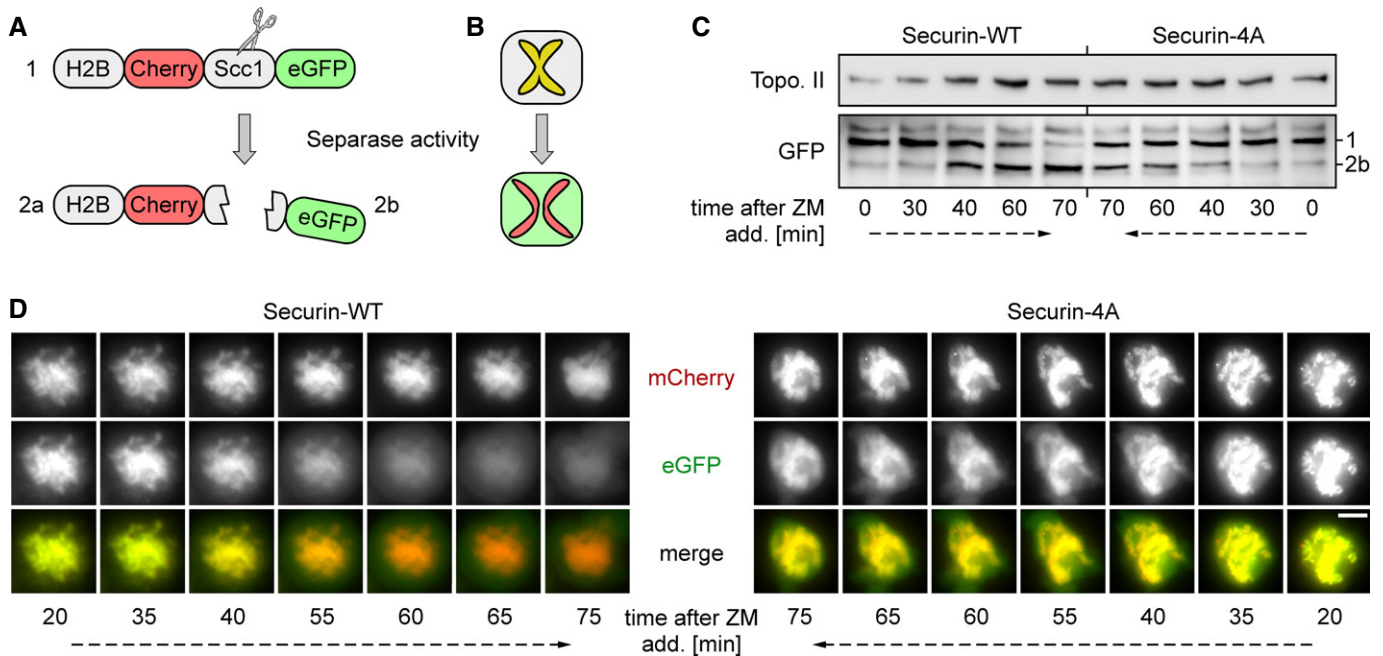


**Figure 5. Phosphorylation site mutant securin impairs timely activation of separase.**

A, B Structure (A) and cell-based read-out (B) of the separase activity sensor as adopted from (Shindo *et al*, 2012). The appearance of the eGFP containing cleavage fragment (2b) in an immunoblot (see (C)) is indicative of separase activity.  
C, D Delayed separase activation in presence of phosphorylation site mutant securin. HeLa cells transiently expressing histone H2B-mCherry-Scc1<sup>107-268</sup>-eGFP were thymidine arrested, released into transgene inducing medium, and re-arrested by taxol. Upon addition of ZM, separase activity was followed by time-resolved immunoblotting analysis of whole cell extracts (C) and live cell fluorescence microscopy (D). Scale bar, 5  $\mu$ m.

indicator of separase activity in these interphasic cells. However, separase not only triggers sister chromatid separation in anaphase but also centriole disengagement in late mitosis/early G1 (Tsou & Stearns, 2006; Schockel *et al*, 2011). Indeed, cells arrested by DRB or RO undergo unscheduled centriole disengagement in an APC/C- and separase-dependent manner (Prosser *et al*, 2012). Synchronization by consecutive treatments with thymidine and DRB or RO were combined with transfection of siRNA against endogenous securin (or GL2 as a control) and induction of transgenic securin-WT or securin-4D (Fig 7A and D, Supplementary Fig S1B). After different times in DRB or RO, cells were harvested and centriole engagement status was quantified by immunofluorescence microscopy of isolated centrosomes stained for the markers centrin-2 (distal) and C-Nap1 (proximal). These analyses not only confirmed the recent findings by the Fry and Morrison laboratories (Prosser *et al*, 2012) but also revealed that substitution of WT securin by the 4D variant aggravates the premature centriole disengagement phenotype. Specifically, cells which expressed securin-4D but lacked the endogenous anaphase inhibitor suffered from 22% centriole disengagement after 5 h in DRB, while the corresponding WT control displayed only 10% disengagement (Fig 7B). Similarly, after 10 h in RO, cells that lacked endogenous securin exhibited 27% versus 11% centriole disengagement, respectively, if they expressed transgenic securin-4D instead of securin-WT (Fig 7C). Despite the omission of CHX in these experiments, securin-4D (but not securin-WT) visibly dropped in abundance once cells were incubated for 5 h in DRB or 14 h in RO (Fig 7A and D). However, the pronounced centriole disengagement in securin-4D-expressing cells lacking endogenous securin became

apparent earlier, that is, prior to a detectable drop of securin-4D levels, which is consistent with the observation made on prometaphase-arrested cells (Fig 6D). We conclude that elevating the turnover of separase-associated securin by mimicking its constitutive phosphorylation is associated with premature activation of separase and cellular defects during checkpoint-mediated cell cycle arrests.

## Discussion

Here, we report that separase-associated securin is longer-lived than free securin, a finding that is consistent with a recent study by Hirota and co-workers (Shindo *et al*, 2012). We expand these findings and provide evidence that differences in phosphorylation status form the basis for this difference in stability. Phosphorylation, which may in part be inflicted by CaMKII, turns free securin into a better UPS substrate. In contrast, the B'56 isoform of PP2A keeps separase-associated securin in a dephosphorylated state, thereby selectively stabilizing this protease-bound pool of the anaphase inhibitor.

Separase-bound securin exhibits a greater half-life than free securin even in G2-arrested cells, in which Cdk1-cyclin B1 activity is low. Furthermore, the four phosphorylation sites mapped herein are not followed by a proline on the +1 position and hence do not match the consensus sequence of Cdk1 substrates. Both notions suggest that securin is phosphorylated on degradation-promoting positions not by Cdk1 but rather by other kinases. CaMKII might represent

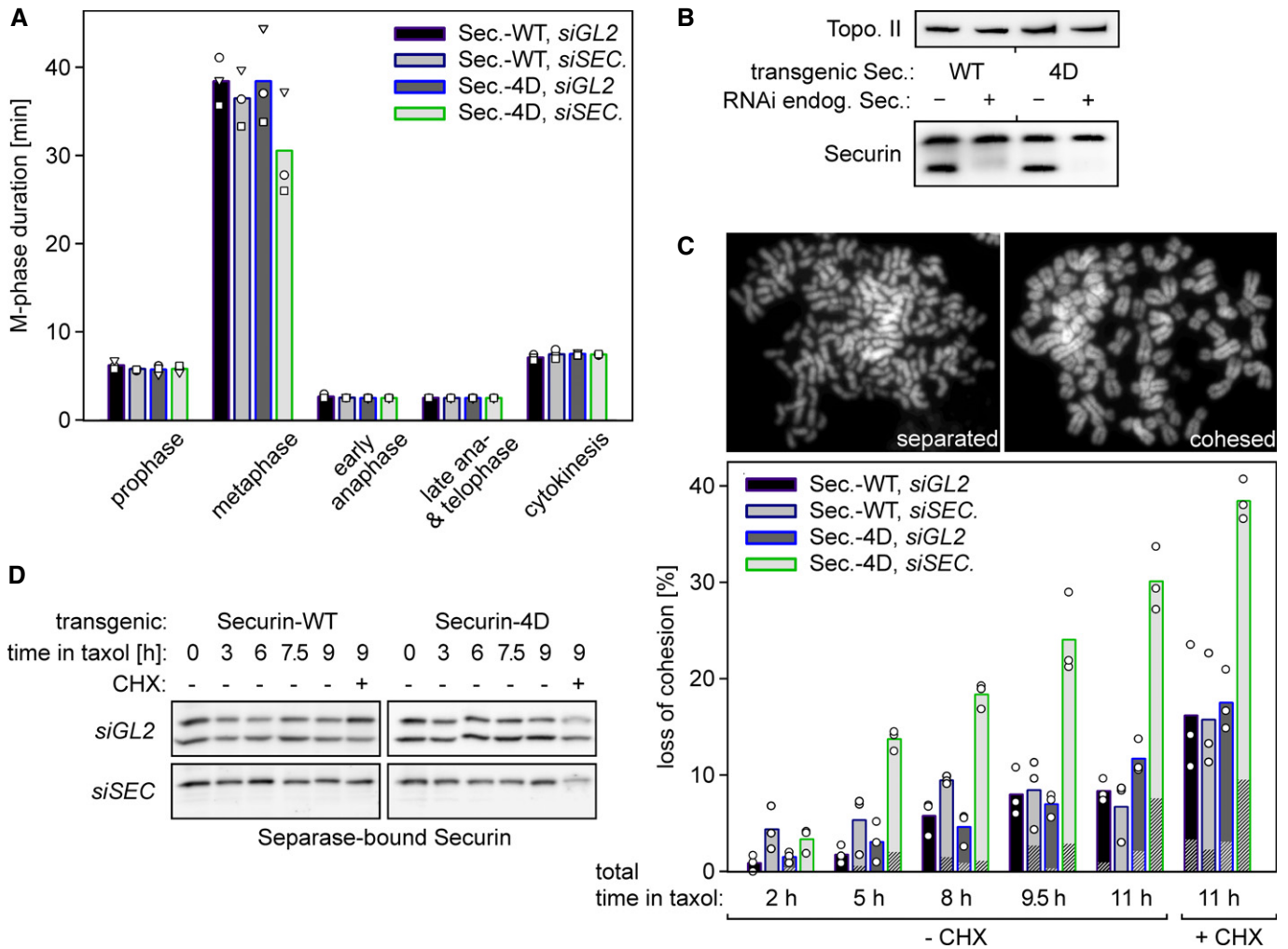


**Figure 6. Mimicking constitutive phosphorylation of securin results in premature sister chromatid separation.**

**A** Video fluorescence microscopy of histone 2B-eGFP-expressing cells reveals a slightly advanced onset of anaphase upon replacement of endogenous securin by securin-4D. Stable HeLa lines were transfected with siRNA against endogenous *SECURIN* or *GL2* 12 h prior to a thymidine block. Following release, cells were transfected to express histone H2B-eGFP and re-arrested with thymidine. Live cell imaging was started 10 h after release from the second block and induction of securin-WT or securin-4D expression. Images were taken in 180-s intervals over a period of 12 h. Shown are mean values (bars) of three independent experiments (dots, triangles, squares) quantifying at least 100 cells per line and siRNA.

**B** Efficient replacement of endogenous securin by (siRNA resistant) transgenic variants as judged by immunoblotting analysis. Cells from (A) were analyzed by immunoblotting 10 h after the second release.

**C, D** Replacing endogenous securin by securin-4D causes sister chromatid separation in prometaphase-arrested cells (C) without a detectable drop in separase-associated securin levels (D). Cells transfected with siRNA against *SECURIN* or *GL2* were released from a thymidine block and induced to express securin-WT or securin-4D expression. 10 h after release and 2 h after addition of taxol, mitotic cells were harvested by shake-off, put in fresh medium with taxol, caspase 1/3 inhibitor and, where indicated, CHX and analyzed by chromosome spreads (C) and immunoprecipitation of separate-bound securin (D) at the indicated times. Shown are mean values (bars) of three independent experiments (dots) quantifying at least 100 cells per line and siRNA. Loss of cohesion was categorized as 'full' (striation) or 'partial', respectively, depending on full separation of all or only some (but at least 3) chromosomes within a given spread.

one such kinase. *In vitro* it efficiently phosphorylates securin-WT (but not securin-4A) and enhances the APC/C<sup>Cdc20</sup>-dependent multi-ubiquitylation of this anaphase inhibitor. *In vivo* CaMKII might accelerate the destruction of free securin. Given that Ser-87, but not the other three identified phosphorylation sites match the consensus sequence of CaMKII substrates, it appears likely that additional kinases (and possibly a different set in G2 than in mitosis) contribute to the modulation of securin's overall stability. Based on a scansite analysis (Obenauer *et al*, 2003), it might be worth

testing whether protein kinase C delta can target Thr-66 of securin (percentile 0.521). Securin is poorly conserved in sequence and exhibits, for example, merely 38% identity (10% gaps) between *Homo sapiens* and *Xenopus laevis*. The divergence within the structurally disordered N-terminal half is even higher and includes most phosphorylation sites. This raises the question whether the preferential destruction of phosphorylated securin is conserved. Beginning to address this issue, we studied the degradation kinetics of human securin-4A and securin-4D in *Xenopus* egg extract and found the

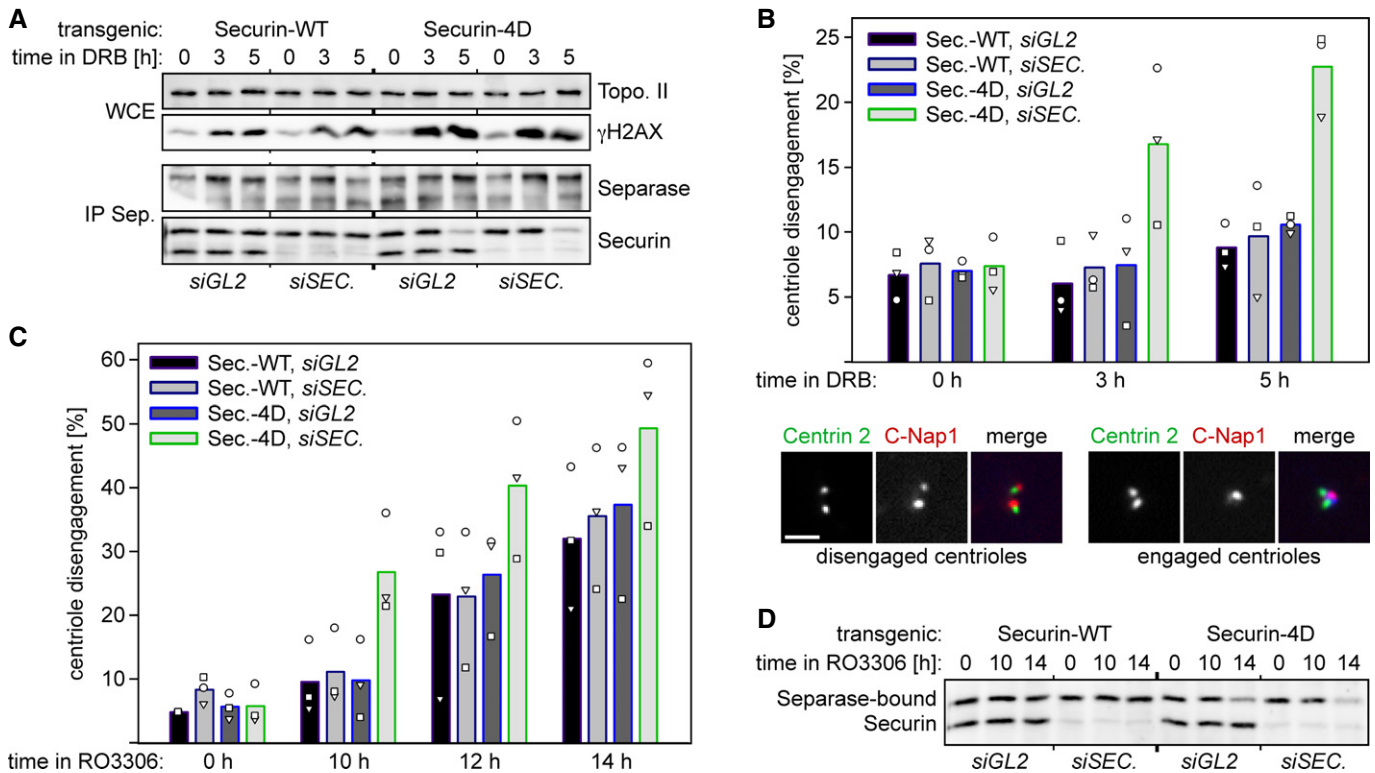


**Figure 7. Mimicking constitutive phosphorylation of securin results in premature activation of separase in G2-arrested cells.**

- A** Separase-bound securin-4D suffers from decreased stability in doxorubicin-treated cells. Transgenic HeLa cells transfected with siRNA against endogenous *SECURIN* or *GL2* and synchronized with thymidine were released and induced to express securin-WT or securin-4D. 8 h thereafter, doxorubicin (DRB) was added to induce DNA damage and G2 arrest (in the absence of CHX). At indicated times, whole cell extracts (WCE) and corresponding separase IPs were immunoblotted as indicated.
- B** Replacing endogenous securin by securin-4D causes premature centriole disengagement during a DNA-damage checkpoint-mediated G2 arrest. WCE from (A) additionally served as starting material for centrosome purification followed by co-staining of centrin-2 and C-Nap1 and IF. Depending on a centrin-2 to C-Nap1 signal ratio of 2:1 or 2:2, centrioles were classified as engaged or disengaged, respectively. In three independent experiments (dots, triangles, squares), the engagement status of at least 100 centrosomes per cell line and condition was analyzed and blotted as mean value (bars). Scale bar, 0.5  $\mu$ m.
- C** Replacing endogenous securin by securin-4D aggravates premature centriole disengagement in RO3306-treated cells. Transgenic HeLa cells were essentially treated as described in (A) except that instead of DRB RO3306 was added 4 h after removal of thymidine. Centriole engagement status was assessed as described in (B). Bars represent mean values of three independent experiments quantifying at least 100 centrosomes per cell line, siRNA and time point.
- D** Degradation of separase-bound securin-4D, but not securin-WT, in G2 arrested cells. Whole cell extracts (WCE) from (C) were subjected to separase IPs and immunoblotting.

phosphorylation-mimetic variant to be less stable—similar to the situation in human cells (Supplementary Fig S6). Thus, the ubiquitin-proteasome system of the frog interprets the additional negative charges within the N-terminal half of human securin just like its human counterpart. This observation argues that the more rapid degradation of phosphorylated versus dephosphorylated securin might indeed be conserved among vertebrates.

Preferred degradation of phosphorylated substrates is usually a hallmark of SCF-type ubiquitin ligases. In fact, it has even been reported that UV irradiation results in SCF <sup>$\beta$ TrCP</sup>-dependent degradation of securin which requires the binding of the F-box protein  $\beta$ TrCP to an unconventional recognition motif (DDAYPE) centered around position 110 of human securin (Limon-Mortes *et al.*, 2008). However, for the proteolysis of phosphorylated securin under the conditions tested herein, the APC/C remains the crucial E3. This is strongly suggested by the following lines of evidence: (i) When OAA is used to force *Xenopus* egg extracts or HeLa cells into a pseudo-anaphase state, WT securin is readily degraded. APC/C's recognition sites

within securin, the KEN- and D-box, can be inactivated by point mutations that do not affect any phosphorylation sites, the OAA-induced hyperphosphorylation of securin, or the integrity of the aforementioned DDAYPE motif. Yet, this exchange of 5 amino acids renders securin completely stable in the presence of OAA. (ii) The same securin-mKEN/mDB is also fully resistant to degradation during a ZM-induced release of pre-synchronized metaphase cells into anaphase, a taxol-induced prometaphase arrest, or a DNA-damage-induced G2 arrest. (iii) siRNA-mediated depletion of Cdc20, the essential co-activator of mitotic APC/C, greatly stabilized securin in prometa- and anaphase cells. (iv) APC/C<sup>Cdc20</sup>-dependent polyubiquitylation of securin is strongly boosted by both CaMKII-dependent phosphorylation and introduction of phosphorylation-mimetic acidic residues. Thus, while we did not address and therefore cannot exclude a minor contribution of SCF <sup>$\beta$ TrCP</sup> to securin degradation, our analyses clearly underline that the preferred proteolysis of phosphorylated securin is largely, if not entirely, dependent on APC/C. Our findings are consistent with those of Clarke and co-workers who

reported that the efficient APC/C-dependent clearance of Mcl-1 from mitotically arrested cells likewise requires prior phosphorylation of this anti-apoptotic Bcl-2 family member (Harley *et al.*, 2010).

How can the effects in the *in vitro* ubiquitylation assay be explained at the mechanistic level? Phosphorylation of securin might increase its affinity toward the APC/C, thereby increasing the processivity of ubiquitin chain formation and, thus, the kinetics of degradation (Rape *et al.*, 2006). Cdc20 and Cdh1 share a WD40 domain that folds into a structurally conserved seven-bladed  $\beta$ -propeller and specifically binds the KEN and D-Box. A recent crystal structure of *S. cerevisiae* Cdh1 in complex with a pseudo-substrate revealed that a conserved basic residue within the WD40 domain faces position +6 (P6) of the D-box (with the Arg of RxxL representing P1), which nicely explains why in APC/C substrates an acidic amino acid is most commonly found at this position (He *et al.*, 2013). Interestingly, P6 of human securin's D-box corresponds to Thr-66. Phosphorylation at this position might therefore stabilize the interaction by giving rise to a salt bridge with the juxtaposed basic residue of APC/C's co-activator. Alternatively or in addition, the enhanced processivity of chain formation might be due to phosphorylation of securin accelerating the frequently rate-limiting initiation of ubiquitylation (Williamson *et al.*, 2011). Interestingly, Ser-87 and Ser-89 lie within the so-called initiation motif of securin that is targeted by UbcH10 (Williamson *et al.*, 2011). Given that initiation efficiency can control the timing of substrate degradation, it is tempting to speculate that phosphorylation of these residues improves the strength of securin's initiation motif. Future experiments will have to clarify whether phosphorylation increases the securin-APC/C affinity or the rate of ubiquitylation initiation or both, and they will have to dissect the relative contributions of the individual phosphorylations at the four different positions within securin's N-terminal half.

As illustrated by the effects of securin-4A expression, abolishing the preferential degradation of free securin dampens the otherwise fitful anaphase and results in aggravated lagging of chromosomes followed by DNA damage. How can these phenotypes be rationalized? If APC/C activity is limiting, then the extended lingering of free securin will competitively delay the degradation of separase-bound securin (Supplementary Fig S7A). Alternatively or in addition to this, surplus securin will re-inhibit any separase which has just been freed, thereby increasing the effective size of the separase-associated pool (Supplementary Fig S7A, gray arrow). Consistent with this second mode of action, the share of securin-4A in the separase-bound securin pool transiently increases after APC/C activation and prior to its complete extinction (Supplementary Fig S7B). Both competitive inhibition of APC/C and re-inhibition of separase are largely prevented by the actual removal of free securin prior to degradation of the separase-bound fraction, thus resulting in a more synchronized, switch-like activation of separase that likely improves the overall fidelity of sister chromatid separation. Another circumstance might add to the abruptness of anaphase onset: Once released from its inhibitor(s), separase immediately undergoes auto-cleavage which abrogates PP2A binding (Supplementary Fig S8A) (Holland *et al.*, 2007). Therefore, any persisting free securin that sequesters previously activated separase is expected to stay phosphorylated and, thus, subject to accelerated degradation (Supplementary Fig S8B). It is therefore tempting to speculate that one function of auto-cleavage might be to minimize

re-inhibition of separase at the metaphase-to-anaphase transition by traces of free securin that have so far evaded destruction. Interestingly, the sharpness of the metaphase-to-anaphase transition in *S. cerevisiae* is also modulated by a phosphorylation-dependent change of securin degradation kinetics. Curiously however, proteolysis of the budding yeast securin is slowed by its (in this case Cdk1-dependent) phosphorylation and sped up by dephosphorylation which occurs only upon activation of Cdc14 phosphatase in early anaphase (Holt *et al.*, 2008). Thus, although the involved kinases, phosphatases, and mechanisms differ, the fine-tuning of late mitotic events by the impact of securin phosphorylation on its APC/C-dependent degradation kinetics is conserved from yeast to man.

At first sight, the expression of securin in excess of separase and the dephosphorylation-dependent stabilization of separase-associated securin seem inconsistent with a sharp metaphase-to-anaphase transition. As outlined above, these characteristics would indeed spoil the anaphase switch if it was not for the preferential degradation of free securin. So why does the cell afford these measures to begin with? Our *in vivo* analyses suggest that preventing unscheduled basal activation of separase during checkpoint-mediated arrests is the answer to this question. This can be illustrated by the exchange of endogenous securin with securin-4D, which exhibits an increased turnover even at times of low APC/C activity. This property of the phosphorylation-mimicking variant suffices to cause premature centriole disengagement and precocious sister separation, respectively, in G2- and prometaphase-arrested cells.

Why PP2A teams up with separase has long remained enigmatic. Our observations now strongly suggest that this interaction constitutes an additional layer of separase regulation that operates through securin and helps to fine-tune the metaphase-to-anaphase transition. Its main purpose, however, is to prevent the unscheduled unleashing of separase's essential but dangerous proteolytic activity.

## Materials and Methods

### Cell lines

For inducible expression of securin-His<sub>6</sub>-Flag-His<sub>6</sub>-Flag (WT: wild-type; mKEN/mDB: K9R/E10D/N11Q and R61A/L64A; 4A: S31A/T66A/S87A/S89A; 4D: S31D/T66D/S87D/S89D) or Myc<sub>6</sub>-separase (WT: wild-type;  $\Delta$ PP2A:  $\Delta$ 1490-93 for Fig 1B and  $\Delta$ 1408-1478 for SILAC-MS experiment and Fig 2C), corresponding transgenes were stably integrated into a HeLa FlpIn TRex cell line. Clones were selected with 400  $\mu$ g/ml hygromycin B (PAA). All cells were cultured in DMEM (PAA) supplemented with 10% FCS (PAA) at 37°C and 5% CO<sub>2</sub>. Growth medium for the transgenic lines was additionally supplemented with 4  $\mu$ g/ml puromycin (Invitrogen) and 62.5  $\mu$ g/ml zeocin (Invitrogen).

### Immunoprecipitation

$1 \times 10^7$  cells were lysed in 1 ml lysis buffer (20 mM Tris-HCl pH 7.7, 100 mM NaCl, 10 mM NaF, 20 mM  $\beta$ -glycerophosphate, 5 mM MgCl<sub>2</sub>, 0.1% Triton X-100, 5% glycerol, 1 mM EDTA) supplemented with complete protease inhibitor cocktail (Roche).

To preserve securin phosphorylation status, lysis buffer was additionally supplemented with 1  $\mu$ M okadaic acid (Sigma-Aldrich) and 1  $\mu$ M microcystin LR (Alexis Biochemicals). Lysates were cleared by centrifugation at 16,000 g for 30 min. For separase and securin IPs, 10  $\mu$ l protein G Sepharose was coupled to 2–5  $\mu$ g of specific antibody for 90 min at room temperature. Coupled beads were washed three times with lysis buffer and incubated with cleared whole cell extracts (WCE) for 4 h at 4°C. Beads were washed three times with lysis buffer, and bound proteins were eluted by boiling in reducing SDS-sample buffer. Note that in several experiments, separase-depleted lysates were subjected to another round of IP with immobilized anti-securin. For anti-Myc and anti-Flag IPs, the corresponding agarose matrices were equilibrated in lysis buffer, incubated with cleared WCE for 4 h at 4°C, and washed three times with lysis buffer before bound proteins were eluted by boiling in non-reducing SDS-sample buffer. For APC/C purification, pre-synchronized HeLa cells were arrested in taxol, harvested by shake-off, and released for 25 min by addition of ZM. Cell lysis and anti-Cdc27 immunoprecipitation were performed as described (Herzog & Peters, 2005) with the following exceptions: The high salt wash of immobilized APC/C was omitted, and the elution was performed in presence of 2 mg/ml antigenic Cdc27 peptide.

#### In vitro ubiquitylation assay

*In vitro* ubiquitylation reactions were performed largely as described (Herzog & Peters, 2005). Immuno-affinity-purified APC/C<sup>Cdc20</sup> (21  $\mu$ l corresponding to half of the cell harvest from one 15-cm petri dish) was combined with 80  $\mu$ g/ml E1 (Boston-Biochem), 50  $\mu$ g/ml recombinant UbcH10-WT or UbcH10-DN (C114S), 1.25 mg/ml ubiquitin (Sigma-Aldrich), energy mix (1 mM ATP, 1 mM MgCl<sub>2</sub>, 0.1 mM EGTA, 7.5 mM creatine phosphate, 30 U/ml creatine phosphokinase type I; Sigma-Aldrich), and 4.5  $\mu$ g recombinant securin-WT, securin-4A, or securin-4D in a total reaction volume of 42  $\mu$ l and incubated at 37°C. After 15–45 min, 7- $\mu$ l reaction aliquots were subjected to SDS-PAGE and anti-securin Western. CaMKII pre-phosphorylation of securin-WT was performed in presence of 400  $\mu$ M ATP in a total reaction volume of 5  $\mu$ l.

**Supplementary information** for this article is available online: <http://emboj.embopress.org>

#### Acknowledgements

We wish to thank Thomas U. Mayer for the HeLa FlpIn TRex cell line and anti-Cdc27; Silke Hauf, Stefan Heidmann, and Klaus Ersfeld for critical reading of the manuscript; Bernd Mayer, Michael Orth, and Martin Wühr for stimulating discussions; and all members of the Stemmann laboratory for help and input. This work was supported by grants (STE 997/3-2 within the priority program SPP1384 and STE 997/4-1) from the Deutsche Forschungsgemeinschaft (DFG) to O.S.

#### Author contributions

FB initiated the project, generated all stable transgenic cell lines, performed the SILAC and the experiments shown in Fig 1A and B, Supplementary Fig S4, and contributed to writing of the manuscript; SH co-designed and performed all experiments (including corresponding quantifications) except for the ones shown in Fig 1A and B, Supplementary Fig S4, and contributed to writing of

the manuscript; CP and MM performed the MS analysis; OS conceived and designed the research, made the figures, and wrote the manuscript.

#### Conflict of interest

The authors declare that they have no conflict of interest.

## References

- Bassermann F, Frescas D, Guardavaccaro D, Busino L, Peschiaroli A, Pagano M (2008) The Cdc14B-Cdh1-Plk1 axis controls the G2 DNA-damage-response checkpoint. *Cell* 134: 256–267
- Boos D, Kuffer C, Lenobel R, Korner R, Stemmann O (2008) Phosphorylation-dependent binding of cyclin B1 to a Cdc6-like domain of human separase. *J Biol Chem* 283: 816–823
- Buheitel J, Stemmann O (2013) Prophase pathway-dependent removal of cohesin from human chromosomes requires opening of the Smc3-Scc1 gate. *EMBO J* 32: 666–676
- Crasta K, Ganem NJ, Dagher R, Lantermann AB, Ivanova EV, Pan Y, Nezi L, Protopopov A, Chowdhury D, Pellman D (2012) DNA breaks and chromosome pulverization from errors in mitosis. *Nature* 482: 53–58
- Eichinger CS, Kurze A, Oliveira RA, Nasmyth K (2013) Disengaging the Smc3/kleisin interface releases cohesin from *Drosophila* chromosomes during interphase and mitosis. *EMBO J* 32: 656–665
- Gil-Bernabe AM, Romero F, Limon-Mortes MC, Tortolero M (2006) Protein phosphatase 2A stabilizes human securin, whose phosphorylated forms are degraded via the SCF ubiquitin ligase. *Mol Cell Biol* 26: 4017–4027
- Gorr IH, Boos D, Stemmann O (2005) Mutual inhibition of separase and Cdk1 by two-step complex formation. *Mol Cell* 19: 135–141
- Haering CH, Farcas AM, Arumugam P, Metson J, Nasmyth K (2008) The cohesin ring concatenates sister DNA molecules. *Nature* 454: 297–301
- Harley ME, Allan LA, Sanderson HS, Clarke PR (2010) Phosphorylation of Mcl-1 by CDK1-cyclin B1 initiates its Cdc20-dependent destruction during mitotic arrest. *EMBO J* 29: 2407–2420
- He J, Chao WC, Zhang Z, Yang J, Cronin N, Barford D (2013) Insights into deproton recognition by APC/C coactivators from the structure of an Acm1-Cdh1 complex. *Mol Cell* 50: 649–660
- Herzig A, Lehner CF, Heidmann S (2002) Proteolytic cleavage of the THR subunit during anaphase limits *Drosophila* separase function. *Genes Dev* 16: 2443–2454
- Herzog F, Peters JM (2005) Large-scale purification of the vertebrate anaphase-promoting complex/cyclosome. *Methods Enzymol* 398: 175–195
- Holland AJ, Taylor SS (2006) Cyclin-B1-mediated inhibition of excess separase is required for timely chromosome disjunction. *J Cell Sci* 119: 3325–3336
- Holland AJ, Bottger F, Stemmann O, Taylor SS (2007) Protein phosphatase 2A and separase form a complex regulated by separase autocleavage. *J Biol Chem* 282: 24623–24632
- Holt LJ, Krutchinsky AN, Morgan DO (2008) Positive feedback sharpens the anaphase switch. *Nature* 454: 353–357
- Huang X, Hatcher R, York JP, Zhang P (2005) Securin and separase phosphorylation act redundantly to maintain sister chromatid cohesion in mammalian cells. *Mol Biol Cell* 16: 4725–4732
- Huang X, Andreu-Vieyra CV, York JP, Hatcher R, Lu T, Matzuk MM, Zhang P (2008) Inhibitory phosphorylation of separase is essential for genome stability and viability of murine embryonic germ cells. *PLoS Biol* 6: e15
- Huang X, Andreu-Vieyra CV, Wang M, Cooney AJ, Matzuk MM, Zhang P (2009) Preimplantation mouse embryos depend on inhibitory phosphorylation of

- separase to prevent chromosome missegregation. *Mol Cell Biol* 29: 1498–1505
- Janssen A, van der Burg M, Suzhai K, Kops GJ, Medema RH (2011) Chromosome segregation errors as a cause of DNA damage and structural chromosome aberrations. *Science* 333: 1895–1898
- Janssens V, Goris J, Van Hoof C (2005) PP2A: the expected tumor suppressor. *Curr Opin Genet Dev* 15: 34–41
- Kumada K, Yao R, Kawaguchi T, Karasawa M, Hoshikawa Y, Ichikawa K, Sugitani Y, Imoto I, Inazawa J, Sugawara M, Yanagida M, Noda T (2006) The selective continued linkage of centromeres from mitosis to interphase in the absence of mammalian separase. *J Cell Biol* 172: 835–846
- Lara-Gonzalez P, Westhorpe FG, Taylor SS (2012) The spindle assembly checkpoint. *Curr Biol* 22: R966–R980
- Lee K, Rhee K (2012) Separase-dependent cleavage of pericentrin B is necessary and sufficient for centriole disengagement during mitosis. *Cell Cycle* 11: 2476–2485
- Limon-Mortes MC, Mora-Santos M, Espina A, Pintor-Toro JA, Lopez-Roman A, Tortolero M, Romero F (2008) UV-induced degradation of securin is mediated by SKP1-CUL1-beta TrCP E3 ubiquitin ligase. *J Cell Sci* 121: 1825–1831
- Matsuo K, Ohsumi K, Iwabuchi M, Kawamata T, Ono Y, Takahashi M (2012) Kendrin is a novel substrate for separase involved in the licensing of centriole duplication. *Curr Biol* 22: 915–921
- Nabti I, Reis A, Levasseur M, Stemmann O, Jones KT (2008) Securin and not CDK1/cyclin B1 regulates sister chromatid disjunction during meiosis II in mouse eggs. *Dev Biol* 321: 379–386
- Obenauer JC, Cantley LC, Yaffe MB (2003) Scansite 2.0: proteome-wide prediction of cell signaling interactions using short sequence motifs. *Nucleic Acids Res* 31: 3635–3641
- Ong SE, Mann M (2007) Stable isotope labeling by amino acids in cell culture for quantitative proteomics. *Methods Mol Biol* 359: 37–52
- Peters JM (2006) The anaphase promoting complex/cyclosome: a machine designed to destroy. *Nat Rev Mol Cell Biol* 7: 644–656
- Prosser SL, Samant MD, Baxter JE, Morrison CG, Fry AM (2012) Oscillation of APC/C activity during cell cycle arrest promotes centrosome amplification. *J Cell Sci* 125: 5353–5368
- Rape M, Reddy SK, Kirschner MW (2006) The processivity of multiubiquitination by the APC determines the order of substrate degradation. *Cell* 124: 89–103
- Schockel L, Mockel M, Mayer B, Boos D, Stemmann O (2011) Cleavage of cohesin rings coordinates the separation of centrioles and chromatids. *Nat Cell Biol* 13: 966–972
- Shindo N, Kumada K, Hirota T (2012) Separase sensor reveals dual roles for separase coordinating cohesin cleavage and cdk1 inhibition. *Dev Cell* 23: 112–123
- Stemmann O, Zou H, Gerber SA, Gygi SP, Kirschner MW (2001) Dual inhibition of sister chromatid separation at metaphase. *Cell* 107: 715–726
- Stemmann O, Gorr IH, Boos D (2006) Anaphase topsy-turvy: Cdk1 a securin, separase a CKI. *Cell Cycle* 5: 11–13
- Sun Y, Yu H, Zou H (2006) Nuclear exclusion of separase prevents cohesin cleavage in interphase cells. *Cell Cycle* 5: 2537–2542
- Tsou MF, Stearns T (2006) Mechanism limiting centrosome duplication to once per cell cycle. *Nature* 442: 947–951
- Uhlmann F, Wernic D, Poupart MA, Koonin EV, Nasmyth K (2000) Cleavage of cohesin by the CD clan protease separin triggers anaphase in yeast. *Cell* 103: 375–386
- Waizenegger IC, Hauf S, Meinke A, Peters JM (2000) Two distinct pathways remove mammalian cohesin from chromosome arms in prophase and from centromeres in anaphase. *Cell* 103: 399–410
- Waizenegger I, Gimenez-Abian JF, Wernic D, Peters JM (2002) Regulation of human separase by securin binding and autocleavage. *Curr Biol* 12: 1368–1378
- Watanabe Y (2005) Shugoshin: guardian spirit at the centromere. *Curr Opin Cell Biol* 17: 590–595
- Williamson A, Banerjee S, Zhu X, Philipp I, Iavarone AT, Rape M (2011) Regulation of ubiquitin chain initiation to control the timing of substrate degradation. *Mol Cell* 42: 744–757
- Wirth KG, Wutz G, Kudo NR, Desdouets C, Zetterberg A, Taghybeeglu S, Seznec J, Ducos GM, Ricci R, Firnberg N, Peters JM, Nasmyth K (2006) Separase: a universal trigger for sister chromatid disjunction but not chromosome cycle progression. *J Cell Biol* 172: 847–860
- Zou H, Stemmann O, Anderson JS, Mann M, Kirschner MW (2002) Anaphase specific auto-cleavage of separase. *FEBS Lett* 528: 246–250

## SUPPLEMENTARY MATERIALS AND METHODS

### Antibodies

The following antibodies were used for immunoblotting according to standard protocols: rabbit anti-separase (Stemmann et al, 2001), mouse anti-securin (1:1,000; MBL), rabbit anti-securin (1:1,000; Epitopics), mouse anti-Flag M2 (1:2,000; Sigma-Aldrich), mouse anti-Myc (1:50; 9E10, DSHB, hybridoma supernatant), rabbit anti-phosphoSer10-histone H3 (1:1,000; Millipore), rabbit anti-phosphoSer139-histone H2A.X (1:1,000; Millipore), mouse anti-cyclin B1 (1:1,000; Millipore), mouse anti-topoisomerase II $\alpha$  (1:1,000; Enzo Life Sciences), mouse anti-Cdc20 (1:2,000; Santa Cruz Biotechnology), goat anti-Cdc27 (1:1000), mouse anti-cyclin A2 (1:200; Santa Cruz Biotechnology), mouse anti-phosphoSer (1:1,000; Invitrogen), mouse anti-PP2A-C (1:1,000; Millipore), rabbit anti-phosphoThr68-Chk2 (1:800; Cell Signaling) and mouse anti- $\alpha$ -tubulin (1:200; 12G10, DSHB, hybridoma supernatant). For immunoprecipitation (IP) experiments, the following affinity matrices and antibodies were used: mouse anti-Myc Agarose (Sigma-Aldrich), mouse anti-Flag M2-Agarose (Sigma-Aldrich), human IgG Sepharose (GE Healthcare), protein G Sepharose (GE Healthcare) loaded with mouse anti-separase (A302-214A, Bethyl; used for PP2A interaction experiments only), rabbit anti-separase (raised against a His<sub>6</sub>-tagged fragment (amino acids 1305-1573) of human separase), rabbit anti-securin (raised against His<sub>6</sub>-tagged human securin), goat anti-Cdc27 (raised against a peptide with the sequence CDADDTQLHAAESDEF) or unspecific rabbit IgG (Bethyl). For immunofluorescence (IF) staining of fixed cells, mouse anti-Hec1 (1:800; Genetex), rabbit anti-phosphoThr68-Chk2 (1:200; Cell Signaling) and mouse anti-phosphoSer139-histone H2A.X (1:2,500; Millipore) were used. Isolated centrosomes were stained with rabbit anti-centrin-2 and guinea-pig anti-C-Nap1 as previously described (Schockel et al, 2011). Secondary antibodies (all 1:500): Cy3 donkey anti-guinea pig IgG (Jackson ImmunoResearch Laboratories), Alexa Fluor 488 goat anti-rabbit and Alexa Fluor 488 goat anti-mouse IgGs (both Invitrogen).

## Cell treatments

For synchronization at the G1/S boundary, cells were treated with 2 mM thymidine (Sigma-Aldrich) for 20 h, released into fresh medium for 10 h, and then exposed to 2 mM thymidine again for additional 18 h. Synchronization of cells in prometaphase was done by addition of nocodazole (Sigma-Aldrich) or taxol (Calbiochem) to 0.2 µg/ml each 6 h after release from a single thymidine block. G2 arrest was achieved by addition of RO3306 (Santa-Cruz Biotechnology) to 10 µM 4 h after release from a previous thymidine treatment. For the taxol-ZM override experiments, taxol-arrested mitotic cells were harvested by shake-off and released for the indicated times by replating into medium supplemented with ZM 447439 (5 µM, Tocris Biosciences), taxol (0.2 µg/ml) and, where indicated, cycloheximide (30 µg/ml, Sigma-Aldrich). For the long-term prometaphase arrest experiment shown in Figure 6C, caspase-1 and -3 inhibitors (5 µM each, Calbiochem) were additionally added after mitotic shake-off. To induce DNA-damage, doxorubicin (0.5 µM, Calbiochem) was added to cells 7 h after release from a double thymidine block. Transgenic securin and separase variants were induced using 0.2-1 µg/ml doxycycline (Sigma-Aldrich) from 10 h up to 3 d. For CaMKII inhibition, KN-93 (4 µM, Calbiochem) was added 4 h before ZM to taxol-arrested cells. For IP of Myc<sub>6</sub>-separase (WT or ΔPP2A) as shown in Figure 2C, taxol-arrested cells were additionally treated with okadaic acid (100 nM; Sigma-Aldrich) 10 min prior to ZM addition. For time-lapse imaging transgenic securin HeLa cells were transiently transfected with plasmids coding for histone H2B-eGFP (BD Pharmingen) or H2B-mCherry-Scc1<sub>aa107-268</sub>-eGFP (separase-sensor). HEK293T and HeLa cells were transfected using calcium phosphate and Lipofectamine 2000 (Invitrogen), respectively.

## Immunofluorescence microscopy

Stable transgenic HeLa cells grown on poly-lysine coated glass coverslips were washed once with 1x PBS, fixed with fixation-solution (1x PBS, 3.7% formaldehyde, 0.3% Triton X-

100) for 10 min at room temperature, and then washed twice with quenching-solution (1x PBS, 100 mM glycine). They were then further permeabilized by treatment with permeabilization-solution (1x PBS, 0.5% Triton X-100) for 5 min which was followed by a PBS wash and an incubation in blocking-solution (1x PBS, 1% (w/v) BSA) for 20 min at room temperature. Coverslips were transferred into a wet chamber and then incubated with primary antibodies for 1 h followed by 4 washes with PBS-Tx (1x PBS, 0.1% Triton X-100). After incubation with fluorescently labeled secondary antibodies for 40 min, samples were washed once, stained for 10 min with 1 µg/ml Hoechst 33342 in PBS-Tx and washed again 4 times. Finally, coverslips were mounted in 78% glycerol, 20 mM Tris-HCl pH 8.0, 2,33% (w/v) 1,4-diazabicyclo(2.2.2)octane on a glass slide. Immunofluorescence microscopy of fixed cells and isolated centrosomes was performed using a HCX PL APO 100x/1.40-0.70 oil objective. To detect DNA bridges or lagging chromosomes (Figure 4B) Z-stacks of 25-30 images at 0.35 µm increments were collected. For digital 3D deconvolution of Z-axis image series, the LAS-AF software was used (20 iterations; blind deconvolution algorithm). For quantification of DNA-damage foci (Figure 4C), Z-stacks series over 4 µM in 0.2 µM increments were collected and projected onto one focus plane using the LAS-AF software. Chromosome spreads were prepared using Carnoy's solution as described (McGuinness et al, 2005). To assess centriole engagement status, centrosomes were isolated from  $4 \times 10^6$  cells and stained as previously described (Schockel et al, 2011).

### **Live-cell imaging**

Cells were seeded into CO<sub>2</sub>-dependent medium without phenol red onto µ-slide 8-well chambered coverslips (Ibidi). Cells were kept in an atmosphere of 37°C and 5% humidified CO<sub>2</sub> during microscopy on a DMI 6000 inverted microscope (Leica). For imaging of unperturbed mitosis, GFP and DIC images were captured in 180 s intervals over a period of 12 h, through a HCX PL APO 40x/0.85 CORR objective. For taxol-ZM override experiments separate sensor expressing cells were imaged at minimal light intensity and every 240-300 s

over a period of 90 min from ZM addition. Changes in focus plane due to mitotic rounding of the cells were compensated by collecting Z-stacks at each time point. Captured images from each experiment were analysed using the corresponding LAS-AF software (Leica).

### **CaMKII kinase assay**

To activate CaMKII autophosphorylation reaction was performed in presence of 200  $\mu$ M ATP, 1.2  $\mu$ M calmodulin and 2 mM  $\text{CaCl}_2$  in 1x protein kinase reaction buffer (all components from NEB) for 10 min at 30°C. For the radioactive phosphorylation assay 1.5  $\mu$ g recombinant securin supplemented with 50  $\mu$ M ATP and 40  $\mu$ Ci  $\gamma$ - $^{33}\text{P}$ -ATP (Hartmann Analytic) were combined with 500 U activated CaMKII and incubated for 1 h at 30°C. Samples were analysed by SDS-PAGE and autoradiography.

### **RNA interference**

For knockdown of human Cdc20 or human securin, cells were transfected with 70-100 nM siRNA duplex (*CDC20*: 5'-CGGAAGACCUGCCGUUACAUU-3', *SECURIN*: 5'-UCUUAGUGCUUCAGAGUUUGUGUGUAU-3') and RNAiMax (Invitrogen) for 48 h according to the manufacturers instructions. Luciferase siRNA (*GL2*) was used as negative control.

### **SILAC and mass spectrometry analysis**

HEK293T cells were calcium phosphate transfected to co-express securin with either separase-WT or separase- $\Delta$ PP2A and arrested in prometaphase by nocodazole (0.2  $\mu$ g/ml). Prior to transient transfection the cells were SILAC labeled as previously described (Cox & Mann, 2008). Briefly, DMEM medium without arginine and lysine (Invitrogen) was supplemented with either  $^{13}\text{C}/^{15}\text{N}$  labeled arginine and  $^{13}\text{C}/^{15}\text{N}$  labelled lysine (R10/K8) or

with the unlabeled amino acids (R0/K0) (Sigma-Aldrich). Cells that were later transfected to express separase-WT and securin were cultivated in R0/K0 medium, while cells that were to express separase- $\Delta$ PP2A and securin were grown in R10/K8 medium over 6 generations prior to transfection.

Following two days of expression, the SILAC-labeled, mitotic HEK293T cells were lysed in lysis buffer (20 mM Tris-HCl at pH 7.7, 100 mM NaCl, 10 mM NaF, 20 mM  $\beta$ -glycerophosphate, 5 mM MgCl<sub>2</sub>, 0.1 % Triton X-100, 5 % glycerol, 1 mM EDTA) supplemented with 1  $\mu$ M okadaic acid and 1  $\mu$ M microcystin LR (both from Alexis Biochemicals) to preserve phosphorylations. Lysates were cleared by centrifugation (45 min, 160,000 g, 4°C) and then rotated with IgG sepharose for 4 h at 4°C to capture separase-securin complexes via the N-terminal ZZ-Tev<sub>4</sub>-tag on separase (Z = IgG binding domain of protein A). Beads were washed three times with lysis buffer before bound separase-securin complexes were eluted by Tev-protease treatment for 2 h at 18°C. Eluates were mixed at a 1:1 ratio and separated by SDS-PAGE. Coomassie-stained separase and securin bands were subjected to in-gel digestion with trypsin or Asp-N according to standard protocol (Shevchenko et al, 2006). Phosphorylated peptides were then enriched by titansphere chromatography. Sample analysis was done by reversed phase LC-MS/MS using the Agilent Technologies 1200 nanoflow system connected to an LTQ Orbitrap XL system (Thermo Electron) with a nanoelectrospray ion source (Proxeon Biosystems) as described (Olsen et al, 2005). Peptides were identified using the Mascot-MatrixScience LLC software and quantified using MSQuant.

### **Extract experiments**

<sup>35</sup>S-labeled securin variants (WT, 4A, 4D or mKEN/mDB) were *in vitro* expressed by combining corresponding pCS2 plasmids with SP6 RNA polymerase supplemented rabbit reticulocyte lysate (TNT SP6 Coupled Transcription/Translation System from Promega) in presence of <sup>35</sup>S-methionine (Hartmann Analytic) according to the manufacturers' instructions.

CSF-arrested *Xenopus* egg extracts were prepared as previously described (Murray, 1991) and combined with cycloheximide (100 µg/ml), recombinant human cyclin B1Δ90 (10 ng/µl), sperm nuclei (2.000 µl<sup>-1</sup>) and <sup>35</sup>S-labeled securin (16 µl/ml). After 20 min at room temperature, extracts were additionally supplemented either with 0.6 mM CaCl<sub>2</sub> and 1 µM okadaic acid (Figure S4B) or with CaCl<sub>2</sub> only (Figure S6). At indicated times thereafter, 3 µl each were analysed by SDS-PAGE and autoradiography. For λ-phosphatase treatment of selected samples (Figure S4B) 3 µl aliquots were treated for 30 min at 30°C with 400 U of λ-phosphatase (NEB) in presence of 2 mM MnCl<sub>2</sub>.

For λ-phosphatase treatment of immunoprecipitated proteins (Figure S4A), the corresponding beads were washed twice with EDTA-, NaF- and β-glycerophosphate-free but MnCl<sub>2</sub> (2 mM) containing lysis buffer and incubated with 400 U λ-phosphatase (NEB) for 30 min at 30°C prior to SDS-PAGE and immunoblotting.

### **Flow cytometry**

For analysis of DNA content, cells were fixed with 70% ethanol (-20°C), washed twice with 1x PBS, 0.1% (w/v) BSA and resuspended in 69 µM propidium iodide, 38 mM tri-sodium citrate, 100 µg/ml RNase A (Qiagen). After incubation for 30 min at 37°C, the cell cycle profiles were analysed on a Cytomics FC 500 flow cytometer using CXP Analysis software (Beckman Coulter)

## SUPPLEMENTARY REFERENCES

Cox J, Mann M (2008) MaxQuant enables high peptide identification rates, individualized p.p.b.-range mass accuracies and proteome-wide protein quantification. *Nat Biotechnol* **26**: 1367-1372

McGuinness BE, Hirota T, Kudo NR, Peters JM, Nasmyth K (2005) Shugoshin prevents dissociation of cohesin from centromeres during mitosis in vertebrate cells. *PLoS biology* **3**: e86

Murray AW (1991) Cell cycle extracts. *Methods Cell Biol* **36**: 581-605

Olsen JV, de Godoy LM, Li G, Macek B, Mortensen P, Pesch R, Makarov A, Lange O, Horning S, Mann M (2005) Parts per million mass accuracy on an Orbitrap mass spectrometer via lock mass injection into a C-trap. *Mol Cell Proteomics* **4**: 2010-2021

Schockel L, Mockel M, Mayer B, Boos D, Stemmann O (2011) Cleavage of cohesin rings coordinates the separation of centrioles and chromatids. *Nature cell biology* **13**: 966-972

Shevchenko A, Tomas H, Havlis J, Olsen JV, Mann M (2006) In-gel digestion for mass spectrometric characterization of proteins and proteomes. *Nat Protoc* **1**: 2856-2860

Stemmann O, Zou H, Gerber SA, Gygi SP, Kirschner MW (2001) Dual inhibition of sister chromatid separation at metaphase. *Cell* **107**: 715-726

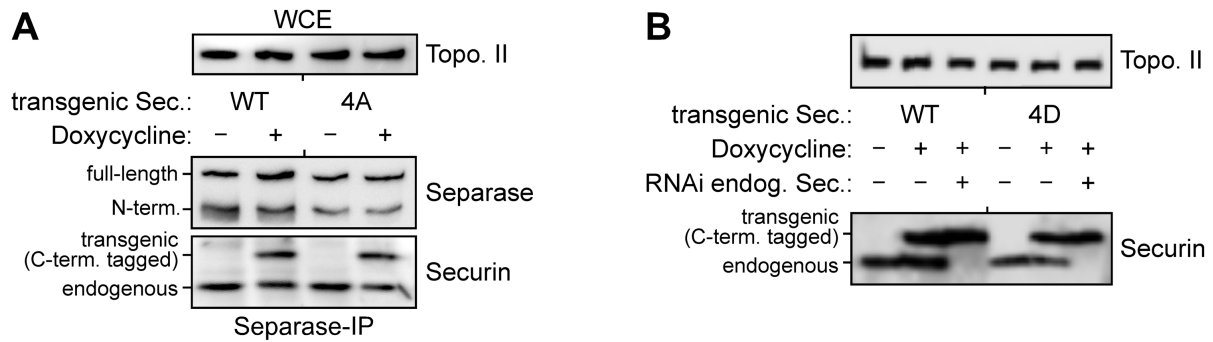


**Figure S1. By combining RNAi and transgene induction, endogenous securin can be efficiently replaced by C-terminally tagged, phosphorylation site mutant variants.**

**(A)** Transgenic HeLa cell lines were left untreated (-) or induced with doxycycline (+) to express C-terminally Flag-tagged securin-WT or -4A. Whole cell extracts (WCE) were prepared 10 h later and subjected to anti-separase immunoprecipitation (IP) to purify separase-securin complexes. Immunoblotting analysis revealed very similar amounts of endogenous securin and transgenic variants in association with separase indicating that tagging and amino acid exchanges left securin's affinity for separase unaffected.

**(B)** Transgenic HeLa cell lines were transfected with siRNA against (endogenous) *SECURIN* (+) or *GL2* (-), induced to express (siRNA resistant) transgenic securin-WT or -4D 38 h later and harvested after an additional 10 h of cultivation. Immunoblotting of whole cell extracts demonstrated efficient depletion of endogenous securin and expression of the transgenic variants at near physiological levels. Topoisomerase II (Topo. II) served as loading control.

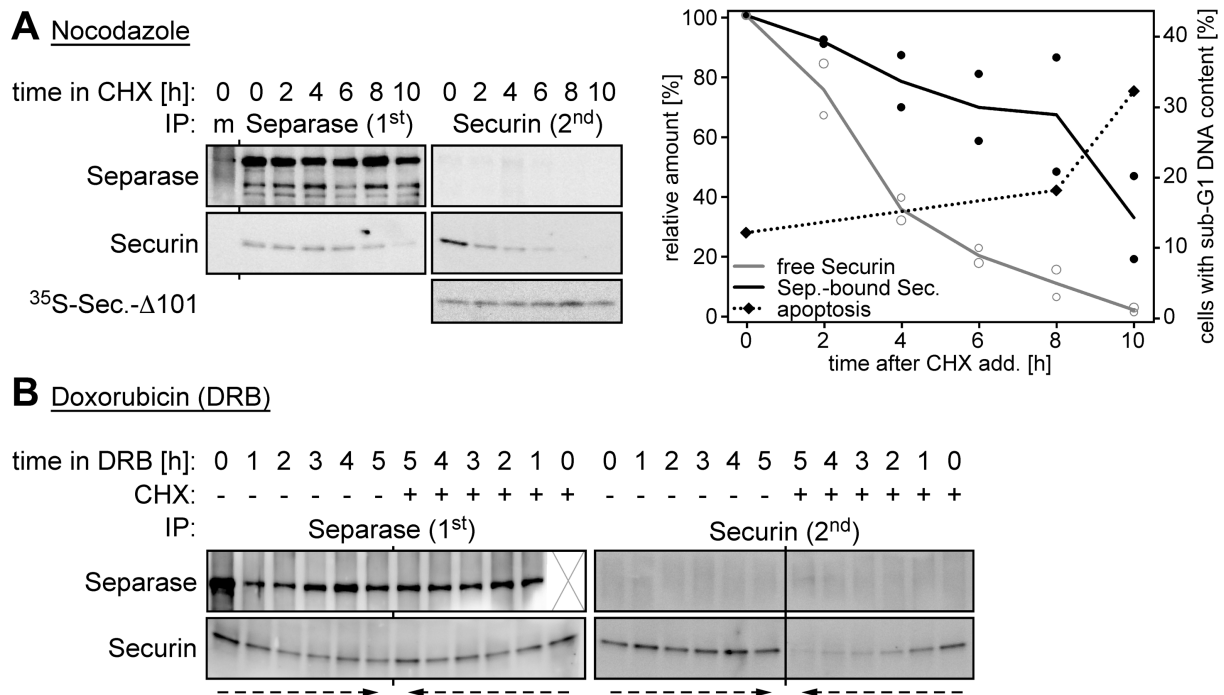


**Figure S2. G2- and prometaphase-arrested cells exhibit decreased stability of free over separase-associated securin.**

(A) HeLa cells were synchronized in prometaphase by consecutive treatments with thymidine and nocodazole, harvested by shake-off and replated in fresh medium supplemented with nocodazole and cycloheximide (CHX). At indicated times cells were lysed and separase-bound and free forms of securin were isolated by immunoprecipitation (IP) with anti-separase and anti-securin, respectively (m = mock IP). Separase-depleted extracts were supplemented with trace amounts of <sup>35</sup>S-labelled securin-Δ101. This non-degradable variant served as an internal control for the efficiency of the IP of free securin. The graph represents mean degradation kinetics of separase-bound and free securin. Western signals of two independent experiments (dots) were quantified by densitometry and blotted as percent of the value at t = 0. Securin levels were normalized against the corresponding signals of separase (1<sup>st</sup>) or securin-Δ101 (2<sup>nd</sup>). Serving as indicators of apoptosis, the percentages of cells with sub-G1 DNA content (diamonds) were determined by propidium iodide staining and flow cytometry.

(B) At t = 0 h, thymidine pre-synchronized HeLa cells were treated with doxorubicin (DRB) in the presence (+) or absence (-) of CHX to induce a DNA-damage checkpoint response in G2 phase (see also Figures 7A and S2). Separase-associated and free pools of securin were isolated as described in (A) and visualized by immunoblotting.

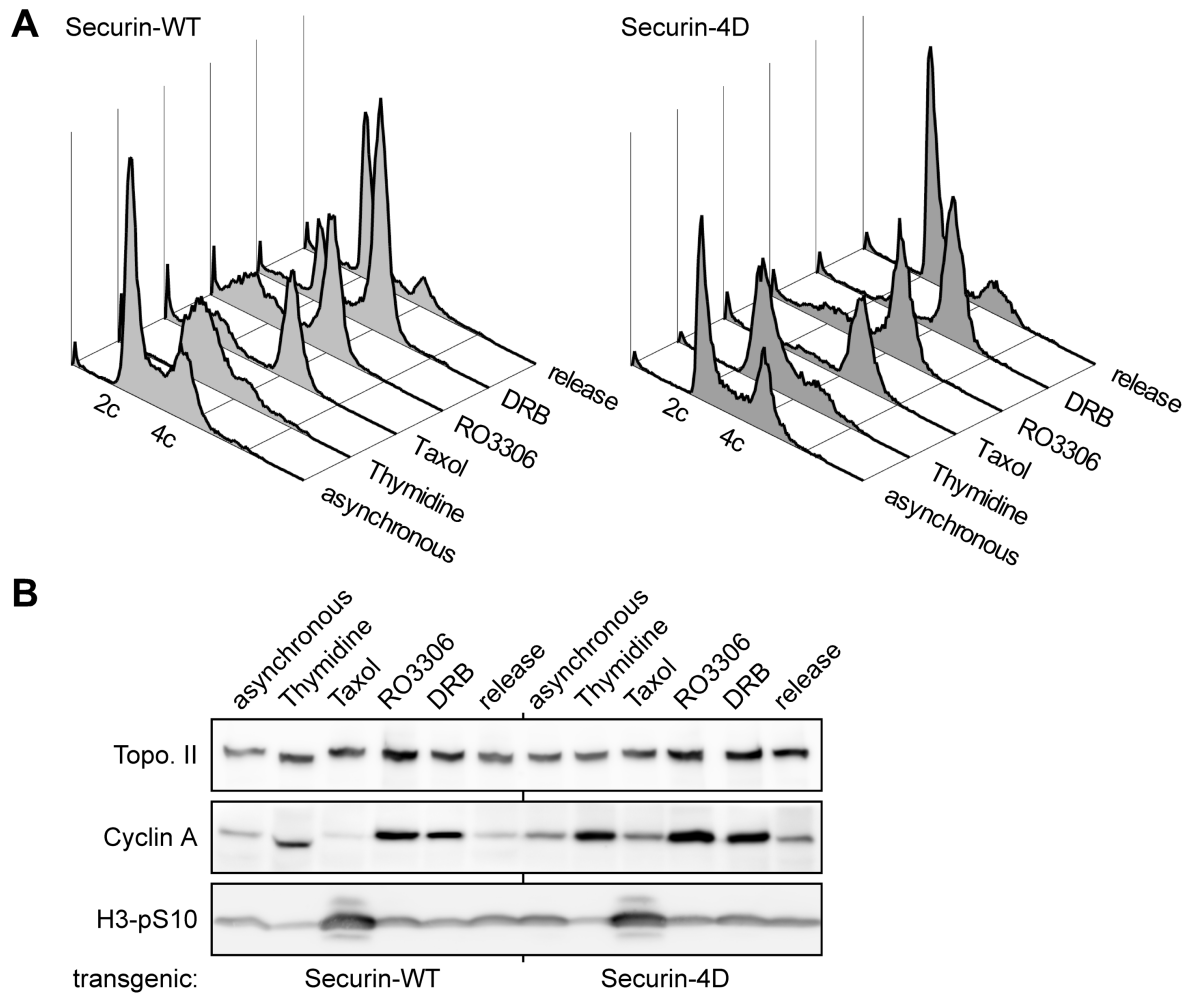


**Figure S3. Efficient synchronization of securin-WT or -4D expressing cells.**

**(A-B)** Sequential thymidine-taxol or thymidine-RO3306/doxorubicin treatments result in efficient cell synchronization in prometa- or G2 phase, respectively. Transgenic HeLa cell lines pre-synchronized by a first thymidine block were released into S-phase and induced with doxycycline to express securin-WT or -4D. 6 h thereafter, cells were exposed to taxol, RO3306, doxorubicin (DRB), or left untreated (release) and incubated for additional 14 h prior to their analysis by propidium iodide-staining and flow cytometry (A) and immunoblotting (B). Despite same DNA contents, G2- and prometaphase-arrested cells could be discerned by immunoblotting for cyclin A and Ser-10 phosphorylated histone H3 (H3-pS10).

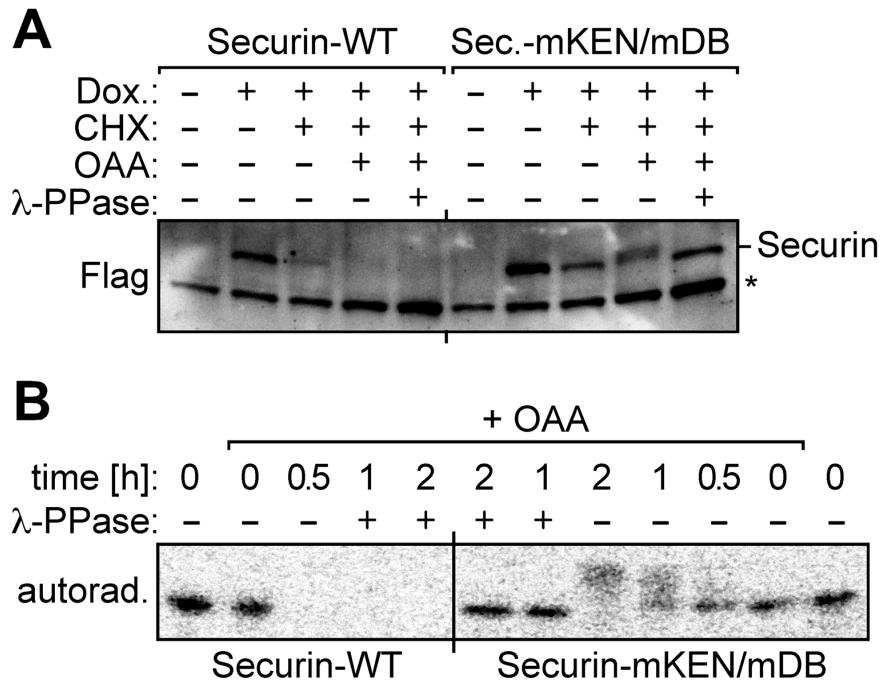


**Figure S4. Okadaic acid induced degradation of securin is blocked by mutation of its KEN- and D-box.**

(A) Stably transgenic HeLa lines were induced with doxycyclin (Dox) to overexpress C-terminally Flag-tagged securin-WT or securin-mKEN/mDB. 4 h thereafter, cycloheximide (CHX, 10  $\mu$ g/ml) was added either alone or together with okadaic acid (OAA) and cells were harvested 3 h later. Securin was affinity purified from corresponding cell lysates using anti-Flag beads and, where indicated, treated with  $\lambda$ -phosphatase prior to analysis by immunoblotting. The asterisk (\*) corresponds to the light chain of the Flag antibody .

(B)  $^{35}$ S-labelled securin was incubated in CHX-supplemented CSF-arrested *Xenopus* egg extract and, where indicated, released from metaphase-II arrest by addition of  $Ca^{2+}$  (t = 0 min) in the presence of OAA. At the indicated times, samples were analysed by SDS-PAGE and autoradiography with (+) or without (-) prior dephosphorylation with  $\lambda$ -PPase.

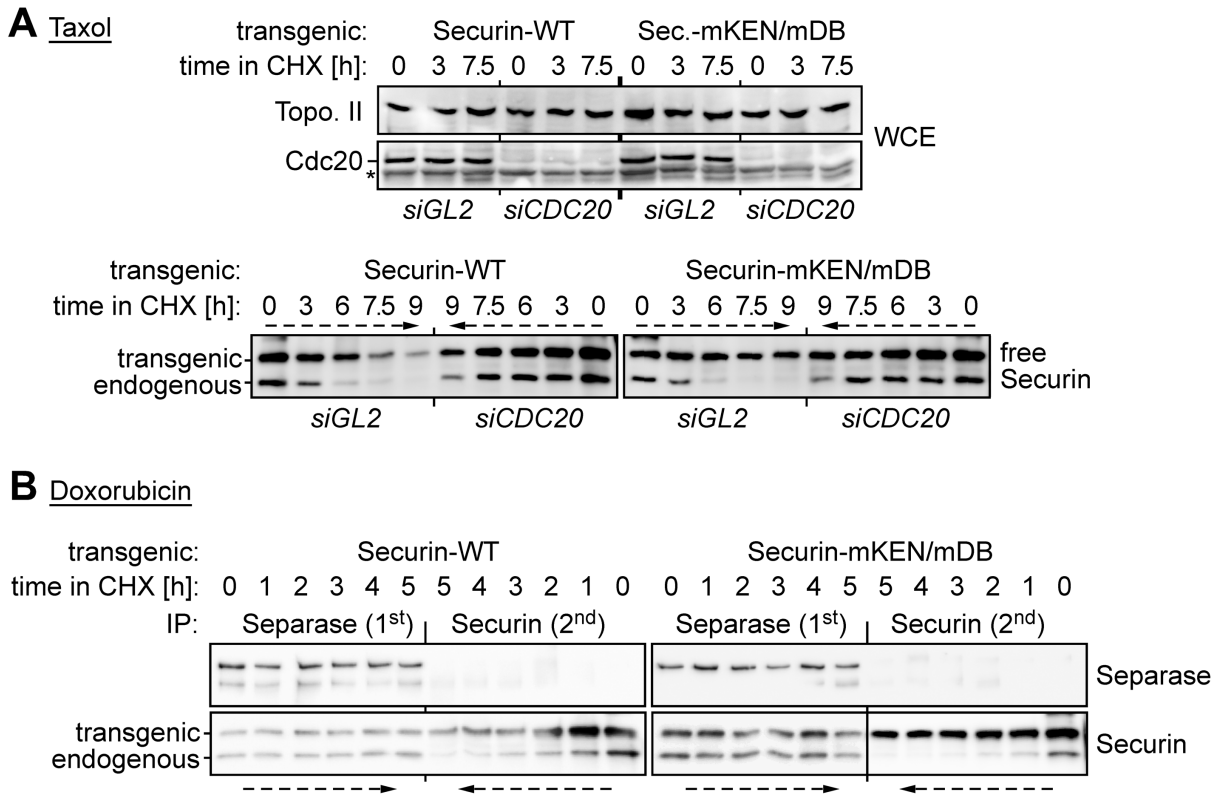


**Figure S5. Slow but APC/C-dependent turnover of free securin in G2 and prometaphase arrested cells.**

(A) Transgenic HeLa cells were transfected with siRNA against *CDC20* or *GL2*, synchronized in prometaphase by sequential thymidine-taxol treatment and induced to express securin-WT or -mKEN/mDB as indicated. Two days after siRNA transfection, mitotic cells were harvested by shake-off and replated in taxol and cycloheximide (CHX) containing medium (t = 0 h). At the indicated time points, whole cell extracts (WCE) were prepared, depleted of separase, and finally used for isolation of free securin as described in figure E1. Despite the fact that Cdc20 depletion was not complete (upper two panels) and cyclin A levels still dropped (data not shown), wild type securin was significantly stabilized at reduced Cdc20 level but degraded in mock-depleted cells (lower left panel). In contrast, securin-mKEN/mDB was stable even in presence of Cdc20 (lower right panel). The asterisk (\*) denotes a crossreactive band in the Cdc20 Western.

(B) Transgenic HeLa cells were released from a thymidine arrest and induced to express securin-WT or securin-mKEN/mDB. 8 h later doxorubicin and CHX were added (t = 0). At the indicated times, two consecutive rounds of immunoprecipitation were conducted to purify separase-bound (1<sup>st</sup>) and free securin (2<sup>nd</sup>). Immunoblotting revealed that only wild type securin experienced considerable degradation, while separase associated securin as well as free securin-mKEN/mDB were stable under these conditions.

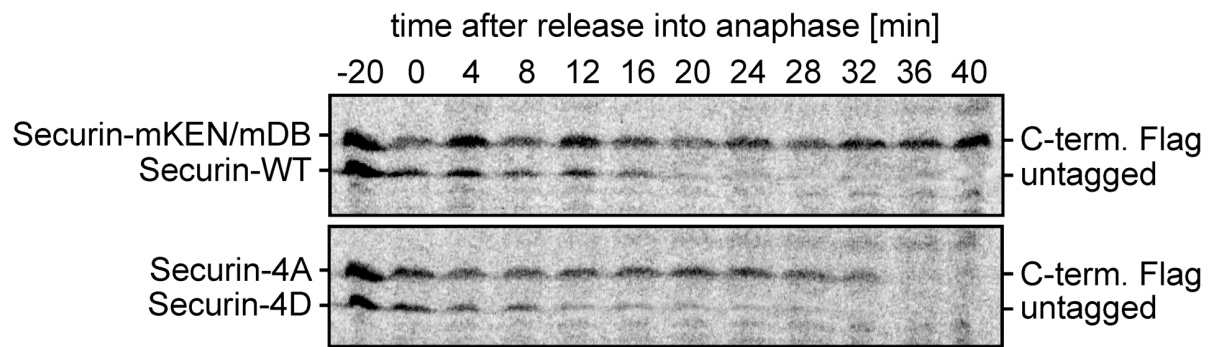


**Figure S6. Preventing or mimicking phosphorylation of human securin is correctly interpreted by *Xenopus* UPS.**

Two aliquots of a CSF-arrested *Xenopus* egg extract were supplemented with an untagged and a C-terminally Flag-tagged version of different <sup>35</sup>S-labeled securin variants as indicated and then released into anaphase by addition of Ca<sup>2+</sup>. After incubation at 16°C for various times, samples were analysed by SDS-PAGE and autoradiography.

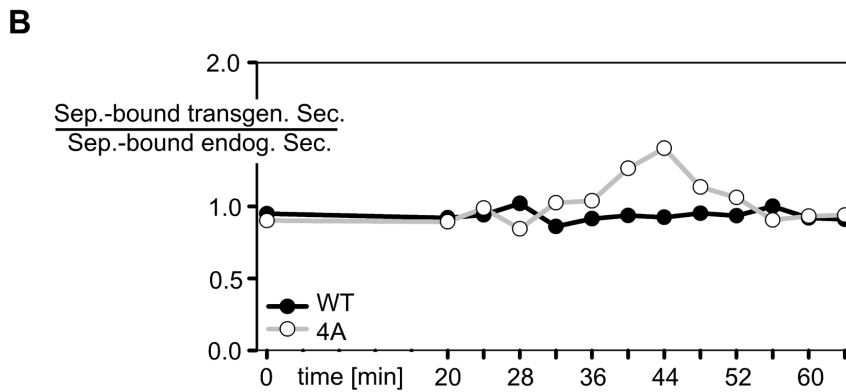
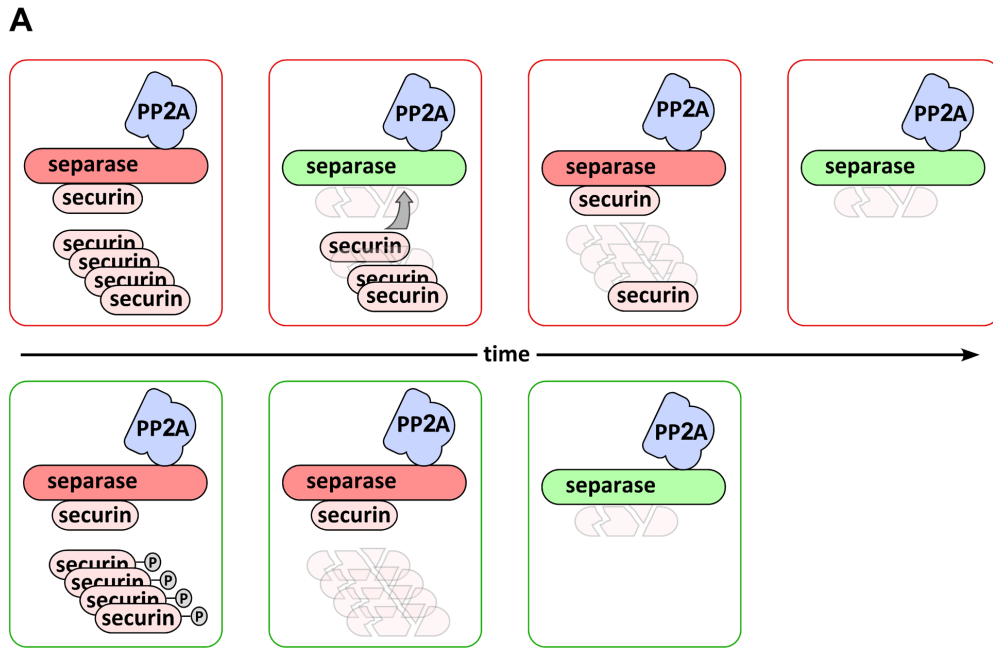


**Figure S7. The phosphorylation status of securin modulates anaphase.**

(A) Model of PP2A-restricted separase activation. Assuming there was no phosphorylation of securin, then the same (slow) degradation kinetics of free and separase-associated securin would cause separase activation to start earlier but take longer (top row). Re-inhibition of separase by remaining free securin would increase the effective pool of separase-associated securin and contribute to a decelerated metaphase-to-anaphase (see (B) and grey arrow). Instead, the actually preferred degradation of free, phosphorylated securin over separase-bound, de-phosphorylated securin ensures that free securin is largely cleared from the cell before separase is rapidly activated in a switch-like manner (lower row, see text for details). Color code: Green = active separase, red = inactive separase.

(B) Within the pool of separase-associated securin the percentage of securin-4A transiently increases upon APC/C activation. Blotted is the amount of separase-bound securin-4A relative to the amount of separase-bound endogenous securin against time after ZM-addition ( $t = 0$  min) to taxol-arrested cells. Averages of densitometric analysis of three independent experiments are shown (compare Figure 2A).

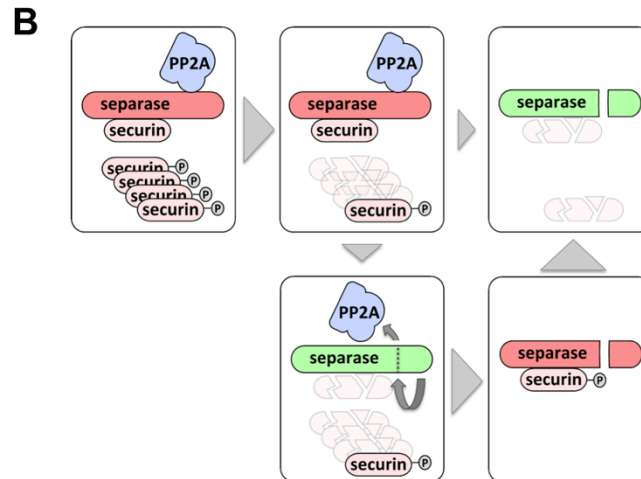
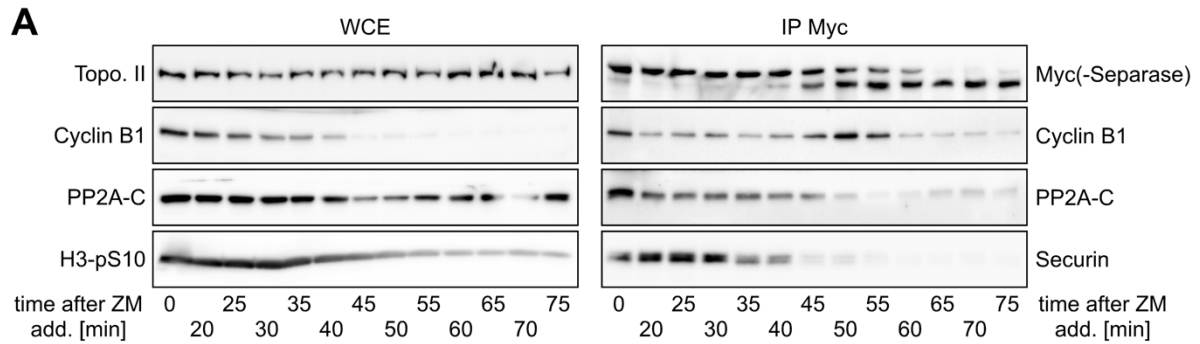


**Figure S8. Auto-cleavage may enhance separase activation at the metaphase-to-anaphase transition.**

**(A)** Auto-cleavage of separase counteracts association with PP2A. Mitotically arrested HeLa cells induced to overexpress Myc-tagged separase-WT were released from taxol arrest by addition of ZM. Cells were harvested at indicated time points and transgenic separase was immunoprecipitated with anti-Myc. Whole cell extracts (WCE) and IPs were analysed by immunoblotting as indicated. Topoisomerase II (Topo. II) and phosphorylated serine 10 of histone H3 (H3-pS10) served as loading control and mitotic marker, respectively, within WCE samples.

**(B)** Model of how auto-cleavage might minimize re-inhibition of previously activated separase. Once liberated, separase will cleave itself, thereby preventing PP2A binding. Any lingering securin that re-binds will now stay phosphorylated and therefore be subject to accelerated APC/C-dependent proteolysis.

# Positive and Negative Regulation of Vertebrate Separase by Cdk1-Cyclin B1 May Explain Why Securin Is Dispensable\*

Received for publication, September 29, 2014, and in revised form, January 30, 2015. Published, JBC Papers in Press, February 6, 2015, DOI 10.1074/jbc.M114.615310

Susanne Hellmuth<sup>‡</sup>, Christopher Pöhlmann<sup>§</sup>, Andreas Brown<sup>‡</sup>, Franziska Böttger<sup>‡</sup>, Mathias Sprinzl<sup>§</sup>, and Olaf Stemmann<sup>‡,1</sup>

From the Chairs of<sup>‡</sup>Genetics and<sup>§</sup>Biochemistry, University of Bayreuth, 95440 Bayreuth, Germany

**Background:** Separase, the trigger protease of eukaryotic anaphase, remains regulated in the absence of its inhibitor, securin.

**Results:** Cdk1-cyclin B1 triggers precipitation of separase by phosphorylation but stabilizes it by inhibitory binding.

**Conclusion:** Only separase that is first complexed by Cdk1-cyclin B1 can later be activated by cyclin B1 degradation.

**Significance:** These minimal requirements of separase regulation could explain the faithful execution of anaphase in the absence of securin.

Sister chromatid cohesion is established during replication by entrapment of both dsDNAs within the cohesin ring complex. It is dissolved in anaphase when separase, a giant cysteine endopeptidase, cleaves the Scc1/Rad21 subunit of cohesin, thereby triggering chromosome segregation. Separase is held inactive by association with securin until this anaphase inhibitor is destroyed at the metaphase-to-anaphase transition by ubiquitin-dependent degradation. The relevant ubiquitin ligase, the anaphase-promoting complex/cyclosome, also targets cyclin B1, thereby causing inactivation of Cdk1 and mitotic exit. Although separase is essential, securin knock-out mice are surprisingly viable and fertile. Capitalizing on our previous finding that Cdk1-cyclin B1 can also bind and inhibit separase, we investigated whether this kinase might be suitable to maintain faithful timing and execution of anaphase in the absence of securin. We found that, similar to securin, Cdk1-cyclin B1 regulates separase in both a positive and negative manner. Although securin associates with nascent separase to co-translationally assist proper folding, Cdk1-cyclin B1 acts on native state separase. Upon entry into mitosis, Cdk1-cyclin B1-dependent phosphorylation of Ser-1126 renders separase prone to inactivation by aggregation/precipitation. Stable association of Cdk1-cyclin B1 with phosphorylated separase counteracts this tendency and stabilizes separase in an inhibited yet activatable state. These opposing effects are suited to prevent premature cleavage of cohesin in early mitosis while ensuring timely activation of separase by anaphase-promoting complex/cyclosome-dependent degradation of cyclin B1. Coupling sister chromatid separation with subsequent exit from mitosis by this simplified mode might have been the common scheme of mitotic control prior to the evolution of securin.

Separase, a giant cysteine endopeptidase, triggers all eukaryotic anaphases (1). It cleaves the Scc1/Rad21 subunit of the ring-shaped cohesin complex, which, up to this point, main-

tains cohesion by entrapping the two sister chromatids of each chromosome (2, 3). Prior to anaphase, separase is held in check by association with securin (4). When the sister kinetochores of every chromosome have acquired a proper amphitelic attachment to microtubules from opposite spindle poles, separase is unleashed in its proteolytically active form by ubiquitin-dependent degradation of securin (4). The relevant E3 ligase is the anaphase-promoting complex/cyclosome, which also sees to the destruction of cyclin B1, the activating subunit of Cdk1 (cyclin-dependent kinase 1) (5). The resulting concomitant activation of separase and inactivation of the master regulatory kinase of mitosis couple sister chromatid separation with mitotic exit.

Securin and separase also influence each other in a positive way. This is illustrated by identical loss-of-function phenotypes for securin and separase in species in which securin is essential and by elevated levels of securin as a result of separase overexpression (6–8). Phosphorylation turns vertebrate securin into a better anaphase-promoting complex/cyclosome substrate. This is counteracted by separase, which mediates the PP2A (protein phosphatase 2A)-dependent dephosphorylation and hence stabilization of associated securin (9). Although this provides an explanation for the positive effect of separase on securin, data are lacking that address how vertebrate securin positively affects separase.

Given the essentiality of separase, it is a surprise that mice and cultured human cells are largely unaffected by the knock-out of securin (1, 10, 11). Could it be that, under these circumstances, regulation of the substrate rather than the protease takes center stage? Indeed, Plk1 (Polo-like kinase 1)-dependent phosphorylation of Scc1 enhances its cleavage by separase (12, 13). However, this phosphorylation is unlikely to be restricted to just the small window of metaphase-to-anaphase transition and does not constitute an absolute requirement for the cleavage of mitotic cohesin by separase. Therefore, regulation at the level of the substrate seems unfit to explain how securin-free mammalian cells maintain proper timing and fidelity of sister chromatid separation in mitosis. Instead, it is likely that, in the absence of securin, at least the inhibitory aspect of separase regulation is taken over by Cdk1-cyclin B1 (14).

\* This work was supported by Deutsche Forschungsgemeinschaft (DFG) Grants STE 997/3-2 (within the priority program SPP1384) and STE 997/4-1 (to O. S.).

<sup>1</sup> To whom correspondence should be addressed: Dept. of Genetics, University of Bayreuth, Universitätsstr. 30, 95440 Bayreuth, Germany. Tel.: 49-921-552701; Fax: 49-921-552710; E-mail: olaf.stemmann@uni-bayreuth.de.

This securin-independent inhibition of human separase requires that Ser-1126 and several residues within a Cdc6-like domain (CLD)<sup>2</sup> centered around position 1370 are phosphorylated by Cdk1-cyclin B1 (and possibly other mitotic kinases) (15, 16). Although necessary, these phosphorylations are not sufficient for inhibition of separase, which additionally requires Cdk1-cyclin B1 to stably associate, via its regulatory cyclin B1 subunit, with the phosphorylated CLD of separase (17). Within the Cdk1-cyclin B1-separase complex, Ser-1126 is probably not in direct contact with the kinase because this residue is dispensable for binding of Cdk1-cyclin B1 to separase fragments (16). However, Ser-1126 phosphorylation is absolutely required for Cdk1-cyclin B1 to associate with full-length separase. Interestingly, securin and Cdk1-cyclin B1 bind to separase in a mutually exclusive manner (17). At the level of an individual separase molecule, they therefore represent alternative rather than synergistic inhibitory mechanisms.

Although most of separase is typically controlled by securin, Cdk1-cyclin B1 can compensate for missing or limited securin. This is illustrated by the fact that murine embryonic stem cells with a combined securin knock-out and (heterozygote) knock-in of a Cdk1-cyclin B1-resistant separase allele quickly lose cohesion in a prometaphase arrest, whereas the isolated defects do not cause such a phenotype (18). Similarly, S1126A and  $\Delta$ CLD variants, but not WT separase, cause premature separation of sister chromatids upon overexpression in HEK293 cells (8). Although Cdk1-cyclin B1 seems able to always compensate for the loss of securin, securin cannot always substitute for Cdk1-cyclin B1 in separase regulation. For unknown reasons, murine early embryonic and post-migratory primordial germ cells express only little securin and fully rely on Cdk1-cyclin B1-dependent control of separase (19, 20). Despite the importance of this securin-independent control of anaphase, it remains enigmatic whether Cdk1-cyclin B1, similar to securin, might exert not only a negative but simultaneously also a positive effect on separase.

Here, we investigated the positive effect of securin on separase and demonstrate that co-translational association of securin with nascent separase coincides with increased solubility of the giant protease, indicating that securin assists separase in achieving a natively folded state. We unraveled two novel and opposing effects of Cdk1-cyclin B1 on separase. Upon entry into mitosis, Cdk1-cyclin B1-dependent phosphorylation of free separase further enhances the protease's tendency to become insoluble and catalytically inactive. This effect is counteracted by a stabilizing association of Cdk1-cyclin B1 with phosphorylated separase. Thus, much like securin, Cdk1-cyclin B1 is both a positive and negative regulator of separase at the same time. Together, these effects of Cdk1-cyclin B1 ensure that only separase, which has been in complex with its inhibitor in early mitosis, can later be activated at anaphase onset. Our findings help explain how anaphase and mitotic exit might have been coupled prior to the evolution of securin and are still coupled today in a securin knock-out.

<sup>2</sup> The abbreviations used are: CLD, Cdc6-like domain; TEV, tobacco etch virus; RNC, ribosome-nascent chain complex.

## EXPERIMENTAL PROCEDURES

**Antibodies**—The following antibodies were used for immunoblotting according to standard protocols: rabbit anti-separase (15), mouse anti-securin (1:1000; MBL International Corp.), mouse anti-Myc (1:50, clone 9E10, hybridoma supernatant; Developmental Studies Hybridoma Bank), rabbit anti-phospho-Ser-10 histone H3 (1:1000; Millipore), mouse anti-cyclin B1 (1:1000; Millipore), goat anti-Cdc27 (1:1000; gift from Thomas U. Mayer), and mouse anti- $\alpha$ -tubulin (1:200, clone 12G10, hybridoma supernatant; Developmental Studies Hybridoma Bank). For immunoprecipitation experiments, the following affinity matrices and antibodies were used: mouse anti-Myc antibody-agarose (Sigma-Aldrich) and protein A-Sepharose (GE Healthcare) coupled to rabbit anti-securin antibody (raised against His<sub>6</sub>-tagged full-length human securin).

**Cell Lines and Treatments**—For stable inducible expression of Myc<sub>6</sub>-tobacco etch virus (TEV)<sub>2</sub>-separase (WT, S1126A, and  $\Delta$ CLD (amino acids 1342–1400 deleted), the corresponding transgenes were stably integrated into an HEK293 Flp-In T-REx cell line. Clones were selected with 150  $\mu$ g/ml hygromycin B (Roth). Induction of transgenic myc<sub>6</sub>-TEV<sub>2</sub>-separase was done using 0.2–1  $\mu$ g/ml doxycycline (Sigma-Aldrich) for 10–14 h. All cells were cultured in DMEM (GE Healthcare) supplemented with 10% FCS (Sigma-Aldrich) at 37 °C and 5% CO<sub>2</sub>. For transient overexpression, HEK293T cells were transfected using the calcium phosphate-based method with pCS2-based plasmids encoding the following proteins: Myc<sub>6</sub>-TEV<sub>2</sub>-separase (WT and S1126A) and untagged WT securin (see Figs. 1B and 2B). For synchronization at the G<sub>1</sub>/S boundary, cells were treated with 2 mM thymidine (Sigma-Aldrich) for 20 h and released into fresh medium. Synchronization of cells in prometaphase was done by addition of nocodazole (Sigma-Aldrich) or Taxol (Calbiochem) at 0.2  $\mu$ g/ml each 6 h after release from a single thymidine block or for 14 h to asynchronous cells. Synchronization in interphase was achieved by addition of 10  $\mu$ M roscovitine (Calbiochem) for 20 h, followed by thymidine treatment for 12 h.

**Separase Pelleting and Activity Assays**—Myc<sub>6</sub>-TEV<sub>2</sub>-separase was expressed by transient transfection or induction of a stably integrated transgene in the presence or absence of securin co-overexpression. Securin-dependent solubility of endogenous separase (see Fig. 1B) was studied by comparing securin<sup>-/-</sup> with the corresponding parental HCT116 cells. Approximately 1  $\times$  10<sup>7</sup> prometaphase-arrested cells were lysed with a Dounce homogenizer in 1 ml of lysis buffer (20 mM Tris-HCl (pH 7.7), 100 mM NaCl, 10 mM NaF, 20 mM  $\beta$ -glycerophosphate, 5 mM MgCl<sub>2</sub>, 0.1% Triton X-100, and 5% glycerol) supplemented with complete protease inhibitor mixture (Roche Applied Science) and incubated for 10 min at 4 °C. Crude lysate (referred to as input) was ultracentrifuged at 66,000  $\times$  g for 35 min and the corresponding supernatant was harvested. The pellet was washed twice with 1 $\times$  PBS, combined with 1 ml of fresh denaturation buffer (8 M urea, 20 mM Tris-HCl (pH 6.8), and 2 mM DTT), and resolubilized by sonification (6 min, 20% power, 50% duty cycle; BANDELIN SONOPULS) on ice. For the separase activity assay (see Fig. 3A), crude lysates were

## Defining the Minimal Requirements of Separase Regulation

treated with Benzonase nuclease (30 units/liters; Santa Cruz Biotechnology) for 1 h at 4 °C. Crude lysate were incubated with anti-Myc beads for 4 h without prior centrifugation. Beads were washed and incubated three times for 5 min in 10 mM Hepes-KOH (pH 7.7), 100 mM KCl, 0.1 mM CaCl<sub>2</sub>, 2 mM MgCl<sub>2</sub>, 50 mM sucrose, 5 mM EGTA, and 0.02% Triton X-100 additionally supplemented with 400 mM NaCl (unless specified otherwise) and subsequently equilibrated in cleavage buffer (10 mM Hepes-KOH (pH 7.7), 50 mM NaCl, 25 mM NaF, 1 mM EGTA, and 20% glycerol) before separase was eluted by incubation with TEV protease. Concomitant with elution in a volume of 30 μl for 30 min at room temperature, separase activity was measured by addition of 2 μl of <sup>35</sup>S-labeled Scc1-GFP. Samples were analyzed by SDS-PAGE, followed by Western blotting or autoradiography.

**RNA Interference and Flow Cytometry**—For knockdown of human securin or separase, 70 nM siRNA duplex (securin, 5'-UCUUAGUGCUUCAGAGUUUGUGUGUAU-3'; and separase, 5'-AUAAGUGCCUGGCUUCACCAAACCC-3') was transfected either with RNAiMAX (Invitrogen) according to the manufacturer's instructions or following a calcium phosphate-based method. Luciferase siRNA (GL2) was used as a negative control. Cells were grown for at least 24 h before synchronization procedures were applied. Analysis of DNA content by flow cytometry was performed as described (9).

**Ribosome-Nascent Chain Complex Formation and Isolation**—The generation of ribosome-nascent chain complexes (RNCs) was based on the translation of truncated synthetic mRNA coding for at least 425 N-terminal amino acids of separase. Plasmids coding for separase or Crm1 (both pCS2-based) were linearized by restriction enzyme digestion at different positions within the coding sequence to create an open reading frame without a stop signal. To create a construct for the transcription of the separase 1–1105 Stop mRNA, a pCS2-based vector containing the coding sequence for full-length separase was linearized with XbaI, filled in with Klenow polymerase (New England Biolabs), and then religated to create a frameshift mutation. For generation of runoff transcripts, plasmids were linearized with a suitable restriction endonuclease, purified by phenol/chloroform extraction and ethanol precipitation, and redissolved in diethylpyrocarbonate/H<sub>2</sub>O. Transcription was carried out with 1 μg of pure linear DNA using an SP6 mMESSAGE mMACHINE kit (Ambion) according to the manufacturer's instructions. TNT rabbit reticulocyte lysate (Promega) was used for the generation of RNCs. A translation reaction was conducted in a volume of 20 μl in the presence of 1 μl of <sup>35</sup>S-labeled securin at 30 °C for 90 min and terminated (when no stop codon was present) by addition of 0.4 μl of 10 mg/ml cycloheximide. Aliquots were taken (referred to as input) before RNCs were further purified as described (21). Translation reaction mixtures were spun through a 80-μl cushion of buffer A (50 mM Tris-HCl (pH 7.0), 500 mM potassium acetate, 25 mM magnesium acetate, 2 mM DTT, 1 M sucrose, 10 μg/ml cycloheximide, and 0.1% Nonidet P-40) supplemented with complete protease inhibitor mixture at 180,000 × g for 90 min. Supernatants were harvested before the RNC pellets were washed twice with buffer B (32.5 mM Tris-HCl (pH 7.0), 125 mM potassium acetate, 26.25 mM magnesium acetate, 1.5 mM DTT,

250 mM sucrose, 100 μg/ml cycloheximide, 0.1% Nonidet P-40, and 0.4 units/μl RNasin) to remove residual soluble contaminants and then resuspended in 20 μl of buffer B. Input, supernatant, and resuspended pellet fractions were finally analyzed by SDS-PAGE and autoradiography.

**Electrochemical Biochip Analysis of mRNA Levels**—Electrochemical biochip analysis of mRNA levels was performed as described previously (22, 23). Capture oligonucleotides were as follows: securin, ACGGTTCCCGAAGGCACATTCTCATTTT-TTTTT (3'-thiol); and separase, TCTGCCCCGAAGGGGAC-GTCTATTTTTTTTT (3'-thiol). The detector oligonucleotide was TTTTTTGGTTGCGCTCGTTGCGGGACTTAACCCA-ACAT (5'-amino). Oligonucleotides used for preparation of complementary mRNA probes (with the T7 RNA polymerase promoter sequence underlined) were as follows: Securin\_1, GGTTGTAATACGACTCACTATAGGTGAGAATGTGCCTT; Securin\_2, GATGGGCACGGTTCCCGAAGGCACATTCTCAC; Securin\_3, CGGGAACCGTGCCCATCCTTAGCAACCACACG; Securin\_4, CTTAACCCAACATGGCACCCGTGTGTTGCTA; Securin\_5, TGCCATGTTGGGTTAAGTCCCGCAACGAGCGC; and Securin\_6, GGTTGCGCTCGTTGCGGGA; Separase\_1, GGTTGGTAATACGACTCACTATAGGTAGGACGTCCCCTT; Separase\_2, CAGCAGCTCTGCCCCGAAGGGGACGTCTCTAC; Separase\_3, CGGGGGCAGAGCTGCTGGTTGCAAGCCCTCAG; Separase\_4, CTTAACCCAACATGCCATCCTGAGGGCTTGCA; Separase\_5, TGGCATGTTGGGTTAAGTCCCGCAACGACGGC; and Separase\_6, GGTTGCGCTCGTTGCGGGA. An untreated gold electrode served as a negative control (blank).

Total RNA was isolated from human securin<sup>-/-</sup> and the parental HCT116 cells using an RNeasy mini kit (Qiagen) following the manufacturer's instructions. The integrity of ribosomal RNA was confirmed by agarose gel electrophoresis, and the quantity and purity of total RNA were spectrophotometrically confirmed. Deviating from the described procedure for microRNA analysis (22), total RNA was fragmented in the presence of 30 mM magnesium acetate, 100 mM potassium acetate, and 40 mM Tris-HCl (pH 8.1) at 95 °C for 15 min before hybridization. Fragmented RNA in 450 mM NaCl, 0.025% Tween 20, 1 mg/ml BSA, 25 mM EDTA, 30 mM NaH<sub>2</sub>PO<sub>4</sub> (pH 7.4), 1 μg of each complementary RNA probe, and 0.2 μM esterase 2-detector oligodeoxynucleotide conjugate was applied to each electrode. Electrode arrays were then incubated at 65 °C for 20 min in a humidity chamber, and the chip was kept at 20 °C for 5 min. After washing with 75 mM NaCl, 0.5 mM EDTA, 0.05% Tween 20, and 5 mM NaH<sub>2</sub>PO<sub>4</sub> (pH 7.4) for 1 min at 25 °C, the chip was inserted onto a multi-potentiostat. Background current reached steady state after flow through 100 mM NaCl and 10 mM sodium phosphate (pH 7.0) for ~1 min. Specific mRNA was detected by *Alicyclobacillus acidocaldarius* esterase 2 molecules bound to the electrode by hybridization. The enzyme substrate *p*-aminophenyl butyrate was delivered through the flow chamber at a flow rate of 250 μl/min. After the flow was stopped, the esterase 2 activity was measured as a change in current intensity (dI) per time (dt) within the first 5 s (22, 23).

**Immunofluorescence Staining of Pelleted Centrosomes**—Stable transgenic HEK293 Flp-In T-REx cells were transfected with separase or GL2 siRNA 24 h prior to synchronization at

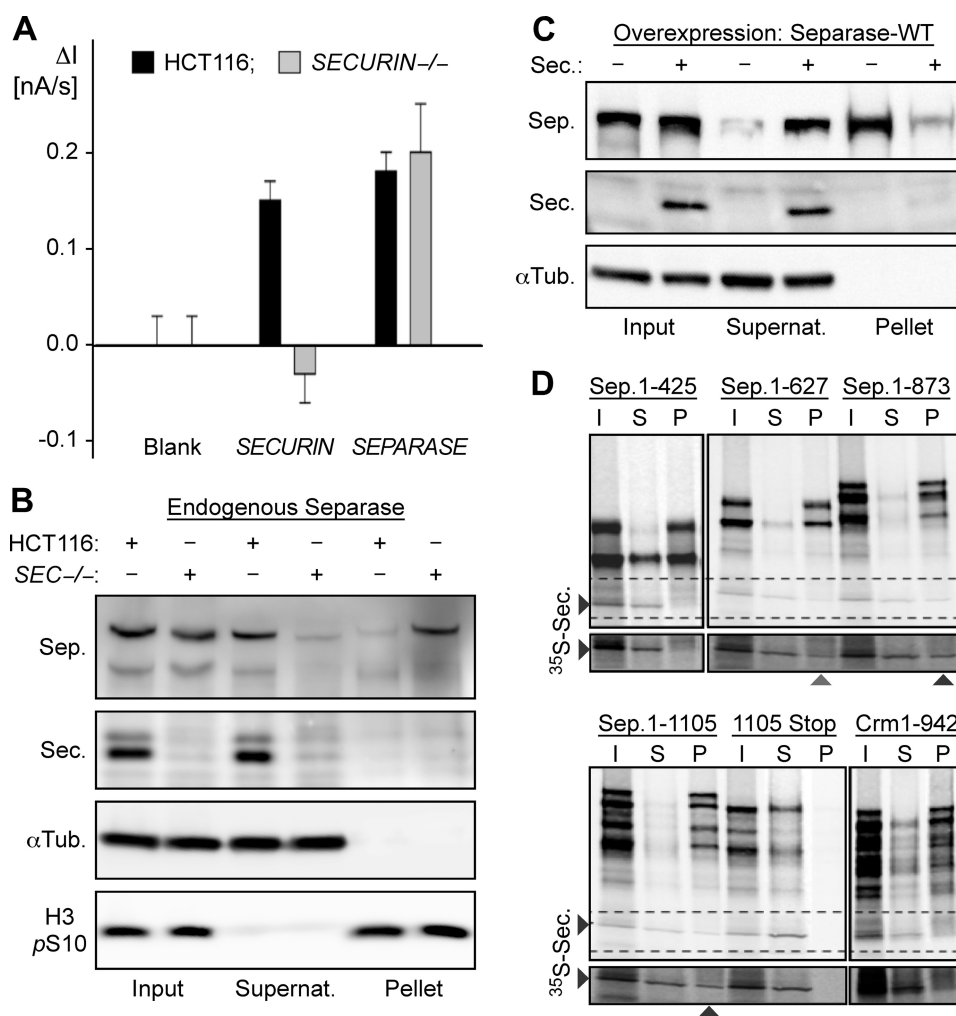


**FIGURE 1. Studying the positive effect of securin on separase.** *A*, securin does not influence the mRNA level of separase. The relative amounts of securin and separase mRNAs in securin<sup>-/-</sup> and parental HCT116 cells were quantified on an electrochemical biochip. *B*, endogenous separase (*Sep.*) is prone to precipitation in the absence of securin (*Sec.*). Lysates (input) of mitotically arrested securin<sup>-/-</sup> (*SEC<sup>-/-</sup>*) and parental HCT116 cells were centrifuged to assess the solubility of separase by Western analysis of the resulting supernatant (*Supernat.*) and pellet fractions.  $\alpha$ -Tubulin ( $\alpha$ *Tub.*) and Ser-10-phosphorylated histone H3 (*H3 pS10*) served as loading controls. *C*, association with securin prevents precipitation of transiently overexpressed separase. Following its overexpression in HEK293T cells with or without co-overexpression of securin, the solubility of separase was determined by centrifugation. *D*, co-translational association of securin with nascent separase. mRNAs lacking or containing a stop codon and coding for amino acids 1–425, 1–627, 1–873, or 1–1105 of human separase or amino acids 1–942 of human exportin-1 (*Crm1*) were translated *in vitro* in the presence of [<sup>35</sup>S]methionine and <sup>35</sup>S-labeled securin. Input (*I*) samples were fractionated by ultracentrifugation into supernatant (*S*) and RNC-containing pellet (*P*) fractions prior to SDS-PAGE and autoradiography. *Crm1* was chosen as a negative control because, similar to the N-terminal half of separase, it contains a superhelical structure.

G<sub>1</sub>/S by addition of thymidine. 20 h thereafter, cells were released into fresh medium, and where indicated, transgene expression was doxycycline-induced 8 h later. 16 h after release into fresh medium, cells were harvested and subjected to immunoblotting, flow cytometry, and centrosome purification. To assess centriole engagement status, centrosomes were isolated from  $4 \times 10^6$  cells and stained as described previously (24).

## RESULTS

Several publications have proposed roles for securin in transcriptional regulation (25–28). To address the possibility that securin might stimulate transcription of separase, the levels of separase mRNA in human securin<sup>-/-</sup> cells and the parental HCT116 line were compared using an electrochemical biochip (22, 23, 29). Here, the complementary binding of the target

mRNA fragment stabilizes the hybridization complex between a capture and a detector oligodeoxynucleotide, thereby bringing a reporter enzyme into the vicinity of an electrode to produce an electrochemical signal. This gap hybridization assay unambiguously revealed that separase mRNA levels are the same in both cell lines (Fig. 1A). This result strongly argues against a positive role of securin in transcription of separase. Immunoblotting consistently showed that the total amounts of separase in securin<sup>-/-</sup> and HCT116 cells are very similar (Fig. 1B, first and second lanes). However, the two cell lines greatly differ in the separase solubility as determined by simple centrifugation of total cell lysates. Although most separase from securin-containing HCT116 cells stayed in the supernatant, most separase from the securin-free knock-out cells pelleted (Fig. 1B, third through sixth lanes). Similarly, the overall level of separase in transiently transfected HEK293T cells was unaffected by co-

## Defining the Minimal Requirements of Separase Regulation

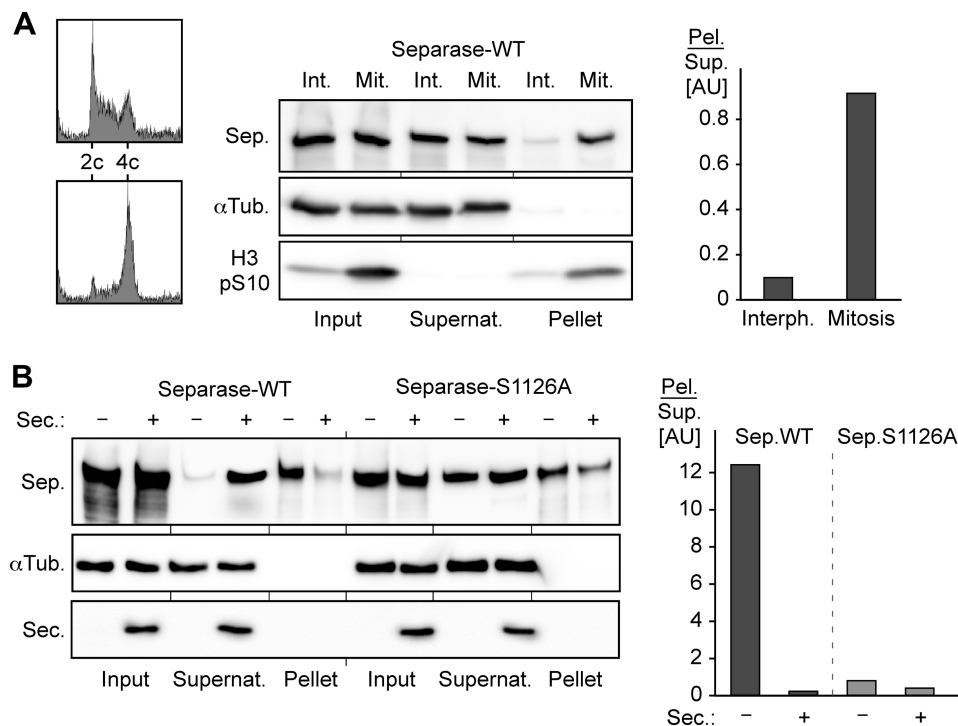


**FIGURE 2. Mitosis-specific phosphorylation of Ser-1126 decreases the solubility of separase.** *A*, aggravated aggregation tendency of separase (*Sep.*) in mitosis. Synchronized interphase (*Int.*, *Interph.*) or prometaphase (*Mit.*) transgenic HEK293 cells induced to express WT separase were stained with propidium iodide and analyzed by flow cytometry or lysed and subjected to ultracentrifugation and Western analysis. Signals for pelleted (*Pel.*) versus soluble (*Sup.*) separase were quantified by densitometry and are depicted as quotients (gray bars).  $\alpha$ Tub.,  $\alpha$ -tubulin; H3 pS10, Ser-10-phosphorylated histone H3; *Supernat.*, supernatant; *AU*, arbitrary units. *B*, preventing phosphorylation of Ser-1126 stabilizes securin-less separase. HEK293T cells transiently overexpressing securin (*Sec.*) and/or Myc-tagged WT separase or S1126A were arrested in prometaphase before the solubility of separase was determined by pelleting assay and quantified as described for *A*.

overexpression of securin, whereas separase solubility was strongly stimulated (Fig. 1C). In summary, we propose that securin has no effect on transcription, mRNA stability, or translation efficiency of separase. Instead, it appears to prevent aggregation/precipitation of separase presumably to keep it in a conformational state, from which it can later be activated by proteasomal degradation of ubiquitylated securin.

To fulfill its dual function as a separase specific chaperone and inhibitor, securin might bind to the protease co-translationally. To clarify this issue, we tested whether recombinant securin added to *in vitro* translation mixtures would associate with RNCs (21) if and only if separase was being translated. Indeed,  $^{35}$ S-labeled securin co-purified with ribosomes stalled in the process of translation on an mRNA that codes for the first 1105 amino acids of separase but lacks a stop codon (Fig. 1D). However, it could not be pelleted if ribosomes were stalled on a control mRNA or if a stop codon within the mRNA allowed for dissociation of the separase fragment from ribosomes. The use of stop codon-less mRNAs that encode increasingly shorter N-terminal separase fragments revealed that securin cannot interact with RNCs displaying the first 425 amino acids but starts to bind to nascent separase 627 amino acids in length (Fig. 1D). These observations suggest that co-translational association of securin with separase serves two purposes: assisting the giant protease in achieving a native fold and inhibiting it at the same time.

Given that vertebrate securin is dispensable for life, a sufficient amount of separase apparently reaches a natively folded

state even in the absence of securin. But who controls separase under these conditions to prevent premature separation of sister chromatids? An obvious candidate is Cdk1-cyclin B1 because, next to securin, this kinase constitutes the only other known inhibitor of vertebrate separase (15, 17). Interestingly, the tendency of overexpressed separase to be spun out from a cell lysate by centrifugation is enhanced in mitosis compared with interphase, consistent with the idea that mitotic phosphorylation renders separase particularly prone to aggregation/precipitation (Fig. 2A). On the basis of this observation and our previous work (16), we speculated that Ser-1126 phosphorylation by Cdk1-cyclin B1 induces a conformational change in native state separase with two opposing consequences. On the one hand, it favors misfolding/aggregation, but on the other hand, it renders the CLD accessible to association with cyclin B1, and this complex formation stabilizes the native fold of separase. This suggestion was easily testable because it predicted that changing Ser-1126 to Ala should prevent the conformational change, thereby rendering separase resistant to precipitation in mitosis. In contrast, preserving Ser-1126 but deleting the CLD should still allow for the conformational switch to occur but abrogate the downstream association with Cdk1-cyclin B1, thereby enhancing the tendency of separase to precipitate.

HEK293T cells were transiently transfected to overexpress WT separase or an S1126A variant and then arrested in mitosis. As before, corresponding lysates were fractionated by centrifugation into a soluble supernatant and insoluble pellet. Subse-

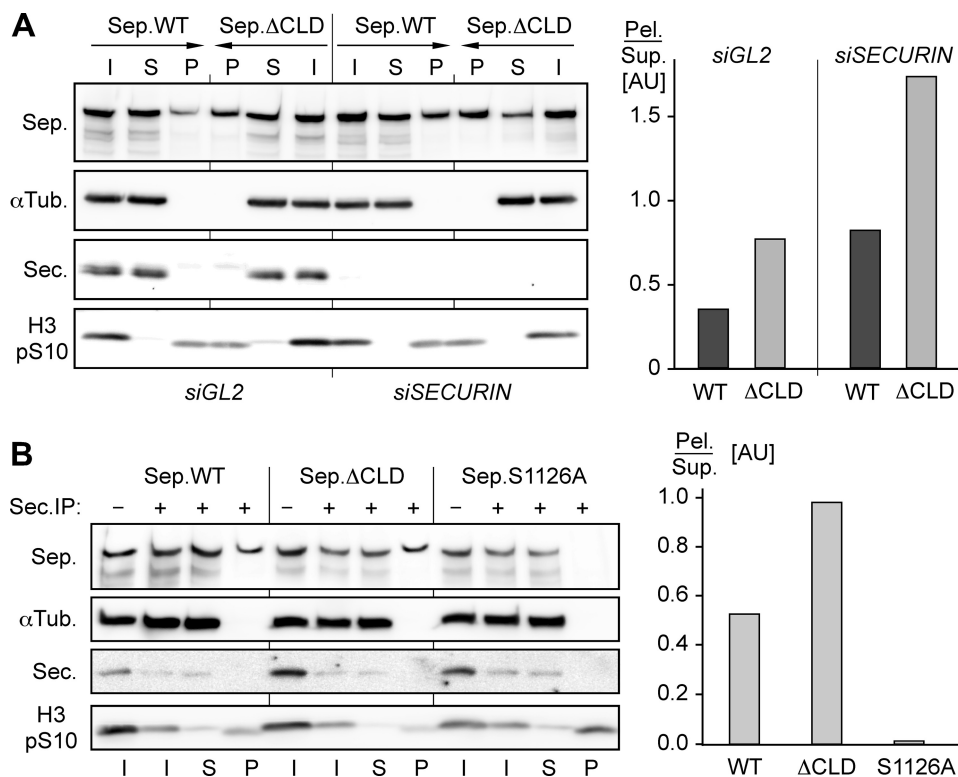


**FIGURE 3. Ser-1126 phosphorylation and binding of Cdk1-cyclin B1 have opposing effects on separase solubility.** *A*, mutational inactivation of its cyclin B1-binding site decreases the solubility of separase (*Sep.*). Transgenic HEK293 cells transfected with securin (*siSECURIN*) or GL2 (*siGL2*) siRNA and expressing WT separase or  $\Delta$ CLD were arrested in prometaphase before the solubility of separase was determined by pelleting assay and quantified as described for Fig. 2*A*. *I*, input; *S*, supernatant; *P*, pellet;  $\alpha$ Tub.,  $\alpha$ -tubulin; *Sec.*, securin; *H3 pS10*, Ser-10-phosphorylated histone H3; *AU*, arbitrary units; *Pel.*, pelleted separase; *Sup.*, soluble separase. *B*, precipitation of separase in mitosis is alleviated by the S1126A mutation but aggravated by CLD deletion. Lysates of transgenic, prometaphase-arrested HEK293 cells expressing the indicated separase variants were immunodepleted of securin before the solubility of securin-free separase was determined by quantitative pelleting assay as described for Fig. 2*A*. *IP*, immunoprecipitation.

quent immunoblotting revealed that the profound aggregation of separase in mitosis was indeed greatly suppressed by changing Ser-1126 to Ala (Fig. 2*B*). Conversely, a  $\Delta$ CLD variant exhibited aggravated insolubility relative to WT separase as revealed by analysis of the corresponding transgenic HEK293 lines by the same pelleting assay (Fig. 3*A*). As expected, siRNA-mediated depletion of securin enhanced the insolubility of overexpressed separase in general and of the  $\Delta$ CLD variant in particular (Fig. 3*A*). Using transiently transfected, nocodazole-arrested HEK293T cells, we also directly compared the aggregation tendencies of WT separase and mutants S1126A and  $\Delta$ CLD after removal of the securin-associated pool. To this end, securin was immunodepleted prior to centrifugation of the lysates. Confirming the previous results, the insolubility of S1126A was again reduced relative to the WT protease, whereas that of the  $\Delta$ CLD variant was again increased (Fig. 3*B*).

The centrifugation of cell lysates quickly determined solubility of separase but did not allow us to draw conclusions about its proteolytic activity. To clarify this issue, Myc-tagged WT separase and mutants S1126A and  $\Delta$ CLD were transiently overexpressed in HEK293T cells with or without simultaneous overexpression of securin. Following cell synchronization in prometaphase, the corresponding lysates were subjected to anti-Myc immunoprecipitation without prior centrifugation to avoid removal of insoluble separase fractions. Finally, the immunoaffinity-purified separase variants were assayed for their ability to cleave cohesin (Fig. 4*A*). When produced under

conditions of limiting amounts of securin, WT separase and S1126A exhibited proteolytic activity toward  $^{35}$ S-labeled Scc1, but  $\Delta$ CLD did not (Fig. 4*A*, lanes 1, 4, and 6). In the case of WT separase, cohesin cleavage activity became apparent only upon displacement of co-purified Cdk1-cyclin B1 by washing with a high ionic strength buffer (compare lanes 1 and 2) (17). As expected, none of the protease variants cleaved Scc1 when securin had been co-overexpressed (lanes 3, 5, and 7). In combination with the pelleting assays, this experiment demonstrates good accordance of solubility and proteolytic activity for securin-less separase. In summary, we interpret our observations as follows. Under conditions of limiting securin, WT separase and  $\Delta$ CLD are switched by Ser-1126 phosphorylation into a precipitation-prone conformation. Although WT separase is protected by association with Cdk1-cyclin B1 and stays soluble and activatable, the  $\Delta$ CLD variant, which cannot form this complex, aggregates/misfolds and quickly becomes inactive. S1126A also cannot bind to Cdk1-cyclin B1, but for another reason. It is already protected from the destabilizing conformational change and hence retains proteolytic activity despite the lack of any binding partner.

Separase also has a chromosome-independent function within the centrosome cycle (30). By cleaving centrosomal cohesin and kendrin/pericentrin B, separase triggers centriole disengagement, which represents a licensing step for subsequent centriole duplication (24, 30–32). In the absence of separase function, centriole disengagement is profoundly delayed,

## Defining the Minimal Requirements of Separase Regulation

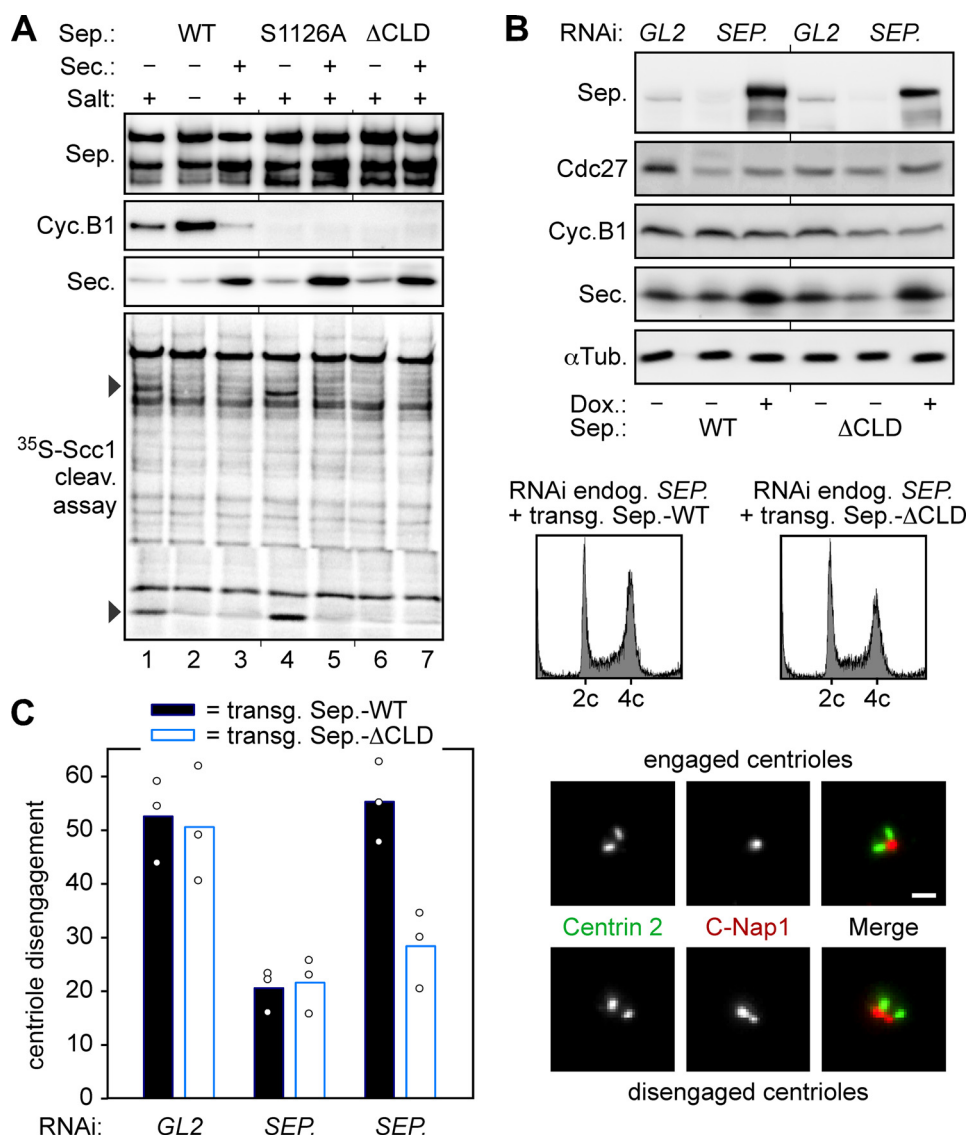


**FIGURE 4. Positive and negative effects of Cdk1-cyclin B1 define the minimal requirements of separase regulation in mitosis.** A, WT separase and mutants S1126A and  $\Delta$ CLD exhibit some, high, or no cohesin cleavage activity upon isolation from prometaphase-arrested cells, respectively. Taxol-treated HEK293T cells transiently overexpressing securin (Sec.) and/or Myc<sub>6</sub>-TEV<sub>2</sub>-tagged WT separase (Sep.), S1126A, or  $\Delta$ CLD were lysed and subjected to anti-Myc immunoprecipitation without prior centrifugation to avoid the removal of insoluble separase fractions. Where indicated, separase-associated Cdk1-cyclin B1 (Cyc.B1) was washed away with a high salt buffer. TEV protease-eluted separases were analyzed by immunoblotting and <sup>35</sup>S-labeled Scc1 cleavage assay/autoradiography. B and C, in  $\Delta$ CLD-expressing cells, the short half-life of proteolytic activity correlates with reduced centriole disengagement. Transgenic HEK293 cells transfected with separase or GL2 siRNA were thymidine-arrested and, where indicated, induced to express WT separase or  $\Delta$ CLD. Cells were harvested 16 h after release into fresh medium and analyzed by immunoblotting, propidium iodide flow cytometry (B), and immunofluorescence microscopy of purified centrosomes (C). Fixed centrosomes were co-stained for centrin-2 and C-Nap1. Depending on a centrin-2 to C-Nap1 signal ratio of 2:1 or 2:2, centrioles were classified as engaged or disengaged, respectively. In three independent experiments (dots), the engagement status of at least 200 centrosomes per cell line and condition was analyzed and blotted as mean values (bars). Scale bar = 1  $\mu$ m.  $\alpha$ Tub.,  $\alpha$ -tubulin; Dox., doxycycline.

but eventually still occurs by an unresolved mechanism that requires Plk1 activity (33). Because centriole disengagement normally takes place after sister chromatid separation at the end of mitosis or in early G<sub>1</sub> phase and because the proteolytic activity of  $\Delta$ CLD seems to exhibit a short half-life, centriole disengagement might be delayed upon replacement of endogenous separase by this deregulated variant. To test this prediction, stable transgenic HEK293 cells depleted of endogenous separase by RNAi were analyzed by immunofluorescence microscopy for their centriole engagement status 16 h after release from G<sub>1</sub>/S arrest and 8 h after induction of WT separase or  $\Delta$ CLD expression by addition of doxycycline. Mock siRNA

(GL2)-transfected, uninduced cells served as an additional control. All separase-expressing cultures exhibited highly similar cell cycle distributions as judged by flow cytometry and immunoblotting (Fig. 4B and data not shown). However, although centrioles were disengaged in ~55% of all WT separase-containing cells, only 28% of  $\Delta$ CLD-expressing cells displayed centriole disengagement on average (Fig. 4C). The above loss-of-function phenotypes do not contradict the observation that overexpression of  $\Delta$ CLD causes premature separation of sister chromatids in prometaphase-arrested cells (8, 16).  $\Delta$ CLD is a hypermorph in that it can no longer be bound and inhibited by Cdk1-cyclin B1, but at the same time, it is a hypomorph because

Ser-1126 phosphorylation renders it aggregation-prone, thus limiting its half-life as an active protease.

## DISCUSSION

Considering its central role in chromosome segregation, it is not surprising that hypo- and hyperactivity of separase both cause aneuploidy and cancer (34–38). Thus, activation of this essential but dangerous protease must be exactly controlled and timed. Here, we found that, *in vitro*, securin associates with nascent separase polypeptides while they are still on ribosomes and that securin-less separase tends to aggregate/precipitate as determined by pelleting assay. Based on these results, the co-translational association of securin with separase both assists the giant protease in achieving a natively folded state and inhibits it at the same time. Interestingly, caspase-activated DNase, another dangerous enzyme that needs tight controlling, also misfolds and aggregates during translation if it does not associate co-translationally with its inhibitor (39, 40). Merging in one protein (securin or caspase-activated DNase inhibitor) the functions of a specific inhibitor and of a specific chaperone therefore appears ideally suited to prevent the unscheduled unleashing of enzymatic activities that would otherwise threaten genome integrity.

We also analyzed the effects of Cdk1-cyclin B1 on separase. By phosphorylating Ser-1126, this chief mitotic kinase increases the tendency of securin-free separase to aggregate and become inactive. Interestingly, this inactivation mechanism involves a conformational change as a result of *cis/trans*-isomerization at Pro-1127, which is catalyzed by the phospho-Ser/Pro-specific peptidyl-prolyl isomerase Pin1.<sup>3</sup> However, although Ser-1126 phosphorylation limits the half-life of the proteolytic activity of separase, Cdk1-cyclin B1 simultaneously counteracts this inactivation mechanism by stable association with the protease in a second step (Fig. 5). Thus, like securin, Cdk1-cyclin B1 also unites the functions of a specific inhibitor and a specific chaperone. Unlike securin, however, it does not assist in folding but rather protects from a “phosphorylation shock” (by analogy to “heat shock”) that it inflicts on separase as the cell enters mitosis (15). In this manner, it is ensured that, even in the absence of securin, any separase, which can later be activated, is first held inactive by association with Cdk1-cyclin B1. This mechanism, plus the fact that chromosomes become accessible to separase only when the nuclear envelope breaks down at the onset of mitosis (41), could explain why vertebrate securin is not essential (10). Our findings furthermore suggest that, in a primordial eukaryotic cell, the control of sister chromatid separation and mitotic exit might have been both mastered by Cdk1-cyclin B1. Then, with the invention of securin, sister chromatid separation was gradually handed over to this folding helper and superior inhibitor but stayed linked to mitotic exit via the simultaneous anaphase-promoting complex/cyclosome-mediated degradation of securin and cyclin B1. In some organisms such as yeast, the Cdk1-cyclin B1-dependent separase regulation appears to have been totally lost during evolution. However, as mouse genetics teach us, this form of

<sup>3</sup> S. Hellmuth, S. Rata, A. Brown, S. Heidmann, B. Novak, and O. Stemmann, submitted for publication.

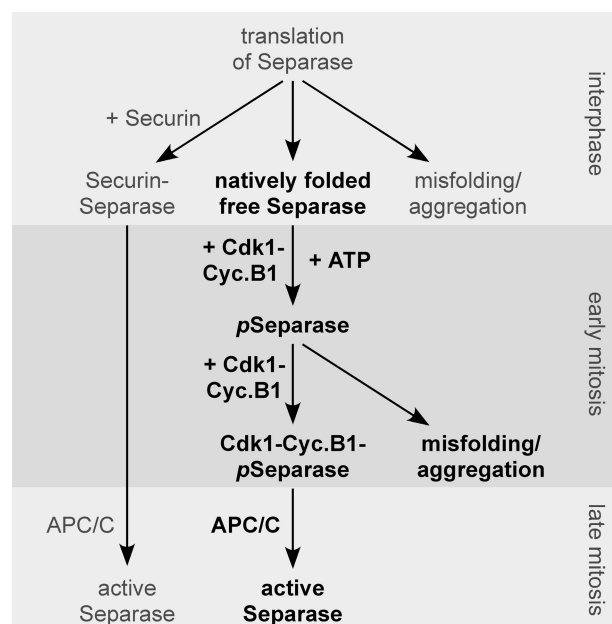


**FIGURE 5. Model of how phosphorylation and mutually exclusive association with securin or Cdk1-cyclin B1 determine the fate of separase across the cell cycle.** The minimal module of separase control (shown in *boldface*) relies only on the positive and negative effects of Cdk1-cyclin B1 (*Cyc.B1*) on separase to maintain faithful chromosome segregation in the absence of securin. *pSeparase*, phosphorylated separase; *APC/C*, anaphase-promoting complex/cyclosome.

anaphase control remains essential in mammals until today (19, 20).

*Acknowledgments*—We thank Stefan Heidmann for critical reading of the manuscript and Dorothea Karalus for helping establish the RNC assay.

## REFERENCES

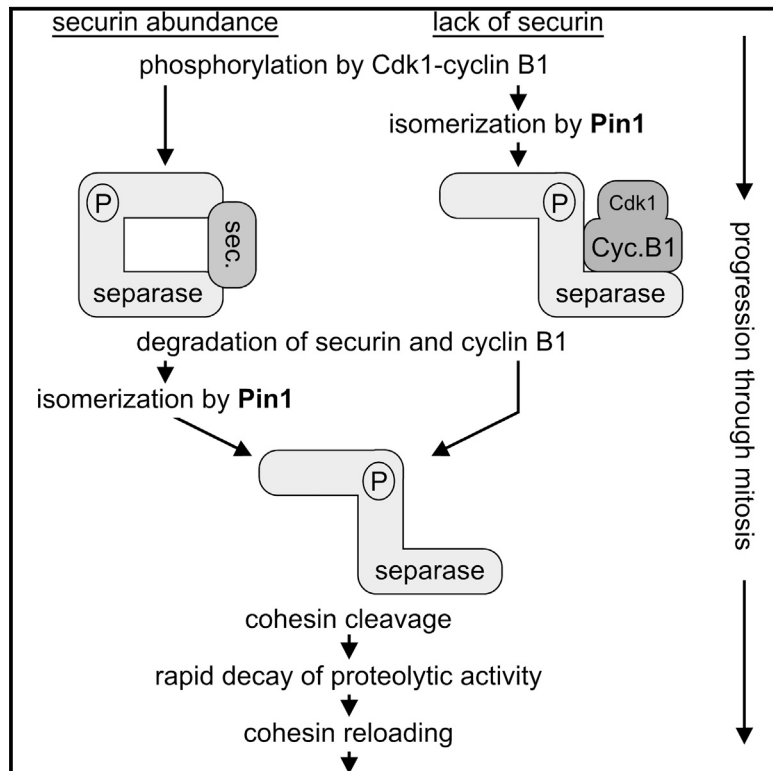
- Wirth, K. G., Wutz, G., Kudo, N. R., Desdouets, C., Zetterberg, A., Taghybeeglu, S., Seznec, J., Ducos, G. M., Ricci, R., Firnberg, N., Peters, J. M., and Nasmyth, K. (2006) Separase: a universal trigger for sister chromatid disjunction but not chromosome cycle progression. *J. Cell Biol.* **172**, 847–860
- Uhlmann, F., Wernic, D., Poupart, M. A., Koonin, E. V., and Nasmyth, K. (2000) Cleavage of cohesin by the CD clan protease separin triggers anaphase in yeast. *Cell* **103**, 375–386
- Haering, C. H., Farcas, A. M., Arumugam, P., Metson, J., and Nasmyth, K. (2008) The cohesin ring concatenates sister DNA molecules. *Nature* **454**, 297–301
- Zou, H., McGarry, T. J., Bernal, T., and Kirschner, M. W. (1999) Identification of a vertebrate sister-chromatid separation inhibitor involved in transformation and tumorigenesis. *Science* **285**, 418–422
- King, R. W., Peters, J. M., Tugendreich, S., Rolfe, M., Hieter, P., and Kirschner, M. W. (1995) A 20 S complex containing CDC27 and CDC16 catalyzes the mitosis-specific conjugation of ubiquitin to cyclin B. *Cell* **81**, 279–288
- Funabiki, H., Kumada, K., and Yanagida, M. (1996) Fission yeast Cut1 and Cut2 are essential for sister chromatid separation, concentrate along the metaphase spindle and form large complexes. *EMBO J.* **15**, 6617–6628
- Jäger, H., Herzig, A., Lehner, C. F., and Heidmann, S. (2001) *Drosophila* separase is required for sister chromatid separation and binds to PIM and THR. *Genes Dev.* **15**, 2572–2584
- Holland, A. J., and Taylor, S. S. (2006) Cyclin-B1-mediated inhibition of excess separase is required for timely chromosome disjunction. *J. Cell Sci.* **119**, 3325–3336

## Defining the Minimal Requirements of Separase Regulation

- Hellmuth, S., Böttger, F., Pan, C., Mann, M., and Stemmann, O. (2014) PP2A delays APC/C-dependent degradation of separase-associated but not free securin. *EMBO J.* **33**, 1134–1147
- Mei, J., Huang, X., and Zhang, P. (2001) Securin is not required for cellular viability, but is required for normal growth of mouse embryonic fibroblasts. *Curr. Biol.* **11**, 1197–1201
- Pfleghaar, K., Heubes, S., Cox, J., Stemmann, O., and Speicher, M. R. (2005) Securin is not required for chromosomal stability in human cells. *PLoS Biol.* **3**, e416
- Alexandru, G., Uhlmann, F., Mechtler, K., Poupart, M. A., and Nasmyth, K. (2001) Phosphorylation of the cohesin subunit Scc1 by Polo/Cdc5 kinase regulates sister chromatid separation in yeast. *Cell* **105**, 459–472
- Hauf, S., Roitinger, E., Koch, B., Dittrich, C. M., Mechtler, K., and Peters, J. M. (2005) Dissociation of cohesin from chromosome arms and loss of arm cohesion during early mitosis depends on phosphorylation of SA2. *PLoS Biol.* **3**, e69
- Stemmann, O., Gorr, I. H., and Boos, D. (2006) Anaphase tropy-turvy: Cdk1 a securin, separase a CKI. *Cell Cycle* **5**, 11–13
- Stemmann, O., Zou, H., Gerber, S. A., Gygi, S. P., and Kirschner, M. W. (2001) Dual inhibition of sister chromatid separation at metaphase. *Cell* **107**, 715–726
- Boos, D., Kuffer, C., Lenobel, R., Körner, R., and Stemmann, O. (2008) Phosphorylation-dependent binding of cyclin B1 to a Cdc6-like domain of human separase. *J. Biol. Chem.* **283**, 816–823
- Gorr, I. H., Boos, D., and Stemmann, O. (2005) Mutual inhibition of separase and Cdk1 by two-step complex formation. *Mol. Cell* **19**, 135–141
- Huang, X., Hatcher, R., York, J. P., and Zhang, P. (2005) Securin and separase phosphorylation act redundantly to maintain sister chromatid cohesion in mammalian cells. *Mol. Biol. Cell* **16**, 4725–4732
- Huang, X., Andreu-Vieyra, C. V., York, J. P., Hatcher, R., Lu, T., Matzuk, M. M., and Zhang, P. (2008) Inhibitory phosphorylation of separase is essential for genome stability and viability of murine embryonic germ cells. *PLoS Biol.* **6**, e15
- Huang, X., Andreu-Vieyra, C. V., Wang, M., Cooney, A. J., Matzuk, M. M., and Zhang, P. (2009) Preimplantation mouse embryos depend on inhibitory phosphorylation of separase to prevent chromosome missegregation. *Mol. Cell Biol.* **29**, 1498–1505
- Beckmann, R., Spahn, C. M., Eswar, N., Helmers, J., Penczek, P. A., Sali, A., Frank, J., and Blobel, G. (2001) Architecture of the protein-conducting channel associated with the translating 80 S ribosome. *Cell* **107**, 361–372
- Pöhlmann, C., and Sprinzl, M. (2010) Electrochemical detection of microRNAs via gap hybridization assay. *Anal. Chem.* **82**, 4434–4440
- Wang, Y., Stanzel, M., Gumbrecht, W., Humenik, M., and Sprinzl, M. (2007) Esterase 2-oligodeoxynucleotide conjugates as sensitive reporter for electrochemical detection of nucleic acid hybridization. *Biosens. Bioelectron.* **22**, 1798–1806
- Schöckel, L., Möckel, M., Mayer, B., Boos, D., and Stemmann, O. (2011) Cleavage of cohesin rings coordinates the separation of centrioles and chromatids. *Nat. Cell Biol.* **13**, 966–972
- Bernal, J. A., Luna, R., Espina, A., Lázaro, I., Ramos-Morales, F., Romero, F., Arias, C., Silva, A., Tortolero, M., and Pintor-Toro, J. A. (2002) Human securin interacts with p53 and modulates p53-mediated transcriptional activity and apoptosis. *Nat. Genet.* **32**, 306–311
- Hamid, T., and Kakar, S. S. (2004) PTTG/securin activates expression of p53 and modulates its function. *Mol. Cancer* **3**, 18
- Pei, L. (2001) Identification of *c-myc* as a down-stream target for pituitary tumor-transforming gene. *J. Biol. Chem.* **276**, 8484–8491
- Tong, Y., and Eigler, T. (2009) Transcriptional targets for pituitary tumor-transforming gene-1. *J. Mol. Endocrinol.* **43**, 179–185
- Jallepalli, P. V., Waizenegger, I. C., Bunz, F., Langer, S., Speicher, M. R., Peters, J. M., Kinzler, K. W., Vogelstein, B., and Lengauer, C. (2001) Securin is required for chromosomal stability in human cells. *Cell* **105**, 445–457
- Tsou, M. F., and Stearns, T. (2006) Mechanism limiting centrosome duplication to once per cell cycle. *Nature* **442**, 947–951
- Matsuo, K., Ohsumi, K., Iwabuchi, M., Kawamata, T., Ono, Y., and Takahashi, M. (2012) Kendrin is a novel substrate for separase involved in the licensing of centriole duplication. *Curr. Biol.* **22**, 915–921
- Lee, K., and Rhee, K. (2012) Separase-dependent cleavage of pericentriolar B is necessary and sufficient for centriole disengagement during mitosis. *Cell Cycle* **11**, 2476–2485
- Tsou, M. F., Wang, W. J., George, K. A., Uryu, K., Stearns, T., and Jallepalli, P. V. (2009) Polo kinase and separase regulate the mitotic licensing of centriole duplication in human cells. *Dev. Cell* **17**, 344–354
- Shepard, J. L., Amatruda, J. F., Finkelstein, D., Ziai, J., Finley, K. R., Stern, H. M., Chiang, K., Hersey, C., Barut, B., Freeman, J. L., Lee, C., Glickman, J. N., Kutok, J. L., Aster, J. C., and Zou, L. I. (2007) A mutation in separase causes genome instability and increased susceptibility to epithelial cancer. *Genes Dev.* **21**, 55–59
- Mukherjee, M., Ge, G., Zhang, N., Huang, E., Nakamura, L. V., Minor, M., Fofanov, V., Rao, P. H., Herron, A., and Pati, D. (2011) Separase loss of function cooperates with the loss of p53 in the initiation and progression of T- and B-cell lymphoma, leukemia and aneuploidy in mice. *PLoS ONE* **6**, e22167
- Mukherjee, M., Ge, G., Zhang, N., Edwards, D. G., Sumazin, P., Sharan, S. K., Rao, P. H., Medina, D., and Pati, D. (2014) MMTV-Esp1 transgenic mice develop aneuploid, estrogen receptor alpha (ER $\alpha$ )-positive mammary adenocarcinomas. *Oncogene* **33**, 5511–5522
- Mukherjee, M., Byrd, T., Brawley, V. S., Bielamowicz, K., Li, X. N., Merchant, F., Maitra, S., Sumazin, P., Fuller, G., Kew, Y., Sun, D., Powell, S. Z., Ahmed, N. M., Zhang, N., and Pati, D. (2014) Overexpression and constitutive nuclear localization of cohesin protease Separase protein correlates with high incidence of relapse and reduced overall survival in glioblastoma multiforme. *J. Neurooncol.* **119**, 27–35
- Meyer, R., Fofanov, V., Panigrahi, A., Merchant, F., Zhang, N., and Pati, D. (2009) Overexpression and mislocalization of the chromosomal segregation protein separase in multiple human cancers. *Clin. Cancer Res.* **15**, 2703–2710
- Sakahira, H., and Nagata, S. (2002) Co-translational folding of caspase-activated DNase with Hsp70, Hsp40, and inhibitor of caspase-activated DNase. *J. Biol. Chem.* **277**, 3364–3370
- Sakahira, H., Iwamatsu, A., and Nagata, S. (2000) Specific chaperone-like activity of inhibitor of caspase-activated DNase for caspase-activated DNase. *J. Biol. Chem.* **275**, 8091–8096
- Sun, Y., Yu, H., and Zou, H. (2006) Nuclear exclusion of separase prevents cohesin cleavage in interphase cells. *Cell Cycle* **5**, 2537–2542

# Human Chromosome Segregation Involves Multi-Layered Regulation of Separase by the Peptidyl-Prolyl-Isomerase Pin1

## Graphical Abstract



## Authors

Susanne Hellmuth, Scott Rata, ...,  
Bela Novak, Olaf Stemmann

## Correspondence

olaf.stemmann@uni-bayreuth.de

## In Brief

Pin1, a peptidyl-prolyl *cis/trans* isomerase that acts on phosphorylated Ser/Thr-Pro motifs, is a crucial regulator of mitosis. Hellmuth et al. identify human separase as a Pin1 substrate. Isomerization determines association with two mutually exclusive binding partners and half-life of enzymatic activity of this essential trigger protease of sister chromatid separation.

## Highlights

- Separase is subject to native-state *cis/trans* isomerization by Pin1
- Once liberated, separase is rendered resistant to remaining securin by Pin1
- When securin is limiting, Pin1 is required for control of separase by Cdk1-cyclin B1
- Isomerization limits the half-life of separase's proteolytic activity in late mitosis

# Human Chromosome Segregation Involves Multi-Layered Regulation of Separase by the Peptidyl-Prolyl-Isomerase Pin1

Susanne Hellmuth,<sup>1</sup> Scott Rata,<sup>2</sup> Andreas Brown,<sup>1</sup> Stefan Heidmann,<sup>1</sup> Bela Novak,<sup>2</sup> and Olaf Stemmann<sup>1,\*</sup>

<sup>1</sup>Chair of Genetics, University of Bayreuth, Universitätsstraße 30, 95440 Bayreuth, Germany

<sup>2</sup>Department of Biochemistry, University of Oxford, South Parks Road, Oxford OX1 3QU, UK

\*Correspondence: [olaf.stemmann@uni-bayreuth.de](mailto:olaf.stemmann@uni-bayreuth.de)

<http://dx.doi.org/10.1016/j.molcel.2015.03.025>

## SUMMARY

Ring-shaped cohesin keeps sister chromatids paired until cleavage of its Scc1/Rad21 subunit by separase triggers chromosome segregation in anaphase. Vertebrate separase is held inactive by mutually exclusive binding to securin or Cdk1-cyclin B1 and becomes unleashed only upon ubiquitin-dependent degradation of these regulators. Although most separase is usually found in association with securin, this anaphase inhibitor is dispensable for murine life while Cdk1-cyclin B1-dependent control of separase is essential. Here, we show that securin-independent inhibition of separase by Cdk1-cyclin B1 in early mitosis requires the phosphorylation-specific peptidyl-prolyl *cis/trans* isomerase Pin1. Furthermore, isomerization of previously securin-bound separase at the metaphase-to-anaphase transition renders it resistant to re-inhibition by residual securin. At the same time, isomerization also limits the half-life of separase's proteolytic activity, explaining how cohesin can be reloaded onto telophase chromatin in the absence of securin and cyclin B1 without being cleaved.

## INTRODUCTION

From their generation in S phase until the onset of anaphase, the two sister chromatids of each eukaryotic chromosome are entrapped and thus paired by ring-shaped cohesin. In somatic cells this heterotetrameric complex consists of Smc1 and 3, Scc1/Mcd1/Rad21, and Stag1 or 2 (Nasmyth and Haering, 2009). The highly elongated coiled-coil SMC proteins interact with each other via a flexible hinge and with both ends of Scc1 to form a tripartite ring 40 nm in diameter. Loading of vertebrate cohesin onto DNA occurs in telophase and involves opening of the Smc1-Smc3 hinge. Most cohesin is removed from chromosomes early in next mitosis by the prophase pathway, which results in phosphorylation-dependent inactivation of the cohesin protector sororin and opening of the Smc3-Scc1 gate (Buheiteil and Stemmann, 2013; Liu et al., 2013). At centromeres, cohesin

rings are protected from opening by protein phosphatase 2A (PP2A)-dependent dephosphorylation of sororin mediated by the adaptor protein shugoshin 1 (Sgo1) (Liu et al., 2013). This centromeric cohesin maintains cohesion until the metaphase-to-anaphase transition, when its Scc1 subunit is cleaved by separase (Waizenegger et al., 2000). In higher eukaryotes, cohesin is reloaded onto chromatin as early as telophase, but strangely, it is no longer cleaved despite unchanged levels of separase (Nasmyth and Haering, 2009; Waizenegger et al., 2000). As known inhibitors of separase are not present at this time (see below), this indicates that separase's proteolytic activity might be short-lived. However, it remains unknown how separase would quickly become inactive in late mitotic cells.

Given separase's essential function in sister chromatid separation, it is clear that both premature and delayed activation of separase would jeopardize faithful execution of anaphase. Thus, cells have to tightly control its proteolytic activity to prevent deleterious chromosome missegregation. Indeed, vertebrate separase is usually kept inactive by mutually exclusive association with either securin or cyclin B1 bound to cyclin-dependent kinase 1 (Cdk1) (Gorr et al., 2005). Separase is released from these inhibitors only when all chromosomes acquire proper amphitelic attachment to spindle microtubules in metaphase. The consequent extinction of a wait-anaphase signal leads to inactivation of the spindle assembly checkpoint followed by derepression of the anaphase-promoting complex/cyclosome (APC/C). This multisubunit ubiquitin ligase then mediates the destruction of securin and cyclin B1 via the ubiquitin-proteasome pathway, thereby releasing active separase. Securin is not only a negative regulator but exerts also a positive effect on separase, possibly by assisting the huge protease to achieve a natively folded state. Most separase is sequestered by securin in a typical eukaryotic cell. Yet mammalian securin is dispensable, while mice with a defect in the Cdk1-cyclin B1-dependent regulation of separase die during early embryogenesis (Huang et al., 2009; Mei et al., 2001). Inhibition of human separase by Cdk1-cyclin B1 requires at least two steps. First, Cdk1-cyclin B1 phosphorylates separase on serine 1126 and (possibly with support from other kinases) on several residues within a Cdc6-like domain (CLD), which centers around amino acid 1370 (Boos et al., 2008; Stemmann et al., 2001). Despite being essential, these phosphorylations are not sufficient for Cdk1-cyclin B1-dependent inhibition of separase (Gorr et al., 2005). Stable (albeit salt-sensitive) binding of the cyclin B1 subunit of

the kinase to the phosphorylated CLD of the protease is also required (Boos et al., 2008; Gorr et al., 2005). Ser1126 proved dispensable for the association of Cdk1-cyclin B1 with separase fragments, but its phosphorylation is absolutely essential for complex formation involving full-length protease (Boos et al., 2008). To explain this conundrum, it was proposed that phosphorylation at this position might induce a conformational change in separase that unmask the CLD, rendering it accessible for cyclin B1 (Boos et al., 2008).

Pin1 is a 17 kDa peptidyl-prolyl *cis/trans* isomerase (PPIase) of the parvulin subfamily. Next to the C-terminal PPIase domain, it also contains an N-terminal WW domain with two conserved tryptophans and a similar peptide binding specificity (see below) (Lu et al., 1999). Despite acting on dozens of substrates and influencing a multitude of processes, Pin1 is, above all, a key regulator of mitosis (Lu et al., 1996; Shen et al., 1998; Yaffe et al., 1997). Like other PPIases, it greatly accelerates the otherwise slow *cis/trans* isomerization of Xxx-Pro peptide bonds, which are special in that the free energy of the *trans*- relative to the *cis*-conformer is not as much lower as for other peptide bonds. However, unlike other PPIases, Pin1 acts only on phosphorylated Ser/Thr-Pro motifs (Liou et al., 2011). Phosphorylation may shift the *cis/trans* populations in equilibrium state but at the same time further slows uncatalyzed isomerization. Together with Ser/Thr-Pro-directed kinases, Pin1 can therefore quantitatively turn proteins into different conformational states of different functions or fates (Liou et al., 2011). Given that kinases and phosphatases usually exhibit *cis/trans* specificity, this molecular switch might, in some cases, operate even in only one direction.

Here, we identify Pin1 as a mitosis-specific interactor of human separase. The WW domain docks onto phosphorylated Ser1153-Pro1154 of separase, thereby positioning the PPIase domain to catalytically act on phosphorylated Ser1126-Pro1127. The resulting conformational change has three consequences. In early mitosis it enables inhibitory binding of Cdk1-cyclin B1 to separase. At metaphase-to-anaphase transition, it renders separase resistant to securin and simultaneously triggers a time fuse, which results in inactivation of separase by telophase.

## RESULTS

### Pin1 Is a Mitosis-Specific Interactor of Human Separase

The binding properties of full-length and partial separase to Cdk1-cyclin B1 differ in their requirement for phosphorylation of Ser1126 (Boos et al., 2008; Gorr et al., 2005). To assess whether this might be due to a conformational change catalyzed by a peptidyl-prolyl *cis/trans* isomerase (PPIase) acting on phosphoSer1126-Pro1127 in full-length separase, we scrutinized a possible involvement of Pin1. First, immunoprecipitations (IP) with anti-separase versus unspecific IgG from mitotic HEK293T cells were analyzed by immunoblotting. Indeed, Pin1 specifically co-purified with endogenous separase, similar to the known interactors securin and cyclin B1 (Figure 1A). Next, transgenic cells arrested in different cell-cycle phases (Figure 1B, upper panels) were subjected to IP of Myc-tagged separase variants. Like cyclin B1, endogenous Pin1 co-purified with wild-type (WT) separase from mitotic but not interphase cells. Unlike cyclin

B1, however, it also bound to Cdk1-resistant separase variants (lower panels).

In addition to the PPIase domain, Pin1 contains a second phosphoSer/Thr-Pro binding module, the WW domain, which usually exhibits greater substrate affinity (Lu et al., 1999). Therefore, the IPs were repeated from mitotically arrested cells that overexpressed either the PPIase or the WW domain in addition to a separase variant (Figure 1C). These analyses revealed (1) that both the PPIase and the WW domain of Pin1 interact with separase and (2) that the PPIase domain had a selective defect in binding to separase-S1126A. Mutation of nearby Ser/Thr-Pro motifs led to the identification of a triple Ala separase variant with compromised WW but normal PPIase binding characteristics (Figure S1A). Changing Ala1153 back to Ser healed this defect (Figure S1B). Consistently, a separase-S1153A single mutant showed greatly reduced association with Pin1's WW domain (Figure 1D). Moreover, binding of bacterially expressed WW domain to separase in a far western assay was compromised by phosphatase treatment prior to SDS-PAGE and extinguished by changing Ser1153 to Ala (Figure 1E). All S1153A-containing separase variants were also impaired in association with endogenous Pin1, demonstrating that under physiological concentrations it is mainly the WW domain that contributes to separase binding of full-length Pin1 (Figure S1B). Together, these observations demonstrate that the WW domain recruits Pin1 to separase by binding to phosphorylated Ser1153, thus enabling the PPIase domain to engage phosphorylated Ser1126-Pro1127 (Figure 1F).

### Pin1 Is Required for Cdk1-Cyclin B1-Dependent Inhibition of Separase

To check for genetic interaction of separase and Pin1 in vivo, induced overexpression of separase-WT was combined with partial depletion of Pin1 by RNAi (Figure 2A). While the individual treatments were well tolerated, simultaneously increasing separase and decreasing Pin1 levels had a strong synthetically lethal effect on HEK293 cells as judged by clonogenic assay. This result suggests a negative regulation of separase by Pin1, which could be explained by a requirement of the isomerase for Cdk1-cyclin B1-dependent inhibition of separase.

To clarify this issue, *Xenopus* egg extracts supplemented with APC/C-resistant, N-terminally truncated ( $\Delta 90$ ) cyclin B1 to maintain an anaphase-like state with constitutively active Cdk1 were rid of Pin1 by immunodepletion or mock treated (Figure 2B). Purified separase-securin complexes were then incubated in these extracts for APC/C-dependent degradation of securin before the protease was re-isolated and probed for associated factors and cohesin cleaving activity. Separase from mock-treated extract hardly cut Scc1 but became proteolytically active when bound cyclin B1 was washed away with high salt prior to the cleavage assay (compare lanes 2 and 5). In contrast, separase re-isolated from a Pin1-depleted extract was active toward Scc1 even without a high salt wash, and this correlated with lack of associated cyclin B1 (lane 3). Demonstrating specificity of the immunodepletion, addition of bacterially expressed GST-tagged Pin1 to depleted extract rescued binding and inhibition of separase by Cdk1-cyclin B1 (lane 4). Thus, Cdk1-cyclin B1-dependent inhibition of separase in vitro requires Pin1.

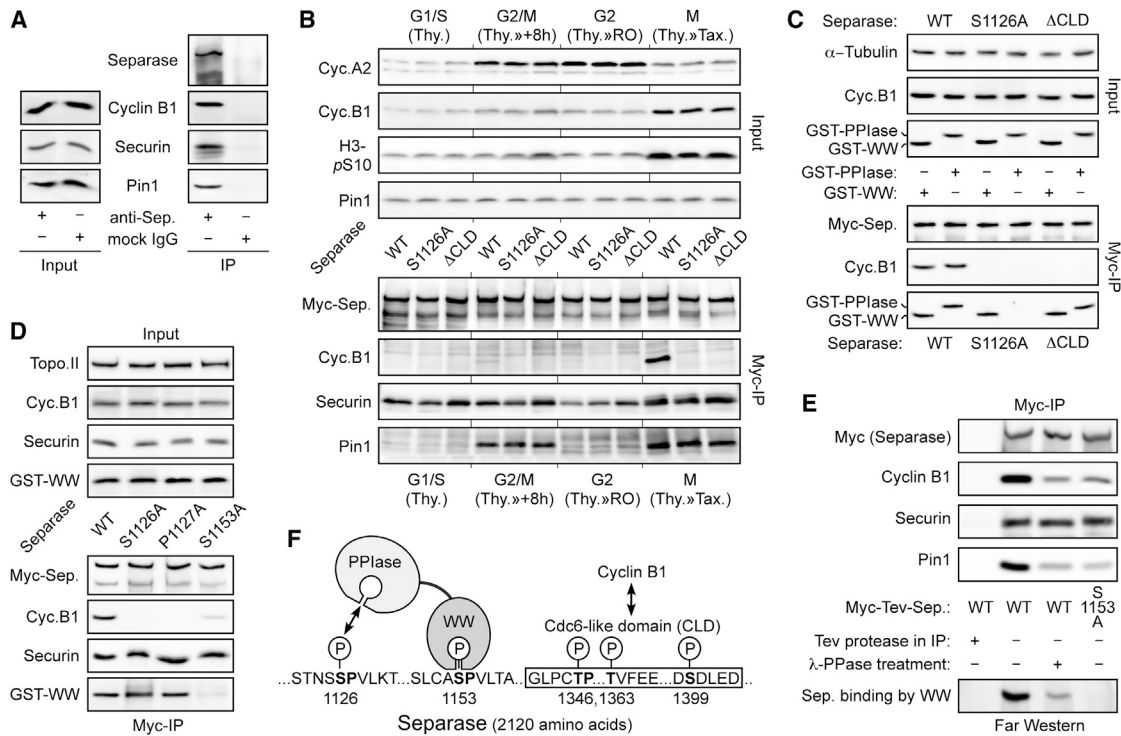


**Figure 1. The Peptidyl-Prolyl Isomerase Pin1 Is a Mitosis-Specific Interactor of Vertebrate Separase**

(A) Mitotic HEK293T lysate (input) was subjected to IP with anti-separase or mock IgG and analyzed by immunoblotting. (B) Myc-separase-variants-expressing HEK293s were synchronized and subjected to Myc IP and immunoblotting. Thy., thymidine; RO, CDK1-inhibitor RO3306;  $\Delta$ CLD, Cdc6-like domain deleted; H3-pS10, Ser10-phosphorylated histone H3. (C) Cells as in (A) and transiently expressing GST-PPIase or -WW were mitotically arrested, lysed, and subjected to Myc IP. (D) Lysates of mitotic HEK293Ts expressing Myc-tagged separase variants together with GST-WW were subjected to Myc IP. (E) Mitotic HEK293Ts expressing Myc-separase variants were subjected to Myc IP and, where indicated,  $\lambda$ -phosphatase treatment. Following additional washing, bound proteins were detected by (far) western analysis. (F) Docking of the WW domain onto phosphorylated Ser1153 recruits Pin1 to separase and facilitates the isomerization of pSer1126-Pro1127 by the PPIase domain.

See also [Figure S1](#).

To test whether the same is true also in vivo, we capitalized on the fact that this form of regulation becomes crucial when securin is titrated out by overexpression of separase (Boos et al., 2008; Holland and Taylor, 2006). Following transfection with *PIN1* or mock (*GL2*) siRNA, transgenic HEK293 cells were induced to over-produce Myc-separase-WT, arrested in prometaphase, and then analyzed by IP-western and chromosome spreading (Figure 2C). Importantly, Pin1 depletion was accompanied by decreased cyclin B1 binding to separase and a 5-fold increased rate of premature sister chromatid separation. Both consequences were specific since they were prevented by simultaneous expression of Flag-Pin1 from an siRNA-resistant transgene. Interestingly, chemical inhibition of Pin1's PPIase activity by epigallocatechin-3-gallate (EGCG) (Urusova et al., 2011) mimicked, and fortified, the RNAi phenotype (Figure 2C). Thus, the catalytic activity of Pin1 appears to be necessary for separase inhibition by Cdk1-cyclin B1 not only in vitro but also in living cells.

The finding that overexpression of WW-binding-deficient separase variants also caused dissociation of cyclin B1 along with premature loss of cohesion (Figures 3A and 3B) enabled us to

address this issue by an independent approach. We reasoned that only with S1153A containing variants should the overexpression phenotypes be suppressible by simultaneous overexpression of Pin1's isolated PPIase domain (see Figure S2A for rationale), thereby providing an assay for the requirement of isomerase activity. Indeed, co-overexpression of PPIase reinstalled cyclin B1 binding and prevented precocious sister separation in separase-S1153A-overexpressing cells, but not in those producing separase-S1126A or -P1127A (Figures 3A and 3B). Importantly, a catalytically inactive PPIase-C113A failed to rescue despite same expression level and normal association with separase (Figures 3A and 3B; see also Figure S2B). The need of catalytic activity strongly implies but does not yet prove that Pin1 changes separase's conformation. Therefore, we used  $\Delta$ 90-cyclin B1-supplemented *Xenopus* egg extracts and high salt washing to produce securin- and cyclin B1-less separase in the absence (EGCG) or presence (DMSO) of Pin1 activity and then subjected both preparations to limited proteolysis by trypsin. Indeed, fragments of 38 and 75 kDa transiently appeared only for separase exposed to active Pin1 (Figure S2C). This differential digestion pattern demonstrates that Pin1 does indeed

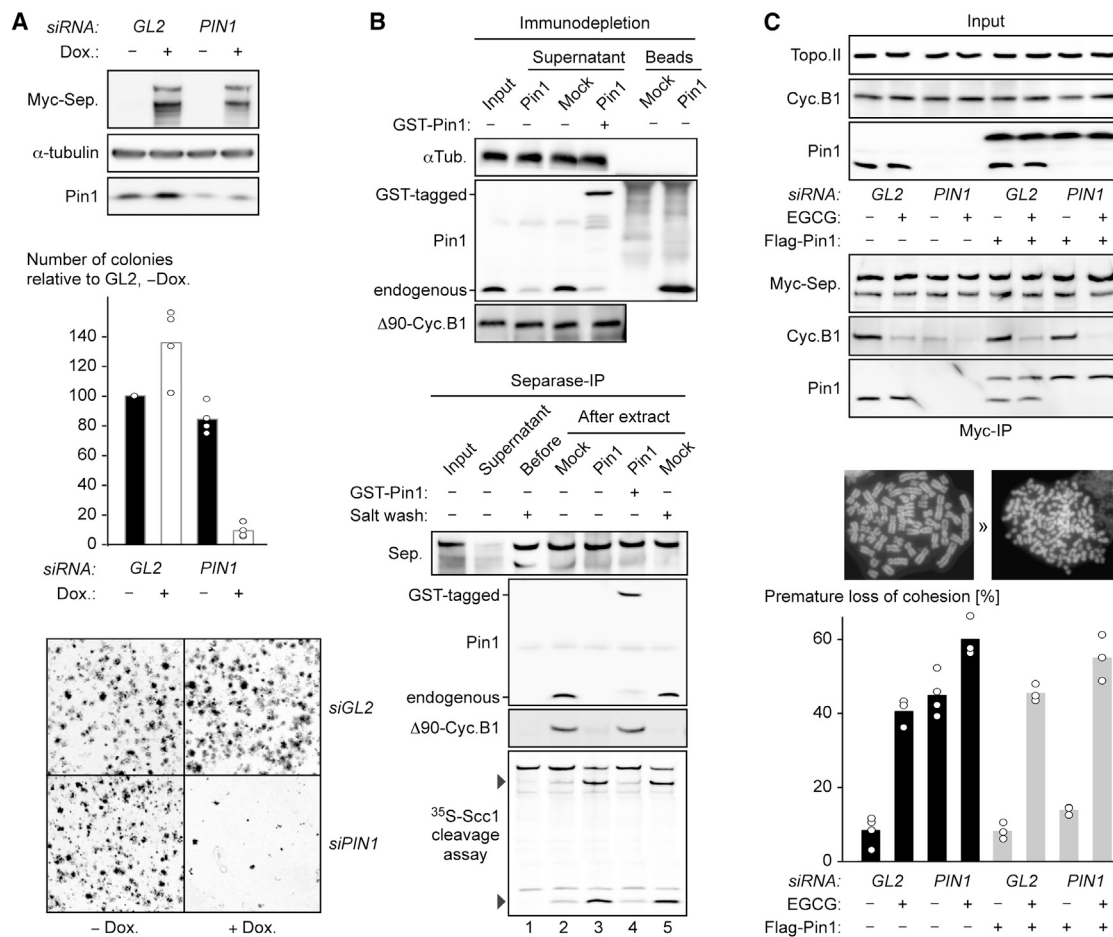


**Figure 2. Pin1 Is a Negative Regulator of Separase**

(A) Transgenic HEK293s transfected with the indicated siRNA were induced with doxycycline (+ Dox.) to overexpress separase-WT or left uninduced and replated. Graph shows mean numbers of stained, automatically counted colonies (bars) of four experiments (dots).

(B) ZZ-Tev-separase-securin from G1/S HEK293Ts was incubated on IgG-sepharose in Pin1- or mock-depleted *Xenopus* egg extract supplemented with  $\Delta$ 90-cyclin B1 and, where indicated, GST-Pin1. Separase beads were re-isolated, washed with high salt (as indicated), and assayed for bound proteins and Scc1 cleavage.

(C) Myc-separase-WT-expressing HEK293s were transfected with siRNA against *PIN1* or *GL2* and a (*PIN1* siRNA-resistant) plasmid encoding Flag-Pin1, treated with nocodazole and EGCG, and analyzed by Myc IP and chromosome spreads. Shown are mean values (bars) of 3–4 experiments (dots) quantifying at least 100 cells each.

alter separase's conformation. Taken together, these data show that phosphorylation of separase by Cdk1 is followed by docking of Pin1 via its WW domain onto phosphorylated Ser1153. This places the PPIase domain at the right position to then catalyze the isomerization of the phosphorylated Ser1126-Pro1127 peptide bond. The resulting conformational change of separase enables Cdk1 to stably bind via its regulatory cyclin B1 to the CLD, thereby blocking separase's proteolytic activity (Figure 3C). In the separase variants S1126A or P1127A, the corresponding Ala-Pro and Ser-Ala peptide bonds likely exist predominantly or almost exclusively in their *trans* conformation, respectively, and both variants bind securin normally but fail to interact with cyclin B1 (Figure 1D). We therefore propose (but stress that we do not prove) that the *trans*-conformer of separase exclusively associates with securin, while the *cis*-conformer exclusively as-

sociates with Cdk1-cyclin B1 (Figure 3C). We will make this assumption for the remainder of this manuscript.

### Pin1 Catalyzes Native State Isomerization of Previously Securin-Inhibited Separase in Anaphase

Is regulation by Pin1 limited to the few percent of separase that are inhibited by Cdk1-cyclin B1 in a standard cell cycle, or does the isomerase also act on securin-associated separase? To address this question, we first assessed whether securin and Pin1 can bind to separase at the same time. Using different tags and antibodies, we can demonstrate that securin and Pin1 co-immunoprecipitate with separase, but that Pin1 does not co-purify with securin and vice versa (Figure 4A). Cyclin B1 was absent from a securin-IP, but present in pull-downs of separase, as previously reported (Gorr et al., 2005). Furthermore, it

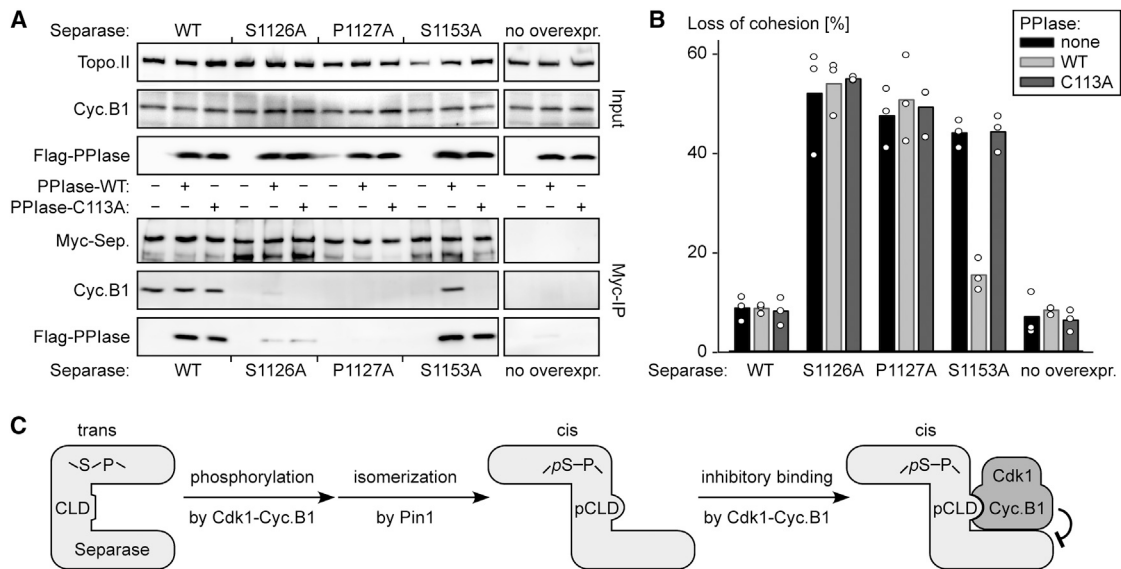


**Figure 3. Catalytically Active Pin1 Is Required for Cdk1-Cyclin B1-Dependent Inhibition of Separase**

(A) HEK293Ts expressing Myc-separase-WT, -S1126A, -P1127A, or -S1153A alone or together with Flag-PPlase-WT or -C113A were synchronized in mitosis, and lysates (input) were subjected to Myc IP and immunoblotting.

(B) Chromosome spreads of cells from (A).

(C) Multi-step, Pin1-dependent assembly of the Cdk1-cyclin B1-separase complex.

See also Figure S2.

was detectable together with separase in a Pin1 pull-down (Figure 4A). Thus, while Pin1 and Cdk1-cyclin B1 can bind separase simultaneously, a heterotrimeric Pin1-separase-securin complex does not exist.

This leaves the possibility that Pin1 acts on the pool of securin-controlled separase only upon APC/C-dependent degradation of securin. To test whether this holds true, we explored association with Cdk1-cyclin B1 to probe for the conversion of previously securin-bound *trans*-separase into the *cis*-isomer in late mitosis. Tax-arrested cells were treated with the aurora B inhibitor ZM447439 (ZM). This drove them synchronously through late mitosis, as evidenced by the decline of cyclin B1 and the dephosphorylation of histone H3 and Cdc27 (Figure 4B). Consistent with previous reports (Hellmuth et al., 2014; Shindo et al., 2012), time-resolved separase IPs followed by western analysis revealed a second wave of cyclin B1 association with separase more than 30 min after ZM addition, i.e., at a time when the overall level of cyclin B1 was already very low (Figure 4B). Importantly, chemical inhibition of Pin1 with EGCG totally abrogated this late peak of Cdk1-cyclin B1-separase complex formation. Thus, at the metaphase-to-anaphase transition, at least part of formerly securin-inhibited separase is switched by Pin1 into its *cis*-conformation.

We reasoned that phosphorylation of Ser1126 would result in a relative increase in the free energy of *trans*- over *cis*-separase, thereby shifting the equilibrium state of Pro1127 from “mostly *trans*” to “mostly *cis*” (Figure 4C). However, securin, while still bound, would lock separase in its *trans*-conformation and prevent Pin1 from converting the protease into its *cis*-isomer. Securin binds with its C-terminal part to an N-terminal region of separase and with further N-terminal residues to the C-terminal

part of the protease (Hornig et al., 2002; Jäger et al., 2004; Viadiu et al., 2005). Thus, bisecting securin might suffice for Pin1-catalyzed isomerization of phosphorylated separase from *trans* to *cis* (see Figure 4D for rationale). To test this hypothesis, we engineered a securin variant with a cleavage site for human rhinovirus 3c (HRV) protease after glutamine 160 but preserved separase binding ability (Figure S3). An APC/C-resistant, N-terminally truncated ( $\Delta 92$ ), and Flag-tagged version of this securin<sup>HRV</sup> was purified in complex with separase and immobilized on anti-Flag agarose. Incubation of the complex in a  $\Delta 90$ -cyclin B1-supplemented, Pin1-containing *Xenopus* egg extract did not allow the cyclin to bind via separase to the securin-loaded beads (Figure S3C). However, upon addition of HRV-protease, securin was cleaved and separase converted into its *cis*-isomer as revealed by the interaction with cyclin B1 that now occurred. This association was largely suppressed when EGCG was added together with HRV-protease to the extract. Importantly, the same result was also observed in a fully defined system, in which the egg extract was replaced by purified Pin1 and Cdk1-cyclin B1 (Figure 4E). Thus, securin-bound, phosphorylated separase is spring loaded and quickly converted by Pin1 from its *trans*- into its *cis*-isomer when securin is destroyed.

### The *cis*-Conformer of Separase Is Resistant against Securin

If securin can only bind to *trans*-separase, then the *cis*-isomer should be resistant to inhibition by securin. To test this prediction, we first produced proteolytically active separases in either *cis*- or *trans*-conformation. Securin-associated separase-WT and -S1126A were incubated in  $\Delta 90$ -cyclin B1 supplemented *Xenopus* egg extract. This resulted not only in degradation of

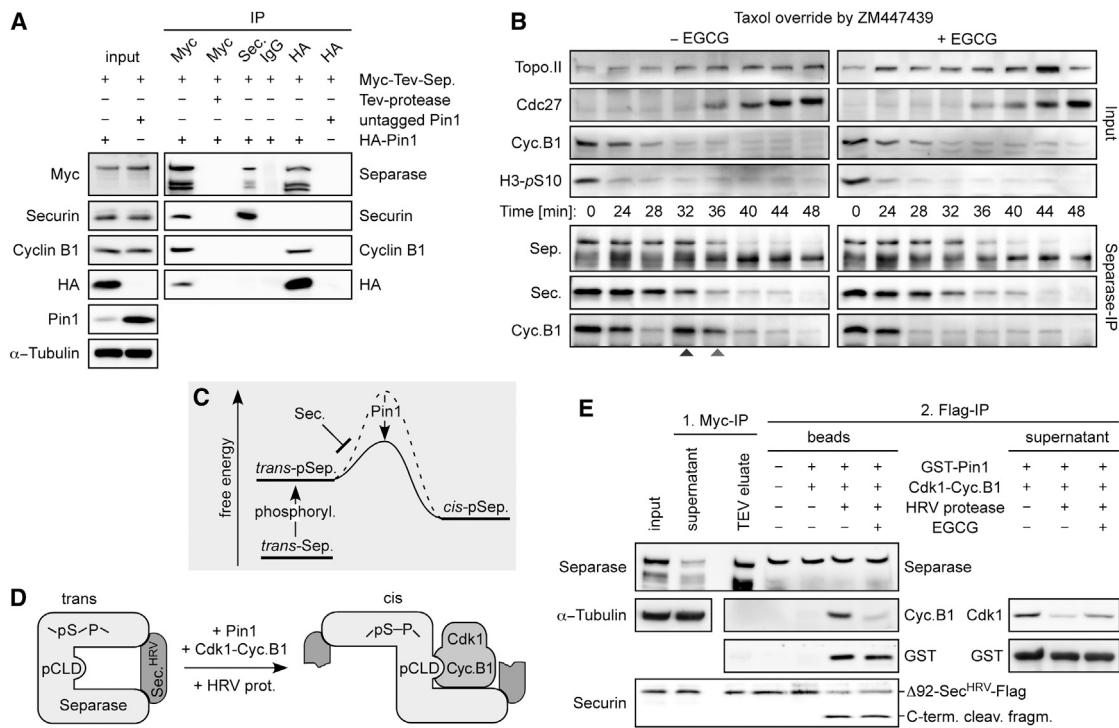


**Figure 4. Pin1 Isomerizes Previously Securin-Inhibited Separase in Anaphase**

(A) Using anti-Myc, -securin, or -HA (hemagglutinin tag), respectively, separase, securin, or Pin1 were IPed from mitotic HEK293Ts overexpressing Myc-Tev-separase and HA-Pin1. Negative controls: Myc IP in presence of TEV-protease, IP with unspecific IgG, or HA IP from cells expressing untagged Pin1. (B) HeLa Ks were released from Tax by ZM ( $t = 0$  min) and analyzed at indicated time points thereafter. Where indicated, EGCG was added prior to release. (C) Cartoon illustrating that phosphorylation energetically favors the *cis*-isomer while securin locks separase in *trans*. (D) Model of how relieving the securin-imposed conformational constraint allows simultaneous binding of securin (fragments) and Cdk1-cyclin B1 to phosphorylated separase. (E) Myc-Tev-separase- $\Delta 92$ -securin<sup>HRV</sup>-Flag was purified by Myc IP and eluted with TEV-protease. After immobilization on anti-Flag agarose, the complex was incubated with Cdk1- $\Delta 90$ -cyclin B1 and ATP, GST-Pin1, EGCG, and/or HRV-protease, as indicated, before unbound (supernatant) and bound proteins (beads) were detected by immunoblotting. See also Figure S3.

securin, but at the same time separase-WT was also phosphorylated and isomerized into *cis* as judged by inhibitory binding of Cdk1-cyclin B1 (Figure 5A). Following re-isolation from the extract and a high salt wash to strip the kinase off WT protease, both preparations displayed similar cohesin cleaving activity, but differed in that separase-WT had been converted into the *cis*-isomer, while separase-S1126A was trapped in the *trans*-conformation. When interrogated for sensitivity toward increasing amounts of recombinant securin, interestingly, separase-S1126A readily re-associated with the inhibitor and was fully inactivated at a securin concentration of 90 nM, while the same amount of separase-WT always bound less inhibitor and retained partial proteolytic activity even at 180 nM securin (Figure 5A). Upon its addition in large excess, securin would be expected to sequester any *trans*-separase, thereby removing it from the *cis/trans* equilibrium. Over time this should result in separase-associated Pin1 to catalyze also the shift of *cis*-separase-WT into its *trans*-isomer (see Figure S4A for rationale). Confirming this reasoning, the presence of EGCG during the incubation with securin further reduced its binding to separase-WT, thus rendering the protease totally resistant to re-inhibition

(Figure 5B). Collectively, these in vitro experiments show that separase acquires resistance against securin upon Pin1-mediated isomerization.

Next, we asked whether Pin1 renders separase resistant to securin also during the metaphase-to-anaphase transition in living cells. Tax-arrested HeLa cells were induced to express non-degradable KEN- and D-box mutated (KDM) securin shortly before they were released from the arrest by ZM addition. At different times thereafter, aliquots were subjected to separase-IP and immunoblotting. This analysis demonstrated that hardly any securin<sup>KDM</sup> associated with separase, although endogenous securin was efficiently degraded (Figures 5C and 5D). Importantly, the picture dramatically changed when EGCG was added to the cells shortly before ZM. Under these conditions of Pin1 inactivity, endogenous separase-bound securin was immediately replaced by securin<sup>KDM</sup> as the former was being degraded (Figures 5C and 5D). The lower panels of Figure 5C allow estimation that roughly 80% of securin inhibited separase undergoes *trans*-to-*cis* isomerization upon destruction of the anaphase inhibitor (see Experimental Procedures). Thus, when APC/C becomes active, the majority of total separase is switched by

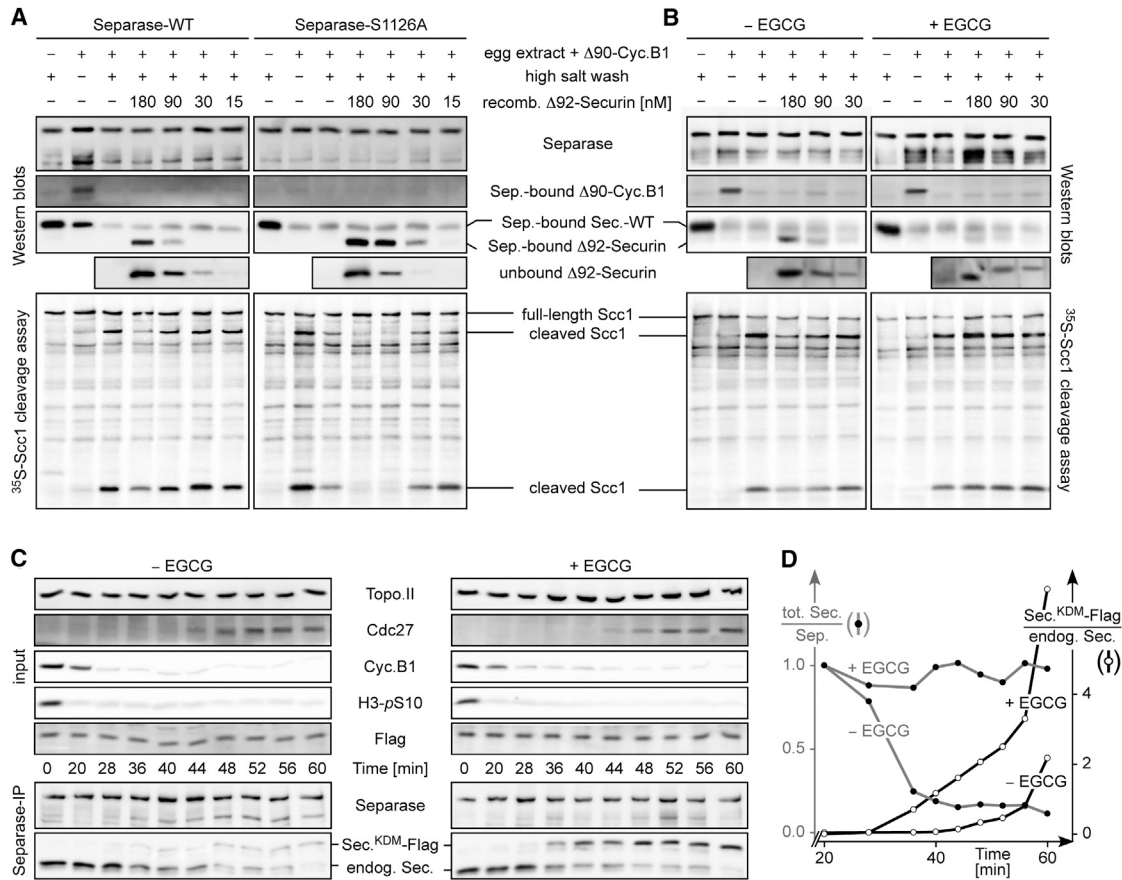


**Figure 5. Pin1 Contributes to the Irreversibility of Separase Activation**

(A) Securin-associated Myc-Tev-separase-WT or -S1126A on anti-Myc beads was incubated in  $\Delta 90$ -cyclin B1-containing *Xenopus* egg extract, re-isolated, and, where indicated, washed with high salt. Separases were then incubated with recombinant  $\Delta 92$ -securin, washed, eluted with TEV-protease, and analyzed by immunoblotting and Scc1 cleavage assay/autoradiography.

(B) Myc-Tev-separase-WT was treated and analyzed as described in (A) except for the addition of EGCG (or DMSO) prior to  $\Delta 92$ -securin.

(C) Tax-arrested HeLa cells were induced to express Flag-securin<sup>KDM</sup>, supplemented with EGCG where indicated, released by ZM (t = 0 min), and subjected to separase-IP at indicated times.

(D) Quantification of the securin immunoblot from (C). Black lines, open circles indicate separase-associated securin<sup>KDM</sup>-Flag relative to endogenous securin. Gray lines, black circles indicate total amount of separase-associated securin relative to separase (set to 1 at t = 0).

See also [Figure S4](#).

Pin1 into a conformation that is highly resistant against securin. This is physiologically relevant, since prometaphase cells contain free securin in about 5-fold excess over separase-bound securin, and about 20% of free securin persist when half of separase-associated securin is degraded (Hellmuth et al., 2014). By catalyzing the *trans*-to-*cis* isomerization, Pin1 renders separase resistant to this lingering free securin.

### Late Mitotic Dephosphorylation of Cyclin B1 Increases Its Affinity for Separase

When separase becomes resistant to securin, it is simultaneously rendered susceptible to the inhibition by remaining Cdk1-cyclin B1. This raises questions regarding the timing of separase activation and cohesin cleavage relative to the formation of Cdk1-cyclin B1-separase complexes in late mitosis. To clarify this issue, transgenic HeLa cells were transiently trans-

ected to express, as a separase activity sensor, histone H2B-mCherry-Scc1<sup>107-268</sup>-eGFP (Hellmuth et al., 2014; Shindo et al., 2012). The same cells were induced to also express Myc-separase and then Tax-ZM treated to synchronously drive them through late mitosis. Proteolytic activity and cyclin B1 binding of separase were followed by immunoblotting of time-resolved anti-GFP- and anti-Myc IPs, respectively. In accordance with an earlier study (Shindo et al., 2012), this analysis demonstrated that the sensor is cleaved prior to formation of the late mitotic Cdk1-cyclin B1-separase peak (Figure S4B). The phenomenon that this peak only forms at a time when total cyclin B1 levels are already very low could be explained if the separase affinity of the remaining trace amounts of Cdk1-cyclin B1 would greatly increase at the end of mitosis. Cyclin B1 is phosphorylated on Ser126, 128, 133, and 147 by Cdk1 itself, polo-like kinase 1 (Plk1), and possibly other mitotic kinases

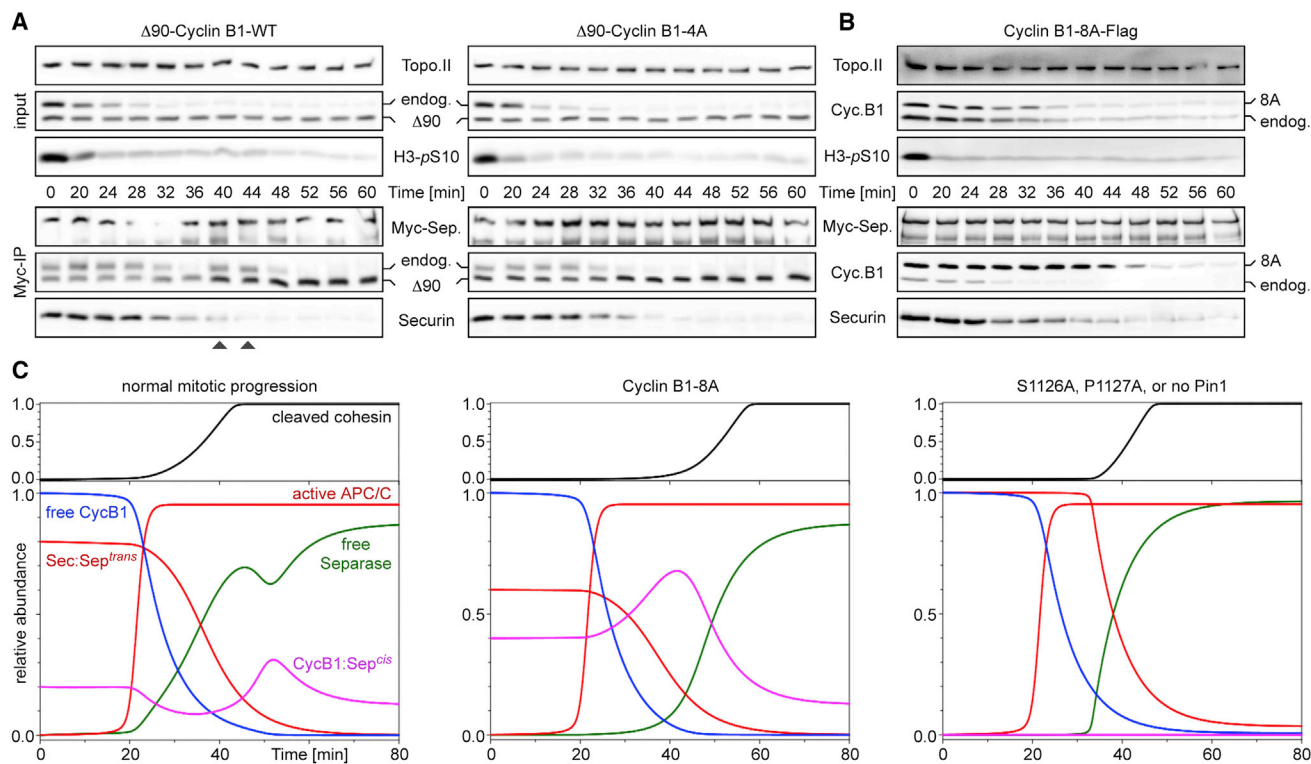


**Figure 6. Dephosphorylation of Cyclin B1 Increases Its Affinity for Separase, thereby Giving Rise to a Second Peak of Cdk1-Cyclin B1-Separase in Late Mitosis**

(A) Myc-separase-WT- and  $\Delta 90$ -cyclin B1-WT- or -4A-expressing HEK293s were Tax-ZM treated. Association of endogenous- and  $\Delta 90$ -cyclin B1 and securin with separase was followed by time-resolved Myc IP.

(B) Myc-separase-WT- and cyclin B1-8A-Flag-expressing HEK293s were treated as in (A).

(C) Mathematical simulation of mitotic progression from an initial checkpoint arrest. Plotted are relative abundances of free Cdk1-cyclin B1, securin-separase, Cdk1-cyclin B1-separase, active APC/C, free separase, and cleaved cohesin for three different scenarios (all without cycloheximide): normal mitotic progression (left), presence of phosphorylation site mutant cyclin B1-8A (middle), and absence of Pin1 or replacement of endogenous separase by a S1126A or P1127A variant (right). Note that absence of isomerization results in premature sister chromatid separation only upon overexpression of separase, which is not considered here.

See also Figure S5.

(Jackman et al., 2003). Ser147 is dephosphorylated during exit from mitosis (Toyoshima-Morimoto et al., 2001), and due to APC/C-dependent inactivation of Cdk1 and Plk1, the other three sites will likely be dephosphorylated at this time, too. To test the provocative idea that dephosphorylation of cyclin B1 might promote Cdk1-cyclin B1-separase complex formation, the four Ser residues were changed to Ala to prevent their phosphorylation. To be able to discriminate the resulting cyclin B1-4A from endogenous cyclin B1, an N-terminally truncated ( $\Delta 90$ ) version was expressed in Myc-separase containing HEK293 cells. Myc IP followed by western analysis demonstrated that cyclin B1-4A indeed represents a gain-of-function variant superior to endogenous cyclin B1 in binding separase in prometaphase-arrested cells (Figure 6A, time 0). This is also illustrated by the fact that its presence prevents re-binding of residual endogenous cyclin B1 to separase in late mitosis. Interestingly,  $\Delta 90$ -cyclin B1-WT cannot suppress the late mitotic peak of endogenous cyclin B1-separase interaction, despite the fact that its binding to separase also improves in late mitosis (arrowheads). This is surprising, because at that time there is only very little endogenous

cyclin B1 left, while  $\Delta 90$ -cyclin B1-WT is, of course, plentiful. Moreover, binding of  $\Delta 90$ -cyclin B1-WT and endogenous cyclin B1 is equally weak in prometaphase. Together, these observations suggested (1) that the first 90 amino acids also contribute to separase binding and (2) that interaction with separase is additionally weakened by phosphorylations within the N-terminal region of cyclin B1. Mitotic phosphorylations are known to occur also at Ser9, 35, 69, and 116 (Daub et al., 2008). Therefore, we generated a full-length cyclin B1-8A variant that had these four residues in addition to Ser126, 128, 133, and 147 changed to Ala and that could be distinguished in size from endogenous cyclin B1 due to a C-terminal Flag tag. Indeed, these additional mutations further fortified the binding of cyclin B1 to separase. Despite apparently normal degradation kinetics, cyclin B1-8A largely replaced endogenous cyclin B1 from separase, and the corresponding complex no longer transiently declined in abundance upon release from a prometaphase arrest (Figure 6B). Together, these data strongly suggest that dephosphorylation of cyclin B1 increases the affinity of Cdk1-cyclin B1 for separase in late mitosis.

### Pin1-Mediated Isomerization of Separase Ensures that Anaphase Commences in the Presence of Residual Cdk1 Activity

The above data suggest that at the metaphase-to-anaphase transition, the majority of separase is switched by Pin1 into the securin-resistant but Cdk1-cyclin B1-susceptible *cis*-conformer. However, because cyclin B1 is phosphorylated and rapidly degraded, separase is not re-inhibited but instead cleaves cohesin. Only thereafter, when dephosphorylation has sufficiently increased cyclin B1's affinity, does separase associate with lingering trace amounts of Cdk1-cyclin B1 (Figure S5A). Considering the known mutual influences (Figure S5B) and using mathematical modeling, we could recapitulate all of these findings, including the transient decline in abundance of the Cdk1-cyclin B1-separase complex, which, however, is prevented in the presence of phosphorylation site mutant cyclin B1-8A (Figure 6C, left and middle). Our model is also consistent with reported inhibition of sister chromatid separation by non-degradable cyclin B1 and explains why it needs to be overexpressed in order to inhibit separase in metaphase, i.e., at a time when its affinity for the protease is reduced due to phosphorylation (Figure S5C) (Hagting et al., 2002; Wolf et al., 2006). If there was no separase isomerization, the model predicts that separase activation would only commence when virtually all free cyclin B1 had disappeared (Figure 6C, right). However, the observation that, in an unperturbed mitosis, cohesin cleavage occurs despite the presence of residual amounts of cyclin B1 (Figure S4) (Hellmuth et al., 2014; Shindo et al., 2012) better fits the model that includes separase isomerization (left). Thus, mathematical modeling provides an independent confirmation that the anaphase transition is shaped by Pin1. By ensuring that anaphase commences before cyclin B1 level and Cdk1 activity are zero, Pin1 might contribute to the ordering of late mitotic events (see Discussion).

### Pin1-Dependent Rapid Inactivation of Separase in Late Mitosis

Even though separase efficiently cleaves chromatin-bound cohesin, the latter re-associates with human chromosomes as early as telophase without being destroyed. This suggests that the burst-like activation of separase is followed by inactivation of the protease shortly thereafter. To investigate whether isomerization of the Ser1126-Pro1127 peptide bond would influence the stability of separase *in vitro*, we produced active separases, which were either in the *trans* or the *cis* conformational state. This was achieved by incubation of securin-bound separase-S1126A or  $\Delta$ CLD in  $\Delta$ 90-cyclin B1-containing anaphase egg extracts. In case of separase- $\Delta$ CLD, this resulted in degradation of securin, Cdk1-dependent phosphorylation, and Pin1-dependent isomerization of Pro1127 into *cis*. Separase-S1126A stayed *trans*-isomer due to resistance against phosphorylation and isomerization. Following pre-incubation for different periods of time, both separase variants were assayed for proteolytic activity towards <sup>35</sup>S-labeled Scc1. Although the two proteases initially displayed similar specific activities, separase- $\Delta$ CLD quickly lost cohesin cleavage capacity ( $t_{1/2} \approx 10$  min) upon pre-incubation, while the proteolytic activity of separase-S1126A did not decay over the course of 60 min (Figure 7A). Next, we produced active separase-WT, but this time added EGCG to the *Xenopus* egg extract

to inhibit Pin1's PPLase activity and, consequently, lock the Ser1126-Pro1127 peptide bond in *trans* beyond the destruction of securin. Following separase re-isolation from the extract, half of the preparation was combined with recombinant Pin1 to facilitate *trans*-to-*cis* isomerization, and the other half was supplemented with fresh EGCG to keep inactive any Pin1 that had co-purified. A subsequent stability assay revealed rapid inactivation (< 10 min) of separase in presence of active Pin1, but only slow decline of its proteolytic capacity ( $t_{1/2} \approx 30$  min) in the presence of EGCG (Figure 7B). Thus, while the activity of *cis*-separase has a short half-life, *trans*-separase is a stable enzyme.

Given that the *trans*- and *cis*-isomer are the predominant forms of separase in early and late mitosis, respectively, the Pin1-facilitated conformational switch of separase may act like a time fuse of self-destruction. If so, then preventing separase from adopting the *cis*-conformation in anaphase cells should prolong its proteolytic activity, which might result in cleavage and displacement of cohesin from telophase chromatin. HEK293T cells expressing either separase-S1126A or  $\Delta$ CLD were synchronously sent through late mitosis by a Tax-ZM regime, and chromatin was isolated and immunoblotted at different times. In separase- $\Delta$ CLD-containing cells, Smc3 disappeared from chromosomes 25 min after the addition of ZM, but re-associated by 50 min (Figure 7C, right panels). This corresponds to the expected normal behavior of cohesin and was also seen in transgenic cells expressing separase-WT (data not shown). Notably, these dynamics were changed in separase-S1126A-expressing cells in that Smc3 did not re-bind to chromatin up to 60 min after the addition of ZM (Figure 7C, left panels). In a complementary approach, EGCG or carrier solvent was added to HeLa K cultures before telophase cells were interrogated by immunofluorescence microscopy (IF) for Scc1 association with chromatin (Figure 7D). In 87%  $\pm$  5% of control telophase cells, Scc1 was bound to chromatin, which still showed signs of condensation. Notably, Pin1 inhibition reduced this value to 34% on average. Assuming that separase has no effect on loading of cohesin onto DNA, these experiments strongly suggest that presence of *trans*-separase prolongs the time of cohesin cleavage in late mitosis. Conversely, the *trans*-to-*cis* isomerization of Pro1127 in separase, which usually occurs at the metaphase-to-anaphase transition, limits the half-life of its proteolytic activity.

## DISCUSSION

We report here three functions for Pin1 in mitosis, all of which revolve around the regulation of separase. When securin is limiting, Pin1 is required for the inhibitory binding of Cdk1-cyclin B1 to separase in early mitosis. In the presence of sufficient amounts of securin, Pin1-dependent isomerization of separase at the metaphase-to-anaphase transition grants previously securin-inhibited separase resistance against re-inhibition by residual securin. However, this also sets a temporal limit to separase's proteolytic activity.

### Separase Might Represent a Crucial *In Vivo* Substrate of Pin1

Mouse mutant embryos, in which half of separase is resistant to Cdk1-cyclin B1 (because of a S1121A-encoding mutation in one

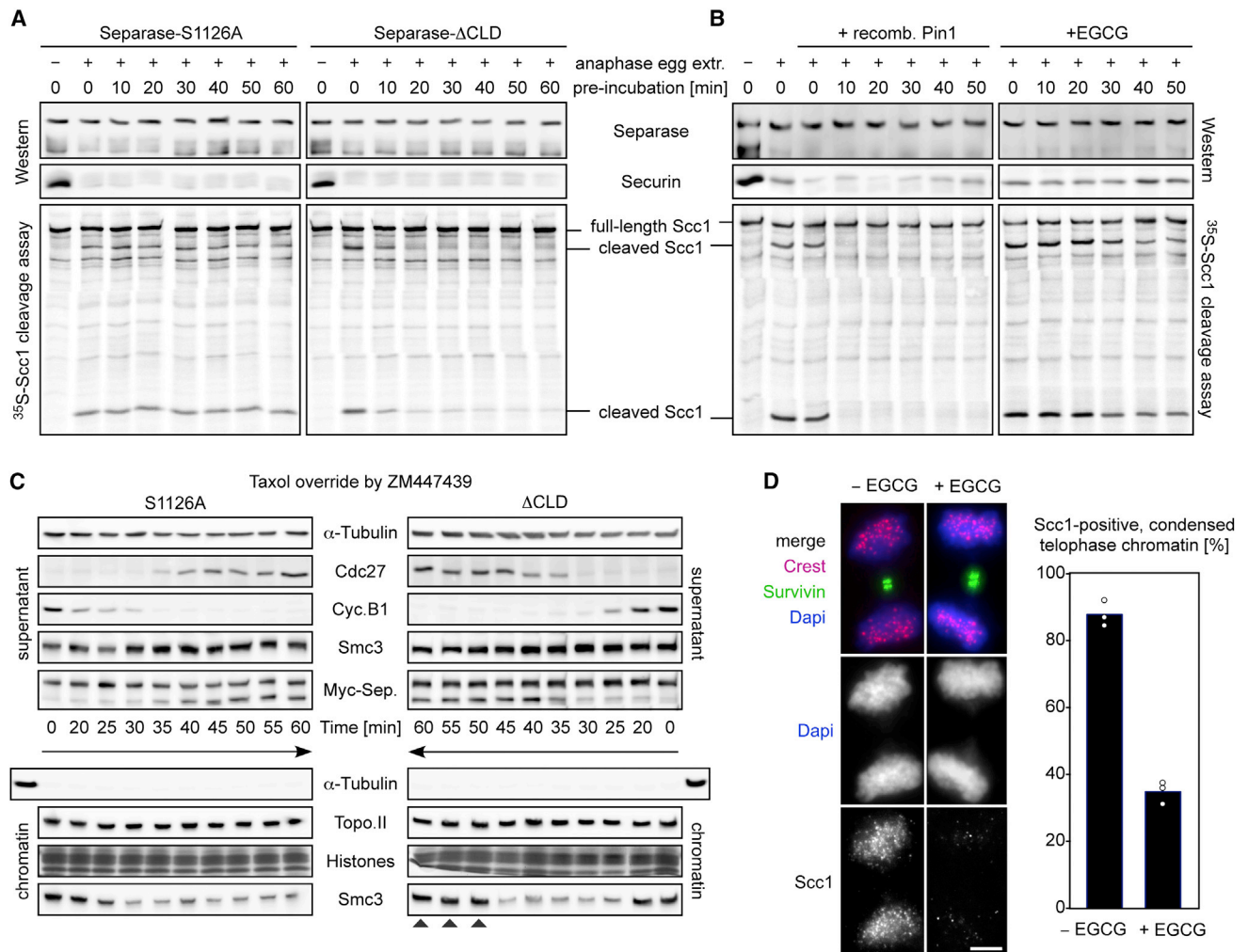


**Figure 7. Pin1-Dependent Rapid Inactivation of Separase in Late Mitosis**

(A) Separase-S1126A and  $\Delta$ CLD were purified as in Figure 5A, shifted to room temperature ( $t = 0$ ), and assessed for proteolytic activity toward  $^{35}\text{S}$ -Scc1 at indicated times.

(B) Separase-WT was purified and treated as in (A), except that EGCG was present until elution with TEV-protease. Separase was combined with recombinant Pin1 or EGCG and then analyzed by immunoblotting and Scc1 cleavage assay/autoradiography. Note that in (A) and (B), gels were blotted and membranes cut and subjected to western analysis prior to reassembly and autoradiography.

(C) Separase-S1126A- or  $\Delta$ CLD-expressing HEK293s were Tax-ZM treated and subjected to chromatin isolation at the indicated time points. Soluble proteins (supernatant) and pelleted chromatin fractions were analyzed by immunoblotting and Coomassie staining (histones). For the  $\alpha$ -tubulin western analysis of chromatin, supernatant was loaded into the outer lanes.

(D) HeLa cells of the Kyoto line (HeLa Ks) were EGCG or DMSO treated prior to IF. Scc1-positive chromatin was scored in telophase cells with condensed DNA (as judged by DAPI staining) and broad midbodies (as judged by the survivin signal). Scale bar = 6  $\mu\text{m}$ .

allele), die between the 8- and 16-cell stage due to premature loss of sister chromatid cohesion (Huang et al., 2009). In contrast, *PIN1*<sup>-/-</sup> mice are viable (Fujimori et al., 1999), which seems to be at odds with our finding that Pin1 is necessary for Cdk1-cyclin B1-dependent inhibition of separase. This discrepancy is likely explained by the existence of murine *PIN1RT1*, a retrogene encoding a protein highly related to Pin1 (Zhu et al., 2007), and/or by overlapping functions of other PP1ases. The most striking phenotype of *PIN1*<sup>-/-</sup> mice is a strong subfertility due to a proliferative defect of postmigratory primordial germ cells (Atchison et al., 2003). Interestingly, a similar albeit more

pronounced effect was observed in *SEPARASE*<sup>+/S1121A</sup> mice (Huang et al., 2008), making it tempting to speculate that separase represents the critical target of Pin1 in developing germ cells. Low levels of securin correlate well with the dependence on Cdk1-cyclin B1-mediated inhibition of separase in murine early embryos and primordial germ cells (Huang et al., 2008, 2009). Why nature relies on this form of separase regulation in these cases but on securin in most others remains enigmatic. Given our finding that mitotic phosphorylations of cyclin B1 weaken its binding to separase, it is tempting to speculate that cells with little or no securin need to upregulate a phosphatase

that removes these phosphates to turn Cdk1-cyclin B1 into a robust separase inhibitor (see below).

### Pin1-Dependent Isomerization of Separase Might Help to Order Late Mitotic Events

Chromosome segregation in anaphase, spindle disassembly, chromosome decondensation, nuclear envelope reformation, and cytokinesis are all negatively regulated by Cdk1, and all of these events are coupled by one trigger event, i.e., the derepression of APC/C. This bears the risk that a supposedly later event might occur too early—with disastrous consequences. Order could be ensured, however, if the execution of later events required a lower Cdk1 threshold activity than earlier ones, and if inactivation of this master regulatory kinase occurred not all at once, but in steps. The Pin1-dependent isomerization of separase into a securin-resistant conformer (Figure 5), together with the weakened binding of mitotically phosphorylated cyclin B1 to separase (Figure 6), results in activation of human separase in the presence of small residual amounts of cyclin B1. Thus, cohesin is cleaved when Cdk1 activity is already low but not yet zero. Interestingly, *trans*-to-*cis* isomerization of separase and dephosphorylation of cyclin B1 result in at least some of the little remaining Cdk1-cyclin B1 to be sequestered by separase after cohesin cleavage. Given that separase is a Cdk1 inhibitor (Gorr et al., 2005), this will result in further drop of Cdk1 activity (Figure S5A). As a result, later events might elegantly be promoted by previous activation of separase. For budding yeast, such a dependence has long been appreciated, the key difference being that, there, free separase is needed not to inhibit Cdk1 directly but to activate Cdc14, a phosphatase that antagonizes residual kinase activity during exit from mitosis (Queralt et al., 2006). It is interesting to note in this context that inhibition of Cdk1 by human separase in anaphase was reported to be required for relocalization of the chromosomal passenger complex from centromeres onto the spindle midzone as well as for cytokinesis at the end of female meiosis I (Gorr et al., 2006; Shindo et al., 2012).

### Formation and Function of Cdk1-Cyclin B1-Separase Complexes in Late Mitosis

Why do Cdk1-cyclin B1-separase complexes reaccumulate so late in mitosis? It was suggested that their efficient formation requires auto-cleavage of separase (Shindo et al., 2012). While we haven't addressed and therefore cannot exclude this possibility, auto-cleavage does not improve Cdk1-cyclin B1 binding to separase in prometaphase-arrested cells (Holland et al., 2007). Based on the findings presented here (Figure 6), we therefore propose that the late peaking of Cdk1-cyclin B1-separase is primarily timed by dephosphorylation of cyclin B1. Its kinetics will depend (1) on the inactivation of Cdk1, Plk1, and possibly additional downstream mitotic kinases and (2) on the activity and/or activation of the relevant, hitherto unknown phosphatase(s). Interestingly, the APC/C-dependent degradation of Plk1 is delayed with respect to disappearance of securin and cyclin B1 (Lindon and Pines, 2004). Moreover, the Cdk1-cyclin B1-controlled, so-called ENSA/Greatwall (EG) timer ensures that the B55 isotype of PP2A, which can dephosphorylate cyclin B1 *in vitro*, is derepressed only at a low cyclin B1 threshold (Borgne et al., 1999; Cundell et al., 2013). Thus, it is tempting to speculate

that the delayed inactivation of Plk1 and the delayed activation of PP2A-B55 might explain why Cdk1-cyclin B1-separase complex reforms only after cohesin has been cleaved.

Separase has an additional chromosome-independent but proteolysis-dependent function in centriole disengagement, which represents the licensing step for later centrosome duplication and occurs only after anaphase (Tsou and Stearns, 2006). This raises the possibility that Cdk1-cyclin B1-separase complexes might form in late mitosis not only to inhibit residual Cdk1 activity, but also to preserve some activatable separase for later. Final destruction of this last cyclin B1 (discernible in Figures 4B and S4B) might give rise to a small pulse of active separase in G1 phase, which could then trigger centriole disengagement but would be excluded from the reformed nucleus and, thus, not pose a threat for reloaded chromosomal cohesin. In line with this, binding of Cdk1-cyclin B1 indeed stabilizes otherwise unstable *cis*-separase, and replacement of endogenous separase by separase- $\Delta$ CLD compromises centriole disengagement (Hellmuth et al., 2015).

### EXPERIMENTAL PROCEDURES

Generation of stable transgenic cell lines inducibly expressing separase variants or securin<sup>DKM</sup> was previously described (Hellmuth et al., 2014). Cell synchronization, RNAi, flow cytometry, chromosome spreads, IPs, IF, *in vitro* expression of <sup>35</sup>S-Scc1, and preparation of *Xenopus* egg extracts were done as previously described (Hellmuth et al., 2014). For far western analysis, the corresponding PVDF membrane was incubated with 10  $\mu$ g/ml recombinant Pin1-WW (aa 1–54) overnight at 4°C prior to detection with rabbit anti-Pin1 antibody. For the clonogenic assay, transgenic HEK293 cells were transfected with *PIN1*- (or *GL2*-) directed siRNAs (40 nM). Seven days after plating 100 cells each in absence or presence of doxycycline, colonies were stained with crystal violet and counted. For chromatin isolation, cells were swollen in hypotonic buffer and then lysed. Chromatin was pelleted through a sucrose cushion, washed, and analyzed by immunoblotting. For tryptic digests purified securin-free preparations of separase in *cis* and *trans* were combined with 80 ng trypsin (sequencing grade, Promega) in a total reaction volume of 50  $\mu$ l and incubated at 4°C for the indicated times. For mathematical modeling the network shown in Figure S5B was converted into a set of nonlinear differential equations that were solved numerically by the freely available software XPPAUT. Kinetic parameter values and initial conditions are specified in the Supplemental Information.

### SUPPLEMENTAL INFORMATION

Supplemental Information includes Supplemental Experimental Procedures and five figures and can be found with this article online at <http://dx.doi.org/10.1016/j.molcel.2015.03.025>.

### AUTHOR CONTRIBUTIONS

S. Hellmuth co-designed and performed all experiments and wrote parts of the manuscript; S.R. and B.N. did the mathematical modeling; A.B. made anti-Pin1 and expression plasmids for GST-PPase and -WW; S. Heidmann suggested the experiments shown in Figures 4D, 4E, and S3C and critically read the manuscript; O.S. conceived and designed the research, made the figures, and wrote the manuscript.

### ACKNOWLEDGMENTS

We wish to thank Markus Herrmann for technical assistance and Franz-Xaver Schmid and Phillip Schmidpeter for fruitful discussions and critical reading of the manuscript. This work was supported by the Deutsche

Forschungsgemeinschaft (DFG) with grants STE 997/3 (within the priority program SPP1384) and STE 997/4 to O.S. and grant HE 2354/3-1 to S.H.. S.R. was supported by the EPSRC with a studentship and B.N. by the EC 7th Framework Program with MitoSys grant 241548.

Received: October 21, 2014  
Revised: January 23, 2015  
Accepted: March 18, 2015  
Published: April 23, 2015

## REFERENCES

- Atchison, F.W., Capel, B., and Means, A.R. (2003). Pin1 regulates the timing of mammalian primordial germ cell proliferation. *Development* **130**, 3579–3586.
- Boos, D., Kuffer, C., Lenobel, R., Körner, R., and Stemmann, O. (2008). Phosphorylation-dependent binding of cyclin B1 to a Cdc6-like domain of human separase. *J. Biol. Chem.* **283**, 816–823.
- Borgne, A., Ostvold, A.C., Flament, S., and Meijer, L. (1999). Intra-M phase-promoting factor phosphorylation of cyclin B at the prophase/metaphase transition. *J. Biol. Chem.* **274**, 11977–11986.
- Buheitel, J., and Stemmann, O. (2013). Prophase pathway-dependent removal of cohesin from human chromosomes requires opening of the Smc3-Scc1 gate. *EMBO J.* **32**, 666–676.
- Cundell, M.J., Bastos, R.N., Zhang, T., Holder, J., Gruneberg, U., Novak, B., and Barr, F.A. (2013). The BEG (PP2A-B55/ENSA/Greatwall) pathway ensures cytokinesis follows chromosome separation. *Mol. Cell* **52**, 393–405.
- Daub, H., Olsen, J.V., Bairlein, M., Gnad, F., Oppermann, F.S., Körner, R., Greff, Z., Kéri, G., Stemmann, O., and Mann, M. (2008). Kinase-selective enrichment enables quantitative phosphoproteomics of the kinome across the cell cycle. *Mol. Cell* **31**, 438–448.
- Fujimori, F., Takahashi, K., Uchida, C., and Uchida, T. (1999). Mice lacking Pin1 develop normally, but are defective in entering cell cycle from G(0) arrest. *Biochem. Biophys. Res. Commun.* **265**, 658–663.
- Gorr, I.H., Boos, D., and Stemmann, O. (2005). Mutual inhibition of separase and Cdk1 by two-step complex formation. *Mol. Cell* **19**, 135–141.
- Gorr, I.H., Reis, A., Boos, D., Wühr, M., Madgwick, S., Jones, K.T., and Stemmann, O. (2006). Essential CDK1-inhibitory role for separase during meiosis I in vertebrate oocytes. *Nat. Cell Biol.* **8**, 1035–1037.
- Hagting, A., Den Elzen, N., Vodermaier, H.C., Waizenegger, I.C., Peters, J.M., and Pines, J. (2002). Human securin proteolysis is controlled by the spindle checkpoint and reveals when the APC/C switches from activation by Cdc20 to Cdh1. *J. Cell Biol.* **157**, 1125–1137.
- Hellmuth, S., Böttger, F., Pan, C., Mann, M., and Stemmann, O. (2014). PP2A delays APC/C-dependent degradation of separase-associated but not free securin. *EMBO J.* **33**, 1134–1147.
- Hellmuth, S., Pöhlmann, C., Brown, A., Böttger, F., Sprinzl, M., and Stemmann, O. (2015). Positive and negative regulation of vertebrate separase by cdk1-cyclin B1 may explain why securin is dispensable. *J. Biol. Chem.* **290**, 8002–8010.
- Holland, A.J., and Taylor, S.S. (2006). Cyclin-B1-mediated inhibition of excess separase is required for timely chromosome disjunction. *J. Cell Sci.* **119**, 3325–3336.
- Holland, A.J., Böttger, F., Stemmann, O., and Taylor, S.S. (2007). Protein phosphatase 2A and separase form a complex regulated by separase auto-cleavage. *J. Biol. Chem.* **282**, 24623–24632.
- Hornig, N.C., Knowles, P.P., McDonald, N.Q., and Uhlmann, F. (2002). The dual mechanism of separase regulation by securin. *Curr. Biol.* **12**, 973–982.
- Huang, X., Andreu-Vieyra, C.V., York, J.P., Hatcher, R., Lu, T., Matzuk, M.M., and Zhang, P. (2008). Inhibitory phosphorylation of separase is essential for genome stability and viability of murine embryonic germ cells. *PLoS Biol.* **6**, e15.
- Huang, X., Andreu-Vieyra, C.V., Wang, M., Cooney, A.J., Matzuk, M.M., and Zhang, P. (2009). Preimplantation mouse embryos depend on inhibitory phosphorylation of separase to prevent chromosome missegregation. *Mol. Cell Biol.* **29**, 1498–1505.
- Jackman, M., Lindon, C., Nigg, E.A., and Pines, J. (2003). Active cyclin B1-Cdk1 first appears on centrosomes in prophase. *Nat. Cell Biol.* **5**, 143–148.
- Jäger, H., Herzig, B., Herzig, A., Sticht, H., Lehner, C.F., and Heidmann, S. (2004). Structure predictions and interaction studies indicate homology of separase N-terminal regulatory domains and *Drosophila* THR. *Cell Cycle* **3**, 182–188.
- Lindon, C., and Pines, J. (2004). Ordered proteolysis in anaphase inactivates Plk1 to contribute to proper mitotic exit in human cells. *J. Cell Biol.* **164**, 233–241.
- Liou, Y.C., Zhou, X.Z., and Lu, K.P. (2011). Prolyl isomerase Pin1 as a molecular switch to determine the fate of phosphoproteins. *Trends Biochem. Sci.* **36**, 501–514.
- Liu, H., Rankin, S., and Yu, H. (2013). Phosphorylation-enabled binding of SGO1-PP2A to cohesin protects sororin and centromeric cohesion during mitosis. *Nat. Cell Biol.* **15**, 40–49.
- Lu, K.P., Hanes, S.D., and Hunter, T. (1996). A human peptidyl-prolyl isomerase essential for regulation of mitosis. *Nature* **380**, 544–547.
- Lu, P.J., Zhou, X.Z., Shen, M., and Lu, K.P. (1999). Function of WW domains as phosphoserine- or phosphothreonine-binding modules. *Science* **283**, 1325–1328.
- Mei, J., Huang, X., and Zhang, P. (2001). Securin is not required for cellular viability, but is required for normal growth of mouse embryonic fibroblasts. *Curr. Biol.* **11**, 1197–1201.
- Nasmyth, K., and Haering, C.H. (2009). Cohesin: its roles and mechanisms. *Annu. Rev. Genet.* **43**, 525–558.
- Queralt, E., Lehane, C., Novak, B., and Uhlmann, F. (2006). Downregulation of PP2A(Cdc55) phosphatase by separase initiates mitotic exit in budding yeast. *Cell* **125**, 719–732.
- Shen, M., Stukenberg, P.T., Kirschner, M.W., and Lu, K.P. (1998). The essential mitotic peptidyl-prolyl isomerase Pin1 binds and regulates mitosis-specific phosphoproteins. *Genes Dev.* **12**, 706–720.
- Shindo, N., Kumada, K., and Hirota, T. (2012). Separase sensor reveals dual roles for separase coordinating cohesin cleavage and cdk1 inhibition. *Dev. Cell* **23**, 112–123.
- Stemmann, O., Zou, H., Gerber, S.A., Gygi, S.P., and Kirschner, M.W. (2001). Dual inhibition of sister chromatid separation at metaphase. *Cell* **107**, 715–726.
- Toyoshima-Morimoto, F., Taniguchi, E., Shinya, N., Iwamatsu, A., and Nishida, E. (2001). Polo-like kinase 1 phosphorylates cyclin B1 and targets it to the nucleus during prophase. *Nature* **410**, 215–220.
- Tsou, M.F., and Stearns, T. (2006). Mechanism limiting centrosome duplication to once per cell cycle. *Nature* **442**, 947–951.
- Urusova, D.V., Shim, J.H., Kim, D.J., Jung, S.K., Zykova, T.A., Carper, A., Bode, A.M., and Dong, Z. (2011). Epigallocatechin-gallate suppresses tumorigenesis by directly targeting Pin1. *Cancer Prev. Res. (Phila.)* **4**, 1366–1377.
- Viadiu, H., Stemmann, O., Kirschner, M.W., and Walz, T. (2005). Domain structure of separase and its binding to securin as determined by EM. *Nat. Struct. Mol. Biol.* **12**, 552–553.
- Waizenegger, I.C., Hauf, S., Meinke, A., and Peters, J.M. (2000). Two distinct pathways remove mammalian cohesin from chromosome arms in prophase and from centromeres in anaphase. *Cell* **103**, 399–410.
- Wolf, F., Wandke, C., Isenberg, N., and Geley, S. (2006). Dose-dependent effects of stable cyclin B1 on progression through mitosis in human cells. *EMBO J.* **25**, 2802–2813.
- Yaffe, M.B., Schutkowski, M., Shen, M., Zhou, X.Z., Stukenberg, P.T., Rahfeld, J.U., Xu, J., Kuang, J., Kirschner, M.W., Fischer, G., et al. (1997). Sequence-specific and phosphorylation-dependent proline isomerization: a potential mitotic regulatory mechanism. *Science* **278**, 1957–1960.
- Zhu, J.X., Dagostino, E., Rejto, P.A., Mroczkowski, B., and Murray, B. (2007). Identification and characterization of a novel and functional murine Pin1 isoform. *Biochem. Biophys. Res. Commun.* **359**, 529–535.

**Molecular Cell**

**Supplemental Information**

## **Human Chromosome Segregation**

**Involves Multi-Layered Regulation of Separase**

**by the Peptidyl-Prolyl-Isomerase Pin1**

**Susanne Hellmuth, Scott Rata, Andreas Brown, Stefan Heidmann, Bela Novak, and Olaf Stemmann**

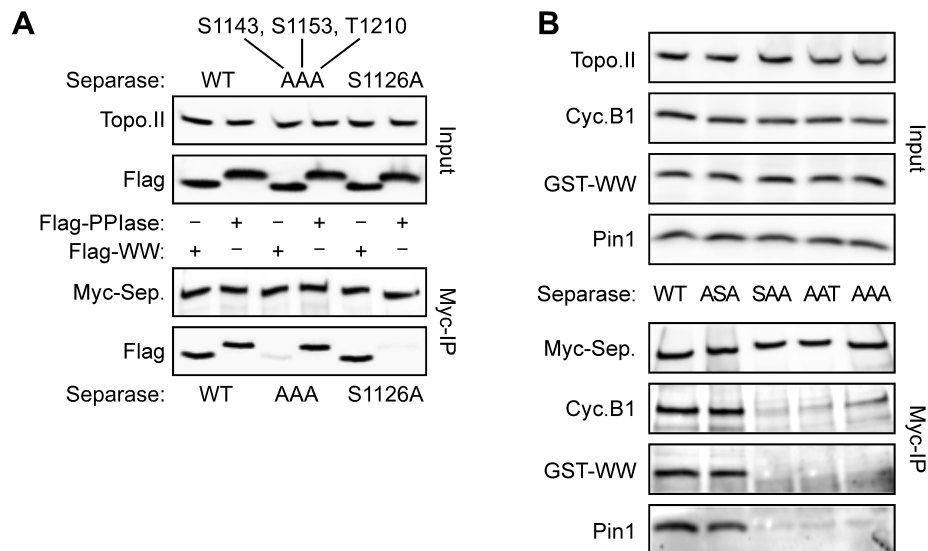


**Figure S1 (Related to figure 1): Mapping the WW binding site on separase.**

(A) The S1143, S1153, T1210A variant of separase (AAA) is defective in binding Pin1's WW domain. Hek293T cells overexpressing Myc-tagged separase-WT, -AAA or -S1126A together with Flag-tagged WW- or PPlase-domain of Pin1 were arrested in prometaphase by nocodazole. Lysates (input) and anti-Myc IPs were analyzed by immunoblotting.

(B) Re-introducing S1153 into separase-AAA (resulting in the ASA variant) is sufficient to restore WW domain binding. Lysates (input) from mitotic Hek293T cells overexpressing Myc-tagged separase-WT, -ASA (S1143A and T1210A), -SAA (S1153A and T1210A), -AAT (S1143A and S1153A) or -AAA together with GST-WW were subjected to anti-Myc IP and immunoblotting. Note that S1153A abolishes also the binding of endogenous Pin1 to separase. Thus, the contribution of the PPlase domain to the affinity of full-length Pin1 for separase is negligible.

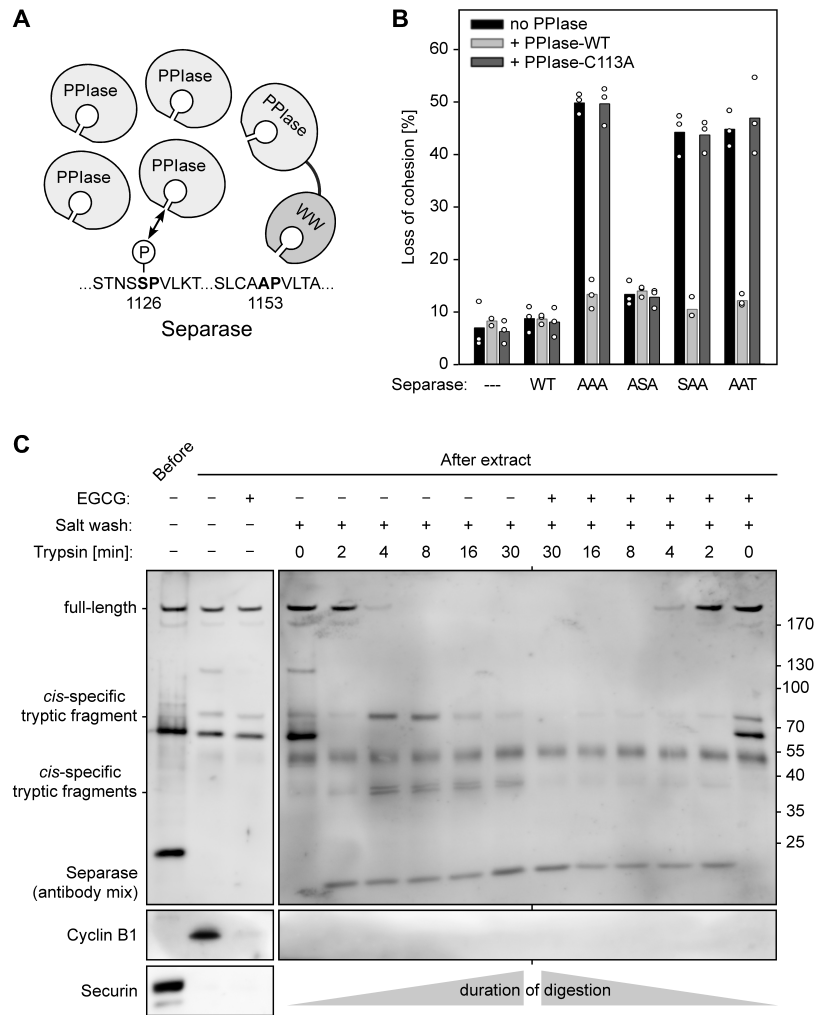


**Figure S2 (related to figure 3):**

(A) Rationale of why the premature loss of cohesion due to overexpression of S1153A containing separase variants can be suppressed by simultaneous overexpression of Pin1's PPlase domain.

(B) Overexpression of WW-binding deficient separase variants causes premature loss of cohesion which can be suppressed by co-overexpression of catalytically active but not inactive PPlase domain. Hek293T cells were transiently transfected to express, as indicated, Myc-tagged separase variants (described in Figure S1) and Flag-tagged PPlase-WT or -C113A. Following mitotic arrest, cells were subjected to chromosome spreading. Represented are mean values (bars) out of three independent experiments (dots) quantifying at least 100 cells per condition.

(C) Differential tryptic digest reveals Pin1-dependent change of separase's conformation. Myc<sub>6</sub>-Tev<sub>2</sub>-separase in complex with securin was bound to anti-Myc beads, incubated in an anaphase like *Xenopus* egg extract supplemented with  $\Delta$ 90-cyclinB1 and, where indicated, EGCG. Following removal of securin and  $\Delta$ 90-cyclinB1 by ubiquitin-dependent degradation and high salt wash, respectively, separase was eluted by TEV-protease treatment, incubated with trypsin for the indicated times, and analyzed by immunoblotting.

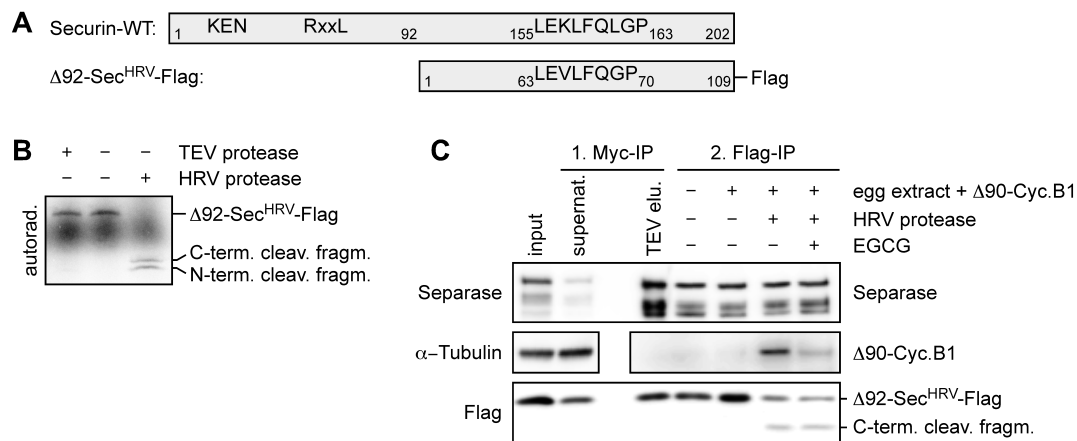


**Figure S3 (related to figure 4): Securin binding arrests separase in the Cdk1-resistant *trans*-conformation.**

(A) Comparison of securin-WT with an APC/C resistant, Flag-tagged securin containing a cleavage site for human rhinovirus 3c protease (HRV). Note that creation of a HRV site in securin merely required changing lysine 157 to valine and deleting leucine 161. The recognition sites for APC/C<sup>Cdc20</sup>, KEN (Lys-Glu-Asn) and RxxL (Arg-Xxx-Xxx-Leu = destruction (D) box), are indicated in their relative positions.

(B)  $\Delta$ 92-securin<sup>HRV</sup>-Flag is efficiently cleaved by HRV- but not TEV-protease. Following incubation of radioactively labeled <sup>35</sup>S- $\Delta$ 92-securin<sup>HRV</sup>-Flag with TEV- or HRV-protease as indicated, samples were separated according to a protocol from Thermo-Scientific on a 15% Tris-SDS-PAG with a Tris-Tricine-SDS electrode buffer and analyzed by autoradiography.

(C) Co-purification of cyclin B1 with securin-associated separase requires bisection of securin<sup>HRV</sup> and Pin1-catalyzed isomerization of separase. Myc<sub>6</sub>-Tev<sub>2</sub>-separase in complex with  $\Delta$ 92-securin<sup>HRV</sup>-Flag was bound to anti-Myc beads and eluted by TEV-protease treatment. The eluted complex was then immobilized on anti-Flag agarose and incubated in an anaphase like *Xenopus* egg extract supplemented with  $\Delta$ 90-cyclin B1 and, where indicated, EGCG and/or HRV-protease. (Note that for treatment with EGCG and HRV-protease, EGCG was added 10 minutes earlier.) Flag-beads were re-isolated from the extract under low salt conditions and associated proteins detected by immunoblotting.

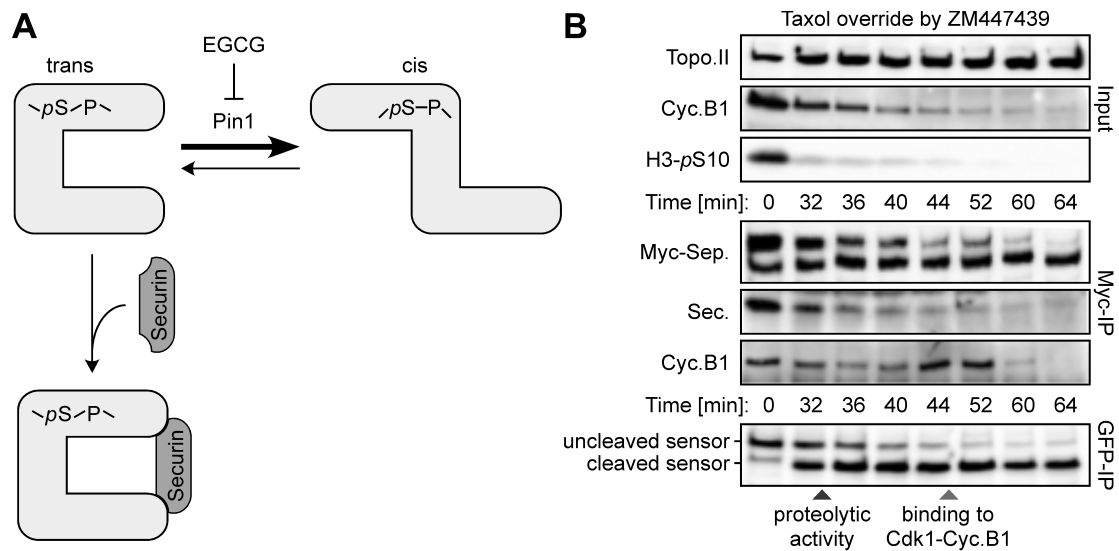


**Figure S4 (related to figure 5): The late mitotic association of separase with Cdk1-cyclin B1 occurs after cohesin cleavage.**

Transgenic HeLa FlpIn TRex cells were transiently transfected to express histone H2B-mCherry-Scc1<sup>107-268</sup>-eGFP, thymidine arrested, released in doxycyclin containing medium to induce Myc<sub>6</sub>-Tev<sub>2</sub>-separase expression and re-arrested by taxol. Upon addition of ZM447439 (t = 0 minutes), proteolytic activity and cyclin B1 binding of separase were followed by immunoblotting of time-resolved anti-GFP- and anti-Myc IPs, respectively. Note that mitosis takes longer in the cell line used here than in the HeLa K cells used in figure 4B, which is why the times of formation of the second Cdk1-cyclin B1-separase peak do not coincide.

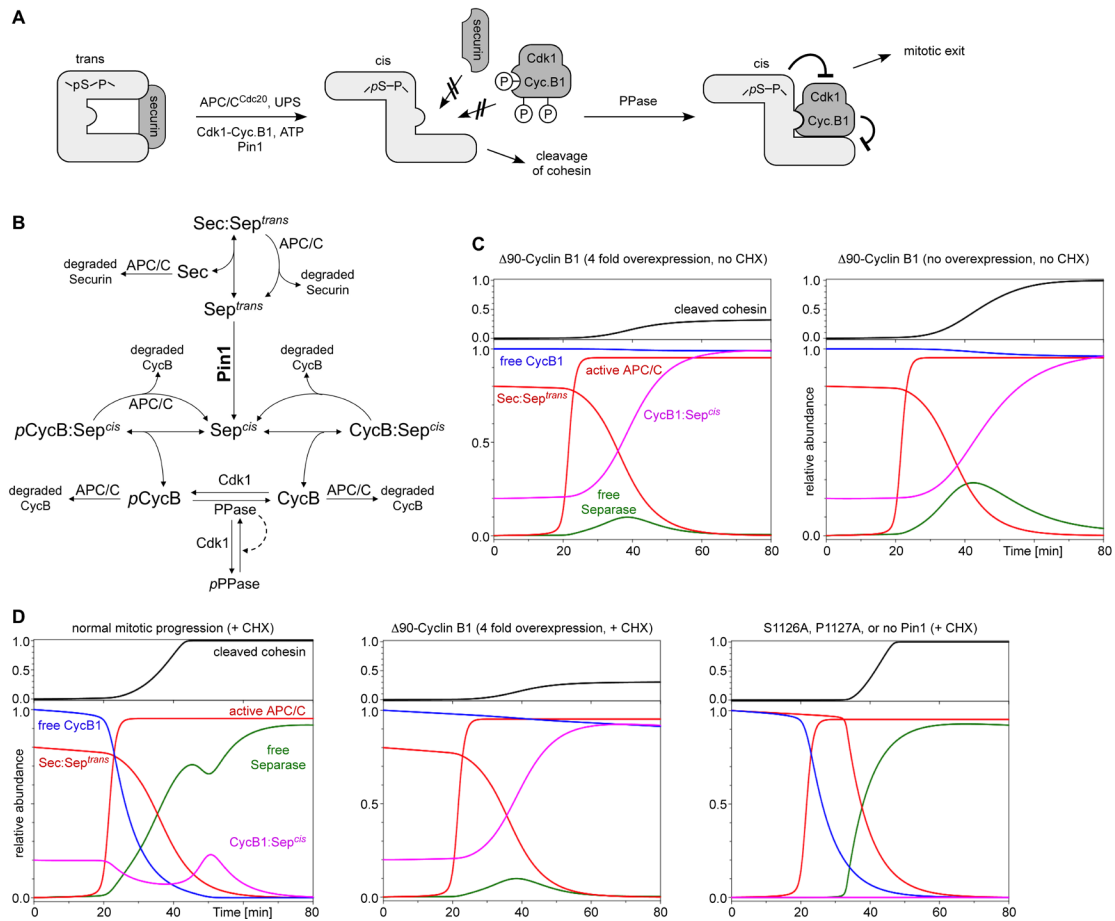


**Figure S5 (related to figure 6): Mathematical modelling of mitotic progression**

(A) Model of separase's conformational states and binding partners across a typical mitosis.

(B) Wiring diagram forming the basis for the mathematical model. For sake of clarity, the network does not show (but the model considers) that the Cdk1-cyclin B1-separase complex is also subject to (de)phosphorylation of cyclin B1.

(C) Mathematical simulations of mitotic progression in presence of non-degradable cyclin B1 at four-fold of physiological (left) and at physiological (right) concentrations in the absence of cycloheximide.

(D) Mathematical simulation of normal mitotic progression (left), the effect of four-fold over-expression of non-degradable cyclin B1 (middle), and the lack of Pin1 or replacement of endogenous separase by a S1126A or P1127A variant (right) in the presence of cycloheximide.

## Experimental Procedures

### Antibodies

The following antibodies were used for immunoblotting according to standard protocols: rabbit anti-separase (Stemmann et al, 2001), mouse anti-securin (1:1,000; MBL), rabbit anti-securin (1:1,000; Epitopics), mouse anti-Flag M2 (1:2,000; Sigma-Aldrich), mouse anti-Myc (1:50; 9E10; hybridoma supernatant), rabbit anti-phosphoSer10-histone H3 (1:1,000; Millipore), mouse anti-cyclin B1 (1:1,000; Millipore), rabbit anti-cyclin B1 (1:1,000; Santa Cruz), mouse anti-topoisomerase II $\alpha$  (1:1,000; Enzo Life Sciences), goat anti-Cdc27 (1:1,000; gift from T. U. Mayer), mouse anti-cyclin A2 (1:200; Santa Cruz Biotechnology), goat anti-GST (1:800; gift from D. Boos), rabbit anti-Pin1 (1:1000; raised against full-length *Xenopus* Pin1), rat anti-HA (1:1,000; 3F10; Roche), mouse anti-RGS-His<sub>6</sub> (1:800; Qiagen), mouse anti-CDK1 (1:1000; Santa Cruz Biotechnology), mouse anti-GFP (1:2,000; gift from D. van Essen and S. Sacconi), rabbit anti-SMC3 (1:1,000; gift from S. Rankin) and mouse anti- $\alpha$ -tubulin (1:200; Developmental Studies Hybridoma Bank; 12G10; hybridoma supernatant). For identification of tryptic separase fragments a mixture of three different separase antibodies was used: rabbit anti-Separase raised against Arg2-Glu16 (Stemmann et al, 2001), Ser1305-Thr1573 (Zou et al, 1999) and Arg1425-Ser1475 (Bethyl Laboratories). For Far Western analysis (Fig. 1F) the corresponding PVDF-membrane was incubated with 10  $\mu$ g/ml recombinant Pin1-WW [aa1-54] over night at 4°C prior to detection with rabbit anti-Pin1 antibody (see above). For immunoprecipitation experiments, the following affinity matrices and antibodies were used: mouse anti-Myc Agarose (Sigma-Aldrich), mouse anti-Flag M2-Agarose (Sigma-Aldrich), rat anti-HA Agarose (Roche), camel anti-GFP (gift from A. Holland) coupled to NHS-sepharose (GE Healthcare), human IgG Sepharose (GE Healthcare), protein G Sepharose (GE Healthcare) coupled to rabbit anti-securin (raised against His<sub>6</sub>-tagged human securin) or unspecific rabbit IgG (Bethyl). For immunofluorescence staining of fixed cells, mouse anti-Scc1 (1:500; Milipore), rabbit

anti-survivin (1:400; Santa Cruz Biotechnology) and human anti-Crest (1:1,000; Immunovision) were used. Secondary antibodies (all 1:500): Cy3 goat anti-human IgG (Bethyl), Cy5 goat anti-mouse IgG (Bethyl) and Alexa Fluor 488 goat anti-rabbit IgG (Invitrogen). Immunofluorescence microscopy was done as previously described (Hellmuth et al., 2014). Pictures shown in figure 7D are representative maximum projections (0.35  $\mu$ M Z-increments over 8  $\mu$ M , HCX PL APO 100x/1.40-0.70 oil objective, DMI 6000 inverted Leica microscope).

### **Cell lines**

For stable, inducible expression of Myc<sub>6</sub>-Tev<sub>2</sub>-separase variants [WT: wild type; S1126A: serine 1126 changed to alanine;  $\Delta$ CLD: amino acids 1342-1400 deleted] corresponding transgenes were stably integrated into Hek293-FlpIn-TRex (Invitrogen). Clones were selected with 150  $\mu$ g/ml hygromycin B (Roth). Induction of transgenic Myc<sub>6</sub>-Tev<sub>2</sub>-separases was done using 0.2-1  $\mu$ g/ml doxycycline (Sigma-Aldrich) for 10-14 hours. For Fig. 5C, securin<sup>DKM</sup>-Flag (more specifically, a transgene encoding for a C-terminally His<sub>6</sub>-Flag-His<sub>6</sub>-Flag-tagged securin with the following changes: K9R, E10D, N11Q, R61A, L64A) was stably integrated and inducibly expressed in HeLa-FlpIn-TRex as described (Hellmuth et al., 2014). All cells were cultured in DMEM (GE Healthcare) supplemented with 10% FCS (Sigma-Aldrich) at 37°C and 5% CO<sub>2</sub>.

### **Cell treatments**

For synchronization at the G1/S boundary, cells were treated with 2 mM thymidine (Sigma-Aldrich) for 20 hours and then released into fresh medium. Synchronization of cells in prometaphase was done by addition of nocodazole (Sigma-Aldrich) or taxol (Calbiochem) to 0.2  $\mu$ g/ml each 6 hours after release from a single thymidine block or for 14 hours to asynchronous cells. G2 arrest was achieved by addition of RO3306 (Santa-Cruz Biotechnology) to 10  $\mu$ M 4 hours after release from a previous

thymidine treatment. For the taxol-ZM experiments shown in figures 4A, 5C, and S4 taxol-arrested mitotic HeLa cells were harvested by shake-off and released for the indicated times by replating into medium supplemented with ZM447439 (5  $\mu$ M, Tocris Biosciences), taxol (0.2  $\mu$ g/ml) and cycloheximide (30  $\mu$ g/ml, Sigma-Aldrich). Where indicated, EGCG (100  $\mu$ M; Sigma-Aldrich) or DMSO (as control) was added 1 hour before ZM. In other cases of Pin1 inhibition, EGCG was added either together with nocodazole for 14 hours (Fig. 2C) or 11 hours after release from a thymidine arrest and 1 hour prior to cell fixation (Fig. 7B).

For transient expressions, Hek293T cells were transfected using a calcium phosphate based method with pCS2-based plasmids encoding the following proteins: Myc<sub>6</sub>-Tev<sub>2</sub>-separase [WT; S1126A;  $\Delta$ CLD; AAA: S1143A, S1153A, T1210A; SAA: S1153A, T1210A; ASA: S1143A, T1210A; AAT: S1143A, S1153A; P1127A; S1153A], ZZ-Tev<sub>4</sub>-separase, Flag<sub>3</sub>-Pin1, GST-Tev<sub>3</sub>-WW [WW: amino acids 1-54], GST-Tev<sub>3</sub>-PPlase [PPlase: amino acids 44-163], FLAG<sub>3</sub>-PPlase [WT; C113A],  $\Delta$ 92-securin<sup>HRV</sup>-Flag (more specifically, a C-terminally His<sub>6</sub>-Flag-His<sub>6</sub>-Flag-tagged securin with the following changes: amino acids 1-92 and 161 deleted, K157V), untagged securin-WT,  $\Delta$ 90-cyclin B1 [WT; 4A: S126,128,133,147A], and cyclin B1-8A-Flag (more specifically, a C-terminally His<sub>6</sub>-Flag-His<sub>6</sub>-Flag-tagged cyclin B1 with the following changes: S9,35,69,116,126,128,133,147A). To obtain separase-securin complexes for *Xenopus* egg-extract experiments (Fig. 2B, 5A-B, 7A-B), transiently transfected, separase and securin co-expressing Hek293T cells were synchronized in S-phase to prevent Cdk1-cyclin B1-separase complex formation. For the experiment shown in figure S4, Lipofectamine 2000 (Life technologies) was used according to manufacturer's instructions to transiently transfect a pCS2-based plasmid encoding H2B-mCherry-Scc1<sup>107-268</sup>-eGFP into transgenic HeLa cells inducibly expressing Myc<sub>6</sub>-Tev<sub>2</sub>-separase-WT.

### **RNA interference and clonogenic assay**

For knockdown of human Pin1 as shown in figure 2C, cells were calcium phosphate transfected for 12 hours with a mixture of two siRNA duplexes (*PIN1* 3'UTR: 5'-UCGCAAAGGUGAACACUCATT-3', *PIN1* 5'UTR: 5'-GAGGGAAGAUGGCGGACGATT-3') at 80 nM, grown for additional 24 hours, and then analysed. Luciferase siRNA (*GL2*) was used as negative control.

For the clonogenic assay (Fig. 2A) transgenic Hek293 cells were transfected with *PIN1* (or *GL2*) directed siRNAs as described above but at a concentration of only 40 nM. Then, 100 cells per condition were replated in medium containing either doxycycline to induce the overexpression of Myc<sub>6</sub>-Tev<sub>2</sub>-tagged separase-WT (+ Dox.) or the corresponding carrier solvent ethanol (- Dox.). Cells were grown for 7 days before colonies were fixed in ice-cold methanol for 10 minutes. Staining with crystal violet was performed as described (Franken et al, 2006) except for the use of ethanol instead of glutaraldehyde. The number of colonies per plate with a minimal area of 20 (circularity 0.00-1.00) was determined automatically with the ImageJ analyze particle software. Corresponding Western samples were also taken after 7 days. To this end, cells were initially plated at higher densities but otherwise under the same conditions.

### **Immunoprecipitation**

1×10<sup>7</sup> cells were lysed in 1 ml lysis buffer 2 (20 mM Tris-HCl pH 7.7, 100 mM NaCl, 10 mM NaF, 20 mM β-glycerophosphate, 5 mM MgCl<sub>2</sub>, 0.1% Triton X-100, 5% glycerol) supplemented with complete protease inhibitor cocktail (Roche). Lysates were cleared by centrifugation at 66,000 g for 35 min (Fig. 2B, 5A-B, and 7A-B) or 16,000 g for 30 min. Separase IPs (Fig. 4B and 5C) were performed as described (Hellmuth et al, 2014). For precipitation of the Histon2B-mCherry-Scc1<sub>107-268</sub>-eGFP fusion protein (Fig. S4) the corresponding lysates were treated with DNase A (50 µg/ml) for 30 minutes at 4°C prior to centrifugation at 1,500 g for 10 minutes. For

Myc-, Flag-, HA-, GFP- and ZZ- (IgG binding domains of protein A) immunoprecipitations, the corresponding agarose matrices were equilibrated in lysis buffer 2, incubated with pre-cleared whole cell lysates (input) for 4 to 12 hours at 4°C, washed three times with lysis buffer 2, and finally eluted by TEV protease treatment in TEV cleavage buffer (10 mM Hepes-KOH pH 7.7, 50 mM NaCl, 25 mM NaF, 1 mM EGTA, 20% glycerol) for 40 min at room temperature or by boiling in non-reducing SDS-sample buffer.

To estimate roughly what percentage of separase is switched from *trans* to *cis* in anaphase, signals of associated securin from figure 5C were quantified and calculated as following:  $100 \times 1 - [\text{Sec.}^{\text{DKM, 48 min, -EGCG}} \div (\text{end.Sec.}^{\text{0 min, -EGCG}} - \text{end.Sec.}^{\text{48 min, -EGCG}})]$ .

### **Recombinant proteins**

Baculoviruses were produced following Invitrogen's instructions for the Bac-to-Bac System. Insect (SF9) cells were infected with individual baculoviral stocks or mixtures thereof, each at an MOI of 1, further cultured for 58 hours, then treated for 2 hours with okadaic acid (0.4  $\mu\text{M}$ ), and finally harvested. For production of human  $\Delta 90$ -cyclin B1 carrying an N-terminal ArgGlySer(His<sub>6</sub>)<sub>2</sub>-TEV<sub>2</sub>-tag corresponding SF9 cells (total of  $5 \cdot 10^8$ ) were dounced in 40 ml lysis buffer 3 (50 mM Na-phosphate buffer pH 8.0, 500 mM NaCl, 5 mM NaF, 5 mM  $\beta$ -glycerophosphate, 0.2% Triton X-100, 0.2 mM DTT) supplemented with 10 mM imidazole. After centrifugation at 16,000 g for 30 minutes, the supernatant was combined with 3 ml of Ni<sup>2+</sup>-NTA-agarose (GE Healthcare) and rotated for 3 hours at 4°C. The affinity matrix was transferred into a column, washed with 15 volumes of lysis buffer 3 supplemented with 20 mM imidazole, and eluted in 8 ml lysis buffer 3 supplemented with 250 mM imidazole (and re-adjusted with HCl to pH 8.0). The protein was dialysed against 10 mM Hepes-KOH pH 7.7, 100 mM KCl, 1 mM MgCl<sub>2</sub>, 50 mM sucrose, 1 mM DTT. To

produce active human Cdk1 complex, SF9 cells co-expressing Cdk1, His-tagged  $\Delta 90$ -cyclin B1 (see above), and Cks1 were subjected to lysis and metal ion affinity chromatography (IMAC) as described above. The eluate was dialysed against 30 mM Tris-HCl pH 8.5, 80 mM NaCl, 1 mM DTT, fractionated on a 1 ml HiTrap-Q column (GE Healthcare) by applying a linear NaCl gradient, and dialyzed against 30 mM HEPES-KOH pH 7.7, 80 mM KCl, 30% glycerol, 1 mM DTT.

His<sub>6</sub>-Sumo1-tagged HRV-protease and His<sub>6</sub>-Sumo3-tagged  $\Delta 92$ -securin were expressed from pET28 plasmid (Novagen) derivatives in *E. coli* strain BL21(DE3). Cells were lysed in 20-fold excess (v/w) of PBS supplemented with additional 400 mM NaCl, 10 mM imidazole, and 0.5 mM DTT. After centrifugation and standard IMAC, the eluates were incubated with His<sub>6</sub>-Senp2. Then, to remove the tag and the Sumo-protease from the target protein, the HRV-protease preparation was run in 50 mM Tris-HCl pH 8.0, 250 mM NaCl, 5 mM EDTA over a Superdex75 (26/60; GE Healthcare) and then adjusted to 20% glycerol.  $\Delta 92$ -securin was dialysed against PBS supplemented with additional 400 mM NaCl, 10 mM imidazole, and 0.5 mM DTT, subjected to a second IMAC (where it stayed in the flow-through), and finally dialysed against 10 mM HEPES-KOH pH 8.5, 150 mM potassium acetate, 2 mM MgCl<sub>2</sub>, 0.1 mM DTT. GST-Pin1 was expressed from a pGEX plasmid (GE Healthcare) derivative in *E. coli* strain BL21. Cleared lysates of the corresponding cells in PBS supplemented with 10 mM DTT were incubated with glutathion-sepharose for 4 hours at 4°C. The affinity matrix was transferred into a column, washed with 15 volumes of PBS supplemented with 10 mM DTT, and eluted by rotation in PBS supplemented with 10 mM DTT and 50 mM glutathione (and re-adjusted to pH 7.7) for 2 hours at 4°C. Finally, the protein was dialysed against CSF-XB supplemented with 0.2 mM DTT. All purified proteins were snap-frozen in aliquots and stored at -80°C.

### Experiments involving *Xenopus* egg extracts

<sup>35</sup>S-labeled Scc1-GFP was *in vitro* expressed by combining a corresponding pCS2 expression plasmid with SP6 RNA polymerase supplemented rabbit reticulocyte lysate (TNT SP6 Coupled Transcription/Translation System from Promega) in presence of <sup>35</sup>S-methionine (Hartmann Analytic) according to the manufacturers' instructions. In parallel, separase-securin complexes immobilized on anti-Myc-, anti-Flag-, or IgG-beads via a corresponding N-terminal tag on separase were combined with a twenty-fold excess (v/v) of anaphase like *Xenopus* egg extract with constitutively high Cdk1 activity. To prepare this extract, a standard CSF-extract (Murray, 1991) was supplemented with cycloheximide (ad 100 µg/ml) and His-tagged human Δ90-cyclin B1 purified from insect cells (ad 39 ng/µl or 550 nM) and released with CaCl<sub>2</sub> (ad 0.6 mM) to trigger securin degradation. For the experiment shown in figure 5B, the extract was additionally supplemented with EGCG (ad 100 µM) prior to its release with calcium. In order to deplete *Xenopus* Pin1 (Fig. 2B), 170 µl protein A Dynabeads-slurry (Life Technologies) were coupled to 40 µg anti-Pin1, washed, and slowly rotated with 80 µl extract for 30 minutes at room temperature. As a negative control, unspecific rabbit IgG was used instead of anti-Pin1. The magnetic beads were removed from the extracts prior to the addition of Ca<sup>2+</sup>. Where indicated, Pin1-depleted extract was supplemented with recombinant human GST-Pin1 ad 0.3 µg/µl (Fig. 2B). After incubation in egg extract for 1 hour at 18°C, separase-beads were re-isolated, washed with CSF-XB containing additional 500 mM NaCl and 0,01% Trition X-100 for 5 min each ("high salt wash") to elute any associated Cdk1-cyclin B1 (unless specified other), and finally eluted by TEV protease treatment. For re-inhibition experiments (Fig. 5A-B), separase-beads were incubated with recombinant Δ92 securin at the indicated concentrations for 1 hour on ice, washed to remove unbound securin and only then eluted with TEV protease. Scc1 cleavage was performed either during TEV elution (Fig. 2B and 5A-B) with 30 µl beads in 30 µl TEV cleavage buffer or after TEV elution (Fig. 7A-B) with 15 µl separase. In each case,

samples were combined with 2.5  $\mu$ l  $^{35}$ S-Scc1-GFP and incubated for 20 to 30 minutes at room temperature. Immunoaffinity purified separase corresponding to one confluent 14.5 cm tissue culture dish of transfected cells was sufficient for up to ten Scc1 cleavage reactions. Samples were analyzed by SDS-PAGE followed by Western blotting or autoradiography.

### **Tryptic digest**

Myc<sub>6</sub>-Tev<sub>2</sub>-tagged separase in complex with securin was immunoprecipitated from Hek293T cells arrested in interphase. Separase-securin complex on Myc-beads was then incubated in anaphase like *Xenopus* egg extract with constitutively high Cdk1 activity in presence or absence of 100  $\mu$ M EGCG. Securin-free separase was re-isolated, subjected to a high salt wash (see above) and equilibrated in 50 mM Tris HCl pH 8.5, 0.5 mM EDTA prior to elution with TEV-protease. Eluates were combined with 80 ng trypsin (sequencing grade, Promega) in a total reaction volume of 50  $\mu$ l and incubated at 4°C. At indicated time points, 10  $\mu$ l each were combined with 10  $\mu$ l 2x SDS-sample buffer. Samples were analyzed by SDS-PAGE followed by Western blotting.

### **Reconstitution of separase isomerization in a purified system**

Myc<sub>6</sub>-Tev<sub>2</sub>-separase in complex with  $\Delta$ 92-securin<sup>HRV</sup>-Flag was isolated from transiently transfected Hek293T cells on anti-Myc beads, washed, and eluted by TEV protease treatment. The complex was then immobilized via securin by incubation of the eluate with anti-Flag beads for 4 hours at 4°C. Beads were washed twice in 1x protein kinase reaction buffer (NEB) and incubated for 30 minutes at room temperature with an active complex of recombinant Cdk1 and His<sub>6</sub>-tagged  $\Delta$ 90-cyclin B1 (40  $\mu$ g/ml) in presence of ATP (300  $\mu$ M). This was followed by addition of recombinant GST-Pin1 (1  $\mu$ g/ $\mu$ l) and incubation for 10 min at room temperature.

Aliquots of the beads were then combined with recombinant HRV protease (10 µg/ml), EGCG (100 µM; was added 10 min prior to HRV protease) and/or reference solutions, as indicated (Fig. 4A). After 1 hour at room temperature beads were washed three times with lysis buffer 2, eluted by boiling in non-reducing SDS-sample buffer, and analyzed by immunoblotting.

### **Chromatin isolation**

Starting from a taxol arrested culture of transgenic Hek293 lines expressing Myc<sub>6</sub>-Tev<sub>2</sub>-tagged separase-S1126A or -ΔCLD, 1×10<sup>6</sup> cells each were harvested at indicated timepoints after ZM addition (Fig. 7C), washed once in PBS, resuspended in 130 µl buffer A (10 mM HEPES-KOH pH 7.9, 10 mM KCl, 1.5 mM MgCl<sub>2</sub>, 10 % glycerol, 1 mM DTT, supplemented with complete protease inhibitor cocktail) and shifted to 4°C. Swollen cells were lysed by the addition of Triton X-100 ad 0.1% and a 10 minutes incubation on ice. The resulting whole cell lysates were centrifuged through a cushion of 200 µl buffer A supplemented with 0.9 M sucrose at 2,900 g for 15 min at 4°C. Following careful removal of the supernatants, which were used for immunoblotting, chromatin pellets were washed once in 100 µl buffer B (3 mM EDTA-NaOH pH 8.0, 0.2 mM EGTA-KOH pH 8.0, 1 mM DTT and complete protease inhibitor cocktail). The isolated chromatin and aliquots of the input were boiled in SDS-sample buffer and analysed by immunoblotting.

### **Chromosome spreads**

For chromosome spreads, stepwise addition of 0.25 and 2 ml hypotonic buffer (40% DMEM medium, 500 ng/ml nocodazole) to 1×10<sup>6</sup> cells were followed by a 5 minutes incubation. The cells were then pelleted for 5 minutes at 100 g and fixed by stepwise addition of 0.25, 0.25, and 2 ml of Canoy's solution (methanol:acetic acid = 3:1). Samples were incubated for 45 minutes at room temperature, washed twice with Canoy's solution and finally resuspended in 100 µl Canoy's solution. Of this cell

suspension 5-7  $\mu$ l were dripped onto a precooled coverslip and then dried at 60°C in a humidified atmosphere. The specimens were then stained with Hoechst 33342 (1  $\mu$ g/ml in PBS) for 10 minutes, washed twice each in PBS and water, and then air-dried. Finally, the coverslips were put face down onto a drop of mounting medium sitting on a glass slide. After sealing with nail-polish, the samples were analyzed by epifluorescence microscopy using a HCX PL APO 100x/1.40-0.70 oil objective.

### Mathematical modelling

The mathematical modelling of mitotic progression was based on the wiring diagram shown in Fig. S5B. The network was converted into a set of nonlinear differential equations which were solved numerically by freely available software XPPAUT (<http://www.math.pitt.edu/~bard/xpp/xpp.html>). Kinetic parameter values and initial conditions are specified in the file below, which can be used directly using XPPAUT:

```
# .ode file of separase activation kinetics

# MMct represents free and APC/C-bound MCC
MCCt' = kasac - (kisac' + kisac*APC)*MCCt

# Total securin
SecT' = kssec*CHX - kdsec'*SecT - Vdsec*(SecT - Complex) - Vdsec*Complex

# Sepfree is separase which is neither bound to securin nor to cyclin B1
Sepfree' = kssep*CHX - kdsep*Sepfree - kass*Sep*Sec + (kdis + kdsec' +
Vdsec)*Complex - kass2*Sepcis*CycB + (kdis2 + kdcycb' + Vdcycb)*Comp2 -
kass3*Sepcis*CycBp + (kdis3 + kdcycb' + Vdcycb)*Comp3

# Complex corresponds to the securin-separase heterodimer
Complex' = kass*Sec*Sep - (kdis + kdsep + kdsec' + Vdsec)*Complex

# Sepcis is the cis isomer of separase not bound to cyclin B1
Sepcis' = pin1*Sep - kdsep*Sepcis - kass2*CycB*Sepcis + (kdcycb' + Vdcycb +
kdis2)*Comp2 - kass3*Sepcis*CycBp + (kdis3 + kdcycb' + Vdcycb)*Comp3

# CycB is free Cdk1-cyclin B1 not bound to separase
CycB' = kscycb*CHX - kpcdk*CycB*(CycB + CycBp) + Vdp*CycBp - (kdcycb' +
Vdcycb)*CycB - kass2*Sepcis*CycB + (kdis2 + kdsep)*Comp2

# Comp2 corresponds to the Cdk1-cyclin B1-separase complex with
unphosphorylated cyclin B1
Comp2' = kass2*Sepcis*CycB - kpcdk*Comp2*(CycB + CycBp) + Vdp*Comp3 -
(kdis2 + kdcycb' + Vdcycb + kdsep)*Comp2
```

```

# CycBp is free Cdk1-cyclin B1 not bound to separase and containing
phosphorylated cyclin B1
CycBp' = kpcdk*CycB*(CycB + CycBp) - Vdp*CycBp - (kdcycb' + Vdcycb)*CycBp -
kass3*Sepcis*CycBp + (kdis3 + kdsep)*Comp3

# Comp3 corresponds to the Cdk1-cyclin B1-separase complex with phosphorylated
cyclin B1
Comp3' = kass3*Sepcis*CycBp + kpcdk*Comp2*(CycB + CycBp) - Vdp*Comp3 -
(kdis3 + kdcycb' + Vdcycb + kdsep)*Comp3

# Cleaved cohesin
CleavCoh' = kcleav*Sepfree*(CohT - CleavCoh)/(Jcoh + CohT - CleavCoh)

# PP is the PPase responsible for cyclin B1 dephosphorylation
PP' = (kapp' + kapp*PP)*(1 - PP) - kipp*(CycB + CycBp)*PP

# MCC:APC/C complexes are calculated based on steady state assumption
BB = MCCT + APCt + kdiss
MCCAPC = 2*MCCT*APCt/(BB + sqrt(BB^2 - 4*MCCT*APCt))
APC = APCt - MCCAPC

# Active APC is total APC minus MCC-inhibited APC
aux APC = APCt - MCCAPC

# Securin and cyclin B1 APC-dependent degradation rate functions
Vdsec = kdsec**APC
Vdcycb = kdcycb**APC

# Rate function for dephosphorylation
Vdp = kdp*(1 - PP) + kdp*PP

# Free securin and free separase in trans form is calculated
Sec = SecT - Complex
Sep = Sepfree - Sepcis

# Normalised free Cdk1-cyclin B1 not bound to separase
aux relCycB = (CycB + CycBp)/(kscycb/kdcycb')

# All Cdk1-cyclin B1-separase complexes
aux CycBcomp = Comp2 + Comp3

# Initial conditions
init MCCT=5, SecT=5, Sepfree=0, Complex=0.8, Sepcis=0, CycB=0, Comp2=0,
CycBP=20, Comp3=0.2, CleavCoh=0, PP=0

p kasac=0.05, kisac=0.1, kisac=1, kdiss=0.005
p APCt=1, CHX=1, kssec=0.005, kdsec'=0.001, kdsec''=0.15
p kass=100, kdis=0.01, kssep=0.001, kdsep=0.001
p pin1=30, kscycb=0.02, kdcycb'=0.001, kdcycb''=0.15
p kass2=2, kdis2=0.05, kass3=0.005, kdis3=0.00001
p kcleav=0.15, Jcoh=0.05, CohT=1
p kpcdk=1, kdp'=0, kdp=1,
p kapp'=0.01, kapp=1, kipp=1

@ total=80,dt=0.1, meth=STIFF,xlo=0,xhi=80,ylo=0,yhi=1.05      done

```

Initial conditions correspond to prometaphase block with high level of Mitotic Checkpoint Complex (MCC) and inactive APC/C. Simulations were started by decreasing MCC activation rate from  $0.5 \text{ min}^{-1}$  to  $0.05 \text{ min}^{-1}$ . In case of non-degradable cyclin B1 its APC/C dependent degradation ( $k_{\text{dcybc}}$ ) was set to zero. In case of cyclin B1 overexpression its initial level was increased four-times higher (80) than the typical value at prometaphase (20) and its rate of synthesis was elevated by a factor of four as well. Protein synthesis inhibition by cycloheximide was simulated by setting the parameter CHX equal to zero. The effect of Pin1 depletion (or replacement of endogenous separase with the S1126A or P1127A variants) was simulated by setting parameter 'pin1' and the initial values of *cis*-separase and its complex with cyclin B1 (Comp3) to zero. Non-phosphorylable cyclin B1-8A was simulated by setting  $k_{\text{pcdk}}$  equal to 0 and by applying the following changes in initial conditions: Complex=0.6, CycB=20, Comp2=0.4, CycBP=0, Comp3=0.

### Supplemental References

Franken NA, Rodermond HM, Stap J, Haveman J, van Bree C (2006) Clonogenic assay of cells in vitro. *Nature protocols* **1**: 2315-2319

Stemmann O, Zou H, Gerber SA, Gygi SP, Kirschner MW (2001) Dual inhibition of sister chromatid separation at metaphase. *Cell* **107**: 715-726

Zou H, McGarry TJ, Bernal T, Kirschner MW (1999) Identification of a vertebrate sister-chromatid separation inhibitor involved in transformation and tumorigenesis. *Science* **285**: 418-422

SOURCE  
DATATRANSPARENT  
PROCESS

# Local activation of mammalian separase in interphase promotes double-strand break repair and prevents oncogenic transformation

Susanne Hellmuth<sup>1</sup>, Cristina Gutiérrez-Caballero<sup>2</sup>, Elena Llano<sup>2,3</sup>, Alberto M Pendás<sup>2,\*</sup> & Olaf Stemmann<sup>1,\*\*</sup>

## Abstract

Separase halves eukaryotic chromosomes in M-phase by cleaving cohesin complexes holding sister chromatids together. Whether this essential protease functions also in interphase and/or impacts carcinogenesis remains largely unknown. Here, we show that mammalian separase is recruited to DNA double-strand breaks (DSBs) where it is activated to locally cleave cohesin and facilitate homology-directed repair (HDR). Inactivating phosphorylation of its NES, arginine methylation of its RG-repeats, and sumoylation redirect separase from the cytosol to DSBs. *In vitro* assays suggest that DNA damage response-relevant ATM, PRMT1, and Mms21 represent the corresponding kinase, methyltransferase, and SUMO ligase, respectively. *SEPARASE* heterozygosity not only debilitates HDR but also predisposes primary embryonic fibroblasts to neoplasia and mice to chemically induced skin cancer. Thus, tethering of separase to DSBs and confined cohesin cleavage promote DSB repair in G2 cells. Importantly, this conserved interphase function of separase protects mammalian cells from oncogenic transformation.

**Keywords** cohesin; DNA double-strand breaks; homology-directed repair; posttranslational modifications; separase

**Subject Categories** Cell Cycle; DNA Replication, Repair & Recombination; Post-translational Modifications, Proteolysis & Proteomics

**DOI** 10.15252/embj.201899184 | Received 6 February 2018 | Revised 17

September 2018 | Accepted 19 September 2018 | Published online 10 October 2018

**The EMBO Journal (2018) 37: e99184**

## Introduction

DNA double-strand breaks (DSBs) pose an enormous threat to genome integrity because they frequently lead to cancer-associated translocations. Therefore, DSBs trigger a DNA damage response (DDR) leading to checkpoint-mediated cell cycle arrest followed by

DSB repair or apoptosis (Polo & Jackson, 2011). DDR involves hierarchical recruitment and diverse posttranslational modifications (PTMs) of proteins at DSBs. Early steps are phosphorylation of histone variant H2AX at Ser139 (resulting in  $\gamma$ H2AX) and Arg-methylation-dependent recognition and resection of DSBs by the MRE11-RAD50-NBS1 (MRN) complex (Polo & Jackson, 2011; Thandapani *et al*, 2013). One branch of the subsequent DNA damage signaling cascade consists of MRN-mediated recruitment and activation of ATM kinase which—together with MDC1, 53BP1, and other mediators—phosphorylates the effector kinase Chk2 (Polo & Jackson, 2011). Non-homologous end joining (NHEJ) and homology-directed repair (HDR) represent the two major pathways of downstream DSB repair. The error-free HDR occurs primarily in S- and G2-phase cells because it usually requires the undamaged sister chromatid as a homologous template (Polo & Jackson, 2011).

The cohesin complex, whose Smc1, Smc3, and Rad21/Scc1 subunits form a 40-nm tripartite ring, also plays an important role in DSB repair (Sjogren & Nasmyth, 2001). However, its canonical functions lie in sister chromatid cohesion and chromosome separation (Nasmyth & Haering, 2009). Loading of cohesin onto chromatin in telophase (higher eukaryotic cells) or late G1 (yeast) is catalyzed by an Scc2-Scc4 complex, known as kollerin, and may involve transient detachment of Smc1 from Smc3 (Nasmyth & Haering, 2009). Concomitant to replication in S-phase, the two arising sister chromatids of each chromosome are then entrapped within cohesin rings and, thus, paired. Cohesion is stabilized by Esco1/2-dependent acetylation of Smc3 and binding of sororin and counteracted by the anti-cohesive factor Wapl (Nasmyth & Haering, 2009). Phosphorylation-dependent inactivation of sororin in early mitosis enables Wapl to somehow open the Smc3-Rad21 gate, thereby displacing cohesin from chromosome arms (Buheitel & Stemmann, 2013; Nishiyama *et al*, 2013). Centromeric cohesin/sororin is stabilized by Sgo1-PP2A-dependent dephosphorylation and removed only at the metaphase-to-anaphase transition when degradation of securin liberates separase to proteolytically cleave Rad21 (Uhlmann *et al*, 2000; Liu *et al*, 2013). Interestingly, a single DSB in yeast triggers the

1 Chair of Genetics, University of Bayreuth, Bayreuth, Germany

2 Centro de Investigación del Cáncer (CSIC-Universidad de Salamanca), Salamanca, Spain

3 Departamento de Fisiología, Universidad de Salamanca, Salamanca, Spain

\*Corresponding author. Tel: +34 923 294809; E-mail: amp@usal.es

\*\*Corresponding author. Tel: +49 921 552701; E-mail: olaf.stemmann@uni-bayreuth.de

replication-independent, genome-wide enforcement of sister chromatid cohesion by *de novo* loading of cohesin. This recruitment was most profound at the break and occurred in a  $\gamma$ H2AX-, MRE11-, and kollerin-dependent manner (Strom *et al*, 2004, 2007; Unal *et al*, 2004, 2007). On the other hand, Aragón *et al* reported a decrease in cohesin from DSBs when re-synthesis of Rad21 was inhibited (McAleenan *et al*, 2013). This decrease coincided with the damage-induced formation of Rad21 fragments and the impairment of DSB repair by expression of a separase-resistant Rad21 variant, observations which had previously been reported also for *Schizosaccharomyces pombe* and which suggested activation of separase during DDR in postreplicative yeast cells (Nagao *et al*, 2004; McAleenan *et al*, 2013). Cohesin accumulates at DSBs also in human cells (Kim *et al*, 2002; Potts *et al*, 2006). However, whether mammalian separase is activated during DDR to cleave cohesin at DSBs remains an unresolved issue.

Overexpression of separase results in aneuploidy and tumorigenesis in the mouse model, occurs in several human cancers, and is associated with poor clinical outcome (Zhang *et al*, 2008; Meyer *et al*, 2009; Finetti *et al*, 2014; Mukherjee *et al*, 2014a,b). Conversely, *SEPARASE* heterozygosity also causes genomic instability and cancer in zebrafish and p53 null mice (Shepard *et al*, 2007; Mukherjee *et al*, 2011) arguing that *SEPARASE* is both an oncogene and a tumor suppressor gene at the same time and that separase's proteolytic activity needs tight control. Whether separase's role in tumorigenesis is due to its role in sister chromatid segregation and/or a hitherto unknown function still needs clarification.

Here, we show that separase associates with DSBs in postreplicative cells, where it is activated to locally cleave cohesin and facilitate HDR. Its recruitment to damaged DNA requires three PTMs of separase: inhibitory phosphorylation of a nuclear export sequence (NES), Arg-methylation of a conserved RG-repeat motif, and sumoylation of Lys1034. Importantly, *SEPARASE* heterozygosity simultaneously results the reduced DDR and heightened predisposition to oncogenic transformation.

## Results

### Separase is recruited to DSBs

Previous yeast studies implied a role of separase in DDR (Nagao *et al*, 2004; McAleenan *et al*, 2013). To address whether human separase might have a similar function, we adopted a system to induce site-specific DSBs (Iacovoni *et al*, 2010; Caron *et al*, 2012). Upon addition of 4-hydroxytamoxifen (OHT), the restriction endonuclease AsiSI fused to an estrogen receptor (ER) re-locates from the cytosol into the nucleus to cleave DNA at 8-bp recognition sites (around 200 per cell; Chailleux *et al*, 2014), thereby triggering formation of  $\gamma$ H2AX- and phosphoChk2-positive foci (Fig EV1A). When ER-AsiSI was expressed in a transgenic HEK293 line that inducibly produces Myc-tagged separase in response to doxycycline (Dox) addition (Boos *et al*, 2008), separase formed nuclear foci that co-localized with  $\gamma$ H2AX—but only when both OHT and Dox were present (Fig EV1B). Similarly, overexpressed separase localized to  $\gamma$ H2AX-positive foci when the topoisomerase II inhibitor doxorubicin (DRB) was used to inflict DSBs (Fig EV1C). Importantly, endogenous separase also co-localized with  $\gamma$ H2AX to sites of DNA

damage as judged by immunofluorescence microscopy (IFM) of DRB-treated HEK293 cells. Demonstrating the specificity of the DRB-induced separase foci, they were absent in separase-depleted and undamaged cells (Figs 1A and EV1D). To independently confirm recruitment of endogenous separase to damaged sites, we conducted chromatin immunoprecipitation (ChIP) experiments followed by multiplex qPCR or qPCR (see Fig EV1E for length and positions of PCR products). These analyses consistently revealed that, much like an anti- $\gamma$ H2AX and unlike non-specific IgG, a separase antibody precipitated DNA close to two different AsiSI sites if and only if OHT was added, while a region that was more than 2.2 Mbp away from the nearest AsiSI site did not co-purify (Fig 1B and C). The specific recruitment of separase to DSBs was further enhanced by induced overexpression of the protease (Fig EV1F).

### Separase functions in HDR but not NHEJ

Is separase of functional importance for DNA damage repair? Indicating that this might indeed be the case, depletion of separase but not mock treatment strongly compromised the ability of HEK293 cells to form colonies in the presence of camptothecin, a topoisomerase I inhibitor that causes replication-dependent DNA single- and double-strand breaks (Fig EV2A and B).

We noted that not all  $\gamma$ H2AX-positive interphase cells showed Myc-separase foci and therefore pre-synchronized ER-AsiSI-expressing cells in either G1- or G2-phase prior to OHT addition and analyses (see Fig EV2C for timeline of the experiment). Successful synchronization was confirmed by measurement of cyclin A2 and DNA contents by immunoblotting and flow cytometry, respectively (Figs 1D and EV2D). Lysates from these different cell populations were benzonase-treated to digest DNA and then subjected to IP using anti-Myc or unspecific IgG. Interestingly,  $\gamma$ H2AX specifically co-purified with Myc-separase from OHT-treated G2- but not G1-phase cells (Fig 1D, lower part). Consistently, IFM revealed that 80% of DSBs containing G2 cells exhibited  $\gamma$ H2AX- and Myc-separase-positive foci as compared to merely 10% in the G1-enriched pool (Figs 1E and EV2E). Due to imperfect synchronization of the HEK293 cells (Fig EV2D), this probably represents an underestimation. These data therefore imply that separase is recruited to DSBs exclusively in postreplicative cells.

Because HDR, but not NHEJ, requires the undamaged sister chromatid as a homologous template, the above result indicates a possible role of separase in HDR rather than NHEJ. To resolve this issue, we adopted *in vivo* assays for HDR versus NHEJ (Pierce *et al*, 1999; Gunn & Stark, 2012). Herein, the homing endonuclease I-SceI in corresponding transgenic U2OS cells introduces a single DSB, the repair of which creates a functional GFP expression cassette only if it occurs by HDR in one reporter line and by NHEJ in the other. Following transfection of a *SEPARASE*-directed (*SEP-1*) or control siRNA (*GL2*), the corresponding cells were again transfected to express I-SceI in fusion with an estrogen receptor (ER) and synchronized in early S-phase. Six hours after release from thymidine arrest, cells were supplemented with OHT to induce nuclear accumulation of the homing endonuclease (or with carrier solvent as a negative control). Two days thereafter, cells were harvested and analyzed for protein content by immunoblotting and for GFP fluorescence and DNA content by flow cytometry. The OHT-induced GFP expression was unaffected by separase in the NHEJ reporter line (Fig 2A and

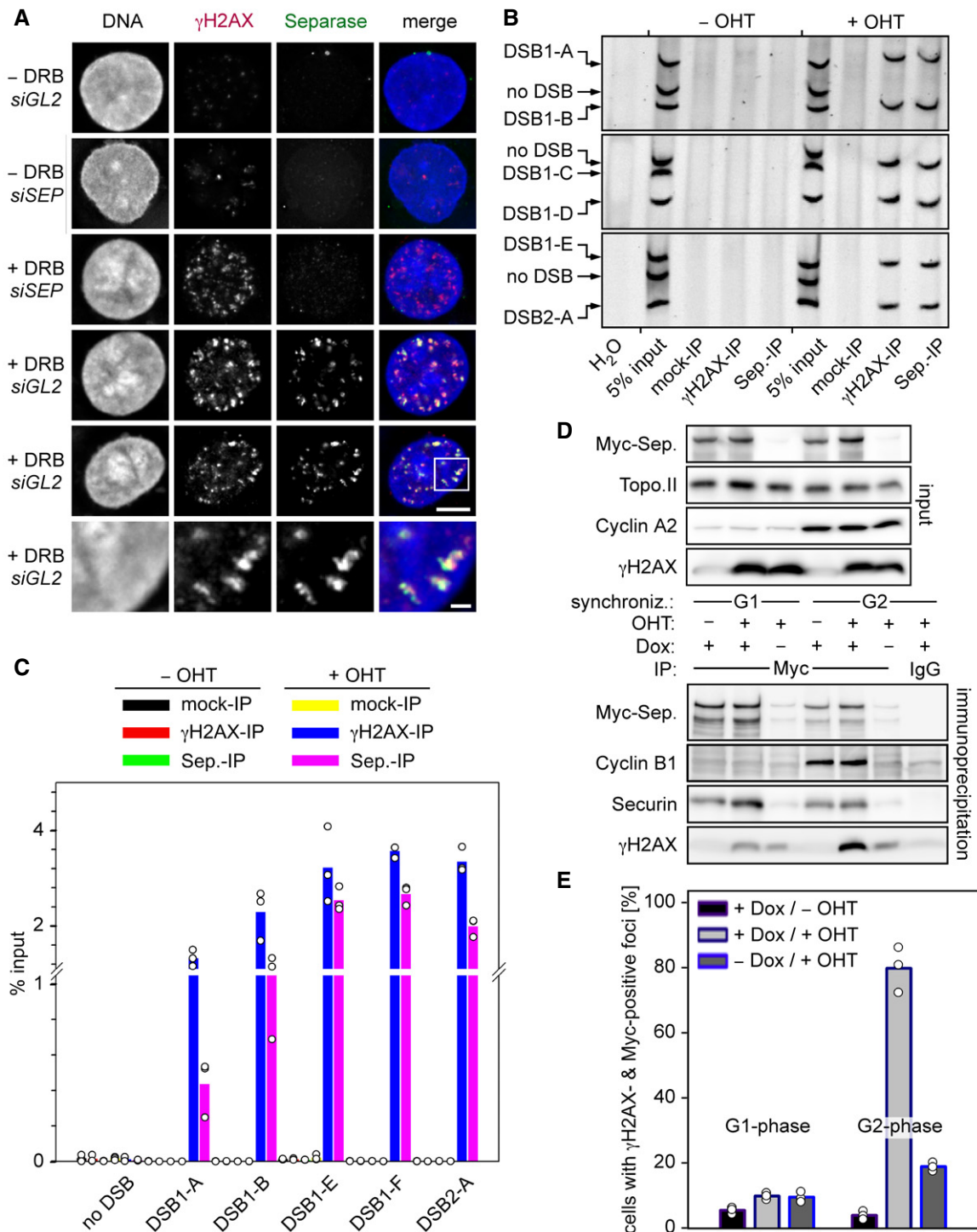


**Figure 1. Human separase localizes to DSBs in postreplicative cells.**

- A Following transfection of given siRNAs and synchronization in G2-phase, Hek293 cells were DRB- or mock-treated and then subjected to IFM using the indicated antibodies. Lower panels display a threefold magnification of the boxed area shown above. Scales bars correspond to 5 and 1  $\mu$ m, respectively. See Fig EV1D for corresponding immunoblot.
- B HEK293 cells were thymidine-arrested for 20 h, mock- or OHT-treated to induce DSBs by nuclear accumulation of ER-AsiSI, and then subjected to ChIP-multiplex PCR.
- C ChIP samples from (B) were analyzed by qPCR. Shown are averages (bars) of three independent experiments (dots).
- D, E Separase interacts with  $\gamma$ H2AX in DSB-containing G2 but not G1 cells. Transgenic HEK293 cells treated with Dox to induce expression of Myc-separase-WT and with OHT to induce nuclear accumulation of ER-AsiSI and infliction of DSBs were synchronized in G1- or G2-phase and analyzed by IP-Western blotting (D) and by IFM for  $\gamma$ H2AX- and Myc-separase-positive foci (see Fig EV2E). The quantification of the IFM in (E) shows averages (bars) of three independent experiments (dots) counting  $\geq 100$  cells each.

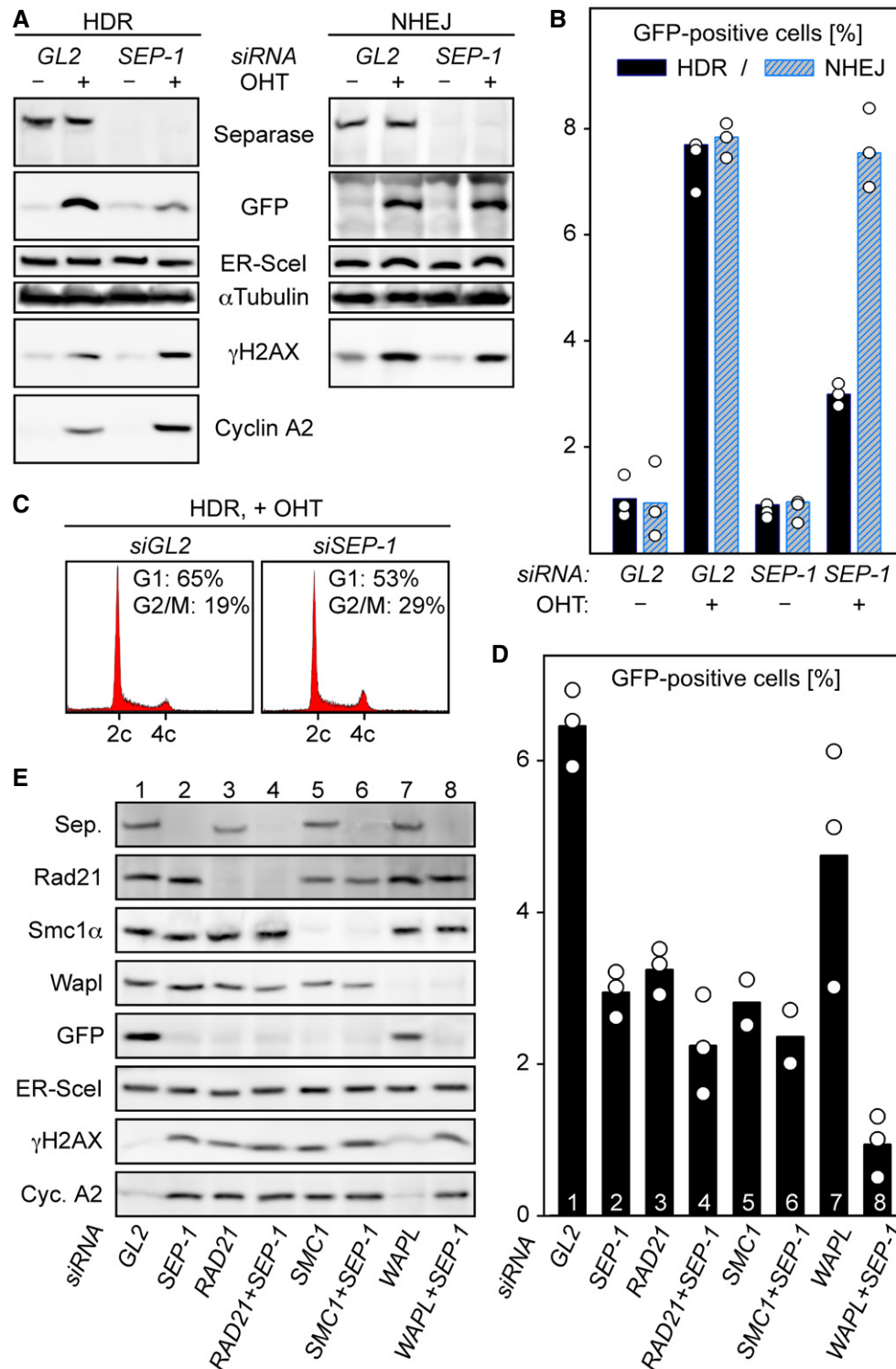


**Figure 2. Separase supports HDR but not NHEJ.**

A–C Separase is required for proper HDR but dispensable for NHEJ. U2OS DR-GFP (HDR reporter) and U2OS EJ5-GFP (NHEJ reporter) cells were separase-depleted by RNAi (*SEP-1*) or control-treated with *GL2* siRNA, transfected to express HA-tagged ER-I-SceI, and then supplemented with OHT in G2-phase to induce nuclear accumulation of the homing endonuclease. Ethanol-supplemented samples served as negative controls. Two days later, cells were subjected to immunoblotting (A) and flow cytometry to quantify the percentage of GFP-positive cells (B) and PI-stained cellular DNA (C). The GFP quantification in (B) displays averages (bars) of three independent experiments (dots).

D, E Co-depletion of Wapl and separase has a synergistic effect on HDR. U2OS DR-GFP cells were transfected with the indicated siRNAs, treated as in (A + B) and analyzed by GFP flow cytometry (D) and immunoblotting (E). Shown in (D) are averages (bars) of two to three independent experiments (dots).

B). However, in the HDR reporter line depletion of separase resulted in a markedly reduced GFP Western signal (Fig 2A) and 2.6-fold less GFP-positive cells (Fig 2B). At the time of analysis, OHT-treated HDR reporter cells lacking separase also displayed slightly enhanced  $\gamma$ H2AX and cyclin A2 signals and a modest accumulation in G2/M (Fig 2A and C; see also Fig EV2F). This is consistent with a compromised repair proficiency and consequent DNA damage checkpoint-dependent delay of mitotic entry. To exclude the possibility that compromised HDR in separase-depleted reporter cells was due to an off-target effect, we tested four additional *SEPARASE*-directed siRNAs (*SEP-2-5*) in the same assay. All reduced the number of GFP-positive cells relative to the GL2 control, and all but one (*SEP-3*) did so to a similar extent as did *SEP-1* (Fig EV2F and G). Consistent with *SEPARASE* being the relevant target, the weaker effect of *SEP-3* correlated with its weaker knock-down efficiency (Fig EV2F). In summary, these results demonstrate that human separase is required for proper HDR but dispensable for NHEJ.

A role of cohesin in HDR is well established (Kim *et al*, 2002; Strom *et al*, 2004; Unal *et al*, 2004; Potts *et al*, 2006). Simultaneous requirement of its antagonist separase in the same repair pathway seems counterintuitive at first. To clarify this issue, we analyzed side by side the effects of cohesin and separase single and double depletions in the abovementioned GFP-based HDR assay. Flow cytometric quantification showed that RNAi of separase, Rad21, or another cohesin subunit, Smc1 $\alpha$ , all reduced the amount of GFP-positive cells to a similar extent and at least by a factor of 2, thereby confirming the requirement of both cohesin and separase for proper HDR (Fig 2D, columns 1–3 and 5). Interestingly, simultaneous knock-down of separase together with Rad21 or Smc1 $\alpha$  only marginally aggravated the HDR defect relative to the single depletions (compare columns 2–6). We believe that effective HDR requires heightening of both density and turnover of cohesin at DSBs (see Discussion). Co-depletion of separase will increase residual cohesion under conditions when cohesin becomes limiting, and this might compensate for the negative effect on HDR of reduced cohesin dynamics due to the sole absence of separase.

We also investigated Wapl, another anti-cohesive factor with key function in proteolysis-independent cohesin removal (Kuong *et al*, 2006). While Wapl depletion alone reduced the GFP formation only mildly, simultaneous knock-down of Wapl and separase had a clear synergistic effect reducing the amount of GFP-positive cells in the individual depletions from 2.8 and 4.6%, respectively, to 1% in the double knock-down (Fig 2D, columns 2, 7, and 8). This suggests that total abrogation of cohesin dynamics by interference with both known anti-cohesive mechanisms leads to maximal impairment of HDR. Immunoblotting not only confirmed the successful and even knock-downs but also the flow cytometric quantification of GFP (Fig 2E). Moreover, it revealed increased levels of  $\gamma$ H2AX and cyclin A2 in the absence of cohesin and/or separase indicating DSB persistence and checkpoint-mediated cell cycle arrest under these conditions (lower two panels).

### Separase is activated at DSBs where it locally cleaves cohesin

Does human separase get activated to cleave cohesin in response to DSBs similar to the situation in yeast? To address this question, histone H2B-mCherry-Rad21<sup>107–268</sup>-eGFP was constitutively expressed in *MYC-SEPARASE* cells (Fig 3A, cartoon at bottom).

Separase-dependent cleavage of this protease activity sensor causes mCherry- and eGFP-positive chromatin to selectively lose its eGFP signal. These doubly transgenic cells were transfected to transiently express also AsiSI-ER, treated with OHT or carrier solvent for different times, and analyzed by immunoblotting (Fig 3A and B). Indeed, this demonstrated DNA damage-dependent proteolysis of the sensor (Fig 3A, bottom panel). Enrichment by IP of its soluble cleavage products revealed that endogenous Rad21 is also cleaved and that these cleavage events increased with duration of DSB induction, i.e., OHT treatment (Fig 3B). Separase activity was only slightly enhanced by Dox-induced overexpression (Fig 3A and B), although this resulted in considerably more protease being recruited to sites of DNA damage as revealed by ChIP-qPCR (compare Figs 1C and EV1F). Under these conditions, the activation of separase therefore seems to be limiting.

When sensor-expressing cells were treated in G2-phase with DRB and the spindle toxin nocodazole, subsequent chromatin spreads displayed some mitotic figures with  $\gamma$ H2AX-positive foci on condensed chromosomes, suggesting that the corresponding cells had slipped from the DNA damage into the mitotic checkpoint arrest (Fig 3C). Notably,  $\gamma$ H2AX foci coincided with regions of decreased eGFP fluorescence (or relative increase in mCherry over eGFP in an overlay) indicative of local separase-dependent sensor cleavage. This net loss of sensor from DSBs does not contradict the reported overall accumulation of cohesin at DSBs because loading mechanisms are fundamentally different for authentic cohesin versus the histone-based sensor. Together, these results strongly indicate that separase is activated at sites of DSBs to locally cleave cohesin during DDR.

### DNA damage- and phosphorylation-dependent inactivation of separase's NES

In undamaged interphase cells, separase is excluded from the nucleus due to the presence of a nuclear export sequence (NES) centered around position 1665 (Sun *et al*, 2006). Therefore, its NES might be inactivated in response to DSBs to retain separase in the nucleus. Interestingly, an NES in p53 is inhibited by DNA damage-induced phosphorylation (Zhang & Xiong, 2001) and separase's NES is immediately flanked by a serine at position 1660. When Myc-separase-WT was immunoprecipitated from cyclin A2-positive, DRB-treated G2-phase cells, separase was detected in an immunoblot by a pan-specific phosphoSer antibody (Fig 4A). This signal was greatly diminished in the absence of DNA damage or when samples were phosphatase-treated prior to SDS-PAGE. Importantly, the phosphoSer signal was also missing when a Ser-1660 to Ala variant instead of separase-WT was immunoprecipitated from DRB-treated G2 cells. At the same time,  $\gamma$ H2AX co-purified with separase-WT but not separase-S1660A from benzonase-treated cell lysates (Fig 4A), suggesting that the phosphorylation site variant is unable to associate with DSBs (see below).

We then raised an antibody that specifically recognized phosphorylated Ser-1660 of separase. Confirming our earlier interpretations, this anti-pS1660 strongly reacted with full-length Myc-separase-WT from DSB-containing cells (Fig 4B). In contrast, Myc-separase-S1660A from accordingly DRB-treated cells and separase-WT from undamaged G2-arrested control cells were hardly recognized. Importantly, this tool also allowed us to detect the NES

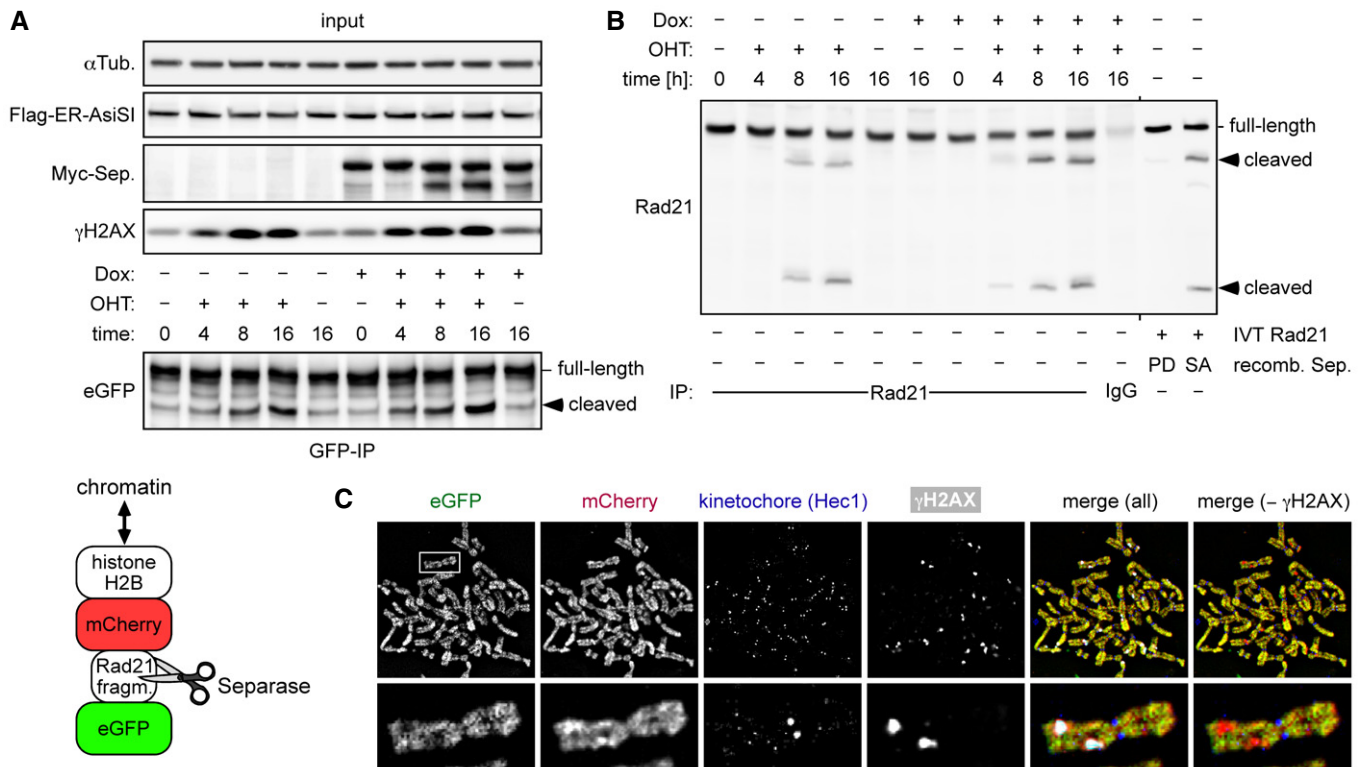


**Figure 3. Human separase locally cleaves Rad21 at DSBs.**

**A** Transgenic HEK293 cells constitutively expressing a separase sensor (cartoon below) and inducibly expressing Myc-separase were transiently transfected to express Flag-AsiSI-ER, Dox- and/or OHT-treated in G<sub>2</sub>-phase, and analyzed by IP–Western blotting.

**B** Cells from (A) were analyzed by IP–Western blotting for cleavage of endogenous Rad21. As a control, *in vitro*-translated (IVT) Rad21 was incubated with hyperactive separase-SA or a protease-dead (PD) variant (Boos *et al*, 2008).

**C** Sensor-expressing cells were treated in G<sub>2</sub>-phase with DRB and nocodazole for 6 and 2 h, respectively, prior to chromosome spreading and IFM using Hec1 and  $\gamma$ H2AX antibodies. The separase sensor was detected based on autofluorescence of eGFP and mCherry, while Hec1 and  $\gamma$ H2AX antibodies were detected with corresponding Cy5- and marina blue-labeled secondary antibodies, respectively. Note that sizes of spread chromosomes vary greatly with buffer conditions, which is why no scale bar is shown.

phosphorylation of endogenous separase upon infliction of DSBs in untransfected, G<sub>2</sub>-arrested HEK293T cells (Fig 4C).

Visible nuclear accumulation of separase (in the absence of DNA damage) requires both mutational inactivation of the NES and fusion of the protease with a nuclear localization sequence (NLS; Sun *et al*, 2006). Transiently expressed NLS-eGFP-separase accumulated in nuclei not only when bulky hydrophobic residues within the NES were replaced by alanines (NESmut) but also when DSBs were inflicted instead (Fig 4D, 2<sup>nd</sup> and 3<sup>rd</sup> panel from top). In contrast, NLS-eGFP-separase-S1660A was absent from nuclei even in DRB-treated cells (6<sup>th</sup> panel from top). Interestingly, an NLS-eGFP-separase variant, in which Ser-1660 was changed to phosphorylation-mimetic Asp, behaved similar to separase-NESmut in that it exhibited nucleoplasmic localization even in the absence of DNA damage (7<sup>th</sup> panel from top). Collectively, these results suggest that DNA damage-induced phosphorylation of separase at Ser-1660 inactivates its NES, thereby facilitating retention of the protease within the nucleoplasm, from where it can then be recruited to DSBs.

Ser-1660 could serve as a substrate for ATM kinase according to a Scansite search, albeit at minimal stringency settings

(Obenauer *et al*, 2003). Recombinant ATM purified from transiently transfected HEK293T cells phosphorylated p53's NES (amino acids 9–22) in fusion with GST, an established model substrate, but not GST alone (Fig 4E; Kim *et al*, 1999). Confirming its specificity, this signal was extinguished in the presence of the ATM-specific inhibitor KU-55933 and greatly diminished when a preparation of a kinase-dead (KD) variant was used instead of ATM-WT. Notably, the same results were observed using separase-WT as a substrate, while separase-S1660A was not phosphorylated at all. Thus, ATM is capable of phosphorylating separase's NES at Ser-1660 *in vitro*. Consistent with these findings, KU-55933 addition to DRB-treated cells strongly reduced Ser-1660 phosphorylation of separase (Fig 4C) and largely compromised the nuclear accumulation of NLS-eGFP-separase-WT but not NLS-eGFP-separase-S1660D (Fig EV3A and B). This is in line with separase's NES being a direct substrate of ATM *in vivo* although we cannot exclude indirect effects. Interestingly, active ATM also enhanced the cleavage of Rad21 by separase *in vitro* (Fig EV3C and D), which fits well to our aforementioned finding of local Rad21 cleavage at DSBs.

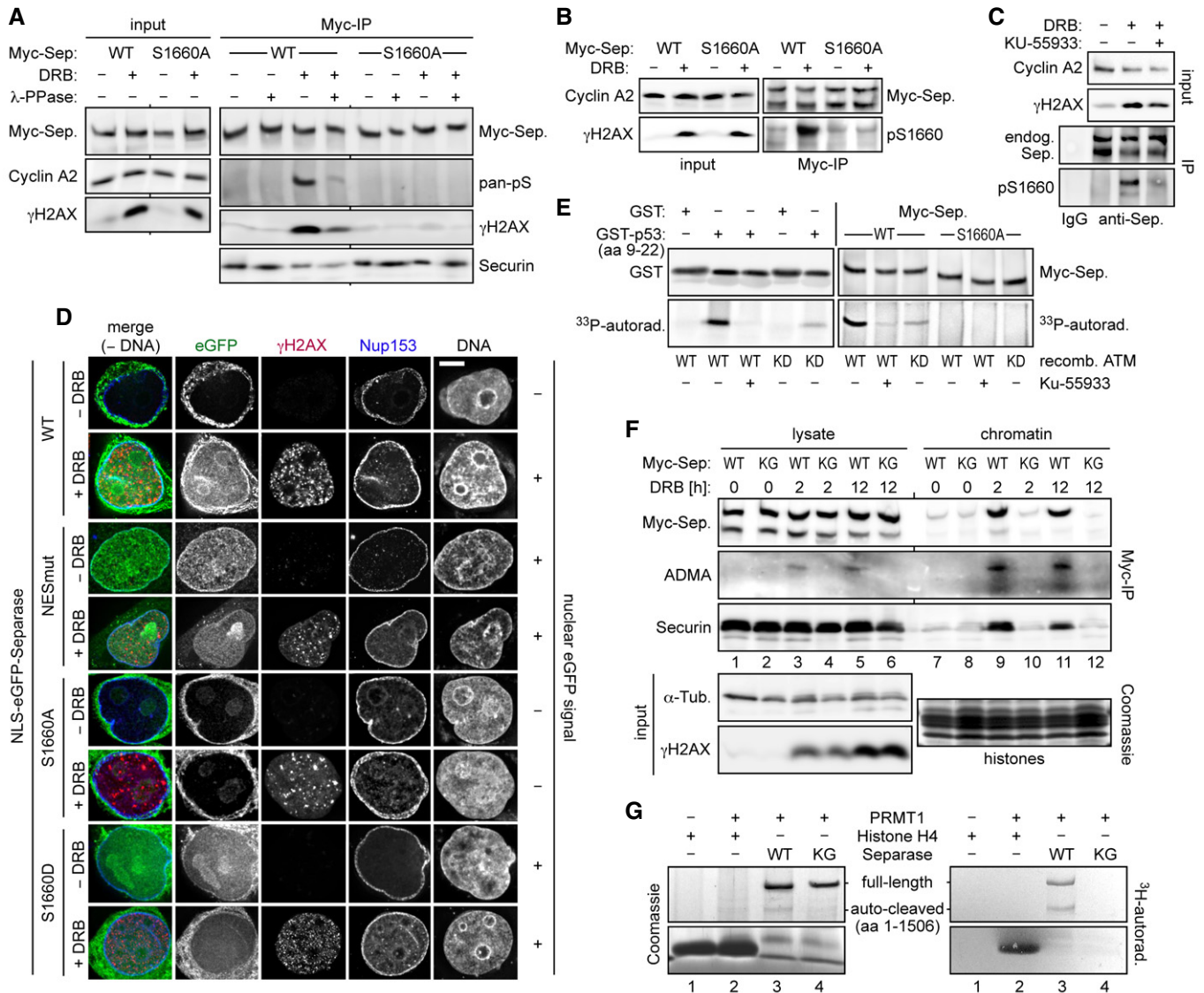


**Figure 4. NES phosphorylation and RG-repeat methylation of separase in response to DSBs.**

**A–C** Ser1660 is phosphorylated in response to DNA damage and required for the interaction of separase with  $\gamma$ H2AX. HEK293 cells were arrested in G2-phase by sequential thymidine and RO-3306 treatment, DRB (+) or mock-treated (–), and then analyzed as indicated. (A and B) Myc-separase-WT or Myc-separase-S1660A-expressing cells were subjected to IP–Western blotting using, among others, a pan-specific antibody against phosphorylated serine (A, pan-pS) or a separase antibody specific for phosphorylated Ser1660 (B, pS1660). (C) DNA damage-induced Ser1660 phosphorylation of endogenous separase is largely blocked by ATM inhibition. G2-enriched HEK293 cells were treated with KU-55933 (0.3  $\mu$ M) and/or DRB and analyzed by IP–Western blotting 12 h thereafter using the indicated antibodies.

**D** Preventing NES phosphorylation spoils nuclear localization of separase in response to DSBs. HeLaK cells expressing N-terminally NLS-eGFP-tagged separase variants were treated with DRB or carrier solvent (– DRB) for 4 h and then subjected to IFM using anti- $\gamma$ H2AX and anti-Nup153 to visualize sites of DNA damage and nuclear pore complexes, respectively. Transgenic separase was detected based on the eGFP autofluorescence. Note that due to their relatively high nuclear concentration, co-localization of separase-WT and separase-S1660D with  $\gamma$ H2AX foci is not discernable. Scale bar = 5  $\mu$ m.

**E** *In vitro* phosphorylation of separase on Ser1660 by ATM kinase. Incubation of GST-p53 (amino acids 9–22), GST, separase-WT, or separase-S1660A with recombinant ATM-WT, ATM-KD (kinase dead), and/or KU-55933 in the presence of [ $\gamma$ -<sup>33</sup>P]-ATP was followed by immunoblotting and autoradiography.

**F** Arg-methylation of RG-repeats mediates recruitment of separase to DSB-containing chromatin. Myc-separase-WT- or Myc-separase-KG-expressing cells were treated with DRB as indicated and analyzed by IP–Western blotting and Coomassie staining.

**G** *In vitro* Arg-methylation of separase's RG-repeats by PRMT1. Incubation of histone H4, separase-WT, or separase-KG with recombinant PRMT1 or reference buffer in the presence of S-adenosyl-L-[methyl-<sup>3</sup>H]-methionine was followed by Coomassie staining and autoradiography.

### RG-repeat methylation tethers separase to DSBs

Once retained in the nucleoplasm, how is separase recruited to DSBs? DNA damage response involves Arg-methylation of several

proteins within RGG- or RG-repeat motifs (Thandapani *et al.*, 2013). For example, the MRN complex component Mre11 can be modified by the protein arginine methyltransferase 1 (PRMT1), and this Arg-methylation was demonstrated to be required for MRN's association

with sites of DNA damage (Boisvert *et al.*, 2005; Dery *et al.*, 2008). Interestingly, vertebrate separases contain a short RG-repeat motif. The RGRGRAR motif centered around position 1426 of the human enzyme was changed to KGK GKAK resulting in separase-KG. Myc-tagged versions of separase-WT or separase-KG were immunoprecipitated from DRB- or mock-treated G2 cells. Subsequent immunoblotting revealed that separase-WT from DSB-containing cells was recognized by an asymmetric dimethylarginine (ADMA)-specific antibody, while the KG variant was not (Fig 4F, lanes 3–6). Enrichment of chromatin prior to the IP demonstrated that separase's association with chromatin depended on both the DNA damage and an intact RG motif and yielded more intense ADMA signals (lanes 9–12). We established *in vitro* Arg-methylation using bacterially expressed human PRMT1, S-adenosyl-L-[methyl-<sup>3</sup>H]-methionine, and histone H4 as a model substrate (Fig 4G, lanes 1 and 2; Wang *et al.*, 2001). Importantly, recombinant separase-WT was readily methylated by PRMT1 in this assay, while the KG variant remained unmodified (lanes 3 and 4). In summary, these data suggest that Arg-methylation of separase's RG motif, possibly by PRMT1, targets the protease to DSBs.

### NES phosphorylation and RG-repeat methylation are required for separase's function in DSB repair

While 87% of HEK293T cells cultivated in continued presence of DRB exhibited  $\gamma$ H2AX- and MDC1-positive foci, this fraction dropped to 32% within 24 h after DRB washout (Fig 5A, compare gray and blue bars in lane 1). Prior depletion of separase by RNAi resulted in persistence of damage foci in 72% of cells (blue bar, column 2), a defect which was fully reversed by Dox-induced expression of Myc-separase-WT from an *siRNA*-resistant transgene (column 3). This rescue offered the possibility to probe separase variants for their retained ability to support DSB repair (see Fig 5B for timeline of the experiment). Notably, separase-S1660A and a variant, in which the NES was replaced by a non-phosphorylatable superNES (Guttler *et al.*, 2010), were unable to support DSB repair in this recovery assay, while the phospho-mimicking separase-S1660D did rescue (Fig 5A, compare columns 6, 9, and 12).  $\gamma$ H2AX- and MDC1-positive foci also persisted after DRB washout when endogenous separase was replaced by the KG variant (column 15). In contrast to separase-WT and separase-S1660D, all other variants failed to form damage-induced foci and to interact with  $\gamma$ H2AX in continued presence of DRB (Fig 5C and D, blue arrowheads). Moreover, separase-WT and separase-S1660D supported recovery from the DNA damage checkpoint-induced G2 arrest as judged by drop in  $\gamma$ H2AX and cyclin A2 levels, while separase-superNES, separase-S1660A, and separase-KG again failed to do so (Fig 5D, red arrows). In summary, separase's ability to localize to DSBs correlates with DNA damage repair proficiency and depends on inhibitory phosphorylation of the NES and Arg-methylation of the RG-repeat motif.

### Sumoylation of Lys1034 supports separase's role in DSB repair

DNA double-strand break recruitment of several proteins, among them 53BP1 and Rad52, is controlled by sumoylation (Sacher *et al.*, 2006; Galanty *et al.*, 2009). We therefore assessed whether separase might also be sumoylated during DDR. Cells that expressed His<sub>6</sub>-separase were DRB- or control-treated and subjected to

denaturing immobilized metal ion affinity chromatography (IMAC). Subsequent comparative separase and Sumo2/3 immunoblotting revealed that separase is indeed sumoylated in response to DSBs (Fig 6A). Conducting a similar pull-down (PD) but starting with His<sub>6</sub>-Sumo2-expressing cells, we could readily detect DNA damage-dependent sumoylation of endogenous separase (Fig 6B). Although separase contains three regions that match the canonical sumoylation consensus motif, the sequence surrounding lysine 1034 was the most likely target according to bioinformatic prediction (Zhao *et al.*, 2014). We therefore transfected cells to co-express His<sub>6</sub>-Sumo2 together with Myc-tagged separase-WT or separase-K1034R. Consecutive DRB treatment, denaturing IMAC and Western blot analysis showed that Myc-separase-WT co-purified with His<sub>6</sub>-Sumo2, while the K1034R variant did hardly at all (Fig 6C). Sumoylation of wild-type separase but not the K1034R variant was detectable even in the absence of Sumo overexpression and upon native isolation of the protease by Myc-IP (Fig 6D). Thus, Lys-1034 is a major, if not the only, target when separase is sumoylated in response to DSBs.

What could be the separase-relevant Sumo E3 ligase? Mms21/Nse2 is the SUMO ligase of the Smc5/6 complex and has an established role in HDR (Potts & Yu, 2005). As a first step toward addressing this issue, we therefore asked whether Mms21 could sumoylate separase *in vitro*. Myc beads were loaded with Myc-separase-WT or Myc-separase-K1034R or left empty, combined with ATP, Sumo2, and the heterodimeric Sumo-activating enzyme (E1: Sae1/Aos1-Sae2/Uba2), and then incubated with recombinant Sumo-conjugating enzyme (E2: Ubc9) and/or Mms21. Analysis of the bead-less supernatant by SDS-PAGE and Coomassie staining revealed that the formation of high molecular weight Sumo conjugates occurred only when both E2 and E3 were present (Fig 6E, lower part). Importantly, Western blot analysis of the (washed) Myc beads demonstrated sumoylation of separase-WT but not separase-K1034R (Fig 6E, upper part). Thus, Lys-1034 can serve as a target of Mms21 in a reconstituted system.

For functional analyses, firstly we assessed separase-K1034R in its ability to associate with chromatin upon DNA damage. In contrast to separase-WT and similar to separase-KG, separase-K1034R was unable to bind damaged,  $\gamma$ H2AX-positive chromatin pelleted by centrifugation from total cell lysates (Fig 6F). Secondly, we interrogated separase-K1034R for its ability to functionally replace endogenous separase in the aforementioned DSB-recovery assay (see above text and Fig 5B). Using separase-WT and the KG variant as positive and negative control, respectively, we could show that separase-K1034R largely failed to support cellular recovery from transient DRB treatment (Fig 6G). Taken together, this set of experiments establishes Lys-1034 sumoylation, possibly by Mms21, as an integral element of separase's recruitment to DSBs and function in DDR.

### SEPARASE<sup>+/-</sup> MEFs suffer from compromised DSB repair

We wanted to assess whether separase participates in HDR also in non-transformed, primary cells and whether this function is conserved in mammals. Therefore, we created *SEPARASE*<sup>+/-</sup> mice and from these MEFs (see Fig EV4A–C and the Materials and Methods section for details). *SEPARASE*<sup>+/-</sup> MEFs were then compared to MEFs from corresponding wild-type mice in their ability to recover

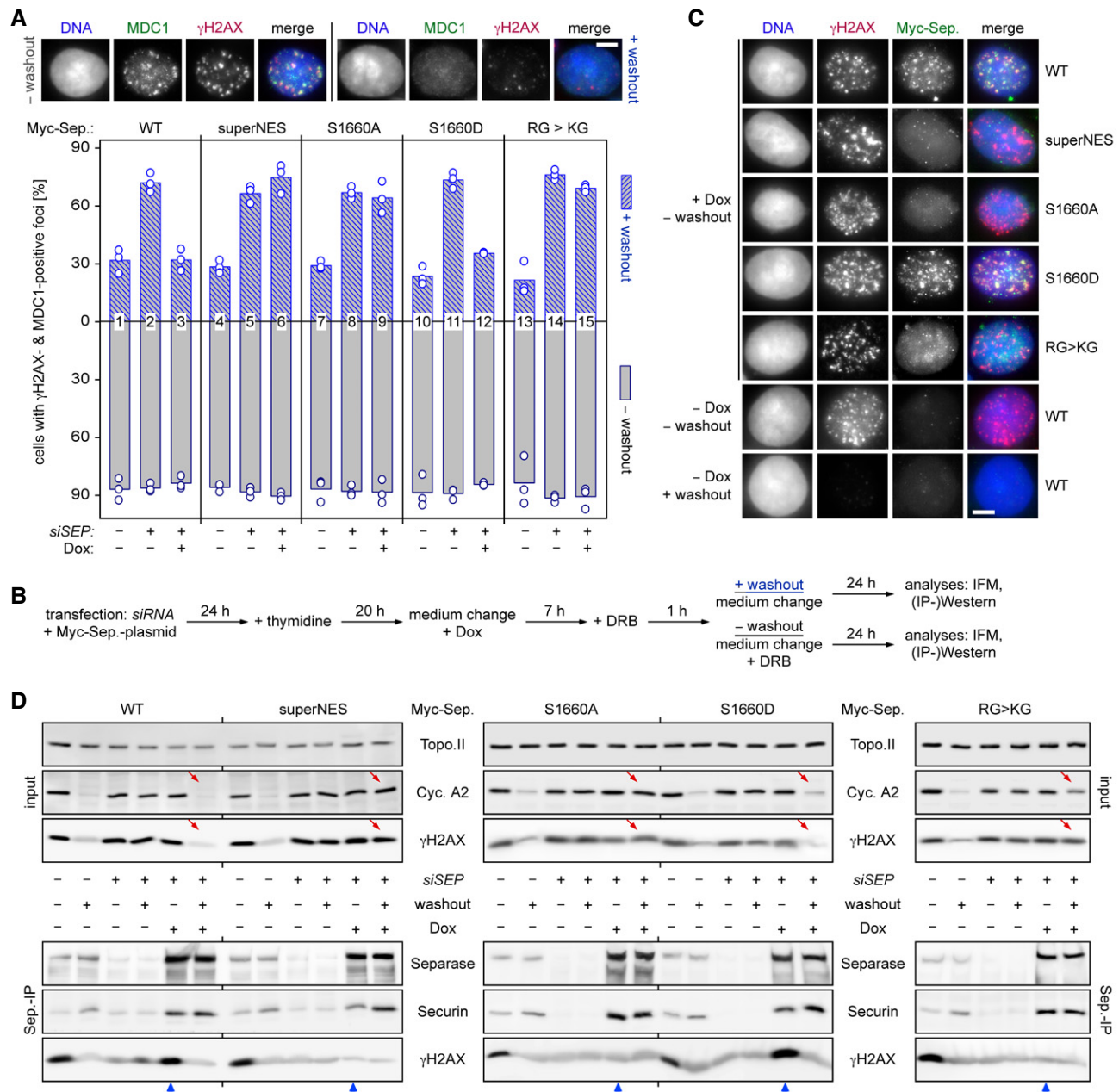


**Figure 5. NES phosphorylation and Arg-methylation of separase are required for proper DSB repair.**

**A** Persistence of  $\gamma$ H2AX- and MDC1-positive foci in the absence of NES phosphorylation or RG-methylation of separase. Transfected HEK293T cells were *siRNA*- and Dox-treated to deplete endogenous separase and induce expression of the indicated, *siRNA*-resistant Myc-tagged separase variants, respectively. Then, they were constitutively (– washout) or transiently exposed to DRB (+ washout) and finally quantitatively assessed by IFM for  $\gamma$ H2AX- and MDC1-positive foci. Shown are averages (bars) of three independent experiments (dots) counting  $\geq 100$  cells each. Scale bar = 5  $\mu$ m.

**B** Schematic of the experiment.

**C** Recruitment of separase-WT and separase-S1660D but not separase-superNES, separase-S1660A, and separase-KG to DSBs. Cells from (A) were treated as indicated and analyzed by IFM for co-localization of Myc-separase with  $\gamma$ H2AX foci. Scale bar = 5  $\mu$ m.

**D** Interaction of separase-WT and separase-S1660D but not separase-superNES, separase-S1660A, and separase-KG with  $\gamma$ H2AX. Cells from (A) were subjected to IP–Western blot analysis as indicated. Lanes that illustrate cellular levels of cyclin A2 and  $\gamma$ H2AX after DRB washout and those that analyze interaction of Myc-separase variants with  $\gamma$ H2AX in the presence of DRB are labeled by red arrows and blue arrowheads, respectively.

from DRB-inflicted DNA damage. In wild-type MEFs, the fraction of cells with foci, which were positive for  $\gamma$ H2AX and another damage marker, 53BP1, declined from 88.5% down to 32% within 24 h after

DRB washout (Fig 7A and B). However, in heterozygotes the percentage of cells with these damage-induced foci dropped from 90.5% to merely 76% during the same period. Consistent with

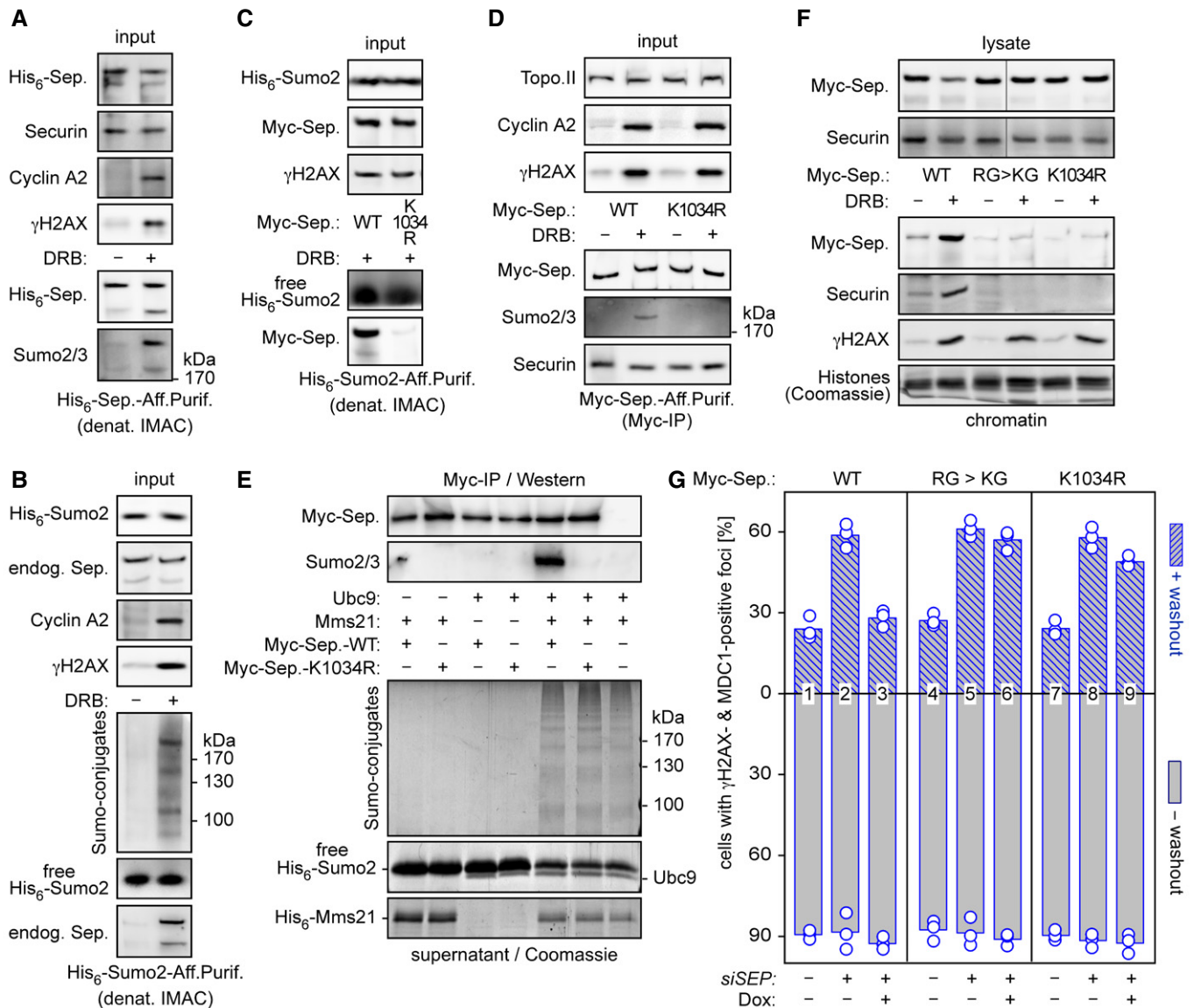


**Figure 6. Sumoylation supports separase's role in DSB repair.**

A, B Separase is sumoylated in response to DSBs. HEK293T cells transfected to express His<sub>6</sub>-separase (A) or His<sub>6</sub>-Sumo2 (B) were treated with DRB or carrier solvent (– DRB) and then subjected to denaturing IMAC followed by immunoblotting of input samples and eluates using the indicated antibodies.

C, D Lys-1034 is a major target of DSB-induced sumoylation of separase. HEK293T cells expressing His<sub>6</sub>-Sumo2 (C) or Myc-separase-WT or separase-K1034R (D) were DRB- or mock-treated and subjected to denaturing IMAC or Myc-IP, respectively. Input samples and eluates were immunoblotted using the indicated antibodies.

E Mms21-dependent *in vitro* sumoylation of separase at Lys-1034. Myc beads were loaded with separase-WT or separase-K1034R or left empty (last lane), combined with recombinant Ubc9 and/or Mms21, as indicated, and incubated in the presence of His<sub>6</sub>-Sumo2, Sae1-Sae2, and ATP. Supernatant and washed beads were analyzed by Coomassie staining (lower panels) and immunoblotting (upper panels), respectively.

F Cells expressing the indicated separase variants were DRB- or mock-treated and then lysed. Lysates and chromatin pelleted therefrom were assessed by immunoblotting and Coomassie staining, as indicated. Note that the lanes shown in the upper panels, although not directly juxtaposed, nevertheless originate from the same gel.

G Preventing sumoylation of Lys-1034 compromises separase's ability to support DSB repair. The indicated variants were probed for their ability to functionally replace endogenous separase in HDR as described in Fig 6A and B. Shown are averages (bars) of three independent experiments (dots) counting  $\geq 100$  cells each.

Source data are available online for this figure.

persistent DNA damage and checkpoint-mediated cell cycle arrest and in marked contrast to the wild type, the levels of  $\gamma$ H2AX, phosphoChk2, and cyclin A2 hardly declined in the *SEPARASE*<sup>+/-</sup> MEFs during the 24 h of recovery from DRB (Fig 7C).

We also assessed damage-induced Rad21 cleavage in *SEPARASE*<sup>+/-</sup> versus *SEPARASE*<sup>+/+</sup> MEFs.  $\gamma$ H2AX and cyclin A2 accumulated comparably with increasing duration of DRB treatment, indicating that the initial steps of damage response and the

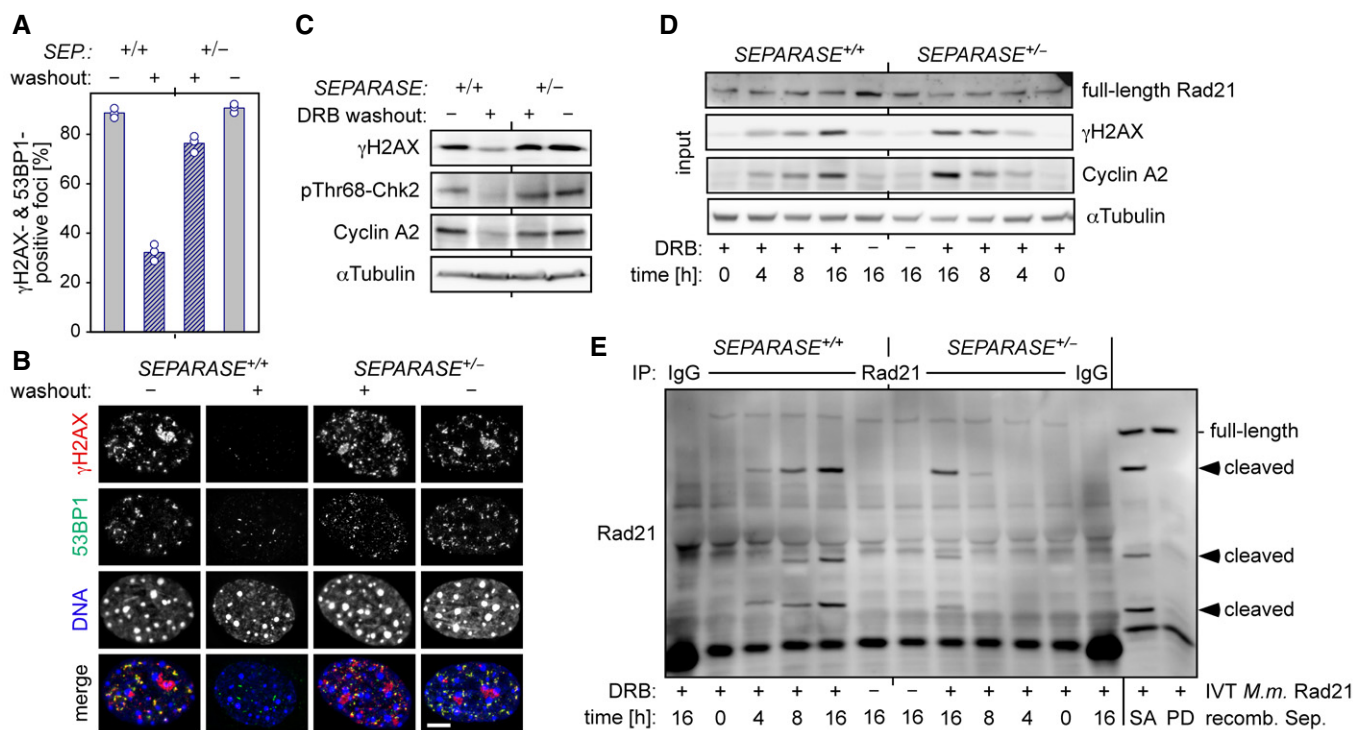


**Figure 7. Compromised DSB repair in *SEPARASE*<sup>+/-</sup> MEFs correlates with reduced damage-induced cleavage of Rad21.**

A, B *SEPARASE*<sup>+/+</sup> and *SEPARASE*<sup>+/-</sup> MEFs were constitutively (– washout) or transiently exposed to DRB (+ washout) and then analyzed by IF for cells with  $\gamma$ H2AX- and 53BP1-positive foci. Shown are averages (bars) of three independent experiments (dots) counting  $\geq 100$  cells each. Scale bar = 5  $\mu$ m.  
 C Cell lysates from one experiment in (A) were analyzed by immunoblotting using the indicated antibodies.  
 D, E *SEPARASE*<sup>+/+</sup> and *SEPARASE*<sup>+/-</sup> MEFs were treated with DRB (+) or carrier solvent (–) for the indicated times and then analyzed by immunoblotting of total cell lysates (D) and IPs using anti-Rad21 or unspecific IgG (E). The lower right two lanes show *in vitro*-expressed mouse Rad21 treated with hyperactive (SA) separase or a protease-dead (PD) variant.

consequent checkpoint-mediated cell cycle arrest were intact in both cell types (Fig 7D). Notably, Rad21-IPs followed by immunoblotting revealed putative cleavage fragments (Fig 7E). Comparison of their mobility pattern with that of murine Rad21, which had been expressed and digested with active (SA) or protease-dead (PD) separase *in vitro* (rightmost two lanes), confirmed their identities as *bona fide* products of separase's proteolytic activity. Importantly, Rad21 cleavage increased with increasing duration of DRB treatment and was always more pronounced in the wild type relative to the heterozygote (Fig 7E). Thus, taking an active part in DDR is not only a conserved feature of mammalian separase; this function is also strikingly dependent on *SEPARASE* dosage.

### Reduced levels of separase predispose murine cells to oncogenic transformation

We have seen above that *SEPARASE* heterozygosity debilitates DSB repair. But does this have any physiological consequences on a cellular and organismal level? No differences in proliferation rate, cell cycle re-entry, or senescence were detected between *SEPARASE*<sup>+/-</sup> and *SEPARASE*<sup>+/+</sup> MEFs (Gutiérrez-Caballero *et al*, unpublished observation). The heterozygous MEFs did also not exhibit any measurable increase in aneuploidies or lagging chromosomes in anaphase relative to wild-type cells (Fig EV4D and E).

Moreover, *SEPARASE*<sup>+/-</sup> mice presented a normal life span and were not predisposed to spontaneous tumorigenesis (Gutiérrez-Caballero *et al*, unpublished observation). Given the strong connection between DSBs and carcinogenesis, we next compared *SEPARASE*<sup>+/-</sup> and *SEPARASE*<sup>+/+</sup> MEFs in a cellular transformation assay, which involved transduction of two cooperating oncogenes, *E1A* and *hRAS*<sup>V12</sup>. Interestingly, we obtained a much higher focus-forming activity of the *SEPARASE*<sup>+/-</sup> MEFs than of their wild-type counterparts (Fig 8A). Thus, reduction in separase increases the susceptibility to neoplastic transformation in primary cell cultures.

Encouraged by this phenotype, we next analyzed tumor initiation and progression in *SEPARASE*<sup>+/-</sup> versus *SEPARASE*<sup>+/+</sup> mice using chemical induction. We chose the two-step skin carcinogenesis protocol based on the use of DMBA as inductor and the mitogen TPA as tumor promoter (Abel *et al*, 2009). The first skin papillomas (initiation) appeared at the 7<sup>th</sup> week after DMBA application in both wild-type and heterozygous mice (Fig 8B). However, the size and number of skin lesions differed markedly between *SEPARASE*<sup>+/+</sup> and *SEPARASE*<sup>+/-</sup> mice during the whole time of the experiment (28 weeks). For instance, at 12 weeks after the beginning of the experiment wild-type mice developed 2.7 tumors per animal compared to a mean of 6 in heterozygotes (2.2 times more). At 28 weeks after DMBA application, *SEPARASE*<sup>+/+</sup> animals showed 1.7 papillomas per mice (mean) and *SEPARASE*<sup>+/-</sup> mice presented

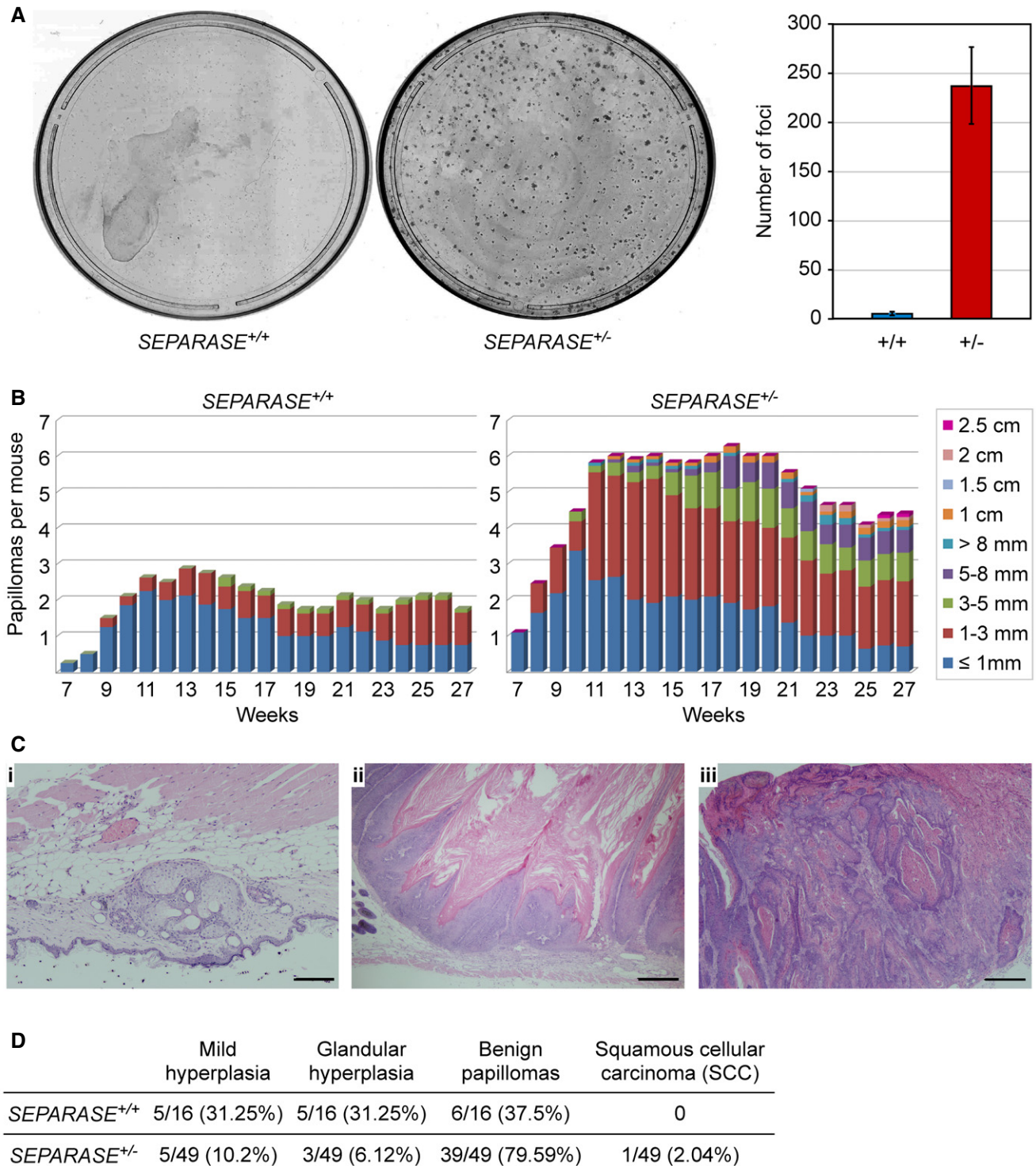


**Figure 8. Reduced levels of separase increases susceptibility to oncogenic transformation in mice.**

**A** Transformation susceptibility of primary MEFs. *SEPARASE*<sup>+/+</sup> versus *SEPARASE*<sup>+/-</sup> MEFs were infected to express E1A and hRas<sup>V12</sup> and then subjected to a colony formation assay. Shown are representative images (left) and the graphical representation of the number of transformed foci (right) from two independent experiments (bars = standard deviations).

**B** Two-stage DMBA (initiation) plus TPA (promotion) skin carcinogenesis. The number and size of skin papillomas are plotted against time for each genotype: *SEPARASE*<sup>+/+</sup> (*n* = 8) versus *SEPARASE*<sup>+/-</sup> (*n* = 11).

**C** Representative hematoxylin- and eosin-stained sections from *SEPARASE*<sup>+/-</sup> biopsies. (i) Glandular hyperplasia; (ii) benign papilloma; (iii) squamous cell carcinoma. Scale bars are 200 μm in (i) and 500 μm in (ii) and (iii).

**D** Quantitative histological assessment of the DMBA-TPA skin carcinogenesis assay. Given are numbers of total, and corresponding percentage in brackets.

4.4 papillomas (2.6 times more). Likewise, the papillomas exhibited a pronounced difference in size (Fig 8B). The majority of the wild-type lesions (95%) were smaller than 3 mm, and none of them exceeded 5 mm. However, 25% of *SEPARASE*<sup>+/-</sup> papillomas were larger than 5 mm. To further investigate malignancy, we analyzed tumor histology (Fig 8C and D). In the wild type, this showed that a high proportion of lesions (62.5%) corresponded to small hyperplasias of the epidermis or glandular tissue, while the rest (37.5%) were defined as benign papillomas. Conversely, in the heterozygous mice only a small percentage (16.3%) of the lesions was classified as mild epidermal or glandular hyperplasias, whereas a large fraction was defined as benign papillomas (79.6%). Furthermore, one tumor (2%) corresponded to a malignant lesion, i.e., a squamous cellular carcinoma (Fig 8C and D). We conclude that *SEPARASE* is haploinsufficient in that the presence of its gene in only one copy strongly promotes formation and progression of chemically induced skin tumors in mice.

## Discussion

We show here that mammalian separase has an important function for the repair of DSBs by HDR. Fulfilling this function involves the tethering of separase to the DNA lesions where it becomes proteolytically active to locally cleave cohesin. Together with previous studies on yeasts (Nagao *et al*, 2004; McAleenan *et al*, 2013), our work now firmly establishes that promotion of HDR is a conserved interphase function of separase. At first sight, these findings seem to be at odds with the well-documented facts that cohesin also accumulates at DSBs and supports their repair (Kim *et al*, 2002; Strom *et al*, 2004; Unal *et al*, 2004; Potts *et al*, 2006). However, when assessing the roles of cohesin and separase side by side in the same *in vivo* assay, we indeed find both to be required for efficient HDR (Fig 2D and E). How can these observations be reconciled with each other? Actually, proteolytic removal of cohesin does not exclude its simultaneous hyper-recruitment but will merely result in heightened turnover of cohesin at DSBs. These increased dynamics might be necessary for effective repair by facilitating close juxtaposition of sister chromatids while simultaneously granting the repair machinery access to catalyze DNA end resection, strand invasion, DNA synthesis and resolution of recombination intermediates. Consistent with this model, Aragón *et al* demonstrated compromised DSB resection and repair efficiency upon expression of separase-resistant, non-cleavable Rad21 in budding yeast (McAleenan *et al*, 2013).

We were able to image some chromosome spreads of DRB-treated cells that expressed a histone-based separase activity sensor and had slipped into mitosis despite persistent DNA damage (Fig 3C). This revealed for the first time that the activation of separase does indeed occur not globally but only locally. Nevertheless, given that separase-dependent reduction in cohesin occurs only within  $\approx 10$  kb around the DSB in *Saccharomyces cerevisiae* (McAleenan *et al*, 2013), the zones of cleaved sensor were surprisingly large, coinciding largely with the  $\gamma$ H2AX signal, which is known to spread up to almost 2 Mb (Iacovoni *et al*, 2010). Remarkably, sensor cleavage, much like the  $\gamma$ H2AX signals, did not spread to the sister but only along the damaged chromatid, arguing that separase might not diffuse freely from the DSB but be recruited over large distances and stay immobilized. Future ChIP-qPCR experiments will clarify this issue.

While the recruitment of yeast separase to DSBs remains enigmatic, we begin here to elucidate this issue for human separase. We identify three novel PTMs, an NES-inactivating phosphorylation, Arg-methylation within a conserved RG-repeat motif, and sumoylation of Lys-1034, all of which are induced by DSBs and necessary for the association of separase with  $\gamma$ H2AX-positive chromatin. Moreover, we reconstitute these separase PTMs *in vitro* by using the DDR-relevant enzymes ATM, PRMT1, and Mms21, respectively. While this answers some questions, others remain to be addressed: Do ATM, PRMT1, and Mms21 act on separase *in vivo*? What represents the anchor for modified separase on damaged DNA? How can the selective recruitment of separase to DSBs of only postreplicative cells be explained? And, most importantly, how is tethered separase activated at DSBs while simultaneously preventing global activation of the protease, which would result in premature loss of cohesion? In regard to this last question, it is interesting to note that an important role of the APC/C coactivator Cdh1 in HDR has recently emerged (Lafranchi *et al*, 2014; Ha *et al*, 2017). Given that the separase inhibitor securin is slowly turned over in DRB-treated G2 cells in an APC/C<sup>Cdh1</sup>-dependent manner (Hellmuth *et al*, 2014), it is tempting to speculate that DSB-associated separase might be activated by the Cdh1-form of this E3 ubiquitin ligase.

Studying cellular transformation in *E1A*- and *hRAS*<sup>V12</sup>-expressing MEFs as well as chemically induced skin carcinogenesis in mice, we demonstrate that *SEPARASE* heterozygosity strongly predisposes murine cells to oncogenic transformation. At the same time, these cells show no signs of numerical chromosomal instability but are clearly compromised in recovery from transient DRB treatment. Thus, HDR seems to be more sensitive to limiting amounts of separase than sister chromatid separation. Replacing *SEPARASE* by our HDR-defective alleles should clarify whether the association of *SEPARASE* heterozygosity with cancer might generally be explained by weakened DSB repair rather than anaphase problems. A recent study reports frequent mutations of *SEPARASE* and the cohesin subunit *STAG2* in transitional cell carcinoma, the predominant form of bladder cancer (Guo *et al*, 2013). With HDR being the only cellular function in which cohesin and its nemesis separase collaborate, it will be interesting to test whether the corresponding alleles might exhibit selective defects in HDR.

## Materials and Methods

### Antibodies

The following antibodies were used for immunoblotting according to standard protocols: rabbit anti-separase (1:1,500; Stemmann *et al*, 2001), mouse anti-securin (1:1,000; MBL), mouse anti-Flag M2 (1:2,000; Sigma-Aldrich), mouse anti-Myc (hybridoma supernatant 1:50; DSHB; 9E10), mouse anti-SUMO2 (protein G-purified hybridoma supernatant conc. 1.67 mg/ml diluted 1:500; DSHB; clone 8A2), mouse anti-RGS-His (1:1,000; Qiagen), rabbit anti-phosphoSer139-histone H2A.X ( $\gamma$ H2AX; 1:5,000; Millipore), rabbit anti-symmetric dimethylarginine (ADMA; 1:100; Acris), mouse anti-cyclin B1 (1:1,000; Millipore), mouse anti-topoisomerase II $\alpha$  (1:1,000; Enzo Life Sciences), mouse anti-cyclin A2 (1:200; Santa Cruz Biotechnology), mouse anti-phosphoSerine (1:1,000;

Invitrogen), rabbit anti-phosphoThr68-Chk2 (1:800; Cell Signaling), mouse anti-Rad21 (1:800; Santa Cruz Biotechnology; B-2), rabbit anti-Rad21 (1:1,000; Bethyl; A300-080A), rabbit anti-Smc1 (1:1,000; Bethyl) mouse anti-Wapl (hybridoma supernatant 1:500; raised against the first 88 aa; clone D9), mouse anti-GFP (hybridoma supernatant 1:2,000; gift from D. van Essen and S. Sacconi), goat anti-GST (1:800; gift from D. Boos), rat anti-HA (1:2,000; Roche; clone 3F10), and mouse anti- $\alpha$ -tubulin (hybridoma supernatant 1:200; DSHB; 12G10). For immunoprecipitation experiments, the following affinity matrices and antibodies were used: mouse anti-Myc agarose (Sigma-Aldrich), mouse anti-Rad21 coupled to protein G sepharose (GE Healthcare), rabbit anti-separase (Hellmuth *et al*, 2014) coupled to protein A sepharose (GE healthcare), and an GFP-binding, *Escherichia coli*-expressed, metal ion affinity-purified camel antibody fragment covalently coupled to NHS-sepharose (GE Healthcare). For ChIP experiments, rabbit anti- $\gamma$ H2AX, rabbit anti-separase (Hellmuth *et al*, 2014), or non-specific rabbit IgG (Bethyl) coupled to protein A agarose containing salmon sperm DNA (Millipore) was used. For non-covalent coupling of antibodies to beads, 10  $\mu$ l of the respective matrix was rotated with 2–5  $\mu$ g antibody for 90 min at room temperature and then washed three times with lysis buffer. For IFM, newly raised rabbit anti-separase (aa1,305–1,573; this study), mouse anti-Hec1 (1:800; Genetex), mouse anti-Myc (1:1,000; Millipore; 4A6), rabbit anti-MDC1 (1:200; Abcam), rabbit anti-53BP1 (1:500; Santa Cruz), mouse anti-Nup153 (1:1,000; Abcam), rabbit anti- $\gamma$ H2AX (1:1,000; Millipore), and mouse anti- $\gamma$ H2AX (1:2,500; Millipore) were used. For the detection of eGFP-tagged separase variants (Figs 4D and EV3A) and eGFP- and mCherry-tagged separase activity sensor (Fig 3C), autofluorescence was imaged. Secondary antibodies (all 1:500) were as follows: Cy3 donkey anti-guinea pig IgG, Cy5 goat anti-rabbit IgG, and Cy5 goat anti-mouse IgG (all from Jackson Immunoresearch Laboratories), and Marina Blue goat anti-rabbit IgG, Alexa Fluor 488 goat anti-rabbit IgG, and Alexa Fluor 488 goat anti-mouse IgG (all from Invitrogen).

### Cell lines

For stable, inducible expression of Myc<sub>6</sub>-separase, a single copy of the corresponding transgene was stably integrated into a HEK293-FlpIn-TRex line (Invitrogen) by selection of clones at 150  $\mu$ g/ml hygromycin B (Figs 1D and E, 3, EV1B, C, and F, and EV2C–E). A second, constitutively expressed transgene encoding histone H2B-mCherry-Rad21<sup>107–268</sup>-eGFP (separase sensor) was integrated via  $\phi$  C31-mediated site-specific recombination followed by selection at 270  $\mu$ g/ml G418 sulfate (Sigma-Aldrich). Induction of transgenic Myc<sub>6</sub>-separase was done using 0.2–1  $\mu$ g/ml doxycycline (Dox; Sigma-Aldrich) for 10–14 h. All human cells were cultured in DMEM (GE Healthcare) supplemented with 10% FCS (Sigma-Aldrich) at 37°C and 5% CO<sub>2</sub>. Mouse embryonic fibroblasts (MEFs) were cultivated in DMEM supplemented with 10% FCS, 1% non-essential amino acids, and 1% glutamine. Experiments shown in Fig 7 were performed during the third passage. For transient, inducible expression of Myc<sub>6</sub>-separase variants [WT, RG>KG (R1423, 1425, 1427, 1429K), NESmut (1661-AQEAPGDAPA-1670 instead of 1661-LQEMPGDVPL-1670), superNES (1749-DIDELALKFAGLDL-1762 instead of 1749-SLQEMPGDVPLARI-1762), S1660A, S1660D, and K1034R], HEK293-FlpIn-TRex (Figs 4A, B, and F, 5, and 6C, D,

F, and G) or HeLaK cells (Figs 4D, and EV3A and B) were transfected with the corresponding pcDNA5-based plasmids using a calcium phosphate-based method or Lipofectamine 2000 (Invitrogen) according to the manufacturer's protocol. To enrich sumoylated separase species, *in vivo* expression plasmids for RGS-His<sub>6</sub>-tagged SUMO2 (kindly provided by S. Müller; Fig 6B and C) or RGS-His<sub>6</sub>-tagged separase-WT (Fig 6A) were transfected into HEK293-FlpIn-TRex cells. To introduce multiple site-specific DSBs, HEK293-FlpIn-TRex cells were transiently transfected with pCS2 plasmid to express FLAG<sub>3</sub>-AsiSI-ER (Figs 1B–E, 3, EV1A–C and F, and EV2E). Alternatively, a single DSB was inflicted by transient transfection of a pcDNA3-based plasmid into U2OS cells (Figs 2, and EV2G and F) to express I-SceI-ER. In both cases, cells were subsequently treated with OHT.

### Cell treatments

For synchronization at the G1/S boundary, cells were treated with 2 mM thymidine (Sigma-Aldrich) for 20 h. To introduce DNA damage specifically in G2, cells released from a single thymidine block for 4–6 h were treated with 0.5–1  $\mu$ M doxorubicin (DRB; LC Laboratories) or, in case of FLAG3-ER-AsiSI or HA-ER-I-SceI expression, with 1  $\mu$ M 4-hydroxytamoxifen (OHT; Sigma-Aldrich) for 4 h unless specified otherwise. Prior to ChIP, cells were exposed to OHT for 12 h. To achieve a DNA damage checkpoint-independent G2 arrest, the Cdk1-inhibitor RO3306 (Santa Cruz Biotechnology) was added to 10  $\mu$ M 4–6 h after release from a thymidine arrest in all cases but the washout (Figs 5, 6G, and 7A–C) and sumoylation experiments (Fig 6A–D). For the inhibition of the ATM kinase, KU-55933 (LC Laboratories) was given at the time of DRB addition for 4 h at 2  $\mu$ M (Fig EV3A and B) or for 12 h at 0.3  $\mu$ M (Fig 4C). To inflict DNA damage on G1 cells, DSB-introducing agents (but no RO3306) were added 13 h after release from a G1/S block. For doxorubicin (DRB) washout experiments, thymidine pre-synchronized cells were DRB-treated for 1 h, detached from the culture plate, and washed five times with fresh medium. Thereafter, cells were divided for the indicated treatments (Figs 5, 6G, and 7A–C) and DRB was re-added to samples “without” DRB washout. Approximately 24 h after DRB removal, cells were analyzed for successful DNA damage repair or persisting  $\gamma$ H2AX- and MDC1- or 53BP1-positive foci.

### Flow cytometry

Flow cytometry of propidium iodide-stained DNA/cells was done as described (Hellmuth *et al*, 2014). To measure the amount of GFP fluorescence (Figs 2B and D, and EV2G) 48 h after infliction of a single DSB by OHT addition, cells were trypsinized, resuspended in fresh media, mixed 2:1 with 10% formaldehyde, and immediately analyzed as described (Gunn & Stark, 2012). The cell population with increased GFP fluorescence above background was gated in a logarithmic FL2/FL1 plot to determine the percentage of GFP-positive cells.

### Immunoprecipitation

1  $\times$  10<sup>7</sup> cells were lysed with a Dounce homogenizer in 1 ml lysis buffer (20 mM Tris-HCl pH 7.7, 100 mM NaCl, 10 mM NaF, 20 mM

$\beta$ -glycerophosphate, 5 mM MgCl<sub>2</sub>, 0.1% Triton X-100, 5% glycerol), combined with Benzonase<sup>®</sup> (ad 30 U/l; Santa Cruz), and incubated on ice for 2 h. To preserve separase phosphorylation status (Fig 4A–C), lysis buffer was additionally supplemented with 1  $\mu$ M okadaic acid (Sigma-Aldrich) and 1  $\mu$ M microcystin LR (Alexis Biochemicals). “Whole cell lysates” were centrifuged at 16,000 g for 30 min to give “high-speed supernatant” and at 2,500 g for 10 min to give “low-speed supernatant” and a chromatin pellet, which was resolubilized in lysis buffer supplemented with additional 400 mM NaCl as well as 50 mM EDTA to give a “chromatin extract”. With few exceptions (see below), 10  $\mu$ l of antibody carrying beads was incubated with 1 ml “whole cell lysate” for 4 h at 4°C and washed 5 $\times$  with lysis buffer before bound proteins were eluted by Tev-protease treatment in Tev-cleavage buffer (10 mM HEPES-KOH pH 7.7, 50 mM NaCl, 25 mM NaF, 1 mM EGTA, 20% glycerol) for 40 min at RT (Fig 4G) or by boiling in non-reducing SDS sample buffer (all other cases). To enrich soluble sensor- and Rad21-cleavage fragments relative to the chromatin-associated full-length proteins (Figs 3A and B, and 7D and E), “low-speed supernatant” instead of “whole cell lysate” was used for the GFP- and Rad21-IPs, respectively. To purify separase as a substrate for Arg-methylation or phosphorylation assays (Fig 4E and G), “high-speed supernatant” instead of “whole cell lysate” was used for the Myc-IP. To enrich Arg-methylated separase (Fig 4F), “chromatin extract” instead of “whole cell lysate” was used for the Myc-IP.

### RNA interference

For efficient knock-down, cells were transfected with calcium phosphate or RNAiMax<sup>®</sup> (Invitrogen) and 70 nM of single siRNA duplex of *SEP-01*: 5'-AACUGUUCUACCUCCAAGGUUAGAUUUU-3' (was generally used unless stated otherwise), *SEP-02*: 5'-GCACUGCCUGCACACCUA-3', *SEP-03*: 5'-GAAGAUCGUUCCUAUACA-3', *SEP-04*: 5'-GAACUUCAGUGAUGACAGU-3', *SEP-05*: 5'-GCUGUCAGAUAGUUGAUUUU-3', or *SMC1\_ORF1*: 5'-AAGAAAGUAGAGACAGA-3'. In case of two siRNAs targeting the identical RNA, 40 nM each was used: (i) *RAD21\_3'UTR1*: 5'-ACUCAGACUUCAGUGUAUA-3', and (ii) *RAD21\_3'UTR2*: 5'-AGGACAGACUGAUGGGAAA-3'; and (i) *WAPL1*: 5'-CGGACUACCCUUAGCACAA-3', and (ii) *WAPL2*: 5'-GGUUAAGU GUUCCUCUUAU-3'. Transfected cells were grown for 12–24 h before synchronization procedures were applied. Luciferase siRNA (*GL2*) was used as negative control in variable concentrations.

### Multiplex PCR

PCRs were performed with the same set of primers and conditions as for qPCR (see below) except for the use of self-made Taq polymerase and 4  $\mu$ l immunoprecipitated DNA or 1  $\mu$ l input DNA as template. Amplified fragments were separated on 6% PAGs (2.7% cross-linker; 8  $\times$  10  $\times$  0.1 cm) in 0.5 $\times$  TBE buffer (44.5 mM Tris, 44.5 boric acid, 1 mM EDTA) at 100 V for 45 min. Gels were stained in ethidium bromide (1  $\mu$ g/ml), destained in H<sub>2</sub>O and finally analyzed under UV light (Gene Flash, Syngene Bio Imaging).

### qPCR

For ChIP-qPCR, immunoprecipitated and input DNA were analyzed in triplicates by real-time qPCR using the following primers:

CGGGTTGGGCTTGAGTGAGG and AACCTGCCCAACCCGATCA for DSB1-A, GGAGTCGGCCGGGATCACAT and CCTTGCAAACC AGTCTCGTCC for DSB1-B, GGAGTCGGCCGGGATCACAT and CCCACAGCTTGCCCATCT for DSB1-C, AGGACTGGTTTGCAA GGATG and ACCCCATCTCAAATGACAA for DSB1-D, GGGACA TGTGAGACTGAAGAAGG and ACGCCTCTCCACTCCCTCT for DSB1-E, AACTTTAGGATGGGGCTGCT and GCCATAACAGA GGGTGGAAA for DSB1-F, TGCCGGTCTCTAGAAGTTTG and GCGCTTGATTCCCTGAGT for DSB2-A, and CCCATCTCAACCTC CACACT and CTTGTCCAGATTCGCTGTGA for “no DSB”. The AsiSI-induced DSB sites are on chromosome 1 (DSB1) and chromosome 6 (DSB2). The AsiSI-negative locus (“no DSB”) maps to chromosome 22. PCRs were assembled with Maxima SYBR<sup>®</sup> Green/ROX master mix (Fermentas), 300 nM forward/reverse primer, and 2  $\mu$ l template DNA in 48-well plates (Applied Bioscience). qPCR was performed at 59°C annealing temperature for 40 cycles in a StepOne Real Time PCR system (Applied Bioscience). IP efficiency was calculated as percentage of input DNA immunoprecipitated (adjusted to 100%) with the following formula:  $100 \times 2^{(\Delta C_i \text{ adjusted input} - \Delta C_i \text{ of IP})}$ .

### Skin chemical carcinogenesis, histology, and immunohistochemistry

For the induction of skin papillomas, a previously described multi-stage carcinogenesis model was followed (Abel *et al*, 2009). Briefly, the back skin of 8-week-old mice was shaved and painted with a single dose of 25  $\mu$ g DMBA (Sigma) dissolved in acetone 24 h later. Forty-eight hours later, tumor growth was promoted by applying 12.5  $\mu$ g of TPA (Sigma) dissolved in acetone twice a week for a period of 12 weeks. The number and characteristics of the skin lesions were annotated twice a week.

Skin papillomas and surrounding skin were fixed in 10% formaldehyde for 24 h and subsequently embedded in paraffin. Serial sections of 5  $\mu$ m were stained with hematoxylin and eosin following standard procedures.

Additional experimental procedures are described in “Appendix Supplementary Materials and Methods”.

**Expanded View** for this article is available online.

### Acknowledgements

We thank Gaëlle Legube, Lisa Mohr, and Stefan Müller for plasmids; Maria Jasin and Jeremy Stark for DR-GFP and EJ5-GFP reporter U2OS cell lines, respectively; Markus Hermann for technical assistance; and Stefan Heidmann, Dominik Boos, and Boris Pfander for critical reading of the manuscript. This work was supported by a grant (STE997/4-2) from the Deutsche Forschungsgemeinschaft (DFG) to O.S. and by a grant (BFU2017-89408-R) from Ministerio de Economía y Competitividad to A.M.P.

### Author contributions

CG-C and EL conducted all the mouse work (Figs 8 and EV4) and isolated the MEFs used for Fig 7. AMP and OS designed the research and wrote the paper. SH co-designed the research, carried out all experiments except for those shown in Figs 8 and EV4 and contributed to writing of the paper.

### Conflict of interest

The authors declare that they have no conflict of interest.

## References

- Abel TW, Clark C, Bierie B, Chytil A, Aakre M, Gorska A, Moses HL (2009) GFAP-Cre-mediated activation of oncogenic K-ras results in expansion of the subventricular zone and infiltrating glioma. *Mol Cancer Res* 7: 645–653
- Boisvert FM, Dery U, Masson JY, Richard S (2005) Arginine methylation of MRE11 by PRMT1 is required for DNA damage checkpoint control. *Genes Dev* 19: 671–676
- Boos D, Kuffer C, Lenobel R, Korner R, Stemmann O (2008) Phosphorylation-dependent binding of cyclin B1 to a Cdc6-like domain of human separase. *J Biol Chem* 283: 816–823
- Buheitel J, Stemmann O (2013) Prophase pathway-dependent removal of cohesin from human chromosomes requires opening of the Smc3-Sccl1 gate. *EMBO J* 32: 666–676
- Caron P, Aymard F, Iacovoni JS, Brioso S, Canitrot Y, Bugler B, Massip L, Losada A, Legube G (2012) Cohesin protects genes against gammaH2AX Induced by DNA double-strand breaks. *PLoS Genet* 8: e1002460
- Chailleux C, Aymard F, Caron P, Daburon V, Courilleau C, Canitrot Y, Legube G, Trouche D (2014) Quantifying DNA double-strand breaks induced by site-specific endonucleases in living cells by ligation-mediated purification. *Nat Protoc* 9: 517–528
- Dery U, Coulombe Y, Rodrigue A, Stasiak A, Richard S, Masson JY (2008) A glycine-arginine domain in control of the human MRE11 DNA repair protein. *Mol Cell Biol* 28: 3058–3069
- Finetti P, Guille A, Adelaide J, Birnbaum D, Chaffanet M, Bertucci F (2014) ESPL1 is a candidate oncogene of luminal B breast cancers. *Breast Cancer Res Treat* 147: 51–59
- Galanty Y, Belotserkovskaya R, Coates J, Polo S, Miller KM, Jackson SP (2009) Mammalian SUMO E3-ligases PIAS1 and PIAS4 promote responses to DNA double-strand breaks. *Nature* 462: 935–939
- Gunn A, Stark JM (2012) I-SceI-based assays to examine distinct repair outcomes of mammalian chromosomal double strand breaks. *Methods Mol Biol* 920: 379–391
- Guo G, Sun X, Chen C, Wu S, Huang P, Li Z, Dean M, Huang Y, Jia W, Zhou Q, Tang A, Yang Z, Li X, Song P, Zhao X, Ye R, Zhang S, Lin Z, Qi M, Wan S et al (2013) Whole-genome and whole-exome sequencing of bladder cancer identifies frequent alterations in genes involved in sister chromatid cohesion and segregation. *Nat Genet* 45: 1459–1463
- Guttler T, Madl T, Neumann P, Deichsel D, Corsini L, Monecke T, Ficner R, Sattler M, Gorlich D (2010) NES consensus redefined by structures of PKI-type and Rev-type nuclear export signals bound to CRM1. *Nat Struct Mol Biol* 17: 1367–1376
- Ha K, Ma C, Lin H, Tang L, Lian Z, Zhao F, Li JM, Zhen B, Pei H, Han S, Malumbres M, Jin J, Chen H, Zhao Y, Zhu Q, Zhang P (2017) The anaphase promoting complex impacts repair choice by protecting ubiquitin signalling at DNA damage sites. *Nat Commun* 8: 15751
- Hayakawa T, Yusa K, Kouno M, Takeda J, Horie K (2006) Bloom's syndrome gene-deficient phenotype in mouse primary cells induced by a modified tetracycline-controlled trans-silencer. *Gene* 369: 80–89
- Hellmuth S, Bottger F, Pan C, Mann M, Stemmann O (2014) PP2A delays APC/C-dependent degradation of separase-associated but not free securin. *EMBO J* 33: 1134–1147
- Iacovoni JS, Caron P, Lassadi I, Nicolas E, Massip L, Trouche D, Legube G (2010) High-resolution profiling of gammaH2AX around DNA double strand breaks in the mammalian genome. *EMBO J* 29: 1446–1457
- Kim ST, Lim DS, Canman CE, Kastan MB (1999) Substrate specificities and identification of putative substrates of ATM kinase family members. *J Biol Chem* 274: 37538–37543
- Kim JS, Krasieva TB, LaMorte V, Taylor AM, Yokomori K (2002) Specific recruitment of human cohesin to laser-induced DNA damage. *J Biol Chem* 277: 45149–45153
- Kueng S, Hegemann B, Peters BH, Lipp JJ, Schleiffer A, Mechtler K, Peters JM (2006) Wapl controls the dynamic association of cohesin with chromatin. *Cell* 127: 955–967
- Lafranchi L, de Boer HR, de Vries EG, Ong SE, Sartori AA, van Vugt MA (2014) APC/C(Cdh1) controls CtIP stability during the cell cycle and in response to DNA damage. *EMBO J* 33: 2860–2879
- Liu H, Rankin S, Yu H (2013) Phosphorylation-enabled binding of SGO1-PP2A to cohesin protects sororin and centromeric cohesion during mitosis. *Nat Cell Biol* 15: 40–49
- McAleenan A, Clemente-Blanco A, Cordon-Preciado V, Sen N, Esteras M, Jarmuz A, Aragon L (2013) Post-replicative repair involves separase-dependent removal of the kleisin subunit of cohesin. *Nature* 493: 250–254
- Meyer R, Fofanov V, Panigrahi A, Merchant F, Zhang N, Pati D (2009) Overexpression and mislocalization of the chromosomal segregation protein separase in multiple human cancers. *Clin Cancer Res* 15: 2703–2710
- Mukherjee M, Ge G, Zhang N, Huang E, Nakamura LV, Minor M, Fofanov V, Rao PH, Herron A, Pati D (2011) Separase loss of function cooperates with the loss of p53 in the initiation and progression of T- and B-cell lymphoma, leukemia and aneuploidy in mice. *PLoS One* 6: e22167
- Mukherjee M, Byrd T, Brawley VS, Bielamowicz K, Li XN, Merchant F, Maitra S, Sumazin P, Fuller G, Kew Y, Sun D, Powell SZ, Ahmed N, Zhang N, Pati D (2014a) Overexpression and constitutive nuclear localization of cohesin protease Separase protein correlates with high incidence of relapse and reduced overall survival in glioblastoma multiforme. *J Neurooncol* 119: 27–35
- Mukherjee M, Ge G, Zhang N, Edwards DG, Sumazin P, Sharan SK, Rao PH, Medina D, Pati D (2014b) MMTV-Espl1 transgenic mice develop aneuploid, estrogen receptor alpha (ERalpha)-positive mammary adenocarcinomas. *Oncogene* 33: 5511–5522
- Nagao K, Adachi Y, Yanagida M (2004) Separase-mediated cleavage of cohesin at interphase is required for DNA repair. *Nature* 430: 1044–1048
- Nasmyth K, Haering CH (2009) Cohesin: its roles and mechanisms. *Annu Rev Genet* 43: 525–558
- Nishiyama T, Sykora MM, Huis in 't Veld PJ, Mechtler K, Peters JM (2013) Aurora B and Cdk1 mediate Wapl activation and release of acetylated cohesin from chromosomes by phosphorylating Sororin. *Proc Natl Acad Sci USA* 110: 13404–13409
- Obenauer JC, Cantley LC, Yaffe MB (2003) Scansite 2.0: proteome-wide prediction of cell signaling interactions using short sequence motifs. *Nucleic Acids Res* 31: 3635–3641
- Pierce AJ, Johnson RD, Thompson LH, Jasin M (1999) XRCC3 promotes homology-directed repair of DNA damage in mammalian cells. *Genes Dev* 13: 2633–2638
- Polo SE, Jackson SP (2011) Dynamics of DNA damage response proteins at DNA breaks: a focus on protein modifications. *Genes Dev* 25: 409–433
- Potts PR, Yu H (2005) Human MMS21/NSE2 is a SUMO ligase required for DNA repair. *Mol Cell Biol* 25: 7021–7032
- Potts PR, Porteus MH, Yu H (2006) Human SMC5/6 complex promotes sister chromatid homologous recombination by recruiting the SMC1/3 cohesin complex to double-strand breaks. *EMBO J* 25: 3377–3388
- Sacher M, Pfander B, Hoegel C, Jentsch S (2006) Control of Rad52 recombination activity by double-strand break-induced SUMO modification. *Nat Cell Biol* 8: 1284–1290
- Shepard JL, Amatruda JF, Finkelstein D, Ziai J, Finley KR, Stern HM, Chiang K, Hersey C, Barut B, Freeman JL, Lee C, Glickman JN, Kutok JL, Aster JC, Zon

- Li (2007) A mutation in separase causes genome instability and increased susceptibility to epithelial cancer. *Genes Dev* 21: 55–59
- Sjogren C, Nasmyth K (2001) Sister chromatid cohesion is required for postreplicative double-strand break repair in *Saccharomyces cerevisiae*. *Curr Biol* 11: 991–995
- Stemmann O, Zou H, Gerber SA, Gygi SP, Kirschner MW (2001) Dual inhibition of sister chromatid separation at metaphase. *Cell* 107: 715–726
- Strom L, Lindroos HB, Shirahige K, Sjogren C (2004) Postreplicative recruitment of cohesin to double-strand breaks is required for DNA repair. *Mol Cell* 16: 1003–1015
- Strom L, Karlsson C, Lindroos HB, Wedahl S, Katou Y, Shirahige K, Sjogren C (2007) Postreplicative formation of cohesin is required for repair and induced by a single DNA break. *Science* 317: 242–245
- Sun Y, Yu H, Zou H (2006) Nuclear exclusion of separase prevents cohesin cleavage in interphase cells. *Cell Cycle* 5: 2537–2542
- Thandapani P, O'Connor TR, Bailey TL, Richard S (2013) Defining the RGG/RG motif. *Mol Cell* 50: 613–623
- Uhlmann F, Wernic D, Poupart MA, Koonin EV, Nasmyth K (2000) Cleavage of cohesin by the CD clan protease separin triggers anaphase in yeast. *Cell* 103: 375–386
- Unal E, Arbel-Eden A, Sattler U, Shroff R, Lichten M, Haber JE, Koshland D (2004) DNA damage response pathway uses histone modification to assemble a double-strand break-specific cohesin domain. *Mol Cell* 16: 991–1002
- Unal E, Heidinger-Pauli JM, Koshland D (2007) DNA double-strand breaks trigger genome-wide sister-chromatid cohesion through Eco1 (Ctf7). *Science* 317: 245–248
- Wang H, Huang ZQ, Xia L, Feng Q, Erdjument-Bromage H, Strahl BD, Briggs SD, Allis CD, Wong J, Tempst P, Zhang Y (2001) Methylation of histone H4 at arginine 3 facilitating transcriptional activation by nuclear hormone receptor. *Science* 293: 853–857
- Zhang Y, Xiong Y (2001) A p53 amino-terminal nuclear export signal inhibited by DNA damage-induced phosphorylation. *Science* 292: 1910–1915
- Zhang N, Ge G, Meyer R, Sethi S, Basu D, Pradhan S, Zhao YJ, Li XN, Cai WW, El-Naggar AK, Baladandayuthapani V, Kittrell FS, Rao PH, Medina D, Pati D (2008) Overexpression of Separase induces aneuploidy and mammary tumorigenesis. *Proc Natl Acad Sci USA* 105: 13033–13038
- Zhao Q, Xie Y, Zheng Y, Jiang S, Liu W, Mu W, Liu Z, Zhao Y, Xue Y, Ren J (2014) GPS-SUMO: a tool for the prediction of sumoylation sites and SUMO-interaction motifs. *Nucleic Acids Res* 42: W325–W330

## **APPENDIX MATERIALS AND METHODS**

### **Table of contents:**

- Appendix materials and methods**
- Appendix references**

## **Immunofluorescence microscopy (IFM)**

HeLaK, mouse embryonic fibroblasts (MEFs) or transgenic Hek293-FlpIn-TRex cells grown on poly-lysine coated glass coverslips were washed once with PBS (all IFMs except for those shown in figures 4D and EV3A) or a digitonin-containing buffer to lower the cytosolic NLS-eGFP-separase signal while leaving the nuclear envelope intact (Figures 4D and EV3A) (Joseph et al, 2002). All samples were fixed with fixation-solution (PBS, 3.7% formaldehyde, 0.3% Triton X-100) for 10 min at room temperature and then washed twice with quenching-solution (PBS, 100 mM glycine). Cells were then further permeabilized by treatment with permeabilization-solution (PBS, 0.5% Triton X-100) for 5 min which was followed by a PBS wash and an incubation in blocking-solution (PBS, 1% (w/v) BSA) for 20 min at room temperature. Coverslips were transferred into a wet chamber and incubated with primary antibodies for 1 h followed by 4 washes with PBS-Tx (PBS, 0.1% Triton X-100). After incubation with fluorescently labeled secondary antibodies for 40 min, samples were washed once, stained for 10 min with 1 µg/ml Hoechst 33342 in PBS-Tx and washed again 4 times. Finally, coverslips were mounted in 20 mM Tris-HCl pH 8.0, 2,33% (w/v) 1,4-diazabicyclo(2.2.2)octane, 78% glycerol on a glass slide.

Immunofluorescence microscopy (IFM) of fixed cells was performed on a DMI 6000 inverted microscope (Leica) using a HCX PL APO 100x/1.40-0.70 oil objective. For the visualization of DNA-damage foci, Z-stacks series over 4 µM in 0.35 µM increments were collected, deconvoluted and projected into one plane using the LAS-AF software.

### **PRMT1 methylation assay**

Hek293T cells were transiently transfected to express Myc<sub>6</sub>-Tev<sub>2</sub>-separase-WT or -KG together with securin-WT, arrested with thymidine to obtain post-translationally unmodified separase and then lysed. Separase-securin complexes were isolated from the corresponding high speed supernatants by Myc-IP and Tev protease elution as described above and stored at -80°C. For the methylation assay, 2 µg purified separase-securin or 2 µg histone H4 (NEB) were incubated with *E. coli*-expressed, metal ion affinity-purified His<sub>6</sub>-Sumo<sub>1</sub>-PRMT1 (8 mg/ml) or reference buffer (25 mM Tris HCl pH 7.4, 0.2 mM EDTA, 100 mM KCl, 20 % glycerol, 0.8 mM DTT) and 0.55 µCi of [methyl-<sup>3</sup>H]-adenosyl-methionine (Hartmann Analytic) in 50 mM Tris-HCl pH 9.0, 5 mM MgCl<sub>2</sub>, 4 mM DTT and a total volume of 50 µl. Reactions were incubated for 2 h at 37°C and stopped by boiling in reducing SDS-sample buffer. Samples were loaded twice onto the same SDS-PAGE. One gel slice was subjected to blotting onto PVDF membrane (0.2 µm pore size; Serva) and the other half was Coomassie-stained. Following transfer, the PVDF was soaked in EN<sup>3</sup>-HANCE (PerkinElmer Life Sciences) for 10 min, dried and exposed to X-ray film (Amersham Hyperfilm<sup>TM</sup> MP; GE Healthcare) for 48 h. Signals were visualized with developing and fixation solution according to manufacturer's recommendation (Dentus F-100; AGFA).

### **ATM kinase assay**

Myc<sub>6</sub>-separase-WT and -S1660A, each associated with securin-WT, were expressed and purified as described for the methylation assay except that the complex was left bound to beads. Active Flag-His<sub>6</sub>-ATM-WT and -KD (kinase-dead; D2870A, N2875K) were over-expressed in Hek293T cells by transient

transfection of corresponding plasmids (Addgene, #31985 and #31986) and purified as described (Rhodes et al, 2001). When supplemented with 10 mM  $\text{MnCl}_2$  and 5  $\mu\text{M}$  ATP, the storage buffer (10 mM Hepes-KOH pH 7.5, 10 mM  $\beta$ -glycerophosphate, 50 mM NaCl, 1 mM DTT, 1 mM  $\text{Na}_3\text{VO}_4$ , 1 mM NaF, 10% glycerol) simultaneously served as kinase reaction buffer. Each reaction was conducted in a total volume of 50  $\mu\text{l}$  containing 5-10  $\mu\text{g}$  separase bound to anti-Myc agarose (25  $\mu\text{l}$ ), 30  $\mu\text{g}$  ATM kinase and 10  $\mu\text{Ci}$  [ $\gamma$ - $^{33}\text{P}$ ]-ATP (Hartmann Analytic). In the positive and negative controls, separase beads were replaced by 5  $\mu\text{g}$  of recombinant GST-p53aa9-22 or GST alone, respectively (Kim et al, 1999). Where indicated, ATM inhibitor Ku55933 (LC Laboratories) was added to 10  $\mu\text{M}$  prior to addition of the kinase. Reactions were stopped after 1 h at 30°C by addition of non-reducing sample buffer and elution of bound separase by boiling. Samples were analyzed by SDS-PAGE followed by immunoblotting and autoradiography. In case of the Rad21 cleavage assay (Figures EV3C and EV3D), 1,5  $\mu\text{l}$  of  $^{35}\text{S}$ -labeled Rad21-GFP IVT were pre-incubated with ATM kinase in presence of 10  $\mu\text{M}$  ATP for 15 min followed by addition of purified active (SA) or inactive (PD) separase in a reaction volume of 7  $\mu\text{l}$  as described (Hellmuth et al, 2015).

### **Sumoylation assay**

Myc<sub>6</sub>-separase-WT and -K1034R were expressed in Hek293T and immunopurified with anti-Myc beads from lysates of asynchronous cells. 10  $\mu\text{l}$  of separase-loaded or empty beads were combined with 45 ng SAE1/SAE2 heterodimer, 2.5  $\mu\text{g}$  of His<sub>6</sub>-Sumo2 (Boston Biochem), 2  $\mu\text{l}$  of energy regeneration mix (10 mM phosphocreatine, 2 mM ATP and 3.5 U creatine kinase), 0.2  $\mu\text{g}$  of Ubc9 and/or 0.5  $\mu\text{g}$  His<sub>6</sub>-Mms21. Reactions were adjusted

to 20  $\mu$ l with 50 mM Tris-HCl (pH 7.5), 5 mM MgCl<sub>2</sub> and incubated for 2 h at 37°C. Afterwards, 10  $\mu$ l supernatant were removed, boiled with SDS sample buffer and analysed by SDS-PAGE and subsequent Coomassie staining. The beads were transferred to 4°C, washed twice with 50 mM Tris-HCl (pH 7.5), 5mM MgCl<sub>2</sub>, eluted in SDS-sample buffer and subjected to SDS-PAGE and subsequent immunoblotting. All components of the Sumo-conjugation system were human proteins expressed in *E. coli* and affinity purified using standard protocols (additional information is provided upon request).

SUMO-conjugates were enriched by denaturing IMAC essentially as described (Rodriguez et al, 1999). Briefly, damaged and undamaged cells were harvested 14 h after DRB-addition, immediately lysed in 6 M guanidinium-HCl (pH 8.0), 5mM imidazole and sonicated for 2 min (Bandelin Sonopuls HD2070, 20% power and 50% duty cycle). Input samples were generated by mixing 50  $\mu$ l sonicated lysate with 2 ml ice-cold ethanol, incubation for 1 h at -20°C, centrifugation at 16.000 g and re-solubilization of the air-dried precipitate in 200 mM Na<sub>2</sub>HPO<sub>4</sub>/NaH<sub>2</sub>PO<sub>4</sub> (pH 6.8), 8 M urea, 5% (w/v) SDS, 1 mM EDTA, 100 mM DTT, and a trace of bromophenol blue. The rest of the sonicated lysates was combined with 80  $\mu$ l Ni<sup>2+</sup>-NTA-agarose beads (Macherey Nagel) and rotated for 2 h at 18°C. Subsequently, beads were successively washed with the following buffers: 6 M guanidinium-HCl, 0.1 M Na<sub>2</sub>HPO<sub>4</sub>/NaH<sub>2</sub>PO<sub>4</sub>, 0.01 M Tris-HCl, 20 mM imidazole (pH 8.0); 8M urea, 0.1 M Na<sub>2</sub>HPO<sub>4</sub>/NaH<sub>2</sub>PO<sub>4</sub>, 0.01 M Tris-HCl, 5 mM  $\beta$ -mercaptoethanol (pH 8.0); 8M urea, 0.1 M Na<sub>2</sub>HPO<sub>4</sub>/NaH<sub>2</sub>PO<sub>4</sub>, 0.01 M Tris-HCl, 5 mM  $\beta$ -mercaptoethanol (pH 6.3) and finally with the latter buffer supplemented with 0.1% Triton X-100. Elution was performed by addition of 200 mM imidazole,

5% SDS, 0.15 M Tris-HCl (pH 6.7), 30% glycerol, 0.72 M  $\beta$ -mercaptoethanol with a trace of bromophenol blue and boiling for 10 min at 95°C. Input and eluate samples were subjected to SDS-PAGE and subsequent immunoblotting.

### **Chromatin immunoprecipitation**

ChIP analysis was performed essentially as described (Carey et al, 2009). Transgenic Hek293-FlpIn-TRex cells transiently expressing AsiSI-ER were grown to confluency, pre-synchronized with thymidine, induced to express Myc<sub>6</sub>-separase or left uninduced and, where indicated, treated with OHT for 12 h. Independent of OHT addition all cells were RO3306-treated to induce a robust G2 arrest. Cross-linking was performed by adding formaldehyde to growing cells to a final concentration of 1% for 10 min. After harvesting, cell lysis, and centrifugation, pelleted nuclei were resuspended in nuclei lysis buffer and sonicated 7x for 40 sec (Bandelin Sonoplus; microtip, 60% power, 80% duty cycle) with rest periods of 1min in between. This resulted in DNA fragmentation to an average length between 300 and 1,000 bp. Nuclear extracts were rotated for 3 h at 4°C with 10  $\mu$ l of salmon sperm DNA protein A agarose (Millipore). After removal of the beads, pre-cleared nuclear extracts (each corresponding to roughly 20 x 10<sup>6</sup> cells) were supplemented with anti-separase, anti- $\gamma$ H2AX, or non-specific IgG (8  $\mu$ g each) and incubated overnight at 4°C. This was followed by addition of 10  $\mu$ l fresh salmon sperm DNA protein A agarose (Millipore) and rotation for 3 h at 4°C. Eluted DNA and aliquots (5%) of nuclear extracts (input) were supplemented with proteinase K (Fermentas) at 20  $\mu$ g/ $\mu$ l and cross-links were reversed overnight at 65°C. Finally, DNA from each sample was further purified with GeneJET PCR Kit

(Thermo Scientific). Purified DNA was analyzed by multiplex- or quantitative PCR.

### **Chromosome spreads for immunofluorescence**

Transgenic Hek293-FlpIn-TRex expressing Myc<sub>6</sub>-separase and histone H2B-mCherry-Rad21<sup>107-268</sup>-eGFP were released from a thymidine arrest (Figure 3C). 6 h and 8 h later, they were treated with DRB and nocodazole (ad 0.2 µg/ml, Sigma-Aldrich), respectively. 10 h after release from thymidine, cells were resuspended in hypotonic buffer I (50 mM sucrose, 30 mM Tris-HCl pH 8.2, 17 mM trisodium citrate, 0.2 µg/ml nocodazole), incubated for 7 min at RT and subsequently centrifuged at 300 g for 3 min. Supernatant was removed and cells were resuspended in a small volume of 100 mM sucrose and immediately spread onto a coverslip that had been dipped into fixation buffer (1% paraformaldehyde, 5 mM sodium tetraborate pH 9.2, 0.15% Triton X-100). Drops of cell suspension were distributed by tilting. Once dried, coverslips were washed several times with PBS and then stored in blocking-solution (1x PBS, 1% (w/v) BSA) at 4°C overnight prior to IF staining.

### **Generation of *SEPARASE* mutant mice**

In an attempt to regulate in a tetracycline-dependent manner the endogenous *SEPARASE*, knock-in mice were generated by introducing a regulatory cassette into the second exon where the initiator methionine is encoded (Figures EV4A and EV4B) (Valbuena-Diez et al, 2012). Mice were derived from positive recombinant ES clones by conventional breeding (see supplementary methods). Unexpectedly, MEFs derived from mutant (+/TG) mice were unable to regulate *SEPARASE* transcription in response to

tetracycline treatment (Gutiérrez-Caballero et al., unpublished observation) but instead showed constitutively reduced transcription of *SEPARASE* in comparison with their wild type control (Figure EV4C). Homozygous mutant *SEPARASE*<sup>tg/tg</sup> mice were never obtained from heterozygous intercrosses (Gutiérrez-Caballero et al., unpublished observation) suggesting lethality of the targeted mutation, as has previously been shown for *SEPARASE*-deficient mice (Kumada et al, 2006; Wirth et al, 2006). We conclude that the knock-in mutation is a null allele of *SEPARASE*, which is why the corresponding heterozygous mice are referred to as *SEPARASE*<sup>+/-</sup>.

### **Clonogenic assays**

Hek293-FlpIn were transfected with siRNA against Separase (*SEP-01*) or *GL2* for 12 h followed by replating of 100 cells per condition in 10-cm dishes and media containing 0.25 nM camptothecin (Abcam) were indicated. Cells were grown for 12 days in continuous presence or absence of camptothecin until colony formation was visible and then fixed in ice-cold methanol for 10 min. Staining was performed as described except for the use of ethanol instead of glutaraldehyde (Franken et al, 2006). The number of colonies per plate with a minimal area of 20 (circularity 0.00-1.00) was determined automatically with the ImageJ particle analysis software (Figures EV2A and EV2B).

MEFs were infected with pLPC E1A-hRas<sup>V12</sup> and selected on puromycin (2 µg/ml) for three days. 4.000 resistant MEFs were plated in 10-cm dishes in complete culture medium for 13 days. The medium was changed every 4 days. On the 13th day, medium was removed and cells were fixed with 10%

formaldehyde, stained with 0.02% Giemsa (SIGMA), and the colonies were quantified.

## APPENDIX REFERENCES

- Carey MF, Peterson CL, Smale ST (2009) Chromatin immunoprecipitation (ChIP). *Cold Spring Harbor protocols* **2009**: pdb prot5279
- Franken NA, Rodermond HM, Stap J, Haveman J, van Bree C (2006) Clonogenic assay of cells in vitro. *Nature protocols* **1**: 2315-2319
- Hellmuth S, Rata S, Brown A, Heidmann S, Novak B, Stemmann O (2015) Human chromosome segregation involves multi-layered regulation of separase by the peptidyl-prolyl-isomerase pin1. *Molecular cell* **58**: 495-506
- Joseph J, Tan SH, Karpova TS, McNally JG, Dasso M (2002) SUMO-1 targets RanGAP1 to kinetochores and mitotic spindles. *The Journal of cell biology* **156**: 595-602
- Kim ST, Lim DS, Canman CE, Kastan MB (1999) Substrate specificities and identification of putative substrates of ATM kinase family members. *The Journal of biological chemistry* **274**: 37538-37543
- Kumada K, Yao R, Kawaguchi T, Karasawa M, Hoshikawa Y, Ichikawa K, Sugitani Y, Imoto I, Inazawa J, Sugawara M, Yanagida M, Noda T (2006) The selective continued linkage of centromeres from mitosis to interphase in the absence of mammalian separase. *The Journal of cell biology* **172**: 835-846
- Rhodes N, Gilmer TM, Lansing TJ (2001) Expression and purification of active recombinant ATM protein from transiently transfected mammalian cells. *Protein expression and purification* **22**: 462-466
- Rodriguez MS, Desterro JM, Lain S, Midgley CA, Lane DP, Hay RT (1999) SUMO-1 modification activates the transcriptional response of p53. *The EMBO journal* **18**: 6455-6461
- Valbuena-Diez AC, Blanco FJ, Oujo B, Langa C, Gonzalez-Nunez M, Llano E, Pendas AM, Diaz M, Castrillo A, Lopez-Novoa JM, Bernabeu C (2012) Oxysterol-induced soluble endoglin release and its involvement in hypertension. *Circulation* **126**: 2612-2624
- Wirth KG, Wutz G, Kudo NR, Desdouets C, Zetterberg A, Taghybeeglu S, Seznec J, Ducos GM, Ricci R, Firnberg N, Peters JM, Nasmyth K (2006) Separase: a universal trigger for sister chromatid disjunction but not chromosome cycle progression. *The Journal of cell biology* **172**: 847-860

## Expanded View Figures

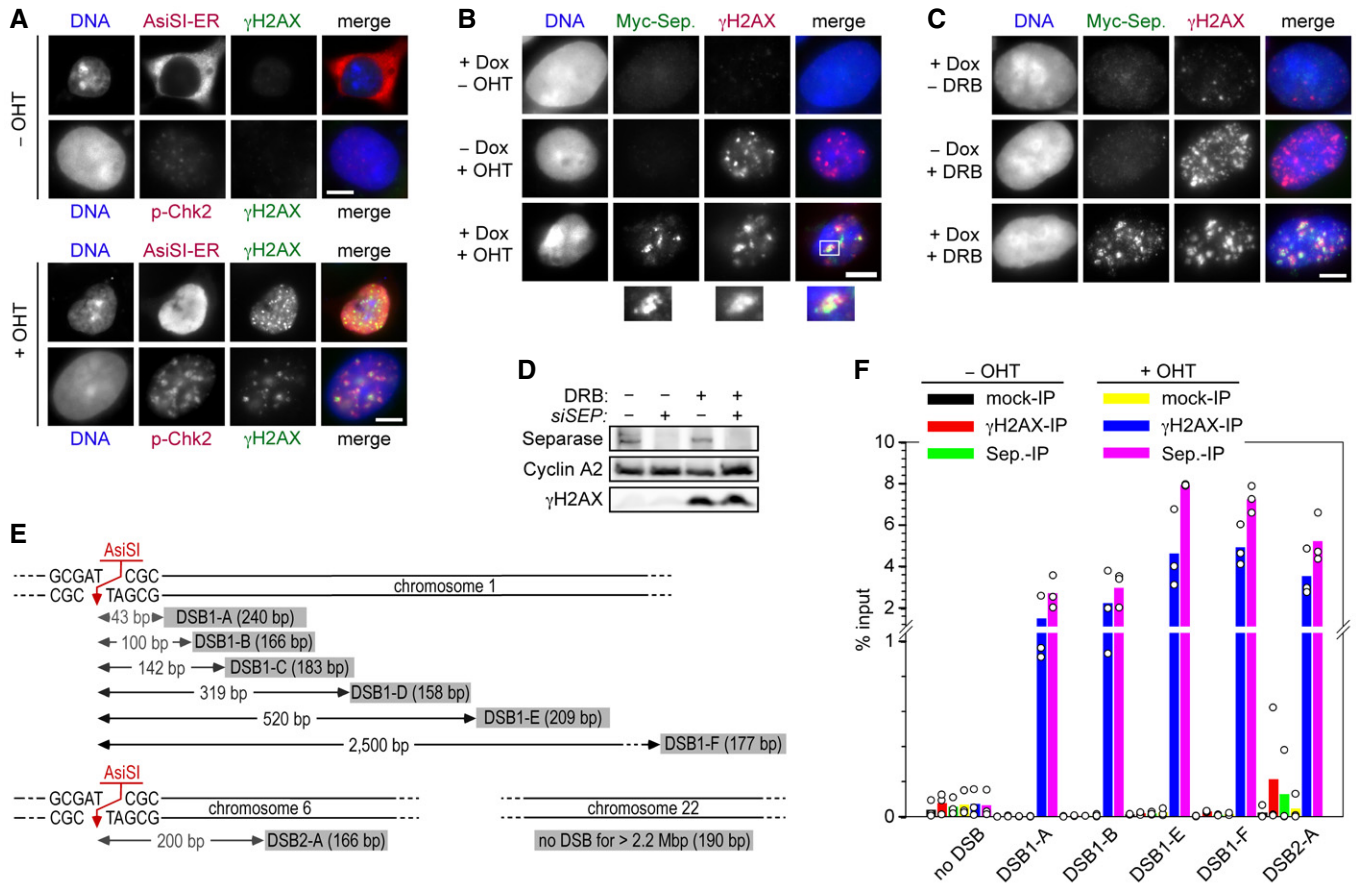


**Figure EV1. Separase localizes to DSBs.**

- A A system for induced introduction of site-specific DSBs. Transgenic HEK293 cells constitutively expressing FLAG-tagged AsiSI-ER were treated with OHT or carrier solvent and then analyzed by IFM as indicated. Scale bar = 5  $\mu$ m.
- B Transgenic HEK293 cells treated with Dox to induce expression of Myc-separase-WT and/or with OHT to induce nuclear accumulation of ER-AsiSI and DSBs were analyzed by IFM as indicated. Scale bar = 5  $\mu$ m.
- C  $\gamma$ H2AX- and separase-positive foci formation in response to DNA damage by DRB. Prior to their analysis by IFM, transgenic HEK293 cells in G2-phase were Dox- and/or DRB-treated to induce the expression of Myc-separase and/or inflict DSBs, respectively. Scale bar = 5  $\mu$ m.
- D Western blot analysis of experiment shown in Fig 1A.
- E Position and sizes of PCR fragments from the ChIP-multiplex PCR and ChIP-qPCR experiments. Schematic is not drawn to scale.
- F Transgenic HEK293 cells supplemented with Dox to induce expression of Myc-separase-WT were mock- or OHT-treated in G2-phase and then subjected to ChIP-qPCR. Shown are averages (bars) of three independent experiments (dots).

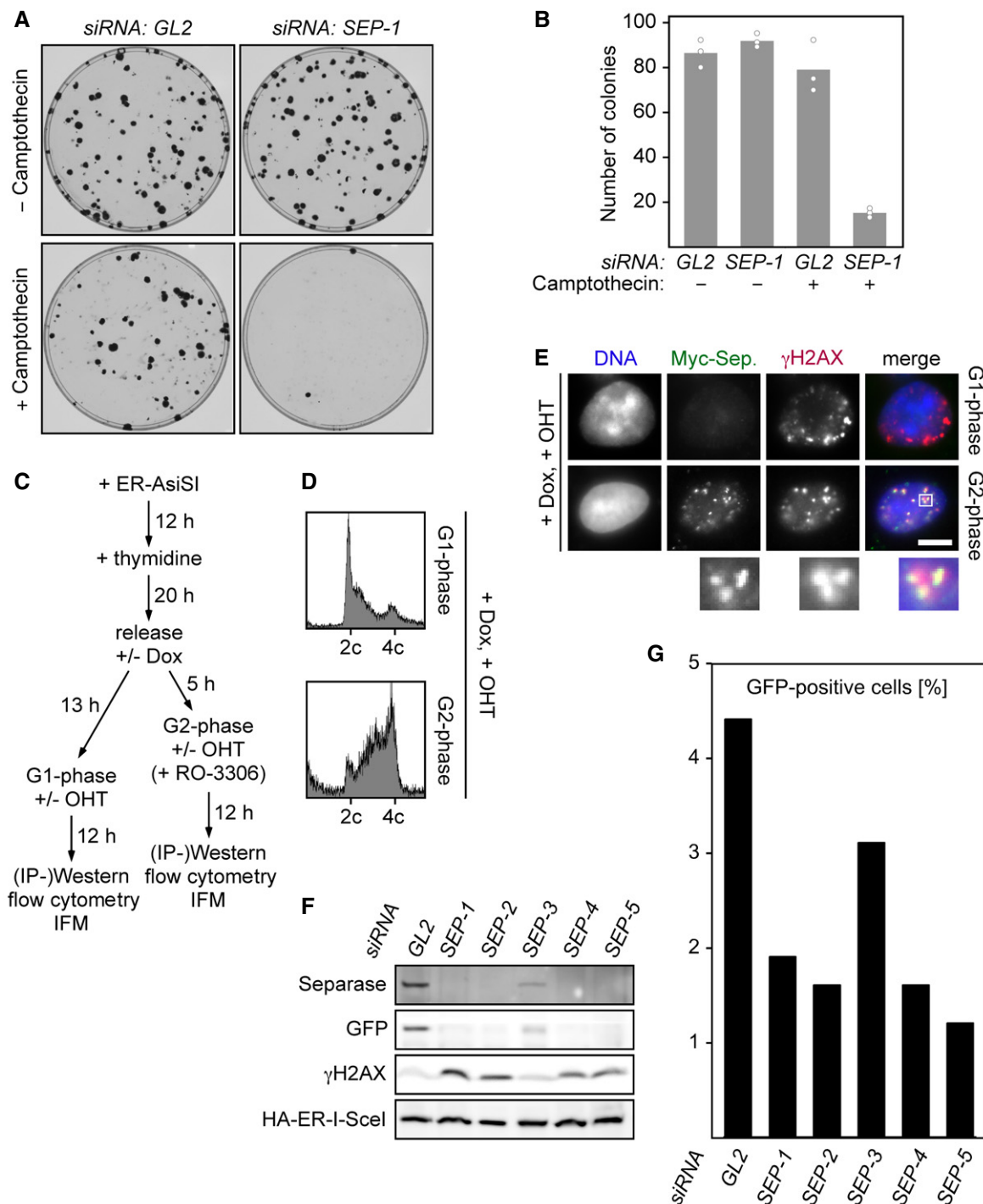


**Figure EV2. Depletion of Separase by RNAi compromises HDR as judged by a GFP-based *in vivo* assay.**

A, B Depletion of separase renders human cells hypersensitive to camptothecin. Twelve hours after transfection of the indicated siRNAs, 100 HEK293 cells each were plated onto 10-cm petri dishes. Another 12 h later, camptothecin (0.25 nM end concentration) or carrier solvent (DMSO) was added. Colonies were stained by crystal violet 12 days thereafter and photographed (A). For each condition, three independent experiments were quantified by ImageJ (dots) and averaged (bars) (B).

C Schematic of the experiment shown in Figs 1D and E, and EV2D and E.

D Dox- and OHT-treated HEK293 cells synchronized in G1- or G2-phase were propidium iodide (PI)-stained and analyzed by DNA content by flow cytometry.

E Representative IFM images of Dox- and OHT-treated HEK293 cells synchronized in G1- or G2-phase. Scale bar = 5 μm.

F, G U2OS DR-GFP (HDR reporter) cells were transfected with GL2 or one of five different SEPARASE-directed siRNAs. Following a second transfection to express ER-tagged I-SceI and addition of OHT to induce nuclear accumulation of the homing endonuclease, cells were subjected to flow cytometry (G) and immunoblotting (F).

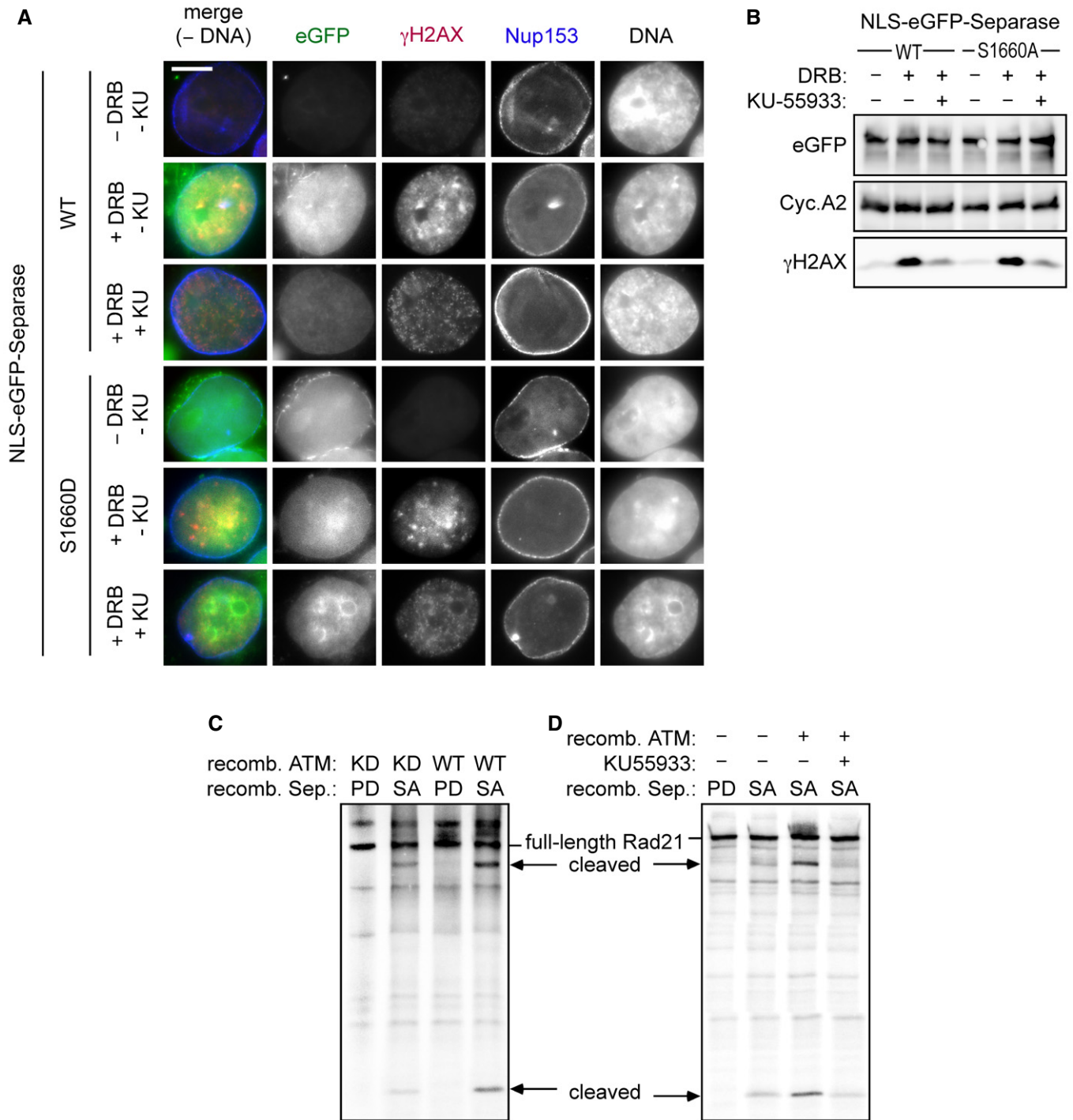


**Figure EV3. ATM kinase activity is required for nuclear accumulation of separase in response to DSBs.**

A, B HeLaK cells expressing N-terminally NLS-eGFP-tagged separase-WT or separase-S1160D were treated with DRB, KU-55933 (2  $\mu$ M), or carrier solvent (-) for 4 h as indicated and then subjected to IFM and Western blot analysis using the indicated antibodies. Transgenic separase was detected based on the eGFP autofluorescence. Note that due to their relatively high nuclear concentration, co-localization of separase-WT and separase-S1160D with  $\gamma$ H2AX foci is not discernable. Scale bar = 5  $\mu$ m.

C, D ATM enhances separase-dependent Rad21 cleavage *in vitro*. Rad21 was  $^{35}$ S-labeled by *in vitro* expression in reticulocyte lysate and treated with recombinant ATM kinase in the presence of KU-55933 (10  $\mu$ M) and/or ATP. Then, samples were incubated with recombinant separase and finally analyzed by SDS-PAGE and autoradiography. Wild-type (WT) or kinase-dead (KD) variants of ATM and hyperactive (SA) or protease-dead (PD) variants of separase were employed as indicated.

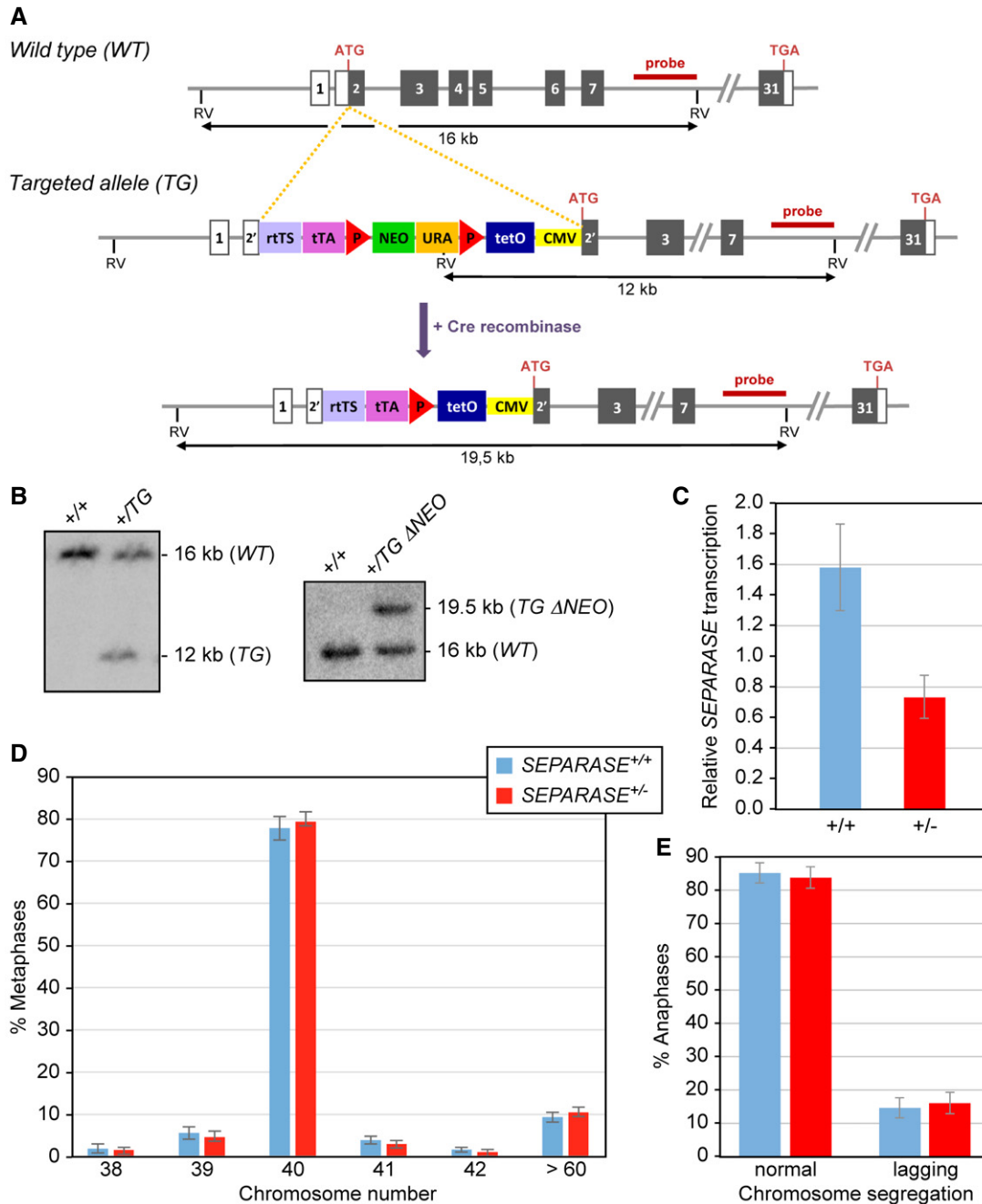


**Figure EV4. Gene targeting of the separase locus.**

A Diagrammatic representation of the relevant 5' region of the *SEPARASE* locus. Exons are depicted as boxes with coding regions in gray. As indicated, the start (ATG) and stop (TGA) codons are located within exons E2 and E31, respectively. The regulating cassette from the TriTAUBi-Bd plasmid is enclosed by a rtTS-tTA cassette (Hayakawa et al, 2006). The selection markers *NEO* and *URA* are flanked by loxP sites (indicated by a P within red arrowheads). The minimum cytomegalovirus promoter (CMV), the tetO repeated sequences (tetO), all EcoRV (RV) sites, and the position of the Southern probe (see B) are indicated.

B Southern blot analysis of EcoRV-digested genomic DNA from tails of wild-type (*WT* = +) mice and those with the targeted mutation (*TG*) before and after Cre-mediated deletion of the selection cassette (*TG* Δ*NEO*). See (A) for expected sizes of EcoRV fragments.

C Separase expression is halved in *SEPARASE*<sup>+/-</sup> MEFs. Northern blot analysis and densitometry were used to quantify the expression of *SEPARASE* mRNA normalized to the expression of *ACTIN* in total RNA preparations from *SEPARASE*<sup>+/+</sup> versus *SEPARASE*<sup>+/-</sup> MEFs (n = 4). Values represent means ± standard deviations.

D No increase in aneuploidy in *SEPARASE*<sup>+/-</sup> MEFs. MEFs were treated with colcemid for 4 h and processed using standard methanol-acetic fixation followed by DAPI staining. MEFs from three embryos of each genotype and more than 100 metaphases per sample were counted. Values represent means ± standard deviations.

E No increase in lagging chromosomes in *SEPARASE*<sup>+/-</sup> MEFs. Cells passaged the day before were directly fixed and stained with DAPI. MEFs from three embryos of each genotype and more than 100 anaphases per sample were counted. Values represent means ± standard deviations.

# Securin-independent regulation of separase by checkpoint-induced shugoshin–MAD2

<https://doi.org/10.1038/s41586-020-2182-3>

Susanne Hellmuth<sup>1</sup>, Laura Gómez-H<sup>2</sup>, Alberto M. Pendás<sup>2</sup> & Olaf Stemmann<sup>1</sup>✉

Received: 22 March 2019

Accepted: 31 January 2020

Published online: 8 April 2020

 Check for updates

Separation of eukaryotic sister chromatids during the cell cycle is timed by the spindle assembly checkpoint (SAC) and ultimately triggered when separase cleaves cohesion-mediating cohesin<sup>1–3</sup>. Silencing of the SAC during metaphase activates the ubiquitin ligase APC/C (anaphase-promoting complex, also known as the cyclosome) and results in the proteasomal destruction of the separase inhibitor securin<sup>1</sup>. In the absence of securin, mammalian chromosomes still segregate on schedule, but it is unclear how separase is regulated under these conditions<sup>4,5</sup>. Here we show that human shugoshin 2 (SGO2), an essential protector of meiotic cohesin with unknown functions in the soma<sup>6,7</sup>, is turned into a separase inhibitor upon association with SAC-activated MAD2. SGO2–MAD2 can functionally replace securin and sequesters most separase in securin-knockout cells. Acute loss of securin and SGO2, but not of either protein individually, resulted in separase deregulation associated with premature cohesin cleavage and cytotoxicity. Similar to securin<sup>8,9</sup>, SGO2 is a competitive inhibitor that uses a pseudo-substrate sequence to block the active site of separase. APC/C-dependent ubiquitylation and action of the AAA-ATPase TRIP13 in conjunction with the MAD2-specific adaptor p31<sup>comet</sup> liberate separase from SGO2–MAD2 in vitro. The latter mechanism facilitates a considerable degree of sister chromatid separation in securin-knockout cells that lack APC/C activity. Thus, our results identify an unexpected function of SGO2 in mitotically dividing cells and a mechanism of separase regulation that is independent of securin but still supervised by the SAC.

In all eukaryotic cells, anaphase is triggered when chromosomal cohesin is cleaved by the essential Cys-endopeptidase separase<sup>3,10</sup>. To prevent the premature loss of sister chromatid cohesion, separase needs to be tightly controlled. Separase is competitively inhibited by association with securin for most of the cell cycle. Only in metaphase does the E3 anaphase-promoting complex or cyclosome (APC/C) mediate the degradation of securin via the ubiquitin-proteasome system, thereby activating separase<sup>11</sup>. The destruction of securin is timed by the SAC, which keeps the APC/C co-activator CDC20 inactive until all kinetochores are properly attached to spindle microtubules<sup>1</sup>.

## SGO2 is a prominent interactor of separase

Unexpectedly, securin is not essential in human cells or mice<sup>4,5</sup>. This can partially be explained by CDK1–cyclin B1-dependent regulation of separase<sup>12–17</sup>. Mouse *Cdc20*<sup>−/−</sup> embryos arrest in metaphase with cohered chromosomes because they cannot degrade either cyclin B1 or securin<sup>18</sup>. Notably, double knockout of *Cdc20* and *Pttg1* (which encodes securin) resulted in arrest with separated sister chromatids; this defect was rescued by constitutive activation of the SAC<sup>18</sup>, which suggests that there is a SAC-dependent but securin-independent mechanism to control separase. Rather than being stimulated by the SAC, the binding of CDK1–cyclin B1 to separase is dampened by

phosphorylation of cyclin B during early mitosis<sup>19</sup>. However, a link between the SAC and the cohesin protector shugoshin (SGO) had previously been identified in that human SGO2—similar to CDC20—is bound by the essential SAC component MAD2<sup>7</sup>. Notably, mouse SGO2 and separase interacted when co-expressed in Hek293 cells (Extended Data Fig. 1a; see, however, Extended Data Fig. 1b). These findings led to the idea that SAC-activated MAD2 could enable SGO2 to bind and inhibit separase. Indeed, when endogenous human separase was isolated by immunoprecipitation (IP) from untransfected, prometaphase-arrested Hek293T or untransformed RPE-1 cells, SGO2 (but not the related SGO1) and MAD2 co-purified, along with the known interactors securin and cyclin B1 (Fig. 1a, Extended Data Fig. 1c). In contrast to separase, SGO2 and MAD2 were undetectable in a securin IP and, vice versa, securin and cyclin B1 were absent from an SGO2 IP (Fig. 1a). With previous results<sup>20</sup>, these data argue that three mutually exclusive complexes co-exist in human mitotic cells: separase–securin, separase–CDK1–cyclin B1 and separase–SGO2–MAD2. Following immunodepletion of the three inhibitors from taxol-arrested Hek293T, HCT116 and HeLa-K cells, we quantified the relative amounts of associated separase. On average, 59, 35, and 6% of total separase was sequestered by securin, SGO2, and cyclin B1, respectively (Extended Data Fig. 1d). Notably, in mitotic *PTTG1*<sup>−/−</sup> cells, most separase (85%) was in complex with SGO2 (Fig. 1b).

<sup>1</sup>Chair of Genetics, University of Bayreuth, Bayreuth, Germany. <sup>2</sup>Molecular Mechanisms Program, Centro de Investigación del Cáncer and Instituto de Biología Molecular y Celular del Cáncer (CSIC-Universidad de Salamanca), Salamanca, Spain. ✉e-mail: olaf.stemmann@uni-bayreuth.de

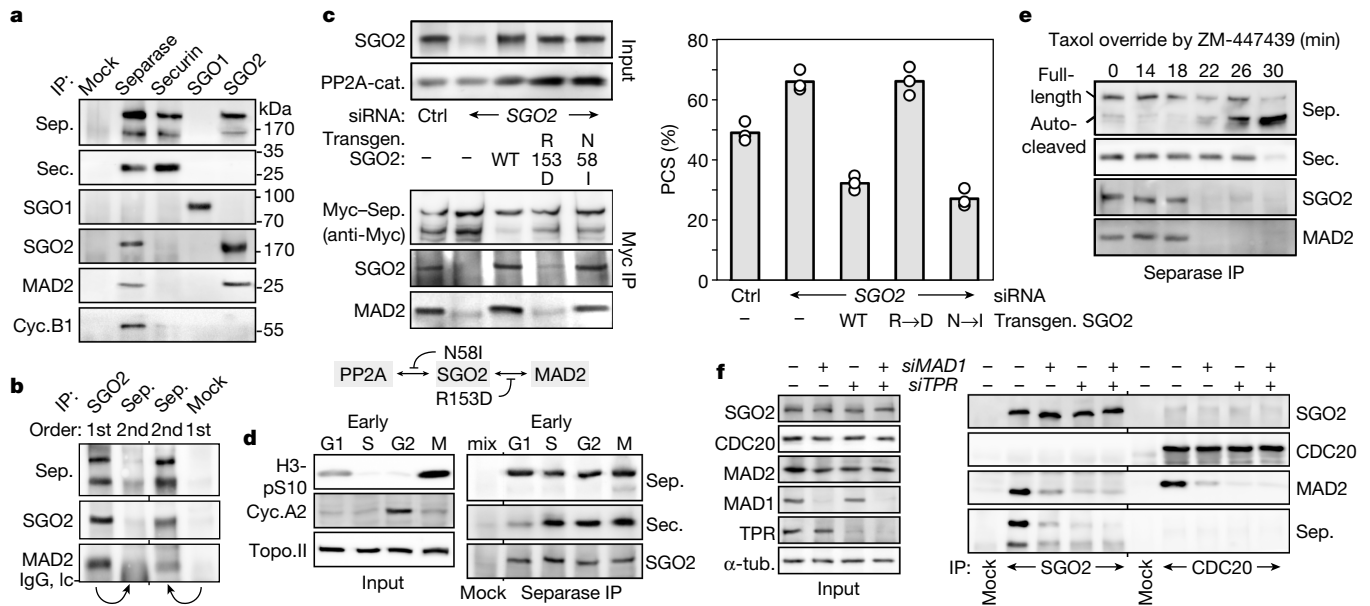


**Fig. 1 | MAD2-dependent binding of human SGO2 to separase.** **a**, Endogenous proteins were immunoprecipitated (IP) from taxol-arrested Hek293T cells and analysed by immunoblotting. Mock, nonspecific IgG. Sep., separase; sec., securin; cyc.B1, cyclin B1. **b**, Lysates from taxol-arrested *PTTGI*<sup>-/-</sup> cells were subjected to consecutive immunodepletions and analysed by immunoblotting. **c**, Transgenic Hek293 cells depleted of SGO2 or control-treated (Ctrl) were transfected to express siRNA-resistant SGO2 variants as indicated (transgen. SGO2: wild-type (WT), R153D or N581), induced with doxycycline to express CDK1–cyclin B1-resistant, stabilized Myc–separase (S1126A), arrested in

prometaphase, and then analysed by IP–immunoblotting (left) and chromosome spreading (right). Bars show mean of three independent experiments (dots). Cat., catalytic subunit. **d**, HeLa-K cells synchronized in the indicated cell cycle phases were subjected to IP–immunoblotting. **e**, Taxol-arrested HeLa-K cells were released with ZM-447439 and subjected to time-resolved IP–immunoblotting. **f**, Control, MAD1-depleted, or TPR-depleted, thymidine-arrested HeLa-K cells were analysed by IP–immunoblotting.  $\alpha$ -tub.,  $\alpha$ -tubulin.

## MAD2 enables SGO to bind separase

To test whether binding of SGO2 to separase required MAD2, we used RNA interference (RNAi) to deplete cells of endogenous SGO2 and replaced it with small interfering RNA (siRNA)-resistant, transgene-encoded variants. Subsequent immunoprecipitation of co-expressed Myc–separase showed that the MAD2-binding-deficient SGO2(R153D) was unable to interact with separase, whereas SGO2(N581), which cannot interact with protein phosphatase 2A (PP2A)<sup>7</sup>, still bound to MAD2 and separase (Fig. 1c). The SAC–shugoshin link is conserved in *Xenopus*, with the difference that here SGO1 rather than SGO2 binds MAD2 and separase<sup>7</sup> (Extended Data Fig. 2). Thus, the separase–shugoshin interaction depends on active MAD2 and is conserved in vertebrates.

The separase–SGO2–MAD2 complex was present in cells arrested in G1, early S, G2, and prometaphase (Fig. 1d) but not in taxol-treated HeLa-K cells that were driven into an anaphase-like state by SAC abrogation with the aurora B kinase inhibitor ZM-447439 (Fig. 1e). This cell cycle distribution mirrored that of CDC20–MAD2, the formation of which in interphase requires MAD1-dependent MAD2 activation at nuclear pore complexes (NPCs)<sup>21</sup>. Consistently, separase–SGO2–MAD2, similar to CDC20–MAD2, became (almost) undetectable in unsynchronized HeLa-K cells depleted of MAD1 and/or the NPC component TPR (Fig. 1f). Thus, conformationally activated MAD2 enables SGO2 to sequester separase through all of the cell cycle except for a short period of SAC inactivity during late mitosis.

## Separase deregulation upon loss of securin and SGO

Overexpression of a CDK1–cyclin B1-resistant and stabilized separase (S1126A) variant causes premature sister chromatid separation (PCS) in Hek293T cells<sup>12,22</sup>. This PCS phenotype was aggravated by siRNA-mediated depletion of endogenous SGO2 and alleviated

by simultaneous slight overexpression of wild-type SGO2 from an siRNA-resistant transgene (Fig. 1c). SGO2(R153D) did not rescue PCS in this cellular assay, whereas transgenic SGO2(N581) remained functional. Together, these findings suggest that SGO2 might indeed have an inhibitory effect on separase and that this effect requires binding of MAD2 but not PP2A to SGO2.

By recruiting PP2A to (peri)centromeres, SGO2 exerts essential cohesin protective functions throughout meiosis I but, similar to securin, it is dispensable in somatic cells<sup>6,7</sup>. If securin and SGO2–MAD2 could functionally replace each other as crucial negative regulators of separase, then co-depletion of securin and SGO2 should result in detrimental deregulation of separase. First, we assessed overall effects on cell viability and proliferation using clonogenic assays. As expected, knockdown of securin or SGO2 alone had no effect or only a small inhibitory effect, respectively, on HeLa-K colony formation (Fig. 2a, Extended Data Fig. 3a). By sharp contrast, hardly any clones grew when both separase interactors were depleted at the same time. Similarly, depletion of SGO2 virtually extinguished colony formation in *PTTGI*<sup>-/-</sup> cells, whereas it only halved colony numbers in the parental HCT116 cell line (Extended Data Fig. 3b). The same tendencies were found for Hek293T cells, although the effects were less pronounced (Extended Data Fig. 3c). Live imaging of histone H2B–eGFP-expressing HeLa-K cells revealed that the individual knockdowns did not affect mitosis; however, when both securin and SGO2 were missing, the ability to form proper metaphase plates was markedly compromised (Extended Data Fig. 4a). HeLa-K cells lacking securin and SGO2 were also marked by the otherwise uncommon absence of cohesin from early mitotic chromatin (Extended Data Fig. 4b). Individual knockdown of securin or SGO2 had no effect on cohesion, whereas simultaneous removal of both resulted in PCS as judged by chromosome spreads from prometaphase-arrested Hek293T cells (Extended Data Fig. 4c, d). The PCS phenotype was further fortified by chemical inhibition (using epigallocatechin-3-gallate (EGCG)) of PIN1, a peptidyl–prolyl–isomerase required for

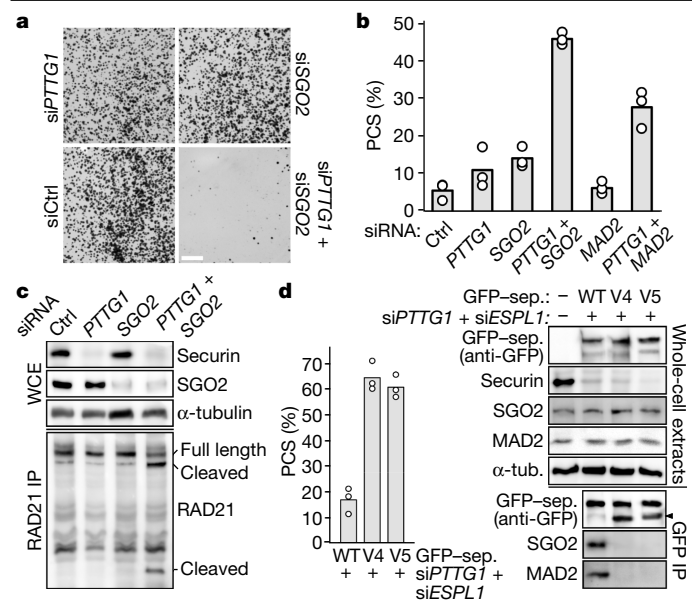


**Fig. 2 | Co-depletion of securin and SGO2 is cytotoxic and results in premature sister chromatid separation and cohesin cleavage.** **a**, Exemplary photographs of clonogenic assay with HeLa-K cells transfected with the indicated siRNAs. Scale bar, 1 cm. **b**, siRNA-transfected Hek293T cells were supplemented with taxol and EGCG and analysed by chromosome spreading. Bars show mean of three independent experiments (dots). **c**, siRNA-transfected HeLa-K cells were taxol-treated and analysed by IP-immunoblotting. WCE, whole-cell extracts. **d**, Securin-depleted (siPTTG1) and separase-depleted (siESPL1) Hek293T cells expressing siRNA-resistant, transgenic separase (wild-type, ΔEEL (V4), or MxxIxEE to AxxAxA (V5)) were treated with taxol and EGCG and analysed by chromosome spreading (left) and IP-immunoblotting (right). Bars show mean of three independent experiments (dots). Arrowhead marks auto-cleaved separase.

CDK1-cyclin B1-dependent inhibition of separase<sup>19</sup> (Fig. 2b, Extended Data Fig. 4c, d). In keeping with the separase-SGO2 interaction being dependent on MAD2, partial removal of MAD2, which alone had no effect, inhibited colony formation and exacerbated PCS in conjunction with RNAi of securin (Fig. 2b, Extended Data Figs. 3, 4c, d). All of these phenotypes could be explained by precocious separase-dependent cleavage of cohesin. Indeed, consistent with a previous study in yeast<sup>23</sup>, the characteristic fragments of the RAD21 subunit of cohesin were detected in prometaphase-arrested cells if—and only if—both securin and SGO2 had been depleted (Fig. 2c). Likewise, a transiently expressed separase activity sensor was already maximally cleaved in securin- and SGO2-depleted HeLa-K cells in a taxol arrest, whereas in mock-depleted cells the sensor was cleaved only upon addition of ZM-447439 (Extended Data Fig. 4e). Screening of separase mutants identified two variants (V4 and V5) that could not interact with SGO2-MAD2 (Extended Data Fig. 5). When endogenous separase was replaced by these variants, depletion of securin was sufficient to induce PCS (Fig. 2d). This indicates that a direct separase inhibitory function of SGO2 works redundantly with securin to prevent PCS.

In interphase, separase is excluded from the nucleus but has an established function in centriole disengagement<sup>24</sup>. Therefore, we assessed this licensing step of centrosome duplication rather than cleavage of chromosomal cohesin upon depletion of securin and SGO2. Premature centriole disengagement in G2-phase was increased threefold in Hek293T cells lacking securin and SGO2 relative to singly- or mock-depleted Hek293T cells (45% versus 10–15%, respectively) (Extended Data Fig. 6). Thus, cells lacking securin and SGO2 already contain active separase in interphase and, hence, are expected to lose sister chromatid cohesion immediately upon breakdown of the nuclear envelope.

Shugoshins are characterized not only by an N-terminal coiled-coil domain but also by a C-terminal SGO-box that binds to BUB1-phosphorylated histone H2A<sup>25</sup>. Phosphorylated, but not unphosphorylated, H2A peptide bound immobilized SGO2 (Extended Data Fig. 7a–c). Notably, pre-incubation with phospho-H2A but not with unphosphorylated H2A or a chemically similar but irrelevant phospho-H3 peptide suppressed the ability of SGO2 to bind MAD2 (Extended Data Fig. 7a–d). Conversely, pre-incubation of immobilized SGO2 with MAD2 prevented subsequent interaction between phospho-H2A and SGO2 (Extended Data Fig. 7e, f). Phospho-H2A did not bind to SGO2 when previous SGO2-MAD2 complex formation was not possible owing to the expression of SGO2(R153D) or a variant of MAD2 lacking the C-terminal domain (MAD2ΔC) instead of the corresponding wild-type proteins. Thus, MAD2 and phospho-H2A bind SGO2 in a mutually exclusive manner. We propose that different pools of SGO2 either associate with chromatin or bind MAD2 and inhibit separase.

### SGO is a pseudosubstrate inhibitor of separase

Incubation of the human separase–securin complex in securin-degrading, anaphase-like *Xenopus laevis* egg extracts followed by affinity purification of separase generates active protease that specifically cleaves <sup>35</sup>S-labelled RAD21<sup>17</sup>. Pre-incubation of this separase with in vitro-expressed SGO2 and MAD2 purified from *Escherichia coli* blocked cleavage of RAD21 (Fig. 3a). The same effect was seen when SGO2(N53I) was used instead of wild-type SGO2, but not when SGO2 or MAD2 was omitted or replaced by SGO2(R153D) or MAD2ΔC, respectively. Thus, the PP2A-independent but MAD2-dependent inhibition of human separase by SGO2 can be recapitulated in vitro.

We investigated whether shugoshin inhibits separase in the same way as securin—by occupying the catalytic site with a non-cleavable pseudo-substrate sequence<sup>8,9</sup>. Using interaction-blocking antibodies, protein fragments and point mutations, we mapped sites within *X. laevis* Sgo1 that are important for separase interaction (Extended Data Fig. 8). Nearby putative pseudosubstrate sites (ϕExxX, with ϕ denoting a hydrophobic residue, x denoting any residue and X denoting any residue except R) were then changed into consensus sites (ϕExxR) and the resulting variants screened for cleavage by active *X. laevis* separase. Notably, *X. laevis* Sgo1(S135R) (but not Sgo1(F288R) or the wild type) was cleaved by separase, and this cleavage was much more pronounced in the presence of wild-type MAD2 than in the presence of MAD2ΔC (Extended Data Fig. 9a).

To confirm this finding independently, we switched back to the human system and tested whether a specific ϕExxX-to-ϕExxR mutation could also turn human SGO2 into a separase substrate. Indeed, <sup>35</sup>S-labelled SGO2(M114R) (but not SGO2(F95R) or SGO2(S126R)) was fragmented in the presence of active separase and wild-type MAD2 (Fig. 3b). Cleavage of SGO2(M114R)—similar to that of RAD21<sup>26</sup>—was further enhanced upon phosphorylation by Polo-like kinase 1. To test in vivo cleavage, we transfected HeLa-K cells to express Flag-tagged variants of SGO2 or securin. Subsequent immunoprecipitation from prometaphase lysates demonstrated that both securin(F118R) (positive control) and SGO2(M114R) were fragmented, whereas the wild-type proteins remained unprocessed (Fig. 3c). Cleavage of SGO2(M114R) was separase-specific because it was suppressed by introduction of a second mutation that compromised the interaction of SGO2 with separase (amino acids 239–242 of SGO2 to Ala; Fig. 3c, Extended Data Fig. 9b). Thus, shugoshin resembles securin in acting as a competitive inhibitor of separase but differs in that it requires MAD2 binding to do so.

*X. laevis* Sgo1 and human SGO2 are very different in sequence (21% similarity) and length (663 versus 1,265 residues). However, the relative order of and distance between functional elements are the same in both proteins (Extended Data Fig. 9c). This suggests that MAD2 binding and separase inhibition evolved before duplication of a primordial SGO gene and were later lost randomly from one SGO gene but retained in the other owing to selective pressure.

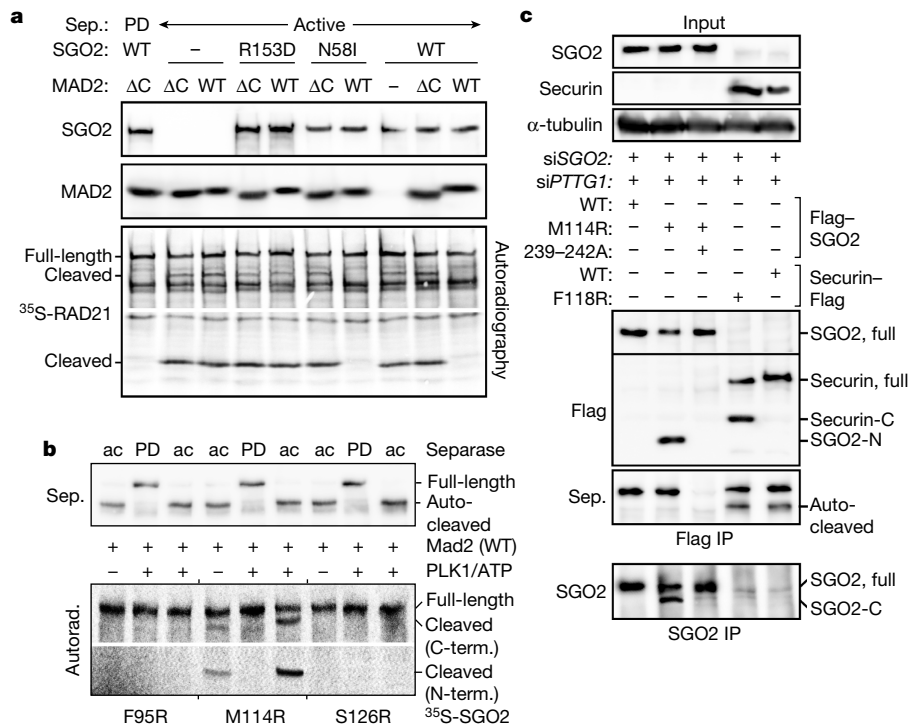


**Fig. 3 | SGO2 is a MAD2-dependent, competitive inhibitor of separase. a,** Protease-dead (PD) or active separase was incubated with variants of recombinant SGO2 and MAD2 and assayed for its ability to cleave <sup>35</sup>S-labelled RAD21. Relevant upper and lower parts of the same gel are shown. **b,** <sup>35</sup>S-labelled SGO2 variants were incubated with MAD2 and, where indicated, Polo-like kinase 1 (PLK1) before being assayed for in vitro cleavage by active (Ac)

separase. Relevant upper and lower parts of the same gel are shown. **c,** SGO2- and securin-depleted HeLa-K cells were transfected to express the indicated siRNA-resistant, Flag-tagged SGO2 or securin variants, taxol-arrested and analysed by IP-immunoblotting. Separase-induced N- and/or C-terminal cleavage fragments of SGO2 and securin are labelled -N and -C.

### TRIP13 liberates separase from SGO2-MAD2

In contrast to securin, human SGO2 is not (or only slowly and incompletely) degraded in late mitosis. This raises the question of how separase is liberated from SGO2-MAD2 when cells are ready to undergo anaphase. The CDC20- and MAD2-containing mitotic checkpoint complex (MCC) is disassembled by the combined action of the AAA-ATPase TRIP13 and its MAD2-specific adaptor p31<sup>comet</sup> (ref. 27). We tested whether this molecular machine could also dismantle the separase-SGO2-MAD2 complex. The complex was immunoprecipitated from securin-depleted, taxol-arrested HeLa-K cells using antibodies against separase and incubated with different combinations of recombinant TRIP13 and p31<sup>comet</sup> variants. Beads were then washed to remove detached proteins, incubated with <sup>35</sup>S-RAD21 to assay for activity of the immobilized separase, and finally analysed for retained proteins. Notably, wild-type TRIP13 and p31<sup>comet</sup> quantitatively displaced SGO2 and MAD2 from separase, thereby leaving it proteolytically active (Fig. 4a). Whereas TRIP13 alone partially disassembled separase-SGO2-MAD2, the Walker-A and -B mutant variants of TRIP13 were inactive even in the presence of p31<sup>comet</sup>. Activation of separase by TRIP13 was also prevented by p31<sup>comet</sup> variants that were defective in MAD2 or TRIP13 interaction. To assess the role of TRIP13 and p31<sup>comet</sup> in vivo, we additionally transfected securin-depleted HeLa-K cells with siRNAs against TRIP13 and p31<sup>comet</sup>, synchronized the cells in prometaphase with taxol and then released them using ZM-447439. Unexpectedly, late mitotic events, such as the de-phosphorylation of CDC27 and histone H3 and the degradation of cyclin B1, were only slightly delayed or occurred largely on schedule in cells lacking TRIP13 and p31<sup>comet</sup> relative to control-treated cells (Fig. 4b, top). By contrast, the separase-SGO2-MAD2 complex was markedly stabilized in the absence of TRIP13 and p31<sup>comet</sup>, as revealed by separase immunoprecipitation

and immunoblotting (Fig. 4b, bottom). Thus, separase-SGO2-MAD2 is actively dismantled by TRIP13 and p31<sup>comet</sup> and might depend on this molecular machine for its disassembly in late mitosis even more than the MCC.

### Sister separation without APC/C activity

The above results suggest that sister chromatid separation in the absence of APC/C<sup>CDC20</sup> activity could be possible when separase is chiefly controlled by SGO2-MAD2 instead of securin. To test this prediction, we supplemented taxol-arrested *PTTG1*<sup>-/-</sup> and parental HCT116 cells with the two APC/C inhibitors proTame and Apcin (or carrier solvent), released the cells by adding ZM-447439, and analysed them by time-resolved immunoprecipitation-immunoblotting and chromosome spreading. Thirty-five minutes after inhibition of aurora B kinase, up to 60% of chromosomes were separated in *PTTG1*<sup>-/-</sup> cells but only 20% on average in parental HCT116 cells, despite the persistence of CDC27 phosphorylation and cyclin B1 in both (Fig. 4c, d). Whereas levels of separase-associated securin also stayed constant in APC/C-inhibited HCT116 cells, SGO2 and MAD2 (which appeared to be overexpressed in *PTTG1*<sup>-/-</sup> cells) disappeared from separase irrespective of securin status (Fig. 4d). Consistent with SGO2-MAD2 being the primary inhibitor of separase, auto-cleavage of separase was strongly increased in *PTTG1*<sup>-/-</sup> cells. Thus, activation of SGO2-MAD2-inhibited separase occurs at least partially independently of APC/C. However, sister chromatid separation was more effective in the absence of proTame and Apcin, even in *PTTG1*<sup>-/-</sup> cells (Fig. 4c). Given that APC/C-associated MCC is disassembled also upon ubiquitylation of CDC20<sup>28</sup>, and given the recent identification of separase and SGO2 as APC/C interactors or substrates<sup>29</sup>, we tested whether separase-SGO2-MAD2

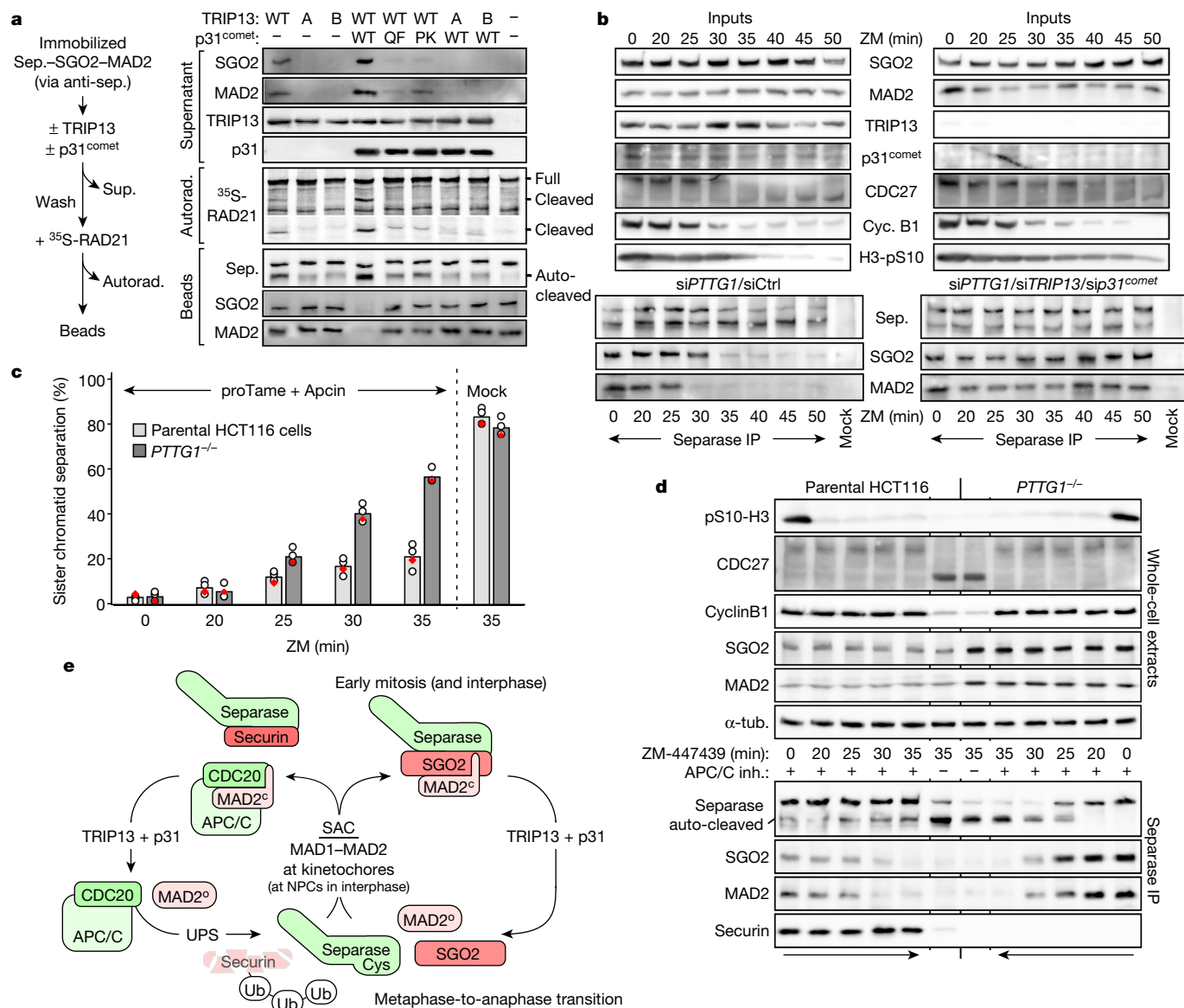


**Fig. 4 | TRIP13–p31<sup>comet</sup>-dependent disassembly liberates separate from SGO2–MAD2.** **a**, Experimental scheme (left) and corresponding immunoblots and autoradiograph (right; relevant upper and lower parts of the same gel are shown). **A**, TRIP13(G184A); **B**, TRIP13(E253Q); **QF**, p31<sup>comet</sup>(Q83A, F191A); **PK**, p31<sup>comet</sup>(P228A, K229A). **b**, siRNA-transfected, taxol-arrested HeLa-C cells were released using ZM-447439 (ZM) and subjected to time-resolved IP-immunoblotting. **c**, **d**, Taxol-arrested PTTG1<sup>-/-</sup> and parental HCT116 cells were supplemented with ZM and APC/C inhibitors or carrier solvent (mock) and analysed by chromosome spreading (**c**) and time-resolved IP-immunoblotting (**d**). Bars show mean of four independent experiments (dots). Red diamonds

indicate experiment shown in **d**. **e**, Model of bifurcated regulation of separate. Activation of MAD2 by SAC signalling inhibits APC/C<sup>CDC20</sup>, thereby stabilizing securin, and enables shugoshin to directly inhibit separate. Liberation of separate from securin requires TRIP13–p31<sup>comet</sup>-dependent dissociation of MAD2 from CDC20 followed by APC/C-dependent degradation of securin. By contrast, TRIP13–p31<sup>comet</sup>-dependent dissociation of MAD2 from shugoshin leads to direct activation of associated separate. The alternative dissociation of MAD2 from its targets by APC/C<sup>CDC20</sup>-dependent ubiquitylation and the CDK1–cyclin B1-dependent inhibition of separate are omitted for clarity.

could also be dismantled by APC/C-dependent ubiquitylation in vitro. Indeed, incubation of the immobilized complex with E1, E2s (UBE2C and UBE2S) and active APC/C<sup>CDC20</sup> in the presence of ubiquitin and ATP displaced SGO2 and MAD2 and rendered separate proteolytically active (Extended Data Fig. 10). Dissociation was accompanied by ubiquitylation of separate. The complex stayed intact, however, when UBE2C was replaced by a dominant-negative variant or when APC/C<sup>CDC20</sup> was omitted. These results suggest that APC/C-dependent ubiquitylation represents a second mode of separate–SGO2–MAD2 disassembly.

We propose a model in which there is bifurcated regulation of separate downstream of the SAC (Fig. 4e). Next to the APC/C<sup>CDC20</sup>–securin

axis, a second major branch is represented by mammalian SGO2 (Sgo1 in amphibians) which is turned into a direct, competitive inhibitor of separate by SAC-activated MAD2. Both branches use TRIP13–p31<sup>comet</sup> (and APC/C-dependent ubiquitylation) for disassembly of their respective MAD2-containing complexes. However, while this liberates separate from shugoshin, the canonical branch additionally requires proteasomal destruction of securin. At least in the cell lines tested here, securin and SGO2 can each compensate for loss of the other. The reason for this seeming redundancy remains to be clarified, but the different requirements for protein degradation might make it beneficial at times to rely on one or the other mode of separate regulation.

## Online content

Any methods, additional references, Nature Research reporting summaries, source data, extended data, supplementary information, acknowledgements, peer review information; details of author contributions and competing interests; and statements of data and code availability are available at <https://doi.org/10.1038/s41586-020-2182-3>.

- Musacchio, A. The molecular biology of spindle assembly checkpoint signaling dynamics. *Curr. Biol.* **25**, R1002–R1018 (2015).
- Nasmyth, K. & Haering, C. H. Cohesin: its roles and mechanisms. *Annu. Rev. Genet.* **43**, 525–558 (2009).
- Uhlmann, F., Wernic, D., Poupard, M. A., Koonin, E. V. & Nasmyth, K. Cleavage of cohesin by the CD clan protease separin triggers anaphase in yeast. *Cell* **103**, 375–386 (2000).
- Mei, J., Huang, X. & Zhang, P. Securin is not required for cellular viability, but is required for normal growth of mouse embryonic fibroblasts. *Curr Biol* **11**, 1197–1201 (2001).
- Pfleghaar, K., Heubes, S., Cox, J., Stemmann, O. & Speicher, M. R. Securin is not required for chromosomal stability in human cells. *PLoS Biol.* **3**, e416 (2005).
- Llano, E. et al. Shugoshin-2 is essential for the completion of meiosis but not for mitotic cell division in mice. *Genes Dev.* **22**, 2400–2413 (2008).
- Orth, M. et al. Shugoshin is a Mad1/Cdc20-like interactor of Mad2. *EMBO J.* **30**, 2868–2880 (2011).
- Boland, A. et al. Cryo-EM structure of a metazoan separase-securin complex at near-atomic resolution. *Nat. Struct. Mol. Biol.* **24**, 414–418 (2017).
- Lin, Z., Luo, X. & Yu, H. Structural basis of cohesin cleavage by separase. *Nature* **532**, 131–134 (2016).
- Wirth, K. G. et al. Separase: a universal trigger for sister chromatid disjunction but not chromosome cycle progression. *J. Cell. Biol.* **172**, 847–860 (2006).
- Zou, H., McGarry, T. J., Bernal, T. & Kirschner, M. W. Identification of a vertebrate sister-chromatid separation inhibitor involved in transformation and tumorigenesis. *Science* **285**, 418–422 (1999).
- Boos, D., Kuffer, C., Lenobel, R., Korner, R. & Stemmann, O. Phosphorylation-dependent binding of cyclin B1 to a Cdc6-like domain of human separase. *J. Biol. Chem.* **283**, 816–823 (2008).
- Hellmuth, S. et al. Positive and negative regulation of vertebrate separase by Cdk1-cyclin B1 may explain why securin is dispensable. *J. Biol. Chem.* **290**, 8002–8010 (2015).
- Huang, X. et al. Preimplantation mouse embryos depend on inhibitory phosphorylation of separase to prevent chromosome missegregation. *Mol. Cell. Biol.* **29**, 1498–1505 (2009).
- Huang, X. et al. Inhibitory phosphorylation of separase is essential for genome stability and viability of murine embryonic germ cells. *PLoS Biol.* **6**, e15 (2008).
- Huang, X., Hatcher, R., York, J. P. & Zhang, P. Securin and separase phosphorylation act redundantly to maintain sister chromatid cohesion in mammalian cells. *Mol. Biol. Cell* **16**, 4725–4732 (2005).
- Stemmann, O., Zou, H., Gerber, S. A., Gygi, S. P. & Kirschner, M. W. Dual inhibition of sister chromatid separation at metaphase. *Cell* **107**, 715–726 (2001).
- Li, M., York, J. P. & Zhang, P. Loss of Cdc20 causes a securin-dependent metaphase arrest in two-cell mouse embryos. *Mol. Cell. Biol.* **27**, 3481–3488 (2007).
- Hellmuth, S. et al. Human chromosome segregation involves multi-layered regulation of separase by the peptidyl-prolyl-isomerase Pin1. *Mol. Cell* **58**, 495–506 (2015).
- Gorr, I. H., Boos, D. & Stemmann, O. Mutual inhibition of separase and Cdk1 by two-step complex formation. *Mol. Cell* **19**, 135–141 (2005).
- Rodriguez-Bravo, V. et al. Nuclear pores protect genome integrity by assembling a premitotic and Mad1-dependent anaphase inhibitor. *Cell* **156**, 1017–1031 (2014).
- Holland, A. J. & Taylor, S. S. Cyclin-B1-mediated inhibition of excess separase is required for timely chromosome disjunction. *J. Cell Sci.* **119**, 3325–3336 (2006).
- Clift, D., Bizzari, F. & Marston, A. L. Shugoshin prevents cohesin cleavage by PP2A(Cdc55)-dependent inhibition of separase. *Genes Dev.* **23**, 766–780 (2009).
- Tsou, M. F. & Stearns, T. Mechanism limiting centrosome duplication to once per cell cycle. *Nature* **442**, 947–951 (2006).
- Kawashima, S. A., Yamagishi, Y., Honda, T., Ishiguro, K. & Watanabe, Y. Phosphorylation of H2A by Bub1 prevents chromosomal instability through localizing shugoshin. *Science* **327**, 172–177 (2010).
- Hauf, S. et al. Dissociation of cohesin from chromosome arms and loss of arm cohesion during early mitosis depends on phosphorylation of SA2. *PLoS Biol.* **3**, e69 (2005).
- Eytan, E. et al. Disassembly of mitotic checkpoint complexes by the joint action of the AAA-ATPase TRIP13 and p31<sup>comet</sup>. *Proc. Natl Acad. Sci. USA* **111**, 12019–12024 (2014).
- Reddy, S. K., Rape, M., Margansky, W. A. & Kirschner, M. W. Ubiquitination by the anaphase-promoting complex drives spindle checkpoint inactivation. *Nature* **446**, 921–925 (2007).
- Bakos, G. et al. An E2-ubiquitin thioester-driven approach to identify substrates modified with ubiquitin and ubiquitin-like molecules. *Nat. Commun.* **9**, 4776 (2018).

**Publisher's note** Springer Nature remains neutral with regard to jurisdictional claims in published maps and institutional affiliations.

© The Author(s), under exclusive licence to Springer Nature Limited 2020

## Methods

## Antibodies

Antibodies generated within this study are from Charles River Laboratories. Antigenic peptides (Bachem) were coupled via terminal Cys to maleimide-activated KLH (ThermoFisher) before immunization. Antibodies were affinity-purified against immobilized antigens (proteins coupled to NHS-activated sepharose (GE Healthcare) or peptides coupled to Sulfo-link (ThermoFisher)). The following antibodies were used for immunoblotting according to standard protocols. Antibodies directed against human proteins: rabbit or guinea pig anti-SGO2 (1.5 µg/ml; 'ab1'; anti-DVPPRESHSHSDQSSKC), rabbit anti-SGO2 (1 µg/ml; 'ab2'; anti-KSEDLSSERTSRRRC), guinea pig anti-TRIP13 (raised against full-length TRIP13), rabbit anti-p31<sup>comet</sup> (raised against isoform 2 of full-length p31<sup>comet</sup>), rabbit anti-separase<sup>17</sup>, mouse anti-securin (1:1,000; MBL, DCS-280), mouse anti-Flag (1:2,000; Sigma-Aldrich, M2), rabbit anti-SGO2 (1:1,000; Bethyl, A301-262A), rabbit anti-SGO1 (1:500, Abcam ab21633), mouse anti-MAD2 (1:800; Santa Cruz Biotechnology, 17D10), rabbit anti-MAD2 (1:1,000; Bethyl, A300-300A), mouse anti-MAD1 (1:1,000; Sigma-Aldrich, 9B10), mouse anti-APC7 (1:800; ThermoFisher, PA5-20948), rabbit anti-phosphoSer10-histone H3 (H3-pS10; 1:1,000; Millipore, 06-570), mouse anti-PP2A-C (1:1,000; Millipore, 1D6), mouse anti-cyclin B1 (1:1,000; Millipore, 05-373), goat anti-CDC2<sup>730</sup>, mouse anti-topoisomerase IIα (1:1,000; Enzo Life Sciences, 1C5), mouse anti-cyclin A2 (1:200; Santa Cruz Biotechnology, 46B11), mouse anti-RAD21 (1:800; Santa Cruz Biotechnology, B-2), rabbit anti-RAD21 (1:1,000; Bethyl, A300-080A). Antibodies directed against *Xenopus* proteins: rabbit anti-Mad2 (raised against full-length protein), four different rabbit anti-Sgo1 (raised against amino acids 200–300, 300–400, 400–500, and 500–600 of *X. laevis* Sgo1)<sup>7</sup>, rabbit anti-separase<sup>31</sup>. Other antibodies: mouse anti-Myc (hybridoma supernatant 1:50; DSHB, 9E10), rat anti-HA (1:2,000; Roche, 3F10), rabbit anti-ovalbumin (1:1,000; ThermoFisher, PA1-196), mouse anti-ubiquitinated proteins (1:1,000; Millipore, FK2), mouse anti-GFP<sup>32</sup>, and mouse anti-α-tubulin (hybridoma supernatant 1:200; DSHB, 12G10). For immunoprecipitation experiments, the following affinity matrices and antibodies were used: mouse anti-Myc agarose (Sigma-Aldrich, 4A6), mouse anti-Flag M2-agarose (Sigma-Aldrich), mouse anti-RAD21 coupled to protein G sepharose (GE Healthcare). Rabbit anti-separase (human), rabbit anti-securin<sup>30</sup>, rabbit anti-SGO2 and rabbit anti-SGO1 (human) were coupled to protein A sepharose (GE healthcare). To precipitate *X. laevis* separase from CSF (cytostatic factor) extract, the corresponding separase antibody or nonspecific rabbit IgG was coupled to magnetic protein A Dynabeads (Invitrogen). For non-covalent coupling of antibodies to beads, 10 µl of the respective matrix was rotated with 2–5 µg antibody for 90 min at room temperature and then washed three times with LP2 lysis buffer. For immunofluorescence microscopy (IFM), rabbit anti-Cap-E (anti-CAKSKAKPPKGAHVEV) and mouse anti-RAD21 (1:500; Millipore, 05-908) were used. Isolated centrosomes were stained with rabbit anti-centrin-2, guinea-pig anti-C-Nap1 and mouse anti-γ-tubulin (Sigma-Aldrich, GTU-88) as previously described<sup>33</sup>. Secondary antibodies (all 1:500): Cy3 donkey anti-guinea pig IgG and Cy3 goat anti-rabbit IgG (Invitrogen), Marina-Blue goat anti-mouse IgG (ThermoFisher), Alexa Fluor 488 goat anti-rabbit IgG, and Alexa Fluor 488 goat anti-mouse IgG (both Invitrogen).

## Cell lines

hTERT RPE-1 cells were purchased from ATCC (CRL-4000). Hek293 Flp-In TRex cells were purchased from Invitrogen (R78007). All other cell lines were gifts: Hek293T from M. W. Kirschner, HeLa-K from D. Gerlich, and securin knockout and parental HCT116 from C. Lengauer. Validation procedures for purchased cell lines are as described by the corresponding manufacturers. All other cell lines were authenticated via visual inspection of typical morphology, immunoblotting analyses (for example, absence of securin), cell synchronization behaviour,

efficiencies of different transfection reagents and resistance to certain antibiotics. Cell lines were not tested for mycoplasma contamination but microscopic inspections of their fluorescently labelled DNA contents were inconspicuous.

All human cells were cultured in Dulbecco's modified Eagle's medium (DMEM; Biowest) supplemented with 10% fetal calf serum (FCS; Sigma-Aldrich) at 37 °C and 5% CO<sub>2</sub>. Generation of a stably transgenic Hek293-FlpIn-TRex line (Invitrogen) expressing Myc<sub>6</sub>-separase(S1126A) upon induction with doxycycline has been described<sup>13</sup>. For transient expression of Flag<sub>3</sub>-Tev<sub>2</sub>-SGO2 variants (WT, R153D, N53I, M114R, RKK124–126A, LSE127–129A, HSDQ239–242A) Hek293T or HeLa-K cells were transfected with the corresponding pCS2-based plasmids using a calcium phosphate-based method or Lipofectamine 2000 (Invitrogen). For time-lapse experiments, HeLa cells stably expressing histone H2B-eGFP were used. In addition, H2B-mCherry-SCC1<sub>107–268</sub>-eGFP<sup>19</sup> was transiently transfected to visualize premature separase activation.

## Cell treatments

For synchronization in early S-phase, cells were treated with 2 mM thymidine (Sigma-Aldrich) for 20 h. Synchronization of cells in prometaphase was done by addition of taxol (LC Laboratories) to 0.2 µg/ml 6 h after release from a single thymidine block. G2 arrest was achieved by addition of 10 µM RO-3306 (Santa-Cruz Biotechnology) 4 h after G1/S release. To analyse cells in G1-phase, cells were collected 15 h after release from a single thymidine block. For the 'taxol-ZM override' experiments, taxol-arrested mitotic HeLa-K cells were collected by shake-off and released for the indicated times by reseeding into medium supplemented with ZM-447439 (5 µM, Tocris Biosciences), taxol (0.2 µg/ml), cycloheximide (30 µg/ml, Sigma-Aldrich) and, where indicated, with proTame (6 µM, Boston Biochemicals) and Apcin (20 µM, Tocris Bioscience). To further enrich the endogenous separase-SGO2-MAD2 complex for later isolation, securin was depleted by RNAi.

## Immunoprecipitation

We lysed 1 × 10<sup>7</sup> cells with a dounce homogenizer in 1 ml LP2 lysis buffer (20 mM Tris-HCl pH 7.7, 100 mM NaCl, 10 mM NaF, 20 mM β-glycerophosphate, 5 mM MgCl<sub>2</sub>, 0.1% Triton X-100, 5% glycerol), combined with benzonase (ad 30 U/l; Santa-Cruz Biotechnology), and incubated them on ice for 1 h. To preserve phosphorylation, lysis buffer was additionally supplemented with 50 nM calyculin A (LC-Laboratories) and 1 µM microcystin LR (Alexis Biochemicals). Corresponding lysates were centrifuged at 2,500g for 10 min followed by incubation of 1 ml cleared lysate with 10 µl of antibody-loaded beads for 4 h or overnight at 4 °C and washed 5× with LP2. In some cases, immobilized human SGO2 variants (purified from G1 cells) or endogenous separase-SGO2-MAD2 complex (purified from mitotic cells) were used as starting material for further experiments before bound proteins were eluted by boiling in SDS-sample buffer. For consecutive immunoprecipitation from *PTTG1*<sup>-/-</sup> cells, the lysate used for the first purification was kept and served as origin for the second precipitation.

For immunoprecipitation of *X. laevis* separase, CSF-arrested *Xenopus* egg extract was prepared as previously described<sup>34</sup> and combined with cycloheximide (100 µg/ml), recombinant human Δ90-cyclin B1 (23 ng/µl ≈ 500 nM)<sup>19</sup> and sperm nuclei (2,000 µl<sup>-1</sup>). After 15 min at room temperature, the egg extract was released into anaphase II by addition of CaCl<sub>2</sub> (0.6 mM). Previously prepared mock- or *X. laevis* separase antibody-coupled magnetic beads were equilibrated in CSF-XB followed by addition of anaphase extract (minimal volume of 500 µl) and consecutive incubation for 45 min at 18 °C. After re-isolation, beads were washed 5× in CSF-XB supplemented with 300 mM NaCl and 0.01% Triton X-100.

## RNA interference

For efficient knockdown, cells were calcium phosphate or RNAiMax (Invitrogen) transfected with 70–100 nM siRNA duplex

of *PTTG1*: 5'-UCUUAGUGCUUCAGAGUUUGUGUGUAU-3'; *SGO2*: 5'-GAA CACAUUUUCUUCGCCUATT-3'; *MAD2*: 5'-GAGUCGGGACCACAGUUUA UU-3'; *MAD1*: 5'-AACCAGCGGCUCAAGGAGGUU-3'; *P31<sup>comet</sup>*: 5'-GGCU GCUGUCAGUUACUUTT-3'; *TRIP13*: 5'-CUGAUGAAGUGUCAGAUCA-3'; *TRP*: 5'-GGGUGAAGAUAGUAAUGAAUUCTT-3'. Transfected cells were grown for 12–24 h before synchronization procedures were applied. *Luciferase* siRNA (GL2) was used as negative control (Ctrl).

### Immunofluorescence staining and microscopy

Hela-K cells transfected with the indicated siRNAs were grown on poly-lysine coated glass coverslips and processed 8 h after thymidine release in the presence of BI-2536 (10 nM) to slow down prophase in early mitotic cells. To remove soluble proteins, cells were pre-extracted (PBS, 0.3% Triton X-100) for 5 min, washed once with PBS and fixed with fixation solution (PBS, 3.7% formaldehyde, 0.3% Triton X-100) for 10 min at room temperature. Subsequently, coverslips were washed twice with quenching solution (PBS, 100 mM glycine), incubated with permeabilization solution (PBS, 0.5% Triton X-100) for 5 min, washed once with PBS and then incubated in blocking solution (PBS, 1% (w/v) BSA) for 1 h at room temperature. Coverslips were transferred into a wet chamber and incubated with primary antibodies for 1 h followed by four washes with PBS-Tx (PBS, 0.1% Triton X-100). After incubation with fluorescently labelled secondary antibodies for 40 min, samples were washed once, stained for 10 min with 1 µg/ml Hoechst 33342 in PBS-Tx and washed again four times. Finally, coverslips were mounted in 20 mM Tris-HCl pH 8.0, 2.33% (w/v) 1,4-diazabicyclo(2.2.2)octane, 78% glycerol on a glass slide. IFM of fixed cells was performed on a DMI 6000 inverted microscope (Leica) using a HCX PL APO 100×/1.40–0.70 oil objective. To identify early mitotic nuclei, DNA morphology (commencing condensation) and condensin staining intensity were examined. For representative images, Z-stack series over 4 µm in 0.2-µm increments were collected, deconvoluted and projected into one plane using the LAS-AF software. Chromosome spreads were prepared using Canoy's solution as described<sup>35</sup>. Spreads were observed with the Zeiss Axioplan 2 Imaging microscope using a Plan-APOCHROMAT 100×/1.40 Oil objective. A cell was counted as suffering from PCS when exhibiting loss of cohesion of >50% of its chromosomes. At least 100 spreads were counted per condition. To assess centriole engagement status, centrosomes were isolated from RO-3306 arrested HeLa-K cells ( $4 \times 10^6$ ) 36 h after transfection of indicated siRNAs and stained as previously described<sup>33</sup>.

### Clonogenic assays

Twelve hours after siRNA transfection, HeLa-K, Hek293T, HCT116 parental or *PTTG1*<sup>-/-</sup> cells were seeded in 10-cm dishes (100 cells per plate and condition). Cells were grown for 10 days and then fixed in ice-cold methanol for 10 min. Staining was performed as described<sup>36</sup> except for the use of ethanol instead of glutaraldehyde. The number of colonies per plate with a minimal area of 20 (circularity 0.00–1.00) was determined with ImageJ particle analysis software.

### In vitro disassembly of separase–SGO2–MAD2 complex

Ten microlitres of immobilized separase–SGO2–MAD2 complex was incubated with 2 mg/ml recombinant variants of TRIP13 (WT; A, Walker A mutant G184A; B, Walker B mutant E253Q) and RGS-His<sub>6</sub>-p31<sup>comet</sup> (WT; QF, Q83A/F191A MAD2-binding deficient; PK, P228A/K229A TRIP13-binding deficient) in EDTA/EGTA-free lysis buffer supplemented with ATP (1 mM) in a final volume of 30 µl for 30 min at 18 °C. Subsequently, 15 µl of the corresponding supernatant was removed for later analysis. Beads were washed three times with LP2 and then equilibrated in cleavage buffer (10 mM Hepes-KOH pH 7.7, 50 mM NaCl, 25 mM NaF, 1 mM EGTA, 20% glycerol). To monitor separase activity, 2 µl of in vitro translated <sup>35</sup>S-RAD21–GFP was added to a volume of 30 µl. Following incubation for 30 min at 30 °C, reactions were stopped by boiling in SDS-sample buffer. Assaying disassembly by in vitro ubiquitylation

(Extended Data Fig. 10) was performed essentially as described<sup>30</sup> with the exception that instead of securin, 10 µl immobilized separase–SGO2–MAD2 complex was added as substrate.

### Bacterially expressed proteins

pET28-vector encoded, His<sub>6</sub>-SUMO<sub>1</sub>-tagged<sup>37</sup> variants of TRIP13 (NP\_004228) and p31<sup>comet</sup> (NP\_055443) were expressed individually in *E. coli* Rosetta 2 DE3 (Novagen). Bacteria were lysed in LP1 (PBS, 5 mM imidazole, 0.5 mM DTT and an additional 400 mM NaCl) and purified over Ni<sup>2+</sup>-NTA-agarose (Qiagen) according to standard procedures. Following elution with PBS supplemented with 250 mM imidazole, 0.5 mM DTT and an additional 400 mM NaCl (pH adjusted to 7.5 with HCl), proteins were dialysed at 4 °C against LP1 in presence of His<sub>6</sub>-SEN2 (10 ng per 100 µg of protein) and then rotated for 3 h over 0.9× the amount of fresh Ni<sup>2+</sup>-NTA-agarose. Supernatants containing pure TRIP13 and p31<sup>comet</sup> were dialysed against 50 mM Hepes-KOH pH 7.7, 10% glycerol, 100 mM NaCl, 5 mM MgCl<sub>2</sub>, 1 mM EDTA and 1 mM DTT. Human MAD2 and *X. laevis* Mad2 were purified as described previously<sup>7</sup>.

### H2A-peptide binding assay

Thr-9-phosphorylated and unmodified histone H2A-peptides (QAVLLP-KKTESHHKAKGK) were obtained from Bachem; Ser-10-phosphorylated or unmodified histone H3-peptides were purchased from Eurogentec (AS-61702 and AS-64611). One milligram of each of the H2A peptides was conjugated to 10 mg/ml maleimide-activated ovalbumin (ThermoFisher) according to the manufacturer's instructions and dialysed against CSF-XB<sup>34</sup> containing 0.5 mM DTT. Reactions (final volume of 30 µl) containing 10 µl immobilized FLAG<sub>3</sub>-Tev<sub>2</sub>-SGO2 and 1 µg ovalbumin-coupled-H2A peptide, 5 µg free H2A or H3 peptide, or 4 µg of recombinant MAD2 were assembled and incubated for 30 min at 18 °C. Unbound peptide or protein was removed by four washes with CSF-XB and the second reaction was assembled with the corresponding counterpart and again incubated for 30 min at 18 °C. Samples were again washed (four times with CSF-XB containing 0.01% Triton X-100) before beads were eluted by boiling in SDS-sample buffer.

### Mapping experiments in *X. laevis* Sgo1

N-terminally tagged Myc<sub>6</sub>- or FLAG<sub>3</sub>-tagged *X. laevis* Sgo1 variants were in vitro translated in rabbit reticulocyte lysate (TNT Quick, Promega) according to the manufacturer's protocol. For mapping with the help of interaction-blocking antibodies, 16 µl Sgo1 was combined with 2.5 µg anti-*X. laevis* Sgo1 and 5 µg recombinant *X. laevis* Mad2 and incubated for 30 min at 18 °C. Then, 10 µl of magnetic beads loaded with *X. laevis* separase (isolated from anaphase egg extract) was added and reactions were incubated for 30 min at 18 °C. Beads were washed four times with CSF-XB, 0.01% Triton X-100 and twice with CSF-XB, 0.01% Triton X-100, 300 mM NaCl and finally eluted by boiling in SDS-sample buffer. In all other cases 12.5 µl Sgo1 and 5 µg Mad2 were pre-incubated in 300 µl CSF-XB, 0.01% Triton X-100 followed by addition of 10 µl immobilized separase.

### Separase inhibition and cleavage assays

For separase inhibition, 10 µl of FLAG<sub>3</sub>-Tev<sub>2</sub>-SGO2 bound to anti-FLAG beads and 4 µg recombinant MAD2 were incubated in cleavage buffer (total volume of 28 µl) for 10 min at 18 °C followed by the addition of 2.5 µl active (Ac, S1126A variant) or protease dead (PD, S1126A and C2029S) separase<sup>17</sup>. After a 10-min incubation at room temperature, 2 µl in vitro translated, <sup>35</sup>S-labelled RAD21–GFP were added. Reactions were stopped after 30 min by boiling in SDS-sample buffer. Samples were separated by SDS–PAGE and blotted onto PVDF membrane (SERVA), which was cut and analysed by immunoblotting before reassembly and autoradiography. For Fig. 3b, 2 µl of each in vitro translated, <sup>35</sup>S-labelled SGO2 variant was combined with 1 µg human MAD2 and, where indicated, 0.1 µg PLK1 (ProQinase; No. O183-0000-1) in modified cleavage buffer (10 mM Hepes-KOH pH 7.7, 50 mM NaCl, 25

# Article

mM NaF, 20% glycerol, 1 mM ATP, 10 mM MgCl<sub>2</sub>) and a total volume of 15 µl. After 15 min at 30 °C, 2.5 µl separase (Ac or PD) was added and reactions were incubated for 30 min at room temperature. For Extended Data Fig. 9a, 2 µl of each in vitro translated, <sup>35</sup>S-labelled *X. laevis* Sgo1 variant was combined with 1 µg *X. laevis* Mad2 (WT or ΔC10) and 10 µl immobilized *X. laevis* separase. Samples were further processed and analysed as described above.

## Live-cell imaging

Cells in phenol red-free medium were seeded into µ-slide 8-well chambered coverslips (Ibidi) and kept in an atmosphere of 37 °C and 5% humidified CO<sub>2</sub> during microscopy on a DMI 6000 inverted microscope (Leica). For imaging of unperturbed mitosis, GFP and DIC images were captured 6 h after release from thymidine arrest at 10-min intervals over a period of 15 h, through a HCX PL APO 40×/0.85 CORR objective. Changes in focus plane due to mitotic rounding of the cells were compensated by collecting Z-stacks at each time point. Captured images from each experiment were analysed using the corresponding LAS-AF software (Leica).

## Statistics and reproducibility

No statistical methods were used to predetermine sample size. The experiments were not randomized. For quantitative analyses of chromosome spreads, clonogenic assays, and IFM specimen the investigators were blinded to sample allocation. Experiments analysed by immunoblotting were repeated 2–4 times with similar results (2–4 biological replicates).

## Reporting summary

Further information on research design is available in the Nature Research Reporting Summary linked to this paper.

## Data availability

All source data for this study are available online.

30. Hellmuth, S., Böttger, F., Pan, C., Mann, M. & Stemmann, O. PP2A delays APC/C-dependent degradation of separase-associated but not free securin. *EMBO J.* **33**, 1134–1147 (2014).
31. Gorr, I. H. et al. Essential CDK1-inhibitory role for separase during meiosis I in vertebrate oocytes. *Nat. Cell Biol.* **8**, 1035–1037 (2006).
32. Hellmuth, S., Gutiérrez-Caballero, C., Llano, E., Pendás, A. M. & Stemmann, O. Local activation of mammalian separase in interphase promotes double-strand break repair and prevents oncogenic transformation. *EMBO J.* **37**, e99184 (2018).
33. Schöckel, L., Möckel, M., Mayer, B., Boos, D. & Stemmann, O. Cleavage of cohesin rings coordinates the separation of centrioles and chromatids. *Nat. Cell Biol.* **13**, 966–972 (2011).
34. Murray, A. W. Cell cycle extracts. *Methods Cell Biol.* **36**, 581–605 (1991).
35. McGuinness, B. E., Hirota, T., Kudo, N. R., Peters, J. M. & Nasmyth, K. Shugoshin prevents dissociation of cohesin from centromeres during mitosis in vertebrate cells. *PLoS Biol.* **3**, e86 (2005).
36. Franken, N. A., Rodermond, H. M., Stap, J., Haveman, J. & van Bree, C. Clonogenic assay of cells in vitro. *Nat. Protocols* **1**, 2315–2319 (2006).
37. Butt, T. R., Edavettal, S. C., Hall, J. P. & Mattern, M. R. SUMO fusion technology for difficult-to-express proteins. *Protein Expr. Purif.* **43**, 1–9 (2005).
38. Holland, A. J., Böttger, F., Stemmann, O. & Taylor, S. S. Protein phosphatase 2A and separase form a complex regulated by separase autocleavage. *J. Biol. Chem.* **282**, 24623–24632 (2007).
39. Schägger, H. Tricine-SDS-PAGE. *Nat. Protocols* **1**, 16–22 (2006).

**Acknowledgements** We thank S. Heidmann and P. Wolf for critical reading of the manuscript, and J. Hübner and M. Hermann for technical assistance. This work was supported by a grant (STE997/4-2) from the Deutsche Forschungsgemeinschaft (DFG) to O.S. and by MINECO (BFU2017-89408-R) and Junta de Castilla y León (CSI239P18). CIC-IBMCC is supported by the Programa de Apoyo a Planes Estratégicos de Investigación de Estructuras de Investigación de Excelencia cofunded by the Castilla–León autonomous government and the European Regional Development Fund (CLC–2017–01).

**Author contributions** L.G.-H. and A.M.P. first discovered the interaction between separase and SGO2. S.H. carried out all experiments except for the one shown in Extended Data Fig. 1a, which was conducted by L.G.-H. S.H. and O.S. co-designed the research and wrote the paper.

**Competing interests** The authors declare no competing interests.

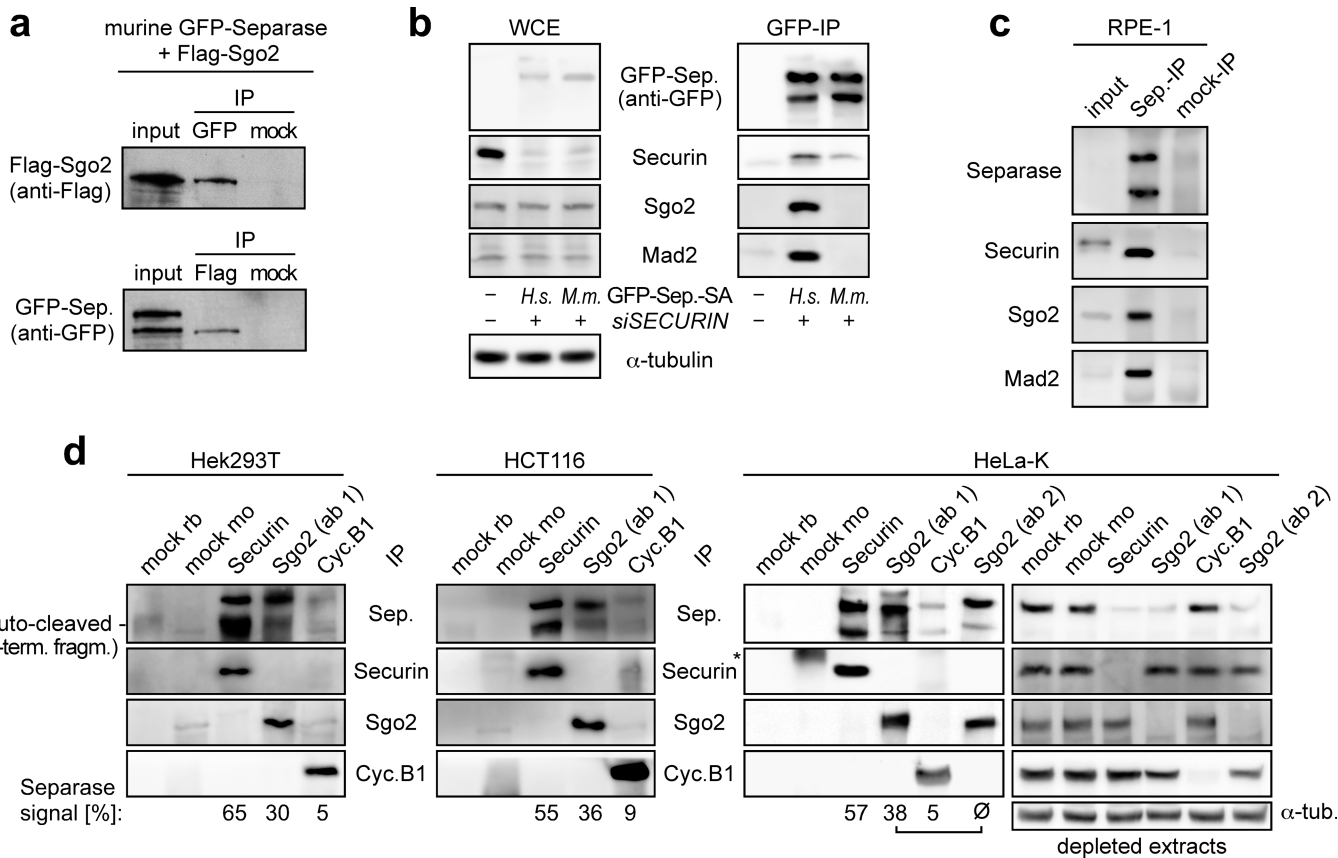
## Additional information

**Supplementary information** is available for this paper at <https://doi.org/10.1038/s41586-020-2182-3>.

**Correspondence and requests for materials** should be addressed to O.S.

**Peer review information** Nature thanks Silke Hauf, Adele Marston and Hongtao Yu for their contribution to the peer review of this work.

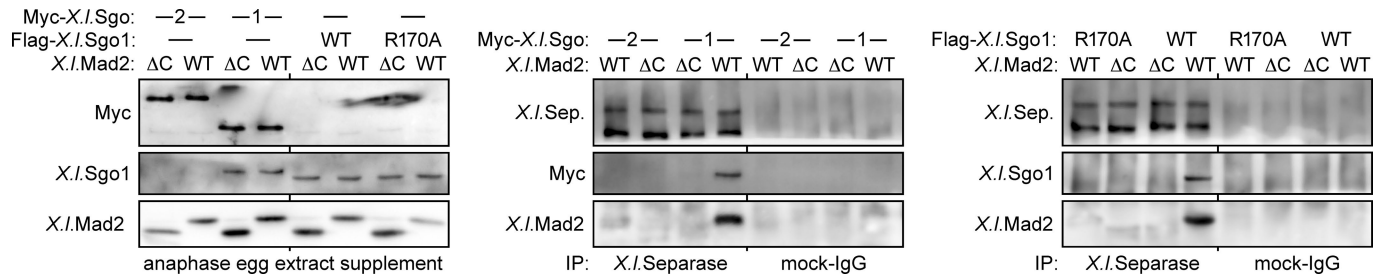
**Reprints and permissions information** is available at <http://www.nature.com/reprints>.



**Extended Data Fig. 1 | Mammalian SGO2 interacts with separase.** **a**, Hek293T cells were co-transfected with expression vectors for the following mouse proteins: GFP-separase, Flag-SGO2 and securin. Immunoprecipitation was carried out from transfected cells with either anti-Flag or anti-GFP antibodies and analysed by immunoblotting with the indicated antibodies. **b**, Mouse separase does not interact with human SGO2 and, therefore, cannot be used to study separase regulation in human cells. Securin-depleted Hek293T cells expressing GFP-tagged human separase(S1126A) or mouse separase(S1121A) were taxol-arrested and then subjected to IP-immunoblotting analyses using the indicated antibodies. **c**, SGO2 and MAD2 interact specifically with separase in untransformed cells. Taxol-arrested RPE1 cells were subjected to IP-

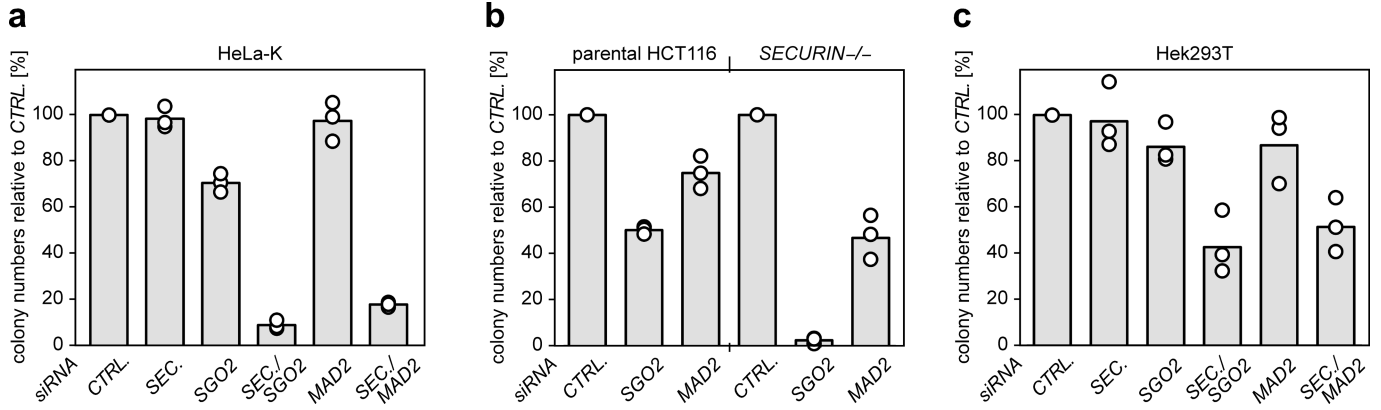
immunoblotting analyses as indicated. **d**, Even in securin-expressing cells, a considerable fraction of separase is sequestered by SGO2. Taxol-arrested Hek293T, HCT116, and HeLa-K cells were subjected to IP-immunoblotting analyses using the indicated antibodies. ab 1, anti-DVPPRESHSHSDQSSKC (corresponding to amino acids 230-245 of human SGO2); ab 2, anti-KSEDLSERTSRRRRC (corresponding to amino acids 1,234-1,249 of human SGO2); rb, rabbit; mo, mouse. Given below are the relative intensities (in per cent) of the separase signals (sum of full-length and N-terminal auto-cleavage fragment). Note the considerable co-depletion of separase upon SGO2 immunoprecipitation from HeLa-K (right).

# Article

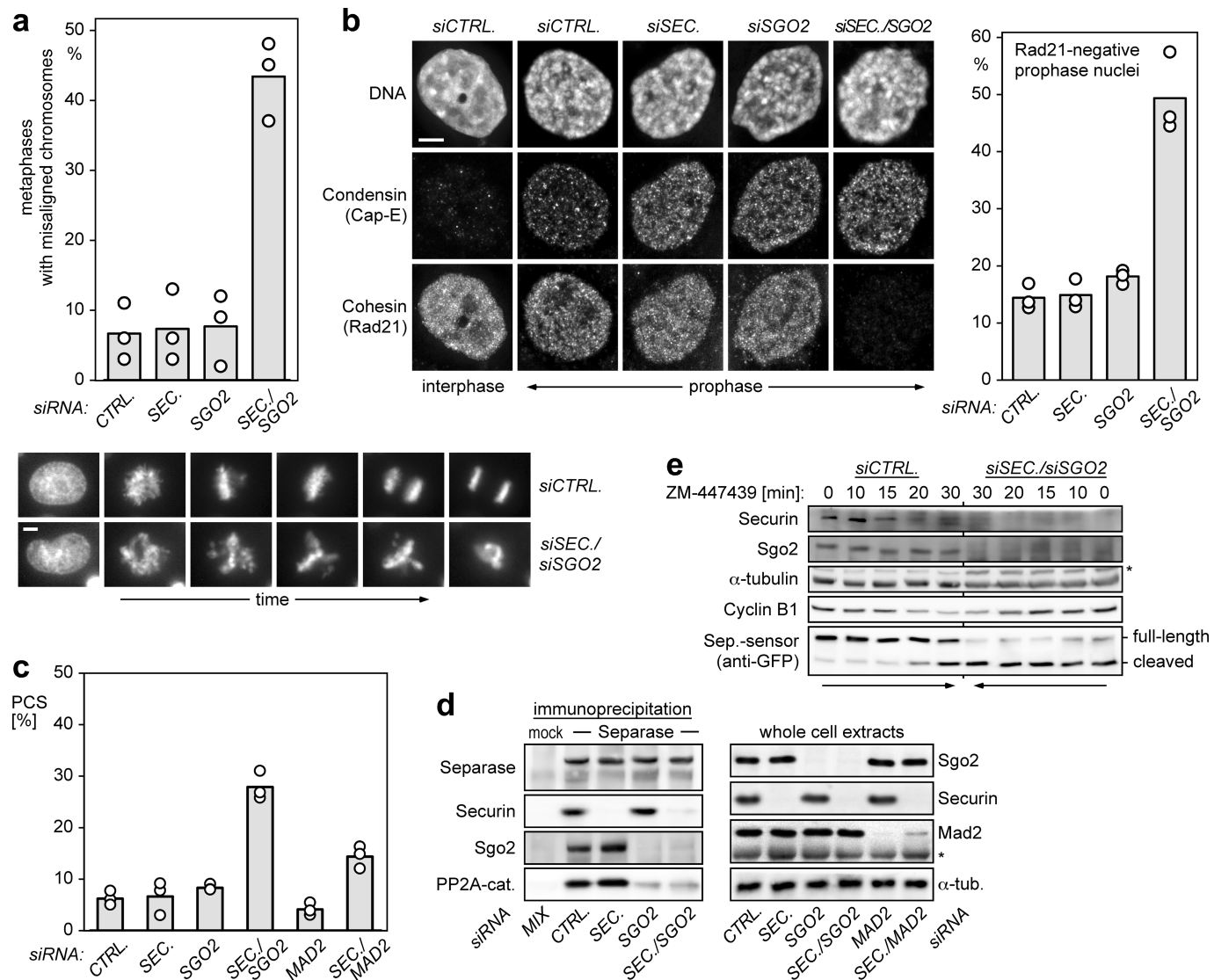


**Extended Data Fig. 2 | Sgo1 rather than Sgo2 interacts with Mad2 and separase in *Xenopus*.** The indicated variants of in vitro-expressed *X. laevis* (*X.l.*) shugoshins and an excess of *E. coli*-expressed Mad2 (to mimic SAC signalling) were incubated in anaphase egg extract (left). Following IP with

anti-*X.l.* separase or mock-IgG from these mixtures, isolated proteins were detected by immunoblotting (middle and right). R170A, Mad2-binding-deficient Sgo1; ΔC, Sgo1-binding-deficient, C-terminally truncated Mad2.

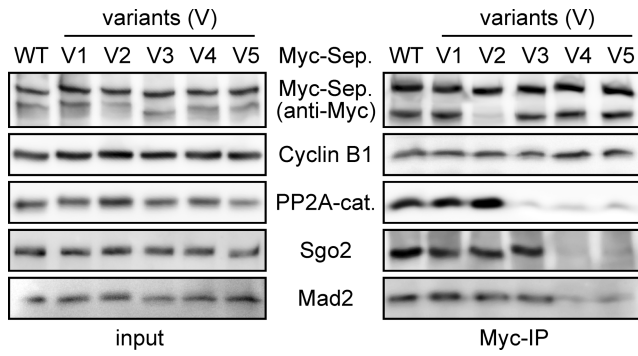


**Extended Data Fig. 3 | Lack of securin and SGO2 or MAD2 have synergistic cytotoxic effects.** a–c, Clonogenic assays with HeLa-K (a), *PTTG1*<sup>+</sup> (*SECURIN*<sup>-/-</sup>) and parental HCT116 cells (b), and Hek293T cells (c) transfected with the indicated siRNAs. Bars show percentages of colony numbers relative to the control of three independent experiments (dots).

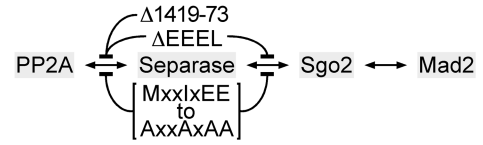


**Extended Data Fig. 4 | Depletion of securin and SGO2, but not the individual knockdowns, results in impaired chromosome alignment, premature loss of chromosomal cohesin and unscheduled separase activity.** **a**, HeLa-K cells transfected with the indicated siRNAs and a histone H2B-eGFP expression plasmid were observed by video fluorescence microscopy to assess metaphase plate formation (bottom). Bars show mean of three independent experiments (dots) counting at least 50 mitotic cells each (top). Scale bar, 5  $\mu$ m. **b**, Eight hours after release from thymidine arrest, HeLa-K cells transfected with the indicated siRNAs were pre-extracted, fixed, and examined by fluorescence microscopy for cohesin-negative early mitotic chromatin. Left, representative images; right, bars show mean of three

independent experiments (dots) counting prophase nuclei that were still round but already stained positive for condensin (100 each). Scale bar, 5  $\mu$ m. **c**, Hek293T cells transfected with the indicated siRNAs were supplemented with taxol (but not EGCG; compare Fig. 2b) and analysed by chromosome spreading. Bars show mean of three independent experiments (dots). **d**, Exemplary immunoblots of cells analysed in **c** and Fig. 2b. Star denotes nonspecific band. **e**, siRNA-transfected HeLa-K cells expressing a separase activity sensor (H2B-mCherry-RAD21<sup>107-268</sup>-eGFP) were released from a taxol arrest by addition of ZM-447439 at time zero and analysed by time-resolved immunoblotting.

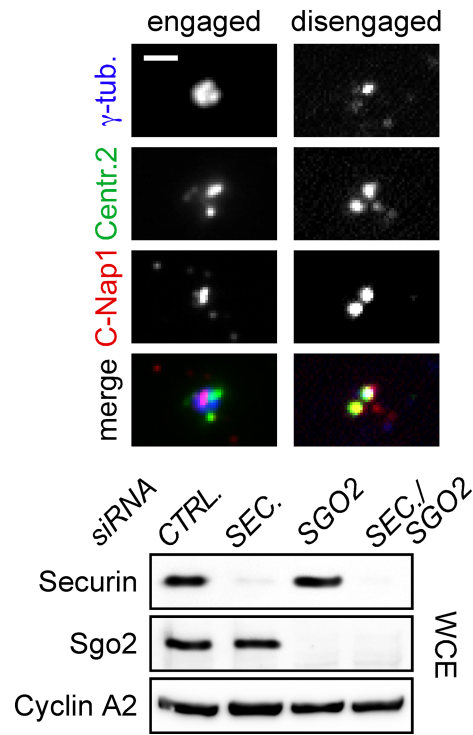
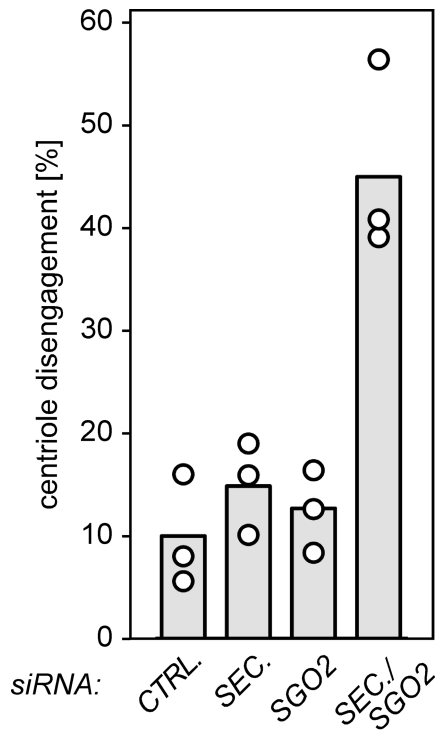


variants:	changes:	amino acid positions:
V1 (ABBA)	FxVFXE to AxAAxA	1362-7
V2 (non-cleavable):	ExxR to RxxE	1483-6, 1503-6, 1532-5
V3 (PP2A-1):	Δ55	1419-73
V4 (PP2A-2):	ΔEEEL	1490-3
V5 (PP2A-3):	MxxlxEE to AxxAxAA	1485-91



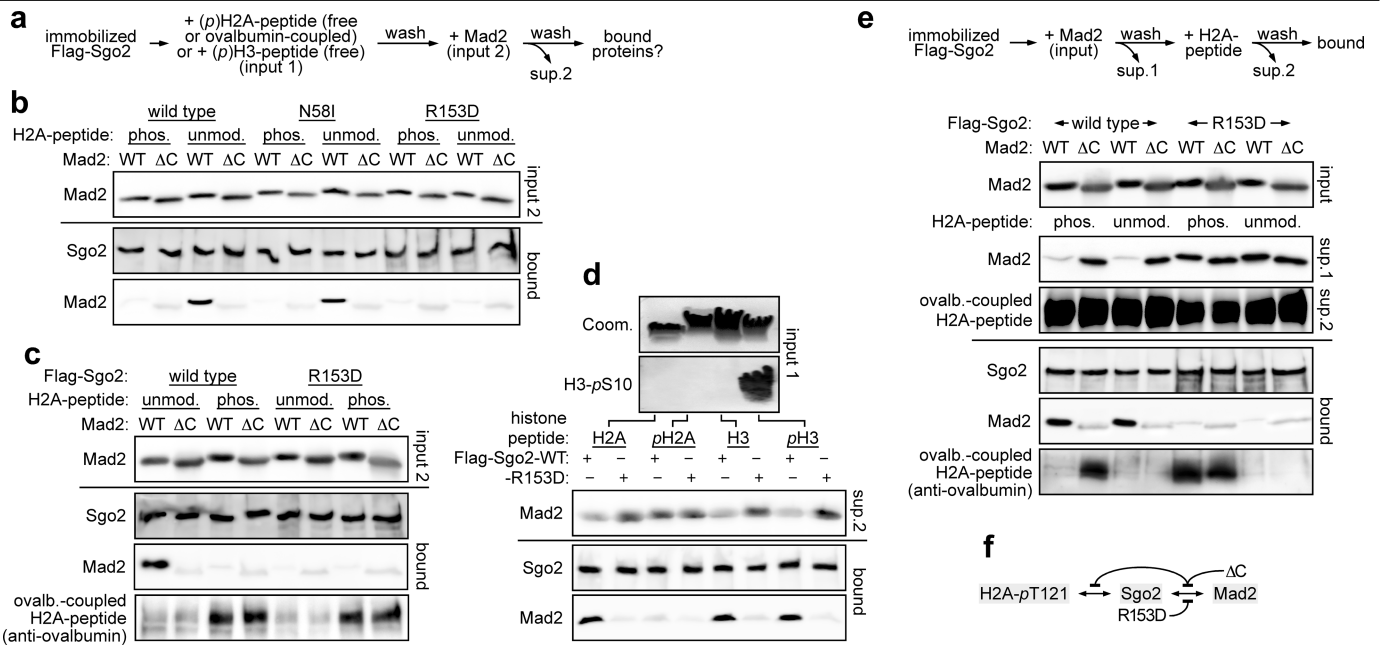
**Extended Data Fig. 5 | Identification of SGO2-binding-deficient separase variants.** Taxol-arrested Hek293T cells expressing transgenic Myc-tagged wild-type separase (WT) or one of the indicated variants (V1-V5) were analysed by IP-immunoblotting using the indicated antibodies. The investigation of

PP2A-binding-deficient variants was motivated by the notion that SGO2-MAD2, like PP2A, preferentially interacts with full-length rather than auto-cleaved separase<sup>38</sup> (see, for example, Fig. 3c). V3 cannot bind PP2A but can bind SGO2-MAD2, indicating overlapping but not identical binding sites.



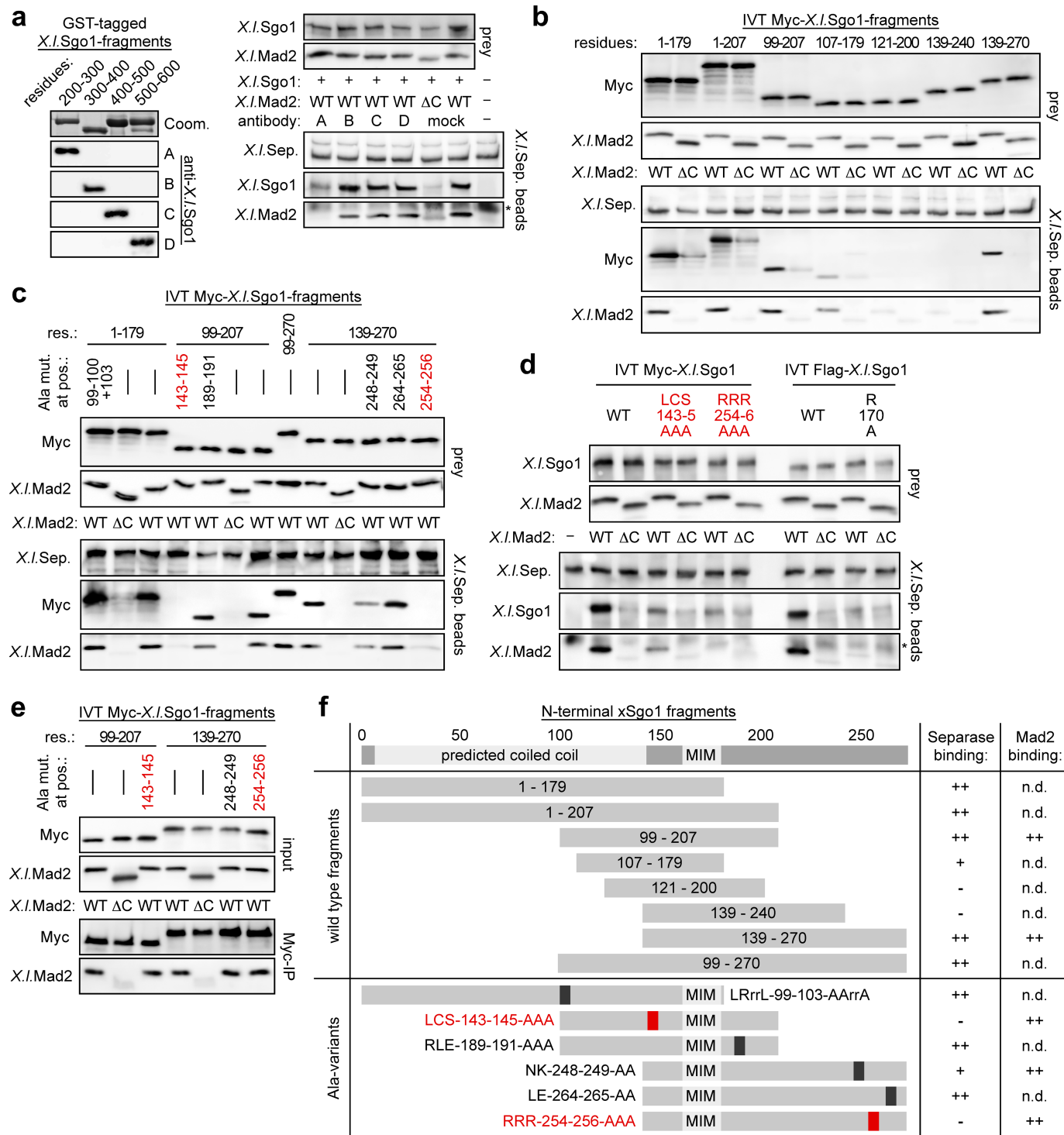
**Extended Data Fig. 6 | Depletion of securin and Sgo2 but not the individual knock-downs result in premature disengagement of centrioles.** HeLa-K cells transfected with the indicated siRNAs were released from a thymidine block and arrested in G2 phase with the CDK1 inhibitor RO-3306. Corresponding lysates were used for immunoblotting (bottom right) and

centrosome isolation followed by immunofluorescence microscopy (top right, representative images) to assess the degree of centriole disengagement as revealed by two C-Nap1 foci. Left, bars show mean of three independent experiments (dots) counting 100 centrosomes each. Scale bar, 1  $\mu$ m.



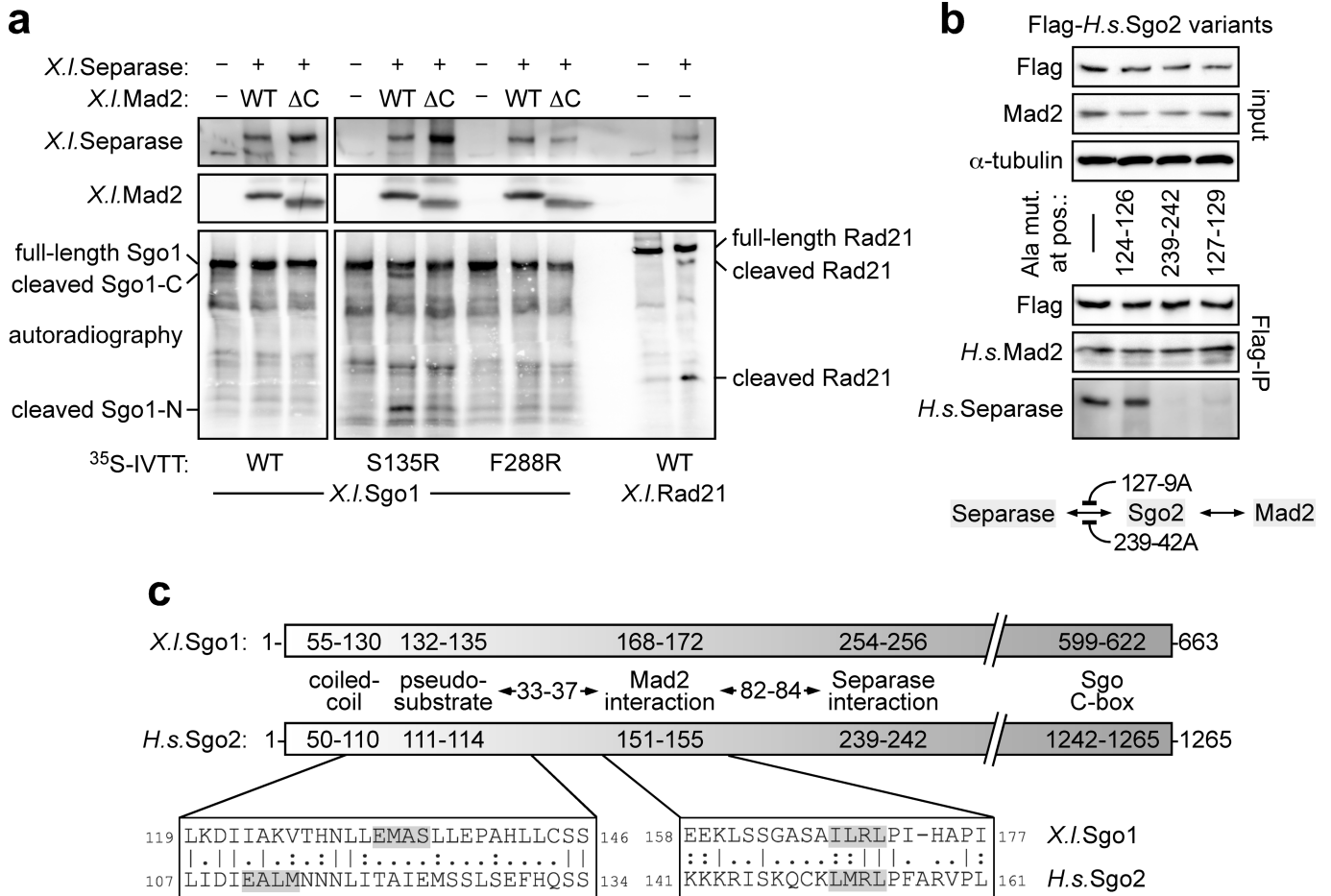
**Extended Data Fig. 7 | Mutually exclusive binding of SGO2 to MAD2 or phosphorylated histone H2A.** **a–d**, Pre-charging of SGO2 with phosphorylated histone H2A blocks subsequent MAD2 binding. **a**, Experimental scheme for experiments shown in **b–d**. Beads loaded with the indicated Flag-SGO2 variants were consecutively incubated first with phosphorylated or unphosphorylated H2A or H3 peptide (input 1) and then with wild-type or, where indicated, C-terminally truncated ( $\Delta$ C) MAD2 (input 2). Following washing (supernatant 2), bound proteins were visualized by immunoblotting. **b**, Usage of free H2A peptides. **c**, Usage of ovalbumin-coupled

H2A peptides to facilitate their detection by standard glycine-SDS-PAGE and immunoblotting. **d**, Phosphorylated histone H3 peptide does not bind to SGO2. Free H2A and H3 peptides, used to interrogate immobilized SGO2, were separated by Tricine-SDS-PAGE<sup>39</sup> and analysed by Coomassie staining and immunoblotting. **e**, Pre-charging of SGO2 with MAD2 blocks subsequent phospho-H2A binding. Experimental scheme (top) and corresponding immunoblotting analysis (bottom). H2A peptides were coupled to ovalbumin for ease of detection. **f**, Cartoon illustrating that SGO2 can bind to H2A phosphorylated on Thr121 or to MAD2 but not both at the same time.



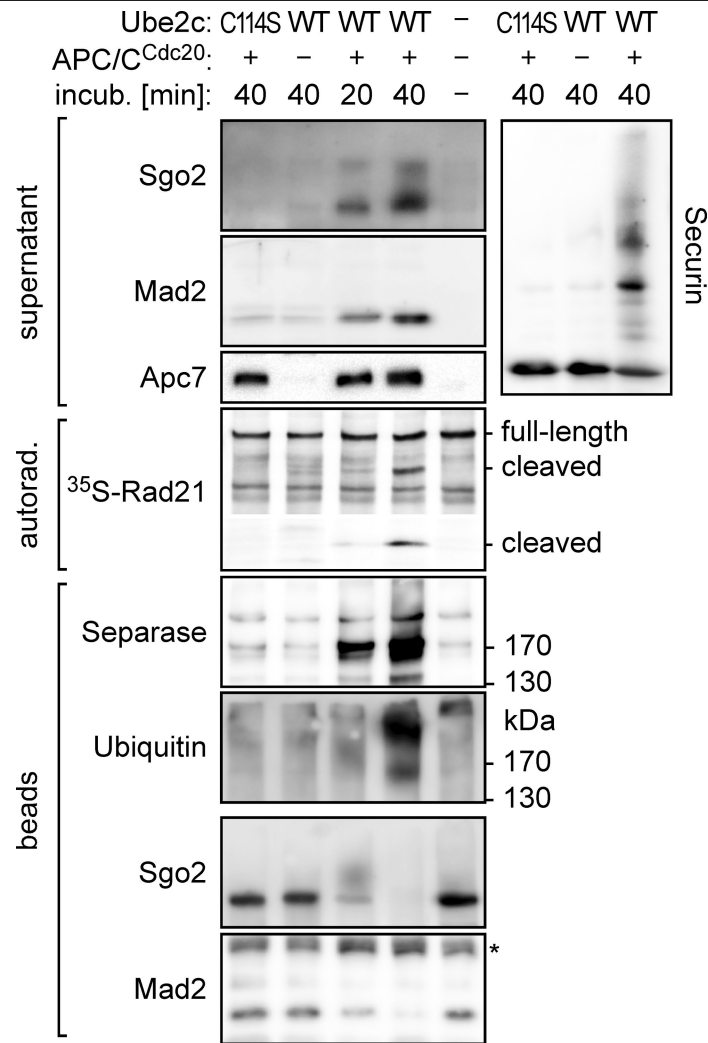
**Extended Data Fig. 8 | Mapping separate-binding sites on *X. laevis* Sgo1. a**, Covering amino acids 200–300 of *X. laevis* Sgo1 with polyclonal antibodies impairs its binding to separate. Region-specific polyclonal *X. laevis* Sgo1 antibodies A–D were characterized (left) and added to in vitro-expressed *X. laevis* Sgo1 and *E. coli*-expressed MAD2 (prey) as indicated. Immobilized *X. laevis* separate isolated by immunoprecipitation from anaphase egg extracts was then added as bait to these mixtures. Separate beads were washed and finally probed for associated proteins by immunoblotting. Mock, unspecific IgG; asterisk, unspecific band. **b, c**, Identification of two sites within *X. laevis* Sgo1 that are relevant for separate binding. Different in vitro translated (IVT) *X. laevis* Sgo1 fragments and variants thereof were combined with wild-type

MAD2 or MAD2-ΔC as indicated (prey). Separate beads as in **a** were combined with these mixtures, washed and analysed for associated proteins by immunoblotting. **d–f**, *X. laevis* Sgo1(143–145A) and Sgo1(254–256A) (red) show compromised separate binding but retain MAD2 binding. **d**, The indicated full-length *X. laevis* Sgo1 variants were assessed for MAD2-dependent separate binding as in **b, c, e**. The indicated *X. laevis* Sgo1 fragments and variants thereof were combined with wild-type MAD2 or MAD2-ΔC, immunoprecipitated via their Myc-tag and assessed for MAD2 binding by immunoblotting. **f**, Summary of the mapping experiments. MIM, Mad2-interaction motif; n.d., not determined.



**Extended Data Fig. 9 | *X. laevis* Sgo1 and human SGO2 share the same order and spacing of separase- and MAD2-binding sites. a**, A point mutation turns *X. laevis* Sgo1 into a Mad2-dependent separase substrate. <sup>35</sup>S-labelled *X. laevis* Sgo1 variants were incubated with wild-type Mad2 or Mad2-ΔC before being assayed for in vitro-cleavage by *X. laevis* separase, which had been immunoprecipitated from anaphase egg extracts. Gels were blotted onto membranes, which were cut and subjected to immunoblotting (top) before reassembly and autoradiography (bottom). **b**, Human (*H.s.*) SGO2(127-129A)

and SGO2(239-242A) show compromised separase binding but retain MAD2 binding. The indicated full-length SGO2 variants were immunoprecipitated via their Flag-tags from transfected, taxol-arrested Hek293T cells and assessed by immunoblotting for binding of MAD2 and separase. See also illustration at bottom. **c**, Cartoon comparing the arrangement of functional domains and alignment of pseudo-substrate and Mad2-binding sites of *X. laevis* Sgo1 and human SGO2. The separase interaction site around position 144 of *X. laevis* Sgo1 and around position 128 of human SGO2 was omitted for clarity.



**Extended Data Fig. 10 | In vitro disassembly of separase-SGO2-MAD2 by APC/C<sup>CDC20</sup>-dependent ubiquitylation.** Immobilized separase-SGO2-MAD2 complex isolated as in Fig. 4a was incubated with ATP, ubiquitin, E1, UBE2S, wild-type or dominant-negative (DN) UBE2C and APC/C<sup>CDC20</sup> (or reference buffer). After removal of the supernatant and washing, the beads were

incubated with <sup>35</sup>S-RAD21 before being analysed by autoradiography and immunoblotting. The autoradiograph shows the relevant upper and lower parts of the same gel. Ubiquitylation of purified securin served as a positive control.

# Separase-triggered apoptosis enforces minimal length of mitosis

<https://doi.org/10.1038/s41586-020-2187-y>

Susanne Hellmuth<sup>1</sup> & Olaf Stemmann<sup>1</sup>✉

Received: 22 March 2019

Accepted: 10 February 2020

Published online: 8 April 2020

 Check for updates

Prolonged mitosis often results in apoptosis<sup>1</sup>. Shortened mitosis causes tumorigenic aneuploidy, but it is unclear whether it also activates the apoptotic machinery<sup>2</sup>. Separase, a cysteine protease and trigger of all eukaryotic anaphases, has a caspase-like catalytic domain but has not previously been associated with cell death<sup>3,4</sup>. Here we show that human cells that enter mitosis with already active separase rapidly undergo death in mitosis owing to direct cleavage of anti-apoptotic MCL1 and BCL-XL by separase. Cleavage not only prevents MCL1 and BCL-XL from sequestering pro-apoptotic BAK, but also converts them into active promoters of death in mitosis. Our data strongly suggest that the deadliest cleavage fragment, the C-terminal half of MCL1, forms BAK/BAX-like pores in the mitochondrial outer membrane. MCL1 and BCL-XL are turned into separase substrates only upon phosphorylation by NEK2A. Early mitotic degradation of this kinase is therefore crucial for preventing apoptosis upon scheduled activation of separase in metaphase. Speeding up mitosis by abrogation of the spindle assembly checkpoint results in a temporal overlap of the enzymatic activities of NEK2A and separase and consequently in cell death. We propose that NEK2A and separase jointly check on spindle assembly checkpoint integrity and eliminate cells that are prone to chromosome missegregation owing to accelerated progression through early mitosis.

The intrinsic pathway of apoptosis is regulated by a balance between pro- and anti-apoptotic BCL2 family proteins that are hallmarked by presence of one to four BCL2 homology (BH) domains<sup>5</sup>. Pore formation by homo-oligomerization of BAK and BAX leads to mitochondrial outer membrane permeabilization (MOMP) and release of cytochrome *c* and other apoptogenic factors from the intermembrane space. MOMP is counteracted by family members such as BCL2 itself, BCL2-like 1 (BCL-XL) and myeloid cell leukaemia 1 (MCL1). These proteins use a hydrophobic groove formed by their BH1–3 domains to sequester the BH3 domain of BAK/BAX and inhibit their self-interaction. BH3-only proteins such as BIM or BAD activate BAK/BAX either directly by transient interaction or indirectly by forcing BAK/BAX off anti-apoptotic BCL2 members through competition<sup>6</sup>. Intrinsic apoptosis in response to excessive cellular stress, such as DNA damage, is initiated by activation of BH3-only proteins, typically via upregulated transcription<sup>5,7</sup>. Other triggers of intrinsic apoptosis are less well understood. Likewise, it remains unclear whether proteins other than BAK/BAX might also be able to form pores and contribute to MOMP.

Separase is the essential trigger protease of all eukaryotic anaphases<sup>4</sup>. Once activated in metaphase, it opens the DNA-embracing cohesin ring complex by cleavage of the kleisin subunit, thus resolving sister chromatid cohesion and enabling chromosome segregation. Separase contains a C-terminal caspase-like proteolytic domain<sup>3</sup>, but it has not been functionally linked to apoptosis. For most of the cell cycle, spindle assembly checkpoint (SAC) signalling ensures that human separase is held inactive by association with securin, SGO2–MAD2 or CDK1–cyclin B1<sup>8,9</sup>. In response to improper attachment of kinetochores to spindle

microtubules, the SAC delays activation of separase and other late mitotic events, thereby giving the cell time for error correction<sup>2,10</sup>. Hyperstimulation of the SAC by spindle toxins such as taxol (paclitaxel) prolongs mitosis<sup>11</sup>. Conversely, SAC impairment results in shortened mitosis, chromosomal instability and tumorigenesis<sup>2</sup>. While prolonged mitosis is known to result in death in mitosis (DiM) or mitotic slippage followed by apoptosis in interphase<sup>1</sup>, it remains unstudied whether shortened mitosis might also trigger intrinsic apoptosis.

## DiM upon premature separase activation

Both depletion of the cohesion-protecting factors SGO1 or sororin and derepression of separase (by co-depletion of SGO2 and securin) result in premature sister chromatid separation<sup>9,12,13</sup> (Extended Data Fig. 1a). This was followed by prolonged mitotic arrest of cells lacking SGO1 or sororin, as previously described<sup>12,13</sup>. However, cells lacking SGO2 and securin exhibited DiM as judged by cleavage of poly(ADP-ribose) polymerase (PARP) and fluorogenic caspase reporters (Extended Data Fig. 1b–h). DiM in cells depleted of SGO2 and securin was specific because it was suppressed by concomitant knockdown of separase (Extended Data Fig. 1g, h). Thus, premature activity of separase rather than premature sister chromatid separation represents an apoptotic stimulus.

## MCL1 and BCL-XL are separase substrates

We speculated that MCL1 and BCL-XL could be relevant targets of separase in DiM because both (1) have previously been linked to apoptosis

<sup>1</sup>Chair of Genetics, University of Bayreuth, Bayreuth, Germany. ✉e-mail: olaf.stemmann@uni-bayreuth.de

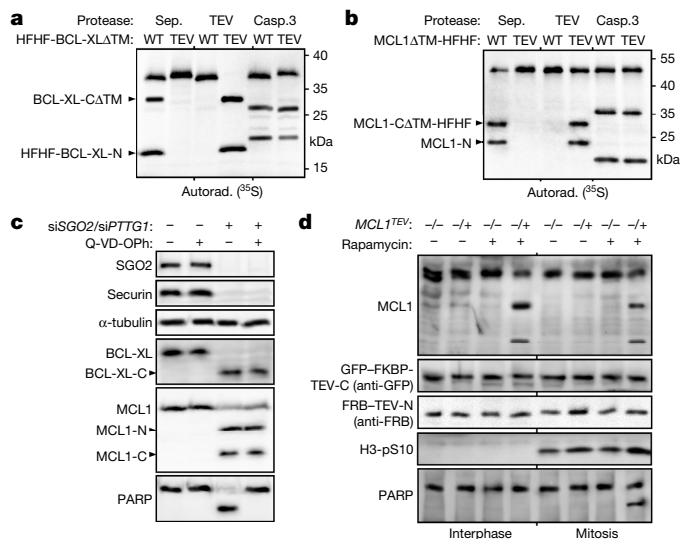


**Fig. 1 | The pro-survival factors MCL1 and BCL-XL are separase substrates.**

**a, b**, Autoradiographies of in vitro cleavage assays in the presence of active NEK2A and ATP. WT, wild type; HFHF, His<sub>6</sub>-Flag-His<sub>6</sub>-Flag tag; ΔTM, transmembrane domain deleted. **c**, siRNA-transfected, taxol-arrested Hek293T cells were treated with Q-VD-Oph or mock-treated and analysed by immunoblotting. siPTTG1, securin depletion. **d**, Immunoblots of parental (−/−) and MCL1<sup>TEV</sup> heterozygous (−/+) hTERT RPE1 cells after (+) or without (−) rapamycin-induced TEV protease complementation. H3-pS10, Ser10-phosphorylated histone H3 (mitotic marker).

after prolonged mitotic arrest<sup>14–17</sup>; (2) have been reported to be cleaved by caspases<sup>18,19</sup>; and (3) contain an ExxR motif that matches the consensus cleavage site of separase close to the caspase cleavage site(s). Indeed, human BCL-XL and MCL1 were cleaved in vitro not only by caspase 3 but also by separase, and the resulting fragments were clearly distinguishable in size (Fig. 1a, b). Replacing 31-ExxR-34 in BCL-XL and 173-ExxR-176 in MCL1 with tobacco etch virus (TEV)-protease cleavage sites required only a few amino acid exchanges (Extended Data Fig. 2a). This rendered both survival factors resistant to separase but susceptible to TEV protease, while leaving cleavage by caspase 3 unaffected (Fig. 1a, b). The proteolytic fragments that were generated by either separase or TEV protease exhibited identical mobilities in SDS-PAGE, thereby indicating that separase cleaves BCL-XL after Arg34 and MCL1 after Arg176. Various in vitro-expressed fragments were used as length standards to confirm the location of the cleavage site for MCL1 (Extended Data Fig. 2b). In mice, the ExxR motif is conserved in BCL-XL but has been replaced with DxxR in MCL1. Still, mouse MCL1 was readily cleaved by separase in vitro (Extended Data Fig. 2c). BCL-XL and MCL1 were also cleaved in human Hek293T, HeLa-K, HCT116, hTERT RPE1 and mouse NIH/3T3 cells during DiM triggered by RNA interference (RNAi) using small interfering RNAs (siRNAs) against *SGO2* and *PTTG1* (which encodes securin) (Extended Data Fig. 2d–g; see also below). Notably, these in vivo cleavages were mediated by separase rather than caspase because (1) Q-VD-Oph, a pan-specific caspase inhibitor, blocked cleavage of PARP but not of BCL-XL and MCL1 (Fig. 1c); (2) fragmentation was not detectable when the endogenous proteins were replaced by their separase-resistant but caspase-sensitive TEV variants (Extended Data Fig. 2d); and (3) MCL1 fragments from Hek293T cells lacking *SGO2* and securin perfectly co-migrated with in vitro-expressed fragments comprising amino acids 1–176 (MCL1-N) and 177–350 (MCL1-C) (Extended Data Fig. 2f). In fact, we never observed caspase-dependent processing of MCL1 or BCL-XL in vivo, although this might be due to our focus on early stages of DiM. Using CRISPR-Cas9 gene editing in hTERT RPE1 cells, we replaced the separase cleavage site with a TEV protease cleavage site in one allele of *MCL1*. Upon activation of ‘split TEV protease’ by

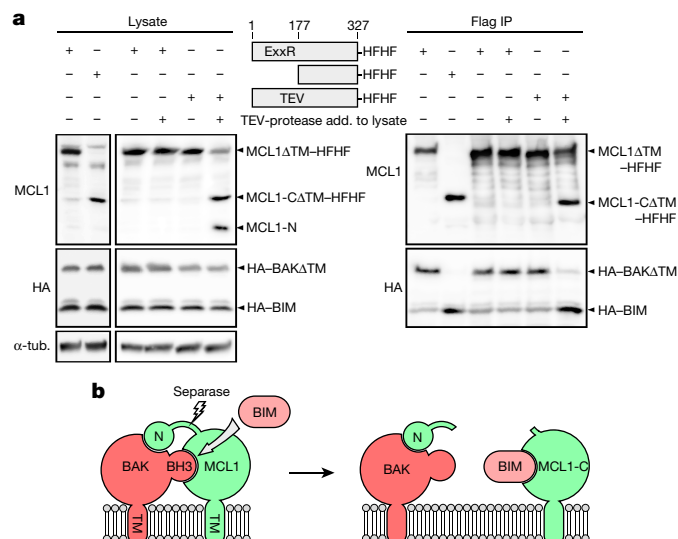


**Fig. 2 | Cleavage of MCL1 by separase enables BH3-only proteins to liberate BAK.**

**a**, Immunoblots of (TEV protease supplemented, +) lysates and Flag immunoprecipitation of transfected, mitotic Hek293T cells expressing the indicated, C-terminally His<sub>6</sub>-Flag-His<sub>6</sub>-Flag (HFHF)-tagged MCL1 fragments together with HA-tagged BAK and BIM. **b**, Model of how separase inactivates MCL1.

rapamycin-induced complementation, half of endogenous MCL1 was cleaved, as expected (Fig. 1d). This was accompanied by considerable PARP cleavage, but only when the cells were in mitosis. Thus, MCL1 cleavage at position 176 is sufficient to initiate DiM during a prometaphase arrest.

### Cleavage of MCL1 and BCL-XL liberates BAK

We investigated whether separase-dependent cleavage affected the interactions of MCL1 and BCL-XL with other BCL2 family members. To this end, we used Flag tags to affinity-purify MCL1 and the corresponding C-terminal separase cleavage fragment from transfected Hek293T cells and analysed them for association with co-expressed BAK relative to the BH3-only protein BIM. Whereas MCL1 preferentially interacted with BAK, as expected, MCL1-C bound only to BIM (Fig. 2a). An analogous experiment was conducted with BCL-XL but using BAD instead of BIM owing to the different binding preference of its C-terminal fragment (Extended Data Fig. 3a). Removal of the N-terminal 34 amino acids switched BCL-XL from binding BAK to binding BAD (Extended Data Fig. 3b). For MCL1, the exchange of binding partners upon cleavage was additionally recapitulated by addition of TEV protease to cell lysate containing the TEV variant of MCL1 (Fig. 2a). The BH4 domain of BCL-2 contributes directly to BAX binding<sup>20</sup>. Similarly, MCL1-N co-purified with BAK from transfected Hek293T cells (Extended Data Fig. 3c), showing that MCL1 contacts BAK not only via its hydrophobic groove but also via its N-terminal domain. We propose that cleavage by separase abolishes the cooperativity of binding, thereby enabling BH3-only proteins such as BIM to supersede BAK from the C-terminal fragment of MCL1 (Fig. 2b). Liberated BAK would then lead to MOMP.

### MCL1-N and MCL1-C actively promote apoptosis

We made the counter-intuitive observation that DiM induced by siRNAs against *SGO2* and *PTTG1* was alleviated by co-depletion of MCL1 (Fig. 3a, b) and almost fully rescued by co-depletion of both MCL1 and BCL-XL (Extended Data Fig. 3d, e). While this showed that these two BCL2 family proteins are the crucial—if not the only—substrates of separase during DiM, it also suggested that the separase cleavage fragments of MCL1

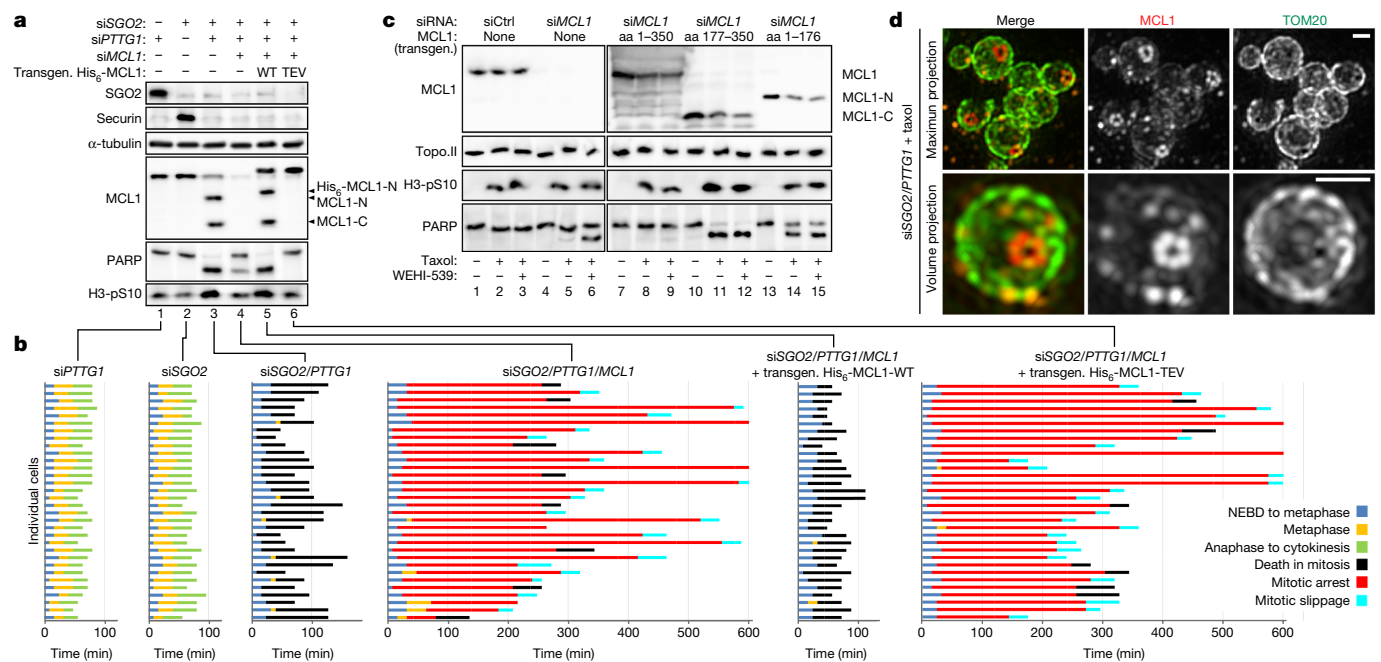


**Fig. 3 | Both separase cleavage fragments of MCL1 are pro-apoptotic and MCL1-C forms macropores during late stages of DiM.** **a, b,** HeLa-K cells transfected with the indicated siRNAs and expression plasmids were released from early S-phase arrest, supplemented with the DNA stain SiR-Hoechst and a fluorogenic caspase-3/7 reporter and analysed by immunoblotting (**a**; 10 h after release) and live cell imaging (**b**; cell fate profiles). **c,** Immunoblots of

MCL1 or control-depleted HeLa-K cells expressing transgenic full-length MCL1 or fragments thereof as indicated. **d,** Immunofluorescence 2D SIM of SGO2- and securin-depleted Hek293T cells undergoing DiM. Note the absence of the mitochondrial outer membrane marker TOM20 from the centres of MCL1 rings. Scale bars, 0.5 μm.

and BCL-XL are apoptogenic. Consistent with this hypothesis, the mitigation of PARP cleavage by depletion of BCL-XL or MCL1 (Extended Data Fig. 2d, lanes 4–6) was reversed by expression of siRNA-resistant transgenic BCL-XL or MCL1 but not their separase-resistant TEV variants (lanes 7–10). Given the stronger effects of MCL1 depletion, we further studied its cleavage fragments individually. Full-length MCL1, MCL1-N or MCL1-C was expressed in Hek293T cells in which endogenous MCL1 (but not SGO2 or securin) was depleted by RNAi. Short-term absence of MCL1 caused very little apoptosis on its own but led to some cell death in conjunction with chemical inhibition of BCL-XL by WEHI-539 (Fig. 3c, lanes 5 and 6). This phenotype was rescued by transgenic full-length MCL1 (lane 9). Notably, expression of MCL1-N or MCL1-C resulted in PARP cleavage even in the absence of WEHI-539, with the C-terminal fragment having the stronger effect (lanes 11 and 14). PARP cleavage correlated with annexin V and propidium iodide staining as additional markers for apoptosis (Extended Data Fig. 3f, g). Induction of apoptosis by MCL1-N or MCL1-C did not occur in interphase but only in taxol-treated cultures (Fig. 3c, Extended Data Fig. 3f). Time-lapse microscopy further illustrated that HeLa-K cells expressing MCL1-N or MCL1-C also underwent DiM in the absence of spindle toxin (Extended Data Fig. 3h, i). Thus, separase-dependent cleavage not only extinguishes the pro-survival activity of MCL1 but also creates two fragments, each of which kills cells upon entry into mitosis without requiring prolonged mitotic arrest. Investigation of MCL1-N-induced apoptosis suggested that it promotes both liberation of BAK and separase-dependent cleavage of BCL-XL by a positive feedback mechanism (Extended Data Fig. 4).

### MCL1-C kills by mitosis-specific MOMP

Interaction analyses of epitope-tagged forms of MCL1 revealed that MCL1-C exhibited homotypic interactions, whereas uncleaved, full-length MCL1 could associate neither with itself nor with MCL1-C (Extended Data Fig. 5a). Self-interaction of MCL1-C and its ability to

induce PARP cleavage were blocked by deletion of the transmembrane domain or presence of the BH3-mimicking MCL1-inhibitor A-1210477, which blocked not only binding of BAK to full-length MCL1 but also binding of BIM to MCL1-C (Extended Data Fig. 5b–d). Tandem affinity purification of co-expressed, differently tagged MCL1-C further revealed that homo-oligomerization and BIM binding are mutually exclusive (Extended Data Fig. 5d), which suggests that BIM interacts with MCL1-C only transiently and disengages upon MCL1-C self-interaction. These observations are reminiscent of the requirements for BAK/BAX-dependent MOMP<sup>21–23</sup> and, thus, are consistent with pore formation by MCL1-C. Notably, homotypic MCL1-C interactions occurred only in extracts from mitotic, and not interphase, cells (Extended Data Fig. 5b); this is consistent with the finding that the pro-apoptotic effect of MCL1-C is cell-cycle-dependent. According to our hypothesis, separase-induced DiM should be delayed or diminished, but still occur, in the absence of BAK and BAX, whereas MCL1-C-induced DiM should be independent of them. Using time-resolved fractionation of chromatin and organelles, including mitochondria, from the cytosol followed by immunoblotting analyses, we compared parental HCT116 and *BAK1<sup>-/-</sup> BAX<sup>-/-</sup>* double-knockout cells as they went synchronously from G2- through M-phase. Whereas the kinetics of MCL1-cleavage were indistinguishable in the absence of SGO2 and securin, the release of cytochrome c into the cytosol and PARP cleavage were delayed, but still occurred, in the absence of BAK and BAX (Extended Data Fig. 6a, b). In fact, PARP cleavage and accumulation of Ser139-phosphorylated histone H2A-X (γH2AX) in the absence of BAK and BAX were less affected during DiM induced by siRNAs against *SGO2* and *PTTG1* than during staurosporine-induced apoptosis<sup>24</sup> (Extended Data Fig. 6c). Notably, the timing and extent of cytochrome c release and PARP cleavage were the same in both cell lines when DiM was induced by MCL1-C expression (Extended Data Fig. 6d).

At later stages of intrinsic apoptosis, the mitochondrial network fragments into globular structures, and BAK and BAX form large rings and macropores within the outer membrane<sup>25–27</sup>. Immunofluorescence

microscopy of MCL1 and the MOM protein TOM20 in taxol-arrested Hek293T cells showed that MCL1 and TOM20 colocalized during DiM, and this colocalization increased when the network dissolved into spheres (Extended Data Fig. 7a, b). Notably, 2D structural illumination microscopy (SIM) revealed the formation of large, typically 0.3- $\mu$ m rings by MCL1-C in SGO2- and securin-depleted cells undergoing DiM (Fig. 3d, Extended Data Fig. 7c). TOM20 appeared largely absent from the centre of the rings, suggesting that they represent macropores.

Phosphorylation might explain why the MOMP activity of MCL1-C is specific to mitosis. A candidate approach identified Thr301. Changing this residue to phosphorylation-mimicking Glu enabled MCL1-C to induce apoptosis also in interphase, whereas changing Thr301 to Ala abrogated the pro-apoptotic and self-interaction properties of MCL1-C (Extended Data Figs. 5d, 7d, e). The detection of affinity-purified MCL1-C by a phospho-Thr-specific antibody was limited to mitosis and abolished by the Thr301Ala mutation, suggesting that this position is phosphorylated in vivo (Extended Data Fig. 7d)—possibly by aurora B (Extended Data Fig. 7f, g). Existing structural information places Thr301 of MCL1 at the end of  $\alpha$ -helix 6, and dimerization of the corresponding helix has been reported to be involved in homo-oligomerization of BAK<sup>28,29</sup>. Sequence alignment implies that the Thr301-equivalent position is occupied by a Glu in BAX (Extended Data Fig. 7h). When we changed this constitutively negatively charged residue at position 146 to Ala, the pro-apoptotic function of BAX was abrogated, whereas changing it to Thr rendered BAX a largely mitosis-specific effector of cell death (Extended Data Fig. 7i). A salt bridge at the end of  $\alpha$ -helix 6 might therefore be required for pore formation (Extended Data Fig. 7j) and explain why MCL1-C becomes pro-apoptotic only upon phosphorylation of Thr301 during mitosis, whereas MOMP by wild-type BAX is independent of the cell cycle.

### Importance of phosphorylation by NEK2A

In unperturbed cells, MCL1 and BCL-XL are present at the onset of anaphase. The question arises of why then cells do not die when separase becomes active on schedule. Considering that cleavage of meiotic kleisin by separase requires its phosphorylation<sup>30</sup>, we tested the effect of various kinases when first establishing MCL1 and BCL-XL cleavage by separase in vitro (Extended Data Fig. 8). These analyses revealed that cleavage of MCL1 by separase essentially requires NEK2A, while cleavage of BCL-XL was enabled by NEK2A and (less so) CDK1/2-cyclin A2 (note that NEK2A was included in Fig. 1a, b and Extended Data Figs. 2b, c, 4c). NEK2A and CDK1/2-cyclin A are special among mitotic kinases and APC/C substrates in that they are degraded early—that is, at a time when separase activation is still blocked by SAC signalling<sup>31,32</sup>.

To identify phosphorylation sites within MCL1 and BCL-XL that are relevant for cleavage, we changed candidate serine and threonine residues to alanine or phosphorylation-mimicking acidic residues and screened corresponding variants in kinase and/or cleavage assays. These analyses revealed the following (Extended Data Fig. 9): (1) the NEK2A-dependent phosphorylation of Ser60 and Thr163 is essential for separase-dependent cleavage of MCL1, and phosphorylation of Ser159 further improves it. (2) NEK2A and CDK1/2-cyclin A2 phosphorylate Ser4 and Ser164, and Ser62, respectively, of BCL-XL to enable its cleavage by separase. (3) The phosphorylation-mimicking variants MCL1(S/T60, I59, I63D/Q) and BCL-XL(S4,62, I64D) are cleaved by separase in the absence of kinases.

The above findings suggested that separase does not trigger DiM at anaphase onset merely because NEK2A (and cyclin A2) is absent by then and MCL1 and BCL-XL—owing to dephosphorylation—no longer represent separase substrates (Fig. 4a, top). As a corollary, any temporal overlap between the enzymatic activities of NEK2A and separase should cause DiM. Indeed, this explains why constitutive activity of separase causes early mitotic cell death and why knockdown of NEK2A largely suppressed DiM induced by siRNAs against SGO2 and

PTTG1 (Extended Data Fig. 1g, h). Extending the window of NEK2A activity until separase activation in anaphase should also cause DiM (Fig. 4a, middle). Live cell imaging of transfected HeLa-K cells revealed that overexpression of wild-type NEK2A was compatible with normal mitosis, whereas production of a C-terminally truncated, stabilized variant ( $\Delta$ MR)<sup>31</sup> triggered DiM, typically shortly after anaphase onset (Extended Data Figs. 3i, 10a). This was confirmed by time-resolved immunoprecipitation and western analysis of cells synchronously undergoing late mitosis. NEK2A- $\Delta$ MR-expressing and mock-treated populations both degraded cyclin B1 and securin and lost SGO2 from separase with similar kinetics (Extended Data Fig. 10b). However, only in NEK2A- $\Delta$ MR-containing cells did activation of separase coincide with cleavage of MCL1 and PARP. Consistent with MCL1 and BCL-XL being the relevant targets, apoptosis in anaphase was also triggered by expression of the constitutive separase substrates BCL-XL(S4,62, I64D) or MCL1(S/T-60, I59, I63D/Q) instead of NEK2A- $\Delta$ MR (Extended Data Fig. 10c, d). Thus, NEK2A must be degraded in early mitosis to prevent separase from killing cells in anaphase.

### Separase-induced DiM increases with MCL1

To investigate whether DiM in response to stabilization of NEK2A was graded with MCL1 dosage, we transfected siRNA or plasmids into Hek293T cells to express wild-type NEK2A or the  $\Delta$ MR variant and, simultaneously, to reduce or increase the amount of MCL1. When transgenic NEK2A was wild-type and, hence, degraded upon entry into mitosis, or when NEK2A- $\Delta$ MR expression was combined with MCL1 depletion, cells showed no signs of apoptosis (Fig. 4b, Extended Data Fig. 11a–c). As seen before, NEK2A- $\Delta$ MR induced some DiM at endogenous levels of MCL1. However, annexin V staining and PARP cleavage increased with increasing levels of (transgene-encoded) MCL1 and cleavage fragments thereof. These data suggest that pharmacological inhibition of early mitotic NEK2A degradation should preferentially kill MCL1-overexpressing cells, which are a hallmark of many cancers<sup>33</sup>.

### A minimal duration of mitosis checkpoint

The SAC is active in each M-phase and chiefly determines its duration<sup>10</sup>. Abrogation of the SAC results in chromosomal instability owing to accelerated progression through mitosis<sup>2</sup>. We investigated whether, under these conditions, separase might become active when NEK2A has not yet been fully degraded (Fig. 4a, bottom). When MAD2 and the SAC kinase BUBR1 were depleted by RNAi, HeLa-K cells that had been released from a thymidine arrest degraded securin and cyclin B1 earlier than control cells; this correlated with earlier auto-cleavage of separase, as expected (Fig. 4c). At the same time, degradation of NEK2A and the disappearance of a corresponding MCL1-S60 phosphorylation mark were delayed, which we attribute to competition by other substrates for the APC/C (Fig. 4c, Extended Data Fig. 11d). Notably, this was accompanied by cleavage of MCL1, BCL-XL and PARP and appearance of a sub-G1 peak in flow cytometry, which is another hallmark of apoptotic cells. As seen before, these phenotypes were largely suppressed by co-depletion of MCL1 and BCL-XL and fully suppressed by additional expression of separase-resistant TEV variants of MCL1 and BCL-XL, but re-installed by transfection with the corresponding wild-type transgenes. Cleavage of MCL1, BCL-XL and PARP also occurred upon individual depletion of MAD2 or BUBR1, albeit to lesser extent (Extended Data Fig. 11e). It also occurred in both mouse and human cells upon chemical inhibition of the SAC kinase MPS1 with reversine (Fig. 4d, Extended Data Fig. 11e). Thus, in mammalian cells SAC abrogation suffices to induce cleavage of MCL1 and BCL-XL by separase and consequent DiM. A corollary is that the few existing SAC-deficient tumour cell lines (unless slowed in mitotic progression

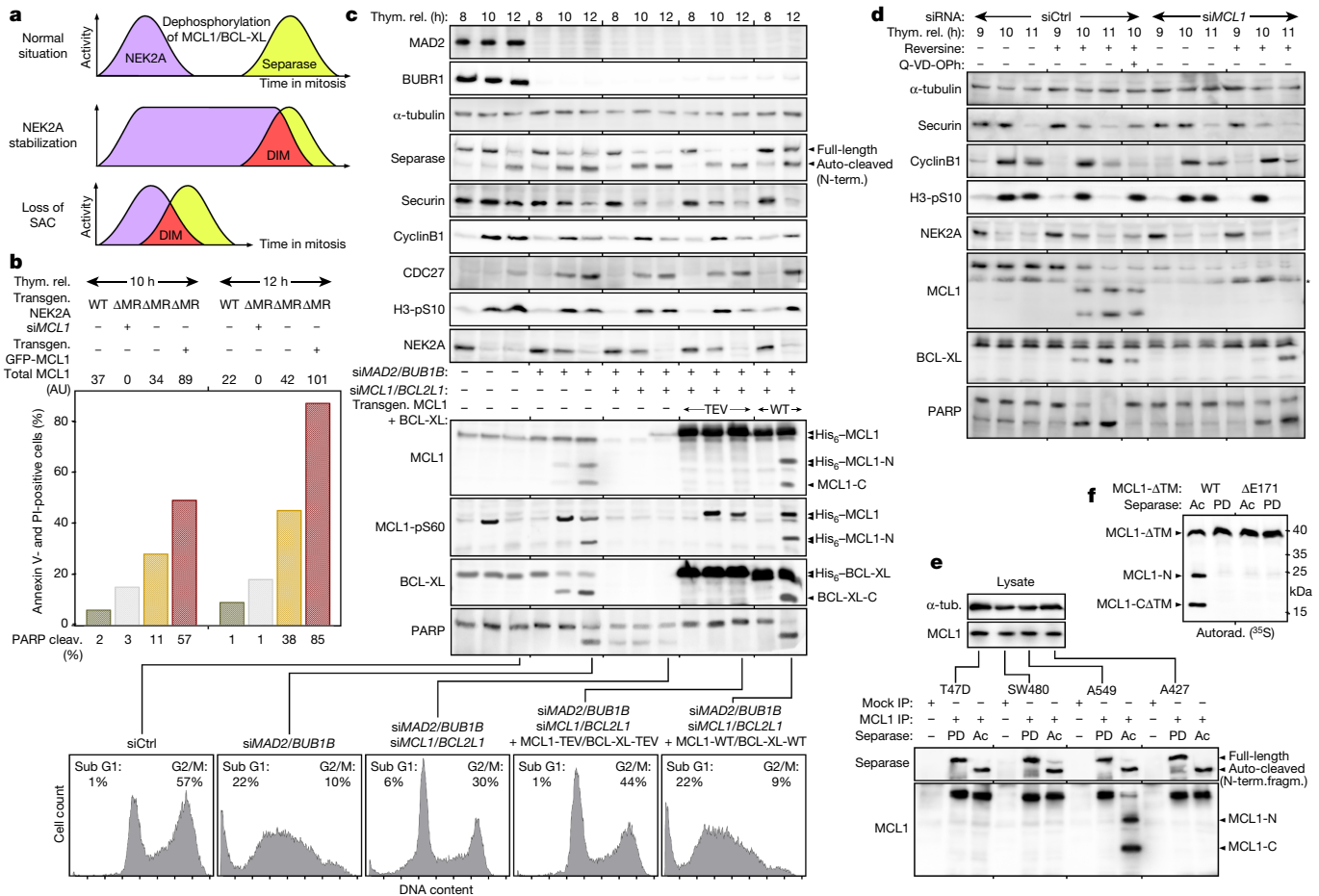


**Fig. 4 | DiM due to simultaneous activity of NEK2A and separase is graded by MCL1 level and triggered by SAC deficiency.** **a**, Both prolonged activity of NEK2A (middle) and speeded-up mitosis due to SAC deficiency (bottom) cause DiM. **b**, Fluorescence microscopic quantification of annexin V- and propidium iodide (PI)-positive Hek293T cells transfected with siMCL1 and expression plasmids for GFP-MCL1 and NEK2A-WT or NEK2A-ΔMR, as indicated, and released for 10–12 h from thymidine arrest (thy. rel.). Expression of MCL1 and degree of PARP cleavage were quantified by densitometry of immunoblots (Extended Data Fig. 11b). **c**, HeLa-K cells transfected with the indicated siRNAs

and expression plasmids were released from thymidine arrest and analysed by immunoblotting and propidium iodide staining with flow cytometry 8–12 h thereafter. siBUB1A, BUBR1 depletion; siBCL2L1, BCL-XL depletion. **d**, Time-resolved immunoblots of NIH/3T3 cells transfected with indicated siRNAs, pre-synchronized with thymidine, and treated with Q-VD-OPh and/or reversine, undergoing mitosis. Asterisk, nonspecific band. **e**, Immunoblots of lysates and NEK2A/separase-treated Mcl1 immunoprecipitations from the indicated cell lines. **f**, Autoradiograph of in vitro-expressed, NEK2A/separase-treated <sup>35</sup>S-MCL1-WT and <sup>35</sup>S-MCL1-ΔE171.

by SAC-independent means<sup>34</sup>) should have found a way to avoid cleavage of MCL1 and BCL-XL. We immunoprecipitated MCL1 from four cancer cell lines: partially SAC-compromised SW480, SAC deficient T47D and A427 and, as a control, SAC-proficient A549 cells<sup>11,35,36</sup>. Notably, only MCL1 from A549 cells was cleaved upon incubation with NEK2A and separase (Fig. 4e). It is unclear how MCL1 from the other three cell lines is rendered separase-resistant, but it is not due to the mere absence of p53 (Extended Data Fig. 11f). Cancer-associated MCL1 variants seem to be rare. However, of the few catalogued in the Catalogue of Somatic Mutations in Cancer (COSMIC) database<sup>37</sup>, deletion of Glu171 is by far the most abundant one, being identified ten times in six studies. Although it leaves the ExxR motif intact, unexpectedly, this mutation renders MCL1 resistant to separase (Fig. 4f).

**Conclusion**

In most cases studied, the intrinsic pathway of apoptosis is triggered by transcriptional upregulation of BH3-only protein expression<sup>5,7</sup>. Here, we describe a mechanism of DiM, which is probably conserved in vertebrates (Extended Data Fig. 12) and consists of separase-dependent

cleavage of MCL1 and BCL-XL and their concurrent transformation from pro-survival into mitosis-specific pro-apoptotic factors. Our results strongly suggest that the deadliest fragment, MCL1-C, permeabilizes the mitochondrial outer membrane by forming pores. Because separase-dependent cleavage of BCL-XL is also sufficient for DiM, the same might be true of BCL-XL-C. Degradation of MCL1 was causally linked to apoptosis upon mitotic arrest, but exactly how MCL1 is removed remains unknown<sup>15,16</sup>. Although we have not done so here, it will therefore be interesting to investigate whether MCL1 somehow becomes phosphorylated and separase-activated during prolonged mitosis. Here we studied shortened mitosis. Our results show that abrogation of SAC results in DiM owing to simultaneous activity of NEK2A and separase (Fig. 4a, bottom). We propose that NEK2A and separase form a surveillance mechanism that eliminates SAC-deficient cells that would otherwise be doomed to massive chromosomal instability and aneuploidy, thereby ensuring the survival of cells with the correct length of M-phase and protecting the organism from tumorigenesis. This ‘minimal duration of early mitosis checkpoint’ (DMC) might explain why mutational inactivation of SAC genes in cancer is rare<sup>35,38</sup>.

## Online content

Any methods, additional references, Nature Research reporting summaries, source data, extended data, supplementary information, acknowledgements, peer review information; details of author contributions and competing interests; and statements of data and code availability are available at <https://doi.org/10.1038/s41586-020-2187-y>.

1. Gascoigne, K. E. & Taylor, S. S. Cancer cells display profound intra- and interline variation following prolonged exposure to antimetabolic drugs. *Cancer Cell* **14**, 111–122 (2008).
2. Michel, L. S. et al. MAD2 haplo-insufficiency causes premature anaphase and chromosome instability in mammalian cells. *Nature* **409**, 355–359 (2001).
3. Lin, Z., Luo, X. & Yu, H. Structural basis of cohesin cleavage by separase. *Nature* **532**, 131–134 (2016).
4. Wirth, K. G. et al. Separase: a universal trigger for sister chromatid disjunction but not chromosome cycle progression. *J. Cell Biol.* **172**, 847–860 (2006).
5. Galluzzi, L. et al. Molecular mechanisms of cell death: recommendations of the Nomenclature Committee on Cell Death 2018. *Cell Death Differ.* **25**, 486–541 (2018).
6. Letai, A. et al. Distinct BH3 domains either sensitize or activate mitochondrial apoptosis, serving as prototype cancer therapeutics. *Cancer Cell* **2**, 183–192 (2002).
7. Villunger, A. et al. p53- and drug-induced apoptotic responses mediated by BH3-only proteins puma and noxa. *Science* **302**, 1036–1038 (2003).
8. Kamenz, J. & Hauf, S. Time to split up: dynamics of chromosome separation. *Trends Cell Biol.* **27**, 42–54 (2017).
9. Hellmuth, S. et al. Securin-independent regulation of separase by checkpoint-induced shugoshin–MAD2. *Nature* <https://www.doi.org/10.1038/s41586-020-2182-3> (2020).
10. Taylor, S. S. & McKeon, F. Kinetochore localization of murine Bub1 is required for normal mitotic timing and checkpoint response to spindle damage. *Cell* **89**, 727–735 (1997).
11. Li, Y. & Benezra, R. Identification of a human mitotic checkpoint gene: hSMAD2. *Science* **274**, 246–248 (1996).
12. Rankin, S., Ayad, N. G. & Kirschner, M. W. Sororin, a substrate of the anaphase-promoting complex, is required for sister chromatid cohesion in vertebrates. *Mol. Cell* **18**, 185–200 (2005).
13. Tang, Z., Sun, Y., Harley, S. E., Zou, H. & Yu, H. Human Bub1 protects centromeric sister-chromatid cohesion through Shugoshin during mitosis. *Proc. Natl Acad. Sci. USA* **101**, 18012–18017 (2004).
14. Bennett, A. et al. Inhibition of Bcl-xL sensitizes cells to mitotic blockers, but not mitotic drivers. *Open Biol.* **6**, 160134 (2016).
15. Haschka, M. D. et al. The NOXA-MCL1-BIM axis defines lifespan on extended mitotic arrest. *Nat. Commun.* **6**, 6891 (2015).
16. Sloss, O., Topham, C., Diez, M. & Taylor, S. Mcl-1 dynamics influence mitotic slippage and death in mitosis. *Oncotarget* **7**, 5176–5192 (2016).
17. Topham, C. et al. MYC is a major determinant of mitotic cell fate. *Cancer Cell* **28**, 129–140 (2015).
18. Clem, R. J. et al. Modulation of cell death by Bcl-XL through caspase interaction. *Proc. Natl Acad. Sci. USA* **95**, 554–559 (1998).
19. Michels, J. et al. Mcl-1 is required for Akata6 B-lymphoma cell survival and is converted to a cell death molecule by efficient caspase-mediated cleavage. *Oncogene* **23**, 4818–4827 (2004).
20. Barclay, L. A. et al. Inhibition of pro-apoptotic BAX by a noncanonical interaction mechanism. *Mol. Cell* **57**, 873–886 (2015).
21. Brouwer, J. M. et al. Conversion of Bim-BH3 from activator to inhibitor of Bak through structure-based design. *Mol. Cell* **68**, 659–672.e659 (2017).
22. Czabotar, P. E. et al. Bax crystal structures reveal how BH3 domains activate Bax and nucleate its oligomerization to induce apoptosis. *Cell* **152**, 519–531 (2013).
23. Dai, H. et al. Transient binding of an activator BH3 domain to the Bak BH3-binding groove initiates Bak oligomerization. *J. Cell Biol.* **194**, 39–48 (2011).
24. Wang, C. & Youle, R. J. Predominant requirement of Bax for apoptosis in HCT116 cells is determined by Mcl-1's inhibitory effect on Bak. *Oncogene* **31**, 3177–3189 (2012).
25. Große, L. et al. Bax assembles into large ring-like structures remodeling the mitochondrial outer membrane in apoptosis. *EMBO J.* **35**, 402–413 (2016).
26. Salvador-Gallego, R. et al. Bax assembly into rings and arcs in apoptotic mitochondria is linked to membrane pores. *EMBO J.* **35**, 389–401 (2016).
27. McArthur, K. et al. BAK/BAX macropores facilitate mitochondrial herniation and mtDNA efflux during apoptosis. *Science* **359**, eaao6047 (2018).
28. Day, C. L. et al. Solution structure of pro-survival Mcl-1 and characterization of its binding by proapoptotic BH3-only ligands. *J. Biol. Chem.* **280**, 4738–4744 (2005).
29. Dewson, G. et al. Bak activation for apoptosis involves oligomerization of dimers via their  $\alpha 6$  helices. *Mol. Cell* **36**, 696–703 (2009).
30. Kudo, N. R. et al. Role of cleavage by separase of the Rec8 kleisin subunit of cohesin during mammalian meiosis I. *J. Cell Sci.* **122**, 2686–2698 (2009).
31. Hayes, M. J. et al. Early mitotic degradation of Nek2A depends on Cdc20-independent interaction with the APC/C. *Nat. Cell Biol.* **8**, 607–614 (2006).
32. Wolthuis, R. et al. Cdc20 and Cks direct the spindle checkpoint-independent destruction of cyclin A. *Mol. Cell* **30**, 290–302 (2008).
33. Beroukhi, R. et al. The landscape of somatic copy-number alteration across human cancers. *Nature* **463**, 899–905 (2010).
34. Wild, T. et al. The spindle assembly checkpoint is not essential for viability of human cells with genetically lowered APC/C activity. *Cell Rep.* **14**, 1829–1840 (2016).
35. Tighe, A., Johnson, V. L., Albertella, M. & Taylor, S. S. Aneuploid colon cancer cells have a robust spindle checkpoint. *EMBO Rep.* **2**, 609–614 (2001).
36. Weitzel, D. H. & Vandré, D. D. Differential spindle assembly checkpoint response in human lung adenocarcinoma cells. *Cell Tissue Res.* **300**, 57–65 (2000).
37. Bamford, S. et al. The COSMIC (Catalogue of Somatic Mutations in Cancer) database and website. *Br. J. Cancer* **91**, 355–358 (2004).
38. Hernandez, E. et al. Molecular analyses of the mitotic checkpoint components hSMAD2, hBUB1 and hBUB3 in human cancer. *Int. J. Cancer* **95**, 223–227 (2001).

**Publisher's note** Springer Nature remains neutral with regard to jurisdictional claims in published maps and institutional affiliations.

© The Author(s), under exclusive licence to Springer Nature Limited 2020

## Methods

## Antibodies

Antibodies generated within this study were raised and purified as described<sup>9</sup>. The following antibodies were used for immunoblotting and immunofluorescence microscopy (IFM): Rabbit anti-separase<sup>39</sup>, rabbit anti-sororin<sup>40</sup>, rabbit anti-PIN1<sup>41</sup>, goat anti-CDC27<sup>42</sup>, mouse anti-GFP<sup>43</sup>, mouse anti-Flag (1:2,000; Sigma-Aldrich, M2), rabbit anti-SGO2 (1:1,000; Bethyl, A301-262A), rabbit or guinea pig anti-SGO2 (1.5 µg/ml; anti-DVPPRESHSHSDQSSKC), rabbit anti-SGO1 (1:500; Abcam, ab21633), mouse anti-securin (1:1,000; MBL, DCS-280), rabbit anti-phosphoSer10-histone H3 ('H3-pS10'; 1:1,000; Millipore, 06-570), mouse anti-cyclin B1 (1:1,000; Millipore, 05-373), rabbit anti-cleaved caspase 3 (Asp175; 1:1,000; Cell Signaling, 5A1E), rabbit anti-BCL-XL (1:1,000; Cell Signaling, 2762), mouse anti-MCL1 (1:800; BioLegend, W16014A), guinea-pig anti-MCL1 (0.75 µg/ml; for IFM 1.5 µg/ml; raised against amino acids 1–327 (ΔTM) of human MCL1), guinea-pig anti-phosphoSer10-MCL1 ('MCL1-pS60'; 0.5 µg/ml; for IFM 1 µg/ml; anti-CVIGGpSAGA, liberated from reactivity towards CVIGGSAGA), anti-TOM20 (1:500; Santa-Cruz Biotechnology, F10), mouse anti-cytochrome c (1:1,000; BD Pharmingen, 7H8.2C12), mouse anti-BubR1 (1:1,000; BD Transduction Laboratories, clone 9), rabbit anti-BAX (1:1,000; Abcam, ab32503), rabbit anti-BAK (1:1,000; Abcam, ab32371), rabbit anti-MAD2 (1:1,000; Bethyl, A300-300A), rabbit anti-PARP (1:800; Cell Signaling, 46D11), mouse anti-PARP (1:1,000; Calbiochem, AM30), anti-MBP monoclonal (1:1,000; NEB Biolabs, E8038S, HRP-conjugated), mouse anti-NEK2 (1:600; BD Transduction Laboratories, clone 20), mouse anti-RGS-His<sub>6</sub> (1:1,000; Qiagen 34610), rabbit anti-phosphoSer139-histone H2A.X ('γH2AX'; 1:5,000; Millipore, EP854(2)Y), mouse anti-topoisomerase IIα (1:1,000; Enzo Life Sciences, IC5), mouse anti-cyclin A2 (1:200; Santa Cruz Biotechnology, 46B11), rat anti-HA (1:2,000; Roche, 3F10) and mouse anti-α-tubulin (hybridoma supernatant 1:200; DSHB, 12G10). Nonspecific rabbit, mouse and guinea pig IgGs were from Sigma-Aldrich. For immunoprecipitation experiments, the following affinity matrices and antibodies were used: mouse anti-Flag agarose (Sigma-Aldrich, M2), rat anti-HA agarose (Roche, clone 3F10), anti-GFP nanobody covalently coupled to NHS-agarose (GE Healthcare), mouse anti-RGS-His<sub>6</sub> or guinea pig anti-MCL1 coupled to protein G sepharose (GE Healthcare) and rabbit anti-BCL-XL coupled to protein A sepharose (GE Healthcare). For non-covalent coupling of antibodies, 10 µl of the respective matrix was rotated with 2–5 µg antibody in the presence of 1% w/v BSA (Roth) for 90 min at room temperature and then washed three times. Secondary antibodies for immunoblotting were horseradish peroxidase (HRP)-conjugated goat anti-rabbit, anti-mouse and anti-guinea pig IgGs (Sigma-Aldrich, all used at 1:20,000). The following secondary antibodies were used for IFM (all 1:500): Cy3 donkey anti-guinea pig IgG, Cy5 goat anti-mouse IgG (both Jackson ImmunoResearch Laboratories), Alexa Fluor 488 goat anti-mouse IgG (Invitrogen). Antisera against mouse SGO2 and mouse securin were gifts from A. M. Pendás.

## Cell lines and plasmids

HeLa-K, Hek293T, hTERT RPE-1, HCT116, HCT116 *BAK*<sup>-/-</sup>, *BAX*<sup>-/-</sup>, HCT116 *TP53*<sup>-/-</sup>, SW480, and NIH/3T3 cells were cultured in Dulbecco's modified Eagle's medium (DMEM) (Biowest), T-47D cells in RPMI-1640 (Biowest) and A427 and A549 cells in essential minimum Eagle's medium (EMEM) (Roth). All media were supplemented with 10% heat-inactivated fetal calf serum (FCS) (Sigma-Aldrich). Cells were cultured at 37 °C in 5% CO<sub>2</sub>. *Xenopus laevis* S3 cells were grown at 27 °C under atmospheric CO<sub>2</sub> in 70% Leibovitz's L-15 medium (Gibco) supplemented with 1% Glutamax (Gibco) and 10% heat-inactivated FCS. *MCL1* (NM\_021960) was PCR-cloned from human testis cDNA (Clontech), *BCL-XL* (*BCL2L1*, NM\_138578), *BAK1* (*BCL2L7*, NM\_001188), *BIM* (*BCL2L11*, NM\_001204106) and *BAD* (*BCL2L8*, NM\_032989) were PCR-cloned from self-made HeLa cell cDNA. *MCL1* from *X. laevis* (NP\_001131055), *Xenopus tropicalis*

(XP\_002935512) and *Danio rerio* (NP\_571674) were PCR-cloned from self-made oocyte cDNA, zygote cDNA (a gift from C. Niehrs) and 72-h embryos (a gift from P. Braaker), respectively. Details about the resulting plasmids and derivatives thereof are available upon request. The ZipGFP plasmid was a gift from X. Shu (Addgene plasmid #81241)<sup>44</sup>. For transient expression of proteins, Hek293T, HeLa-K or hTERT RPE-1 cells were transfected with corresponding pCS2- or pDNA5-based plasmids using a calcium phosphate-based method or Lipofectamine 2000 (Invitrogen) according to the manufacturer's protocol. *X. laevis* S3 cells were transfected using PEI (Polysciences; 3 µl of 1 µg/µl per 1 µg DNA). *MCL1*<sup>+/TEV</sup> hTERT RPE1 cells were generated using the co-CRISPR approach<sup>45</sup> with 0.8 µM ouabain octahydrate (Sigma) 72 h after transfection with 30 pmol ssODN *MCL1*<sup>TEV</sup> (5'-GCTGGAGTTGGTCGGGGAATC TGGAATAACACCAGTACGGACGGGTACTACCCTCGACGCCGCCGCC AGCAGAGGAGGAGGAGGAGGAGACTGTACTTCCAGTCGCTCGAGA TTATCTCTCGGTACCTTCGGGAGC-3'), 10 pmol ssODN *ATPIA1* and 1 µg eSpCas9-ATPIA1\_G3\_Dual\_sgRNA (a gift from Y. Doyon, Addgene plasmid #86613) encoding the corresponding sgRNA for *MCL1*<sup>TEV</sup> (5'-CGAGTTGTACCGGCAGTCGC-3'). Ouabain-resistant clones were screened by PCR with oligonucleotides (fwd: 5'-GAGTTC GCTGGCGCCACCCCGTAGGACT-3', rev: 5'-GGGAGTGAGCCTTGG CGATTAATGAACCCCTT-3') and the resulting 871-bp fragment was further analysed for the presence of a XhoI site.

## Cell treatments

For synchronization in early S-phase, human and frog cells were treated with 2 mM thymidine (Sigma-Aldrich) for 20 h. Upon release/wash-out, cells entered mitosis within 8–10 h. Synchronization of cells in prometaphase was done by addition of taxol (LC Laboratories) to 0.2 µg/ml 6 h after release from thymidine block. G2 arrest was achieved by addition of 10 µM RO-3306 (Santa-Cruz Biotechnology) 4 h after release from thymidine arrest for 6–10 h. For release from G2 arrest, cells were trypsinized, washed 5× with fresh medium and reseeded for the indicated incubation times. To inhibit MCL1, BCL-XL, caspases or MPS1 kinase, cells were supplemented with A-1210477 (2.5 µM, Abcam), WEHI-539 (0.5 µM, Cayman Chemicals), Q-VD-OPh (20 µM, BD Pharmingen) or reversine (1 or 5 µM, Cayman Chemicals), respectively, at the time of taxol addition and incubated for 6 h. To assess apoptosis in interphase, cells were arrested with thymidine for 20 h together with simultaneous transfection of corresponding plasmids or siRNA, released for 15 h, re-supplemented with thymidine and analysed 10 h thereafter. To assess apoptosis in mitosis, cells were transfected 10–12 h before thymidine addition, released and treated with taxol as described above, and collected when morphological signs of apoptosis first became visible (typically 10–13 h after thymidine wash-out). When studying depletion of MCL1 and BCL-XL without separase deregulation, the taxol arrest was prolonged to 12 h before cells were analysed. As control, cells were treated with 1 µM staurosporine (Abcam) for 8–12 h. To address DiM in SAC-abrogated HeLa-K cells, the corresponding plasmids were transfected first. Ten hours later, siRNA was transfected. Thymidine was added 14 h thereafter. (In the case of NIH/3T3 cells, thymidine (4 mM) was added immediately after siRNA transfection and washed away 18 h thereafter. This was followed by a second thymidine block 10 h later.) After 20 h, cells were released, re-seeded, supplemented with reversine (5 µM unless stated otherwise) and incubated for the indicated times without addition of taxol. For the 'taxol-ZM override' experiments, taxol-arrested HeLa-K cells were collected by shake-off and released for the indicated times by replating into medium supplemented with ZM447439 (5 µM, Tocris Biosciences), taxol (0.2 µg/ml) and cycloheximide (30 µg/ml, Sigma-Aldrich). To induce FRB-FKBP heterodimerization of the split TEV<sup>46</sup>, rapamycin (100 nM, Sigma) was added 10 h before cells were collected.

## Immunoprecipitation and subcellular fractionation

Cells (1 × 10<sup>7</sup>) were lysed with a dounce homogenizer in 1 ml LP2 lysis buffer (20 mM Tris-HCl (pH 7.7), 100 mM NaCl, 10 mM NaF, 20 mM



# Article

supplemented with taxol 24–48 h thereafter and collected 12 h later. Lysates in LP2 (including protease and phosphatase inhibitors) were cleared by centrifugation for 30 min at 16,500g and rotated for 4 h at 4 °C with anti-GFP nanobody beads (0.1 ml corresponding to 1 mg nanobody). Immobilized kinases were washed three times in LP2 (200g, 1 min, 4 °C), transferred into cleavage buffer (10 mM Hepes-KOH (pH 7.7), 50 mM NaCl, 25 mM NaF, 1 mM EGTA, 20% glycerol) and incubated with 40 µg His<sub>6</sub>-SUMOstar protease<sup>52</sup> for 45 min at 18 °C. Eluates (80 µl) were snap-frozen and stored in aliquots at –80 °C. His<sub>6</sub>-SUMO1–MCL1ΔTM was expressed from a pET28-derivative in *Escherichia coli*. Rosetta 2 DE3 (Novagen). Bacteria were lysed in LP1 (PBS, 5 mM imidazole, 0.5 mM DTT and an additional 400 mM NaCl) and purified over Ni<sup>2+</sup>-NTA-agarose (Qiagen) according to standard procedures. The eluate in PBS supplemented with 250 mM imidazole, 0.5 mM DTT and an additional 400 mM NaCl (pH adjusted to 7.5 with HCl) was dialysed against LP1 for 12 h at 4 °C in the presence of 10 ng His<sub>6</sub>-Senp2<sup>53</sup> per 100 µg MCL1 and then rotated for 3 h over 9/10th the amount of fresh Ni<sup>2+</sup>-NTA-agarose. The flow-through containing pure MCL1ΔTM was dialysed against PBS and stored in aliquots at –80 °C.

## Flow cytometry

To measure apoptosis in vivo, Hela-K cells transfected with corresponding siRNAs and plasmids were collected by gentle trypsination, washed once with medium, and then stained with annexin V-FITC and propidium iodide according to the manufacturer's protocol (Abcam, ab14085). Samples were analysed immediately on a Cytomix FC 500 (Beckman Coulter) using an FL1 signal detector for FITC and FL2 for propidium iodide and counting at least 20,000 single cells per condition. Flow cytometry of propidium iodide-stained cells was done as described<sup>42</sup>.

## Statistics and reproducibility

No statistical methods were used to predetermine sample size. Experiments analysed by immunoblotting or autoradiography were repeated 2–4 times with similar results (2–4 biological replicates). For quantitative analyses of chromosome spreads, clonogenic assays, and IFM specimens, the investigators were blinded to sample allocation. Otherwise, experiments were not randomized.

## Reporting summary

Further information on research design is available in the Nature Research Reporting Summary linked to this paper.

## Data availability

The data that support the findings of this study are available within the paper. Source Data for Figs. 1–4 and Extended Data Figs. 1–12 are provided with the paper. Data or other materials are available from the corresponding author upon reasonable request.

39. Stemmann, O., Zou, H., Gerber, S. A., Gygi, S. P. & Kirschner, M. W. Dual inhibition of sister chromatid separation at metaphase. *Cell* **107**, 715–726 (2001).
40. Wolf, P. G., Cuba Ramos, A., Kenzel, J., Neumann, B. & Stemmann, O. Studying meiotic cohesin in somatic cells reveals that Rec8-containing cohesin requires Stag3 to function and is regulated by Wapl and sororin. *J. Cell Sci.* **131**, jcs212100 (2018).
41. Hellmuth, S. et al. Human chromosome segregation involves multi-layered regulation of separase by the peptidyl-prolyl-isomerase Pin1. *Mol. Cell* **58**, 495–506 (2015).
42. Hellmuth, S., Böttger, F., Pan, C., Mann, M. & Stemmann, O. PP2A delays APC/C-dependent degradation of separase-associated but not free securin. *EMBO J.* **33**, 1134–1147 (2014).
43. Hellmuth, S., Gutiérrez-Caballero, C., Llano, E., Pendás, A. M. & Stemmann, O. Local activation of mammalian separase in interphase promotes double-strand break repair and prevents oncogenic transformation. *EMBO J.* **37**, e99184 (2018).
44. To, T. L. et al. Rational design of a GFP-based fluorogenic caspase reporter for imaging apoptosis in vivo. *Cell Chem. Biol.* **23**, 875–882 (2016).
45. Agudelo, D. et al. Marker-free coselection for CRISPR-driven genome editing in human cells. *Nat. Methods* **14**, 615–620 (2017).
46. Wehr, M. C. et al. Monitoring regulated protein–protein interactions using split TEV. *Nat. Methods* **3**, 985–993 (2006).
47. Murray, A. W. Cell cycle extracts. *Methods Cell Biol.* **36**, 581–605 (1991).
48. McGuinness, B. E., Hirota, T., Kudo, N. R., Peters, J. M. & Nasmyth, K. Shugoshin prevents dissociation of cohesin from centromeres during mitosis in vertebrate cells. *PLoS Biol.* **3**, e86 (2005).
49. Lukinavičius, G. et al. SiR-Hoechst is a far-red DNA stain for live-cell nanoscopy. *Nat. Commun.* **6**, 8497 (2015).
50. Hanson, K. M. & Finkelstein, J. N. An accessible and high-throughput strategy of continuously monitoring apoptosis by fluorescent detection of caspase activation. *Anal. Biochem.* **564–565**, 96–101 (2019).
51. Gorr, I. H., Boos, D. & Stemmann, O. Mutual inhibition of separase and Cdk1 by two-step complex formation. *Mol. Cell* **19**, 135–141 (2005).
52. Liu, L., Spurrier, J., Butt, T. R. & Strickler, J. E. Enhanced protein expression in the baculovirus/insect cell system using engineered SUMO fusions. *Protein Expr. Purif.* **62**, 21–28 (2008).
53. Butt, T. R., Edavettal, S. C., Hall, J. P. & Mattern, M. R. SUMO fusion technology for difficult-to-express proteins. *Protein Expr. Purif.* **43**, 1–9 (2005).
54. Hames, R. S. & Fry, A. M. Alternative splice variants of the human centrosome kinase Nek2 exhibit distinct patterns of expression in mitosis. *Biochem. J.* **361**, 77–85 (2002).
55. Inoshita, S. et al. Phosphorylation and inactivation of myeloid cell leukemia 1 by JNK in response to oxidative stress. *J. Biol. Chem.* **277**, 43730–43734 (2002).
56. Maurer, U., Charvet, C., Wagman, A. S., Dejardin, E. & Green, D. R. Glycogen synthase kinase-3 regulates mitochondrial outer membrane permeabilization and apoptosis by destabilization of MCL-1. *Mol. Cell* **21**, 749–760 (2006).

**Acknowledgements** We thank T. U. Mayer for suggesting the concept of the DMC, R. Youle and M. Orth for cell lines, D. Pfeiffer for help with the 2D SIM, S. Heidmann, T. Klecker, and P. Wolf for critical reading of the manuscript, and J. Hübner and M. Hermann for technical assistance. This work was supported by a grant (STE997/4-2) from the Deutsche Forschungsgemeinschaft (DFG) to O.S.

**Author contributions** S.H. carried out all experiments. S.H. and O.S. co-designed the research and wrote the paper.

**Competing interests** The authors declare no competing interests.

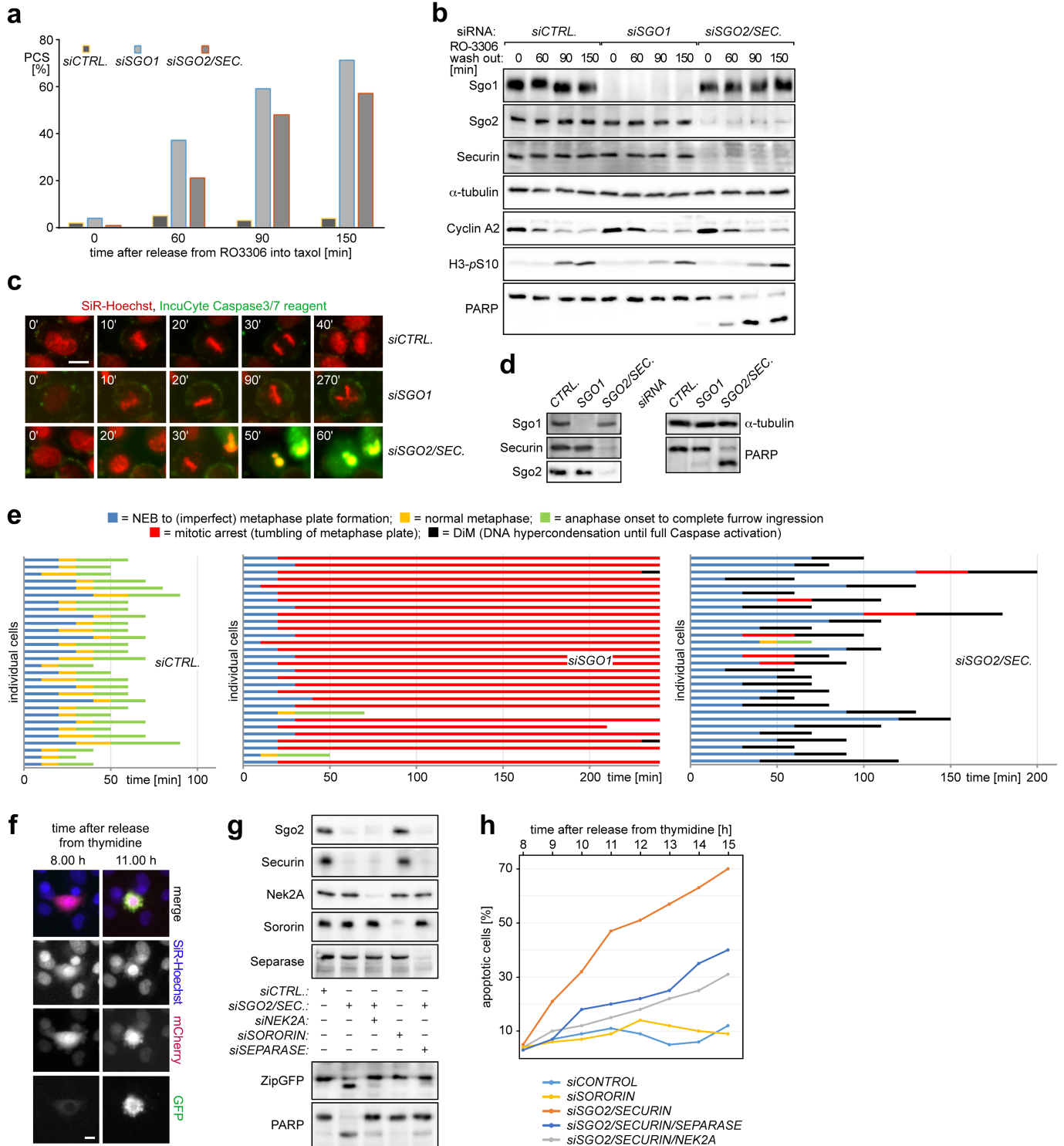
## Additional information

**Supplementary information** is available for this paper at <https://doi.org/10.1038/s41586-020-2187-y>.

**Correspondence and requests for materials** should be addressed to O.S.

**Peer review information** Nature thanks Andreas Villunger, Hongtao Yu and the other, anonymous, reviewer(s) for their contribution to the peer review of this work.

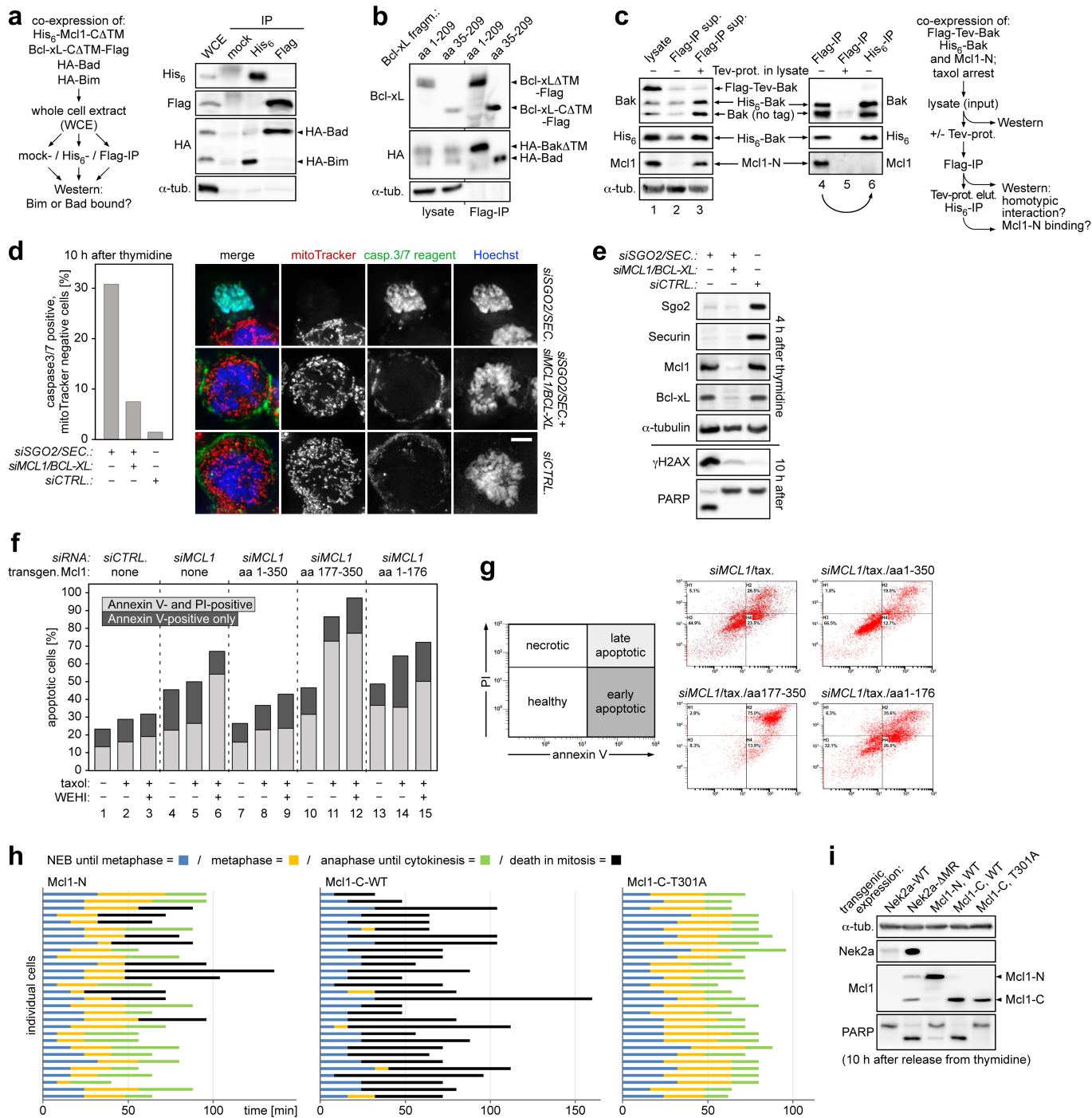
**Reprints and permissions information** is available at <http://www.nature.com/reprints>.



**Extended Data Fig. 1 | Premature activation of separase rather than loss of cohesion triggers DiM.** **a**, Premature sister chromatid separation (PCS) was quantified by chromosome spreading from siRNA-transfected HeLa-K cells at different times after release from RO-3306/G2 arrest. **b**, Immunoblots of cells from **a**. **c-e**, HeLa-K cells transfected with the indicated siRNAs and cultured in the presence of SiR-Hoechst<sup>49</sup> and a fluorogenic caspase 3/7 reporter<sup>50</sup> were analysed by video fluorescence microscopy. Shown are representative stills

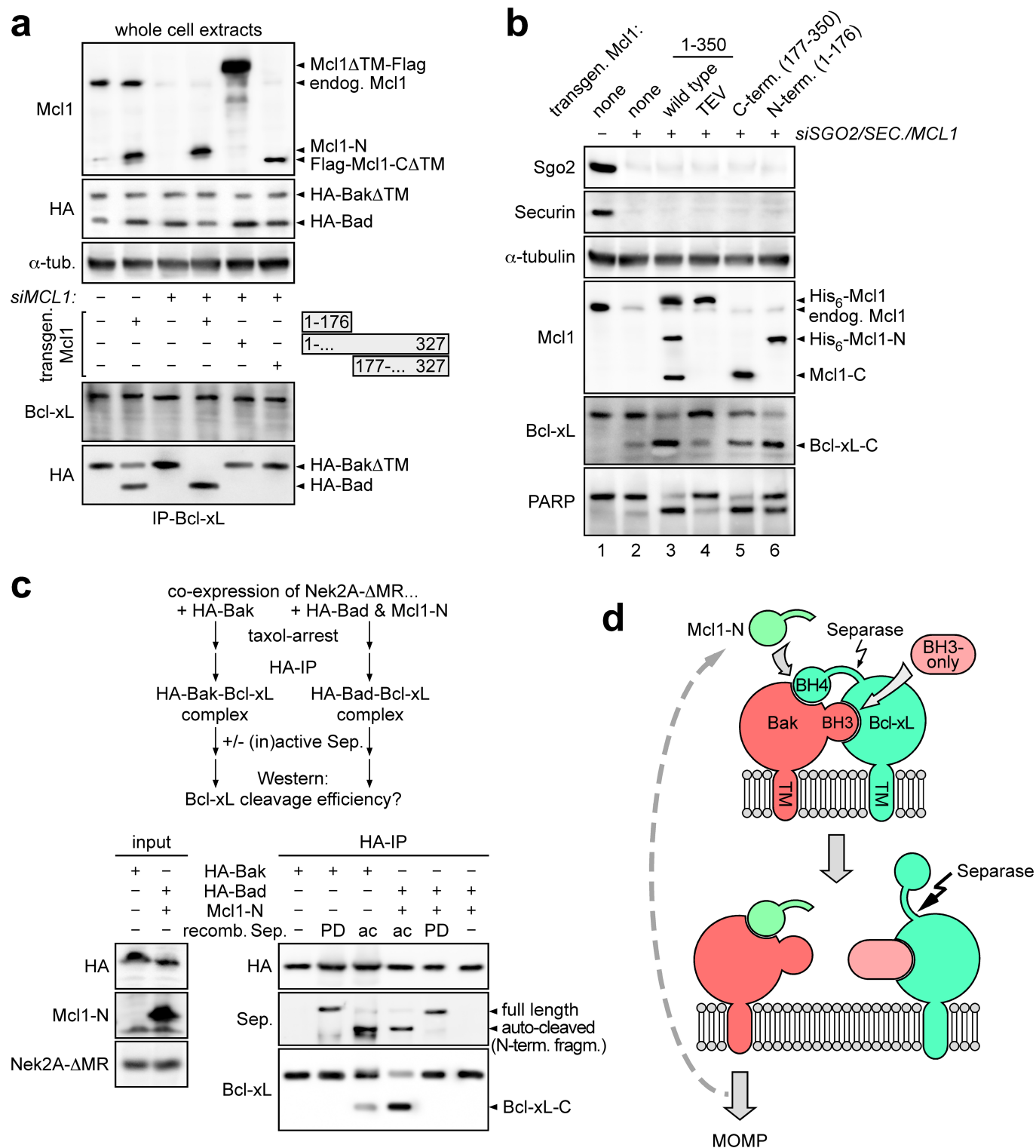
(**c**; scale bar, 10  $\mu$ m), immunoblots (**d**), and cell fate profiles (**e**). **f-h**, HeLa-K cells expressing the caspase 3 reporter ZipGFP<sup>44</sup> were transfected with the indicated siRNAs, supplemented with SiR-Hoechst and followed by video microscopy. At least 100 cells were counted per time point and condition. Shown are representative stills (**f**), immunoblots (**g**), and line graphs (**h**) of the percentages of GFP-positive (apoptotic) cells. The ZipGFP plasmid also expresses mCherry as a control. Scale bar, 10  $\mu$ m.





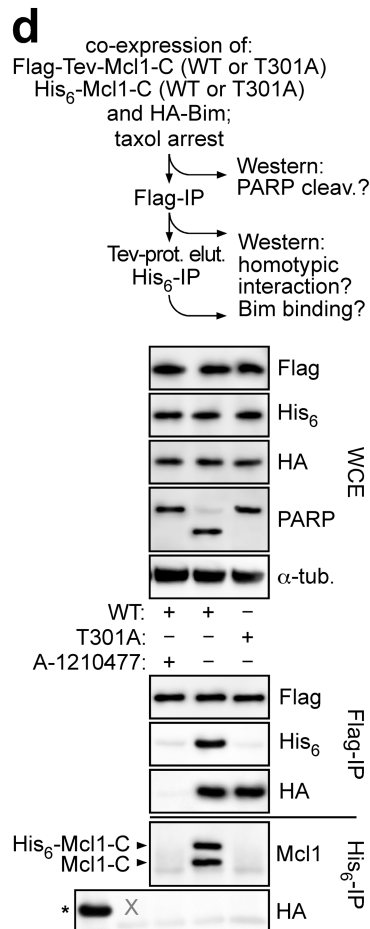
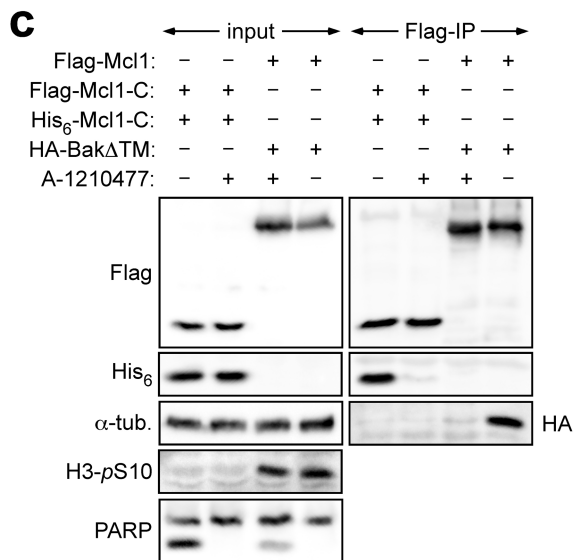
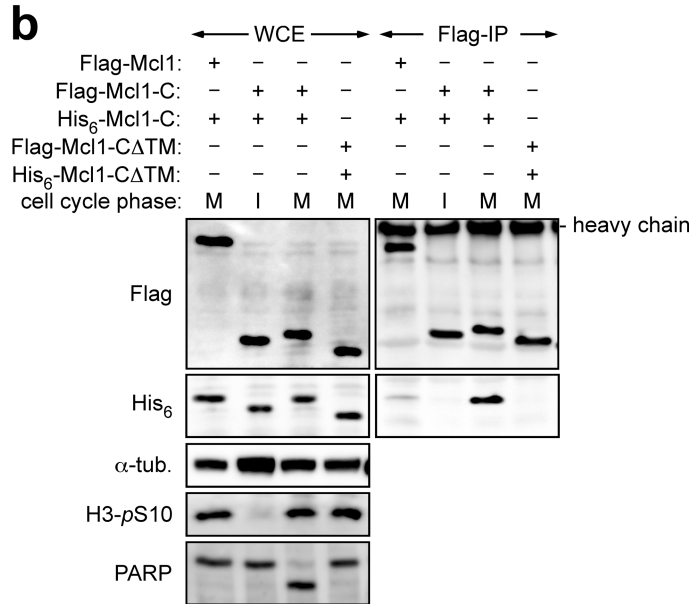
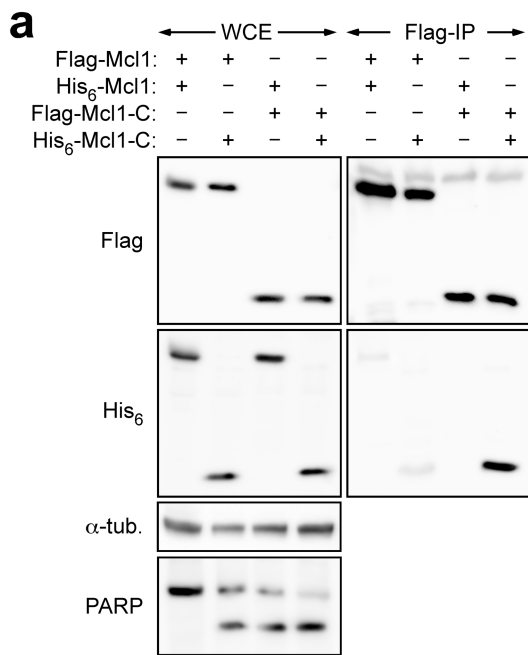
**Extended Data Fig. 3 | Characterization of separate cleavage fragments of MCL1 and BCL-XL.** **a**, The C-terminal separate cleavage fragments of MCL1 and BCL-XL preferentially bind BIM and BAD, respectively. Experimental setup and immunoblots of the indicated immunoprecipitation from taxol-arrested Hek293T cells co-expressing His<sub>6</sub>-MCL1-ΔCATM, BCL-XL-ΔCATM-Flag, HA-BAD, and HA-BIM. **b**, BCL-XL and BCL-XL-C bind BAK and BAD, respectively. Immunoblots of Flag immunoprecipitation from transfected, mitotic Hek293T cells expressing the indicated Flag-tagged BCL-XL fragments together with HA-tagged BAK and BAD. **c**, MCL1-N interacts with BAK. Experimental setup and immunoblots of lysate and consecutive Flag and His<sub>6</sub> immunoprecipitations from transfected, mitotic Hek293T cells co-expressing Flag-TEV-BAK, His<sub>6</sub>-BAK, and MCL1-N. TEV protease supplementation of lysate served as a negative control. Self-interaction of BAK is mutually exclusive with binding of MCL1-N. **d**, Separate-induced DiM is suppressed by knock-down of

MCL1 and BCL-XL. Quantification and representative images of siRNA-transfected, mitotic Hek293T cells cultivated in the presence of mitoTracker and a fluorogenic caspase 3/7 reporter before fixation and Hoechst staining. At least 100 cells each were counted. Scale bar, 5 μm. **e**, Immunoblots of cells from **d**. **f**, MCL1-N and -C promote DiM. Plot of early (dark grey) and late (light grey) apoptosis as judged by flow cytometric analysis of propidium iodide and annexin V staining of Hek293T cells transfected with siRNAs and expression vectors for transgenic MCL1 (fragments) and supplemented with taxol and BCL-XL inhibitor WEHI-539 (WEHI) as indicated. **g**, Representative 2D scatter plots of cells from **f** and their interpretation. **h**, Induction of DiM by MCL1-C does not require taxol treatment but does require Thr301. Cell fate profiles of HeLa-K cells expressing the indicated MCL1 fragments and cultured in the presence of SiR-Hoechst and a fluorogenic caspase 3/7 reporter. **i**, Immunoblot of cells from **h** and Extended Data Fig. 10a.



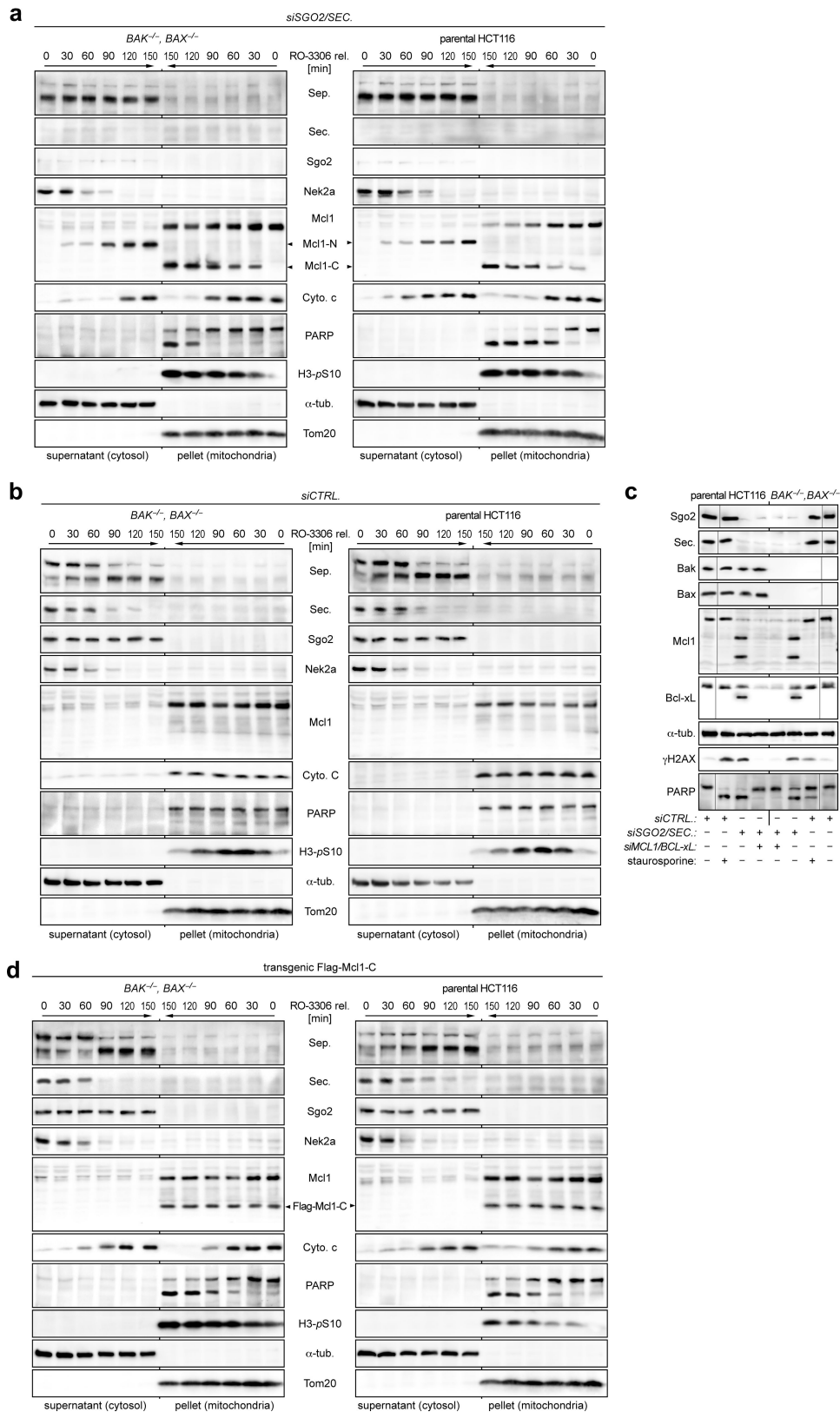
**Extended Data Fig. 4 | MCL1-N enables BAD to replace BAK as an interactor of BCL-XL and enhances cleavage of BCL-XL by separase.** **a**, MCL1-N causes a switch in the binding partner of BCL-XL from BAK to BAD. Immunoblots of BCL-XL immunoprecipitation from MCL1-depleted or control-treated, mitotic Hek293T cells co-expressing HA-BAK, HA-BAD and, where indicated, various MCL1 fragments. Separase was not deregulated in this experiment, which is why BCL-XL is not cleaved. **b**, Separase-dependent BCL-XL cleavage in cells is primarily stimulated by MCL1-N. Immunoblots of SGO2/securin/MCL1 triple-depleted or control-treated, prometaphase Hek293T cells expressing the indicated transgenic MCL1 variants. **c**, Separase prefers BCL-XL in complex with BAD as a substrate rather than BAK. Experimental setup and immunoblots

of HA immunoprecipitation from taxol-arrested Hek293T cells expressing NEK2A-ΔMR and either HA-BAK or HA-BAD plus MCL1-N. Before SDS-PAGE, samples were incubated with inactive (PD) or active (ac) separase or control treated (-). **d**, MCL1-N promotes apoptosis by a positive feedback mechanism. MCL1-N competitively displaces the BH4 domain of BCL-XL from BAK, resulting in BH3-only proteins, such as BAD, excluding BAK from BCL-XL. At the same time, this renders BCL-XL a better separase substrate. MCL1-N acts catalytically, being released from BAK upon self-interaction and pore formation by the latter (dotted arrow; Extended Data Fig. 3c).



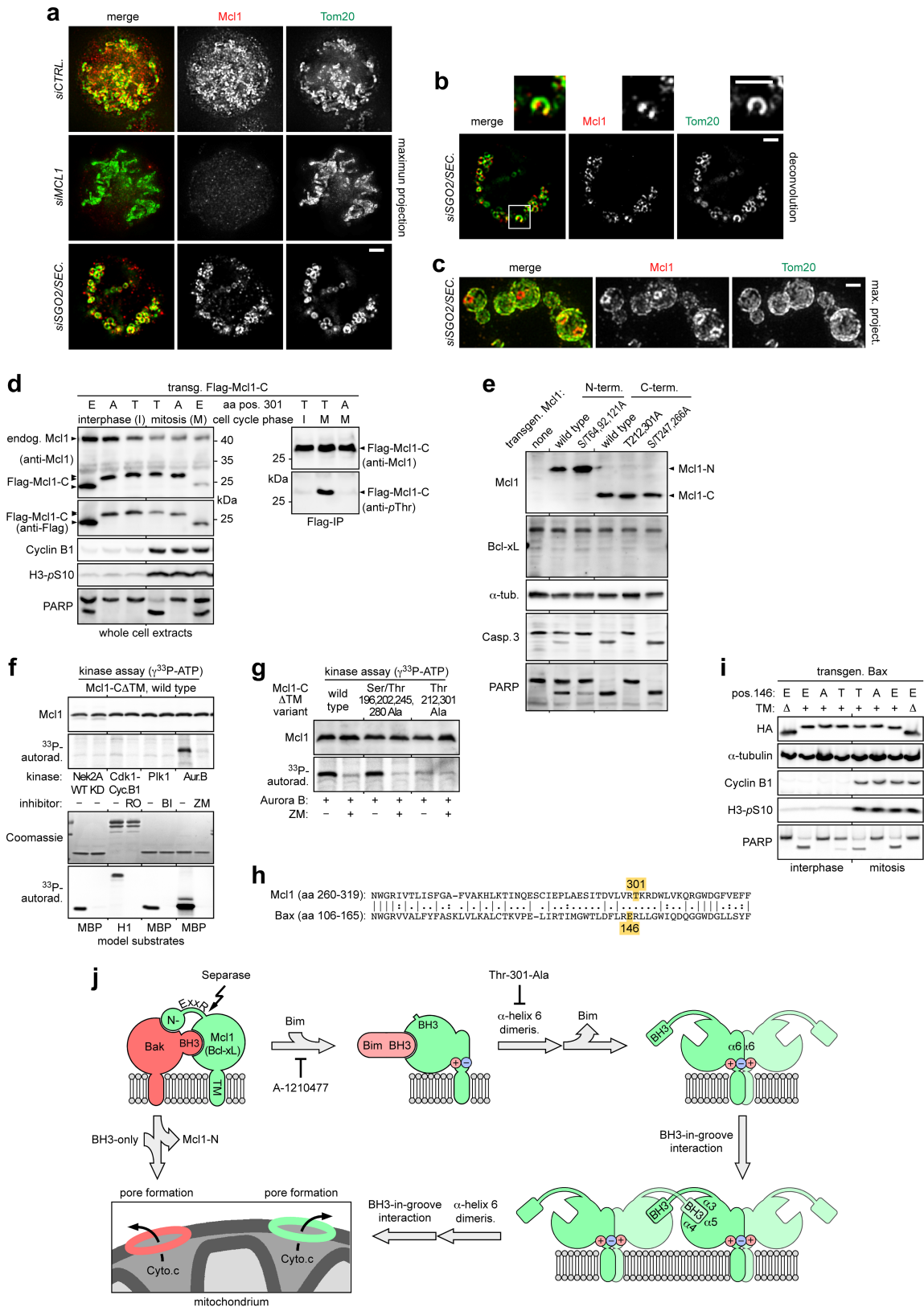
**Extended Data Fig. 5 | Self-interaction of pro-apoptotic MCL1-C shares characteristics with pore formation by BAK/BAX but requires mitosis-specific phosphorylation. a-c.** MCL1-C exhibits mitosis-specific self-interaction, which requires the transmembrane domain and an accessible BH3-binding groove. Immunoblots of Flag immunoprecipitation from mitotic or interphase Hek293T cells expressing MCL1 variants and supplemented with the MCL1 inhibitor A-1210477 as indicated. Blockade of the MCL1-BAK interaction served as a control for the effectiveness of A-1210477. **d.** The

homotypic interaction of MCL1-C is mutually exclusive with BIM binding. Top, experimental setup; bottom, immunoblots of consecutive Flag and His<sub>6</sub> immunoprecipitations from Hek293T cells expressing HA-BIM together with Flag-TEV- and His<sub>6</sub>-tagged forms of either wild-type MCL1-C or the T301A variant. X, irrelevant lane between HA-BIM control (asterisk) and His<sub>6</sub> immunoprecipitation samples. The T301A mutation prevents self-interaction of MCL1-C but not its association with BIM.



**Extended Data Fig. 6 | BAK/BAX-independent release of cytochrome c by separate deregulation or MCL1-C expression.** **a, b**, Time-resolved immunoblots of cytosol and mitochondria-containing fractions from SGO2/securin-depleted or mock-transfected *BAK<sup>-/-</sup>, BAX<sup>-/-</sup>* and parental HCT116 cells released from a G2-arrest at  $t = 0$  min. **c**, Immunoblots of taxol-arrested *BAK<sup>-/-</sup>, BAX<sup>-/-</sup>* and parental HCT116 cells that were transfected with siRNA and supplemented with staurosporine as indicated. Note the absence of MCL1 and

BCL-XL cleavage during staurosporine-induced apoptosis and suppression of *siSGO2/siPTTG1*-induced DiM by co-depletion of MCL1 and BCL-XL. Grey lines within panels are between lanes that were not directly juxtaposed but nevertheless originated from the same gel. **d**, Time-resolved immunoblots of cytosol and mitochondria-containing fractions from Flag-MCL1-C-expressing *BAK<sup>-/-</sup>, BAX<sup>-/-</sup>* and parental HCT116 cells released from G2-arrest at  $t = 0$  min.

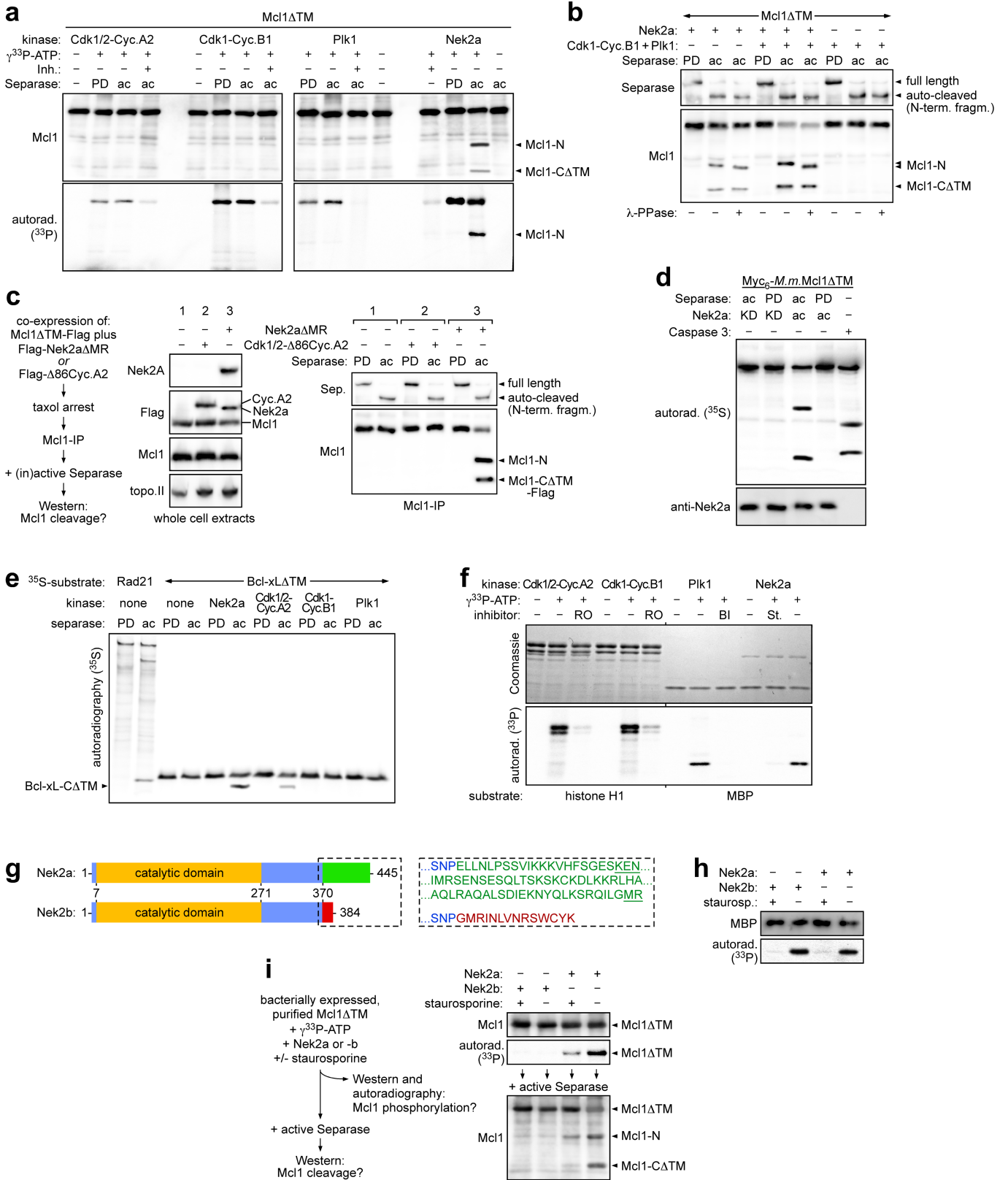


Extended Data Fig. 7 | See next page for caption.

# Article

**Extended Data Fig. 7 | The pro-apoptotic effect of MCL1-C and BAX requires a negative charge at the end of  $\alpha$ -helix 6.** **a, b**, Immunofluorescence micrographs of taxol-arrested Hek293T cells transfected with the indicated siRNAs. Shown are maximum projections of 20 z-stacks (**a**) or a single, deconvoluted plane (**b**). The interruption of TOM20 rings by MCL1 dots is consistent with a cross-section through a fragmented mitochondrion containing an MCL1 ring. Scale bars, 3  $\mu\text{m}$ . **c**, MCL1-C is likely to form macropores into the mitochondrial outer membrane. Immunofluorescence 2D SIM of SGO2/securin-depleted Hek293T cells undergoing DiM. Note the absence of the mitochondrial outer membrane marker TOM20 from the centres of MCL1 rings. Scale bar, 0.5  $\mu\text{m}$ . **d**, Immunoblots of extracts and Flag immunoprecipitations from interphase or mitotic Hek293T cells expressing Flag-tagged MCL1-C-WT (T), MCL1-C(T301A) (A), or MCL1-C(T301E) (E). **e**, Identifying serine and threonine residues that affect the pro-apoptotic nature of MCL1-N and MCL1-C. Immunoblot of MCL1-depleted, taxol-arrested Hek293T cells expressing the indicated siRNA-resistant variants of MCL1-N or MCL1-C. BCL-XL is not cleaved during apoptosis if separase remains inhibited.

**f, g**, Aurora B kinase phosphorylates MCL1-C in vitro, probably at position 301 primarily. Immunoblots and autoradiographs of in vitro-translated wild-type MCL1-C $\Delta$ TM and variants thereof after incubation with the indicated kinases and inhibitors in the presence of  $\gamma^{33}\text{P}$ -ATP. Activity of the recombinant kinase was confirmed using model substrates (**f**, lower panels). KD, kinase-dead; RO, RO-3306; BI, BI-2536; ZM, ZM-447439; MBP, myelin basic protein; H1, histone H1. **h**, Local alignment of MCL1 and BAX. Vertical lines and colons mark identical and chemically similar residues, respectively; dashes represent gaps. **i**, Immunoblots of interphase or mitotic Hek293T cells expressing BAX with (+) or without ( $\Delta$ ) TM and with Glu (E), Ala (A), or Thr (T) at position 146. **j**, Model of MOMP by MCL1-C homo-oligomerization. The indicated conformational changes are inspired by knowledge about BAK/BAX pore formation and their hierarchy was chosen to best explain our data; that is, why the T301A mutation abolished self-interaction of MCL1-C but left BIM binding unaffected (Extended Data Fig. 5d). Minus signs represent phosphorylated Thr301 and plus signs represent a nearby basic residue.

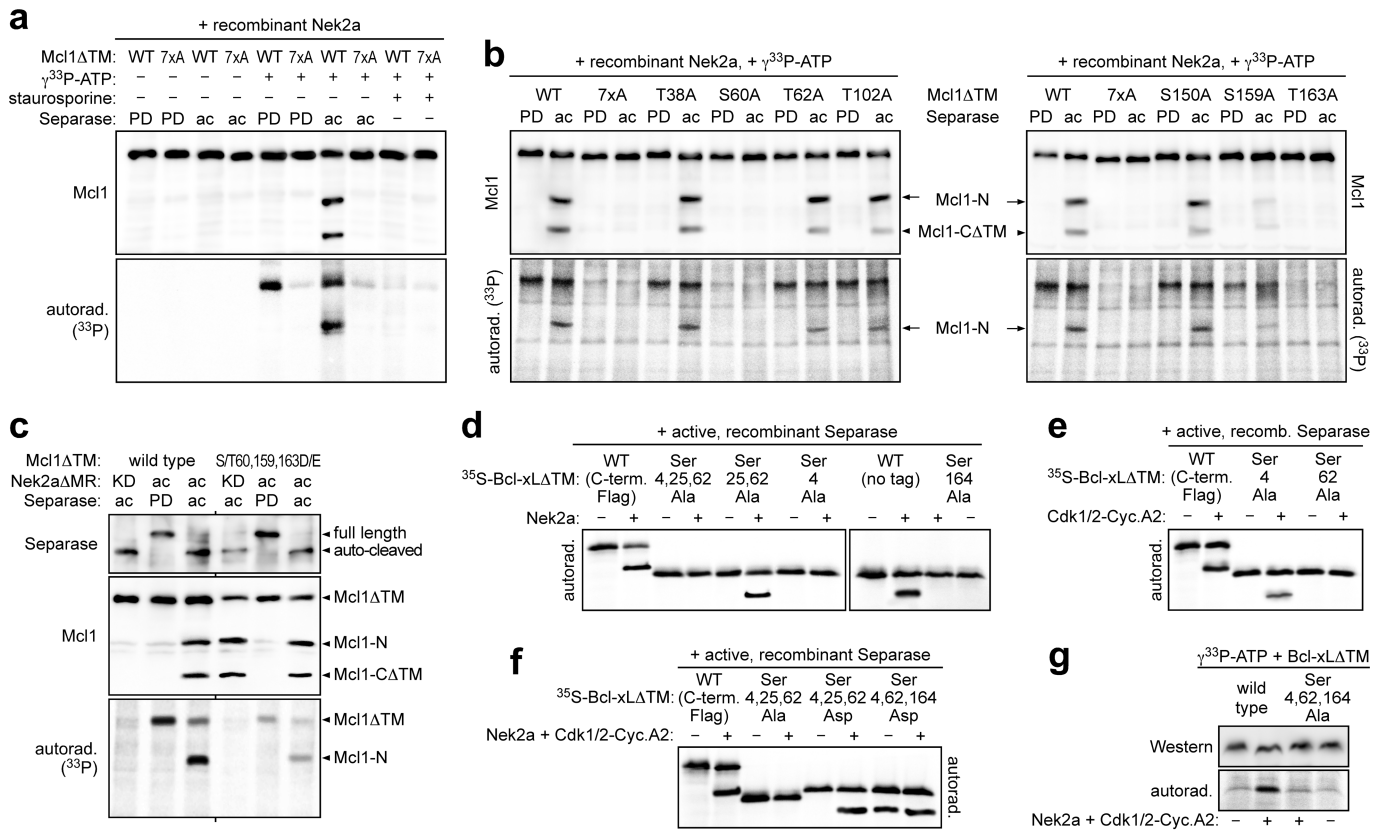


Extended Data Fig. 8 | See next page for caption.

## Article

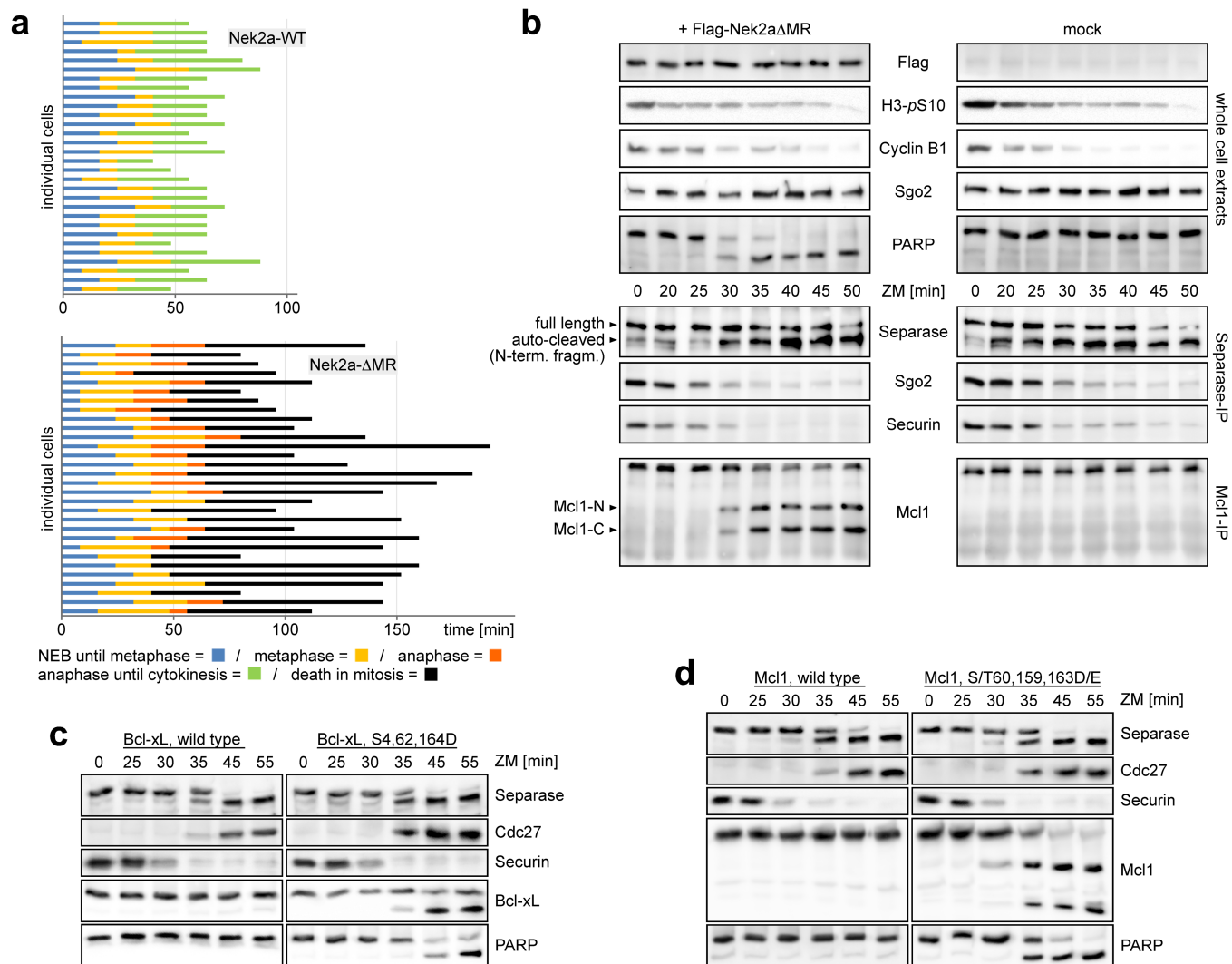
**Extended Data Fig. 8 | NEK2A kinase turns MCL1 and BCL-XL into separase substrates.** **a**, Autoradiographs and immunoblots of combined kinase ( $^{33}\text{P}$ -labelling) and cleavage (fragment-generation) assays using bacterially expressed, purified MCL1 $\Delta\text{TM}$  and kinases, specific inhibitors and active (ac) or inactive (PD) separase, as indicated. **b**, CDK1–cyclin B1 and PLK1 enhance separase-dependent cleavage of NEK2A-phosphorylated MCL1. Immunoblots of cleavage assays using bacterially expressed, purified MCL1 $\Delta\text{TM}$  and the indicated combination of kinases and separase variants. **c**, When immunoprecipitated from NEK2A- $\Delta\text{MR}$ -expressing, SAC-arrested cells, endogenous MCL1 is efficiently cleaved by separase in vitro. Left, experimental setup; right, immunoblots of cleavage assay combining active or inactive separase with MCL1 immunoprecipitation from prometaphase Hek293T cells expressing MCL1 $\Delta\text{TM}$ –Flag and, where indicated, Flag–NEK2A- $\Delta\text{MR}$  or N-terminally truncated ( $\Delta\text{86}$ ) Flag–cyclin A2. **d**, Cleavage of mouse (*M.m*) MCL1 by separase also requires NEK2A-dependent phosphorylation. In vitro-translated  $^{35}\text{S}$ -MYC6-*M.m*.MCL1 $\Delta\text{TM}$  was incubated with separase,

caspase 3 and NEK2A/ATP as indicated. Reactions were resolved by SDS–PAGE and analysed by autoradiography and immunoblotting. KD, kinase-dead (K37M). **e**, NEK2A and (to a lesser extent) CDK1/2–cyclin A2 sensitize BCL-XL to separase. Autoradiography of cleavage assay combining in vitro-translated  $^{35}\text{S}$ -RAD21 (positive control) or  $^{35}\text{S}$ -BCL-XL $\Delta\text{TM}$  with kinases/ATP and separase variants as indicated. **f**, Autoradiography of kinase assays ( $^{33}\text{P}$ -labelling) using model substrates and the kinases from **d**. **g–i**, The NEK2A-related NEK2B does not support separase-dependent MCL1 cleavage. **g**, Schematics and C-terminal sequences (dashed box) of NEK2A and NEK2B, which arise by alternative splicing of the same gene<sup>54</sup>. NEK2A-specific, C-terminal degrons (KEN box and MR-tail) are underlined. **h**, Both NEK2A and NEK2B can phosphorylate the model substrate MBP. **i**, NEK2B cannot phosphorylate MCL1. Left, experimental setup; top right, kinase assay; bottom right, cleavage assay combining MCL1 $\Delta\text{TM}$  with NEK2A, NEK2B, staurosporine (kinase inhibitor) and active separase as indicated.



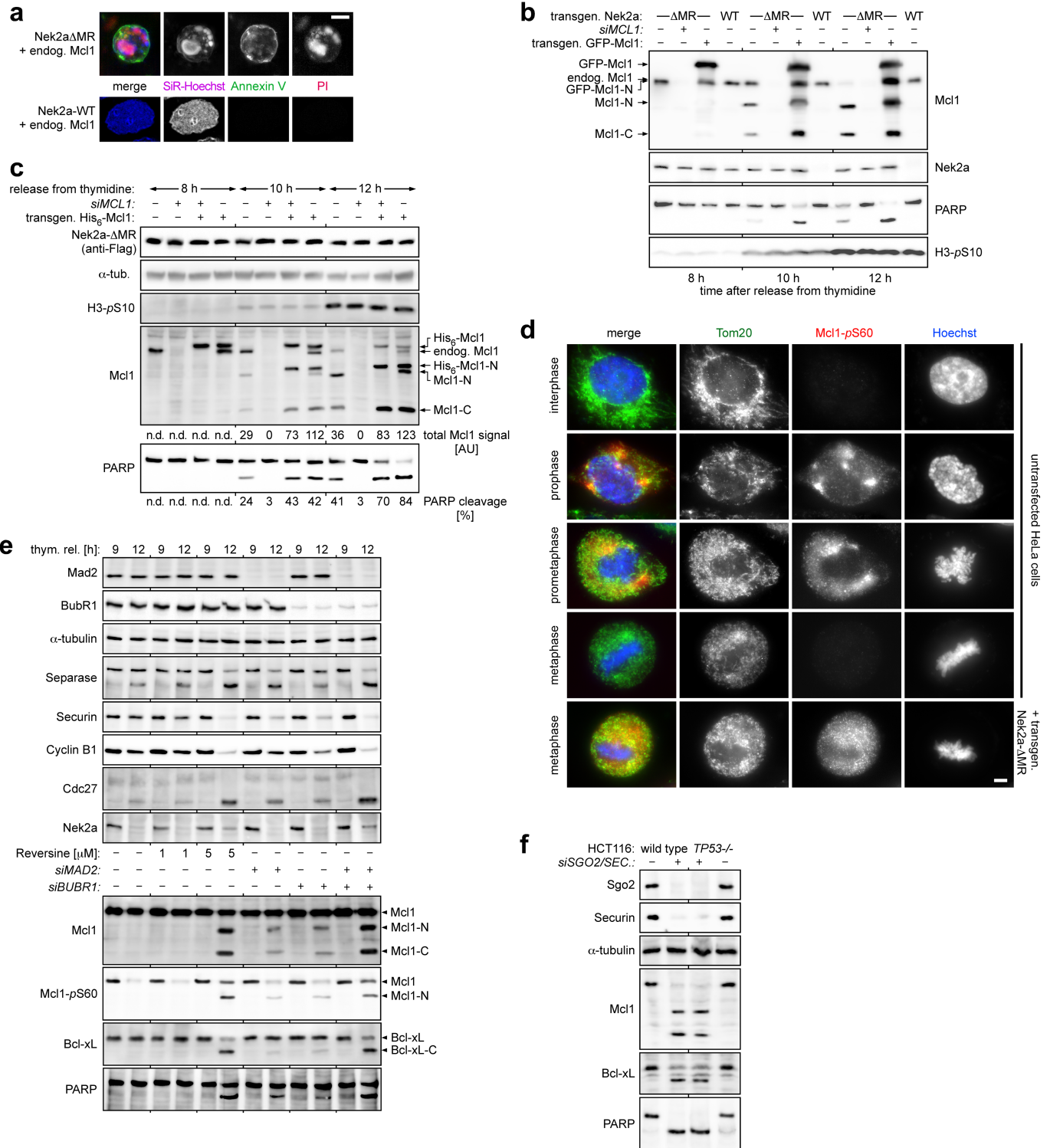
**Extended Data Fig. 9 | Mapping cleavage-relevant phosphorylation sites within MCL1 and BCL-XL. a, b,** Cleavage of MCL1 by separase essentially requires NEK2A-dependent phosphorylation of Ser60 and Thr163. Autoradiographs and immunoblots of combined kinase (<sup>33</sup>P-labelling) and cleavage (fragment-generation) assays. Prior to analysis, in vitro-translated, wild-type MCL1ΔTM and variants thereof were incubated with active NEK2A, γ<sup>33</sup>P-ATP, staurosporine, and active (ac) or inactive (PD) separase as indicated. In vivo phosphorylation of Ser159 and Thr163 has previously been reported<sup>55,56</sup>. In vivo phosphorylation of Ser60 was detected by a phosphorylation-specific antibody (Fig. 4c, Extended Data Fig. 11d, e). **c,** Separase-dependent cleavage of MCL1(S/T60,159,163D/E) is independent of NEK2A. Immunoblots and

autoradiography of combined kinase (<sup>33</sup>P) and cleavage assay. **d-f,** In vitro-translated, <sup>35</sup>S-labelled wild-type BCL-XLΔTM and variants thereof were incubated with the indicated kinases (+) or reference buffers (-) and active separase before SDS-PAGE and autoradiography. **d,** NEK2A-stimulated cleavage of BCL-XL by separase essentially requires Ser4 and Ser164. **e,** CDK1/2-cyclin A2-stimulated cleavage of BCL-XL by separase essentially requires Ser62. In vivo phosphorylation of Ser62 has been previously reported<sup>48</sup>. **f,** Separase-dependent cleavage of BCL-XL(S4,62,164D) occurs independently of NEK2A and CDK1/2-cyclin A2. **g,** Autoradiograph and immunoblot of kinase assay using in vitro-translated, wild-type BCL-XLΔTM or its S4,62,164A variant and γ<sup>33</sup>P-ATP in combination with the indicated kinases (+) or reference buffers (-).



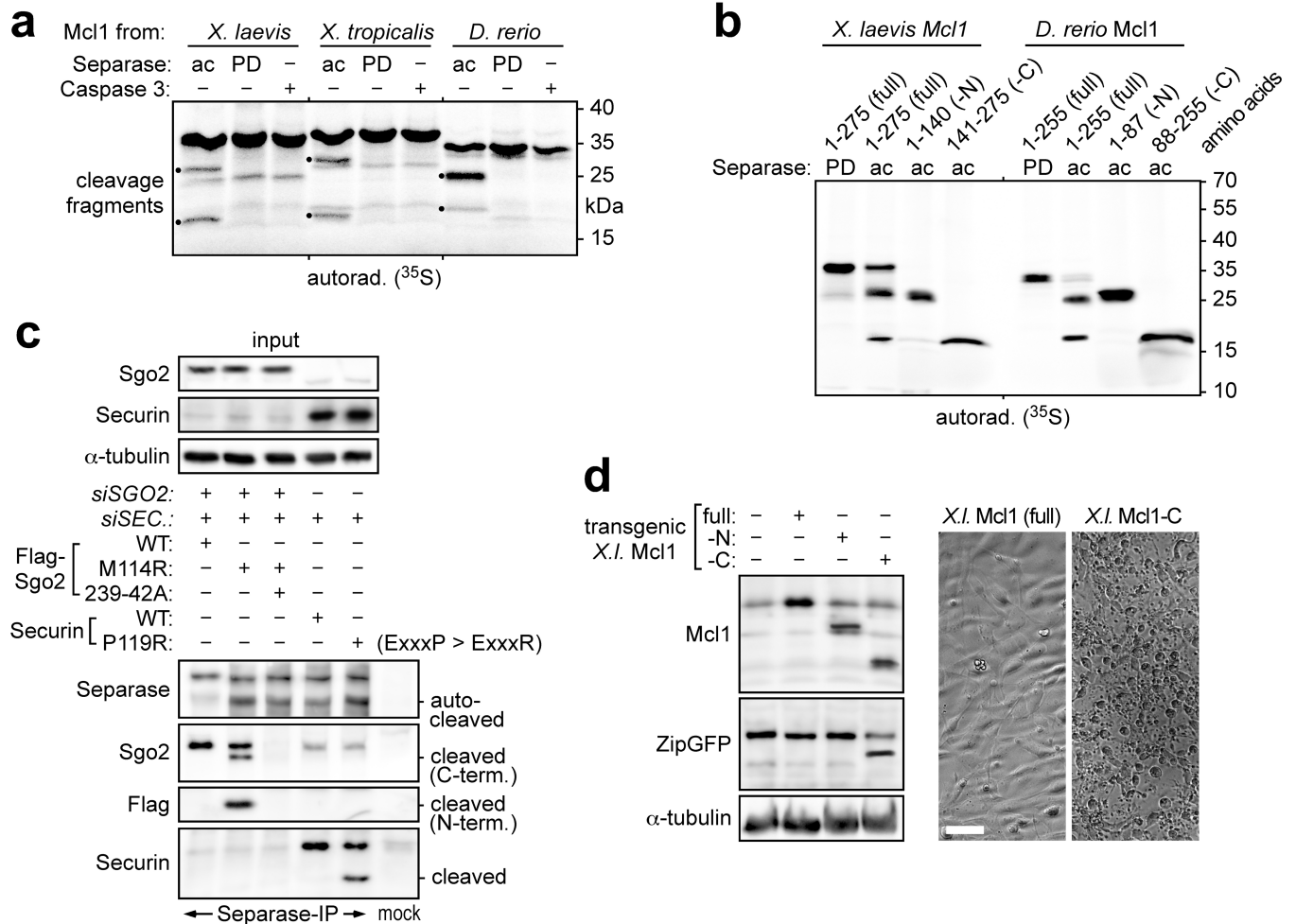
**Extended Data Fig. 10 | Stabilized NEK2A and constitutively cleavable MCL1- and BCL-XL variants result in DiM upon activation of separase in anaphase. a**, Cell fate profiles of HeLa-K cells expressing NEK2A-WT or NEK2A-ΔMR and cultured in the presence of SiR-Hoechst and a fluorogenic caspase 3/7 reporter. **b**, Immunoblots of time-resolved separase and MCL1

immunoprecipitations from NEK2A-ΔMR-expressing or control HeLa-K cells released from taxol arrest by addition of ZM-447439 (ZM) at  $t = 0$  min. **c, d**, HeLa-K cells expressing the indicated variants of MCL1 and BCL-XL were analysed as in **a**. (Dephosphorylated) CDC27 served as a marker for late mitosis.



**Extended Data Fig. 11 | NEK2A stabilization preferentially kills MCL1-overexpressing cells.** **a, b**, Representative images and immunoblots of quantitative analysis shown in Fig. 4b. Scale bar, 5  $\mu$ m. **c**, Immunoblots of NEK2A- $\Delta$ MR-expressing Hek293T cells transfected with siMCL1 and expression plasmids for His<sub>6</sub>-MCL1 as indicated. MCL1 and PARP cleavage were quantified densitometrically. n.d., not determined. **d**, MCL1-Ser60 is phosphorylated in early mitosis only. Untransfected or NEK2A- $\Delta$ MR-expressing HeLa-K cells were

released from thymidine arrest for 8 h and then analysed by (immuno) fluorescence microscopy using Hoechst and the indicated antibodies. Scale bar, 5  $\mu$ m. **e**, Chemical abrogation of the SAC triggers DiM. Immunoblots of reversine- or siRNA-treated HeLa-K cells synchronized as in Fig. 4c. Dephosphorylation of CDC27 into a sharp, fast-migrating band serves as a marker of late mitosis. **f**, TP53<sup>-/-</sup> cells and parental HCT116 cells were depleted of SGO2 and securin, taxol-arrested and analysed by immunoblotting.



**Extended Data Fig. 12 | MCL1 cleavage by separase and the pro-apoptotic effect of MCL1-C is conserved in non-mammalian vertebrates.**

**a**, <sup>35</sup>S-labelled, NEK2A/ATP-treated full-length Mcl1 from *X. laevis*, *X. tropicalis* and *D. rerio* were incubated with separase variants and caspase 3 as indicated, and analysed by autoradiography. **b, c**, Separase can cleave after ExxxR motifs. **b**, *X. laevis* and *D. rerio* Mcl1 are cleaved by separase after 136-ExxxR-140 and 84-ExxR-87, respectively. The indicated full-length Mcl1 or fragments thereof

were analysed as in **a, c**. Changing the pseudo-substrate sequence of securin to ExxxR turns it into a separase substrate. Endogenous human SGO2 and securin were depleted by RNAi and replaced by the indicated variants<sup>9</sup>. These were then assessed for cleavage by immunoprecipitation and western blotting.

**d**, *Xenopus* S3 cells transfected to express ZipGFP and the indicated forms of *X. laevis* Mcl1 were analysed by immunoblotting (left) and video microscopy (representative phase contrast images on right). Scale bar, 50 μm.

## List of all own publications

- 1) Hellmuth, S., Bottger, F., Pan, C., Mann, M. & Stemmann, O.  
PP2A delays APC/C-dependent degradation of separase-associated but not free securin.  
EMBO J 33, 1134-1147, doi:10.1002/embj.201488098 (2014).
- 2) Hellmuth, S., Pohlmann, C., Brown, A., Bottger, F., Sprinzl, M. & Stemmann, O.  
Positive and negative regulation of vertebrate separase by Cdk1-cyclin B1 may explain why securin is dispensable.  
J Biol Chem 290, 8002-8010, doi:10.1074/jbc.M114.615310 (2015a).
- 3) Hellmuth, S., Rata, S., Brown, A., Heidmann, S., Novak, B. & Stemmann, O.  
Human chromosome segregation involves multi-layered regulation of separase by the peptidyl-prolyl-isomerase Pin1.  
Mol Cell 58, 495-506, doi:10.1016/j.molcel.2015.03.025 (2015b).
- 4) Wild, T., Budzowska, M., Hellmuth, S., Eibes, S., Karemore, G., Barisic, M., Stemmann, O. & Choudhary, C.  
Deletion of APC7 or APC16 Allows Proliferation of Human Cells without the Spindle Assembly Checkpoint.  
Cell Rep 25, 2317-2328 e2315, doi:10.1016/j.celrep.2018.10.104 (2018).
- 5) Hellmuth, S., Gutierrez-Caballero, C., Llano, E., Pendas, A. M. & Stemmann, O.  
Local activation of mammalian separase in interphase promotes double-strand break repair and prevents oncogenic transformation.  
EMBO J 37, e99184, doi:10.15252/embj.201899184 (2018).
- 6) Henschke, L. Frese, M., Hellmuth, S., Marx, A., Stemmann, O. & Mayer, T. U.  
Identification of Bioactive Small Molecule Inhibitors of Separase.  
ACS Chem Biol 14, 2155-2159, doi:10.1021/acscchembio.9b00661 (2019).
- 7) Hellmuth, S., Gomez-H, L., Pendas, A. M. & Stemmann, O.  
Securin-independent regulation of separase by checkpoint-induced shugoshin-Mad2.  
Nature 580, 536-541, doi: 10.1038/s41586-020-2182-3 (2020).
- 8) Hellmuth, S. & Stemmann, O.  
Separase-triggered apoptosis enforces minimal length of mitosis  
Nature 580, 536-541, doi: 10.1038/s41586-020-2187-y (2020).
- 9) Gómez-H, L., Herrán, Y., Nikalayevich, E., Hellmuth, S., Felipe-Medina, N., Gómez, R., Warif El Yakoubi, W., Melmeh, S., Ángel Suja, J., Maestre, C., Barbero, J. L., Malumbres, M., Sánchez-Martín, M., Stemmann, O., Wassmann, K., Llano, E. & Pendás, A. M.  
Securin promotes complete resolution of cohesion during the second meiotic division and safeguards spermatozooids from aneuploidy.  
*In preparation.*

## Danksagung

Zu allererst möchte ich mich bei Prof. Dr. Benedikt Westermann bedanken, der meine Promotion gegenüber der Fakultät offiziell vertritt und den Vorsitz des Prüfungsausschusses übernommen hat.

Der Grund, warum Wissenschaft mein Leben geworden ist, ist vor allem der ansteckenden Begeisterung und der absoluten Hingabe meines Doktorvaters Prof. Dr. Olaf Stemmann geschuldet. Die Begleitung und Betreuung durch die gesamte Doktorzeit war ausnahmslos unglaublich wertvoll. Bei jedem wissenschaftlichen Problem waren einem Anregungen und experimentelle Hilfe gewiss. Ohne die Unterstützung und die große Expertise von Prof. Dr. Olaf Stemmann, hätte ich meine Promotion nicht so erfolgreich beenden können.

Hervorheben möchte ich die tolle Zusammenarbeit mit den Mitgliedern des Lehrstuhls für Genetik. Mein Dank gilt Jutta Hübner und Kerstin Kapp, für die Hilfe beim Klonieren sowie Markus Herrmann für die Unterstützung bei der Mikroskopie, FACS-Bedienung und Aufreinigung rekombinanter Proteine. Natürlich wäre ein Arbeiten in der Zellkultur ohne den stetigen Nachschub an sterilen, gestopften Glaspipetten durch Petra Helies unmöglich gewesen. Liebe Petra, wir kennen uns nun schon so lange, vielen Dank, dass Du so bist wie Du bist. Auch Brigitte Jaunich möchte ich nicht vergessen, die immer alles unternimmt, um unser Bestells-Wirrwarr zu ordnen und in allen Belangen des Labors eine große Hilfe ist. Auch persönlich bist Du ein ganz toller Mensch, mit großem Herz und ehrlicher Stimme.

Danke auch allen Doktoranden/innen des Lehrstuhls für die Zusammenarbeit und den praktischen und wissenschaftlichen Rat.

Zu Beginn meiner Doktorzeit waren vor allem Dr. Lisa Mohr, Dr. Bu, Dr. Peter Wolf, Dr. Laura Schöckel, Philip Kahlen und Dr. MO vertraute Wegbegleiter zu denen ich aufschauen konnte, mit denen ich viel gelacht habe, und die mir damit lange Abende im Labor verkürzten. Es war eine schöne Zeit mit Höhen und Tiefen. Auch beim aktuellen Team möchte ich mich bedanken. Besonders `meine drei Männer´ Alex, Marcel und Bald-Doktorand Basti möchte ich hervorheben. Eure Unterstützung, Ehrlichkeit und unser gemeinsamer Humor haben mir sehr in stressigen Zeiten geholfen. Ich hoffe unsere Freundschaft besteht über die Doktorarbeit hinaus.

Auch Du, liebe Mama, hast einen großen Anteil daran, dass ich diese Doktorarbeit geschafft habe. Du hast mir die Kraft geschenkt, in vielen schwierigen Momenten den Kopf zu bewahren, und hast mir neue Blickwinkel vermittelt. Du bist mein Vorbild. Meine beiden Mäuse, Klara und Marie, wenn Ihr einmal diese Zeilen lesen könnt, sollt Ihr wissen, dass auch Ihr mir geholfen habt. Als Babys wart Ihr mit mir im Labor und habt in der Babytrage mit mir zusammen experimentiert. Ihr seid mein größtes Glück und ich bin dankbar Eure Mama zu sein.

Zuletzt möchte ich mich bei Dir, Olaf, als meinem Partner bedanken. Ich bewundere Dich und bin dankbar, Dich gefunden zu haben. Auch in stürmischen Zeiten warst Du immer an meiner Seite. Danke für Deine Unterstützung und Liebe.

## **(Eidesstattliche) Versicherungen und Erklärungen**

(§ 8 Satz 2 Nr. 3 PromO Fakultät)

*Hiermit versichere ich eidesstattlich, dass ich die Arbeit selbstständig verfasst und keine anderen als die von mir angegebenen Quellen und Hilfsmittel benutzt habe (vgl. Art. 64 Abs. 1 Satz 6 BayHSchG).*

(§ 8 Satz 2 Nr. 3 PromO Fakultät)

*Hiermit erkläre ich, dass ich die Dissertation nicht bereits zur Erlangung eines akademischen Grades eingereicht habe und dass ich nicht bereits diese oder eine gleichartige Doktorprüfung endgültig nicht bestanden habe.*

(§ 8 Satz 2 Nr. 4 PromO Fakultät)

*Hiermit erkläre ich, dass ich Hilfe von gewerblichen Promotionsberatern bzw. –  
vermittlern oder ähnlichen Dienstleistern weder bisher in Anspruch genommen habe  
noch künftig in Anspruch nehmen werde.*

(§ 8 Satz 2 Nr. 7 PromO Fakultät)

*Hiermit erkläre ich mein Einverständnis, dass die elektronische Fassung der  
Dissertation unter Wahrung meiner Urheberrechte und des Datenschutzes einer  
gesonderten Überprüfung unterzogen werden kann.*

(§ 8 Satz 2 Nr. 8 PromO Fakultät)

*Hiermit erkläre ich mein Einverständnis, dass bei Verdacht wissenschaftlichen  
Fehlverhaltens Ermittlungen durch universitätsinterne Organe der wissenschaftlichen  
Selbstkontrolle stattfinden können.*

.....